National Research Council Canada

Conseil national de recherches Canada

NRC · CNRC

Canadian Journal of Fisheries and Aquatic Sciences

Journal canadien des sciences halieutiques et aquatiques

http://cjfas.nrc.ca

http://jcsha.cnrc.ca

ISSN 0706-652X / CJFSDX 61(11) 2025–2266 (2004)

The *Canadian Journal of Fisheries and Aquatic Sciences*, previously published as *Contributions to Canadian Biology* 1901–1925, *Contributions to Canadian Biology and Fisheries* 1926–1934, *Journal of the Biological Board of Canada* 1934–1937, and *Journal of the Fisheries Research Board of Canada* 1938–1979, is issued monthly to form annual volumes of 12 numbers plus supplements.

Editorial policy. The Journal publishes original research articles, perspectives (syntheses, critiques, re-evaluations), discussions (comment and reply), and rapid communications. Manuscripts may concern cells, organisms, populations, communities, ecosystems, or processes that affect aquatic systems. They may cover a range of disciplines including biology and ecology of marine and freshwater organisms, limnology, oceanography, physiology, toxicology, genetics, economics, disease, and management. Preference will be given to manuscripts that emphasize understanding of observed phenomena and interpretation of experimental results. The Journal encourages papers that lead from clearly stated purpose or rationale and from testable hypotheses, concepts, or questions to identifiable conclusions or syntheses. Such papers may amplify, modify, question, or redirect accumulated knowledge embodied in contemporary perceptions of a particular state of aquatic sciences. The Journal discourages papers that are essentially descriptive, except in emerging disciplines; have only site-specific or local applications (a certain year, place, taxon, chemical compound, etc.); only confirm previously established principles; or apply standard techniques without breaking new methodological ground.

Manuscripts for publication should be submitted to the Senior Editor, *Canadian Journal of Fisheries and Aquatic Sciences*, Department of Organismal Biology, Ecology and Evolution, University of Guelph, Guelph, ON N1G 2W1, Canada (519-824-4120 ext. 52646; fax: 519-767-9798; e-mail: cjfas@uoguelph.ca).

Submissions in either English or French are acceptable. The information must be original, that is, not copyrighted, published, or submitted elsewhere except in abstract form or unless by written consent of the Editor.

Correspondence concerning accepted manuscripts and corrected proofs should be sent to NRC Research Press, National Research Council of Canada, Ottawa, ON K1A 0R6, Canada (fax: 613-952-7656; e-mail: pubs@nrc-cnrc.gc.ca).

Instructions to Authors are published once a year in the first issue of each volume. Copies are available from NRC Research Press or at http://cjfas.nrc.ca. The **Publication Policy** of NRC Research Press is available at http://pubs.nrc-cnrc.gc.ca.

Microfilm. Issues from 1934 through the current volume can be purchased on 16- or 35-mm microfilm. Photocopies of individual articles or issues can be purchased from University Microfilms International, 330 North Zeeb Road, Ann Arbor, MI 48106, USA.

US periodical postage paid at Champlain, NY 12919, USA, and at additional mailing offices. Attention U.S. POSTMASTER: Send address changes to **Canadian Journal of Fisheries and Aquatic Sciences**, c/o USACAN Media Distribution Center, P.O. Box 2888, Plattsburgh, NY 12901, USA.

Publié sans interruption depuis 1901, le *Journal canadien des sciences halieutiques et aquatiques* a paru sous plusieurs titres : *Contributions to Canadian Biology* 1901–1925, *Contributions to Canadian Biology and Fisheries* 1926–1934, *Journal of the Biological Board of Canada* 1934–1937, et *Journal of the Fisheries Research Board of Canada* 1938–1979. Le Journal paraît tous les mois, formant ainsi un volume de 12 numéros, et offre en plus jusqu'à deux suppléments par année.

Politique éditoriale. On publie, dans le Journal, des articles rendant compte de recherche originale, des perspectives (synthèses, critiques et réévaluations), des discussions (commentaires et réponses) et des communications rapides. Les documents peuvent porter sur les cellules, organismes, populations, communautés, écosystèmes ou processus qui affectent les systèmes aquatiques. Ils peuvent relever de divers domaines y compris la biologie et l'écologie des organismes marins et d'eau douce, la limnologie, l'océanographie, la physiologie, la toxicologie, la génétique, l'économie, la pathologie et la gestion. On accorde la préséance aux articles qui contribuent à la compréhension de phénomènes observés et à l'interprétation de résultats expérimentaux. On invite les auteurs à soumettre des articles ayant des objectifs précis ou relevant d'hypothèses, de concepts ou de questions vérifiables et se terminant par de solides conclusions ou d'utiles synthèses. Ces articles enrichissent, changent, mettent en question ou réorientent les connaissances acquises sur divers aspects des sciences aquatiques. On décourage toutefois la soumission d'articles simplement descriptifs (à moins qu'il ne s'agisse de nouvelles disciplines), d'application très limitée (applicables à une seule année, une seule région ou un seul taxon, portant sur un unique composé chimique, etc.); d'articles qui ne font que reprendre les principes énoncés dans des articles précédents; et d'articles rendant compte de l'application de normes sans gain de méthodologie.

Les auteurs voudront adresser leurs **manuscrits** à la directrice scientifique principale, *Journal canadien des sciences halieutiques et aquatiques*, Department of Organismal Biology, Ecology and Evolution, University of Guelph, Guelph, ON N1G 2W1, Canada (519-824-4120 poste 52646; télécopieur : 519-767-9798; courriel : cjfas@uoguelph.ca).

Les contributions peuvent être en anglais ou en français. Elles doivent être originales, c.-à.-d. qu'elles ne doivent pas avoir fait l'objet d'un copyright, avoir été publiées ou soumises ailleurs, sauf sous forme abrégée ou avec le consentement du rédacteur. Le CNRC ne se tient en aucune façon responsable des opinions exprimées par un collaborateur ou des déclarations qui pourrait faire ce dernier.

La correspondance ayant trait aux manuscrits acceptés et les **épreuves corrigés** doivent être envoyées aux Presses scientifiques du CNRC, Conseil national de recherches du Canada, Ottawa, ON K1A 0R6, Canada (télécopieur : 613-952-7656; courriel : pubs@nrc-cnrc.gc.ca).

Les Recommandations aux auteurs sont publiées une fois par année dans le premier numéro de chaque volume. Des copies sont disponibles auprès du Bureau de la rédaction aux Presses scientifiques du CNRC ou au http://jcsha.cnrc.ca. **La Politique de publication** est disponible auprès des Presses scientifiques du CNRC ou au http://pubs.nrc-cnrc.gc.ca.

Microfilms. On peut acheter sur microfilms de 16 ou 35 mm tous les numéros depuis 1934. Des photocopies d'articles ou de numéros individuels sont aussi en vente auprès de University Microfilms International, 330 North Zeeb Road, Ann Arbor, MI 48106, É.-U.

This Journal is indexed or abstracted in / Cette revue est signalée ou résumée dans

ABSEARCH, Applied Science and Technology Index and Abstracts, Aquatic Sciences and Fisheries Abstracts, Biological Abstracts, Biological and Agricultural Abstracts, CAB Abstracts, Chemical Abstracts, Current Contents, Elsevier BIOBASE, Environmental Abstracts, ETDE Energy Database, General Science Index and Abstracts, GEOBASE, GeoRef, Life Sciences Collection, Meteorological and Geoastrophysical Abstracts, Oceanic Absiracts, PASCAL Database, and Science Citation Index.

Volume 61, Number 11, November 2004

Canadian Journal of Fisheries and Aquatic Sciences

Published by the National Research Council of Canada

Volume 61, numéro 11, novembre 2004

Journal canadien des sciences halieutiques et aquatiques

Publié par le Conseil national de recherches du Canada

Senior Editor / Directrice scientifique principale **Moira M. Ferguson**

Editors / Directeurs

Jeffrey A. Hutchings, *Dalhousie University, Halifax*
Pierre Pepin, *Northwest Atlantic Fisheries Centre, DFO/MPO, St. John's, Newfoundland*
W. Gary Sprules, *University of Toronto at Mississauga*
Assistant to the Editors / Adjointe aux directeurs scientifiques **Holly Foster**

Associate Editors / Directeurs scientifiques associés

D. Boisclair, *Université de Montréal*
U. Borgmann, *Environment Canada, Burlington*
M.J. Bradford, *DFO/MPO and Simon Fraser University*
S.E. Campana, *DFO/MPO, Dartmouth*
R. Carignan, *Université de Montréal*
J.J. Dodson, *Université Laval*
G.T. Evans, *DFO/MPO, St. John's, Newfoundland*
K.T. Frank, *DFO/MPO, Dartmouth*
J.W.A. Grant, *Concordia University*
M.M. Hansen, *Danish Institute for Fisheries Research, Silkeborg, Denmark*
R. Hilborn, *University of Washington*
A. Hontela, *Université du Québec à Montréal*
D.F. Houlihan, *University of Aberdeen*
F.A. Huntingford, *University of Glasgow*
G.S. Jamieson, *DFO/MPO, Nanaimo*
J.M. Jech, *NFSC/NOAA, Woods Hole, Mass.*
B. Jonsson, *Norwegian Institute for Nature Research, Oslo, Norway*
D.L. MacLatchy, *University of New Brunswick, Saint John*
P. Magnan, *Université du Québec à Trois Rivières*
C.T. Marshall, *University of Aberdeen*
R.B. Millar, *University of Auckland, New Zealand*
W.P. Patterson, *University of Saskatchewan*
Y.T. Prairie, *Université du Québec à Montréal*
T.J. Quinn II, *University of Alaska–Fairbanks, Juneau, Alaska*
T.P. Quinn, *University of Washington*
C.W. Ramcharan, *Laurentian University*
R.D. Robarts, *Environment Canada, Saskatoon*
B. Sainte-Marie, *DFO/MPO, Mont-Joli*
D.W. Schindler, *University of Alberta*
R.E.H. Smith, *University of Waterloo*
S.J. Smith, *DFO/MPO, Dartmouth*
W.F. Vincent, *Université Laval*
R.D. Vinebrooke, *University of Alberta*
C.J. Walters, *University of British Columbia*
R.D. Ward, *CSIRO Marine Research, Australia*
B. de Young, *Memorial University of Newfoundland*

NRC Research Press / Presses scientifiques du CNRC

Editor-in-Chief / Directeur scientifique en chef **Bruce P. Dancik**
Assistant Editor-in-Chief / Adjoint au directeur scientifique en chef **Iain E.P. Taylor**

Journals Program / Programme des revues

Fax / Télécopieur : 613-952-7656; e-mail / courriel : pubs@nrc-cnrc.gc.ca; URL / URL : pubs.nrc-cnrc.gc.ca
Director / Directeur **Cameron D. Macdonald**
Acting Business Manager / Gestionnaire des affaires par intérim **Mike Boroczki**
Manager, Journals Program / Gestionnaire, Programme des revues **Carolyn Brown**
Managing Editor / Rédactrice administrative **Cecily M. Pearson** (613-993-9099)
Publication Officers / Agents de publication **Jennifer McColl, Thad Costigan**
Advertising and reprints / Annonces publicitaires et tirés à part **Roxanne Landriault** (613-990-2254)
Subscriptions / Abonnements **Eileen Evans-Nantais** (613-990-7873)

The National Research Council of Canada accepts no responsibility for statements or opinions expressed by a contributor. Acceptance of an advertisement, announcement, or other material does not imply endorsement by either the Journal's Senior Editor or the National Research Council.

© National Research Council of Canada 2004. All rights reserved.

No part of this publication may be reproduced, stored, or transmitted in any form or by any means, without the written permission of the publisher, except as stated below.

The National Research Council of Canada grants **permission*** to individuals to make single copies of articles for personal use. Any person may reproduce short excerpts from articles in the journal for any purpose that respects the moral rights of authors, provided that the source is fully acknowledged. As a courtesy, the consent of authors of such material should be obtained directly from the author.

Authorization to reproduce items for other than personal use, as stated above, is granted by the National Research Council of Canada provided that the copyright fee of $7.00 per copy is paid directly to CANCOPY, One Yonge Street, Suite 1900, Toronto, ON M5E 1E5, Canada.

*The above permission does not extend to other kinds of copying, such as copying for general distribution, for advertising, or promotional purposes, for creating new collective works, or for resale. For such copying, arrangements must be made with the publisher, National Research Council of Canada, Ottawa, ON K1A 0R6, Canada.

Subscription information

The *Canadian Journal of Fisheries and Aquatic Sciences* (ISSN 0706-652X) is published monthly by the National Research Council of Canada. The 2005 annual subscription rates (second class postage) for Canada are $892CAN institutional and $276CAN personal, for US & foreign $892US institutional and $276US personal. For air mail add $175US to foreign rate. Canadian customers please include 7% GST (business no. 12149 1807 RT 0275). Subscriptions are entered for the calendar year. Remittances should be made payable to the Receiver General for Canada, credit NRC. Price for regular single issues: institutional, $110.00; personal, $35.00. Supplements will be priced separately. Special rates apply to members of Canadian scientific and engineering societies if they subscribe through their respective societies.

There are no refunds on cancelled subscriptions once delivery has begun. Claims for missing issues should be made within four months (N. America) or six months (outside N. America) following the date of publication. The publisher expects to supply missing issues only when losses have occurred in transit and when the reserve stock will permit. For change of address and subscription enquiries: Subscription Office, NRC Research Press, National Research Council of Canada, Ottawa, ON K1A 0R6, Canada; tel.: 613-993-9084; fax: 613-952-7656; e-mail: pubs@nrc-cnrc.gc.ca.

Microform backfiles are available from UMI, P.O. Box 1346, Ann Arbor, MI 48106-1346, USA, and Micromedia Ltd., 20 Victoria St., Toronto, ON M5C 2N8, Canada.

All issues of the *Canadian Journal of Fisheries and Aquatic Sciences* since 1996 are available on the Web. Pricing information can be found at http://pubs.nrc-cnrc.gc.ca.

Le Conseil national de recherches du Canada ne se tient en aucune façon responsable des opinions exprimées par un collaborateur ou des déclarations que pourrait faire ce dernier. La publication d'annonces publicitaires, d'avis et autres n'implique pas l'endossement de leur contenu par la directrice principale de la Revue ou le CNRC.

© Conseil national de recherches du Canada 2004. Tous droits réservés.

Il est interdit de reproduire, de sauvegarder ou de transmettre quelque partie de la présente publication dans quelque format ou de quelque façon sans le consentement écrit de l'éditeur, à l'exception des conditions suivantes.

Le Conseil national de recherches du Canada accorde aux particuliers le droit de faire des copies individuelles pour leur usage personnel. Toute personne peut reproduire de courts extraits des articles de la Revue pour autant que les droits moraux de l'auteur soient respectés et que la mention de provenance soit clairement indiquée. Il est de convenance de demander le consentement de l'auteur avant de faire mention de son travail.

On obtiendra l'autorisation de reproduire des articles à d'autres fins que l'usage personnel (tel qu'on l'a décrit ci-dessus) auprès du Conseil national de recherches du Canada pour autant que des redevances de droits d'auteurs de 7,00 $/copie soient versées au CANCOPY, 1, rue Yonge, bureau 1900, Toronto, ON M5E 1E5, Canada.

*La permission ci-dessus ne s'applique pas à la reproduction à grande échelle, telle que la reproduction aux fins de distribution générale, publicitaire ou promotionnelle, de compilation de nouveaux ouvrages collectifs ou de revente. Dans de tels cas, il faudra ratifier une entente particulière avec l'éditeur, le Conseil national de recherches du Canada, Ottawa, ON K1A 0R6, Canada.

Renseignements sur l'abonnement

Journal canadien des sciences halieutiques et aquatiques (ISSN 0706-652X) est une publication mensuelle du Conseil national de recherches du Canada. Le prix de l'abonnement annuel en 2005 au Canada (courrier de deuxième classe) est de 892 $CAN pour les organismes et de 276 $CAN pour les particuliers. À l'étranger (y compris les É.-U.), le prix de l'abonnement est de 892 $US pour les organismes et de 276 $US pour les particuliers. L'expédition par avion exige des frais de 175 $US en sus du prix d'abonnement à l'étranger. Les clients du Canada doivent ajouter la TPS de 7 % (numéro d'entreprise 12149 1807 RT 0275). Les abonnements sont pour l'année civile. Tout paiement doit être adressé au Receveur général du Canada, crédit du CNRC. Le prix par numéro est de 110 $ pour les organismes et de 35 $ pour les particuliers. Le prix des hors-série varie. Les membres des sociétés canadiennes de sciences et de génie bénéficient de taux préférentiels en s'abonnant via leurs sociétés respectives.

Aucun remboursement ne sera accordé ni aucune annulation acceptée une fois que les livraisons auront commencé. Les réclamations de numéros manquants devront être soumises dans les quatre mois (Amérique du Nord) ou dans les six mois (à l'extérieur de l'Amérique du Nord) suivant la date de publication. L'éditeur ne fournira de numéros manquants que si le document a été perdu pendant l'expédition et que si le stock le permet. Adressez tout changement d'adresse ou toute question quant à l'abonnement au : Bureau des abonnements, Presses scientifiques du CNRC, Conseil national de recherches Canada, Ottawa, ON K1A 0R6, Canada; téléphone : 613-993-9084; télécopieur : 613-952-7656; courriel : pubs@nrc-cnrc.gc.ca.

On peut obtenir les fichiers rétrospectifs sur **microforme** auprès de UMI, P.O. Box 1346, Ann Arbor, MI 48106-1346, É.-U., et auprès de Micromedia Ltée, 20, rue Victoria, Toronto, ON M5C 2N8, Canada.

À partir de 1996, tous les numéros de *Journal canadien des sciences halieutiques et aquatiques* sont accessibles sur le Web. On trouvera des renseignements sur les tarifs à http://pubs.nrc-cnrc.gc.ca.

Response by trout populations in alpine lakes to an experimental halt to stocking

Trip W. Armstrong and Roland A. Knapp

Abstract: Trout are often stocked into alpine lakes based on the generally untested assumption that resident populations would go extinct without stocking. The objectives of our study were to estimate the proportion of currently or formerly stocked alpine lakes in the Sierra Nevada, California, containing naturally reproducing trout populations (*Oncorhynchus mykiss*, *Oncorhynchus mykiss aguabonita*, *Oncorhynchus clarki henshawi*), identify characteristics of lakes associated with successful reproduction, and quantify the effects of stocking termination on trout density and individual growth rates in reproducing populations. We surveyed trout populations in 95 lakes in the John Muir Wilderness before and after a 4- to 8-year stocking halt and in 84 lakes in Sequoia–Kings Canyon National Park after a ≥20-year stocking hiatus. Based on recruitment during the no-stocking period, 70% and 68% of study lakes in the John Muir Wilderness and Sequoia–Kings Canyon National Park, respectively, contained reproducing populations. Results indicated that lakes with >2.1 m^2 of spawning habitat and at elevations <3520 m nearly always showed evidence of reproduction. For reproducing populations, stocking termination did not result in significant changes in population density, but may have increased individual growth rates. We conclude that most trout stocking in Sierra Nevada alpine lakes could be permanently halted with only minimal impact on the recreational fishery.

Résumé : Il arrive souvent que l'on ensemence des truites dans les lacs alpins, parce que l'on croit, généralement sans preuves, que les populations résidantes pourraient disparaître sans ces ensemencements. Les objectifs de notre étude sont d'estimer la proportion de lacs alpins dans la Sierra Nevada, Californie, contenant des populations de truites à reproduction naturelle (*Oncorhynchus mykiss*, *O. m. aguabonita*, *O. clarki henshawi*) qui sont actuellement ensemencés ou qui l'ont été dans le passé; nous voulons aussi identifier les caractéristiques des lacs dans lesquels la reproduction est réussie et étudier quantitativement les effets de l'arrêt des ensemencements sur la densité des truites et les taux individuels de croissance dans les populations qui se reproduisent. Nous avons fait l'inventaire de 95 lacs dans la région sauvage John Muir (JMW) avant et après un arrêt de 4–8 ans des l'ensemencements et de 84 lacs du parc national de Sequoia–Kings Canyon (SEKI) après un arrêt de ≥20 ans. D'après le recrutement observé durant l'arrêt des ensemencements, 70 % des lacs étudiés à JMW et 68 % de ceux de SEKI maintiennent des populations qui se reproduisent. Les lacs qui possèdent >2,1 m^2 d'habitat de fraye et qui sont situés à <3520 m d'altitude montrent presque toujours des indices de reproduction. Chez les populations qui se reproduisent, l'arrêt des ensemencements ne cause pas de changement significatif de la densité de population et peut augmenter les taux individuels de croissance. En conclusion, la plupart des ensemencements de poissons dans les lacs alpins de la Sierra Nevada peuvent être abandonnés de façon permanente et l'impact sur la pêche sportive sera minime.

[Traduit par la Rédaction]

Introduction

The stocking of non-native trout into naturally fishless alpine lakes of western North America has been a common fisheries-management practice for the past century. The fundamental motivation behind this practice is the creation and maintenance of recreational fisheries where none formerly existed (Cowx 1994). Although it is estimated that fewer than 5% of high-elevation lakes in western North America originally contained fish, more than 95% of the larger (>2 ha surface area) and deeper (>3 m maximum depth) lakes now contain non-native trout populations as a result of these stocking programs (Donald et al. 1980; Bahls 1992). Since the introduction of aerial stocking in the early 1950s, the majority of lakes capable of supporting trout populations have been stocked on a regular basis (Bahls 1992; Pister

Received 31 July 2003. Accepted 31 May 2004. Published on the NRC Research Press Web site at http://cjfas.nrc.ca on 15 January 2005.
J17679

T.W. Armstrong.[1,2] Wildlife, Fish, and Conservation Biology, University of California, Davis, 1 Shields Avenue, Davis, CA 95616, USA.
R.A. Knapp. Sierra Nevada Aquatic Research Laboratory, University of California, HCR 79, Box 198, Mammoth Lakes, CA 93546, USA.

[1]Corresponding author (e-mail: twarmstrong@ucdavis.edu).
[2]Present address: Sierra Nevada Aquatic Research Laboratory, University of California, HCR 79, Box 198, Mammoth Lakes, CA 93546, USA.

 doi: 10.1139/F04-144 © 2004 NRC Canada

2001). A central assumption underlying this intensive stocking program is that most introduced trout populations would disappear if stocking was halted. For example, fisheries managers in the western USA estimated that only 25% of high-elevation lakes harboring introduced trout populations showed levels of natural reproduction sufficient to maintain these populations without supplemental stocking (Bahls 1992). The assumption that most trout populations are not self-sustaining has rarely been tested, however, despite the fact that continued supplemental stocking of lakes that already contain self-sustaining fish populations may provide little or no benefit to these fisheries (Parsons and Pereira 2001).

The objectives of this study were to (*i*) use an experiment in which lakes were subjected to a 4- to 8-year stocking hiatus to determine what proportion of currently stocked lakes in the John Muir Wilderness (JMW) study area (California, USA) contain naturally reproducing populations of introduced trout (rainbow trout, *Oncorhynchus mykiss*; golden trout, *Oncorhynchus mykiss aguabonita*; Lahontan cutthroat trout, *Oncorhynchus clarki henshawi*), (*ii*) determine what proportion of *Oncorhynchus* spp. populations in lakes in Sequoia–Kings Canyon National Park (SEKI; California, USA) show evidence of natural reproduction following a ≥20-year stocking hiatus, (*iii*) identify the habitat factors associated with successful reproduction in the JMW study lakes, and (*iv*) quantify the effects of halting stocking in the JMW study area on density and individual growth rates of naturally reproducing populations. Based on our common observation of young-of-the-year trout in lakes in both study areas, we hypothesized that a majority of currently stocked trout populations are in fact at least partially maintained by natural reproduction. We included the data from SEKI to determine whether the rates of natural reproduction by trout populations observed in the JMW study area were similar to those in other parts of the high-elevation Sierra Nevada. We also hypothesized that the probability of successful natural reproduction is directly related to the total spawning area available to trout populations. For trout populations showing evidence of successful natural reproduction, we predicted that halting stocking would have either no effect or a positive effect on fish growth rates. A positive effect on growth rates might occur if halting stocking reduced fish densities (Donald and Anderson 1982).

Materials and methods

Study area

This study was conducted in the southern Sierra Nevada of California, and included lakes on both the east and west sides of the Sierra Nevada crest (JMW study area: 67 125 ha in the Inyo and Sierra national forests; the center of the study area is at 37°20′N, 118°48′W; SEKI study area: 348 833 ha, the center of the study area is at 36°45′N, 118°30′W). All of the study lakes are of glacial origin and are located primarily within watersheds composed of intrusive igneous bedrock (California Division of Mines and Geology 1958). As a result, these lakes all have similar physical and chemical properties (Melack et al. 1985; Knapp and Matthews 2000). They are located in the alpine and subalpine zones (>2800 m), remain ice-free for approximately 4 months each year, are oligotrophic, and rarely reach maximum temperatures greater than 17 °C (Melack et al. 1985; Bradford et al. 1998; Knapp and Matthews 2000). Most of the precipitation entering these lakes is in the form of snow, which falls from November to April. All lakes in the JMW and SEKI study areas were historically fishless, but most have been stocked repeatedly with fingerlings (young-of-the-year trout <50 mm fork length) since at least the 1950s as part of the aerial stocking program conducted by the California Department of Fish and Game (CDFG) (Knapp 1996).

The JMW study area contains 216 lakes (water bodies with surface area ≥1.0 ha; maximum depth ≥3 m), 173 of which harbor introduced trout populations (80%; R.A. Knapp, unpublished data). During 1990–2000, 118 (84%) of these lakes were stocked with either *O. mykiss* (10 lakes), *O. m. aguabonita* (84 lakes), or *O. c. henshawi* (1 lake). The median number of times each lake was stocked during this period was 4 (range = 1–11) and the median stocking density was 553 fish·ha^{-1} (range = 57–6289 fish·ha^{-1}). Of the 1157 lakes in SEKI, 548 lakes harbor introduced trout populations (47%; R.A. Knapp, unpublished data). Although the National Park Service discontinued nearly all stocking in 1977, 84 lakes were stocked with either *O. mykiss* (29 lakes), *O. m. aguabonita* (53 lakes), or both species (2 lakes) between 1960 and 1977. During this period the median number of times each lake was stocked was 2 (range = 1–4) and the median stocking density was 988 fish·ha^{-1} (range = 91–9886 fish·ha^{-1}).

Most golden trout in the Sierra Nevada are actually golden trout × rainbow trout hybrids (R.A. Knapp, personal observation; Cordes 2001; Cordes et al. 2003). Because they are phenotypically more similar to golden trout, we refer to them as such throughout this paper.

Study design

The portion of our study conducted in the JMW involved the survey of trout populations in a series of lakes during 1995–1996, the use of these data to quantify premanipulation characteristics of fish populations and to select experimental lakes (in which stocking was temporarily halted) and reference lakes (in which regular stocking continued), and then the resurvey of trout populations in the experimental and reference lakes in 2001 and 2002 (Fig. 1). Trout captured during the lake resurveys were aged using otoliths, and the presence of fish born during the stocking hiatus was used as evidence of successful natural reproduction by the resident trout population. To select experimental lakes, we used CDFG stocking records and data from field surveys to identify all lakes (N = 61) that met the following requirements: (*i*) contained only *Oncorhynchus* spp. (*O. mykiss*, *O. m. aguabonita*, or *O. c. henshawi*), (*ii*) were stocked at least biennially, and (*iii*) were separated from other stocked lakes located upstream or downstream by natural barriers or ≥500 m of stream. The first requirement was necessary to eliminate the potentially confounding effect of the presence of brook trout (*Salvelinus fontinalis*), because this species generally precludes self-sustainability by *Oncorhynchus* spp. in Sierra Nevada lakes (Boiano 1999). The second requirement was necessary to ensure that stocking frequencies prior to the stocking halt were high enough to allow us to test the effect of halting stocking on fish population densities and growth rates. The third requirement was necessary to mini-

© 2004 NRC Canada

Fig. 1. Map of the John Muir Wilderness (JMW) study area showing the locations of the experimental lakes (solid circles) and reference lakes (shaded circles). The inset map shows the State of California, USA (solid), the Sierra Nevada (open), and the location of the study area within the Sierra Nevada (●).

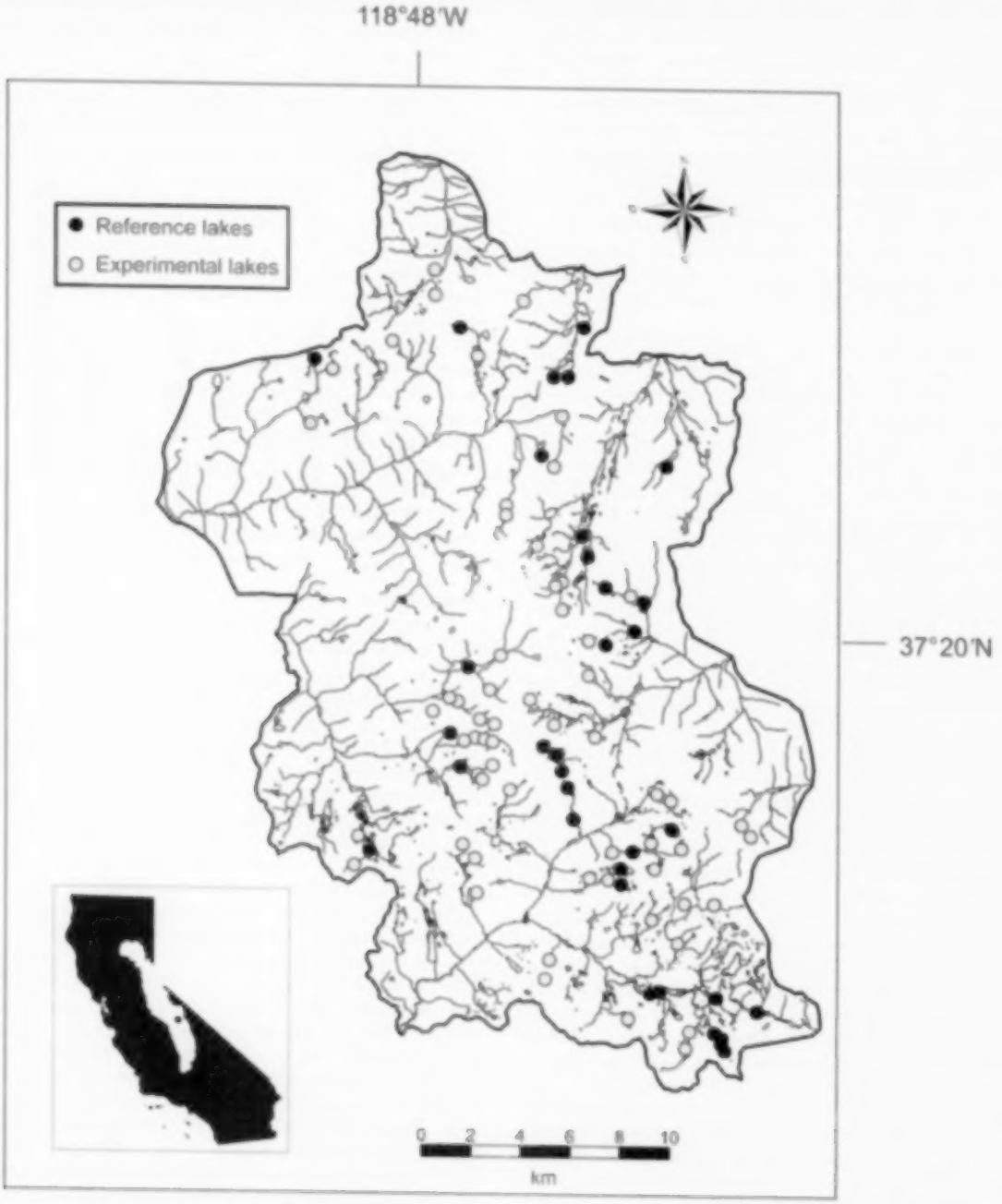

mize the possibility that fish population dynamics in the experimental lakes would be influenced by stocking in adjacent lakes (e.g., stocked fish moving into adjacent unstocked lakes). While some literature suggests that trout are able to move distances >2000 m through streams (Gowan and Fausch 1996), golden trout in Sierra Nevada streams have only been documented moving relatively short distances (<600 m; Matthews 1996). Trout populations in 54 (89%) of our experimental lakes were isolated from other stocked trout populations by impassible barriers. In the remaining seven experimental lakes (11%), trout populations were separated from adjacent stocked trout populations by 500–3600 m (median = 500 m). As a consequence of the generally high degree of isolation of trout populations in our experimental

© 2004 NRC Canada

lakes from any stocked lakes, stocking of reference lakes during the study should have had little or no influence on the structure of trout populations in the experimental lakes. Following the initial sampling of fish populations in all JMW study lakes, the CDFG ceased stocking experimental lakes for at least 4 consecutive years between 1994 and 2001 (range = 4–8 years, median = 5 years).

Reference lakes ($N = 34$) were randomly chosen from the remaining lakes that met requirements *i* and *ii* but not *iii*. These lakes continued to be regularly stocked for the duration of the experiment. Reference lakes were used for two reasons in this study: (1) to facilitate assessment of the effects of halting stocking on population densities and individual growth rates, and (2) to allow us to apply our model of those factors determining whether or not trout populations were able to reproduce naturally to a broader subset of JMW lakes.

In addition to the short-term experiment in the JMW, we also conducted a longer term study in which we evaluated whether introduced *Oncorhynchus* spp. populations in SEKI lakes had maintained themselves through natural reproduction after a ≥20-year halt to stocking. We identified 84 lakes in SEKI that were not stocked after 1977, had been stocked at least once between 1962 and 1977, and contained only *Oncorhynchus* spp. Fish populations in these lakes were sampled in 1997, 2000, 2001, or 2002, and the capture of any trout was taken as evidence of successful natural reproduction. We used the results of this analysis to evaluate the generality of our findings regarding the rate of successful natural reproduction in the JMW study area.

Fish-population sampling

We sampled fish populations in JMW and SEKI lakes using gill nets. During the JMW resurveys, gill nets were set in the same locations and generally during the same time of day as sets made during the initial surveys. Gill nets used in all surveys were sinking monofilament nets 36 m long and 1.8 m tall. Each net had six 6 m long panels with bar mesh sizes of 10, 12.5, 18.5, 25, 33, and 38 mm. The five largest mesh size panels are effective at catching >120 mm long trout, while the smallest mesh size panel can successfully capture trout as small as 80 mm (Hall 1991*b*). A single net was set in each lake so that the smallest mesh size panel was closest to shore and the largest mesh size panel was farthest out in the lake. This arrangement was chosen to allow the capture of trout <120 mm in length, fish that are found primarily in nearshore habitats (Landry et al. 1999). Nets were anchored to shore and set perpendicular to the lake shoreline. We set gill nets in either the early morning or the late evening and pulled them after 8–12 h. Every captured fish was weighed to the nearest gram and measured to the nearest millimetre (fork length). Catch per unit effort (CPUE; i.e., the number of fish captured per hour in each net) from nets set during the day versus at night were similar ($X_{day} = 3.1$, $X_{night} = 2.6$; two-sample t test, $t = 0.628$, df = 93, $P = 0.532$).

We used sagittal otoliths to age fish captured during the 2001–2002 JMW lake resurveys (Campana and Neilsen 1985). In 70 lakes, we captured <40 fish and in these cases we removed the pair of sagittal otoliths from all captured fish. In 25 lakes, we captured >40 fish. For these lakes, otoliths were extracted from 40 fish that represented the full range of size classes captured in the gill net. Otoliths were taken to the laboratory, where they were cleaned, mounted on a glass microscope slide sulcus-side up, ground to the sagittal midplane, polished, and aged using the methods of Secor et al. (1992).

Annuli on sagittal otoliths are commonly used to age fish from a wide variety of salmonid species (Kruse et al. 1997; Hining et al. 2000), including trout from alpine lakes (Hall 1991*a*; Boiano 1999). Annular-increment formation has been validated in *O. mykiss* (Graynoth 1996) but not in *O. m. aguabonita*. To test the hypothesis that increments from golden trout in our JMW study lakes are in fact produced annually, we conducted a validation experiment using one of our reference lakes. In August 1999, we clipped adipose fins from 2000 golden trout fingerlings (~30 days old) immediately prior to their being stocked into Summit Lake (37°14′N, 118°41′W). When the Summit Lake fish population was surveyed in 2002 using gill nets, fish without adipose fins were identified and otoliths from all captured fish were returned to the laboratory for aging. Aging was conducted without any information on whether or not the fish being aged had or did not have an adipose fin. Based on the assumption that sagittal otoliths from golden trout contain increments produced annually, we expected that these adipose-fin-clipped fish would contain otoliths with three annuli.

Habitat characterization

In addition to resurveying fish populations in 2001 and 2002 in the JMW, we also characterized physical lake properties for each of the 95 JMW study lakes. Maximum lake depth was measured by sounding with a weighted line, and lake area was obtained from US Geological Survey 1 : 24 000 topographic maps. We characterized littoral zone substrate composition by visually estimating the dominant substrate type along approximately fifty 3 m long shoreline transects that were evenly spaced around the lake perimeter and were perpendicular to shore. Substrates were categorized as silt (<0.5 mm diameter), sand (0.5–2 mm), gravel (<2–75 mm), cobble (>75–300 mm), boulder (>300 mm), or bedrock. To assess the amount of potential spawning habitat available to each trout population, we measured the area of suitable spawning habitat in the first 100 m of each inlet and outlet stream, as well as of in-lake spawning habitat associated with inlet and outlet streams. We focused spawning-habitat measurements on stream and stream-associated habitats because successful embryo development in *Oncorhynchus* spp. depends on continuous water flow (Bjornn and Reiser 1991). For the stream portion of surveys, we limited our measurements to the first 100 m of stream because analysis of preliminary spawning-habitat data collected during the 1995–1996 lake surveys indicated a significant association between the amount of spawning habitat in the first 100 m of stream and successful natural reproduction by lake-resident trout. Suitable spawning habitat was defined as gravel particles 0.5–4 cm in diameter and not cemented into the streambed, water depths of 10–50 cm, and water velocities of 20–60 cm·s^{-1} (Bjornn and Reiser 1991; Knapp and Preisler 1999). We also estimated the average width and depth of the first 100 m of each inlet and outlet stream.

© 2004 NRC Canada

Fig. 2. Frequency histogram showing the amount of trout (*Oncorhynchus* spp.) reproduction that occurred in the JMW experimental lakes during the stocking hiatus. The *x* axis shows the number of trout captured in the gill net whose ages indicated that they were born during the stocking hiatus. The number of trout captured was divided by the number of years of the stocking hiatus to standardize the catch amongst lakes subject to no stocking for differing numbers of years. The number of captured fish that were born per year of the stocking hiatus ranged from 0 to 9.

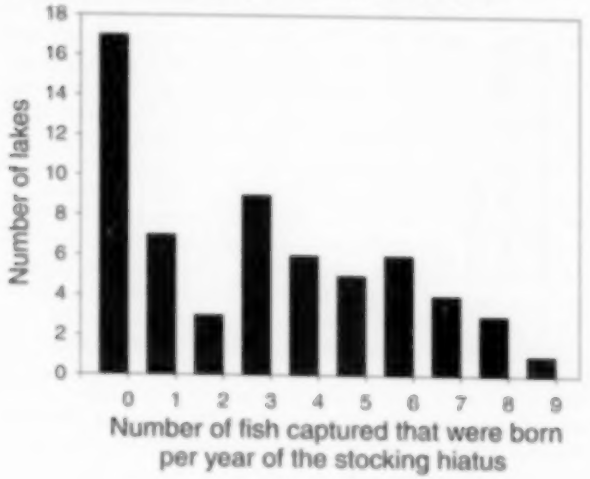

Data analysis

Determination of reproductive status

We used two different criteria to categorize JMW trout populations as reproductive or non-reproductive. Under the first criterion, a trout population was categorized as reproductive if the gill-net catch from the 2001–2002 fish surveys included any trout whose age indicated that it was born during the stocking hiatus, and non-reproductive if no such trout were captured. Because low levels of successful natural reproduction might not be sufficient to maintain trout populations over the long term, we also included a second, more conservative criterion. Under this criterion, a trout population was categorized as reproductive only if the gill-net catch included an average of >1 fish born per year of the stocking hiatus. This division point was chosen based on an obvious break in the distribution of the number of captured fish born per year of the stocking hiatus for all experimental lakes (Fig. 2). The number of fish is expressed on a per-year basis to standardize the numbers captured from lakes with different durations of stocking termination. Because SEKI lakes had not been stocked for ≥20 years and *Oncorhynchus* spp. in Sierra Nevada alpine lakes rarely live longer than 10 years (Knapp et al. 2001), fish populations in SEKI lakes were categorized as reproductive if 1 or more trout were captured during the gill-net survey and non-reproductive if no trout were captured.

Habitat effects on reproductive status

We used stepwise logistic regression and tree regression to model the effect of physical lake characteristics on the reproductive status of trout populations in the JMW. Independent variables used in both models included maximum lake depth, elevation, total area of spawning habitat, total width of all inlet and outlet streams, and littoral zone substrate composition. Before including the littoral zone substrate data in the regression analyses, we used principal components analysis to reduce their dimensionality to two principal components (PC1, PC2), which together explained 53% of the variation in substrate characteristics (Table 1). Although tree regression is still rarely used in ecological studies, it is a useful method to identify the relationships between predictor variables and the response variable by producing an easily interpretable hierarchy of decision processes, as well as identifying the levels at which these variables become important (De'ath and Fabricius 2000). Because the two regression models produced similar results (see Results), we used the tree-regression results to estimate the proportion of naturally reproducing populations in reference lakes. We then combined this estimate with the number of experimental lakes with naturally reproducing populations to obtain a single estimate of the proportion of naturally reproducing trout populations for all currently stocked lakes in the study area.

Table 1. Loadings for the first two principal component axes of littoral zone substrate composition.

Substrate type	PC1	PC2
Silt	–0.269	–0.749
Sand	–0.262	0.474
Gravel	–0.469	0.354
Cobble	0.000	0.119
Boulder	0.691	0.230
Bedrock	0.390	–0.151

Note: PC1 and PC2 explained 29% and 24%, respectively, of the variance in littoral zone substrate characteristics.

Our regression analyses indicated that the amount of spawning habitat was of primary importance in determining population reproduction (see Results). However, measuring this variable requires visits to each lake, and measurements of spawning-habitat quantity are therefore not widely available for lakes outside our study area. During the 1950s and 1960s, the CDFG conducted qualitative habitat and fish-population surveys for many of the lakes on national forest lands in the Sierra Nevada, including nearly all of our JMW study lakes. These surveys included a categorization of trout spawning habitat as none, poor, fair, good, or excellent. These CDFG estimates were available for 55 of the 61 experimental lakes. Only one lake had been categorized as having excellent spawning habitat, so we combined this category with the "good" category. To determine whether this widely available measure of spawning habitat could be used to predict trout population reproduction, we used a χ^2 test to quantify the strength of the association between the CDFG spawning-habitat categories and our lake-specific determination of trout population reproductive status in the experimental lakes from our JMW study area.

Effects of halting stocking on densities and growth rates

We quantified the effect of halting stocking on trout populations in the JMW by comparing population densities and

© 2004 NRC Canada

lake-specific individual fish growth rates in reference and experimental lakes before and after the stocking hiatus. We used two different measures to quantify individual fish growth: size-at-age and maximum fish size. For size-at-age analyses, we used age-4 fish because this was the most frequently encountered age class. All age-4 fish from each gill-net sample were used in these growth-rate determinations. Although size-at-age is a commonly used measure of salmonid growth rate (Quinn and Deriso 1999), this analysis was dependent on having fish from a particular age class present in every gill-net sample. Therefore, we used maximum fish size as a second measure of individual growth rate because it allowed us to include every JMW study lake in our analyses. Although maximum fish size is only rarely used as a measure of individual growth rate, based on our study data, average size of age 4 fish and maximum fish size were highly correlated ($N = 42$, $r = 0.56$, $P < 0.0001$). We used CPUE as a measure of fish density. The validity of this method of estimating population density is suggested by the results of Schindler et al. (2001), which demonstrate a positive linear relationship between CPUE (measured as gill-net catches) and actual population density for *O. m. aguabonita* in high-elevation Sierra Nevada lakes.

We used two different comparisons to determine whether the halt to fish stocking resulted in changes in population density and growth rate. First, we used two-sample *t* tests to compare CPUE, size-at-age, and maximum fish size in experimental versus reference lakes using data collected after the several-year halt to stocking (2000–2001 survey). To determine whether observed differences in CPUE, size-at-age, and maximum fish size were likely a consequence of the halt to stocking and not attributable to preexisting differences between fish populations in experimental and reference lakes, we also used two-sample *t* tests to compare CPUE, size-at-age, and maximum fish size in experimental and reference lakes before the stocking hiatus began (using data from the 1995–1996 survey). Second, we used paired *t* tests to compare CPUE, size-at-age, and maximum fish size for each fish population measured before and after the stocking hiatus. Only those experimental lakes containing trout populations categorized as reproductive were included in this analysis.

To determine whether these statistical tests could identify potential changes in population density and maximum fish size, given our study design, we conducted power analyses. Power analysis allowed us to determine whether a lack of statistically significant changes in CPUE, size-at-age, and maximum fish size was the result of a lack of real change in these metrics or an inability to detect such a change as a consequence of small sample sizes and (or) high variability (Steidl et al. 1997). For all power analyses, we measured our ability to identify a change in mean values of at least 25% ($\alpha = 0.05$). High power (≥0.8) indicates that the sampling design used was likely sufficient to allow us to detect significant changes in CPUE and maximum fish size. All statistical analyses were conducted using S-Plus (S-Plus 1999) and the α level for all statistical tests was 0.05.

Results

Validation of annular-increment formation

In the 2002 gill-net sample from Summit Lake, we captured 6 golden trout lacking adipose fins. Independent counts of increments on sagittal otoliths from these fish made by both authors indicated that otoliths from all 6 fish contained three obvious increments. Therefore, increments in these otoliths appear to be produced annually.

Fish population reproductive status

Trout populations in 43 of our 61 JMW experimental lakes (70%) contained trout with ages which indicated that they were born during the stocking hiatus. Therefore, based on our first criterion for determining reproductive status, 70% of the experimental lakes contained trout populations that were categorized as reproductive. Using our second, more conservative criterion to identify only those lakes with abundant natural reproduction, in 37 of 61 experimental lakes (61%) we captured an average of >1 fish born per year of the stocking hiatus (Fig. 2). The age structure of two representative trout populations that were categorized as nonreproductive and reproductive are provided (Fig. 3). For the SEKI lakes, 57 of 84 lakes (68%) contained trout populations categorized as reproductive. Therefore, the majority of study lakes in the JMW and SEKI showed evidence of substantial natural reproduction. In SEKI, the fact that trout populations persisted after ≥20 years of no stocking suggests that the level of natural reproduction in lakes categorized as reproductive is sufficient to maintain these populations over the long term.

Habitat factors influencing reproductive status

Regression analyses of the factors that influence trout population reproductive status and the analyses of the effects of stocking termination on CPUE and fish size were conducted on data categorized using both criteria for determining trout population reproductive status. Results were similar regardless of which criterion was used, and we therefore present only the results from the more conservative estimate of the percentage of populations categorized as reproductive (61%).

Logistic regression indicated that the probability of trout population reproduction was a positive function of the total amount of spawning habitat and a negative function of lake elevation (Table 2). The effects of maximum lake depth, littoral zone substrate composition (PC1, PC2), and stream width on population reproduction were not significant. The tree regression yielded similar results, again indicating the positive influence of the amount of spawning habitat and the negative influence of elevation on population reproduction (Fig. 4). Ninety-five percent of lakes with >2.1 m^2 of spawning habitat contained reproductive trout populations, while only 41% of lakes with <2.1 m^2 of spawning habitat contained reproductive trout populations. For lakes with <2.1 m^2 of spawning habitat, none of the 10 trout populations occurring in lakes above 3520 m were reproductive, while 55% of those in lakes below 3520 m were reproductive (Fig. 4).

Before using the tree-regression model to predict natural reproduction in the reference lakes, we compared the physical habitat characteristics of experimental and reference lakes to ensure that they were similar. Experimental and reference lakes were compared using Wilcoxon's rank-sum tests and showed no significant differences in any of the measured habitat variables, including maximum depth (Fig. 5*a*),

© 2004 NRC Canada

Fig. 3. Age–frequency histograms for two JMW experimental lakes, (*a*) Jawbone Lake and (*b*) Upper Honeymoon Lake, chosen to illustrate trout (*Oncorhynchus* spp.) populations with different levels of natural reproduction. The solid box above the bars indicates the period during which the lake was stocked and the open box indicates the period of the stocking hiatus. The trout population depicted in *a* shows no evidence of natural reproduction, while the trout population depicted in *b* shows substantial natural reproduction during the stocking hiatus.

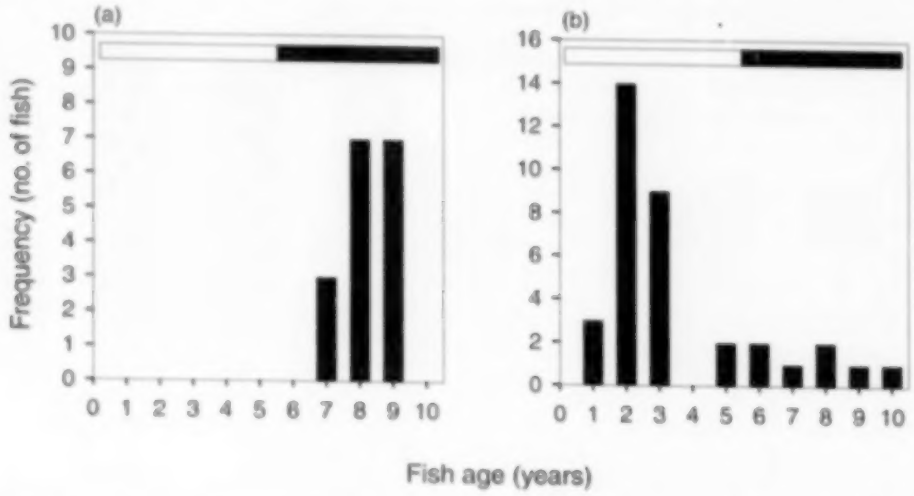

Table 2. Results of stepwise logistic regression analysis of the effect of lake habitat characteristics on the reproductive status of trout (*Oncorhynchus* spp.) populations in the experimental lakes (reproductive, non-reproductive) in the John Muir Wilderness.

Variable	Regression coefficient	*P*
Total spawning habitat area	0.383	0.0004
Elevation	–0.007	0.006
Maximum depth	0.004	0.773
Total stream width	–0.0002	0.657
PC1	–0.009	0.967
PC2	–0.261	0.420

Fig 4. Tree-regression results for all 61 JMW experimental lakes, displaying the effects of habitat variables on the reproductive status of trout (*Oncorhynchus* spp.) populations (reproductive, non-reproductive). The number of reproductive populations (*Y*) and the number of non-reproductive (*N*) populations is given at each node as *Y*/*N*, together with the percentage of lakes that were reproductive.

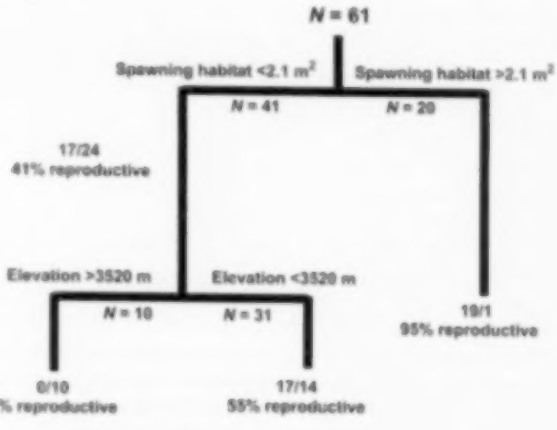

total stream width (Fig. 5*b*), elevation (Fig. 5*c*), lake surface area (Fig. 5*d*), total spawning area (Fig. 5*e*), PC1 (Fig. 5*f*), and PC2 (Fig. 5*g*). Therefore, despite the fact that experimental lakes were not chosen at random, they were physically similar to the reference lakes. We next applied the results from our tree-regression model to all 34 reference lakes used in our JMW study area. Our model predicted that 19 of these populations would be reproductive (56%). We combined these predictions with our determination of reproductive populations in the experimental lakes (based on the more conservative criterion), which resulted in 59% of our JMW study lakes being categorized as reproductive. Therefore, the majority of lakes that were stocked during the past decade in our JMW study area contain naturally reproductive *Oncorhynchus* spp. populations.

After determining which of the experimental-lake populations were reproductive, we analyzed whether qualitative CDFG estimates of spawning-habitat quality could also be used to predict successful population reproduction. The qualitative spawning-habitat categories were significantly associated with population reproductive status (Pearson's χ^2 test, $\chi^2 = 10.79$, df = 3, $P = 0.013$; Fig. 6). Of the lakes with poor, fair, or good/excellent spawning habitat, 71% contained trout populations categorized as reproductive. In contrast, of the 20 lakes with spawning habitat categorized as none, only 25% showed evidence of natural trout reproduction (Fig. 6). These results suggest that the qualitative CDFG estimates of spawning-habitat quality that are currently available for many Sierra Nevada lakes could be used to identify naturally reproductive trout populations.

© 2004 NRC Canada

Fig. 5. Box plots showing (*a*) maximum lake depth, (*b*) total stream width, (*c*) lake elevation, (*d*) lake surface area, (*e*) total area of spawning habitat, (*f*) littoral zone substrate principal component axis 1 (PC1), and (*g*) littoral zone substrate principal component axis 2 (PC2) for reference ($N = 34$) and experimental ($N = 61$) lakes. The line within each box represents the median, the bottom and top of each box indicate the 25th and 75th percentiles, the whiskers represent the 10th and 90th percentiles, and the data points below and above the whiskers indicate values outside the 10th and 90th percentiles; "ns" indicates that the difference between reference and experimental lakes is not statistically significant (Wilcoxon's rank-sum test, $P > 0.05$).

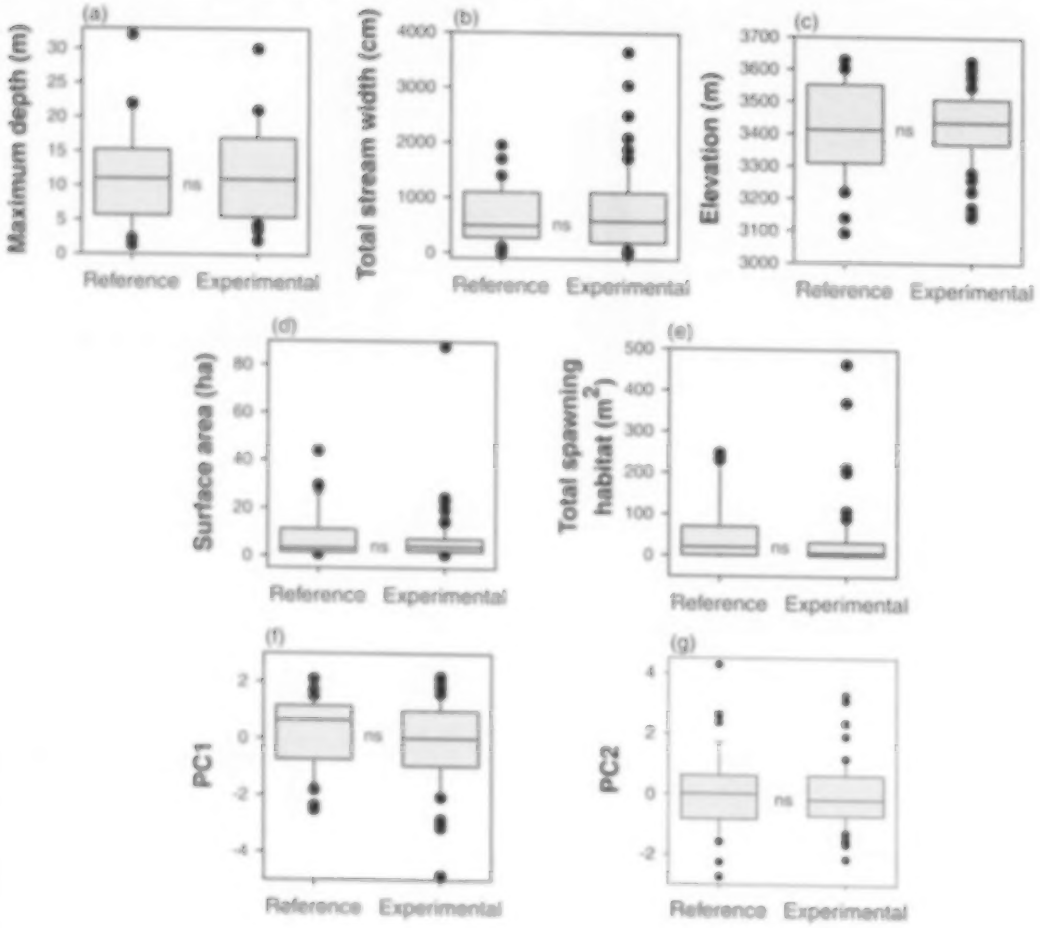

Effects of halting stocking on reproducing populations

Prior to the stocking hiatus, neither CPUE (two-sample *t* test, $t = 0.049$, df = 93, $P = 0.96$; Fig. 7*a*), size at age 4 (two-sample *t* test: $t = -0.595$, df = 64, $P = 0.554$; Fig. 7*b*), nor maximum fish size (two-sample *t* test, $t = 0.824$, df = 93, $P = 0.412$; Fig. 7*c*) differed significantly between reference and experimental lakes. Based on a hypothetical difference of 25% between the means, the power of these tests was high in two cases (CPUE: power = 0.7; maximum fish size: power = 1.0), indicating that both statistical tests had a relatively strong ability to detect a difference, given the sample sizes and sample variances that characterized these data. The power of the size-at-age test was relatively low (0.12), which was likely a result of a smaller sample size. After the stocking hiatus, CPUE (two-sample *t* test, $t = 0.646$, df = 93, $P = 0.520$; Fig. 7*d*), size-at-age (two-sample *t* test, $t = -0.638$, df = 41, $P = 0.267$; Fig. 7*e*), and maximum fish size (two-sample *t* test: $t = -1.036$, df = 93, $P = 0.303$; Fig. 7*f*) again did not differ significantly between reference and experimental lakes. Again, the power of two of these tests was high (CPUE: power = 0.7; maximum fish size: power = 1.0), whereas the power of the third test was relatively low (size-at-age: power = 0.16). The high power values suggest that we likely would have been able to detect a difference of 25% in CPUE and maximum fish size had there been a real difference of this magnitude. The low power in the size-at-age *t* test is also likely a result of the smaller sample size.

For experimental lakes categorized as reproductive, comparisons of CPUE and maximum fish size for the same lakes before and after the stocking hiatus indicated no significant change in CPUE (paired *t* test, $t = 2.1$, df = 36, $P = 0.978$; Fig. 8*a*) or maximum fish size (paired *t* test, $t = -1.82$, df =

© 2004 NRC Canada

Fig 6. Percentages of JMW experimental lakes that contained reproductive trout (*Oncorhynchus* spp.) populations as a function of qualitative categories of spawning-habitat suitability obtained from the California Department of Fish and Game. The number at the base of each bar is the sample size.

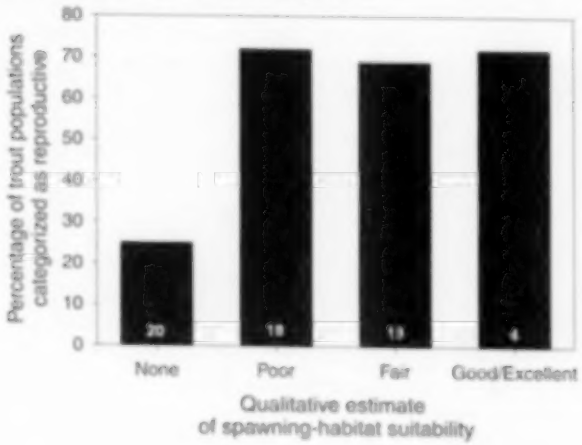

36, $P = 0.962$; Fig. 8*c*). However, size at age 4 was significantly higher after the stocking hiatus (paired *t* test, $t = 2.99$, df = 21, $P = 0.0035$; Fig. 8*b*). The power of the CPUE and maximum fish size tests was also relatively high (CPUE: power = 0.64; maximum fish size: power = 1.0), indicating that the paired *t* tests had a relatively strong ability to detect a difference of 25% between the means, given the sample size of 37 lakes and sample variances that characterized these data. We conclude that while the experimental halt to stocking had no effect on population densities, individual growth rates of naturally reproducing trout populations increased after stocking was halted, at least when the growth rate was measured as size at age 4.

Discussion

The practice of supplemental stocking in high-elevation lakes in the Sierra Nevada of California and elsewhere in western North America has historically been predicated on the assumption that few or none of these introduced trout populations are self-sustaining (Bahls 1992). However, results from our stocking-termination experiment indicate that the majority of *Oncorhynchus* spp. populations in our JMW and SEKI study areas showed evidence of substantial natural reproduction. Based on the more conservative criterion that we used to categorize experimental lakes as reproductive, we estimated that 61% of our JMW experimental lakes and 68% of our SEKI study area lakes contained naturally reproductive trout populations. The tree-regression model predicted that 56% of the reference lakes in the JMW also contained reproductive populations. Adding our determinations of reproduction in experimental-lake populations to our predictions from the reference-lake populations resulted in an overall estimate of natural reproduction in the JMW study lakes of 59%. The high degree of concordance between estimates of natural reproduction in JMW and SEKI populations suggests that the results from the JMW can be extrapolated across both a longer time scale and a broader spatial scale.

The relatively short time scale of the experimental halt to stocking in the JMW study area was not sufficient to allow a definitive determination of self-sustainability in these populations. In contrast, the much longer (20+ years) halt to stocking in SEKI lakes was likely sufficient for determining population self-sustainability. Many of these populations in SEKI experienced low levels of natural reproduction (measured as CPUE), yet the populations remained self-sustaining over a long period of time. In addition, the presence of fish populations in SEKI lakes indicates that angling pressure probably has little or no effect on population self-sustainability. These low levels of reproduction in SEKI populations suggest that most or all of the JMW populations identified as reproductive are likely to be self-sustaining over the long term as well.

Given that the majority of currently stocked lakes in the JMW study area show evidence of successful natural reproduction, the consequences to the recreational fishery of even a complete and permanent halt to stocking in this area are likely to be small. For example, there are 216 large lakes (≥1 ha, ≥3 m deep) in the JMW study area, 173 of which contain trout populations. Sixty-three of these lakes contain self-sustaining S. fontinalis populations and are not stocked, while another 15 contain *Oncorhynchus* spp. populations and are not stocked for various reasons. Our results predict that of the remaining 95 *Oncorhynchus* spp.-containing lakes (all of which were stocked until our study began), approximately 39 are non-reproductive and will likely revert to a fishless condition without supplemental stocking and 56 are reproductive and would maintain themselves in the absence of any further stocking. The 39 populations that would disappear represent only 23% of the total fish populations ($N = 173$) in the JMW study area. Therefore, the results from both study areas indicate that even a complete halt to stocking in the southern Sierra Nevada would likely result in only a relatively small decrease in the overall number of fish-containing lakes. These results suggest that a reevaluation of the need for continued fish stocking to maintain trout fisheries in other high-elevation lake systems may be necessary. One of the most effective methods to determine the proportion of naturally reproducing fish populations in high-elevation areas, as demonstrated in our experiment, is to halt stocking for several consecutive years. In addition to being a simple tool for evaluating reproductive potential, halting stocking is inexpensive and any negative effects are easily reversible.

The logistic-regression and tree-regression models both identified the amount of spawning habitat and elevation as being the only two factors from our study that significantly influenced the reproductive status of trout populations. Results from the tree regression further suggested that as little as 2.1 m^2 of spawning habitat was sufficient to produce naturally reproducing trout populations. Other studies have also documented the overriding importance of spawning habitat in allowing successful reproduction by trout introduced into mountain lakes. For example, Donald (1987) reported that the probability of trout populations becoming established after being introduced into naturally fishless alpine lakes was directly related to the size of outlet streams, presumably because the amount of available spawning habitat is an increasing function of outlet size. Boiano (1999) also identified

© 2004 NRC Canada

Fig. 7. Box plots showing (*a*) catch per unit effort (CPUE), (*b*) size at age 4, and (*c*) maximum fish size for reference and experimental lakes in 1995–1996 (i.e., before the stocking hiatus), and (*d*) catch per unit effort (CPUE), (*e*) size at age 4, and (*f*) maximum fish size for reference and experimental lakes in 2001–2002 (i.e., after the stocking hiatus). The line within each box represents the median, the bottom and top of each box indicate the 25th and 75th percentiles, the whiskers represent the 10th and 90th percentiles, and the data points below and above the whiskers indicate values outside the 10th and 90th percentiles; "ns" indicates that the difference between reference and experimental lakes is not statistically significant (two-sample *t* test, $P > 0.05$). In the comparisons between CPUE and maximum fish size, sample sizes are 34 and 61 for reference and experimental lakes, respectively. Sample sizes for size-at-age before the stocking hiatus are 20 and 46 for reference and experimental lakes, respectively; sample sizes for size-at-age after the stocking hiatus are 15 and 28 for reference and experimental lakes, respectively.

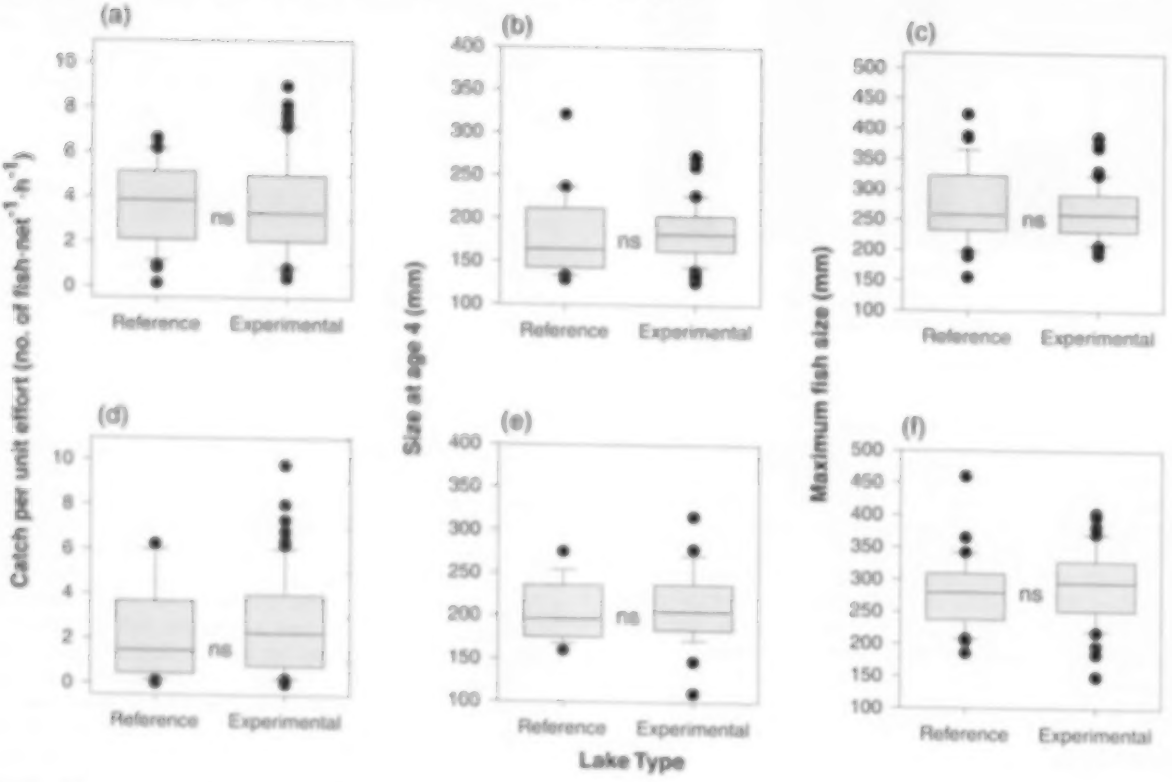

spawning-habitat area as a significant factor in allowing successful natural reproduction by introduced *O. mykiss* populations in high-elevation lakes in Yosemite National Park. Most high-elevation Sierra Nevada lakes contain at least some spawning habitat (R. Knapp, unpublished data), which supports the idea that the majority of currently stocked trout populations are in fact able to reproduce and would not require additional stocking to persist. Although our surveys included all spawning habitat in the first 100 m of each stream, as well as all in-lake stream-associated spawning habitat, it is important to note that measurements of the total amount of spawning habitat at each lake likely vary from year to year depending upon the amount of winter precipitation as well as the time of year the lake is surveyed. As a result of this interannual variation, the minimum amount of spawning habitat we identified in this study as necessary for successful reproduction is unlikely to be an absolute limitation, but rather a relative number indicating the small area actually required by trout populations. It should also be recognized that by restricting our measurements of stream spawning habitat to the first 100 m of stream, we undoubtedly missed some spawning habitat that was available to the trout populations.

The significant association we found between the likelihood of successful natural reproduction and qualitative estimates of spawning-habitat quality in our JMW study area suggests not only that qualitative estimates of spawning-habitat availability may provide a reasonably accurate means of categorizing the reproductive status of trout populations, but also that in the absence of quantitative measures of recruitment magnitude and habitat characteristics, a prudent management strategy may be to simply categorize those trout populations in lakes with any spawning habitat as reproductive. The qualitative assessments needed to make this determination are currently available for many Sierra Nevada lakes.

Our regression models also suggest that in addition to depending on the amount of spawning habitat, the probability of successful reproduction by trout populations decreases with increasing elevation. Specifically, the tree regression indicated that lakes above 3520 m were unlikely to contain reproductive trout populations. One possible explanation for

© 2004 NRC Canada

Fig. 8. Box plots showing (*a*) catch per unit effort (CPUE), (*b*) size at age 4, and (*c*) maximum fish size for trout (*Oncorhynchus* spp.) populations in JMW experimental lakes categorized as reproductive from initial surveys (1995–1996) and resurveys (2001–2002). The line within each box represents the median, the bottom and top of each box indicate the 25th and 75th percentiles, the whiskers represent the 10th and 90th percentiles, and the points below and above the whiskers indicate values outside the 10th and 90th percentiles; "ns" indicates that the difference between reference and experimental lakes is not statistically significant (paired *t* test, $P > 0.05$); ** indicates that the difference is significant (paired *t* test, $P < 0.005$). Sample sizes are 37 for the first two groups and 22 for the third group.

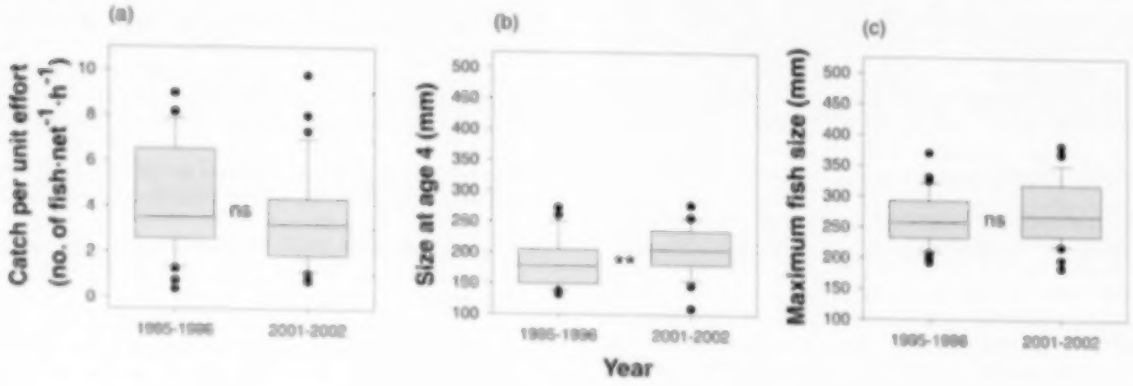

this inability of trout populations at the highest elevations to reproduce is that the ice-free growing season in these lakes may be too short to allow successful recruitment. Lakes at these high elevations usually remain ice-free for only a few weeks each summer. A short ice-free season forces spawning to occur later in the summer, which would likely result in a truncated growing season for emerging fry. These small fry may be subject to strong size-selective mortality, as has been documented for fry of other salmonids (e.g., West and Larkin 1987). If emerging trout fry in our high-elevation lakes are subject to slow growth and size-selective mortality based on some minimum size threshold, then it is possible that fish in the highest elevation lakes are spawning successfully but that this spawning results in little or no recruitment.

For the naturally reproducing populations in our JMW study area, the results of our experiment show that there were no effects of a halt to stocking on population density or maximum fish size, but that there was an increase in fish growth rates as measured by size at age 4. Together, these results suggest that supplemental stocking of the study lakes provides no benefit when populations reproduce on their own, and in fact may reduce growth rates. Several other studies have examined the effects that stocking can have on existing fish populations in species other than *Oncorhynchus* spp., and have also concluded that supplemental stocking may often contribute little to fishery quality. Cortes Rui et al. (1996) and Bohlin et al. (2002) found that stocking brown trout (*Salmo trutta*) into streams with resident S. trutta populations increased mortality resulting from intraspecific competition. Stocking walleye (*Stizostedion vitreum*) into Minnesota lakes with self-sustaining *S. vitreum* populations resulted in decreases in abundance of adjacent year classes and decreases in the weights of resident fish (Li et al. 1996*b*) yet had no effect on overall population abundance (Li et al. 1996*a*). Similarly, Parsons and Pereira (2001) concluded that the stocking of *S. vitreum* fingerlings into self-sustaining *S. vitreum* populations was ineffective in boosting year-class strength.

The lack of a density response following stocking termination in our study lakes that contained reproductive populations suggests that at higher trout densities (resulting from the stocking of fry) an increasing mortality rate may compensate for the increase in density. This compensation may result in an essentially constant number of adult fish within each population. Salmonid populations are well known to be subject to such density-dependent mortality (Elliot 1985; Keeley 2001). Studies of population regulation in salmonids have nearly all been conducted in streams, and in these habitats it seems likely that the mechanism underlying density-dependent mortality is territory formation by age-0 fish that places an upper limit on their density (Elliot 1990; Grant and Kramer 1990). Whether a similar mechanism is responsible for population regulation in lake-dwelling salmonids remains unknown.

Individual growth rates and population density are often negatively correlated in salmonids (e.g., Jenkins et al. 1999; Schindler et al. 2001; Vollestad et al. 2002). Although we did not detect a significant change in trout density and maximum fish size in our experimental lakes after stocking termination, size-at-age increased. One possibility as to why the two growth-rate measures responded differently to stocking termination is that a rapid response in maximum fish size was prevented by the presence of fish cohorts that remained from the prestocking-hiatus period. If competition for food is strongest within cohorts, then density and growth of cohorts from the stocking period may be relatively unaffected by changes in the density of younger cohorts resulting from the stocking hiatus. In contrast, growth of age-4 fish may have increased as a result of even slight decreases in the density of this cohort. Longer term studies will be necessary to elucidate whether stocking termination did in fact increase fish growth rates and if so, the mechanism underlying these changes.

© 2004 NRC Canada

In conclusion, the majority of lake-dwelling *Oncorhynchus* spp. populations in our JMW and SEKI study areas showed evidence of successful reproduction, and relatively few JMW lakes will revert to a fishless condition even with a complete halt to stocking. The findings from this study indicate that cessation of stocking had no effect on population density but may have had a positive effect on fish growth rates. These results should encourage fisheries managers to reevaluate current mountain lake stocking programs, as the level of successful natural reproduction by trout populations in other high-elevation lakes in western North America may also be considerably higher than is currently believed (e.g., Bahls 1992).

Acknowledgements

This research was supported by grants to R. Knapp from the California Department of Fish and Game (P01800021), the U.S. Forest Service (PSW-95-001-CCS, PSW-96-0007CA, PSW-98-0009CA), and the National Park Service (USDI NPS 8550-002), a donation to R. Knapp from Trout Unlimited, and a grant to P. Moyle from the University of California Water Resources Center (Project W-955). Numerous field assistants were critical to the success of this study and their diligence is much appreciated. Thanks are also extended to the California Department of Fish and Game for altering their stocking program to allow us to conduct the stocking-termination experiment in the John Muir Wilderness.

References

Bahls, P. 1992. The status of fish populations and management of high mountain lakes in the western United States. Northwest Sci. **66**:183–193.

Bjornn, T.C., and Reiser, D.W. 1991. Habitat requirements of salmonids in streams. Am. Fish. Soc. Spec. Publ. No. 19. pp. 83–138.

Bohlin, T., Sundstrom, L.F., Johnsson, J.I., Hojesjo, J., and Pettersson, J. 2002. Density-dependent growth in brown trout: effects of introducing wild and hatchery fish. J. Anim. Ecol. **71**: 683–692.

Boiano, D.M. 1999. Predicting the presence of self-sustaining trout populations in high elevation lakes of Yosemite National Park, California. M.S. thesis, Humboldt State University, Humboldt, Calif.

Bradford, D.F., Cooper, S.D., Jenkins, T.M., Jr., Kratz, K., Sarnelle, O., and Brown, A.D. 1998. Influences of natural acidity and introduced fish on faunal assemblages in California alpine lakes. Can. J. Fish. Aquat. Sci. **55**: 2478–2491.

California Division of Mines and Geology. 1958. Geologic atlas of California. California Department of Conservation, Sacramento.

Campana, S.E., and Neilsen, J.D. 1985. Microstructure of fish otoliths. Can. J. Fish. Aquat. Sci. **42**: 1014–1032.

Cordes, J.F. 2001. Genetic purity of California golden trout populations in the headwater of Golden Trout Creek. Available from the web site of the University of California Genomic Research Laboratory: http://genome-lab.ucdavis.edu/People/Ian's%20Web%20Pages/CGT%20project%20page1.htm [accessed 5 May 2002].

Cordes, J.F., Stevens, M.R., and May, B.P. 2003. Genetic status of California golden trout in the South Fork Kern River and transplanted populations. Report to the Threatened Trout Committee, California Department of Fish and Game, Sacramento.

Cortes Rui, M.V., Teixeira, A., and Pereira, C.A. 1996. Is supplemental stocking of brown trout (*Salmo trutta*) worthwhile in low productive streams? Folia Zool. **45**: 371–381.

Cowx, I.G. 1994. Stocking strategies. Fish. Manag. Ecol. **1**: 15–30.

De'ath, G., and Fabricius, K.E. 2000. Classification and regression trees: a powerful yet simple technique for ecological data analysis. Ecology, **81**: 3178–3192.

Donald, D.B. 1987. Assessment of the outcome of eight decades of trout stocking in the mountain national parks, Canada. N. Am. J. Fish. Manag. **7**:545–553.

Donald, D.B., and Anderson, R.S. 1982. Importance of environment and stocking density for growth of rainbow trout in mountain lakes. Trans. Am. Fish. Soc. **111**: 675–680.

Donald, D.B., Anderson, R.S., and Maywood, D.W. 1980. Correlations between brook trout growth an environmental variables for mountain lakes in Alberta, Canada. Trans. Am. Fish. Soc. **109**: 603–610.

Elliot, J.M. 1985. Population regulation for different life-stages of migratory trout *Salmo trutta* in a Lake District stream, 1966–1983. J. Anim. Ecol. **54**: 617–638.

Elliot, J.M. 1990. Mechanisms responsible for population regulation in young migratory trout, *Salmo trutta*. III. The role of territorial behaviour. J. Anim. Ecol. **59**: 803–818.

Gowan, C., and Fausch, K.D. 1996. Mobile brook trout in two high-elevation Colorado streams: re-evaluating the concept of restricted movement. Can. J. Fish. Aquat. Sci. **53**: 1370–1381.

Grant, J.W.A., and Kramer, D.L. 1990. Territory size as a predictor of the upper limit to population density of juvenile salmonids in streams. Can. J. Fish. Aquat. Sci. **47**: 1724–1737.

Graynoth, E. 1996. Determination of the age of brown and rainbow trout in a range of New Zealand lakes. Mar. Freshw. Res. **47**: 749–756.

Hall, D.L. 1991*a*. Age validation and aging methods for stunted brook trout. Trans. Am. Fish. Soc. **120**: 644–649.

Hall, D.L. 1991*b*. Growth, fecundity, and recruitment responses of stunted brook trout populations to density reduction. Doctoral dissertation, University of British Columbia, Vancouver, B.C.

Hining, K.J., West, J.L., Kulp, M.A., and Neubauer, A.D. 2000. Validation of scales and otoliths for estimating age of rainbow trout from southern Appalachian streams. N. Am. J. Fish. Manag. **20**: 978–985.

Jenkins, T.M., Jr., Diehl, S., Kratz, K.W., and Cooper, S.D. 1999. Effects of population density on individual growth of brown trout in streams. Ecology, **80**: 941–956.

Keeley, E.R. 2001. Demographic responses to food and space competition by juvenile steelhead trout. Ecology, **82**: 1247–1259.

Knapp, R.A. 1996. Nonnative trout in natural lakes of the Sierra Nevada: an analysis of their distribution and impacts on native aquatic biota. Vol. III. Centers for Water and Wildlands Resources, University of California, Davis.

Knapp, R.A., and Matthews, K.R. 2000. Non-native fish introductions and the decline of the mountain yellow-legged frog from within protected areas. Conserv. Biol. **14**: 428–438.

Knapp, R.A., and Preisler, H.K. 1999. Is it possible to predict habitat use by spawning salmonids? A test using California golden trout (*Oncorhynchus mykiss aguabonita*). Can. J. Fish. Aquat. Sci. **56**: 1576–1584.

Knapp, R.A., Matthews, K.R., and Sarnelle, O. 2001. Resistance and resilience of alpine lake fauna to fish introductions. Ecol. Monogr. **71**: 401–421.

Kruse, C.G., Hubert, W.A., and Rahel, F.J. 1997. Using otoliths and scales to describe age and growth of Yellowstone cutthroat trout in a high-elevation stream system, Wyoming. Northwest Sci. **71**: 30–38.

Landry, F., Post, J.R., and Parkinson, E.A. 1999. Spatial ontogeny of lentic age-0 rainbow trout, *Oncorhynchus mykiss*: whole-lake

© 2004 NRC Canada

manipulations of population size structure. Can. J. Fish. Aquat. Sci. **56**: 1916–1928.

Li, J., Cohen, Y., Schupp, D.H., and Adelman, I.R. 1996*a*. Effects of walleye stocking on population abundance and fish size. N. Am. J. Fish. Manag. **16**: 830–839.

Li, J., Cohen, Y., Schupp, D.H., and Adelman, I.R. 1996*b*. Effects of walleye stocking on year-class strength. N. Am. J. Fish. Manag. **16**: 840–850.

Matthews, K.R. 1996. Diel movement and habitat use of California golden trout in the Golden Trout Wilderness, California. Trans. Am. Fish. Soc. **125**: 78–86.

Melack, J.M., Stoddard, J.L., and Ochs, C.A. 1985. Major ion chemistry and sensitivity to acid precipitation of Sierra Nevada lakes. Water Resour. Res. **21**: 27–32.

Parsons, B.G., and Pereira, D.L. 2001. Relationship between walleye stocking and year-class strength in three Minnesota lakes. N. Am. J. Fish. Manag. **21**: 801–808.

Pister, E. 2001. Wilderness fish stocking: history and perspective. Ecosystems, **4**:279–286.

Quinn, T.J., and Derison, R.B. 1999. Quantitative fish dynamics. Oxford University Press, New York.

Schindler, D.E., Knapp, R.A., and Leavitt, P.R. 2001. Alteration of nutrient cycles and algal production resulting from fish introductions into mountain lakes. Ecosystems, **4**: 308–321.

Secor, D.H., Dean, J.M., and Laban, E.H. (*Editors*). 1992. Otolith removal and preparation for microstructural examination. Can. Spec. Publ. Fish. Aquat. Sci. No. 117.

S-Plus. 1999. User's manual. Data Analysis Products Division, Math Soft, Seattle, Wash.

Steidl, R.J., Hayes, J.P., and Schauber, E. 1997. Statistical power analysis in wildlife research. J. Wildl. Manag. **61**: 270–279.

Vollestad, L.A., Olsen, E.M., and Forseth, T. 2002. Growth-rate variation in brown trout in small neighboring streams: evidence for density-dependence? J. Fish Biol. **61**: 1513–1527.

West, C.J., and Larkin, P.A. 1987. Evidence for size-selective mortality of juvenile sockeye salmon *Oncorhynchus nerka* in Babine Lake, British Columbia, Canada. Can. J. Fish. Aquat. Sci. **44**: 712–721.

© 2004 NRC Canada

Spatial and temporal variability of the phytoplankton community structure in the North Water Polynya, investigated using pigment biomarkers

Francesca Vidussi, Suzanne Roy, Connie Lovejoy, Marie Gammelgaard, Helge Abildhauge Thomsen, Beatrice Booth, Jean-Eric Tremblay, and Behzad Mostajir

Abstract: Phytoplankton taxonomic pigments were measured by high-performance liquid chromatography (HPLC) during a 3-month survey (April–June 1998) in the North Water (NOW) Polynya (Canadian Arctic) to investigate changes in phytoplankton biomass and composition and the physical–chemical factors that influence these changes. A phytoplankton bloom with high chlorophyll *a* (Chl *a*) concentrations (up to 17.45 mg·m^{-3} at 15 m) occurred in mid-May along the Greenland coast in the southeastern part of the NOW Polynya. The initiation of the phytoplankton bloom was linked to shallow mixed-layer depths. The contribution of the different phytoplankton groups to Chl *a* inferred using a factorization program (CHEMTAX) indicated that the bloom was diatom-dominated (maximum 94% diatoms). The phytoplankton community structure was influenced by the water mass characteristics and the surface circulation pattern. Autotrophic flagellates dominated in April and May along the Canadian coast, where cold Arctic waters with relatively deep mixed layers were found. In contrast, diatoms dominated in May along the Greenland coast in warmer water masses of Atlantic origin and during June in the whole polynya, except in the southernmost part.

Résumé : Nous avons mesuré par chromatographie liquide à haute performance (HPLC) les pigments taxonomiques du phytoplancton durant un inventaire de 3 mois (avril–juin 1998) dans la polynie des eaux du nord (NOW) de l'Arctique canadien, afin d'étudier les changements de biomasse et de composition du phytoplancton et les facteurs physico-chimiques qui influencent ces changements. À la mi-mai, il s'est produit une prolifération du phytoplancton avec de fortes concentrations de chlorophylle *a* (Chl *a*) (pouvant atteindre 17,45 mg·m^{-3} à 15 m) le long de la côte du Groenland, dans la partie sud-est de la polynie NOW. Le début de la prolifération du phytoplancton est associé à des faibles profondeurs de la couche de mélange. La détermination de la contribution des différents groupes du phytoplancton à chl *a* au moyen d'un logiciel de factorisation (CHEMTAX) indique que la prolifération est dominée par les diatomées (un maximum de 94 % de diatomées). La structure de la communauté phytoplanctonique est influencée par les caractéristiques de la masse d'eau et par le pattern de circulation d'eau en surface. Les flagellés autotrophes dominent en avril et en mai le long de la côte canadienne, où il y a des eaux froides arctiques avec des couches de mélange relativement profondes. En revanche, les diatomées prédominent en mai le long de la côte du Groenland dans des masses d'eau plus chaudes provenant de l'Atlantique, ainsi qu'en juin dans toute la polynie, sauf dans la partie la plus australe.

[Traduit par la Rédaction]

Received 4 March 2003. Accepted 12 March 2004. Published on the NRC Research Press Web site at http://cjfas.nrc.ca on 18 January 2005.
J17376

F. Vidussi[1,2] **and S. Roy.** Institut des sciences de la mer de Rimouski, Université de Québec à Rimouski, Rimouski, QC G5L 3A1, Canada.
C. Lovejoy. Département de Biologie, Université Laval, Québec, QC, G1K 7P4, Canada.
M. Gammelgaard and H.A. Thomsen. Danish Institute for Fisheries Research, Department of Marine Ecology and Aquaculture, 2920 Charlottenund, Denmark.
B. Booth. School of Oceanography, University of Washington, Seattle, WA 98195, USA.
J.-E. Tremblay. Department of Biology, McGill University, Montréal, QC, H3A 1B1, Canada.
B. Mostajir. Réseaux trophiques pélagiques (GDR 2476) and UMR 5119 Écosystèmes lagunaires, Centre national de la recherche scientifique (CNRS) – Université Montpellier II, 34095 Montpellier cedex 5, France.

[1]Corresponding author (e-mail: vidussi@univ-montp2.fr).
[2]Present address: Réseaux trophiques pélagiques (GDR 2476) and UMR 5119 Écosystèmes Lagunaires, CNRS – Université Montpellier II, 34095 Montpellier cedex 5, France.

 doi: 10.1139/F04-152 © 2004 NRC Canada

Introduction

Polynyas are regions of open water or thin ice cover surrounded by pack ice. Polynyas form in winter, when air temperatures are below the freezing point of seawater, under conditions where we would expect ice cover (Smith and Sakshaug 1990). Polynyas support high production at various trophic levels, from phytoplankton to marine mammals (Stirling 1981). Two types of polynyas, with two mechanisms of formation and maintenance, are recognized (Smith and Sakshaug 1990): (*i*) a "latent heat" polynya, when the forming ice is mechanically advected by wind and (or) currents; and (*ii*) a "sensible heat" polynya, when warm upwelled water melts the ice cover and thus prevents ice formation. Although one mechanism can be dominant, in many cases both mechanisms are responsible for the formation and the maintenance of the polynya. North Water (NOW) Polynya is a recurrent polynya situated between Greenland and Ellesmere Island (Canada) and extending from 75°N to 78.5°N. Although the NOW surface is 95% covered by ice in January, the ice does not consolidate in winter and the open area starts to expand in late March–April and reaches its maximum extent in July. The NOW Polynya is generally considered a latent heat polynya (Melling et al. 2001), although the sensible heat mechanism can be significant for its maintenance (Melling et al. 2001). The NOW Polynya is known to be the most productive polynya in the Canadian Arctic, supporting an abundance of birds and mammals (Stirling 1981). Lewis et al. (1996) reported a diatom bloom in May 1991 (up to 506 mg·m^{-2} of chlorophyll *a* (Chl *a*)) starting in the eastern part of the NOW Polynya near the Greenland coast and moving westward and progressively exhausting nutrients. Lewis et al. (1996) hypothesized that bloom initiation was linked to the absence of ice cover. Considering the significance of polynyas for the Canadian Arctic ecosystem and the lack of data of their bio-geochemical functioning, the NOW international program was undertaken over 3 years (August 1997, March to July 1998, and September to November 1999) with the goal of understanding the formation and maintenance of the polynya as well as the bio-geochemical consequences of its presence in this Arctic environment. One of the hypotheses of the NOW Polynya program was that the physical mechanism of formation of the polynya, latent versus sensible heat, controls the structure of the water column and as a consequence the intensity and timing of the biological processes. The sensible heat mechanism induces surface ice melt and therefore the release of fresh water, which forms a thin surface layer and helps stratify the water column. This stratification causes a longer residence time of phytoplankton in the surface layer and therefore favors phytoplankton blooms. In contrast, the latent heat mechanism induces a deep mixing of the water column; thus phytoplankton should be more limited by light. The mechanism of formation of the polynya and linked physical processes can also be of significance in determining the phytoplankton community structure, which has a key role in trophic food webs (Legendre and Rassoulzadegan 1995). Large diatoms are at the base of herbivorous food webs, supporting such renewable marine resources as herbivorous zooplankton and fish. In contrast, small phytoplankton, mainly cyanobacteria and autotrophic flagellates, are at the base of the microbial food web, which includes heterotrophic bacteria and protozoa. Phytoplankton community structure has also been implicated in the control and fate of biogenic carbon in the ocean (Michaels and Silver 1988). Particulate organic matter often sinks rapidly following diatom blooms, whereas recycling and weak export of particulate organic matter occurs when small phytoplankton and the microbial food web dominate.

The present study was undertaken in the NOW Polynya from April to June 1998. Its main objective was to study the temporal and spatial composition and distribution of the phytoplankton community, inferred using pigment biomarkers (chlorophylls and carotenoids) analyzed by high-performance liquid chromatography (HPLC), and the relationship between the phytoplankton community structure and physical–chemical processes that control the timing and the development of the spring phytoplankton bloom in the NOW Polynya.

Materials and methods

Study site and sampling

A 3-month study was undertaken during April–June 1998 over the NOW Polynya as part of the international North Water project (NOW project). A number of stations (between 23 and 31, Fig. 1) were visited once a month during three legs: leg 1 (8 April – 6 May), leg 2 (7 May – 1 June), and leg 3 (2 June – 29 June), referred to as April, May, and June respectively. Most stations were visited three times during the study period, except a few stations that were sampled only once or twice (see Fig. 1). Temperature and salinity were measured with a conductivity, temperature, and depth meter (mocel ICTD, Falmouth Scientific Inc., Cataumet, Massachusetts) equipped with a Sea Tech fluorometer (Sea-Bird Electronics, Inc., Bellevue, Washington) mounted on a rosette sampler. The mixed layer depth Z_{mld} was defined as the deepest depth where the potential density did not exceed surface (2.5 dbar; 1 bar = 100 kPa) density by a given threshold. Thresholds of 0.01, 0.02, 0.03, 0.04, and 0.05 were examined, and thresholds of 0.01 or 0.04 were retained as detailed in Tremblay et al. (2002*a*). Samples for the analysis of the chemical and biochemical parameters (nutrients, pigments, and phytoplankton abundance) were collected using Niskin bottles mounted on the rosette. Water samples were taken from optical depths corresponding to 100%, 45%, 30%, 20%, 10%, 1%, 0.1%, and 0.01% of surface irradiance and at the subsurface chlorophyll maximum when it occurred.

Nutrients

The concentrations of nitrite plus nitrate, orthophosphate, and silicate were determined in fresh samples using an ALPKEM autoanalyzer with routine colorimetric methods as reported in Tremblay et al. (2002*a*). A nutrient-based tracer (Tremblay et al. 2002*a*) derived from silicate–nitrate relationships in the upper 100 m was used to characterize water masses in the upper mixed layer. This tracer was designated Si^{ex}, as it is a measure of the concentration of silicate in excess of nitrate (Tremblay et al. 2002*a*, 2002*b*). This tracer can be used to determine the distribution of water masses of Pacific origin, referred to as silicate-rich Arctic water, and water masses of Atlantic origin, referred to as Baffin Bay water in the NOW Polynya. Following Tremblay et al. (2002*a*, 2002*b*), we grouped the stations into three catego-

© 2004 NRC Canada

Fig. 1. Location of the sampling stations in the North Water Polynya (Canadian Arctic) during April (A), May (B), and June (C) 1998.

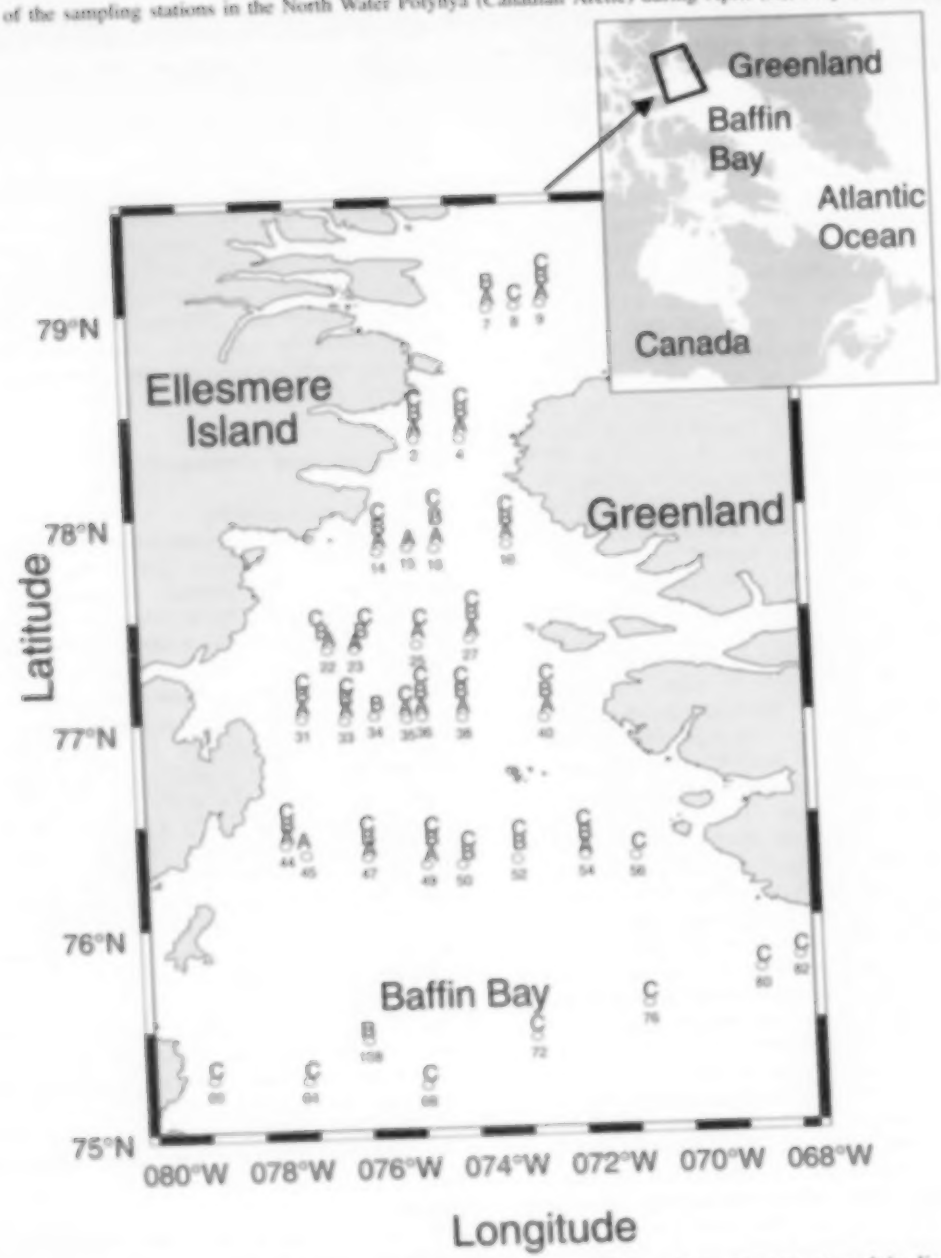

ries according to Si^{ex} values: (*i*) Si^{ex} > 70%; water masses were dominated by silicate-rich Arctic water; (*ii*) Si^{ex} < 30%; water masses were dominated by Baffin Bay water; and (*iii*) Si^{ex} values ranging from 30% to 70%; water masses were of intermediate origin.

Pigments

For pigment analysis, 2–5 L of water were sampled at three–seven depths selected among the standard optical depths listed above by examining the fluorometer profiles obtained during the downcast. Samples were immediately filtered onto 47-mm glass fiber filters (GF/F, Whatman Inc., Clifton, New Jersey), stored in liquid nitrogen, and then kept frozen (–80 °C) until analysis. Pigments were extracted in 3–12 mL of MeOH – ammonium acetate (98:2, *v/v*) and then sonicated for a few seconds. Extracts containing pigments were then filtered onto 0.2-µm Gelman acrodisc filters (Pall Gelman Sciences, Ann Arbor, Michigan). The extract was analyzed by HPLC using a modified method of Wright et al. (1991) using as eluent solution A (MeOH – ammonium acetate 0.5 mol·L^{-1}, pH = 7.1, 85:15, *v/v*), solution B (acetonitrile–H_2O, 90:10, *v/v*), and solution C (ethyl acetate, 100%) at a flow rate of 0.8 mL·min^{-1}. The elution program was as follows (minutes, % solvent A, % solvent B,

© 2004 NRC Canada

Table 1. Phytoplankton groups and corresponding specific accessory pigments.

Phytoplankton group	Specific pigment	References
Prasinophytes 1	Prasinoxanthin, Chl *b*	Jeffrey 1976; Simon et al. 1994
Prasinophytes 2	Lutein, zeaxanthin, Chl *b*	Ricketts 1970
Chlorophytes	Lutein, zeaxanthin, Chl *b*	Jeffrey 1976
Dinoflagellates	Peridinin	Johansen et al. 1974; Jeffrey et al. 1975
Cryptophytes	Alloxanthin	Jeffrey and Vesk 1997; Gieskes and Kraay 1983
Prymnesiophytes 1	Chl c_3, Hex-fuco, fucoxanthin	Jeffrey and Wright 1994
Prymnesiophytes 2	Chl c_3, Hex-fuco, But-fuco, fucoxanthin	Jeffrey and Wright 1994
Chrysophytes–Pelagophytes	Chl c_3, But-fuco, fucoxanthin	Bjørnland and Liaaen-Jensen 1989; Wright and Jeffrey 1987; Andersen et al. 1993
Fuco-containing flagellates[a]	Fucoxanthin	Stuart et al. 2000
Diatoms	Fucoxanthin	Bjørnland and Liaaen-Jensen 1989; Wright and Jeffrey 1987; Hooks et al. 1988

Note: Chl *b*, chlorophyll *b*; Chl c_3, chlorophyll c_3; Hex-fuco, 19′-hexanoyloxyfucoxanthin; But-fuco, 19′-butanoyloxyfucoxanthin.
[a]Flagellates containing fucoxanthin as major accessory pigment.

% solvent C): (0, 100, 0, 0), (2, 50, 50, 0), (8, 0, 100, 0), (13, 0, 80, 20), (28, 0, 30, 70), (34, 0, 30, 70), (35, 0, 0, 100), (45, 100, 0, 0). The HPLC system consisted of an automatic sampler (model AS 3000, Thermo Separation Products, Thermo Electron Corporation, Waltham, Massachusetts), which injects the sample into a 100-µL loop, a pump (model SP8800, Spectra Physics, Mountain View, California), a Spherisorb ODS2 (Richard Scientific, Novato, California) column (150 mm × 4.6 mm, 5 µm particle size), and two detectors: a fast-scanning, spectrophotometric detector (Spectra Focus, Spectra Physics) for screening the absorbance from 380 to 700 nm with a monitoring wavelength set at 450 nm, and a fluorometric detector (model Spectroflow 980, Applied Biosystems, Foster City, California) set at 412 nm for excitation and 650 nm for emission. Carotenoids, chlorophyll *b* (Chl *b*), and chlorophyll c_3 were quantified using the spectrophotometric detector, while Chl *a* allomers and epimers, chlorophyll c_{1+2}, and Chl *a* degradation products (chlorophyllides, pheophorbides, and pheophytins) were quantified using the fluorometric detector. The HPLC was calibrated using external standards obtained commercially (Sigma Chemical Co., St. Louis, Missouri, and DHI, Copenhagen, Denmark) or prepared in-house from algal cultures as recommended by SCOR UNESCO (Repeta and Bjørnland 1997).

Pigment results are presented as volumetric concentrations ($mg \cdot m^{-3}$) at surface and (or) at the depths within the euphotic layer (Z_e). Z_e was defined as the depth of 1% incident surface irradiance given in Mei et al. (2002). Integrated water column pigment concentrations were not given, as we sampled too few depths (three or four) for several stations, which would cause a bias in integrated concentrations. However, there was a significant relationship ($r = 0.88$, $p < 0.001$) between HPLC-measured surface Chl *a* concentrations and integrated Chl *a* concentrations from fluorometric measurements in the euphotic layer (Klein et al. 2002) where 6–10 depths were used. The concentration of total pheopigments was calculated as the sum of pyropheophorbide *a*, pheophorbide *a* derivatives (a_1, a_2, a_3, and a_4), pheophytin *a*, and pyropheophytin *a*.

The CHEMTAX program (Mackey et al. 1996) is a factorization program that uses a number of algal classes (defined according to the pigment composition; Table 1) and accessory pigment/Chl *a* ratios to infer the contribution of the different phytoplankton classes to Chl *a*. Initial ratios were assumed for the different algal classes according to the literature (Mackey et al. 1996; Wright et al. 1996; Schlüter et al. 2000). These ratios were iteratively modified by CHEMTAX to minimize the sum of squares of differences between the observed and calculated pigment concentrations. Since the accessory pigment/Chl *a* ratio varied with species, irradiance, and nutrient conditions, it was necessary to subdivide the pigment data set into subgroups with relatively stable pigment ratios. These different subgroups were then processed separately by the CHEMTAX program. Cluster analysis (Bray–Curtis) performed on pigment concentrations was used to identify three groups: (*i*) early spring (April) stations located in the northwestern part of the polynya (identified as a no-bloom situation); (*ii*) stations from throughout the study period but that were not yet involved in the bloom (identified as the prebloom situation); and (*iii*) stations visited during May and June where there was an active phytoplankton bloom (identified as bloom stations). Each of these three groups was subdivided into two subgroups according to depth: the surface subgroup included data taken at 100%, 45%, 30%, and 20% of surface irradiance and the deep subgroup included samples from ≤1% to ≤0.01% of surface irradiance. Because there is little information in the literature on pigment/Chl *a* ratios of phytoplankton in Arctic waters, and since we have direct information for only one prasinophyte isolated during the study and cultured (see below), we tested different combinations of taxonomic groups (e.g., one with one group of prasinophytes and one with two groups) having different initial pigment/Chl *a* ratios taken from the literature for the different cluster-derived groups to obtain consistent results (Goericke and Montoya 1998). At the same time, different initial pigment/Chl *a* ratios were used according to the literature for each of the surface and deep subgroups. We reported final results on accessory pigment/Chl *a* ratio from CHEMTAX (Table 2). It should be noted that the southernmost stations of the NOW Polynya, sampled only in June, represent a cluster group different from the others. These stations were very different in terms of pigments, and there were too few samples (<30) to compute taxonomic characteristics within this group by the CHEMTAX program.

© 2004 NRC Canada

Table 2. Range of the accessory pigment/Chl *a* ratio ($g \cdot g^{-1}$) calculated from CHEMTAX.

Phytoplankton group	Range	Chl c_3	Perid	But-fuco	Fuco	Hex-fuco	Pras	Allo	Lut	Zea	Chl *b*
Prasinophytes 1	Min.	0	0	0	0	0	0.029	0	0	0	0.095
	Max.	0	0	0	0	0	0.121	0	0	0	0.929
Prasinophytes 2	Min.	0	0	0	0	0	0	0	0.004	0.002	0.478
	Max.	0	0	0	0	0	0	0	0.008	0.014	0.997
Chlorophytes	Min.	0	0	0	0	0	0	0	0.105	0.087	0.073
	Max.	0	0	0	0	0	0	0	0.201	0.094	—
Dinoflagellates	Min.	0	0.600	0	0	0	0	0	0	0	0
	Max.	0	—	0	0	0	0	0	0	0	0
Cryptophytes	Min.	0	0	0	0	0	0	0.673	0	0	0
	Max.	0	0	0	0	0	0	—	0	0	0
Prymnesiophytes 1	Min.	0.020	0	0	0.294	0.800	0	0	0	0	0
	Max.	0.055	0	0	0.538	1.416	0	0	0	0	0
Prymnesiophytes 2	Min.	0.708	0	0.012	0.500	0.011	0	0	0	0	0
	Max.	0.918	0	—	—	0.039	0	0	0	0	0
Chrysophytes–Pelagophytes	Min.	0.031	0	0.197	0.398	0	0	0	0	0	0
	Max.	0.197	0	0.992	—	0	0	0	0	0	0
Fuco-flagellates	Min.	0	0	0	0.285	0	0	0	0	0	0
	Max.	0	0	0	0.285	0	0	0	0	0	0
Diatoms	Min.	0	0	0	1.067	0	0	0	0	0	0
	Max.	0	0	0	1.391	0	0	0	0	0	0

Note: Chl c_3, chlorophyll c_3; Perid, peridinin; But-fuco, 19′-butanoyloxyfucoxanthin; Fuco, fucoxanthin; Hex-fuco, 19′-hexanoyloxyfucoxanthin; Pras, prasinoxanthin; Allo, alloxanthin; Lut, lutein; Zea, zeaxanthin; Chl *b*, chlorophyll *b*; —, max. value was same as min.

The contribution of the different algal classes to Chl *a* was estimated using the CHEMTAX software, considering a number of algal classes defined according to the pigment composition (Table 1), information from microscopic identification of species, and pigment ratios taken from the literature. Prasinophytes were separated into two types: prasinophytes-1 consisted of Prasinophyceae that contained prasinoxanthin, whereas prasinophytes-2 were prasinophytes, such as *Micromonas pusilla*, that lack prasinoxanthin. *Micromonas pusilla* was the dominant picoeukaryote in the NOW Polynya (Lovejoy et al. 2002*a*) and was isolated and cultured during the study. This alga contained only traces of prasinoxanthin, and lutein, zeaxanthin, Chl *b*, and siphonaxanthin were the major accessory pigments (F. Vidussi and C. Lovejoy, unpublished data). Zeaxanthin is the major accessory pigment of cyanobacteria (*Synechococcus* and *Prochlorococcus*) and a minor pigment in prasinophytes and chlorophytes. *Prochlorococcus* was not detected by flow cytometry in the NOW Polynya surface samples (Mostajir et al. 2001). *Synechococcus*, although detected by microscopy, accounted for an extremely low biomass (Lovejoy et al. 2002*a*). Thus, zeaxanthin, which was detected in low concentrations during this study (average 0.006 $mg \cdot m^{-3}$), was exclusively associated with prasinophytes and chlorophytes. The dinoflagellate group was limited to Dinophyceae that contained peridinin. Other dinoflagellates with pigments typical of other classes (e.g., fucoxanthin and its derivatives; Jeffrey and Vesk 1997) were not identified as dinoflagellates by the CHEMTAX method. Cryptophytes included only Cryptophyceae that contained alloxanthin. Prymnesiophytes were separated into two types: (*i*) type 1 identified prymnesiophytes containing 19′-hexanoyloxyfucoxanthin (Hex-fuco) and fucoxanthin, such as *Chrysochromulina* (Barlow et al. 1993), which was detected by microscopy (Lovejoy et al. 2002*a*), and (*ii*) type 2 identified prymnesiophytes containing Hex-fuco, 19′-butanoyloxyfucoxanthin (But-fuco), and fucoxanthin. Some prymnesiophytes contained only fucoxanthin and lacked fucoxanthin derivatives (Hex-fuco and But-fuco; Jeffrey and Wright 1994). This is the case for *Phaeocystis pouchetii* in the Labrador sea (Stuart et al. 2000) and may be also the case in the NOW Polynya for *P. pouchetii*, which was relatively abundant at a few stations (Lovejoy et al. 2002*a*). These prymnesiophytes were grouped with flagellates designated as fucoxanthin-containing flagellates (abbreviation Fuco-flagellates): these flagellates contained solely fucoxanthin as specific accessory pigment (Table 1) and had a relatively low fucoxanthin:Chl *a* ratio (Vaulot et al. 1994). This last group also included the Chrysophyceae that contained fucoxanthin (such as *Ochromonas* sp.), Dictyochophyceae, Pedinophyceae, and those Dinophyceae that contain fucoxanthin instead of peridinin as an accessory pigment. Chrysophyceae containing But-fuco and fucoxanthin, such as *Dinobryon* (Booth and Marchant 1987), which was detected by microscopy during NOW, were included with the pelagophytes–chrysophytes (Table 1). Other Chrysophyceae, such as Parmales (Booth and Marchant 1987), containing But-fuco, Hex-fuco, and fucoxanthin, which were identified by microscopy during NOW, were not distinguished from the prymnesiophyte 2 group, since they share the same pigments. Finally, a group that contained a relatively high fucoxanthin:Chl *a* ratio was identified as Diatoms (Table 1). Thus, Diatoms and Fuco-flagellates were identified by the same pigment (fucoxanthin) and were distinguished in the CHEMTAX matrix by lower fucoxanthin/ Chl *a* initial ratios for Fuco-flagellates than for Diatoms.

Pearson linear correlations were performed between microscopic results and CHEMTAX results as well as among the contribution to Chl *a* of Diatoms, Fuco-flagellates, and prymnesiophytes 2 and different environmental variables, namely temperature, contribution of water mass of Arctic or-

© 2004 NRC Canada

igin, and nutrients. Spatial autocorrelation structures of the different variables listed before were tested separately for the 3 studied months of different distance classes and measured using Moran's *I* coefficient corrected with the Bonferroni adjustment (Legendre and Legendre 1998). The number of distance classes for the spatial autocorrelation analysis between sampling stations were calculated using Sturge's rule. All statistical tests were performed using the multivariate and spatial analysis program R Package (available from www.fas.umontreal.ca/biol/Legendre) and $\alpha = 0.05$ was used as a critical level of significance.

Results

Physical–chemical trends

The physical and chemical oceanographic conditions of the water column in the NOW Polynya over the 3-month survey have been described elsewhere (e.g., Melling et al. 2001; Bâcle et al. 2002; Tremblay et al. 2002*a*). Here, we summarize only the trends relevant to understanding the pigment distribution during this study. Surface temperature increased from April to June and ranged from –1.84 to –1.53 °C in April, from –1.83 to –0.26 °C in May, and from –1.50 to +1.64 °C in June (Fig. 2). The surface temperature increase started in May in the southeastern part of the polynya along the Greenland coast. Surface salinity ranged from 31.70‰ to 33.56‰, and decreased from April to June (Fig. 2). Surface salinity showed an east–west gradient, with increased salinity along the Greenland coast in April and May. Surface nitrate concentrations were high in April (from 9.0 to 11.69 μmol·L^{-1}; Fig. 2). In May, surface nitrate was exhausted to undetectable levels (<0.05 μmol·L^{-1}) along the Greenland coast, while along the Canadian coast concentrations showed a maximum of 11.01 μmol·L^{-1}. In June, surface nitrate concentrations ranged from undetectable levels (<0.05 μmol·L^{-1}) to 10.86 μmol·L^{-1} (Fig. 2).

Phytoplankton pigment distribution

Surface Chl *a* concentrations in the polynya varied from 0.03 to 16.30 mg·m^{-3} (average 2.50 mg·m^{-3}) during the 3-month survey (Fig. 3). In April, surface Chl *a* concentrations were on average 15 times lower than in May and 10 times lower than in June. However, relatively high Chl *a* concentrations at the surface (>1 mg·m^{-3}) were detected in late April in the eastern part of the polynya along the Greenland coast (Fig. 3). In May, high Chl *a* concentrations at the surface and at subsurface depths were detected in the southeastern part of the polynya near the Greenland coast (up to 17.45 mg·m^{-3} at 15 m), which indicates the presence of a well-developed phytoplankton bloom. In late May, Chl *a* concentrations were relatively high along the Canadian coast, and in June Chl *a* concentrations were relatively high over several areas of the polynya, suggesting the bloom had spread to the west and north along the Canadian coast. The southernmost part of the polynya was not sampled in April and May because of ice cover; in June, Chl *a* concentrations were relatively low (≤0.50 mg·m^{-3}) in that region.

Fucoxanthin showed the highest concentration of all accessory pigments (average 1.7 mg·m^{-3}), and concentrations were on average 14 times greater in May and June compared with April (Table 3). The surface distribution of fucoxanthin followed the general pattern of Chl *a*, with higher concentrations along the Greenland coast in May and at various locations in the polynya in June (Fig. 3). Other accessory pigments (e.g., Chl *b*; Fig. 3) had lower concentrations (always less than 0.12 mg·m^{-3}) and were less variable among months (Table 3). The surface distribution of Chl *b* differed from that of Chl *a* and fucoxanthin during the 3-month survey; the increase of Chl *b* along the Greenland coast started in April, earlier than Chl *a*, and higher Chl *b* concentrations were found in the north of the polynya and along the Canadian coast during May (Fig. 3). In addition, the southernmost stations of the polynya sampled in June showed relatively high Chl *b* concentrations (Fig. 3) and anomalous accessory pigments/Chl *a* ratios (data not shown). Total pheopigment concentration in the euphotic layer increased from April to June and ranged from undetectable levels to 2.33 mg·m^{-3} (data not shown). The average ratios of total pheopigments to Chl *a* in the euphotic layer increased through the year and were 0.015, 0.093, and 0.174 g·g^{-1} in April, May, and June, respectively (data not shown).

Three periods can be distinguished according to Chl *a* and nutrient concentrations in the euphotic zone: (*i*) the prebloom period with relatively low Chl *a* and high nutrient concentrations; (*ii*) the bloom period with relatively high Chl *a* concentrations and low nutrients; and (*iii*) the late-bloom period with relatively low Chl *a* and low nutrient concentrations. The prebloom period was encountered at stations visited in April and northern and western areas in May. The bloom period occurred in May along the Greenland coast and in June in several regions. Late-bloom conditions were encountered at several stations in June.

Phytoplankton group distribution

Results of phytoplankton group concentrations (and contribution) in terms of Chl *a* calculated by CHEMTAX were compared with phytoplankton group concentrations (and contribution) in terms of carbon derived from microscopic counts made by two different laboratories (Fig. 4). CHEMTAX and microscopic results were significantly correlated ($p < 0.01$) except for dinoflagellates (data shown only for Diatoms; Fig. 4). The percent contribution of Diatoms to the chlorophyll biomass calculated by CHEMTAX was generally lower than the diatom contribution to the total carbon biomass estimated by microscopy (Fig. 4*b*), while flagellate contribution was higher (not shown).

Results from the CHEMTAX surface subgroup indicated that the relative contribution of Diatoms to Chl *a* increased about twofold from April to June, whereas the flagellate contribution decreased (Table 4). Flagellates generally dominated in April and May, while Diatoms became dominant in June where their average contribution to Chl *a* was 62% (maximum contribution = 94%). However, Diatoms were also dominant at bloom stations during May; their contribution to Chl *a* then ranged from 60% to 70%. Among flagellates, prymnesiophytes 1 and 2 were the groups that contributed most to Chl *a* during April, while the Fuco-flagellate group was dominant during May and June. The diatom contribution to Chl *a* in the euphotic layer was positively correlated with temperature during May and June ($p < 0.05$, $n = 18$, $r = 0.55$ and 0.59 respectively; Fig. 5*a*), while no significant relationship or a negative relationship was found between the auto-

© 2004 NRC Canada

Fig. 2. Surface temperature (*a*, *b*, *c*), salinity (*d*, *e*, *f*), and nutrient concentration (NO_3^-) (*g*, *h*, *i*) in the North Water Polynya during April (1st column), May (2nd column), and June (3rd column) 1998. Note that NO_3^- concentrations in April ranged from 9 to 10 μmol·L^{-1} and differ from those of May and June (see the figure legend).

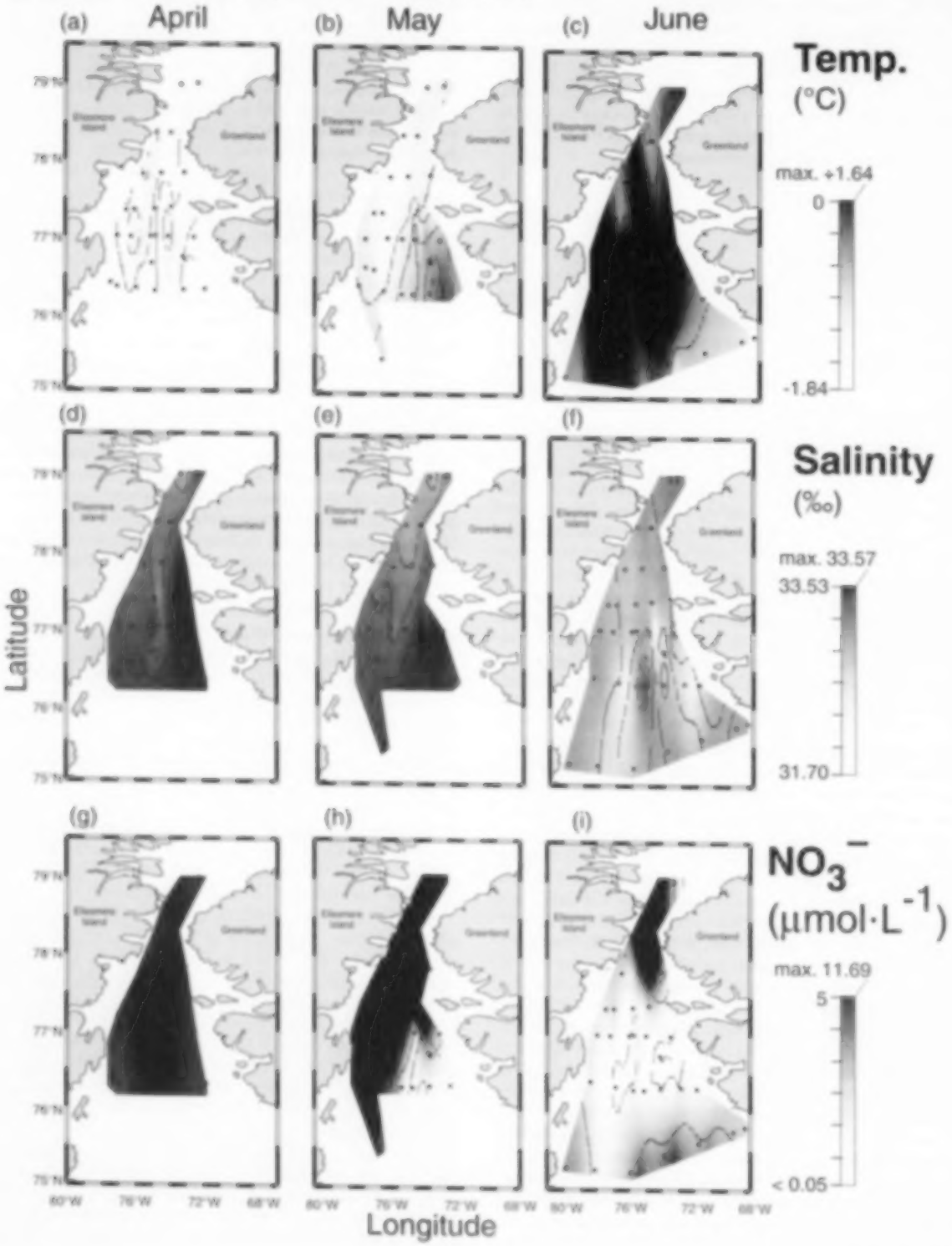

© 2004 NRC Canada

Fig. 3. Surface chlorophyll *a* (Chl *a*) (*a*, *b*, *c*), fucoxanthin (Fuco) (*d*, *e*, *f*), and chlorophyll *b* (Chl *b*) (*g*, *h*, *i*) concentrations in the North Water Polynya during April, May, and June 1998. Note that the scales are different according to the pigment.

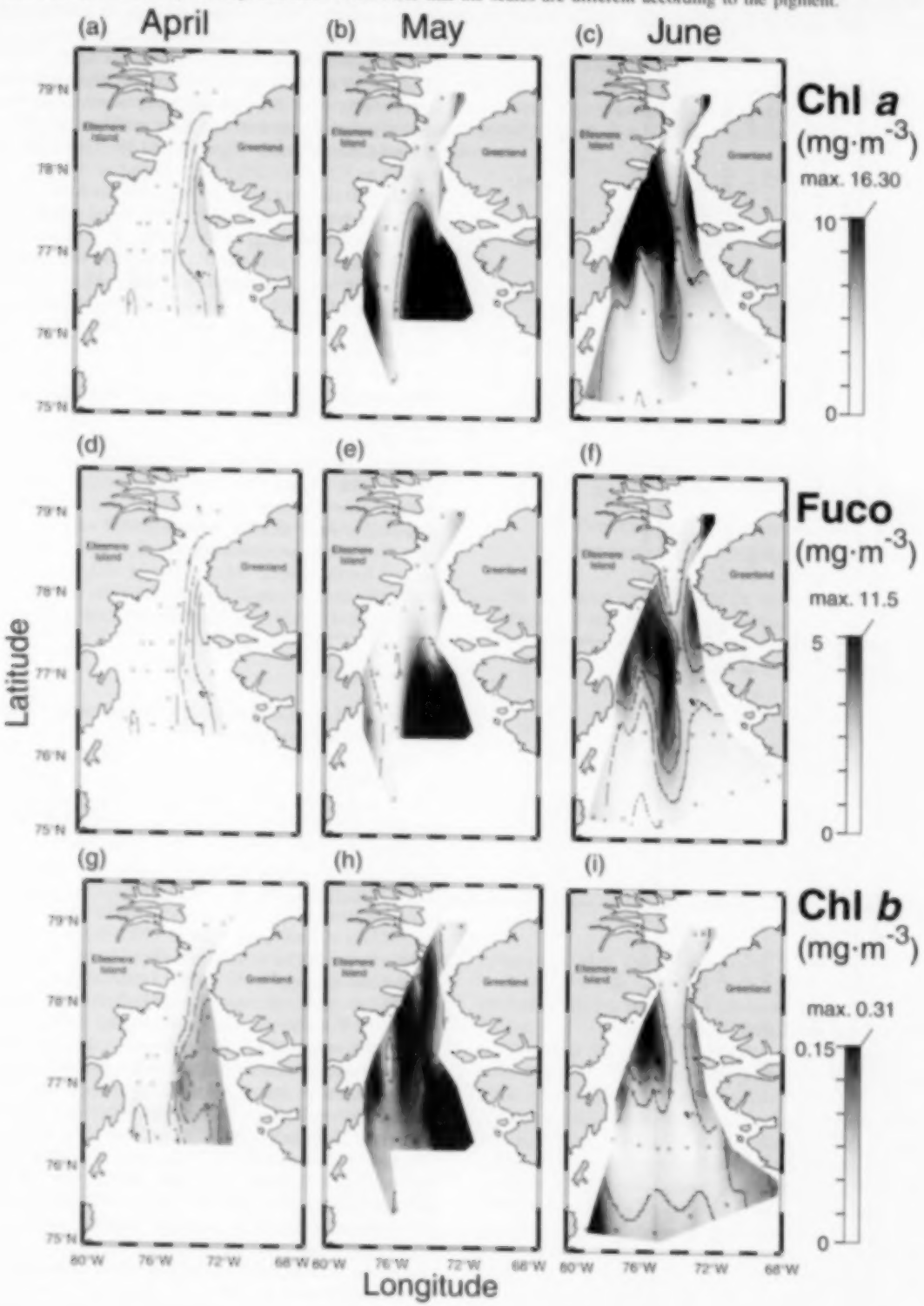

© 2004 NRC Canada

Table 3. Average physical and biochemical parameters (±SE) at the surface during April, May, and June 1998 in the North Water Polynya.

Period	Temp. (°C)	Salinity (‰)	Z_{mld} (m)	Z_{eu} (m)	NO_3^- (μmol·L^{-1})	$Si(OH)_4$ (μmol·L^{-1})	PO_4^{3-} (μmol·L^{-1})	Chl *a* (mg·m^{-3})	Fuco (mg·m^{-3})	Chl *b* (mg·m^{-3})	Hex-fuco (mg·m^{-3})	But-fuco (mg·m^{-3})	Peri (mg·m^{-3})	Allo (mg·m^{-3})	Prasino (mg·m^{-3})
April	−1.774	33.142	57	54	10.1	16.5	1.4	0.317	0.170	0.028	0.012	0.011	0.009	0.004	0.003
(*n* = 23)	(0.081)	(0.239)	(34)	(4)	(0.7)	(5.0)	(0.2)	(0.45)	(0.26)	(0.033)	(0.010)	(0.010)	(0.012)	(0.004)	(0.005)
May	−1.431	33.107	36	39	6.1	15.4	1.1	4.482	2.783	0.122	0.022	0.020	0.041	0.008	0.019
(*n* = 22)	(0.433)	(0.274)	(21)	(17)	(4.4)	(8.2)	(0.4)	(5.111)	(3.530)	(0.082)	(0.024)	(0.018)	(0.046)	(0.005)	(0.028)
June	−0.065	32.504	13	27	1.7	6.4	0.8	2.716	2.065	0.062	0.022	0.022	0.039	0.009	0.016
(*n* = 31)	(0.898)	(0.356)	(7)	(18)	(2.9)	(6.9)	(0.4)	(2.672)	(2.063)	(0.052)	(0.014)	(0.025)	(0.039)	(0.013)	(0.013)

Notes: Z_{mld}, mixed layer depth; Z_{eu}, euphotic layer depth; NO_3^-, nitrate plus nitrite; $Si(OH)_4$, silicate; PO_4^{3-}, phosphate; Chl *a*, chlorophyll *a*; *n*, number of samples. For accessory pigment abbreviations, see Table 2.

trophic flagellate contribution to Chl *a* and temperature (data shown only for prymnesiophytes 2 and Fuco-flagellates; Figs. 5*c* and 5*e*). The diatom contribution to Chl *a* was negatively correlated to the inflow of Arctic waters over the 3 months ($p < 0.001$, $n = 19$, $r = 0.77$ in April; $p < 0.01$, $n = 13$, $r = 0.69$ in May; and $p < 0.05$, $n = 18$, $r = 0.57$ in June, respectively; Fig. 5*b*). In contrast, autotrophic flagellates were not significant correlated or positive correlated to the inflow of Arctic water (Figs. 5*d* and 5*f*). High diatom contributions to Chl *a* (>70%) were found at relatively shallow mixed-layer depths ($Z_{mld} < 25$ m), whereas high contributions of prymnesiophytes 2 (>20%) were found at relatively deep mixed-layer depth ($Z_{mld} > 70$ m; Fig. 6). The diatom contribution to total Chl *a* in the euphotic layer was negatively related to nutrient concentrations during May and June ($p < 0.001$, $n = 18$, $-0.69 \leq r \leq -0.80$), while prymnesiophytes 2 and Fuco-flagellates contributions were positive related to nutrient concentrations during May ($p < 0.01$, $n = 18$, $0.63 \leq r \leq 0.72$) and during June ($p < 0.001$, $n = 18$, $0.71 \leq r \leq 0.80$), respectively (Fig. 7). No significant relationships were found between Diatoms or autotrophic flagellates and nutrients for the other months. The other flagellate groups showed the same general trends as prymnesiophytes 2 (data not shown). The spatial autocorrelation analysis results showed spatial autocorrelation structures of the studied variables only during June where all the different variables (Diatoms, Fuco-flagellates, prymnesiophytes 2, temperature, % of waters of Arctic origin, NO_3^-), except PO_4^{3-}, were spatially autocorrelated at small and (or) medium–large distances (80 km and 180–250 km, respectively; data not shown).

Discussion

Chlorophyll biomass and physico-chemical control of the phytoplankton bloom

The phytoplankton bloom in the NOW Polynya during spring 1998 started in late April along the Greenland coast (Chl *a* around 1 mg·m^{-3}) and reached high chlorophyll concentrations (Chl *a* > 5 mg·m^{-3}) in mid-May (this study; Klein et al. 2002; Mei et al. 2002; Tremblay et al. 2002*b*). Maximum Chl *a* concentrations at the subsurface maximum found here (17.45 mg·m^{-3}) were in the same range as those reported previously (19.8 mg·m^{-3}; Klein et al. 2002; Mei et al. 2002) and during May 1991 (19.5 mg·m^{-3}; Lewis et al. 1996). It should be noted that when comparing Chl *a* concentrations derived from HPLC measurements (this study) and Chl *a* concentrations measured fluorometrically during the NOW Polynya studies (Lewis et al. 1996; Klein et al. 2002; Mei et al. 2002), discrepancies can arise because of methodological biases in addition to spatio-temporal variation (as might be the case for Lewis et al. 1996). Chl *a* concentrations measured fluorometrically include allomers, epimers, and degradation products of Chl *a* (e.g., chlorophyllides), while Chl *a* measured by HPLC does not. The sum of chlorophylls *a* (true Chl *a* plus allomers and epimers) during this study was up to 15% higher (maximum 20.34 mg·m^{-3}) than Chl *a* alone, which is 3% higher than chlorophyll measured fluorimetrically in the same cruise (Klein et al. 2002; Mei et al. 2002). The relatively high Chl *a* concentration in the NOW Polynya was also observed in 1999 and 2000 by SeaWIFS satellite-derived chlorophyll

© 2004 NRC Canada

Fig. 4. (*a*) Comparison between the diatom chlorophyll *a* (Chl *a*) concentrations derived from CHEMTAX and diatom carbon biomass estimated by microscopic counts. (*b*) Comparison between the relative contribution of diatoms to Chl *a* derived from CHEMTAX and the relative contribution of diatom carbon biomass to total phytoplankton carbon biomass estimated by microscopic counts. Data for both panels were taken from different depths in the euphotic zone of the North Water Polynya during the 3-month survey. Solid (●) and open (○) circles are data from two different laboratories. Diatom Chl *a* concentrations were calculated as the product of the contribution of diatoms to Chl *a* derived from CHEMTAX and Chl *a* concentrations measured by high-performance liquid chromatography (HPLC). Diatom carbon biomass as well as the contribution of diatoms to total phytoplankton biomass in term of carbon were estimated by microscopy using volume to carbon conversion factors as reported in Booth et al. (2002). *r* is Pearson's coefficient of linear correlation ($n = 40$). Note that the axes in Fig. 4*a* are in log scale format.

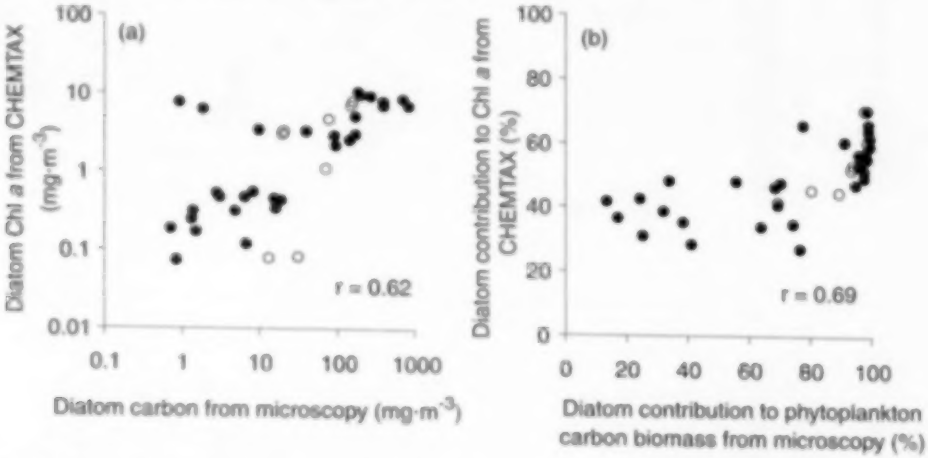

Table 4. Mean (SE) different phytoplankton group contribution to Chl *a* (%) calculated from CHEMTAX during April, May, and June and in water mass of Arctic, Baffin Bay, and intermediate (Int.) origin during the 3 months in the North Water Polynya.

Phytoplankton group	April	May	June	SRAW	Int.	BBW
Prasinophytes 1	8 (6)	9 (9)	2 (3)	9 (4)	6 (7)	4 (5)
Prasinophytes 2	7 (7)	5 (5)	2 (2)	4 (3)	4 (3)	3 (2)
Chlorophytes	0.4 (0.9)	2 (2)	0.6 (2)	1 (2)	1 (1)	1 (2)
Dinoflagellates	6 (3)	3 (3)	1 (1)	4 (5)	4 (4)	2 (2)
Cryptophytes	4 (3)	2 (2)	0.4 (0.7)	3 (4)	3 (3)	1 (2)
Prymnesiophytes 1	9 (6)	3 (2)	0.8 (1)	5 (5)	7 (8)	2 (2)
Prymnesiophytes 2	14 (7)	7 (7)	4 (4)	6 (5)	8 (7)	4 (4)
Chrysophytes–Pelagophytes	7 (4)	2 (3)	0.1 (0.3)	4 (5)	5 (5)	1 (2)
Fuco-flagellates	18 (11)	24 (12)	26 (13)	30 (14)	20 (10)	22 (11)
Diatoms	27 (15)	44 (15)	62 (17)	35 (16)	41 (23)	60 (17)

Note: SRAW, silicate-rich Arctic water; BBW, Baffin Bay water.

distributions (Bélanger 2001). High chlorophyll biomass up to 15 mg·m^{-3}, as measured during the NOW studies in 1991 and in 1998, was also reported from other adjacent regions (Head et al. 1988; Longhurst and Head 1989). However, as noted by Tremblay et al. (2002*b*), the phytoplankton bloom in the NOW Polynya started earlier than in adjacent, seasonally ice-covered regions, and the duration of the phytoplankton bloom was particularly long (1.5 months). The magnitude of the phytoplankton bloom in the NOW Polynya during spring depends on the initial nutrient inventories and on physical forcing (Tremblay et al. 2002*b*). In fact, Tremblay et al. (2002*b*) suggest that storm events that disrupt the pycnocline and thus inject additional nutrients in the upper mixed layer can enhance phytoplankton productivity to levels above what would be expected from the initial nutrient concentrations. Despite similar maximum Chl *a* concentrations (including epimers and allomers) during the bloom in the NOW Polynya in May 1991 (19.5 mg·m^{-3}; Lewis et al. 1996) and in May 1998 (20.34 mg·m^{-3}; this study), nitrates were not exhausted during May 1991 (minimum NO_3 concentration = 3.7 μmol·L^{-1}; Table 2 in Lewis et al. 1996), while they were exhausted in May 1998 (Tremblay et al. 2002*b*). This indicates that the bloom in 1991 was still ongoing, while in 1998 the bloom had reached a maximum.

The phytoplankton bloom during spring 1998 in the NOW Polynya started in relatively warmer and saltier surface waters that originate from Baffin Bay and are located along the Greenland coast (this study; Mei et al. 2002; Tremblay et al. 2002*a*). In this region, a shallow mixed layer associated with partial ice cover (Mei et al. 2002) favored optimal irradiance conditions and as a consequence the development of the phytoplankton bloom. These physical conditions were linked to the surface circulation and to the wind regime in the NOW Polynya (Mei et al. 2002; Tremblay et al. 2002*b*). The

© 2004 NRC Canada

Fig. 5. Relationship between temperature and the water mass index (i.e., inflow of Arctic water (%)) and the relative contribution of diatoms (*a*, *b*), prymnesiophytes 2 (prymnesio 2) (*c*, *d*), and Fuco-flagellates (*e*, *f*) to chlorophyll *a* derived from CHEMTAX in the North Water Polynya in samples from depths of 100%, 45%, 30%, and 20% surface irradiance during April (■), May (△), and June (○) 1998.

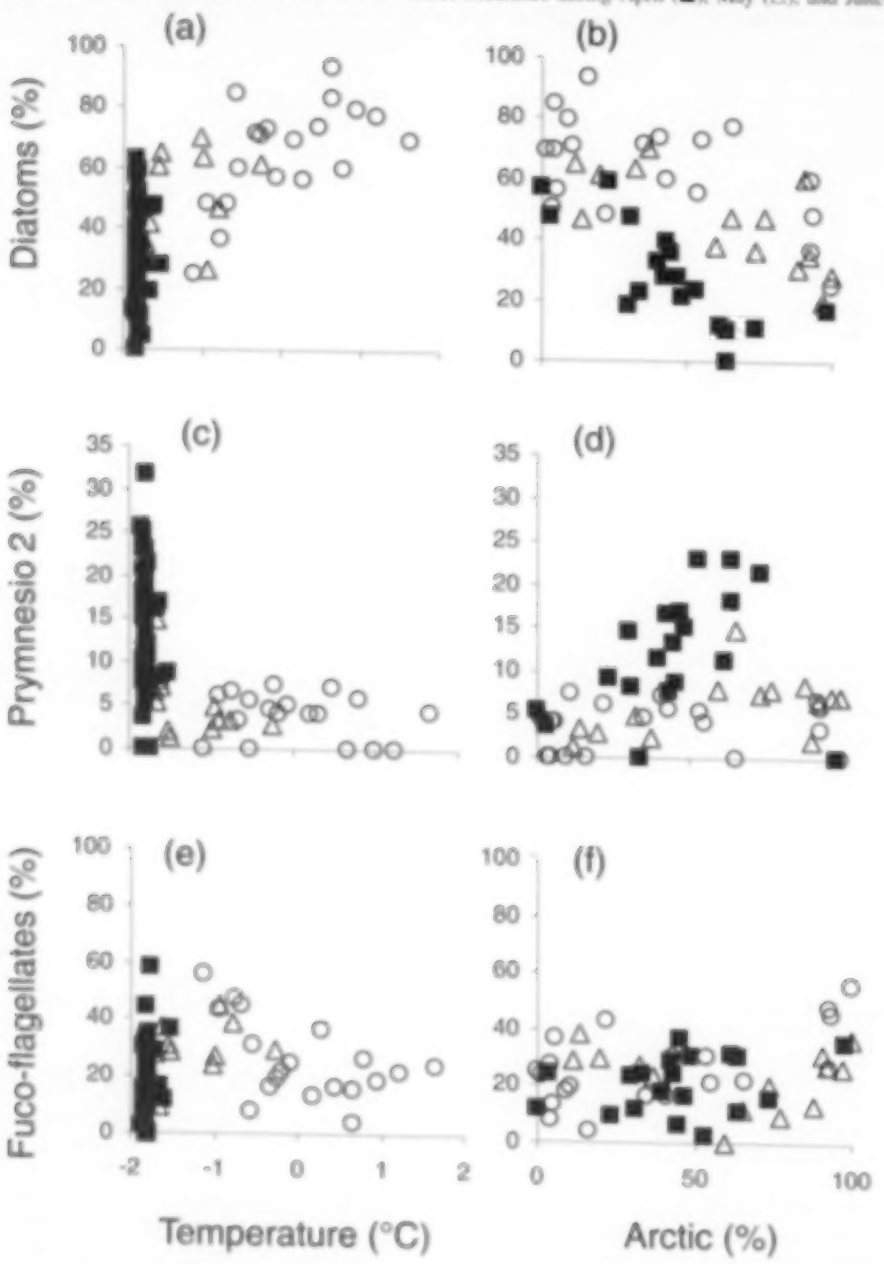

NOW Polynya circulation is characterized by strong northerly winds and southward flow of cold water and ice from the Arctic Ocean, promoting strong convection and deep mixing in the western sector of the polynya (Melling et al. 2001). In contrast, in the southeastern sector of the polynya, a northward flow of a branch of the West Greenland Current drives warm waters along the Greenland coast, which promotes reduced convection and a shallow mixed layer (Melling et al. 2001).

Factors controlling the phytoplankton composition

During this study, the contribution of different phytoplankton groups to total Chl *a* was estimated using the CHEMTAX program. CHEMTAX and microscopic results

© 2004 NRC Canada

Fig. 6. Relationship between the mixed-layer depth (Z_{mL}) and the relative contribution of diatoms (*a*), prymnesiophytes 2 (prymnesio 2) (*b*), and Fuco-flagellates (*c*) to chlorophyll *a* derived from CHEMTAX in the North Water Polynya in samples from depths of 100%, 45%, 30%, and 20% surface irradiance during April (■), May (△), and June (○) 1998.

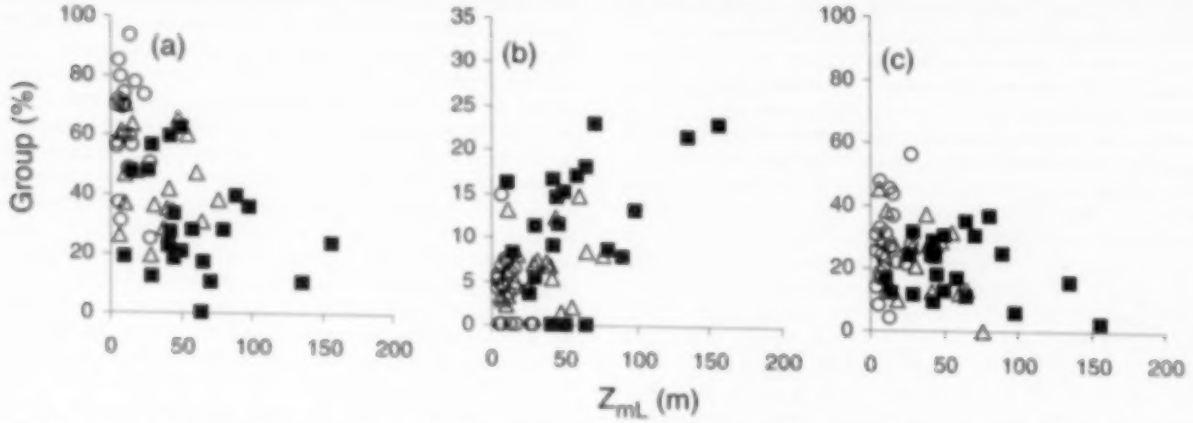

Fig. 7. Relationship between NO_3^-, $Si(OH)_4$, and PO_4^{3-} concentrations and the relative contribution of diatoms (*a*, *b*, *c*), prymnesiophytes 2 (prymnesio 2) (*d*, *e*, *f*), and Fuco-flagellates (*g*, *h*, *i*) to chlorophyll *a* derived from CHEMTAX in the North Water Polynya in samples from depths of 100%, 45%, 30%, and 20% surface irradiance during April (■), May (△), and June (○) 1998.

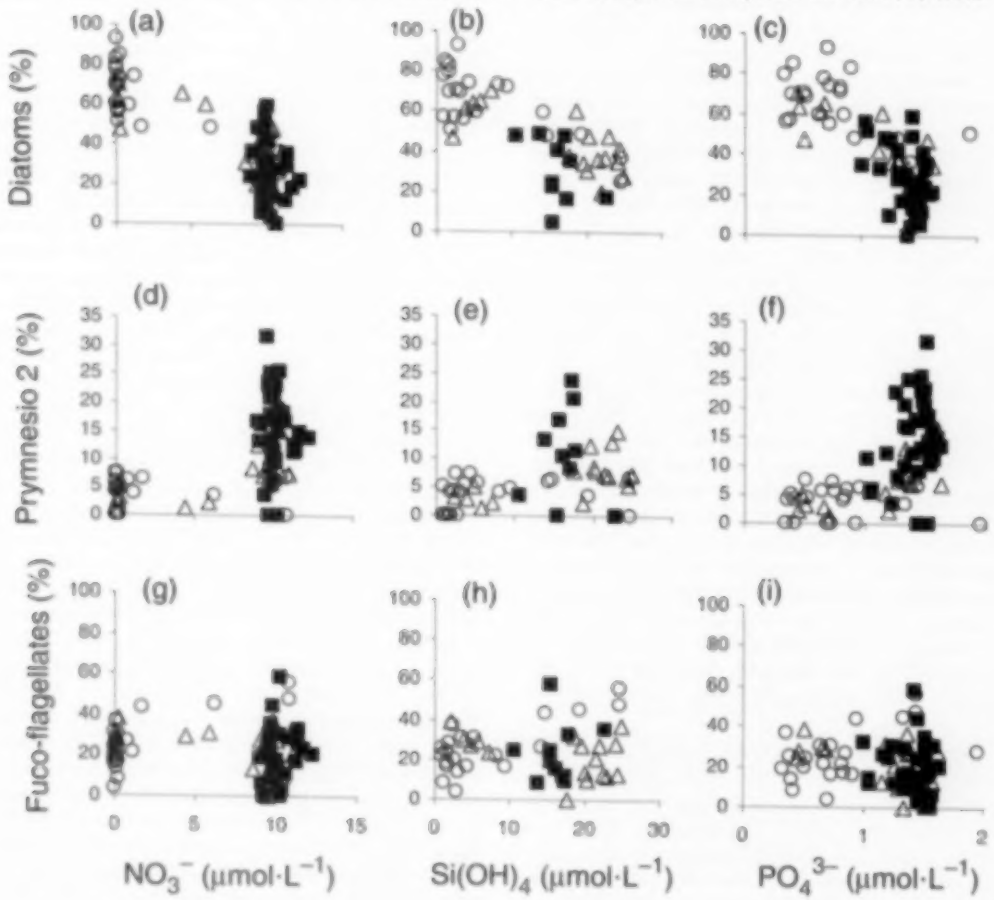

© 2004 NRC Canada

were generally significantly correlated, but there were discrepancies between the diatom contribution to Chl *a* derived from CHEMTAX and the diatom contribution to total carbon biomass estimated on the basis of microscopic analysis. There were also inconsistencies in the microscopic estimates of the contribution of diatoms to the total phytoplankton biomass coming from different laboratories associated with this research program (not shown). It should be noted that pigment samples and microscopic samples did not necessarily come from the same Niskin bottle, and for some stations they were not sampled at exactly the same depth (sometimes separated by 10 m). This can partially explain the divergence between CHEMTAX and microscopic results, since Lovejoy et al. (2002*b*) found that interleaving water masses were associated with different taxonomic groups over closely spaced depths. Discrepancies can also be explained by methodological limitations for both methods. During this study, good CHEMTAX results were obtained only when we included two groups with fucoxanthin as the single specific pigment (Fuco-flagellates and Diatoms). We assumed that Fuco-flagellates corresponded only to fucoxanthin-containing flagellates. However some diatoms with a low fucoxanthin/Chl *a* ratio, like that calculated by CHEMTAX for Fuco-flagellates, may also be included in this group. This may have caused an underestimation of the contribution of Diatoms to Chl *a* estimated by CHEMTAX. This can partially explain the lower contributions of Diatoms to Chl *a* calculated by CHEMTAX when compared with those calculated by microscopy. Discrepancies between the relative contribution of Diatoms to phytoplankton biomass estimated by CHEMTAX and microscopy may also be explained by the difficulty in preserving and counting some fragile, small and (or) rare flagellates (e.g., Roy et al. 1996; Guillou et al. 1999), thus overestimating diatoms compared with flagellates estimated by microscopy. In addition, comparisons of biomass in terms of chlorophyll (CHEMTAX) and in terms of carbon (microscopy) include intrinsic discrepancies due to the variability in the carbon to chlorophyll *a* ratio, which varies with species, light, and nutrients (Falkowski and Raven 1997).

The relationship between dinoflagellate carbon biomass estimated using microscopic counts and dinoflagellate Chl *a* estimated by CHEMTAX was not significant. It is likely that some dinoflagellates do not contain peridinin but other accessory pigments, such as fucoxanthin or its derivatives, and would thus have been included in the Fuco-flagellate group by CHEMTAX. In addition, nonphotosynthetic heterotrophic dinoflagellates were also included in the microscopic counts (Lovejoy et al. 2002*a*), and these would not have contained diagnostic pigments. For the other phytoplankton groups, the relationship between group-specific Chl *a* estimated by CHEMTAX and the carbon biomass estimated by microscopic counts associated to the same group were all significant ($p < 0.01$; data not shown).

Accessory pigment concentrations and CHEMTAX results indicate that the phytoplankton bloom in the NOW Polynya was diatom dominated. This result is consistent with the microscopic data (Booth et al. 2002; Lovejoy et al. 2002*a*). In the NOW Polynya, centric diatoms (especially *Thalassiosira* spp.) dominate the phytoplankton community with a succession: from centric diatoms (*Thalassiosira* spp.) in May and June to *Chaetoceros* spp. in July (Booth et al. 2002; Lovejoy et al. 2002*a*). The dominance of diatoms is consistent with high primary and new production as well as with the dominance of the chlorophyll biomass in large-sized cells, as observed in the NOW Polynya (Klein et al. 2002; Tremblay et al. 2002*b*). The peak in abundance of diatoms and autotrophic flagellates occurred at the same time in the NOW Polynya, as indicated by the maximum concentrations of accessory pigments during May along the Greenland coast. Contrary to the notion that flagellate blooms precede or follow diatom blooms (e.g., as in the North Atlantic; Barlow et al. 1993), there was no obvious succession of different groups during this study. However, the initiation of the bloom of autotrophic flagellates (e.g., green algae) seemed to precede the diatom bloom when comparing the dynamics of fucoxanthin (diatoms) and Chl *b* (green flagellates). The bloom of green algae apparently spread to the west and to the north in May, earlier than that of the diatoms. Diatoms eventually dominated the bloom, however, consistent with an intrinsic capacity for diatoms to grow faster than smaller flagellates during favorable conditions (Agawin et al. 2000). Ciliate grazing pressure, which may be coupled to the phytoplankton development, could also be significant in controlling the biomass of small cells such as autotrophic flagellates (Lovejoy et al. 2002*b*).

The phytoplankton bloom progressively exhausted nutrients and the surface waters became nutrient limited at some stations in May and June (Tremblay et al. 2002*a*, 2002*b*). In the present study, at the stations where nitrate was exhausted (i.e., <0.05 μmol·L^{-1}), silicate remained in excess. Thus, even if the phytoplankton were primarily diatoms, nitrate rather than silicate was the principal limiting nutrient in the NOW Polynya during spring 1998. Spatial autocorrelation between different variables in June indicates a spatial structure in the NOW Polynya, which can be interpreted as the causal relationship between the environmental variables and the phytoplankton groups' development. For example, the diatom development exhausted nitrates in June, underlying the complementary spatial structure of diatoms (e.g., fucoxanthin) and nitrates concentrations. The phytoplankton community structure was also influenced by the water mass characteristics and by the surface circulation. The contribution of diatoms increased along with increasing temperature and increased proportion of Baffin Bay waters characterized by low Z_{eu}. In contrast, autotrophic flagellates dominated in colder waters of Arctic origin where the mixed layer was deeper. The dominance of autotrophic flagellates, notably prymnesiophytes 2, in waters of Arctic origin, especially during April in the northern part of the polynya, is confirmed by microscopic counts during the same study, which report a dominance by *Phaeocystis* and other flagellates (Lovejoy et al. 2002*a*). As pointed out by Lovejoy et al. (2002*a*), this phytoplankton community is similar to a typical Arctic community. The relative dominance of diatoms versus autotrophic flagellates supports their need for more favorable irradiances, obtained when the mixed layer was relatively shallow. For example, blooms of *Phaeocystis* in Antarctic waters were observed in less stratified, deeply mixed waters, while blooms of diatoms occurred in well-stratified waters (e.g., Arrigo et al. 1998; Goffart et al. 2000). This has been attributed to greater photoadaptative and photophysiological properties of *Phaeocystis* at low ir-

© 2004 NRC Canada

radiances compared with diatoms (Palmisano et al. 1986; Arrigo et al. 1999; Moisan and Mitchell 1999). However, Stuart et al. (2000) found increased photoadaptation at relatively high light intensity for a population dominated by *Phaeocystis* near Greenland. In contrast, the diatom population they found near Labrador showed lower photoadaptation characteristics than the *Phaeocystis*-dominated population. These results differ from those found in the present work, as the diatom-dominated community near Greenland was apparently acclimated to high light levels, and the flagellate-dominate community near the Canadian coast was acclimated to low light levels. Even if the influence of ice cover on the control of the phytoplankton bloom initiation was not demonstrated during this study, it is clear that in Polar waters higher irradiance conditions are favored by the decrease in ice cover (Mei et al. 2002). Nonetheless, during this study it seems that a shallow mixed-layer depth was the essential factor that allowed optimal irradiance conditions for the initiation of the diatom bloom. The overall duration of the diatom bloom was likely determined by the nutrient supply rates (Lovejoy et al. 2002*c*; Tremblay et al. 2002*a*).

The greatest diatom contribution in this study was in the late-bloom period (June). Flagellates, mainly dinoflagellates, replaced diatoms only in July (Lovejoy et al. 2002*a*). Unfortunately, there were no pigment data from July because of space limitation on board the ship. The southernmost stations of the NOW Polynya, which were sampled only in June, showed some peculiarities. Microscopic counts showed that this region differed radically from the polynya proper and that the majority of the algal biomass was composed of dinoflagellates, the only diatom being *Melosira arctica*, a bottom sea-ice diatom (Lovejoy et al. 2002*a*).

In summary, the results of this study show that water mass characteristics and surface circulation influenced the phytoplankton distribution and the community structure as well as the timing and development of the phytoplankton bloom in the NOW Polynya. A diatom-dominated phytoplankton bloom developed where sensible heat favored the shallowing of the mixed layer. Diatoms rather than flagellates were favored by these conditions, and this can explain the high productivity of the NOW Polynya and its significance for the higher trophic levels in the Canadian Arctic. It would be expected that interannual and long-term changes in physical factors that influence mixing-layer depth, circulation, and water mass contributions in the polynya will also affect the phytoplankton community structure and perhaps the magnitude and significance of the phytoplankton bloom in the polynya.

Acknowledgements

This work was funded by the Natural Sciences and Engineering Research Council of Canada (NSERC Research Network grant to L. Fortier et al. and individual grant to SR) and is a contribution to the NOW Research Network (International North Water Polynya Study). We thank the captains and crews of the CCGS *Pierre Esprit Radisson* (Canadian Coast Guard) and L. Fortier and M. Gosselin, chief scientists of the 1998 NOW cruise from April to June. We thank B. Klein for the chlorophyll fluorimetric data, Y. Gratton for mixed-layer depth calculations, G. Ouellet for pigment standards, and M. Troussellier for help in statistic tests. FV was supported by a post-doctoral fellowship of "Ministère de l'Éducation du Québec, Relations internationales" and CL by NSERC postgraduate fellowships. Support was provided by GDR 2476 (BM and FV) and CNRS under a "chercheur associé" grant (FV).

References

Agawin, N.S.R., Duarte, C.M., and Agusti, S. 2000. Nutrient and temperature control of the contribution of picoplanckton to phytoplankton biomass and production. Limnol. Oceanogr. **45**: 591–600.

Andersen, R.A., Sauders, G.W., Paskind, M.P., and Sexton, J.P. 1993. Ultrastructure and 18S rRNA gene sequence for *Pelagomonas calceolata* nov. gen. et spec. nov., and the description of a new algal class, the Pelagophyceae classis nov. J. Phycol. **29**: 701–715.

Arrigo, K.R., Weiss, A.M., and Smith, W.O., Jr. 1998. Physical forcing of phytoplankton dynamics in the southwestern Ross Sea. J. Geophys. Res. [Oceans]. **103**: 1007–1021.

Arrigo, K.R., Robinson, D.H., Worthen, D.L., Dunbar, R.B., DiTullio, G.R., VanWoert, M., and Lizotte, M.P. 1999. Phytoplankton community structure and the drawdown of nutrients and CO^2 in the Southern Ocean. Science (Washington, D.C.), **283**: 365–367.

Bâcle, J., Carmack, E.C., and Ingram, R.G. 2002. Water column structure and circulation under the North Water Polynya during spring transition: April–July 1998. Deep-Sea Res. Part II, **49**: 4907–4925.

Barlow, R.G., Mantoura, R.F.C., Gough, M.A., and Fileman, T.W. 1993. Pigment signatures of the phytoplankton composition in northeastern Atlantic during the 1990 spring bloom. Deep-Sea Res. **40**: 2229–2242.

Bélanger, S. 2001. Analyse spatio-temporelle des patrons de chlorophylle dans la Polynye NOW par teledetection du capteur SeaWIFS. M.Sc. thesis, University of Sherbrooke, Que.

Bjørnland, T., and Liaaen-Jensen, S. 1989. Distribution pattern of carotenoids in relation to chromophyte phylogeny and systematics. *In* The chromophyte algae: problems and perspectives. *Edited by* G.C. Green, B.S.C. Leaderbeater, and W.L. Diver. Clarendon, Oxford. pp. 37–60.

Booth, B., and Marchant, H.J. 1987. Parmales, a new order of marine crysophytes, with description of three new genera and seven new species. J. Phycol. **23**: 245–260.

Booth, B.C., Larouche, P., Bélanger, S., Klein, B., Amiel, D., and Mei, Z.-P. 2002. Dynamics of *Chetoceros socialis* blooms in the North Water. Deep-Sea Res. Part II, **49**: 5003–5025.

Falkowski, P.G., and Raven, J.A. 1997. Aquatic photosynthesis. Blackwell Science Ltd., Oxford, UK.

Gieskes, W.W.C., and Kraay, G.W. 1983. Dominance of Cryptophyceae during the phytoplankton spring bloom in the central North Sea detected by HPLC analysis of pigments. Mar. Biol. **75**: 179–185.

Goericke, R., and Montoya, J.P. 1998. Estimating the contribution of microalgal taxa to chlorophyll *a* in the field-variations of pigment ratios under nutrient and light-limited growth. Mar. Ecol. Progr. Ser. **169**: 97–112.

Goffart, A., Catalano, G., Hecq, J.H. 2000. Factors controlling the distribution of diatoms and *Phaeocystis* in the Ross Sea. J. Mar. Syst. **27**: 161–175.

Guillou, L., Moon-van der Staay, S.-Y., Claustre, H., Partensky, F., and Vaulot, D. 1999. Diversity and abundance of Bolidophyceae (Heterokonta) in two oceanic regions. Appl. Environ. Microbiol. **65**: 4528–4536.

Head, E.J.H., Bedo, A., and Harris L.R. 1988. Grazing, defecation and excretion rates of copepods from inter-island channels of Canadian Arctic Archipelago. Mar. Biol. **99**: 333–340.

© 2004 NRC Canada

Hooks, C.E., Bidigare, R.R., Keller, M.D., and Guillard, R.R.L. 1988. Coccoid eukaryotic marine ultraplankters with four different HPLC pigment signatures. J. Phycol. **24**: 571–580.

Jeffrey, S.W. 1976. A report of green algal pigments in the central North Pacific Ocean. Mar. Biol. **37**: 33–37.

Jeffrey, S.W., and Vesk, M. 1997. Introduction to marine phytoplankton and their pigment signatures. *In* Phytoplankton pigments in oceanography. *Edited by* S.W. Jeffrey, R.F.C. Mantoura, and S.W. Wright. United Nations Educational, Scientific and Cultural Organization, Paris. pp. 407–428.

Jeffrey, S.W., and Wright, S.W. 1994. Photosynthetic pigments in the Prymnesiophyceae. *In* The Haptophyte algae. *Edited by* J.C. Green and B.S.C. Leadbeater. Clarendon Press, Oxford. pp. 111–132.

Jeffrey, S.W., Sielicki, M., and Haxo, F.T. 1975. Chloroplast pigment patterns in dinoflagellates. J. Phycol. **11**: 374–385.

Johansen, J.E., Svec, W.A., Liaaen-Jensen, S., and Haxo, F.T. 1974. Carotenoids of the Dinophyceae. Phytochemistry, **13**: 2261–2271.

Klein, B., LeBlanc, B., Mei, Z.-P., Beret, R., Michaud, J., Mundy, C.-J., von Quillfeldt, C.H., Garneau, M.-E., Roy, S., Gratton, Y., Cochran, J.K., Bélanger, S., Larouche, P., Pakulski, J.D., Rivkin, R.B., and Legendre, L. 2002. Phytoplankton biomass, production and potential export in the North Water. Deep-Sea Res. Part II, **49**: 4983–5002.

Legendre, L., and Rassoulzadegan, F. 1995. Plankton and nutrient dynamics in coastal waters. Ophelia, **41**: 153–172.

Legendre, P., and Legendre, L. 1998. Numerical ecology. 2nd ed. Elsevier Science BV, Amsterdam.

Lewis, E.L., Ponton, D., Legendre, L., and LeBlanc, B. 1996. Springtime sensible heat, nutrients and phytoplankton in the Northwater Polynya, Canadian Arctic. Cont. Shelf Res. **16**(14): 1775–1792.

Longhurst, A., and Head, E. 1989. Algal production and variable herbivore demand in Jones Sound, Canadian High Arctic. Polar Biol. **9**: 281–286.

Lovejoy, C., Legendre, L., Martineau, M.-J., Bâcle, J., and von Quillfeldt, C.H. 2002*a*. Distribution of phytoplankton and other protists in the North Water. Deep-Sea Res. Part II, **49**: 5027–5047.

Lovejoy, C., Carmack, E.C., Legendre, L., and Price, N.M. 2002*b*. Water column interleaving: a new physical mechanism determinig protist communities and bacterial states. Limnol. Oceanogr. **47**: 1819–1831.

Lovejoy, C., Price, N.M., and Legendre, L. 2002*c*. Prolonged diatom blooms and microbial food web dynamics: experimental results from Arctic Polynya. Aquat. Microb. Ecol. **39**: 267–278.

Mackey, M.D., Mackey, D.J., Higgins, H.W., and Wright, S.W. 1996. CHEMTAX — a program for estimating class abundances from chemical markers: application to HPLC measurements of phytoplankton. Mar. Ecol. Progr. Ser. **144**: 265–283.

Mei, Z.-P., Legendre, L., Gratton, Y., Tremblay, J.-E., LeBlanc, B., Mundy, C.-J., Klein, B., Gosselin, M., Larouche, P., Papakyriakou, T.N., Lovejoy, C., and von Quillfeldt, C.H. 2002. Physical control of spring–summer phytoplankton dynamics in the North Water, April–July 1998. Deep-Sea Res. Part II, **49**: 4959–4982.

Melling, H., Gratton, Y., and Ingram, R.G. 2001. Oceanic circulation within the North Water Polynya in Baffin Bay. Atmos.-Ocean, **39**: 301–325.

Michaels, A.F., and Silver, M.W. 1988. Primary production, sinking fluxes and the microbial food web. Deep-Sea Res. Part A, **35**: 473–490.

Moisan, T.A., and Mitchell, B.G. 1999. Photophysiological acclimation of *Phaeocystis antarctica* Karsten under light limitation. Limnol. Oceanogr. **44**: 247–258.

Montajir, B., Gosselin, M., Gratton, Y., Booth, B., Vasseur, C., Garneau, M.-E., Fouilland, E., Vidussi, F., and Demers S. 2001. Surface water distribution of pico- and nanophytoplankton in relation to two distinctive water masses in the North Water, northern Baffin Bay, during fall. Aquat. Microb. Ecol. **23**: 205–212.

Palmisano, A.C., SooHoo, J.B., SooHoo, S.L., Kottmeier, S.T., Craft, L.L., and Sullivan, C.W. 1986. Photoadaptation in *Phaeocystis pouchetii* advected underneath annual sea ice in McMurdo Sound, Antartica. J. Plankton Res. **8**: 891–906.

Repeta, D.J., and Bjornland, T. 1997. Preparation of carotenoid standards. *In* Phytoplankton pigments in oceanography. *Edited by* S.W. Jeffrey, R.F.C. Mantoura, and S.W. Wright. United Nations Educational, Scientific and Cultural Organization, Paris. pp. 239–260.

Ricketts, T.R. 1970. The pigments of the Prasinophyceae and related organisms. Phytochemistry, **9**: 1835–1842.

Roy, S., Chanut, J.-P., Gosselin, M., and Sime-Ngando, T. 1996. Characterization of phytoplankton communities in the lower St. Lawrence Estuary using HPLC-detected pigments and cell microscopy. Mar. Ecol. Progr. Ser. **142**: 55–73.

Schlüter, L., Møhlenberg, F., Havskum, H., and Larsen, S. 2000. The use of phytoplankton pigments for identifying and quantifying phytoplankton groups in coastal areas: testing the influence of light and nutrients on pigment/chlorophyll *a* ratios. Mar. Ecol. Progr. Ser. **192**: 49–63.

Simon, N., Barlow, R.G., Marie, D., Partensky, F., and Vaulot, D. 1994. Characterization of oceanic photosynthetic picoeukaryotes by flow cytometry. J. Phycol. **30**: 922–935.

Smith, W.O., and Sakshaug, E. 1990. Polar phytoplankton. *In* Polar oceanography, part B: chemistry, biology and geology. *Edited by* W.O. Smith. Academic Press Inc., New York.

Stirling, I. 1981. Polynyas in the Canadian Arctic. Canadian Wildlife Service, Ottawa, Ont. Occas. Pap. No. 45.

Stuart, V., Sathyendranath, S., Head, E.J.H., Platt, T., Irwin, B., Maass, H. 2000. Bio-optical characteristics of diatom and prymnesiophyte populations in the Labrador Sea. Mar. Ecol. Progr. Ser. **201**: 91–106.

Tremblay, J.-E., Gratton, Y., Fauchot, J., and Price, N.M. 2002*a*. Climatic and oceanic forcing of new, net and diatom production in the North Water. Deep-Sea Res. Part II, **49**: 4927–4946.

Tremblay, J.-E., Gratton, Y., Carmack, E.C., Payne, C.D., and Price, N.M. 2002*b*. Impact of the large-scale Arctic circulation and the North Water Polynya on nutrient inventories in Baffin Bay. J. Geophys. Res. **107**: C8.

Vaulot, D., Birrien, J., Marie, D., Casotti, R., Veldhuis, M.J.W., Kraay, G.W., and Chretiennot-Dinet, M.-J. 1994. Morphology, ploidy, pigment composition, and genome size of cultured strains *Phaeocystis* (Prymnesiophyceae). J. Phycol. **30**: 1022–1035.

Wright, S.W., and Jeffrey, S.W. 1987. Fucoxanthin pigment markers of marine phytoplankton analysed by HPLC and HPTLC. Mar. Ecol. Prog. Ser. **38**: 259–266.

Wright, S.W., Jeffrey, S.W., Mantoura, R.F.C., Llewellyn, C.A., Bjornland, T., Repeta, D., and Welschmeyer, N.A. 1991. Improved HPLC method for the analysis of chlorophylls and carotenoids from marine phytoplankton. Mar. Ecol. Prog. Ser. **77**: 183–196.

Wright, S.W., Thomas, D.P., Marchant, H.J., Higgins, H.W., Mackey, M.D., and Mackey, D.J. 1996. Analysis of phytoplankton of the Australian sector of the Southern ocean: comparisons of microscopy and size frequency data with interpretations of pigment HPLC data using the "CHEMTAX" matrix factorization program. Mar. Ecol. Prog. Ser. **144**: 285–298.

© 2004 NRC Canada

Fishing and the impact of marine reserves in a variable environment

Lynda D. Rodwell and Callum M. Roberts

Abstract: We use discrete-time models to investigate the impact of marine reserve establishment on fishery catch and biomass levels in open-access and quota-regulated fisheries under conditions of recruitment variability and natural mortality events. We find that under the conditions of variability tested, reserves can increase the probability of achieving target levels of biomass (60%, 35%, and 5% of carrying capacity) and can reduce catch variability in neighbouring fisheries, making future planning in the fishery more efficient. The size of the reserve required to meet each objective will depend on the initial condition of the stock and the exploitation rate in the fishery. Reserve coverage of between 20% and 40% prevent stock collapse in most cases. In heavily exploited fisheries, reserves are also likely to enhance mean catches, particularly in highly variable systems. If the stock has previously been heavily exploited, large reserves (≥60%) may be required to significantly increase the probability of achieving target biomass levels. However, once stocks have recovered, reserve coverage may be reduced without a reduction in this probability of success.

Résumé : Nous utilisons dans notre étude un modèle en temps discret pour étudier l'impact de l'établissement de réserves marines sur les captures de pêche et les niveaux de biomasse dans les pêches commerciales à accès libre et avec quota réglementé sous diverses conditions de variabilité du recrutement et d'événements de mortalité naturelle. Dans les conditions de variabilité testées, la présence de réserves peut permettre d'atteindre les valeurs de biomasse ciblées (60 %, 35 % et 5 % du stock limite) et elle peut réduire la variabilité des captures dans les pêches des régions avoisinantes, ce qui rend la planification de la pêche plus efficace. La taille de la réserve nécessaire pour atteindre chaque objectif dépend de la condition initiale du stock et du taux d'exploitation de la pêche. Dans la plupart des cas, une réserve qui représente entre 20 % et 40 % de la surface peut empêcher l'effondrement des stocks. Dans les pêches fortement exploitées, les réserves vont aussi vraisemblablement faire augmenter les captures moyennes, particulièrement dans les systèmes très variables. Si le stock a déjà été fortement exploité, il peut être nécessaire d'établir de grandes réserves (≥60 %) pour augmenter significativement la probabilité d'atteindre les niveaux de biomasses souhaités. Cependant, un fois les stocks rétablis, on peut réduire la surface de la réserve sans diminuer la probabilité de succès.

[Traduit par la Rédaction]

Introduction

The marine environment is highly variable. Some events are unpredictable, such as red tides, disease outbreaks, and seawater warming (Mann and Lazier 1996). Other events, often termed regime shifts, may be variable from year to year but follow some long-cycle underlying pattern (Steele 1998). These sources of variability and uncertainty pose serious problems for fisheries management (Mangel 2000*b*).

Managers make fish stock assessments at intervals and base recommendations for future catch limits. Changing environmental conditions that affect stock growth rates can render those predictions inaccurate, leading to over- or under-fishing, both of which carry economic costs. Adding to problems, capital invested during productive periods may not be easy to redeploy elsewhere as production levels fall. For example, year-to-year variation in the strength of upwelling in Peru drives the productivity of anchovy stocks. During strong El Niño conditions, upwelling virtually shuts down, greatly reducing productivity and concentrating remaining anchovy schools close to the coast (Longhurst and Pauly 1987). Stock assessments in the 1970s and 1980s failed to take upwelling strength into account. Continued high levels of fishing at a time of intense El Niño in the early 1970s drove the stock to collapse (Longhurst and Pauly 1987).

Regime shifts from cool to warm conditions in the North Pacific (Francis et al. 1998) and Atlantic Oceans (Alheit and Hagen 1997) drive underlying changes in productivity of fish stocks over decadal time scales. Stocks fluctuate from year-to-year against this background. While greater understanding of regime shifts can improve predictions of production levels, scientific sampling cannot remove or reduce

Received 29 May 2003. Accepted 17 May 2004. Published on the NRC Research Press Web site at http://cjfas.nrc.ca on 15 January 2005.
J17556

L.D. Rodwell.[1] Marine and Coastal Policy Research Group, University of Plymouth, Drake Circus, Plymouth, Devon, PL4 8AA, UK.
C.M. Roberts. Environment Department, University of York, Heslington, York YO10 5DD, UK.

[1]Corresponding author (e-mail: Lynda.Rodwell@plymouth.ac.uk).

 doi: 10.1139/F04-142 © 2004 NRC Canada

stochastic variation. Consequently, fisheries management must operate with what have been termed "irreducible uncertainties" (Cohen 1966, 1967), making management error prone and risky. Marine reserves (i.e., areas that are permanently off limits to fishing) have been proposed as tools that can reduce the impact of uncertainty in fisheries management (Clark 1996; Lauck et al. 1998; Mangel 2000*a*). By protecting some fraction of fish stocks, it is argued that they increase the ability of managers to maintain target stock levels in the face of fluctuating productivity and to deliver less variable catches to the fishing industry. Using models, we explore these predictions for fisheries operating across a range of environmental variability and for different levels of management control.

There have been few attempts to model the effects of marine reserves that consider stochastic and variable events. Lauck et al. (1998) directly addressed the question of uncertainty and sustainability in fisheries management, focusing on irreducible scientific uncertainty. They used a simple model to explore the probability of maintaining a target population level under various scenarios of reserve size, levels of protection, and catch rates. They found that the chances of successfully maintaining 60% of the carrying capacity (an "Optimal Sustainable Population") over a 40-year time horizon fell dramatically when the total area available for exploitation exceeded 30%. An alternative to the reserve scenario would be to reduce catch rates to 10% of the stock level. They found that reserve protection can simultaneously achieve stock protection and a higher level of catch by intensifying fishing in the smaller fishing ground, but only at high levels of protection. They recommended marine reserves as a hedge against the prevailing uncertainties of biological, management, and economic systems.

Sumaila (1998) used a dynamic bioeconomic model to determine the optimal size of a marine reserve for the Barents Sea cod fishery with respect to economic rent, catches, and standing stock. Variability focused on recruitment failure events. That author found that reserves will only be bioeconomically beneficial when both transfer rates between protected and unprotected regions are high and the reserves are large. However, reserves increased biomass under all circumstances. The findings fully supported those of Lauck et al. (1998), who found that reserves hedge against biological losses. However, no consideration of the influence of reserve size on transfer rate was made. Furthermore, the model was developed in a way to suggest that the productivity of the stock increased with the size of the reserve. This may explain why it concluded that large reserves are necessary.

Mangel (2000*a*) developed stochastic methods to determine how much habitat needs to be set aside as reserve, once reserve objectives are decided. In this model, stochastic calculations are based on the harvest fraction being a random variable. "Persistence" of the stock is characterized by the probability that the stock stays above a critical level (35% or 60% of carrying capacity). Mangel found that reserves provided a buffer that increased the chances of sustainability of the stock and may not necessarily reduce harvest. He concluded that the fraction of management area that should be allocated to reserves will depend on biological, economic, and social conditions. In a second paper, Mangel (2000*b*) developed a model for a marine reserve for an open population subject to environmental uncertainty where natural mortality was a correlated random process, fishing mortality fluctuated, and recruitment was episodic. Catch was calculated as a fraction of the fish that disappeared each year (the rest attributed to natural mortality). Recruitment was episodic. The probability of maintaining the population at a level at or above 35% of carrying capacity was calculated. Probabilities were also calculated as a function of the fraction of habitat protected. Smaller reserves led to larger but more variable catches (i.e., there was a mean–variance trade-off). In this study, Mangel predicted that implementing a reserve will not increase catch but will decrease variability in catch and so help avoid boom and bust fishery cycles (e.g., Clark 1990).

In his stochastic model, Conrad (1999) introduced a linear total allowable catch function and presumed that fishery managers can measure biomass and can enforce the total allowable catch regulation. He introduced a random variable that influenced the growth of the fish stock. He found that through the movement process, biomass variability can be lower with a reserve of 40%–60% of the original grounds compared with the no-reserve case.

Each of these studies has addressed the variability of the marine environment and exploitation of marine resources in different ways. In this paper, we use discrete-time models to investigate the impact of marine reserve establishment in two contrasting fishery regimes: an otherwise open-access fishery and a regulated fishery (regulated by total allowable catch (TAC) quotas). Impacts of reserve establishment on fishery catch and biomass levels under conditions of both recruitment variability and natural mortality events are explored. Our aim is to assess the potential contribution of marine reserves to managing fisheries in variable environments. We will address the questions can marine reserves (*i*) increase probability of maintaining target biomass levels in the fishery, (*ii*) enhance mean catches over a given time period, and (*iii*) reduce the variability of catches in the fishery? For each question, we compare results of the open-access regime with the quota regime. We examine these questions in the context of both a previously unexploited fish stock (initially at carrying capacity) and a heavily exploited stock (initially one fifth of carrying capacity) facing varying levels of recruitment and natural mortality variability.

We compare the results of a highly variable system with those of a system where natural mortality and recruitment are deterministic. The highly variable system experiences stochastic recruitment with underlying regime shifts and stochastic natural mortality, with pulses representing catastrophic events such as disease or red tides. We examine the role of reserves in achieving stated management objectives, such as increasing the probability of total biomass remaining above target levels 60%, 35%, and 5% of carrying capacity for at least 25%, 50%, and 100% of the time, respectively, enhancing mean catches and reducing the variability of catches. We also consider how large an area should be protected to achieve these objectives. We do not consider explicit random exploitation functions but rather that exploitation is variable because of variability in the stock level and, in the open-access case, because of changing fishing effort. Results for

© 2004 NRC Canada

both the open-access and quota-regulated fishery regimes are compared and contrasted.

Methods

The general models

We chose to examine the role of marine reserves in both the open-access fishery regime and the quota-regulated fishery to compare the outcome of variable effort and fixed effort regimes. These two regimes may approximate to a fishery with relative ease of entry and exit such as a low cost fishery and a commercial fishery regulated by strict quotas, respectively.

An open-access fishery

The conditions for open access are met when rents in the fishery are dissipated (i.e., profits are reduced to zero)

$$\pi_t = pH_t - cE_t = 0$$

where p is a unit price, H_t is the catch, c is a unit cost of fishing effort, E_t is fishing effort, and π_t is profit in time period t. E_t responds to profit levels in a previous time period. The change in effort is expressed as a function of profits in time period t and an effort adjustment parameter, ϕ, which reflects the ease of exit or entry to the industry (eq. 2).

Complete open access

The system of open access in the whole fishery is described by the two dynamic equations:

$$X_{t+1} - X_t = -nX_t + R_t - H_t \quad (1)$$

$$E_{t+1} - E_t = \phi(pH_t - cE_t) \quad (2)$$

where the growth of the stock is described by a spawner–recruit relationship. R_t is the recruitment (a function of biomass X_t) and n is natural mortality expressed as a proportion of total biomass (X_t). Equation 1 describes a biomass-dynamic relationship in which a change in X accounts for a change in both the number and size of individual fish.

Equilibrium is reached when $X_{t+1} - X_t = 0$ and $E_{t+1} - E_t = 0$. Using a Gordon–Schaefer catch function, $H_t = qE_tX_t$, where q is the catchability coefficient, the equilibrium biomass is $X^* = c/qp$.

Marine reserve and open access (in remaining fishing grounds)

The stock now is composed of two distinct substocks, X_1 and X_2, which occupy the reserve (proportion of management area, α) and the fishing grounds (proportion of management area, $1 - \alpha$), respectively. Though for modelling simplicity we specify two areas (i.e., a marine reserve and a fishing ground), the "reserve" corresponds to coverage of the management area with areas that are permanently off limits to fishing. That is, it represents a network of reserves covering a proportion of a management area rather than just one marine reserve. As the reserve is fully protected from fishing, there is only catch from the fishing grounds (H_2). The dynamics between the reserve and the fishing grounds are described by the transfer of recruits due to larval dispersal (T) and the movement of fish (M). T and M can be positive or negative depending on the relative biomasses inside and outside of the reserve and so represent movement in or out of the reserve.

The system with a reserve and a fishing ground is expressed by three dynamic equations:

$$X_{1,t+1} - X_{1,t} = -n_1X_{1,t} + R_{1,t} - M_t - T_t \quad (3)$$

$$X_{2,t+1} - X_{2,t} = -n_2X_{2,t} + R_{2,t} - H_{2,t} + M_t + T_t \quad (4)$$

$$E_{2,t+1} - E_{2,t} = \phi(pH_{2,t} - cE_{2,t}) \quad (5)$$

where the recruitment functions $R_{1,t}$ and $R_{2,t}$ are based on the Beverton–Holt recruitment function (Beverton and Holt 1957).

Equilibrium is reached when $X_{1,t+1} - X_{1,t} = 0$, $X_{2,t+1} - X_{2,t} = 0$, and $E_{2,t+1} - E_{2,t} = 0$. The Gordon–Schaefer function in this case is $H_{2,t} = qE_{2,t}X_{2,t}$, and so equilibrium biomass is $X_2^* = c/qp$. Therefore, the equilibrium level of biomass in the fishing ground (not total biomass) will be the same with or without reserve if costs, prices, and catchability are unchanged. n_1 and n_2 represent natural mortality in the reserve and fishing ground, respectively. These may reflect differences in stock composition or habitat quality in the two areas (Rodwell et al. 2003).

A quota-regulated fishery

In this case, we consider a fishery that has an imposed TAC quota policy. The quota is set as a fixed proportion of available fish biomass (i.e., a fixed exploitation rate) in the fishing ground (similar to the linear production function of Conrad (1999) and equivalent to the model used in Rodwell et al. (2002, 2003)).

Quota-regulated fishery without a reserve

This model can simply be expressed in terms of the catch function, which, if a linear catch quota, can be written as

$$H = uX_t \quad (6)$$

where u represents a fixed exploitation rate or the total allowable proportion of biomass to be extracted subject to stock dynamics in eq. 1, ($X_{t+1} - X_t = -nX_t + R_t - H_t$).

Quota-regulated fishery with a reserve

In this case, the model is simply expressed using the catch function

$$H_{2,t} = uX_{2,t} \quad (7)$$

subject to stock dynamics in eqs. 3 and 4 ($X_{1,t+1} - X_{1,t} = -n_1X_{1,t} + R_{1,t} - M_t - T_t$ and $X_{2,t+1} - X_{2,t} = -n_2X_{2,t} - H_{2,t} + R_{2,t} + M_t + T_t$, respectively).

Functional forms

Using the two formulations of the model, we can examine the impact of reserve establishment on biomass and catch levels and variability over a given time horizon. However, we must first specify the functional forms for movement of adult and juvenile fish (M) and transfer of recruits (T). The movement functions are the same as those used by Rodwell et al. (2002, 2003).

Fish movement, M_t

The movement of fish between the reserve and the fishing ground is a function of the biomasses in the two areas.

© 2004 NRC Canada

(8) $$M_t = \sigma[(1-\alpha)X_1 - \alpha X_2]$$

where σ is the mobility coefficient of fish and $0 \le \sigma \le 1$. If $\sigma = 0$, fish are assumed to be sedentary; if $\sigma = 1$, fish are highly mobile. Equation 8 is equivalent to

$$M_t = \sigma A\alpha(1-\alpha)[X_1/A\alpha - X_2/A(1-\alpha)]$$

where A represents the management area, and α represents reserve coverage (the proportion of management area protected) (see Rodwell et al. 2002 for full explanation). Note that if $X_1/A\alpha > X_2/A(1-\alpha)$, then M is positive and fish move out of the reserve. If $X_1/A\alpha < X_2/A(1-\alpha)$, then M is negative and fish move into the reserve.

Recruit transfer, T_t

Larval movement patterns are taken as a function of the larval retention factor, θ. The recruit transfer function is given by

(9) $$T_t = (1-\theta)[(1-\alpha)R_{1,t} - \alpha R_{2,t}] \quad \text{for } 0 \le \theta \le 1$$

where θ is the proportion of larvae retained. If $\theta = 0$, then there is no larval retention and the larvae disperse uniformly. If $\theta = 1$, then full retention of larvae occurs. This results in no transfer of recruits between the reserve and the fishing ground.

The recruitment functions R_t, $R_{1,t}$, and $R_{2,t}$ are based on the Beverton–Holt recruitment function (Beverton and Holt 1957). However, they take different forms depending on the level of variability in the marine environment. These are described in detail in the Methods section.

Simulations

The models were set up with the two cases of recruitment and natural mortality variability described below. In each case, fish biomass and catch levels were considered for both the reserve and no-reserve cases.

Biomass analysis

In the biomass analysis, three biomass management objectives were stated, and the probability of achieving each of them were evaluated under the different fishery regimes and with reserve coverage ranging from 0% to 100%. The three objectives were (*i*) to maintain the stock at 60% of carrying capacity at least 25% of the time, (*ii*) to maintain the stock at 35% of carrying capacity at least 50% of the time, and (*iii*) to maintain the stock at 5% of carrying capacity 100% of the time.

These levels were chosen based on the recommendations that stocks should be kept at (*i*) 60% of carrying capacity — an economically optimal level of biomass (Lauck et al. 1998), (*ii*) 35% of carrying capacity — a level of biomass sufficient to prevent recruitment overfishing (in most cases) (Mangel 2000*b*), and (*iii*) 5% of carrying capacity, representing likely stock collapse.

The percentage of time for which the target level is to be achieved is a little more arbitrary. In a highly variable system to achieve an economic optimum, 100% is unlikely, whereas 25% of the time may be realistic and achievable. Maintaining the stock at 35% of carrying capacity at least 50% of the time also seems realistic. 5% carrying capacity 100% of the time is necessary to guarantee that the stock will not collapse.

The probability that the objective will be reached, in the variable system, is based on 200 runs of the model. In each run, the number of years the target biomass is reached is calculated and then the proportion of runs in which the objective is achieved forms the basis of the probability of success. In the deterministic system, there is just one run for which the target biomass objective is either achieved or not, so the probability is either 0 or 1.

Catch analysis

The catch objectives for management in this case were stated as (*i*) to increase mean catches over the management time horizon and (*ii*) to reduce catch variability over the management time horizon. Each scenario tested was evaluated on the criteria of meeting these objectives. Catch variability was measured in terms of standard deviation and also percentage variability (SD/mean catch × 100).

The findings of Rodwell et al. (2003) suggest that the impact of marine reserves on a fishery may be highly dependent on the condition of the stock at the time of reserve establishment. We therefore consider two contrasting initial stock conditions. The first is the case where the stock is initially at its carrying capacity and has high reproductive capacity, consistent with not having been previously exploited. The second illustrates the case when the stock is initially one fifth of its carrying capacity and low reproductive capacity consistent with previous heavy exploitation.

Cases of variability

We modelled the cases of a deterministic and a highly variable system to determine whether they would produce any significantly different outcomes in terms of the contributions of reserves to the fishery management objectives.

Deterministic system

For the case of deterministic and stable recruitment, the Beverton–Holt recruit production function for the reserve is

(10) $$R_{1,t} = \frac{\varepsilon_1 X_{1,t}}{\gamma_1 \varepsilon_1 X_{1,t} + \beta_1}$$

where $R_{1,t}$ is recruit production of the reserve fish stock in time period t, $X_{1,t}$ is reserve fish biomass in time period t, γ_1 and β_1 are recruitment parameter estimates for the reserve stock for a given initial growth rate, and ε_1 is the proportion of the reserve stock that is reproductively mature. ε_1 will vary with time since protection (i.e., $\varepsilon_1 = f(t)$). $\varepsilon_1 X_1$ is taken as a proxy for spawning stock biomass in the reserve.

For the fishing ground stock, the Beverton–Holt recruit production function is

(11) $$R_{2,t} = \frac{\varepsilon_2(X_{2,t} - \psi H_{2,t})}{\gamma_2 \varepsilon_2(X_{2,t} - \psi H_{2,t}) + \beta_2}$$

where ε_2 is the proportion of the fishing ground stock that is reproductively mature. This is a function of the exploitation rate in the fishing ground (i.e., $\varepsilon_2 = f(u)$ in the quota fishery, or $\varepsilon_2 = f(qE)$ in the open-access fishery). ψ is the proportion of exploitation taking place before recruitment (i.e., $0 \le \psi \le 1$). The only spawners are those remaining after a proportion of catch takes place (i.e., $\varepsilon_2(X_2 - \psi H_2)$) in each time period

© 2004 NRC Canada

where $0 \leq \psi \leq 1$. See Rodwell et al. (2002) for discussion. The equivalent recruit production function for the no-reserve case is

$$R_t = \frac{\varepsilon(X_t - \psi H_t)}{\gamma\varepsilon(X_t - \psi H_t) + \beta}$$

Natural mortality is assumed to be a constant proportion of biomass.

Stochastic system

Recruitment is stochastic with underlying regime shifts

If recruitment is stochastic against a background of regime shifts, the functions are given by eqs. 12 and 13

$$(12) \quad R_{1,t} = z_1 \exp(w_1)\left(\frac{\varepsilon_1 X_{1,t}}{\gamma_1 \varepsilon_1 X_{1,t} + \beta_1}\right)$$

$$(13) \quad R_{2,t} = z_2 \exp(w_2)\left[\frac{\varepsilon_2(X_{2,t} - \psi H_t)}{\gamma_2 \varepsilon_2(X_{2,t} - \psi H_t) + \beta_2}\right]$$

where w_i is a random normal variable and so the errors have a lognormal distribution (Hilborn and Walters 1992). We take $w = w_1 = w_2$ (i.e., the reserve and the fishing ground face the same stochastic events) so that the true effects of the reserve can be determined. However, in reality different w values could represent spatial heterogeneity between reserve and fishing ground, reflecting better or worse conditions for recruitment. z_i represents the regime shift following a sine motion

$$(14) \quad z_{i,t} = g_i + d_i \sin(tl_i)$$

where g_i is a constant, d_i is the depth of the phase, l_i is the length of the phase for area i where $i = 1, 2$ (reserve and fishing ground). Note that we take $z = z_1 = z_2$ for comparability between reserve and no-reserve results. The combination of the stochastic element ($\exp(w)$) and the underlying regime shift (z) is illustrated (Fig. 1*a*). This pattern of regime shifts illustrated is for $g_i = 1$, $d_i = 0.2$, and $l_i = 0.2$ and $-0.2 < w_i < 0.2$, with a mean of $w = 0$ (i.e., $\exp(w) = 1$). This is the underlying random process for all the simulations. The equivalent recruit production function for the no-reserve case is

$$R_t = z \exp(w) \frac{\varepsilon(X_t - \psi H_t)}{\gamma\varepsilon(X_t - \psi H_t) + \beta}$$

Natural mortality is stochastic with pulses

We also consider that natural mortality is likely to experience random fluctuations as well as sudden pulses brought about by disease or other natural events such as red tides, storms, and regional anoxia (i.e., a highly variable system). The general equation including a pulse is given by eq. 15, where n_0 is the base level of natural mortality, a random normal variable.

$$(15) \quad n = \exp(n_0 + [\text{pulse}(\text{year}, \text{duration})] \times \text{intensity}$$

The natural mortality pulses (represented in Fig. 1*b*) were set up as shown in eqs. 16 and 17.

Fig. 1. (*a*) Recruitment variability factor ($z \exp(w)$) indicating an underlying regime shift (broken line) and stochastic fluctuations following a lognormal distribution (solid line). (*b*) Natural mortality variability indicated by stochastic fluctuation about a base level of 0.2, with pulses representing catastrophic mortality events.

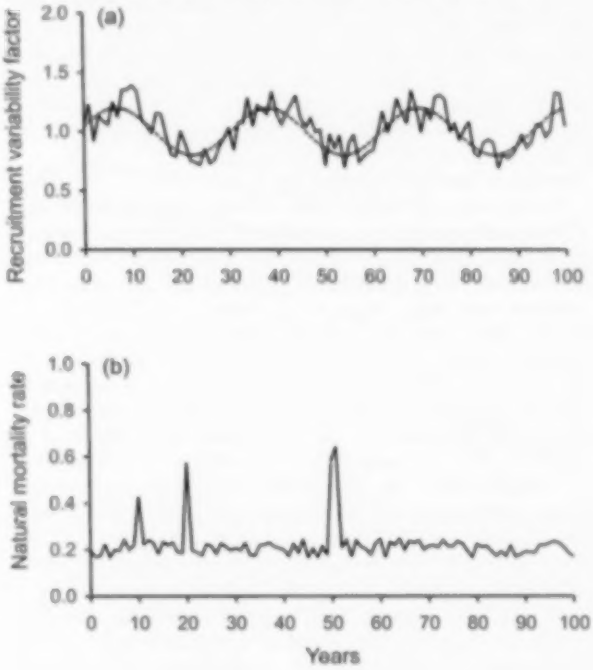

$$(16) \quad n = \exp(n_0) + [\text{pulse}(10,1)]0.3 + [\text{pulse}(20,1) + \text{pulse}(50,20)]0.5$$

$$(17) \quad n_0 = \text{random normal}(-1.8, -1.4, -1.6, s)$$

where n is the proportion of biomass dying naturally each year, and s is the noise seed that varies for each simulation run. –1.8, –1.4, and –1.6 are the minimum, maximum, and mean values used in the random normal distribution, respectively. They approximate to a natural mortality rate between 0.16 and 0.24 and a mean of 0.2. The function represents a base natural mortality of 0.2 (20% per annum), with sudden pulses in years 10, 20, and 50 for 1-, 1-, and 2-year periods, respectively, at intensities of 0.3, 0.5, and 0.5, increasing natural mortality to 0.5, 0.7, and 0.7, respectively (50%, 70%, and 70%). Note that $n = n_1 = n_2$ (i.e., all stocks whether protected or unprotected are assumed to be subject to same natural mortality pulses).

Life history and fishery model parameters

Two scenarios of initial stock condition were tested: one where the stock was previously unexploited and another where the stock was previously heavily exploited. This was done to determine whether different management strategies are appropriate in each case. The growth patterns of both the previously unexploited stock and the previously heavily exploited stocks for the two cases of variability under the scenario of zero exploitation are illustrated (Fig. 2). Note that

© 2004 NRC Canada

we do not specify units, since this is a simulation exercise to compare with and without reserve scenarios.

Previously unexploited stock

In this case, the initial total biomass level is set at X_1 = 2000 where carrying capacity of the stock is also 2000 (i.e., X_c = 2000). Hence $X_{1,0} = 2000\alpha$ and $X_{2,0} = 2000(1 - \alpha)$. In the open-access regime, π_0 = 1000 and ϕ = 0.01. Therefore $E_{2,0} = E_0 = 10$. The growth parameters used are n_1, n_2, n = 0.2 (deterministic only); β_1, β_2, β = 0.1; ε_1 = 0.7; ε_2, ε = 0.7 $\exp(-3u)$; γ = 0.00243; $\gamma_1 = 0.00243/\alpha$; $\gamma_2 = 0.00243/(1 - \alpha)$.

Previously heavily exploited stock

In this case, the initial total biomass level is set at X_1 = 400 in each scenario — one fifth of the carrying capacity X_c = 2000. Hence $X_{1,0} = 400\alpha$ and $X_{2,0} = 400(1 - \alpha)$. π_0 = 1000 and ϕ = 0.01. Therefore $E_{2,0} = E_0 = 10$. The growth parameters used are n_1, n_2, n = 0.2 (deterministic only); β_1, β_2, β = 0.3 (the choice of β influences the time taken to return to carrying capacity); $\varepsilon_1 = 0.20+0.05t$ (for t = 0 to 10) and 0.7 (for t = 11 to 100) (we assume the reproductive capacity of stock at carrying capacity is 0.7, and it takes 10 years of protection for the stock to reach this level; see Rodwell et al. 2003); ε_2, ε = 0.2 $\exp(-3u)$; γ = 0.00229; $\gamma_1 = 0.00229/\alpha$; $\gamma_2 = 0.00229/(1 - \alpha)$. Note from this that we assume that heavy exploitation affects recruitment rather than natural mortality, since exploitation reduces the average size of individual fish and so their fecundity. We also assume that the reproductive capacity of the stock continues to decline after heavy exploitation even if exploitation is reduced to a TAC of 10%, because even low levels of exploitation will result in the removal of the largest and most fecund fish, reducing overall reproductive capacity of the stock.

In both scenarios, the following parameters were used: σ = 0.2 (moderate fish movement); θ = 0.5 (50% larval retention); ψ = 1 (all exploitation before spawning); g_1, g_2, g = 1; d_1, d_2, d = 0.2; l_1, l_2, l = 0.2; u = 0.1 to 0.5; p = 0.2; and c = 0.1. Reserves covering 0%, 20%, 40%, 60%, 80%, and 100% of the management area were tested (i.e., α = 0, 0.2, 0.4, 0.6, 0.8, and 1, respectively).

The simulation software package Vensim DSS® was used for the simulations. Simulations were run over a 120-year time horizon with a time step of 1 year. The first 20 years were taken as an adjustment period and the years 21–120 were analysed. We then compared results to the 1- to 100-year period. 200 runs were simulated with different levels of noise in each (noise seed s is a random variable).

Results

Impacts on biomass

What is the impact of reserve establishment on total biomass levels?

One main objective of establishing marine protected areas may be to allow stocks to recover or rebuild. In an open-access fishery, total biomass in both deterministic and highly variable marine systems is enhanced by a reserve whether the stock was previously unexploited or heavily exploited. The larger the reserve, the greater the biomass level (Fig. 3). The graphs compare the case of no-reserve against those of 20% and 40% reserve coverage (given the 20%–40% range of recommendations for reserve coverage suggested to maximize fishery benefits in Roberts and Hawkins (2000), NRC (2001), and Gell and Roberts (2003)). In the case of previous heavy exploitation and a highly variable system (Fig. 3*b*), the presence of a reserve covering 20% or 40% of the management area appears to prevent the stock plummeting to near zero levels. Note that over a longer time period, the biomass levels stabilize.

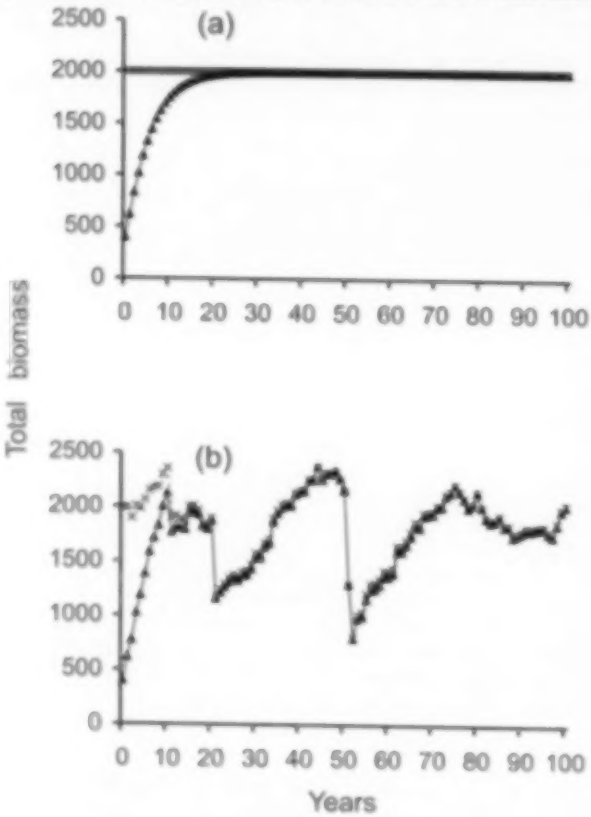

Fig. 2. Growth scenarios for previously unexploited stock (○) and previously heavily exploited stock (▲) in (*a*) a deterministic system and (*b*) a highly variable system for the scenario of zero exploitation. The carrying capacity of the stock is 2000 in each case.

In a TAC-regulated fishery, total biomass levels are also always higher with a reserve (Fig. 4 shows biomass levels with a TAC of 10%, 30%, 50%), and the larger the reserve, the higher the biomass. Total biomass levels also decrease with an increase in the quota level. However, without a reserve and in a previously heavily exploited fishery, the stock will collapse if the TAC reaches 20% or above (Fig. 4*b*). In a previously unexploited stock, total biomass levels will fall from the initial level with the imposition of a quota fishery with or without a reserve (Fig. 4*a* shows the results of one sample run). At low levels of exploitation (TAC 10%), the difference between biomass levels with and without reserve are small (with a mean level of 1243 without reserve and 1467 with a 40% reserve). The differences in biomass are, however, considerable at TAC 50% (with a mean level of 70 without a reserve and 702 with a 40% reserve). In a previously heavily exploited stock with a TAC of 50%, a reserve

© 2004 NRC Canada

Fig. 3. Total biomass levels in an open-access fishery for two stocks: (*a*) previously unexploited and (*b*) previously heavily exploited. No reserve (solid line), 20% reserve (×), and 40% reserve coverage (△) are shown in deterministic and highly variable systems. The figures for the highly variable case represent one sample run (out of 200 runs).

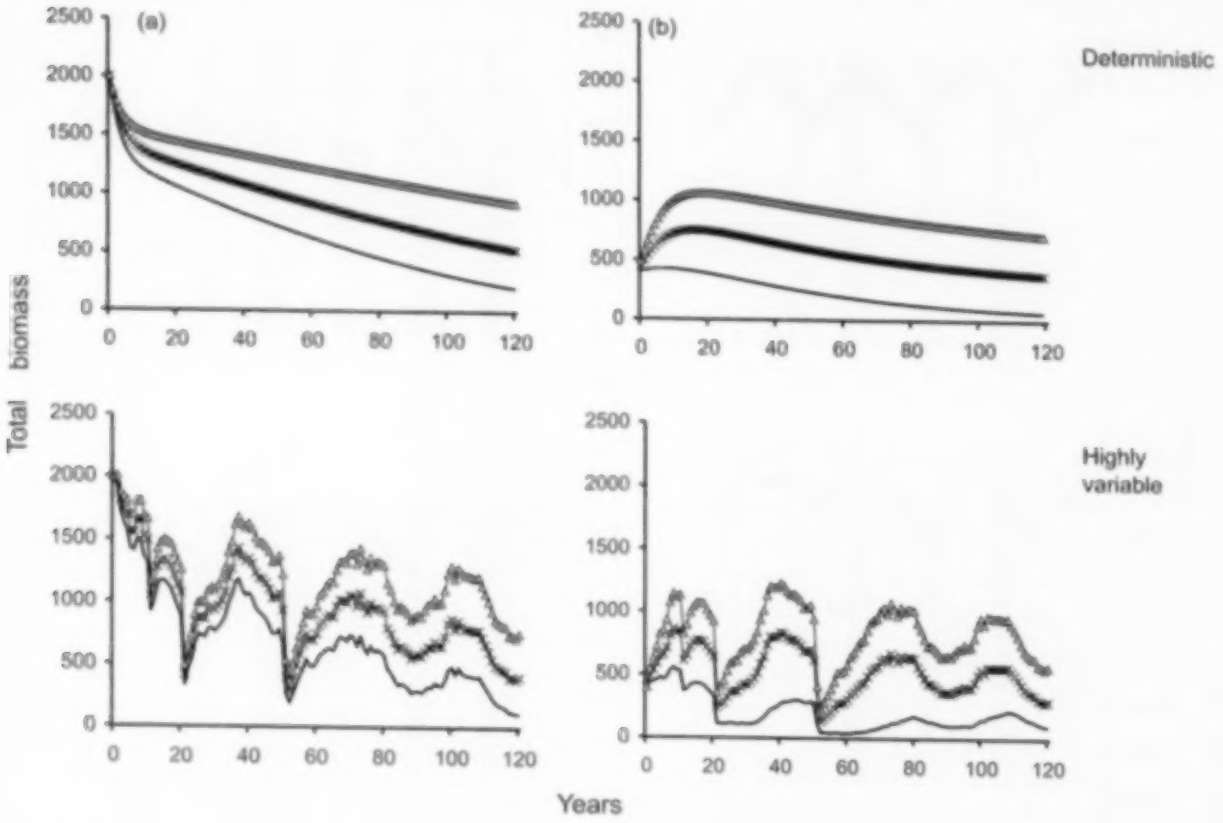

coverage of 40% of the management area can increase total biomass levels from the initial level of 400, but total biomass falls far short of the carrying capacity of the stock because of the prevailing high exploitation rate in the fishery (Fig. 4*b*).

How does the reserve affect the probability of achieving management biomass objectives?

For the open-access fishery, we present results for the deterministic and highly variable systems to compare probabilities of achieving target biomass levels stated in the management objectives (Fig. 5). Both deterministic and variable systems showed similar patterns of increasing probabilities with reserve coverage. We find that the probabilities of achieving target biomass level are slightly greater in the deterministic system, though for these target objectives, this is only evident in the previously unexploited stock. If the objectives were more risk averse, such as 60% of carrying capacity 60% of the time and 35% of carrying capacity 80% of the time, the probabilities of achieving each target biomass level would be significantly higher in the deterministic system. This is not surprising given that the natural mortality pulses in the variable conditions increase natural mortality rate. This does suggest, however, that ignoring such plausible events inherent in a variable environment may result in an overestimation of total biomass levels in a fishery. When the stock is initially at its carrying capacity, reserves greatly increase the probabilities of achieving even the highest target levels of biomass (Fig. 5*a*). For example, in a highly variable system, a 20% reserve coverage increases the probability of achieving 35% of carrying capacity (50% of the time) from 0 without a reserve to 1, whereas 40% reserve coverage would increase the probability of achieving 60% of carrying capacity (25% of the time) from 0 without a reserve to 1.

When the stock has previously been heavily exploited (Fig. 5*b*), it takes larger reserves to increase the probability of achieving target biomass levels. For example, in the highly variable system, it takes 40% reserve coverage before 35% carrying capacity is guaranteed (50% of the time) and 60% reserve coverage to guarantee 60% carrying capacity (25% of the time). This compares to 20% and 40% reserve coverage if the stock was previously unexploited. Without the reserve, the previously heavily exploited stock will collapse (i.e., the 5% carrying capacity objective is not guaranteed). If previously unexploited, however, there is a probability of 0.93 that 5% carrying capacity can be maintained (Fig. 5*a*).

© 2004 NRC Canada

Fig. 4. Total biomass levels in a total allowable catch (TAC)-regulated fishery in a highly variable system, with TAC 10%, TAC 30%, and TAC 50% for (*a*) previously unexploited stock and (*b*) previously heavily exploited stock. No reserve (solid line), 20% reserve (×), and 40% reserve coverage (△) are shown. The figures represent one sample run (out of 200 runs).

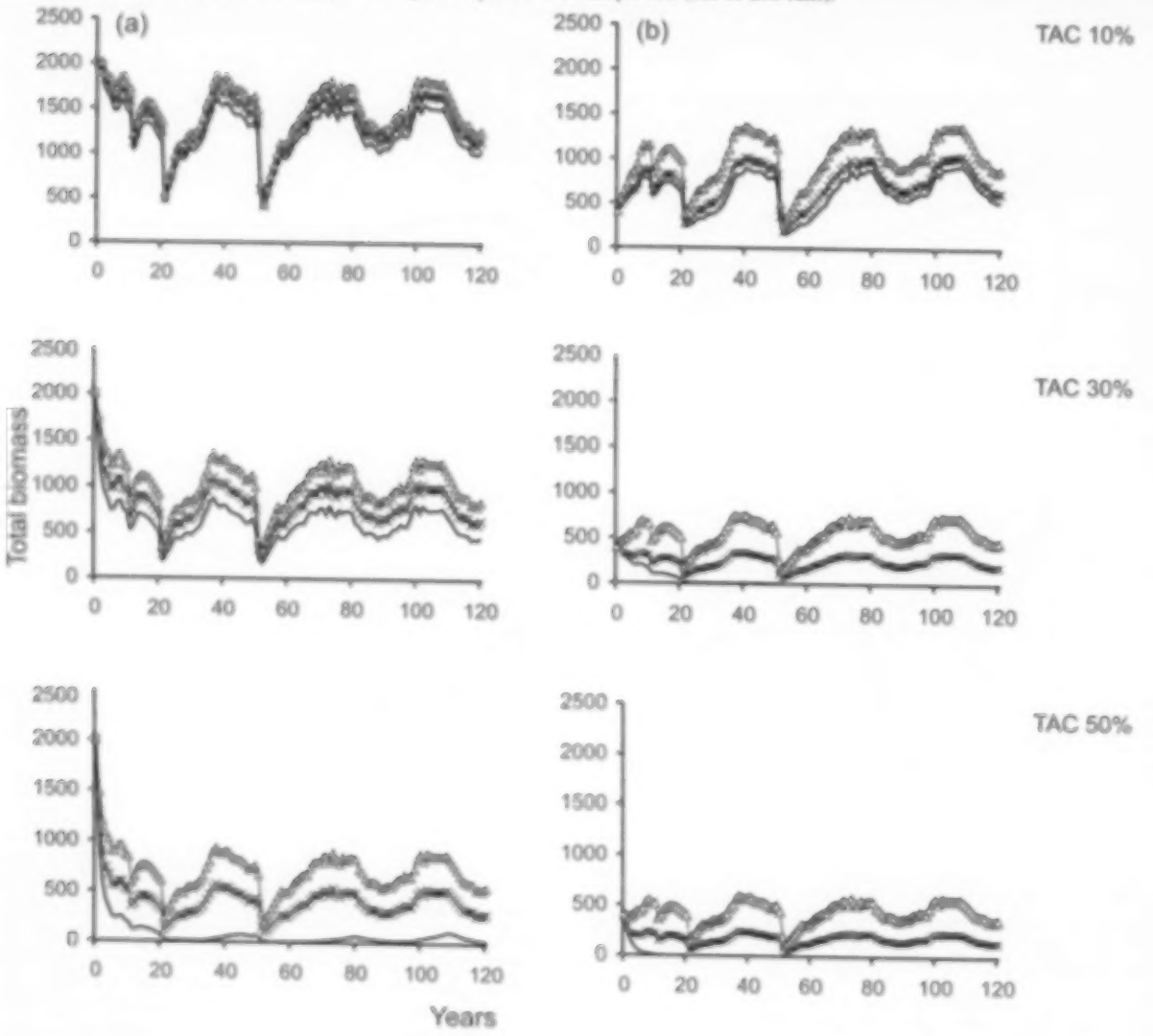

In the TAC-regulated fishery, the probabilities of achieving target biomass levels are again increased with a reserve in most cases if the system is highly variable (Fig. 6). In the highly variable system at low levels of exploitation (TAC 10%), a previously unexploited stock can achieve all biomass objectives even without a reserve. If, however, the stock has previously been heavily exploited, a 20% reserve is required to guarantee the 35% carrying capacity objective and a 60% reserve to guarantee the 60% carrying capacity objective. The probabilities of achieving biomass management objectives generally decline as the TAC level increases to 30% and then 50%. However, with a previously exploited stock, the probabilities are the same for the TAC 30% and 50% case. With a TAC of 50%, a reserve coverage of 40% can only guarantee that the stock does not collapse (fall below 5% carrying capacity), 60% reserve coverage would guarantee the 35% carrying capacity objective is met, and 80% reserve would be required to achieve the 60% carrying capacity objective for both previously unexploited and heavily exploited stocks (Fig. 6).

It is worth noting that the management objective of achieving 60% carrying capacity (25% of the time) in a previously unexploited stock can be achieved by maintaining a low TAC of 10% in the whole fishing ground, by establishing 60% reserve coverage and allowing a TAC of 30% in the remaining (40%) fishing grounds, or by establishing an 80% reserve coverage and allowing a TAC of 50% in the remaining (20%) fishing grounds. In the case of a previously heavily

© 2004 NRC Canada

Fig. 5. Probabilities of achieving management objectives of target biomass levels in an open-access fishery in a deterministic and a highly variable system for a (*a*) previously unexploited stock and (*b*) previously heavily exploited stock for various coverages of marine reserves. 60% carrying capacity 25% of time, solid bars; 35% of carrying capacity 50% of time, hatched bars; and 5% of carrying capacity 100% of time, open bars.

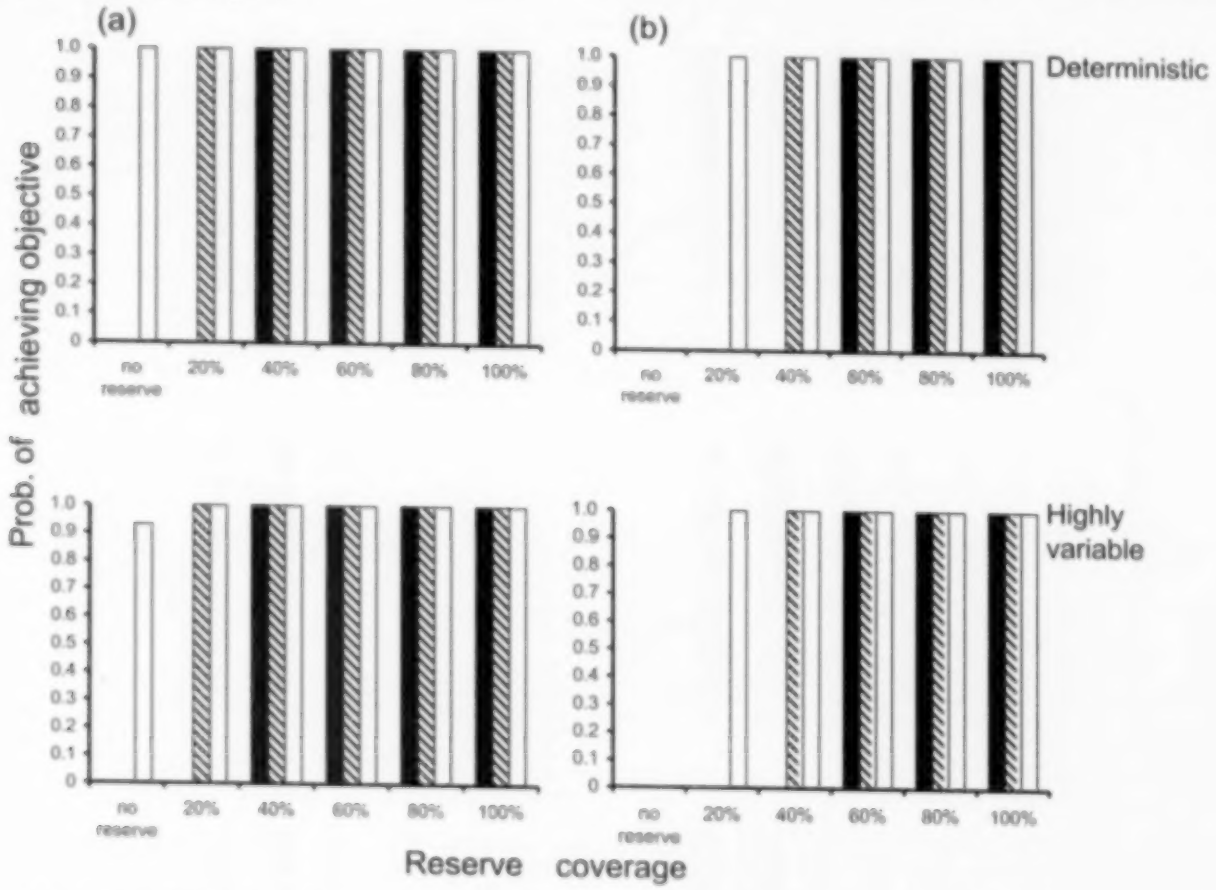

exploited stock, the objective of preventing stock collapse (5% carrying capacity 100% of the time) can be achieved either by maintaining TAC of 10% in the whole management area or by allowing a TAC of 50% in 60% of management area (i.e., with a 40% reserve coverage).

Similar patterns of increasing probabilities with reserve size are found in the deterministic and variable systems, but in general the probability of achieving target biomass levels for all reserve sizes is higher in the deterministic system (as expected because of natural mortality pulses). This highlights the impact of variability on reducing the probability of achieving target biomass levels and reinforces the need for reserves to counter the effects of environmental variability.

Impacts on catch

What is the impact of reserve establishment on the levels and variability of catches in the fishery?

In an open-access fishery, where the system is highly variable, if the stock is previously unexploited, the no-reserve case can produce higher mean catches than 20% and 40% reserve coverage (as seen in Fig. 7) but also more variable catches (Table 1). However, without a reserve, the trend in catch in both the deterministic and variable cases appears to be towards zero, whereas the 20% and 40% reserves appear to stabilize catches at a higher level towards the end of the time period (Fig. 7). Mean catches are approximately 159 (±50) without the reserve compared with 153 (±39) with 20% reserve coverage and 125 (±32) with 40% reserve coverage (Table 1). Percent variability (SD/mean catch × 100) is lower with the reserve (24%–26%) compared with without the reserve (31%) but does not decline uniformly with reserve size.

If the stock was previously heavily exploited, a reserve of 40% in the open-access fishery produces the highest catches of 59 (±17) compared with 18 (±9) of no reserve. Mean catches with reserve coverages up to 80% are higher than those without the reserve and in terms of percent variability are less variable (Table 1). If we take the percent variability as the measure of variability, the larger the reserve, the less variable the catches — ranging from 50% without the reserve to 26% with an 80% reserve. Furthermore, in the pre-

© 2004 NRC Canada

Fig. 6. Probabilities of achieving management objectives of target biomass levels in a total allowable catch (TAC)-regulated fishery in a highly variable system for fisheries regulated by TAC 10%, 30%, and 50% in (*a*) previously unexploited and (*b*) previously heavily exploited stocks. 60% carrying capacity 25% of time, solid bars; 35% of carrying capacity 50% of time, hatched bars; and 5% of carrying capacity 100% of time, open bars.

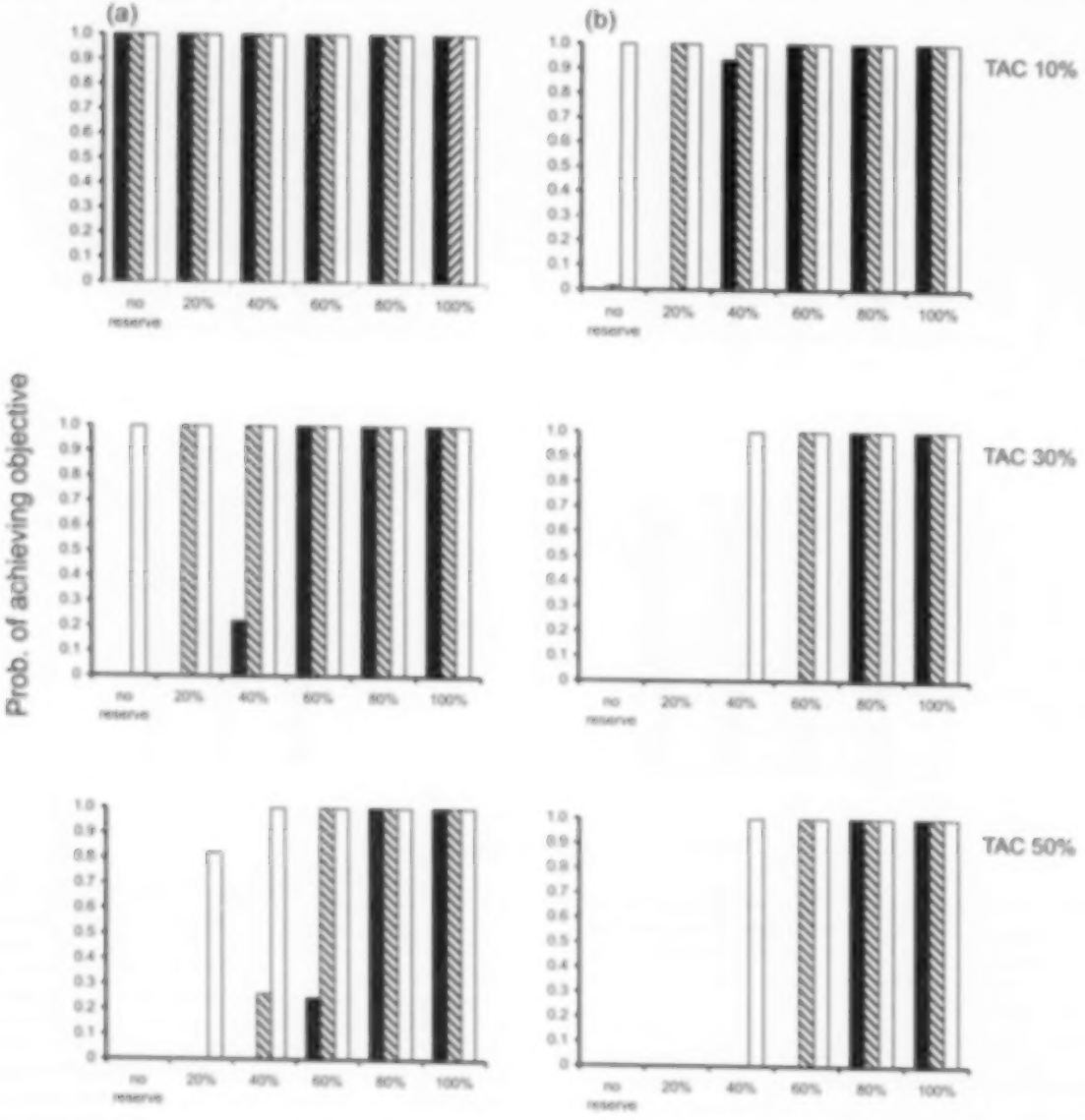

viously heavily exploited fishery, if there is no reserve, catches plummet to near zero levels by year 120 in both the deterministic and the variable systems (Fig. 7*b*).

In the TAC-regulated fishery (Fig. 8) with a previously unexploited stock, catches are higher with no reserve if the TAC is 10%, 20%, or 30%. For TACs of 40% and 50%, catches with the 20% reserve are higher and also less variable (Table 1). For example, mean catches with a TAC of 40% in a previously unexploited stock are 133 (±33%) without a reserve, 143 (±27%) with a 20% reserve, and 132 (±24%) with a 40% reserve. With a TAC of 50%, mean catches in a previously unexploited stock are 18 (±66%) without a reserve, 103 (±31%) with a 20% reserve, 114 (±26%) with a 40% reserve, and even 100 (±23%) with a 60% reserve.

If the stock has previously been heavily exploited, catches without the reserve fall to zero once the TAC is 20% or higher (Table 1). Therefore, reserves of 20%, 40%, 60%, and even 80% will produce higher catches under conditions of previous heavy exploitation combined with continuing moderate to heavy exploitation. Even for low TAC levels (TAC

© 2004 NRC Canada

Fig. 7. Catch levels in an open-access fishery for two stocks: (*a*) previously unexploited and (*b*) previously heavily exploited. No reserve (solid line), 20% reserve (×), and 40% reserve coverage (△) are shown for deterministic and highly variable systems.

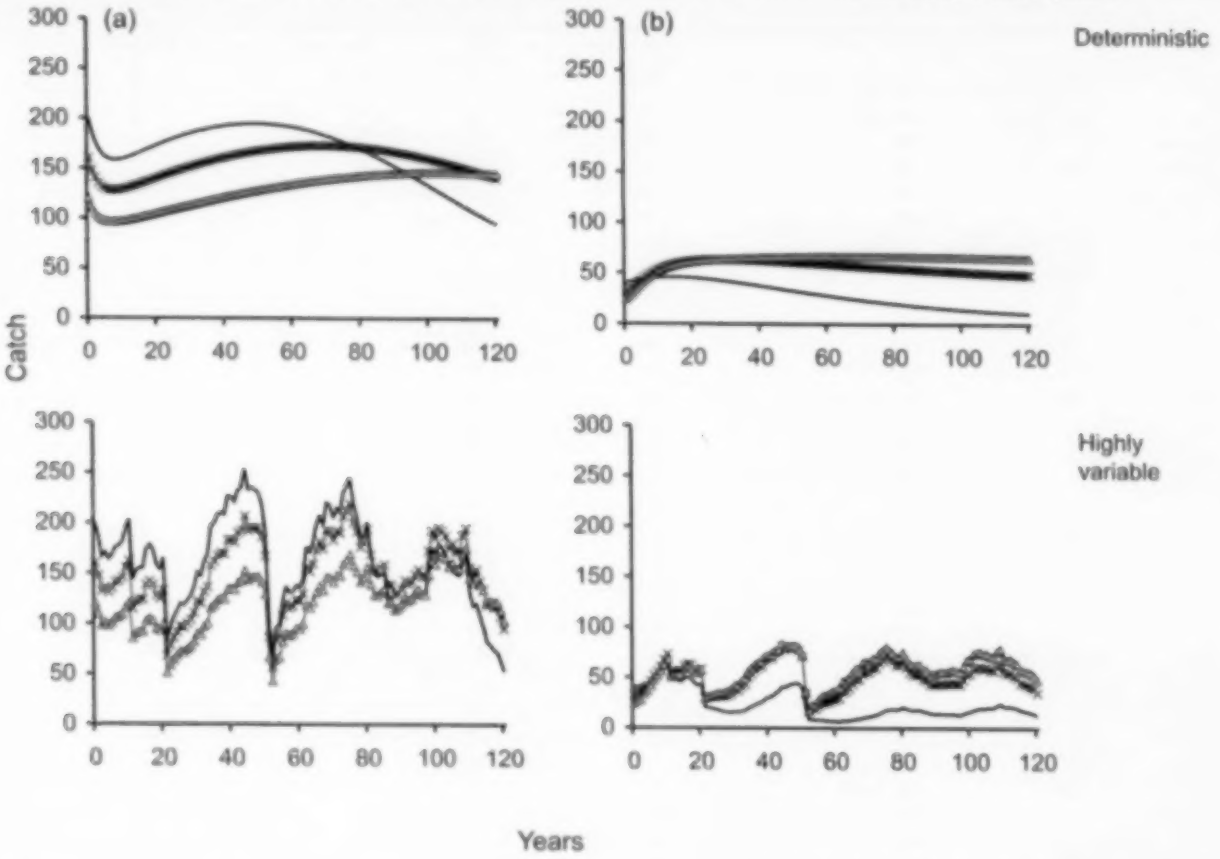

10%), mean catches are higher with a 20%, 40%, and 60% reserve than without the reserve: 53 (±30%), 51 (±27%), and 41 (±27%) compared with 36 (±39%), respectively.

Sensitivity of results

We chose some of the parameters used in the previous analysis based on previous studies (e.g., reproductive capacity from Rodwell et al. 2002), the literature (natural mortality from Pauly and Ingles 1981), and others on what we believe are reasonable estimates (e.g., movement rates of fish and larvae). However, we accept that some of the outcomes of the analysis may be sensitive to some assumptions and parameter choices made. Two main assumptions are the movement rates of larvae and fish and the initial stock condition and growth rate.

Movement rates of larvae and fish

The nature of the movement of fish and larvae between a reserve and fishing ground is a common and important question and one with implications for reserve design and location. The case shown is a system with moderate fish movement and 50% larval retention. This was chosen as a middle ground, assuming that the reserve in question would export some fish and some larvae in response to changing biomass levels in the fishing ground and the reserve.

Clearly if the mobility of fish and larvae were significantly different from that assumed, the simulation results may be quite different. For example, if mobility were increased such that there is uniform larval dispersal ($\theta = 0$) and high fish movement ($\sigma = 1$), reserves are likely to produce higher catches than suggested, with a less dramatic reduction in catch variability. For example, for the case of a previously unexploited stock with a reserve coverage of 40% and TAC of 30% in the remaining fishing grounds, mean catches increased from 134 ± 30 to 152 ± 34 because of the higher movement rate. There may also be a lower probability of meeting biomass target levels because more of the biomass will be moving out of the protected area. Note that for the same example above, the probabilities of reaching each of the target levels remained unchanged.

If the system was closed, however, with complete larval retention ($\theta = 1$) and no fish mobility ($\sigma = 0$), the reserve will reduce mean catches, since there is no replenishment effect from the reserve to the fishing ground. For example, for the case of a previously unexploited stock with a reserve coverage of 40% and TAC of 30% in the remaining fishing grounds, mean catches decreased from 134 ± 30 to 105 ± 26 because of the lower movement rate. Catches are likely to be just as variable (in terms of percent) with or without the reserve because of the lack of spillover from the reserve pro-

© 2004 NRC Canada

Table 1. Mean catch levels with standard deviation (SD) and percent variability (var.) for previously unexploited and previously heavily exploited stocks for a highly variable system in an open-access and total allowable catch (TAC) quota fishery.

		Previously unexploited			Previously heavily exploited		
Fishery regime	Reserve coverage (%)	Mean	SD	% var.	Mean	SD	% var.
Open-access	No reserve	159	50	31	18	9	50
	20	153	39	25	50	16	32
	40	125	32	26	59	17	29
	60	82	21	26	50	14	28
	80	36	9	24	27	7	26
TAC (%)							
10	No reserve	121	26	21	36	14	39
	20	100	21	21	53	16	30
	40	78	17	22	51	14	27
	60	54	11	20	41	11	27
	80	28	6	21	24	6	25
20	No reserve	170	38	22	0	0	—
	20	146	32	22	44	14	32
	40	118	25	21	59	17	29
	60	84	18	21	54	14	26
	80	45	10	22	35	9	26
30	No reserve	175	43	25	0	0	—
	20	159	37	23	36	10	28
	40	134	30	22	56	15	27
	60	100	21	22	58	15	26
	80	55	12	21	40	10	25
40	No reserve	133	44	33	0	0	—
	20	143	38	27	33	9	27
	40	132	31	24	55	14	25
	60	104	23	22	60	14	23
	80	61	13	22	43	10	23
50	No reserve	18	12	66	0	0	—
	20	103	31	31	32	8	25
	40	114	29	26	55	13	24
	60	100	23	23	62	14	23
	80	62	14	22	46	10	23

viding a stabilizing effect. The probability of achieving total biomass target levels may increase because part of the stock will be permanently protected. For the example above, the probability of reaching the target level of 60% carrying capacity (25% of the time) rose from 0.22 to 1. This extreme case of a closed system may occur if the reserve is sited around isolated habitat patches rather than in places where habitat is contiguous with fishing grounds.

In general, there must be bidirectional or source dynamics in order for reserves to feed fishing grounds (L.D. Rodwell, unpublished data). However, though alternative movement patterns, such as a reserve sink or lower fish and larval mobility, can reduce catch levels, catches are likely to still be less variable with a reserve if the fishery is heavily exploited.

Initial stock condition and growth rate

We have chosen two scenarios of initial stock condition. One is the extreme of an unexploited stock operating at carrying capacity, which is then subjected to fishery exploitation with or without a reserve. The second is taken as a heavily exploited stock at one fifth of its carrying capacity, which if left unexploited, would reach its carrying capacity after approximately 20 years. We take this to reflect a realistic scenario. However, if the previously heavily exploited stock were to grow at a slower rate, reaching the carrying capacity after 40 years if left unexploited (achieved by changing β to 2.5 and γ to 0.0007), catches would be much lower than recorded (Table 1). For example, with 40% reserve coverage and a TAC of 30%, catches would be as low as 6 ± 3 compared with 56 ± 15. Catches would still be zero without the reserve. We also found that if the stock were much slower growing, reserves must be much larger to increase the probability of achieving target biomass levels. For example, in a previously heavily exploited fishery with a TAC of 30% in fishing grounds, a 40% reserve can no longer prevent stock collapse. The reserve would have to be 60% of management area to prevent stock collapse and a 100% closure would be required to guarantee all biomass target objectives are met (previously 80% coverage would have met all three objectives). The more the exploitation rate exceeds the replenishment rate, the more extensive protection is required. The stock in this case requires a large refuge simply to survive. If the stock is faster growing, smaller

© 2004 NRC Canada

Fig. 8. Catch levels in a quota-regulated fishery with total allowable catch (TAC) of 10%, 30%, and 50% for two stocks: (*a*) previously unexploited and (*b*) previously heavily exploited. No reserve (solid line), 20% reserve (×), and 40% reserve coverage (△) are shown. Note different scales on *y* axes for each TAC level.

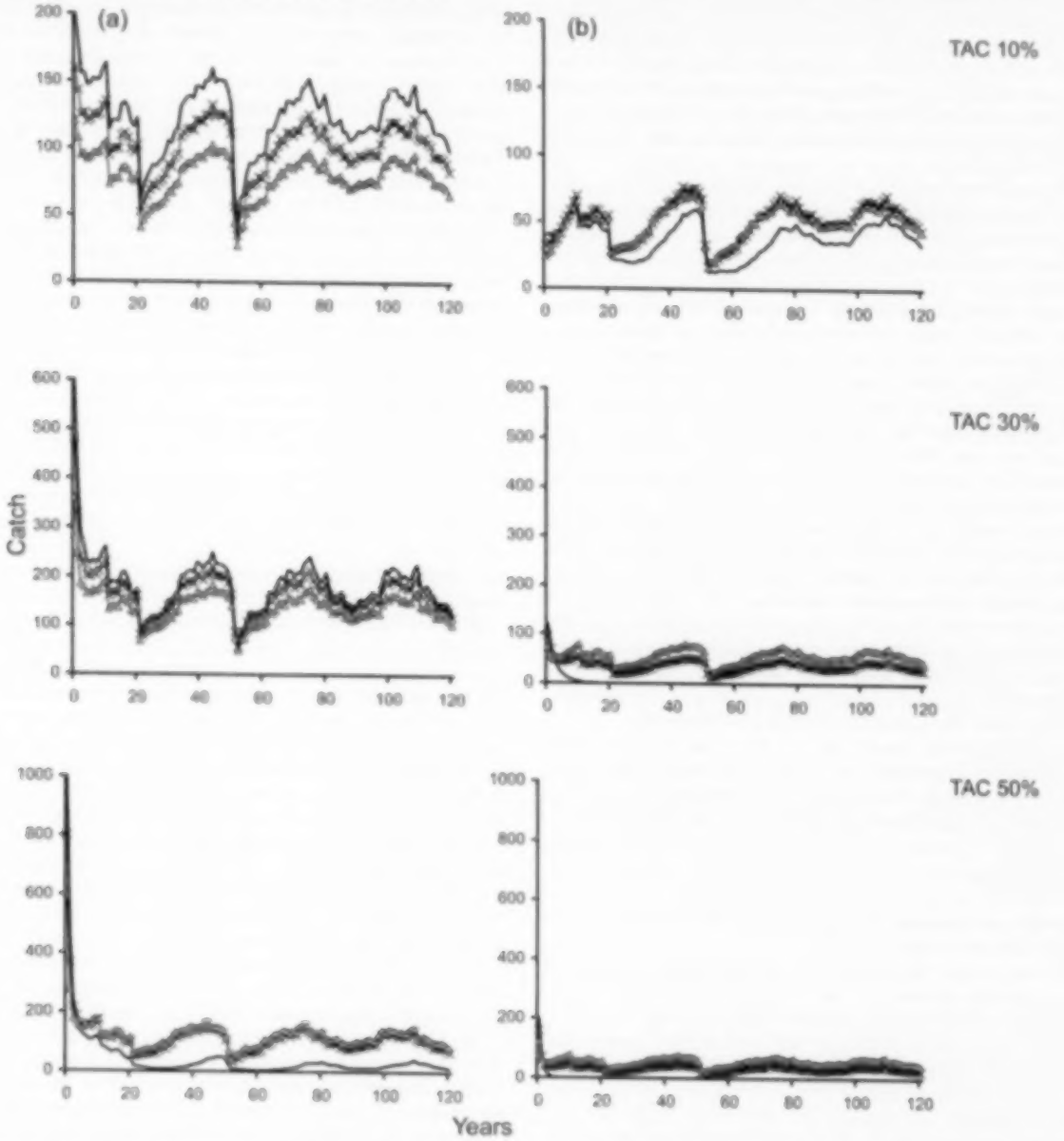

reserves will produce the same benefits. The stock is still able to replenish itself at a quicker rate than exploitation and so requires less protection.

Implications of other assumptions and parameter choices

The stocks described have reproductive capacities that reflect their condition: 0.7 (70% reproductive mature at carrying capacity) and 0.2 (20% reproductively mature if heavily exploited). These values are taken from Rodwell et al. (2002, 2003). We assume that if reproductive capacity remains at 0.2, the stock will not reach carrying capacity. Only if allowed to increase to 0.7 is this possible. Assumptions made about the relative reproductive capacity of reserve and fishing ground stocks can influence the relative effectiveness of reserves in increasing catches. For example, if $\varepsilon_1 = \varepsilon_2 = \varepsilon$ (i.e., reproductive capacity is uniform throughout management area), which is extremely unlikely in practice, then mean catches are more likely to be lower with the reserve.

In the simulations, recruitment in the fishing ground is assumed to be a function of fish biomass post-exploitation (i.e., all exploitation takes place before spawning $\psi = 1$). However, recruitment may take place before some or any ex-

© 2004 NRC Canada

ploitation occurs (i.e., $\psi = 0$ (no exploitation before spawning) or 0.5 (50% exploitation before spawning)). This may occur in a seasonal fishery. The timing of exploitation can have important implications, particularly in a regulated fishery. If a fishery operates in such a way as to allow recruitment to take place before exploitation, then the fishery can be more productive and there is less argument for a reserve as catch enhancement grounds. However, in reality the variability in recruitment patterns may make this type of regulation ineffective.

We considered years 21–120 as a 100-year period of analysis. This was designed to eliminate extreme adjustment periods and to concentrate more on the equilibrium results on catch, biomass, and variability. However, we did analyse the results for a 1- to 100-year period to check if this influenced the conclusions considerably. The probabilities of achieving target biomass levels remained unchanged for most reserve coverages and TAC or open-access cases. However, for a TAC of 10% in a previously heavily exploited stock, 40% reserve coverage had a probability of 0.94 of achieving the 60% carrying capacity objective if years 21–120 were considered but only 0.24 if years 1–100 were considered. This indicates the tendency for biomass to build up over time with reserve protection. Also, for both TAC and open-access regimes, catches for the no-reserve case were slightly higher and more variable if years 1–100 were considered (i.e., years 1–20 are those before catches responded fully to exploitation); catches with a reserve remained very similar, and the comparative catch status of reserve and no-reserve case remained unchanged. The time frame of 100 years was taken as realistic. However, some may view 20 or 50 years to be more realistic in management terms. The shorter the management time frame considered, the less favourable the reserve contributions would appear. Reserves produce long-term benefits. Therefore, the longer the management horizon, the more likely reserves are to be useful as management tools from both fishery catch and fish biomass perspectives.

Discussion

Reserves can increase the probability of achieving target biomass levels

The mean total fish biomass level was found to be higher with a reserve regardless of the initial condition of the stock, variability, or the fishery regime. Total biomass levels increased with reserve coverage. The probability of the stock remaining above target levels of biomass generally increased with the presence of the reserve in both deterministic and variable systems. The greater the reserve coverage and the better the initial condition of the stock, the greater the probability would be of reaching targets levels of fish biomass in the fishery.

The highly variable system had lower probabilities of reaching target biomass levels for most reserve scenarios and an increased chance of stock collapse in the absence of a reserve. However, the probability of achieving each target level was generally greater with a reserve than without, and probabilities increased as reserve coverage increased. If the stock had previously been heavily exploited, larger reserves may have been required to replenish stocks (i.e., sufficiently increase probability of attaining target biomass levels). The results of this study suggest, however, that once stocks have recovered, reserve coverage could be reduced without reducing the probability of maintaining target biomass levels (i.e., the stock moves from the state of previously heavily exploited to the state of previously unexploited after protection).

In a quota-regulated fishery with a high TAC, the reserve would have to be large to make a real difference to probabilities of attaining target stock levels. However, if the TAC were reduced, small reserves could substantially increase this probability. In each scenario, reserves showed the potential to eliminate the possibility of stock collapse even in a highly variable system.

Higher movement rates out of the reserve may reduce the probability of achieving target biomass levels, and lower movement may increase probabilities. The probability of achieving target biomass levels will also fall with the growth rate of the stock. Slower growing stocks will need larger reserves to achieve target biomass levels. The findings that reserves increase the probability of achieving target biomass levels and that they can prevent stock collapse in heavily exploited fisheries are sound regardless of the assumptions regarding reproductive capacity of reserve and fishing ground stocks, recruitment timing, or movement patterns. The reserve coverage required to achieve this objective, however, increases with exploitation rate in the remaining fishery.

Reserves can enhance mean catches in a fishery over time

Mean catches can be enhanced with a reserve, but the biological and economic conditions in the fishery will determine at what level of exploitation reserves will enhance catches and what coverage reserves need to achieve this objective. We can say that the higher the exploitation rate in the fishery, the more likely that catches will be enhanced by the presence of a reserve but only if there is some moderate movement of larvae and (or) fish out of the reserve. In closed systems, reserves will clearly not enhance catches.

If the stock has previously been unexploited (or experienced low exploitation), the establishment of the reserve may lead to lower catch levels than with the no-reserve case. This will depend on the fishery regime. Open-access results show lower mean catches with reserves. In the quota-regulated fishery, if TAC remains low then mean catches will again be lower with reserves. As the TAC increases, mean catches with small reserve coverage can exceed mean catches without the reserve. Even large reserve coverage could produce greater catches than catches without a reserve if the stock has previously been heavily exploited. In the open-access fishery, the effectiveness of the reserve in enhancing catches is highly dependent on the condition of the stock prior to protection. This may be explained by the fact that under conditions of open access, a previously heavily exploited stock will not have the opportunity to recover to levels at which catch can be enhanced (unlike a fishery regulated by strict quotas). However, in a quota-regulated fishery, the TAC levels would have to be high for a small reserve coverage to increase mean catches. These results are consistent with other modelling efforts that suggest that marine reserves will enhance catches in heavily exploited fisheries (e.g., Holland and Brazee 1996; Sanchirico and Wilen 2001; Rodwell et al. 2003).

© 2004 NRC Canada

In an open-access fishery, mean catches with a reserve were only higher in the case where the stock was previously heavily exploited. In a quota-regulated fishery, a small reserve coverage could prevent fishery catches from collapsing completely, even when the TAC was set high, regardless of the previous condition of the stock or high level of variability. Given that in the 1980s and 1990s in the North Sea, 2- to 8-year-old cod (http://www.cefas.co.uk/fsmi/roundfish-cod.htm) and 2- to 6-year-old haddock (http://www.cefas.co.uk/fsmi/roundfish-haddock.htm) were estimated to be exploited at a rate of approximately 50%–60%; our results support the suggestion that collapse of these stocks may be imminent in the absence of reserve protection or effective measures in fishing effort reduction.

Higher movement rates from the reserve increased the mean catch levels in the fishing ground, and lower movement reduced mean catches. Mean catches will be lower if the growth rate of the stock is slower than simulated for the previously heavily exploited stock.

Reserves can reduce the variability of catches in the fishery

Depending on the initial condition of the stock and the fishery regime in place, reserves can reduce the variability of catches. In general, we found that if the stock was previously unexploited in an open-access fishery, the level of variability (in terms of percent variability) declined with reserve coverage. This was also true in a quota fishery with moderate to high TAC levels. However, if TAC levels were low, the levels of variability were not significantly different with or without the reserve.

If the stock had been previously heavily exploited variability, in catches declined with reserve coverage. However, for a fishery with moderate to high TACs, catches without the reserve were zero and so stable. Therefore, we conclude that even in a highly variable system, reserves can reduce variability of catches if the fishery is moderately to heavily exploited, a finding consistent with those of Mangel (2000*a*, 2000*b*) and Pezzey et al. (2000). Under some conditions (e.g., low exploitation), mean catches can be reduced because of reserve establishment resulting in a mean–variance trade-off (e.g., Dixit and Pindyck 1994). It may be desirable in some fisheries to accept lower catches in return for more predictable catches.

Lower levels of fish or larval movement will reduce the impact of the reserve on variability. In the extreme case of a zero movement rate, we found that percent variability with or without the reserve was the same. The movement of fish and larvae from the reserve can have a stabilizing effect on the catches in the fishing ground. If growth of the stock is slower, the catches are likely to be lower and perhaps more variable in term of percentage. However, the results for catch variability are not conclusive for very slow-growing stocks.

Two fishery regimes compared

Although in general, results were similar between open-access and quota management regimes, there were some notable differences. Firstly, the open-access fishery did not collapse completely in the time period tested, but in the quota fishery, the stock could collapse after as little as 10 or 20 years. This suggests that under open-access conditions, the stock is able to bounce back from low biomass levels because of a reduction in fishing effort. However, in reality these low levels of biomass may be insufficient for some species to recover. Secondly, we assume that fishing effort has a reasonably high response. High capital investment in boats and fishing gear may in fact make fishing effort less flexible than assumed. In the quota fishery, even if biomass drops to critical levels, a proportion will still be removed. If quotas are set too high (because of lack of knowledge of stock condition, for example), the stock can collapse. High levels of exploitation in an open-access fishery may be due in part to government subsidies making fishing costs artificially low. High quotas may arise from politicians seeking to avoid economic hardship that lower quotas might entail.

The danger of setting quotas based on estimates of biomass is clear. The quotas are a fixed proportion of biomass, but the stock is variable. In a quota fishery, there is a far greater danger of stock collapse without a marine reserve. As noted previously, reserves of between 20% and 40% have been suggested by scientists as the range needed to assure fishery benefits (Roberts and Hawkins 2000; NRC 2001; Gell and Roberts 2003). This recommended range of reserve coverage as a tool to prevent stock collapse is supported by the findings of this study, though we acknowledge that the conditions in each fishery will require individual consideration. Larger reserves would create greater buffers but may result in lower catches. Furthermore, we find that a very slow-growing stock may require full protection from fishing if previously heavily exploited.

The variability and uncertainty of marine environments strengthens the argument for marine reserves as refuges from exploitation. This study supports others that suggest that the presence of fully protected marine reserves can insure against stock collapse (Lauck et al. 1998; Mangel 2000*a*). Reserves could increase the ability of fishery managers to achieve target levels of biomass, particularly in variable environments, and reduce the variability in catches in neighbouring fisheries, making future planning in the fishery more efficient. In heavily exploited fisheries, reserves are also likely to enhance mean catches so long as fish and (or) larvae are moderately mobile.

Acknowledgements

Lynda Rodwell was funded by the Economic and Social Research Council, UK, Research Fellowship number T02627. Callum Roberts was supported by a Pew Fellowship in Marine Conservation from The Pew Charitable Trusts. We thank two anonymous reviewers for their very constructive comments on an earlier version of this manuscript.

References

Alheit, J., and Hagen, E. 1997. Long-term climate forcing of European herring and sardine populations. Fish. Oceanogr. **6**: 130–139.

Beverton, R.J.H., and Holt, S.J. 1957. On the dynamics of exploited fish populations. 1st ed. Chapman and Hall, London.

Clark, C.W. 1990. Mathematical bioeconomics: the optimal management of renewable resource. 2nd ed. John Wiley & Sons, New York.

Clark, C.W. 1996. Marine reserves and the precautionary management of fisheries. Ecol. Appl. **6**(2): 369–370.

© 2004 NRC Canada

Cohen, D. 1966. Optimizing reproduction in a randomly varying environment. J. Theor. Biol. **12**: 119–129.

Cohen, D. 1967. Optimizing reproduction in a randomly varying environment when correlation may exist between the conditions at the time a choice has to be made and a subsequent one. J. Theor. Biol. **26**: 1–14.

Conrad, J.M. 1999. The bioeconomics of marine sanctuaries. J. Bioecon. **1**: 205–217.

Dixit, A.K., and Pindyck, R.S. 1994. Investment under uncertainty. Princeton University Press, Princeton, N.J.

Francis, R.C., Hare, S.R., Hollowed, A.B., and Wooster, W.S. 1998. Effects of interdecadal climate variability on the oceanic ecosystems of the NE Pacific. Fish. Oceanogr. **7**: 1–21.

Gell, F., and Roberts, C.M. 2003. The fishery effects of marine reserves and fishery closures. World Wildlife Fund, Washington, D.C. Tech. Rep.

Hilborn, R., and Walters, C.J. 1992. Quantitative fisheries stock assessment: choice, dynamics and uncertainty. Chapman and Hall, New York.

Holland, D.S., and Brazee, R.J. 1996. Marine reserves for fisheries management. Mar. Res. Econ. **11**: 157–171.

Lauck, T., Clark, C., Mangel, M., and Munro, G.R. 1998. Implementing the precautionary principle in fisheries management through marine reserves. Ecol. Appl. **8**: S72–S78.

Longhurst, A.R., and Pauly, D. 1987. Ecology of tropical oceans. Academic Press, San Diego, Calif.

Mangel, M. 2000*a*. Irreducible uncertainties, sustainable fisheries and marine reserves. Evol. Ecol. Res. **2**(4): 547–557.

Mangel, M. 2000*b*. On the fraction of habitat allocated to marine reserves. Ecol. Lett. **3**(1): 15–22.

Mann, K.H., and Lazier, J.R. 1996. Dynamics of marine ecosystems: biological-physical interactions in the oceans. 2nd ed. Blackwell Science Ltd., Oxford.

National Research Council (NRC). 2001. Marine protected areas: tools for sustaining ocean ecosystems. National Research Council, National Academy Press, Washington, D.C.

Pauly, D., and Ingles, J. 1981. Aspects of growth and natural mortality of exploited coral reef fishes. *In* Proceedings of the 4th International Coral Reef Symposium, Manila, Philippines. Vol. 1. Marine Sciences Center, University of the Philippines, Quezon City, Philippines. pp. 89–98.

Pezzey, J.C.V., Roberts, C.M., and Urdal, B.T. 2000. A simple bioeconomic model of a marine reserve. Ecol. Econ. **33**(1): 77–91.

Roberts, C.M., and Hawkins, J.P. 2000. Fully protected marine reserves: a guide. WWF Endangered Seas Campaign, Washington, D.C.

Rodwell, L.D., Barbier, E.B., Roberts, C.M., and McClanahan, T.R. 2002. A model of tropical marine reserve – fishery linkages. Nat. Res. Mod. **15**(4): 453–486.

Rodwell, L.D., Barbier, E.B., Roberts, C.M., and McClanahan, T.R. 2003. The importance of habitat quality for marine reserve – fishery linkages. Can. J. Fish. Aquat. Sci. **60**(2): 171–181.

Sanchirico, J., and Wilen, J. 2001. A bioeconomic model of marine reserve creation. J. Environ. Econ. Manag. **42**: 257–276.

Steele, J.H. 1998. Regime shifts in marine ecosystems. Ecol. Appl. **8**: S33–S36.

Sumaila, U.R. 1998. Protected marine reserves as fisheries management tools: a bioeconomic analysis. Fish. Res. **37**: 287–296.

© 2004 NRC Canada

Experimental evaluation of ontogenetic diet transitions in summer flounder (*Paralichthys dentatus*), using stable isotopes as diet tracers

David A. Witting, R. Christopher Chambers, Keith L. Bosley, and Sam C. Wainright

Abstract: We examined the rate of isotopic change of nitrogen (N) and carbon (C) and isotopic fractionation at two temperatures during several ontogenetic diet transitions in summer flounder (*Paralichthys dentatus*). We examined prefeeding larvae as they metabolize the maternal source of nutrition and evaluated three diet transitions in the early life stages of this species: (*i*) yolk dependency to first feeding on zooplankton, (*ii*) one zooplankton (rotifers) to another (*Artemia*), and (*iii*) zooplanktivory to piscivory. We used experimental results and simulations to contrast time- versus growth-based models for estimating parameters of isotopic change and fractionation. All rates of isotopic change were lowest for the transition between zooplanktivory and piscivory, most rapid for the transition from yolk dependency to first feeding, and generally lower at cooler temperatures. Estimates of fractionation were greater for N (2.8‰–3.8‰) than for C (0.23‰–0.91‰) but appeared to be unaffected by water temperature or fish life stage. Simulation results suggested that parameter estimates of isotopic change and fractionation may be compromised when growth rates are low unless sampling design is modified to address slow growth rates. We conclude that sampling strategy and the model used can influence the accuracy and precision of estimates of isotopic change and fractionation.

Résumé : Nous avons mesuré les taux de variation des isotopes d'azote (N) et de carbone (C), ainsi que la fractionation isotopique, à deux températures, durant plusieurs changements ontogéniques de régime alimentaire chez le cardeau d'été (*Paralichthys dentatus*). Nous avons d'abord étudié les larves avant leur première alimentation alors qu'elles métabolisent leur réserve alimentaire maternelle, puis durant trois changements de régime dans les premiers stades du cycle de l'espèce, soit (*i*) de l'utilisation de la vésicule vitelline jusqu'à la première alimentation dans le zooplancton, (*ii*) durant la substitution d'un type de proie zooplanctonique (rotifères) à un autre (*Artemia*) et (*iii*) durant la transition de la zooplanctonophagie à l'ichtyophagie. Les résultats expérimentaux et des simulations nous ont permis de comparer les modèles basées sur le temps et ceux basés sur la croissance pour l'estimation des paramètres de la variation isotopique et de la fractionation. Tous les taux de variation isotopique sont minimaux lors de la transition de la zooplanctonophagie à l'ichtyophagie et ils sont maximaux lors du passage de l'alimentation vitelline à la première alimentation dans le milieu; ils sont aussi plus bas aux températures plus fraîches. Les estimations de la fractionation sont plus élevées pour N (2,8‰–3,8‰) que pour C (0,23‰–0,91‰), mais elles ne semblent pas affectées par la température de l'eau, ni par le stade de développement des poissons. Les résultats des simulations indiquent que les estimations des paramètres de la variation isotopique et de la fractionation sont faussées lorsque les taux de croissance sont faibles, à moins que le plan d'échantillonnage ne soit modifié pour tenir compte de ces faibles taux de croissance. En conclusion, le plan d'échantillonnage et le choix des modèles peuvent affecter la justesse et la précision des estimations de la variation isotopique et de la fractionation.

[Traduit par la Rédaction]

Introduction

Knowledge of the identities and sources of items in a fish's diet is fundamental to understanding trophic relationships in aquatic ecosystems. This information is often difficult to obtain because of seasonal, spatial, and ontogenetic changes in the fish's diets. Most fish encounter a series of complex assemblages of prey (Checkley 1982; Jenkins

Received 29 July 2003. Accepted 2 July 2004. Published on the NRC Research Press Web site at http://cjfas.nrc.ca on 25 January 2005.
J17672

D.A. Witting[1] and R.C. Chambers. Northeast Fisheries Science Center, National Marine Fisheries Service, Howard Marine Sciences Laboratory, 74 Magruder Road, Highlands, NJ 07732, USA.
K.L. Bosley. Fishery Resource Analysis and Monitoring Division, Northwest Fisheries Science Center, National Marine Fisheries Service, 2032 SE OSU Drive, Newport, OR 97365, USA.
S.C. Wainright. US Coast Guard Academy, New London, CT 06320, USA.

[1]Corresponding author (e-mail: david.witting@noaa.gov).

 doi: 10.1139/F04-156 © 2004 NRC Canada

1987; McClaren and Avendano 1995) as they undergo habitat shifts that are often related to their life stage (Grover et al. 1998). The occurrence and frequency of prey items in stomachs of fish when fish are collected offer at best only a recent snapshot of the prey consumed, a snapshot that may be distorted by the prey digestibility and environmental factors affecting digestion rate.

Naturally occurring stable isotopes of nitrogen (N) and carbon (C) have proven to be powerful tools for identifying trophic relationships in food webs (Fry and Sherr 1984; Owens 1987; Peterson and Fry 1987). The stable-isotope ratio of the tissues of a consumer can substantially extend inferences about trophic relationships beyond those based on stomach contents to include a time-integrated description of the diet and the sources of prey. Moreover, the general habitat occupied by a consumer may be identified isotopically because, for example, the ratio of C isotopes often varies between habitats that differ in their primary producers (Fry and Sherr 1984). The trophic level of a consumer can also be estimated because heavier isotopes, particularly ^{15}N, are differentially retained in the tissues of a consumer relative to those of its prey, a process known as trophic enrichment or fractionation (DeNiro and Epstein 1981).

The utility of isotopic analysis in food web studies depends on knowledge about the rate at which the isotopic profile of the consumer's tissues changes as new prey are consumed and assimilated (Fry and Arnold 1982; Herzka and Holt 2000; Bosley et al. 2002). A change in a consumer's isotopic profile requires that new tissues are formed and that new prey or mixtures of prey are isotopically distinct from the former prey. The rate of change of the isotopic profile of the consumer after it experiences a new diet, however, depends on the joint rates of metabolic breakdown of old ones, including the loss of breakdown by-products from the body, and also on the formation of new tissues. When these rates are equal, isotopic change will occur but without an increase in mass of the consumer (tissue replacement or turnover). If the rates of tissue replacement are equal and high, isotopic change will occur at a faster rate than if they are equal and low. An increase in mass (i.e., growth) results if the rate of formation of new tissue exceeds that of tissue breakdown. The rates of isotopic change and growth can be expected to depend on prey digestibility, the life stage of the consumer, and environmental factors.

Various models have been used to describe the joint effects of the formation and breakdown of tissues on the rate, direction, and magnitude of isotopic change after a diet transition (Fry and Arnold 1982; Hesslein et al. 1993). The decay model depicts isotope ratios as an exponential function of time. Decay models are appropriate for adult organisms near their maximum size and especially for those taxa whose metabolism is largely independent of environmental factors (e.g., endotherms such as birds and mammals (Hobson and Clark 1992)). The dilution model depicts isotope ratios as a power function of relative growth. Dilution models are appropriate for organisms or life stages that exhibit rapid growth (e.g., shrimp and juvenile fish (Fry and Arnold 1982; Herzka and Holt 2000; Bosley et al. 2002)).

Few studies have addressed rates of isotopic change in fish during their early life histories. This period for fish is one in which multiple nutritional sources are used, beginning with the early dependency of larvae on maternal nutrition and continuing to include zooplanktivory and piscivory on a variety of prey types. Concurrent with ascension in trophic level is the expectation of fractionation, as has been shown in other taxa (Macko et al. 1982; Waser et al. 1999).

Here we provide analysis and experimental validation of the stable-isotope technique and associated models used to infer trophic change. We performed a series of controlled diet-transitions experiments on multiple early life stages of summer flounder (*Paralichthys dentatus*). Our objectives were threefold: (*i*) to estimate the parameters of isotopic change and trophic enrichment based on multiple forced diet transitions in the early ontogeny of a marine fish, (*ii*) to evaluate the role of lifetime water temperature on these estimates, and (*iii*) to compare models and sampling methods that might be used for estimating and interpreting these parameters.

Methods

Species used

Summer flounder undergo a series of diet and habitat transitions during their first few months of life. Spawning occurs in shelf waters of the western Atlantic Ocean during autumn to midwinter. After hatching, larvae depend on yolk reserves for 2–10 days depending on water temperature and food availability. From hatching to settlement, larvae grow from approximately 3 to 12 mm total length (TL) and from 0.1 to 3.1 mg dry weight. In nature, the diets of larvae are likely to change as the zooplankton assemblages available to them changes. A transition from pelagic shelf waters to benthic estuarine habitats occurs coincidentally with the ontogenetic transition from the larval to the juvenile stage. The sources and identities of prey also change before and after larval ingress into estuarine habitats. Juvenile summer flounder undergo a subsequent diet and trophic transition once they become sufficiently large (~25–30 mm TL) to consume small fish.

General laboratory procedures

Summer flounder adults were maintained in the laboratory for greater than 1 year prior to spawning on a diet of frozen squid (*Loligo* spp.) (>90% of total diet), menhaden (*Brevoortia tyrannus*), and Atlantic herring (*Clupea harengus*). Adults were brought into reproductive maturation by simulating autumnal light and temperature and injecting females with carp pituitary hormone (0.011 $mg \cdot g^{-1}$ wet weight; Smigelski 1975). Gametes were stripped from four ripe adults and mixed to produce two full sibships, which were used as replicates in all experiments described below. Three fin ray samples were collected from each of the two female parents (caudal, anal, and dorsal fin) to determine the maternal stable-isotope profile of N and C. Eggs were maintained at 19 °C in 34 ppt seawater and were checked twice daily for hatchlings. Larvae used in this study hatched within a 12-h period.

The three diet-transition experiments evaluated in this study (described below) required the production and analyses of four different diets. Squid (*Loligo* spp.) used as food for the parent summer flounder was purchased as frozen blocks from a local source. The maternal isotopic signature, as well as that of the yolk-sac larvae, was expected to reflect the

© 2004 NRC Canada

squid diet. Marine rotifers (*Brachionus plicatilis*) were used as zooplankton prey for first-feeding summer flounder larvae. Rotifers were produced in house on a diet of yeast and a nutritional supplement (DHA Selco®). *Artemia* (var. Great Salt Lake) were used as the second and larger zooplankton prey for advanced summer flounder larvae and young juveniles. *Artemia* were purchased in bulk as cysts, decapsulated, hatched, enriched with DHA Selco for at least 2 h, and fed as instar II nauplii. Recently settled juvenile winter flounder (*Pseudopleuronectes americanus*) (8–12 mm TL) were used as the fish prey for advanced summer flounder juveniles. The winter flounder were reared in a method similar to that used for the summer flounder larvae. Winter flounder had been fed exclusively with enriched *Artemia* for 3–6 weeks prior to their use as prey.

Diet transitions

Overview

We examined four sequential sources of nutrition, including three diet transitions, during the early life history of summer flounder. We began by assessing the change in isotopic profile of N and C of unfed yolk-sac larvae during yolk absorption. Subsequently, the first diet transition was for larvae when they changed from exclusive dependence on yolk to obtaining nutrition from zooplankton (rotifers). The second diet transition was also for larvae and occurred when they were forced to change from rotifers to a second species of zooplankton (*Artemia*). The third diet transition was for juveniles and consisted of a change from zooplantivory (*Artemia*) to piscivory (recently settled juvenile winter flounder). Each diet transition experiment was conducted at two temperatures (13 and 22 °C) that were known to be within the range experienced by early life stages of wild summer flounder in nature and to result in different growth rates of summer flounder (C. Chambers and D. Witting, unpublished data).

Yolk absorption

This experiment was designed primarily to establish a baseline for the first-feeding experiment. At 2 days prior to hatching, two samples of 40 eggs were obtained from each of the two replicates to estimate the weights of eggs and their N and C stable-isotopic profiles. Each sample was analyzed as an aggregate sample, and individual egg weights were estimated by division of the total weight by 40. Similarly, on the day of hatching, two samples of 40 larvae from each family were collected to estimate the weights of just-hatched larvae and their stable-isotopic profile. Eight sets of 50 larvae from each family were placed in 100-mL glass beakers and were not fed. Five of these beakers were maintained at 13 °C and three at 22 °C (slower development in the cooler bath dictated more beakers needed for sample coverage). All larvae in a beaker were sampled for each family and temperature starting at hatching and ending when feeding was observed by contemporaneous larvae in tanks that were supplied with food. Samples were collected at 1, 2, and 3 days after hatching from the 22 °C bath and at 1, 2, 3, 5, and 7 days after hatching from the 13 °C bath. Ten of the larvae from each of these samples were preserved in 4% seawater-buffered formalin to estimate the time course of changes in larval sizes and the amount of yolk remaining. Forty larvae were frozen (–20 °C) as an aggregate sample for estimating the time course of changes in dry weights and stable-isotope values.

First-feeding larvae

Two sets of 1000 just-hatched larvae from each replicate were assigned to separate, 80-L black plastic cylindrical rearing containers filled with 60 L of seawater. One container per replicate was maintained at 13 °C and one at 22 °C. Rotifers were provided as prey (5 mL^{-1}-day^{-1}), and larvae were checked daily for evidence of first feeding. Samples of 50 larvae were collected from each of the four populations (2 temperatures × 2 replicates) at 0.25, 0.5, 1, 2, 4, 8, and 16 days after the morning evaluation (0900) for evidence of a first feeding. Ten larvae from each sample were preserved in 4% seawater-buffered formalin to assess the time course of changes in larval sizes and to assess developmental state. Forty larvae were frozen (–20 °C) as an aggregate sample for estimating the time course of changes in dry weights and stable-isotopic values.

Zooplankton transition

Larvae for this experiment were drawn from the two containers held at 22 °C in the previous experiment on first-feeding larvae. When larvae reached a size known to be capable of consuming *Artemia* (~8 mm TL), two sets of 110 larvae were removed from each replicate and placed into 8-L black plastic cylindrical containers filled with 6 L of seawater. One container per replicate was held at 13 °C while the other was held at 22 °C. We chose to use larvae from a common thermal history (22 °C) to test for temperature effects on diet transitions to avoid confounding current with historical temperature effects. The discrete diet transition from rotifers to *Artemia* was imposed upon the larvae moved to the smaller rearing containers by offering them only *Artemia* as prey. Samples of 7–10 larvae were collected from each of the four larval populations (2 temperatures × 2 replicates) at the time of their transfer to their new containers and then again at 0.25, 0.5, 1, 2, 4, 16, and 32 days after the transfer. Five larvae from each sample were preserved in 4% seawater-buffered formalin in for estimating the time course of changes in larval sizes and to assess developmental state.

Zooplanktivory to piscivory

Juvenile summer flounder used for this transition were reared as larvae in the two 80-L containers held at 22 °C. Before their use in this experiment, these larvae had been fed exclusively with *Artemia* for at least 40 days to ensure that they had reached an isotopic equilibrium with their *Artemia* diet. During this 40-day period, the summer flounder grew from 6–8 mm TL pelagic larvae to 30–45 mm TL settled juveniles (TL, at start of this experiment = 37.4 ± 3.9 mm (mean ± SD)). The winter flounder to be used as prey in this experiment had, as larvae, been maintained on a rotifer diet until they were large enough to capture *Artemia*, (~7 mm TL). Once they reached that size, the winter flounder were fed only *Artemia* nauplii until their use in the experiment. Once settled, the winter flounder juveniles were maintained at 5–6 °C to slow their growth and thus prolong the period during which they could be used as prey in this experiment.

© 2004 NRC Canada

The experiment was initiated by assigning 64 premeasured summer flounder (32 from each replicate) to separate plastic cylindrical containers (17 cm in diameter, filled with 6 L of seawater). One half of these containers was maintained at 13 °C and the other half at 22 °C. Eight of these fish were immediately sacrificed (frozen individually at –20 °C) to give an estimate of dry weight and isotope profile of N and C for juvenile summer flounder that were fed *Artemia*. The remaining 56 fish were held for 3 days without food to ensure that all previously consumed *Artemia* had cleared the digestive tract and that all the summer flounder had recovered from the handling during their measurement and weighing. After this 3-day digestion–recovery period (Day 0 of the experiment), eight summer flounder (two from each temperature × family combination) were measured and sacrificed (frozen individually at –20 °C) to give an initial estimate of dry weight and isotope signature for juvenile summer flounder at the start of the experiment. Each of the remaining summer flounder was then offered three–five recently settled winter flounder each morning. The number of winter flounder offered was adjusted upward as the summer flounder grew in an attempt to ensure that each summer flounder was satiated. Prior to introducing the daily allotment of prey, we removed the winter flounder remaining from the previous day and counted them. Juvenile summer flounder were sampled 1, 2, 4, 8, 16, and 32 days after their shift to a winter flounder diet. Live lengths of juveniles were taken, then the juveniles were frozen individually at –20 °C for later processing to estimate dry weight and isotope profile.

Sample preparation and isotopic analysis

Dry weights of individual or aggregate samples were obtained by rinsing the thawed fish with deionized water and drying them in a preweighed tin capsule (Microanalysis, Inc., Manchester, Massachusetts) at 55 °C for 24 h. The samples plus capsules were then reweighed to 0.001-mg precision and the final dry weight of the fish calculated by difference. The capsules were gently crushed into small balls and stored in a desiccator until analysis. Estimates of the initial dry weights of all fish were based on a relationship between initial wet (ww_{t0}) and dry weight (dw_{t0}) derived from the eight t_0 fish ($dw_{t0} = 186.8 \times ww_{t0} - 2.95$, $r^2 = 0.92$). Estimates of the initial dry weight, the observed final dry weight, and the known time between when these weights were taken were used to estimate the growth in dry weight for each fish.

The rotifers and *Artemia* were prepared for isotopic analysis by first rinsing the samples in deionized water, placing them into precombusted glass vials, and drying at 55 °C for 24 h or until completely dried. After drying, these samples were ground to a fine powder using an automated mortar and pestle. Approximately 0.8 mg of sample was loaded into tin capsules for isotope analysis.

Stable-isotope analyses were performed on a Europa Scientific ANCA-GSL elemental analyzer (Crewe, Cheshire, UK) coupled to a Europa Scientific 20/20 stable-isotope mass spectrometer in the continuous-flow mode, with ultra-high-purity helium as the carrier gas. The stable-isotope ratios ($^{15}N:^{14}N$ and $^{13}C:^{12}C$) are reported as $\delta^{15}N$ and $\delta^{13}C$ with units of per mil difference relative to standards (N_2 in air for nitrogen and PDB, the fossil *Belemnitella americana* from the Peedee formation of South Carolina (Craig 1957), for carbon). Secondary standards (egg powder and aquatic plant) were included in each batch for quality control.

Parameter estimation

Overview

Two models were used to estimate the rate of isotopic change and the magnitude of fractionation. One model is based on the rate of isotopic change with respect to time; the other model relates isotopic change to growth. Each model includes a rate constant to be estimated (c_t, c_g, respectively) from which half-life constants, the magnitude of fractionation, and equilibrium isotopic values are calculated. For both models, the parameter estimates for each temperature regime can be computed and compared in order to assess temperature effects. Each model was fit using nonlinear regression, which is not without user-dependent choices that may affect parameter estimates (Bates and Watts 1988). Results of nonlinear regression are often affected by the selection of the starting values in the iteration method and by the coverage of data on the independent axis. Regarding the latter, time of collection is easily controlled in isotope studies, and hence observations for the time-dependent model can be set by the experimental design. Systematic coverage of a range of growth rates is difficult to obtain, and hence nonlinear regression is more likely to be problematic when applied to the growth-based model.

Time-based model

Hobson and Clark (1992) describe a time-based model of isotopic change

$$(1) \qquad \delta_t = \delta_f + (\delta_i - \delta_f)\exp(c_t t)$$

where δ_t is the isotopic value of the consumer at time t since the diet transition, δ_f is the consumer's equilibrium (i.e., final) isotopic value on the new diet, δ_i is its equilibrium (i.e., initial) isotopic value on the old diet, and c_t is a rate constant. A study such as ours provides observations on δ_t and δ_i (the average values of each are used here), whereas δ_f and c_t are parameters to be estimated. The model is nonlinear in its parameters because of the rate constant c_t and thus is fit with nonlinear regression. To avoid problems inherent in nonlinear regression caused by a parameter appearing twice in the model (Bates and Watts 1988), we substituted $\Delta\delta = \delta_f - \delta_i$ into eq. 1, leaving

$$(2) \qquad \delta_t = \delta_f + \Delta\delta\exp(c_t t)$$

Estimates of δ_f, $\Delta\delta$, and c_t were then obtained using nonlinear regression. Fractionation was estimated as the difference between the predicted asymptotic isotopic value of the consumer after the diet switch, δ_f, and the isotopic value of the new diet. We also used the average isotopic value of fish sacrificed in the final collection of the experiment, δ_d, to approximate δ_f in calculating fractionation. A half-life with respect to time, H_t, that provides an estimate of the time scale of isotopic change was calculated from the estimate of c_t

$$(3) \qquad H_t = \ln(0.5)/c_t$$

The estimates of isotopic change are time-specific and are therefore a result of the rates of production of new tissues and the breakdown of old tissues. Both rates are expected to

© 2004 NRC Canada

depend on temperature. We tested for this by using a t test for differences in the estimated parameters at the two temperatures.

Growth-based model

Fry and Arnold (1982) describe a growth-based model of isotopic change wherein growth is quantified as the relative increase in (dry) weight, W_R, at the time of sampling relative to the initial weight (i.e., $W_{R,t} = W_t/W_i$), resulting in

$$\delta_t = \delta_f + (\delta_i - \delta_f)(W_{R,t})^{c_g} \quad (4)$$

where the parameters δ_f and δ_i are as in eq. 1, and c_g is a rate constant for the growth model. We again substituted $\Delta\delta = \delta_f - \delta_i$ into eq. 4 for purposes of obtaining a more robust convergence of the nonlinear regression, leaving

$$\delta_t = \delta_f + \Delta\delta(W_{R,t})^{c_g} \quad (5)$$

As in the time-based model, our study provides observations on $W_{R,t}$, δ_t, and δ_i (average values used for each term), whereas δ_f and c_g are estimated using nonlinear regression. As before, fractionation is estimated as the difference between the predicted asymptotic isotopic value of the consumer after the diet switch, δ_f, and the isotopic value of the new diet. The estimate of W_i can be estimated either from an average dry weight of individuals destructively sampled at the time of the diet switch or from the predicted value from relationships between it and wet weight or length. We used both methods in our experiments. Fractionation was estimated as in the time-based model.

The parameter c_g from the growth-based model can be used to partition isotopic change into growth and tissue replacement. This partitioning of c_g can be calculated using a growth-based half-life constant, H_g

$$H_g = \exp[\ln(0.5)/c_g] \quad (6)$$

where H_g is the value of $W_{R,t}$ when the isotopic value of the consumer's tissue is halfway between the equilibrium values for the old and new food sources. If the change in isotopic value is due entirely to growth (i.e., $c_g = -1$), half of the consumer's tissue is derived from the new food source when the consumer doubles its weight (i.e., $H_g = 2$). We then calculated the fraction of new tissue derived from growth, T_g, and the fraction due to tissue replacement (also known as metabolic turnover), T_m, at the midpoint between the old and new diet values

$$T_g = \frac{H_g - 1}{H_g} \quad (7)$$

$$T_m = \frac{1 - 0.5H_g}{H_g} \quad (8)$$

The significance of the contribution of tissue replacement was evaluated by comparing T_m with –1 using a one-tailed t test with a critical value of 0.05. For all t tests that did not reject the hypothesis of $c_g = -1$ (i.e., all isotopic change is caused by growth), the statistical power of being able to detect a difference when tissue replacement constitutes ≥10% of the total amount of isotopic change (i.e., when $c_g \leq -1.43$) was calculated to buttress our inferences based on the magnitude of T_m (Zar 1984).

Sensitivity analysis

We used simulations to evaluate the influence of growth rate on parameter estimates of isotopic change and fractionation. This was done to aid our interpretation of our experimental results and to identify optimal experimental designs for future studies on changes in stable-isotope values following diet transitions. We made the following assumptions: (*i*) growth in dry weight, W, is an exponential function of time, t (i.e., $W_t = W_0 \exp(gt)$, where W_0 is a standardized initial size, g is a growth constant, and t is time), (*ii*) growth is measured without error, and (*iii*) error in the measured isotopic values is independent of growth rate. Although the second assumption is unlikely in reality, the addition of an error term to the growth constant would reduce our ability to resolve the effect of variable growth rates. In the simulation, samples were collected at 1, 2, 4, 8, 16, and 32 days after the transition to a new diet, as was the case in our experiments.

Isotopic values were calculated using the growth-based model (eq. 5) with a random error term. The error term was based on an earlier analysis of diet-driven isotopic change (Bosley et al. 2002). The parameters of isotopic change were set to $\delta_f = 6.4‰$, $\Delta\delta = -9.5‰$, and $c_g = -1.5$ — values within those reported for $\delta^{15}N$ in the literature (e.g., Bosley et al. 2002; Herzka and Holt 2000) or from our own work (the choice of N or C is arbitrary). Next, we created 30 data sets for each of 20 values of g ranging from 0.005 day^{-1} to 0.1 day^{-1} in increments of 0.005, resulting in a total of 600 simulated turnover experiments. Each of the 3600 values for $\delta^{15}N$ in this simulation (six sample dates × 20 g values × 30 runs) was calculated with an independent error term drawn from a normal distribution (mean = 0, SD = 0.49‰) based on analysis of our experimental results.

We used nonlinear regression to estimate rates of isotopic change and fractionation for each of the 600 simulated turnover experiments. Using standard starting values of $\delta_f = 10$, $\Delta\delta = -10$, and $c_g = -1$, we examined the effect of growth rate on the estimates of δ_f, which we view as a proxy for fractionation given that fractionation is calculated as the difference between δ_f and the isotopic value of the new diet. Finally, we determined the sensitivity of estimating the known parameter values (above) to growth rate variation. Accuracy of the estimate was quantified as the difference between the known and average estimated parameter value ($n = 30$ estimates per level of growth rate). Precision of the estimate was quantified using the standard error of the parameter estimates within each growth rate level.

Results

Our analyses of changes in the stable-isotope values of N and C and our estimates of fractionation are predicated on distinct isotopic profiles of the diet items fed to adult summer flounder and to the early life stages of their offspring. These diets (squid, rotifers, *Artemia*, and winter flounder) proved to be isotopically distinct (Table 1). The separation of isotopic values among diet sources was greater for N than for C. The isotopic profiles of the two female parents of our experimental specimens were similar to each other but dis-

© 2004 NRC Canada

Table 1. Estimates of isotopic values of diet items used in summer flounder diet transition experiments, also including estimates of isotopic values of tissue of the two females that produced the experimental specimens and isotopic values for the adult diet.

Source	$\delta^{15}N$	SD	$\delta^{13}C$	SD
Diet item				
Rotifer	2.7	0.5	−15.7	1.0
Artemia	14.7	0.1	−22.1	0.1
Winter flounder	13.8	1.4	−19.1	0.8
Adult tissue				
Female 1 (fin clip)	15	0.1	−17.3	0.2
Female 2 (fin clip)	15.4	0.1	−16.9	0.4
Adult diet (squid)	11.2	0.8	−19.1	0.4

tinct from that of their diet and the items fed to their offspring.

Yolk absorption

The isotopic profiles of prefeeding larvae differed from those of maternal tissue. The maternal $\delta^{15}N$ and $\delta^{13}C$ signals were enriched over (i.e., isotopically different from) their squid diet by 3.72‰ and 1.85‰, respectively, for female 1 and by 4.16‰ and 2.24‰ for female 2 (Table 1). The $\delta^{15}N$ values did not differ significantly among samples taken from fertilized eggs, larvae at hatching, larvae after yolk-sac absorption, or the adult females, whereas the $\delta^{13}C$ values did differ significantly among these stages (Figs. 1 and 2). The $\delta^{13}C$ values of the eggs and larvae at hatching were 2.0‰ and 2.5‰ lower, respectively, than the average maternal signal. The $\delta^{13}C$ values of larvae by the time they absorbed their yolk were similar at the two temperatures and 0.9‰ greater than those of the just-hatched larvae (Fig. 2). The increase in the $\delta^{13}C$ value was linear with respect to time for larvae at both temperatures and occurred more rapidly at the warmer one. The time to yolk depletion was shorter for larvae held at 22 °C (~3 days) than for those held at 13 °C (~7 days). The dry weight of larvae at hatching was lower than the dry weight of the eggs prior to hatching (Fig. 2). Dry weights of larvae decreased slightly but not significantly (linear regression, $p > 0.05$) during the period of yolk depletion.

First-feeding larvae

Tissues of young larvae displayed a clear transition from a maternal isotopic profile to one reflecting the rotifer prey (Figs. 1 and 3). Larvae grew from 3.76 mm (±0.06 SD) to 5.52 mm (±0.21) TL at 13 °C and from 3.64 mm (±0.05) to 6.08 mm (±0.21) TL at 22 °C during the 16-day experiment. The isotopic transition was slower for larvae at 13 °C than for those at 22 °C (Table 2). At 13 °C, the isotopic signal was halfway between the maternal and rotifer values after 7.5 days for $\delta^{15}N$ and 9.2 days for $\delta^{13}C$. The midpoint was reached about three times more quickly at 22 °C (3.2 days and 2.9 days for $\delta^{15}N$ and $\delta^{13}C$, respectively).

The differences in the rate of isotopic transition of larvae held at the two temperatures are largely attributable to their growth rates (Table 3). Summer flounder larvae held at 13 °C grew at about half the rate as those held at 22 °C. The increase in dry weight during the 16-day experiment was ~six-fold for larvae at 13 °C and 12-fold for larvae at 22 °C. The

Fig. 1. Joint distributions of $\delta^{15}N$ and $\delta^{13}C$ values for diet items and tissues of adult summer flounder (*Paralichthys dentatus*, SF) and the early life stages of their offspring. Diet items were squid (Sq) for adults (maternal signal, M-Sq); rotifers (R) and *Artemia* (A) for larvae; and *Artemia*-fed winter flounder (WF-A) for juveniles. (*a*) Vectors indicate isotopic transitions during early life stages — egg (E) to hatchling (H) to late yolk-sac larvae (SF-Y) to larvae feeding on rotifers (SF-R). (*b*) Isotopic transitions during larval and juvenile life stages feeding on rotifers to *Artemia* (SF-R) to *Artemia*-fed winter flounder (SF-WF). Ellipses represent 95% bivariate confidence intervals around each data centroid (solid line). Arrows indicate the vector of isotopic change for each diet shifts. Asterisks (*) indicate a significant correlation between $\delta^{13}C$ and $\delta^{15}N$.

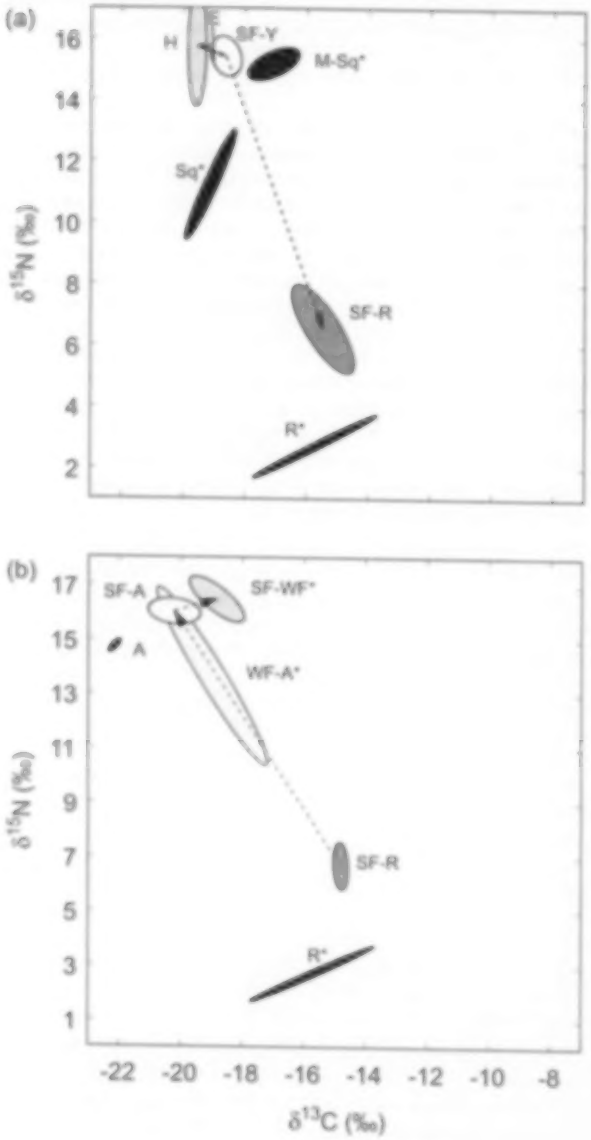

© 2004 NRC Canada

Fig. 2. Changes in dry weight (*a*), $\delta^{15}N$ (*b*), and $\delta^{13}C$ (*c*) in summer flounder (*Paralichthys dentatus*) eggs and unfed larvae. Sampling began with eggs at 2 days prior to hatching (time = –2 days) and continued through yolk depletion (time = 7 days for larvae at the cooler temperature (13 °C)). Triangles represent hatching larvae, circles represent eggs, diamonds represent larvae held at 13 °C, and squares represent larvae held at 22 °C.

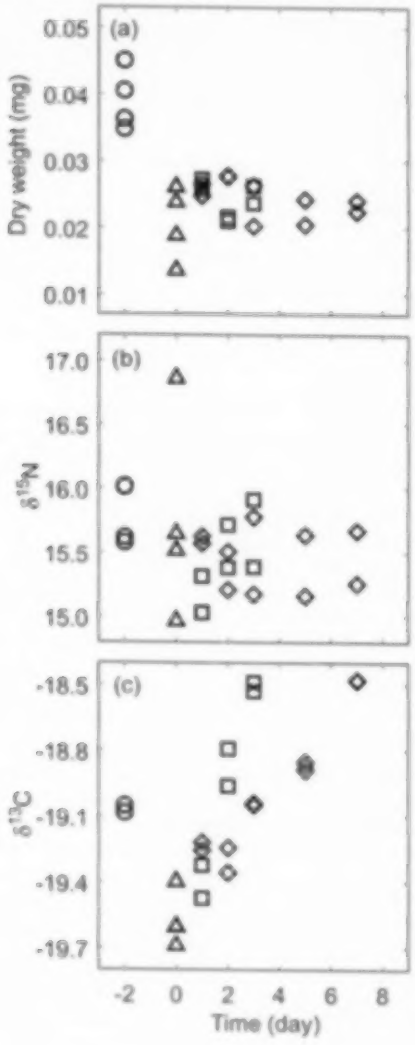

estimates of the equilibrium isotopic value and the contribution of tissue replacement tended to be higher at 13 °C than at 22 °C (Table 4). Estimates of the growth rate constant c_g were <-1 ($p < 0.05$ for both temperatures combined), meaning that for both temperatures, 50% of body tissues were derived from the new diet after only a 60% increase in dry weight.

The fractionation of both elements during the period of first-feeding resulted in the isotopic profile of larvae differing substantially from that of their rotifer prey (Fig. 1). The estimate of fractionation f_t of $\delta^{15}N$ exceeded that of $\delta^{13}C$, and both estimates varied with the temperature at which the fish were held and the estimation method used (Tables 2 and 4). The estimate of fractionation for $\delta^{15}N$ tended to be lower for larvae held in cooler water (1.59‰ and 2.79‰ at 13 and 22 °C, respectively) when the time-based model was used. Furthermore, estimates of fractionation of $\delta^{15}N$ were higher at both temperatures when the fish from the terminal collection, f_{tf}, were used to compute fractionation in the time-based model (Table 2). Estimates of $\delta^{15}N$ fractionation obtained using the growth-based model, f_g, tended to be higher at both temperatures (significantly so at 13 °C) than those derived from the time-based model. The growth-based estimates of $\delta^{15}N$ fractionation were not affected by temperature and did not differ from estimates based on fish from the terminal collection f_{tf}. The estimates of fractionation of $\delta^{13}C$ were higher and more variable when calculated using the time-based model compared with the growth-based one (Tables 2 and 4). Similar to results for $\delta^{15}N$, estimates of $\delta^{13}C$ fractionation for fish experiencing the two temperatures were more similar when derived from the growth-based model than when the time-based one was used.

Zooplankton transition

The isotopic profile of late-stage summer flounder changed after a diet transition from rotifers to *Artemia* (Figs. 1 and 4). Prior to the diet transition, the isotopic profile was nearly identical to the estimates of post-transition (rotifer) equilibrium from the first-feeding experiment described above. The isotopic shift occurred much more slowly for fish held at the cooler temperature — the half-life for N and C at 13 °C that was about half of those for 22 °C (Table 2, Fig. 4).

The change in the isotopic profile appears to be largely due to the increase in mass rather than the replacement of existing tissues (>90% due to growth vs. <10% due to replacement; Table 4). None of the estimates of the rate constant for the growth-based model c_g differed from –1, suggesting that isotopic change was attributable to growth alone with no tissue replacement. The statistical power of these tests, however, ranged from 0.32 to 0.65, so this conclusion is conditional until a more robust experimental design can be implemented.

As was found in the first-feeding experiment, the effect of temperature on estimates of half-life of isotopic change was largely mediated through effects on larval growth rates (Table 3). Summer flounder larvae held at 13 °C grew at one-third the rate of those held at 22 °C. The increase in dry weight during the 32-day experiment was approximately ninefold for larvae at 13 °C and 23-fold for larvae at 22 °C (corresponding to an increase in dry weights of 278.3-fold and 725.2-fold from the point of hatching). Rates of isotopic change relative to growth were similar for fish held at 13 °C and 22 °C (Fig. 4), as were estimates of the equilibrium values using either the time- or growth-based models for parameter estimation.

As in the first-feeding experiment, differences in the isotopic profile of the new prey (*Artemia*) and the flounder tissue at equilibrium with the new prey permitted estimates of fractionation for $\delta^{15}N$ and $\delta^{13}C$ (Fig. 1). Fractionation was consistently greater for $\delta^{15}N$ than for $\delta^{13}C$; however, the estimate of fractionation depended on the method used to derive the estimate (Tables 2 and 4). Estimates of fractionation for $\delta^{15}N$ and $\delta^{13}C$ at the two temperatures were much more con-

© 2004 NRC Canada

Fig. 3. Changes in $\delta^{15}N$ (*a*, *b*) and $\delta^{13}C$ (*c*, *d*) in summer flounder (*Paralichthys dentatus*) larvae that were fed rotifers for 16 days after first feeding (time = 0) relative to time (*a*, *c*) and to increase in relative biomass (*b*, *d*). Diamonds and solid lines represent larvae held at 13 °C; squares and dashed lines represent larvae held at 22 °C. Predicted isotopic values versus time are derived from the time-based model (eq. 2) for each temperature. Predicted isotopic values versus growth are derived from the growth-based model (eq. 5) for both temperatures combined (solid line).

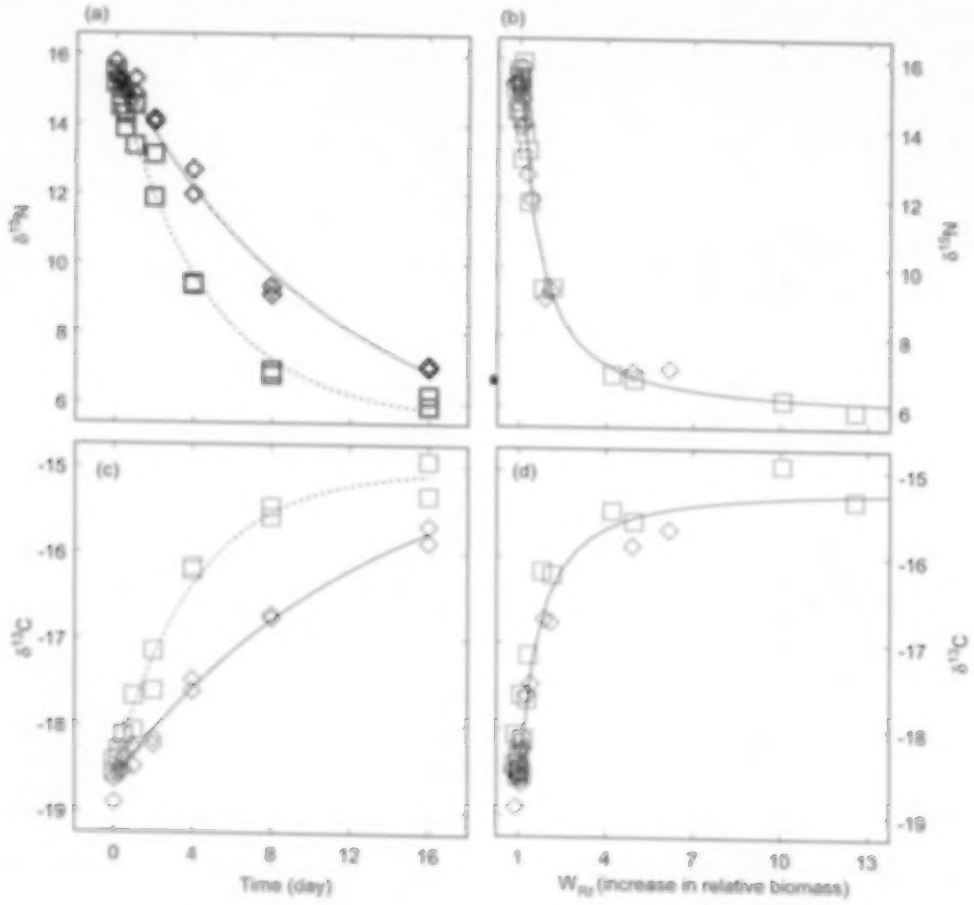

sistent when derived from the growth-based model rather than from the time-based one. Fractionation estimates did not differ between temperature treatments and varied by 0.27‰ ($\delta^{15}N$) and 0.39‰ ($\delta^{13}C$) for the two temperatures when derived from the growth-based model. The time-based model resulted in fractionation estimates that were affected by temperature, differing by 1.68‰ ($\delta^{15}N$) and 1.36‰ ($\delta^{13}C$) between the two temperatures. Estimates of fractionation of $\delta^{15}N$ based on the terminal samples, δ_d, were less than estimates based on the time- and growth-based models, whereas fractionation estimates for $\delta^{13}C$ based on the terminal samples were greater than estimates based on the time- and growth-based models.

Zooplanktivory to piscivory

The change in isotopic profile of the summer flounder after a diet transition from *Artemia* to winter flounder was more complicated than that observed in the other diet transition experiments (Fig. 5). The data centroids created by the winter flounder isotopic values for $\delta^{15}N$ and $\delta^{13}C$ are similar to the vector of isotopic change expressed by the summer flounder when shifted from rotifers to *Artemia*. This transition resulted in the isotopic profile of the summer flounder tissues shifting from an uncorrelated bivariate distribution of $\delta^{15}N$ and $\delta^{13}C$ that reflected the *Artemia* food source to a correlated distribution that is nearly parallel to that of its new prey but with a higher level of $\delta^{15}N$ and $\delta^{13}C$.

The estimates of rate and fractionation parameters varied considerably among the temperatures and methods used (Tables 2 and 4). Estimates of fractionation with respect to N had large errors when derived from predicted equilibrium values from the time-based model. Better estimates (i.e., smaller standard errors (SEs)) were obtained for fractionation with respect to C. Using the terminal samples of this experiment to calculate N fractionation resulted in estimates of 3.23 and 3.70 for the fish held at 13 and 22 °C, respectively. The estimates for C fractionation from the time-based model suggest that a reduction in $\delta^{13}C$ occurred at 13 °C, whereas it increased at 22 °C. A similar pattern occurred when the terminal samples were used to estimate fraction-

© 2004 NRC Canada

Table 2. Parameter estimates of isotopic change of N and C in summer flounder tissues in the diet-transition experiments using the time-dependent model.

Experiment	Isotope	Temp. (°C)	δ_f	SE	$\Delta\delta$	SE	c_t	SE	r^2	H_t	f_t	δ_{ti}	SD	f_{ti}
First-feeding larvae	δ^{15}N	13	4.3	1.0	11.4	1.0	–0.09	0.02	0.98	7.5	1.6	7.0	0.05	4.33
		22	5.5	0.4	9.9	0.4	–0.22	0.03	0.98	3.2	2.8	6.0	0.22	3.34
	δ^{13}C	13	–14.5	0.5	–4.1	0.5	–0.08	0.02	0.98	9.2	1.2	–15.8	0.13	–0.07
		22	–15.0	0.1	–3.5	0.1	–0.24	0.02	0.98	2.9	0.7	–15.1	0.29	0.57
Zooplankton transition	δ^{15}N	13	19.0	1.6	–12.4	1.5	–0.05	0.02	0.96	13.6	4.3	16.2	0.36	1.53
		22	17.3	0.6	–10.6	0.6	–0.11	0.02	0.96	6.1	2.6	16.6	0.34	1.88
	δ^{13}C	13	–22.3	0.8	7.3	0.8	–0.06	0.01	0.95	11.6	–0.1	–21.0	0.16	1.15
		22	–20.9	0.3	6.2	0.3	–0.14	0.02	0.96	5.0	1.2	–20.6	0.05	1.53
Zooplanktivory to piscivory	δ^{15}N	13	18.4	5.9	–2.4	1.0	–0.01	0.03	0.63	63.0	5.4	16.7	0.14	3.70
		22	19.4	16.7	–3.6	16.7	–0.01	0.04	0.54	99.0	6.4	16.2	0.31	3.23
	δ^{13}C	13	–18.9	0.7	–1.0	0.7	–0.04	0.06	0.38	16.9	–0.3	–19.2	0.06	–0.52
		22	–18.6	0.2	–1.4	0.2	–0.12	0.04	0.76	6.0	0.1	–18.6	0.21	0.11

Note: Parameters estimated are as follows: δ_f, asymptotic isotopic value; $\Delta\delta$, change in isotopic value after diet shift; c_t, time-model-specific turnover constant; R^2, proportion of variance explained by time-dependent model; H_t, half-life in days; f_t, fractionation; δ_{ti}, the average isotopic value of the final sample in the experiment; f_{ti} (a second estimate of fractionation) is based on the difference between δ_{ti} and the isotopic value of the new diet; SD, standard deviation; SE, standard error.

ation. The growth-based model could not be fit to the diet transition data for δ^{15}N. Slightly better estimates of rate parameters were generated for C when the growth-based model was used. Estimated values of the growth rate constant c_g suggest that tissue replacement contributed 22% at 13 °C and 47% at 22 °C (average of 34%) of the change in isotopic value of C, while growth contributed 50%–70%. Estimates of c_g differed from –1 for fish at 22 °C and when the data for fish from both temperatures were combined. Estimates of c_g did not differ from –1 for fish at 13 °C; however, the statistical power for that test was low (power = 0.10 to detect 10%, 0.11 to detect 20%, and 0.27 to detect 50% metabolic turnover), so some tissue replacement may have occurred but was not detected because of error in our estimates of c_g.

The growth rate (mg·day^{-1}) of summer flounder in the piscivory transition was much higher than that of earlier stage fish in the previous diet transitions (Table 3). When growth rate was scaled to the dry weight at the beginning of the experiment, W_i or as proportional increase in dry weight, G, it was considerably lower than those observed in the previous diet transitions. All measures of growth rates of summer flounder in the piscivory transition showed small differences in their growth between temperature treatments, with slightly faster growth in weight and length for flounder held at 22 °C.

Sensitivity analysis

Our simulations suggest that when growth rates are low, estimates of isotopic rate of change and fractionation will be inaccurate and imprecise (Fig. 6). The range of growth constants used in this simulation (0.0005–0.1 day^{-1}) translated to relative weight increases ranging from less than twofold to more than sixfold at the end of the 32-day simulation. When instantaneous growth rates were <0.05 day^{-1}, estimates of the asymptotic value overestimated the magnitude of change from the old value (i.e., an increase in absolute value of the new isotopic equilibrium). Precision of the estimated asymptotic value increased when growth rate was >0.05 day^{-1}. Estimates of c_g were less sensitive to growth rate; however, when growth rates were low (<0.02 day^{-1}), the growth-based model underestimated c_g. The precision in the estimates of c_g was also highly variable when growth rates were <0.02 day^{-1}.

Discussion

Our results add to a small but growing literature on the dynamics of isotopic change in the early life stages of fishes (Herzka and Holt 2000, 2001; Bosley et al. 2002). Not only do these ectothermic vertebrates have characteristically fast growth rates during this early part of their lives, but their rate processes are highly dependent upon environmental variables. Such subjects are likely to exhibit patterns in their constituent stable-isotope values that differ considerably from endothermic vertebrates, whose capacity for growth is relatively small. We confirmed that the isotopic composition of summer flounder in all life stages (adult, egg, yolk sac, post yolk sac, and juvenile) reflects the diet upon which it is feeding. We also found that the isotopic composition of an individual can change through processes other than feeding, as evidenced by the significant change in the δ^{13}C signal between eggs and just-hatched larvae, as well as the slight increases in the δ^{13}C values during yolk-sac period.

While the data presented here provide clear evidence that isotopic data can be used to infer feeding relationships, the accuracy of parameter estimates based on nonlinear regression or difference calculations were clearly sensitive to differences in the distribution of samples along the isotopic transition curve. An advantage of conducting experiments at several temperatures was that the two temperatures focused on different portions of the growth-dependent transition curve. This resulted in excellent coverage of the entire curve when both temperatures were combined, resulting in reasonable estimates of average values for the parameters of isotopic change. This differential coverage of the curve by the two temperatures, however, limited our ability to make direct comparisons of parameters between temperatures. This result

© 2004 NRC Canada

Table 3. Growth estimates for summer flounder in diet transition experiments.

Experiment	Temp. (°C)	Duration (days)	Mean dry weight (mg)		SL (mm)		Growth rate				
			T_0	T_f	T_0	T_f	mg·day^{-1}	G	W	W_b	min·day^{-1}
First-feeding larvae	13	16	0.0	0.1	—	—	0.01	0.11	5.6	5.6	—
	22	16	0.0	0.3	—	—	0.02	0.17	12.3	11.5	—
Zooplankton transition	13	32	0.7	6.3	—	—	0.17	0.07	8.7	278.3	—
	22	32	0.7	16.5	—	—	0.49	0.10	22.8	725.2	—
Zooplanktivory to piscivory	13	32	72.1	340.8	37.8	57.7	8.40	0.05	4.7	15 005.0	0.62
	22	32	81.0	429.0	40.1	61.3	10.87	0.05	5.3	18 880.1	0.66

Note: Experiments began on the day of the diet transition T_0 and continued for either 16 or 32 days to the final sampling day T_f. An initial length (SL) is recorded only for the piscivory experiment. Growth is expressed as (*i*) an increase in dry weight per day, mg·day^{-1}; (*ii*) an instantaneous growth rate (day^{-1}), G; (*iii*) a multiple of the initial dry weight, W; (*iv*) a multiple of the dry weight at hatching, W_b; and (*v*) min·day^{-1} (zooplankton to piscivory only).

highlighted the risks associated with evaluating temperature-dependent fractionation with a single sample after a common time period for all temperatures. We saw these results as a highlight of the pitfalls one could experience if time-series data were not collected when the details of isotopic turnover were being investigated.

Evaluation of the effect of life stage and water temperature on isotopic change

The decrease we observed in $\delta^{13}C$ values at hatching and during yolk-sac absorption likely reflect differences in isotopic composition of the egg chorion and the embryo within it and the fractionation of the contents of the yolk sac as they are assimilated into body tissue. Yúfera et al. (1999) determined that the chorion of Senegal sole, *Solea senegalensis*, is composed largely of proteins, which are likely to have a higher $\delta^{13}C$ value relative to lipids (DeNiro and Epstein 1977). Sole embryos, yolk, and oil globules had a higher lipid fraction compared with the chorion (Yúfera et al. 1999). The decreases we observed in the $\delta^{13}C$ signal between pre- and post-hatching, therefore, are likely due to the disproportionate loss of carbon in the chorion at hatching. The subsequent increase in $\delta^{13}C$ values with advancing age in the prefeeding larvae and a stable $\delta^{15}N$ value is consistent with the finding that prefeeding larvae principally catabolize carbon-rich compounds (primarily lipids) while nitrogen-rich compounds (proteins) remain practically unaltered from hatching to the time of first feeding (Yúfera et al. 1999).

Our estimates of the rates of isotopic change varied among the three exogenous-feeding life stages (first-feeding, late-larval, early juvenile) and between the two temperatures. The temperature effect on isotopic change appears to result entirely from the thermal effects on growth rate, as has been found previously for the early life stages of other marine fishes (Herzka and Holt 2000; Bosley et al. 2002). The between-life-stage differences in the contribution of tissue replacement differed from earlier results that could not resolve a significant component of tissue replacement (Herzka and Holt 2000; Bosley et al. 2002). We found a significant contribution of tissue replacement to overall isotopic change in the first-feeding experiment, with ~25% of the new tissue resulting from tissue replacement when 50% of the fish's tissues were derived from the new diet.

As in earlier studies of isotopic change in the early life stages of marine fish, we did not resolve a significant contribution of tissue replacement for the late larval stages (i.e., zooplankton transition experiment). While we cannot conclude that tissue replacement is not occurring, this result suggests a difference in energy allocation between the first-feeding and later larval stages. Higher rates of surplus tissue production during the late larval period may result from a variety of causes. Relatively more tissue rebuilding during the first-feeding stage may result from the development of new organs, ossification of bones, etc. Alternatively, the absolute allocation to tissue rebuilding may remain the same, but more energy is available, so surplus production of tissue (growth) is much greater. Increased available energy could result from increased consumption because of more efficient foraging or increased stomach capacity. Our growth data suggest that relative growth rates were similar between the two experiments conducted on feeding larval stages (first-

© 2004 NRC Canada

Table 4. Parameter estimates of isotopic change of N and C in summer flounder tissues in the diet-transition experiments using the growth-dependent model.

Experiment	Isotope	Temp. (°C)	δ_i	SE	$\Delta\delta$	SE	c_g	SE	r^2	H_g	T_g	T_m	f_g
First-feeding larvae	δ^{15}N	13	6.5	0.6	9.5	0.5	–1.7	0.3	0.97	1.5	0.66	0.34	3.8
		22	5.6	0.7	10.0	0.7	–1.4	0.3	0.95	1.7	0.80	0.20	2.9
		Combined	5.9	0.4	10.0	0.4	–1.5	0.2	0.96	1.6	0.75	0.25	3.2
	δ^{13}C	13	–15.5	0.2	–3.2	0.2	–1.4	0.2	0.98	1.6	0.79	0.21	0.2
		22	–15.1	0.2	–3.5	0.2	–1.6	0.4	0.94	1.6	0.71	0.29	0.6
		Combined	–15.2	0.2	–3.5	0.2	–1.4	0.2	0.95	1.6	0.78	0.22	0.5
Zooplankton transition	δ^{15}N	13	17.5	1.7	–11.0	1.6	–1.0	0.4	0.92	2.0	0.99	0.01	2.8
		22	17.8	1.6	–11.6	1.6	–1.0	0.3	0.85	2.0	0.99	0.01	3.1
		Combined	17.7	1.1	–11.4	1.0	–1.0	0.2	0.89	2.0	0.99	0.01	3.0
	δ^{13}C	13	–21.6	0.9	6.7	0.8	–1.2	0.4	0.92	1.8	0.91	0.09	0.5
		22	–21.2	0.8	6.7	0.9	–1.2	0.4	0.89	1.8	0.90	0.10	0.9
		Combined	–21.4	0.6	6.7	0.6	–1.2	0.3	0.89	1.8	0.90	0.10	0.8
Zooplanktivory to piscivory	δ^{15}N	13	26.0	80.6	–10.0	80.6	–0.1	0.5	0.73	—	—	—	—
		22	17.5	1.1	–1.5	1.1	–0.6	0.6	0.78	—	—	—	—
		Combined	30.0	743.2	–14.0	743.1	0.0	2.1	0.56	—	—	—	—
	δ^{13}C	13	–19.1	0.2	–1.3	0.2	–2.6	1.3	0.63	1.3	0.47	0.53	–0.4
		22	–18.7	0.2	–1.9	0.4	–5.9	2.8	0.61	1.1	0.22	0.78	–0.1
		Combined	–18.9	0.2	–1.6	0.2	–3.7	1.5	0.58	1.2	0.34	0.66	–0.3

Note: Parameters estimated are as follows: δ_i, asymtotic isotopic value; $\Delta\delta$, change in isotopic value after diet shift; c_g, weight-specific turnover constant; R^2, proportion of variance explained by growth-dependent model; H_g, relative increase in dry weight to produce an isotopic value of $\delta_i - \Delta\delta/2$ (weight-specific half-life); T_g, proportion of isotopic turnover explained by growth (i.e., increase in dry weight); T_m, proportion of isotopic turnover explained by metabolic activity that does not result in an increase in dry weight; f_g, fractionation; SE, standard error.

© 2004 NRC Canada

Fig. 4. Changes in $\delta^{15}N$ (*a*, *b*) and $\delta^{13}C$ (*c*, *d*) in summer flounder (*Paralichthys dentatus*) from the time of switching diet from rotifers to *Artemia* (time = 0) relative to time (*a*, *c*) and to increase in relative biomass (*b*, *d*). Diamonds and solid lines represent larvae held at 13 °C, and squares and dashed lines represent larvae held at 22 °C. Predicted isotopic values versus time are derived from the time-based model (eq. 2) for each temperature. Predicted isotopic values versus growth are derived from the growth-based model (eq. 5) for both temperatures combined (solid line).

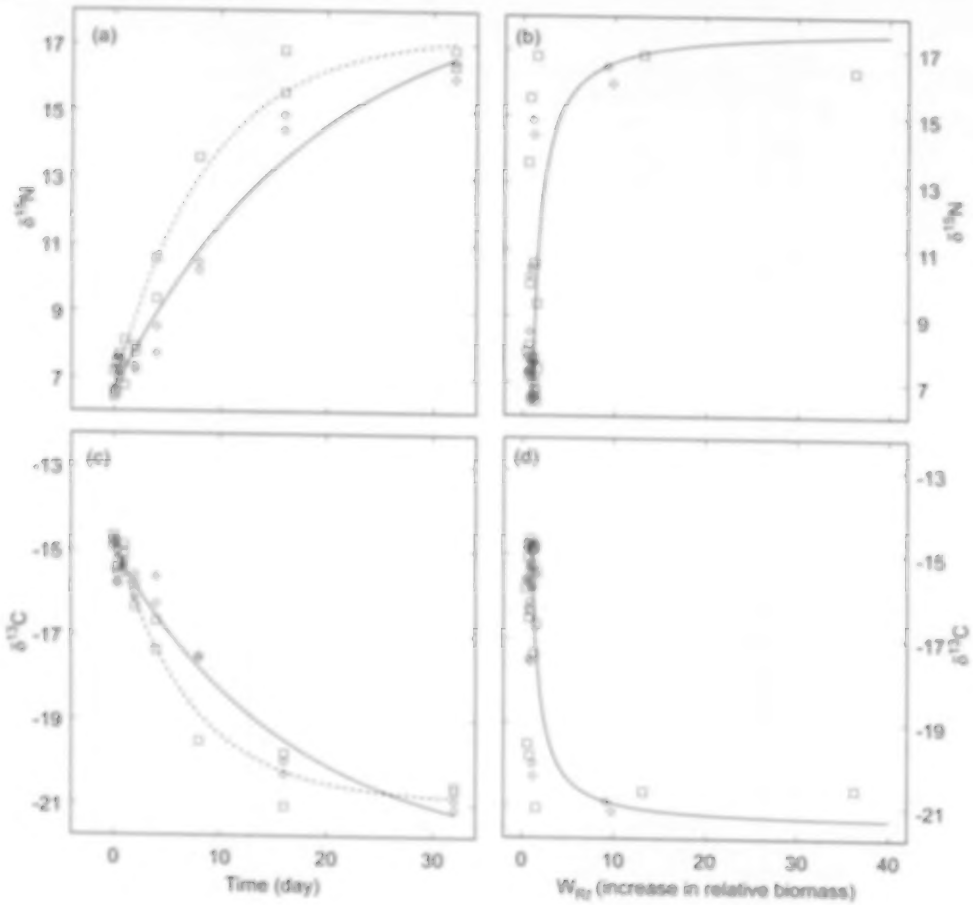

feeding and zooplankton transition). This coupled with lower values for c_g in the first-feeding larvae lends support for the former conclusion that tissue replacement is relatively higher during the first-feeding larval stage.

The zooplankton-to-piscivory experiment resulted in estimates of c_g that were considerably less than –1. However, we were not able to reject the null hypothesis of $c_g = -1$ as a result of the high error term associated with our estimate of c_g. While the possibility that a relatively large amount of tissue replacement contributed to isotopic change is worth noting, the juvenile summer flounder in our trophic-level-shift experiment grew relatively slowly (~0.6 mm·day^{-1}). Earlier experiments suggest that juvenile summer flounder are capable of growing at >1 mm·day^{-1} (Malloy and Target 1991; Szedlmayer et al. 1992) at the temperatures used in our experiments, suggesting that the juvenile summer flounder in our experiments were not growing maximally. In our experiments, nearly every winter flounder offered was consumed within a short time, and our supply of small winter flounder was limited. If it were possible to provide an unlimited food supply, it is likely that we would have observed higher growth rates and consequently a higher relative contribution of added tissues.

The experiment that evaluated the effect of a trophic-level shift on isotopic value involved complexities that reflect those that are likely to occur in nature. In our experiment, the diet of the winter flounder prey appeared to be in isotopic transition between a rotifer-based signal and an *Artemia*-based signal. While both flounders were reared in the laboratory on the same diet of rotifers followed by *Artemia*, the isotopic profile of the winter flounder had not reached equilibrium with their *Artemia* diet prior to their use as prey for summer flounder. The juvenile summer flounder, therefore, switched from feeding on one trophic level with a single, relatively stable, uncorrelated isotopic signature to a higher trophic level that reflected a mixed isotopic signal. As a result, they had a more variable and highly correlated isotopic signal. This variation in the isotopic signal in the winter

© 2004 NRC Canada

Fig. 5. Changes in $\delta^{15}N$ (*a*, *b*) and $\delta^{13}C$ (*c*, *d*) in summer flounder from the time of switching diet from *Artemia* to *Artemia*-fed winter flounder (time = 0) relative to time (*a*, *c*) and to increase in relative biomass (*b*, *d*). Diamonds and solid lines represent larvae held at 13 °C, and squares and dashed lines represent larvae held at 22 °C. Predicted isotopic values versus time are derived from the time-based model (eq. 2) for each temperature. Predicted isotopic values versus growth are derived from the growth-based model (eq. 5) for both temperatures combined (solid line).

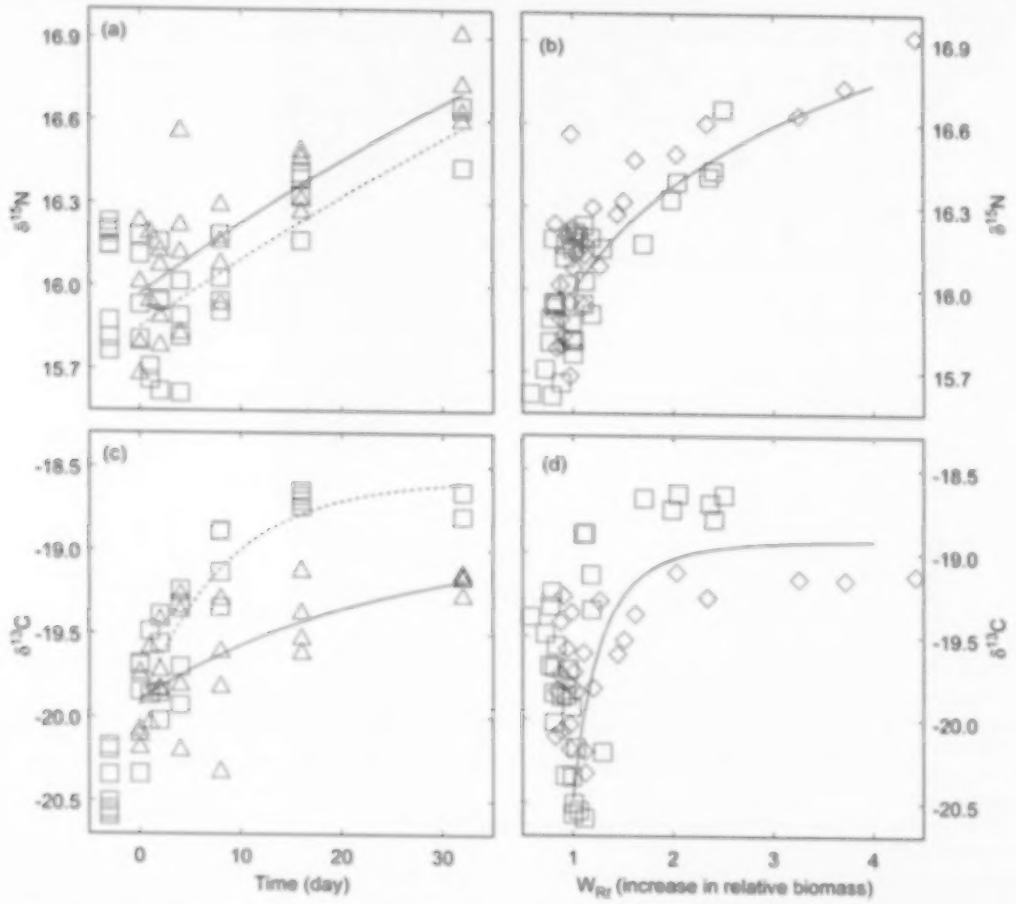

flounder was reflected in that of the summer flounder, but was shifted in a positive direction as a result of the fractionation of each isotope.

Isotopic fractionation

Our estimates for fractionation for the first two diet transitions derived from the asymptotic value predicted by the growth-based model and that of the parents are within the range of previously reported estimates for fishes (Hesslein et al. 1993; Pinnegar and Polunin 1999; Herzka and Holt 2000). They are also similar to the fractionation estimates that have been used in trophic-level studies of more diverse aquatic consumers (Vander Zanden et al. 1997). Our fractionation estimates for $\delta^{15}N$ in the first-feeding and rotifer-to-*Artemia* transitions were close to the ~3.5‰ reported in earlier literature (DeNiro and Epstein 1981; Minagawa and Wada 1984), but they exceeded those for the early life stages of red drum (*Sciaenops ocellatus*) reported by Herzka and Holt (2000), who found values of ~1.6‰. Bosley et al. (2002) investigated diet transitions in winter flounder and found fractionation of $\delta^{15}N$ to be 1‰–2‰. Our estimates of $\delta^{13}C$ fractionation (~0.50‰) were also similar to those reported previously. Macko et al. (1982) reported values of $\delta^{13}C$ fractionation as low as −1.0‰ for marine amphipods, whereas Pinnegar and Polunin (1999) found values as high as 2.2‰ for rainbow trout (*Salmo gairneri*).

Parameter estimation methods

We used and evaluated three methods of calculating fractionation, and all involved subtracting an estimate of the equilibrium isotopic value of the consumer's tissues from an average isotopic value of the diet. We obtained the most consistent estimates of fractionation by using the growth-based model to predicted equilibrium value on the new diet. This determination was consistent with our simulations that supported this method when growth rates were >5%·day^{-1}. Lower growth rates, including entire life stages or species with characteristically low growth rates, may require a dif-

© 2004 NRC Canada

Fig. 6. Changes in estimates of parameters of isotopic change with increasing growth rate (G ($\times 10^2$·day^{-1})) at two trajectories of isotopic change based on simulation analysis. The asymptotic value is used as a proxy for fractionation. Results are shown for a relative increase (dashed line) and decrease (solid line) in the isotopic value because of a new diet item. Estimates of the asymptotic value (*a*) and the growth-based turnover constant (*b*) with their standard errors, SE (*c*, *d*) are plotted against growth constants. Arrows and horizontal reference lines in (*a*) indicate direction of isotopic change and the known parameter values used in the simulation, respectively. The horizontal line in (*b*) indicates the known turnover parameter value used in the simulation.

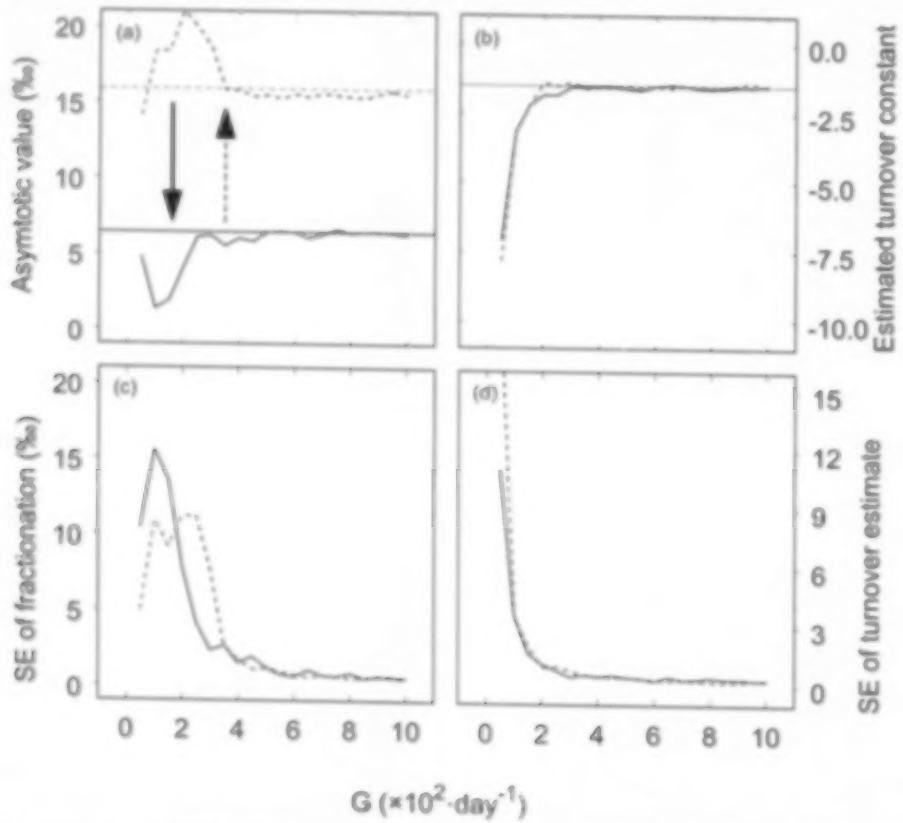

ferent and more prolonged sampling design than employed in this study. Low growth rate in the juvenile stage of summer flounder was likely a factor limiting our ability to estimate the growth constant c_g.

The time-based estimates of fractionation appeared to be affected by the direction of isotopic change. Fractionation was lower relative to growth-based estimates when the isotopic value of the new diet exceeded that of the old one, and it was higher when the isotopic value of the new diet was lower than that of the old one. This pattern was clear in the rotifer–*Artemia* transition, particularly at cooler temperatures when growth rates were slower. The time-based estimate of fractionation for δ^{15}N was significantly higher at 13 °C than at 22 °C. The δ^{13}C fractionation estimates had the opposite pattern. This temperature-specific difference in estimates of fractionation was not evident in results from the growth-based model and was likely an artifact of the parameter estimation method rather than a true temperature effect. It appeared that δ^{15}N and δ^{13}C were still changing for the 13 °C treatment, and the time-based asymptote was not fully achieved at the last sample.

The error associated with rate parameter estimates in asymptotic models is linked with that of the asymptotic value (Bates and Watts 1988). Error estimates of both rate and asymptote parameters can be reduced when more post-asymptotic time points are included in the analysis. One advantage of the time-based model is that the half-life constant provides an estimate of appropriate time scale for field and experimental studies. For example, a half-life of 3.5 days at a given temperature would predict that ~7 days are required for a consumer to be 75% toward isotopic equilibrium with its diet. The time-based half-life constant is particularly useful for slow-growing species or life stages. However, the same prediction may be made with higher accuracy for fast-growing species or life stages using the growth-based model if the growth history of the consumer can be estimated from otolith increment analysis or from growth models.

Although our estimates of the growth constant c_g were similar in magnitude to others reported previously for early life stages of fish (Herzka and Holt 2000; Bosley et al. 2002), these prior studies did not find c_g to differ from –1. Hence, previous investigators concluded that the isotopic transition in the tissues of early life stages of fish was attributable to growth with only a minor contribution from tissue replacement. This conclusion represents an inference based on failure to reject the null hypothesis and therefore should

© 2004 NRC Canada

Fig. 7. Contour plot of statistical power to detect the metabolic component of turnover. Isoclines are lines of equal statistical power. c_g is a rate constant to determine isotopic change for the growth model.

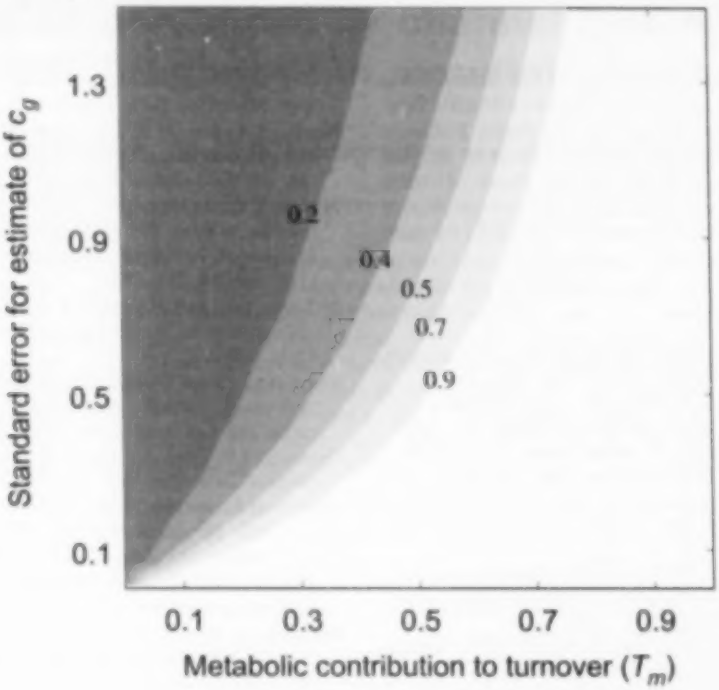

be coupled with an estimate of power to detect significant differences. We found that the estimated value of c_g was significantly less than –1 for the first-feeding transition, suggesting that tissue replacement contributed to 20%–30% of the overall isotopic change at the midpoint of the transition (i.e., when 50% of the body tissues are composed of the new diet). In the rotifer-to-*Artemia* transition, c_g was not significantly different from –1, but the statistical power of our test was low (<50% to detect a contribution of 10%). Our simulation analysis of the statistical power of such tests suggests that given the range of standard errors associated with estimates of c_g, it would be improbable to detect contributions of tissue replacement to isotopic change unless it accounted for >50% of the total isotopic change (Fig. 7).

Future directions

The probability that a consumer will exploit multiple sources of carbon and nitrogen increases with higher trophic levels, resulting in increasingly variable isotopic signals. In natural communities, higher trophic levels are occupied by consumers that may feed opportunistically on prey of variable trophic status, while primary consumers are not. Thus, a quantification of within-trophic-level isotopic autocorrelations in field collections is needed to be used as a baseline for evaluating food-web connectivity (Vander Zanden and Rasmussen 1999). This, combined with more traditional approaches, such as stomach content analysis, allows for a more complete interpretation of isotopic variation with respect to food-web dynamics (Vander Zanden et al. 1997).

Differences among studies in fractionation estimates for both elements could be related to the lipid and (or) protein composition of the diets that were used, the inherent level of isotopic variability in the diets, and the experimental design. In diet-transition studies such as ours, the estimates of fractionation depend largely on the extent to which the consumer has achieved equilibrium with its diet. We found and indeed expected a large error in the fractionation estimates in cases where equilibrium was not achieved. As described above, the magnitude and perhaps even the direction of this error may depend on the direction of isotopic change. These differences in fractionation estimates emphasize the need for further studies that quantify diet- and tissue-specific fractionation. It is important to note that studies of fractionation should always involve a time series of data that allow for a careful evaluation of an equilibrium state.

In summary, growth appears to be a better predictor of isotopic change than time for the early life stages of fish. This result will likely hold for life stages of other taxa that are in an exponential phase of a growth. Our data also suggest that the extent to which growth explains isotopic change will vary with the subject's life stage. We view these results as robust, but nevertheless argue for additional and improved experimental investigations into the processes that underlie the dynamics of isotopic change. We suggest that these future experiments be designed such that collection of data points is scheduled using predicted growth intervals rather than regular time intervals. This would help promote a more consistent coverage of the isotopic transition curve among treatments and consequently result in a more reliable comparison of parameter estimates. We especially encourage further experimental analyses that use isotopically stable diets to better evaluate hypotheses about the relative contribution

© 2004 NRC Canada

of tissue replacement and growth to isotopic change in ectothermic vertebrates under a range of natural conditions.

Acknowledgements

We are grateful to the National Oceanic and Atmospheric Administration (NOAA) – Rutgers Cooperative Marine Education and Research Program and the Northeast Fisheries Science Center of the National Marine Fisheries Service (NMFS) for support of this work. We also thank Michelle Walsh, Steve Lewis, and staff of the Coastal Ecology Branch at the Howard Marine Sciences Laboratory (NMFS) for their efforts.

References

Bates, D.M., and Watts, D.G. 1988. Nonlinear regression analysis and its applications. John Wiley & Sons, New York.

Bosley, K.L., Witting, D.A., Chambers, R.C., and Wainright, S.C. 2002. Estimating turnover rates of carbon and nitrogen in recently metamorphosed winter flounder, Pseudopleuronectes americanus, with stable isotopes. Mar. Ecol. Prog. Ser. **236**: 233–240.

Checkley, D.M. 1982. Selective feeding by Atlantic herring (*Clupea harengus*) larvae on zooplankton in natural assemblages. Mar. Ecol. Prog. Ser. **9**(3): 245–253.

Craig, H. 1957. Isotopic standards for carbon and oxygen and correction factors for mass-spectrometric analysis of carbon dioxide. Geochim. Cosmochim. Acta, **12**: 133–149.

DeNiro, M.J., and Epstein, S. 1977. Mechanism of carbon isotope fractionation associated with lipid synthesis. Science (Washington, D.C.), **197**: 261–263.

DeNiro, M.J., and Epstein, S. 1981. Influence of diet on the distribution of nitrogen isotopes in animals. Geochim. Cosmochim. Acta, **45**: 341–351.

Fry, B., and Arnold, C. 1982. Rapid $^{13}C/^{12}C$ turnover during growth of brown shrimp (Panaeus aztecus). Oecologia, **54**: 200–204.

Fry, B., and Sherr, E.X. 1984. $\delta^{13}C$ measurements as indicators of carbon flow in marine and freshwater ecosystems. Contrib. Mar. Sci. **27**: 13–47.

Grover, J.J., Eggleston, D.B., and Shenker, J.M. 1998. Transition from pelagic to demersal phase in early-juvenile Nassau grouper, Epinephelus striatus: pigmentation, squamation, and ontogeny of diet. Bull. Mar. Sci. **62**(1): 97–113.

Herzka, S.Z., and Holt, G.J. 2000. Changes in isotopic composition of red drum (Sciaenops ocellatus) larvae in response to dietary shifts: potential applications to settlement studies. Can. J. Fish. Aquat. Sci. **57**: 137–147.

Herzka, S.Z., and Holt, G.J. 2001. Documenting the settlement history of individual fish larvae using stable isotope ratios: model development and validation. J. Exp. Mar. Biol. Ecol. **265**: 49–74.

Hesslein, R.H., Hallard, K.A., and Ramlal, P. 1993. Replacement of sulfur, carbon, and nitrogen in tissue of growing broad whitefish (Coregonus nasus) in response to a change in diet traced by $\delta^{34}S$, $\delta^{13}C$, and $\delta^{15}N$. Can. J. Fish. Aquat. Sci. **50**(10): 2071–2076.

Hobson, K.A., and Clark, R.G. 1992. Assessing avian diets using stable isotopes I: turnover of ^{13}C in tissues. Condor, **94**: 181–188.

Jenkins, G.P. 1987. Comparative diets, prey selection, and predatory impact of co-occurring larvae of two flounder species. J. Exp. Mar. Biol. Ecol. **110**(2): 147–170.

Macko, S.A., Lee, W.Y., and Parker, P.L. 1982. Nitrogen and carbon isotope fractionation by two species of marine amphipods: laboratory and field studies. J. Exp. Mar. Biol. Ecol. **63**(2): 145–150.

Malloy, K.D., and Targett, T. 1991. Feeding growth and survival of juvenile summer flounder *Paralichthys dentatus*: experimental analysis of the effects of temperature and salinity. Mar. Ecol. Prog. Ser. **72**: 213–223.

McLaren, I.A., and Avendano, P. 1995. Prey field and diet of larval cod on Western Bank, Scotian Shelf. Can. J. Fish. Aquat. Sci. **52**(3): 448–463

Minagawa, M., and Wada, E. 1984. Stepwise enrichment of ^{15}N along food chains: Further evidence and the relation between d ^{15}N and animal age. Geochem. Cosmochim. Acta, **48**: 1135–1140.

Owens, N.J.R. 1987. Natural variations in ^{15}N in the marine environment. Adv. Mar. Biol. **24**: 390–451.

Peterson B.J., and Fry, B. 1987. Stable isotopes in ecosystem studies. Annu. Rev. Ecol. Syst. **18**: 293–320.

Pinnegar, J.K., and Polunin, N.V.C. 1999. Differential fractionation of $\delta^{13}C$ and $\delta^{15}N$ among fish tissues: implications for the study of trophic interactions. Funct. Ecol. **13**: 225–231.

Smigelski, A.S. 1975. Hormone-induced spawnings of the summer flounder and rearing of the larvae in the laboratory. Prog. Fish. Cult. **37**(1): 3–8.

Szedlmayer, S.T., Able, K.W., and Rountree, R.A. 1992. Growth and temperature-induced mortality of young-of-the-year summer flounder (*Paralichthys dentatus*) in southern New Jersey. Copeia, 1992: 120–128.

Vander Zanden, M.J., and Rasmussen, J.B. 1999. Primary consumer $\delta^{13}C$ and $\delta^{15}N$ and the trophic position of aquatic consumers. Ecology, **80**(4): 1395–1404.

Vander Zanden, M.J., Cabana, G., and Rasmussen, J.B. 1997. Comparing trophic position of freshwater fish calculated using stable nitrogen isotope ratios ($\delta^{15}N$) and literature dietary data. Can. J. Fish. Aquat. Sci. **54**: 1142–1158.

Waser, N.A., Yu, Z., Yin, K., Nielsen, B., Harrison, P.J., Turpin, D.H., and Calvert, S.E. 1999. Nitrogen isotopic fractionation during a simulated diatom spring bloom: importance of N-starvation in controlling fractionation. Mar. Ecol. Prog. Ser. **179**: 291–296.

Yúfera, M., Parra, G., Santiago, R., and Carrascosa, M. 1999. Growth, carbon, nitrogen and caloric content of *Solea senegalensis* (Pisces: Soleidae) from egg fertilization to metamorphosis. Mar. Biol. **134**: 43–49.

Zar, J.H. 1984. Biostatistical analysis. 2nd ed. Prentice-Hall, Inc., Englewood Cliffs, N.J.

© 2004 NRC Canada

Basin-scale availability of salmonid spawning gravel as influenced by channel type and hydraulic roughness in mountain catchments

John M. Buffington, David R. Montgomery, and Harvey M. Greenberg

Abstract: A general framework is presented for examining the effects of channel type and associated hydraulic roughness on salmonid spawning-gravel availability in mountain catchments. Digital elevation models are coupled with grain-size predictions to provide basin-scale assessments of the potential extent and spatial pattern of spawning gravels. To demonstrate both the model and the significance of hydraulic roughness, we present a scenario for optimizing the spatial extent of spawning gravels as a function of channel type in Pacific Northwest catchments. Predictions indicate that hydraulic roughness could control more than 65% of the potential available spawning habitat at our study sites. Results further indicate that bar roughness can be important for maintaining spawning gravels in lower mainstem reaches, while wood roughness may be required for spawning-gravel maintenance in steeper, upper mainstem channels. Our analysis indicates that wood loss and consequent textural coarsening could deplete up to one third of the potentially usable spawning area at our study sites.

Résumé : Nous présentons ici un cadre général pour l'examen des effets du type de chenal et de la rugosité hydraulique associée sur la disponibilité de graviers pour la fraye des saumons dans les bassins versants de montagne. Le couplage de modèles digitaux d'altitude et de prédictions des tailles des particules fournit une évaluation à l'échelle du bassin versant de l'étendue potentielle et de la répartition spatiale des graviers de fraye. Comme illustration du fonctionnement du modèle et de l'importance de la rugosité hydraulique, nous présentons un scénario pour l'optimisation de l'étendue spatiale des graviers de fraye en fonction du type de chenal dans les bassins versants de la région pacifique du nord-ouest. Les prédictions indiquent que la rugosité hydraulique peut contrôler plus de 65 % des habitats de fraye potentiellement disponibles dans nos sites d'étude. Les résultats indiquent de plus que la rugosité due aux seuils peut être importante pour le maintien des graviers de fraye dans les sections d'aval du cours principal, alors que la rugosité due au bois est nécessaire pour le maintien des graviers de fraye dans les cours principaux d'amont à pente plus forte. Notre analyse montre que la perte du bois et la texture plus grossière qui en résulterait pourraient éliminer jusqu'à un tiers de la surface utilisable potentielle de fraye dans nos sites d'étude.

[Traduit par la Rédaction]

Introduction

Channel characteristics such as temperature, depth, velocity, percent fines, and intragravel flow affect selection of salmonid spawning sites (Bjornn and Reiser 1991), but perhaps the most important characteristic is the size of sediment in which an adult salmonid can excavate a redd. As a family, salmonids prefer to spawn in sediments ranging in size from small gravel to cobble (Kondolf and Wolman 1993). The availability of sediment suitable for spawning depends on two geomorphic factors: (*i*) channel hydraulics and (*ii*) sediment supply. Channel hydraulics control the shear stress and competence of the river (largest size of sediment that the channel can carry) and are modified by channel type and associated hydraulic roughness (Buffington and Montgomery 1999*a*). Sediment supply controls the size and volume of material available to be transported and hydraulically sorted into suitable spawning habitats. In this paper, we assess the influence of hydraulic roughness on sediment size and spawning habitat availability.

Theory

The following theoretical development is an extension and modification of concepts originally proposed by Dietrich et al. (1996) and Montgomery et al. (1998).

Surface grain size in gravel- and cobble-bed rivers is strongly controlled by channel hydraulics and the consequent

Received 26 November 2003. Accepted 10 June 2004. Published on the NRC Research Press Web site at http://cjfas.nrc.ca on 18 January 2005.
J17862

J.M. Buffington.[1,2] Department of Civil Engineering, Ecohydraulics Research Group, University of Idaho, 800 Park Boulevard, Suite 200, Boise, ID 83712, USA.
D.R. Montgomery and H.M. Greenberg. Department of Earth and Space Sciences, University of Washington, Seattle, WA 98195-1310, USA.

[1]Corresponding author (e-mail: jbuffington@fs.fed.us).
[2]Present address: USDA Forest Service, Rocky Mountain Research Station, 316 E. Myrtle Street, Boise, ID 83702, USA.

 doi: 10.1139/F04-141 © 2004 NRC Canada

Fig. 1. Reach-average median surface grain size (D_{50}) as a function of total bank-full shear stress (τ) and channel type (modified from Buffington and Montgomery 1999*a*). Circles represent plane-bed channels, triangles represent wood-poor pool–riffle channels, and squares represent wood-forced pool–riffle channels. Right side of figure shows D_{50} ranges preferred by different salmonid species (Kondolf and Wolman 1993), with solid circles indicating median values and open circles indicating inner and outer quartiles of each distribution. Gray area defines typical range of suitable D_{50} values based on overall range of quartiles.

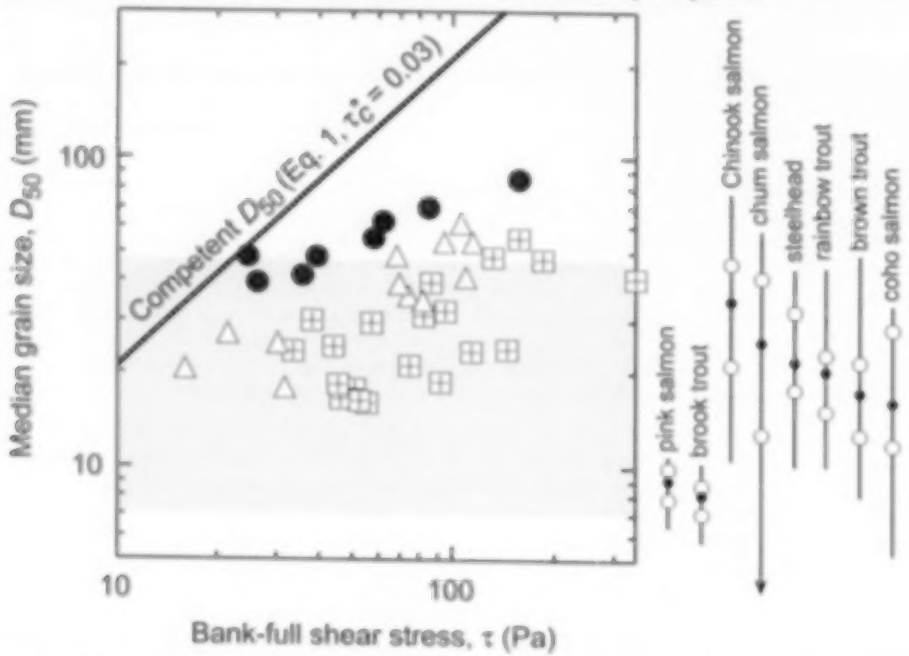

boundary shear stress that is imparted to the streambed (Buffington and Montgomery 1999*b*). In particular, the bank-full flow is the dominant discharge influencing sediment transport, surface grain size, and channel morphology in many alluvial rivers (e.g., Wolman and Miller 1960; Parker 1978; Andrews 1984; Andrews and Nankervis 1995). The median surface grain size (D_{50}) that can be mobilized by the bank-full flow can be predicted from the Shields (1936) equation

$$(1) \qquad D_{50} = \frac{\tau}{(\rho_s - \rho)g\tau_c^*} = \frac{\rho hS}{(\rho_s - \rho)\tau_c^*}$$

where τ is the total bank-full shear stress defined from the depth–slope product (ρghS), ρ_s and ρ are sediment and fluid densities, respectively, g is gravitational acceleration, h is bank-full depth, S is channel slope, and τ_c^* is the critical Shields stress for movement of D_{50} (see review by Buffington and Montgomery 1997). All values in eq. 1 are reach-average quantities.

Equation 1 is a theoretical prediction of competence (largest mobile D_{50}), assuming that particle size is not limited by local sediment supply. Although surface grain size can be modified by local sediment supply (Dietrich et al. 1989; Buffington and Montgomery 1999*b*), particle abrasion (Dietrich and Dunne 1978; Parker 1991), and chemical decomposition (Bradley 1970), downstream variations in substrate size in mountain rivers are principally driven by spatial changes in shear stress and channel competence (Constantine et al. 2003; Brummer and Montgomery 2003; Mueller and Pitlick 2005). That is to say, rivers hydraulically sort the sediment that is supplied to them. However, the supply of sediment in mountain basins can be punctuated in both space and time. In particular, local point sources of sediment from tributaries and hillslope mass wasting can interrupt and reset downstream fining trends (Rice 1998; Cui and Parker 2005) and may have significant influences on faunal distributions (Rice et al. 2001*a*, 2001*b*). Wood jams and other flow obstructions can also dam sediment, forcing textural changes that disrupt or modify larger-scale downstream fining trends (Rice and Church 1996).

Equation 1 predicts the competent D_{50} as a function of the total boundary shear stress (τ). However, rivers contain a variety of roughness elements (such as bars, wood, and bank irregularities) that extract momentum from the flow and reduce the reach-average shear stress acting on the streambed. Consequently, it is expected that channels with greater hydraulic roughness will have relatively smaller substrate sizes. Field data from forest gravel-bed rivers in western Washington and southeastern Alaska support this hypothesis (Fig. 1). For a given τ, observed values of D_{50} systematically decrease as one moves from plane-bed to pool–riffle to wood-forced pool–riffle channel types (morphologic definitions of Montgomery and Buffington 1997, 1998; Buffington et al. 2003). The observed decrease in surface grain size is due to a systematic increase in hydraulic roughness and a consequent reduction of channel competence (Buffington and Montgomery 1999*a*). Plane-bed channels generally have the least amount of roughness, with resistance primarily due to

© 2004 NRC Canada

bank irregularities, bed-surface grains, and occasional pieces of wood debris. Wood-poor pool–riffle channels have an additional source of roughness because of topographic form drag (bars). Wood-forced pool–riffle channels have the greatest roughness because of the addition of abundant wood debris and the combined effects of grain, bank, bar, and wood resistance.

Because these data come from forest rivers, wood debris is present in each of the channel types. Although the sites were selected to minimize wood abundance in the plane-bed and pool–riffle channels, there is a systematic increase in wood loading from plane-bed to pool–riffle to wood-forced pool–riffle sites. The increase in wood loading across the sites forces a higher frequency of bed and bank scour, causing greater bank and bed topography and a systematic increase in form drag that reduces channel competence and surface grain size (see Buffington and Montgomery 1999*a* for further detail). Systematic increases in roughness due to greater particle form drag (lower relative submergence) and lower channel width–depth ratios at steeper slopes are also incorporated in each data set (see Buffington and Montgomery 2001).

Figure 1 demonstrates that channel type and associated hydraulic roughness alter channel competence and observed substrate size relative to that predicted by eq. 1. Moreover, comparison of the range of roughness effects to the size of salmonid spawning gravels shows that these effects may have important implications for the availability of salmonid spawning habitat in mountain catchments. The right side of Fig. 1 shows ranges of median grain sizes preferred by different salmonid species for spawning (Kondolf and Wolman 1993). Comparison of observed median grain sizes with those preferred by spawning salmonids suggests that bar and wood roughness can produce suitable substrate in channels that might otherwise be too coarse. We explore this issue by coupling the above theory and observations with digital elevation models (DEMs) to predict the potential spatial distribution of salmonid spawning gravels as a function of channel type and hydraulic roughness in mountain catchments. Our intent is to provide a general framework for assessing spawning habitat availability, which can be modified, as needed, for basin-specific and species-specific concerns.

Analysis framework

Here, we describe the general procedure for evaluating parameters in eq. 1 and for assessing potential spawning-gravel availability at basin scales. We then present an application of our analysis framework that systematically examines the potential influence of channel type and hydraulic roughness.

Assuming that sediment and water densities are known (typically 2650 and 1000 $kg \cdot m^{-3} \cdot s^{-1}$, respectively), the only remaining unknown parameters for predicting D_{50} from eq. 1 are channel slope (S), bank-full depth (h), and critical Shields stress (τ_c^*); all reach-average quantities. We obtain S from DEMs, predict h from local hydraulic geometry relationships, and predict τ_c^* as an empirical function of channel type and associated roughness.

Bank-full depth can be predicted from region-specific hydraulic geometry relationships (Leopold et al. 1964; Dunne and Leopold 1978). In these relationships, bank-full depth is expressed as a power function of drainage area (a surrogate for bank-full discharge)

$$h = \alpha A^{\beta} \qquad (2)$$

where A is drainage area, and α and β are empirical values representing local physiography (geology, topography, and climate), basin hydrology, and sediment supply.

To evaluate the Shields stress, we assume a bank-full threshold for significant sediment transport (e.g., Henderson 1963; Parker 1978; Buffington and Montgomery 1999*a*), such that the critical Shields stress can be approximated by the mean bank-full value ($\tau_c^* \approx \tau_{bf}^* = \tau / [(\rho_s - \rho) g D_{50}]$). This is a reasonable assumption for coarse-grained channels typically used by salmonids. In particular, many authors have shown that gravel- and cobble-bed rivers have a near bank-full threshold for sediment transport (e.g., Leopold et al. 1964; Parker 1978; Andrews 1984) and that the bank-full flow is the dominant discharge (that which controls channel morphology and transports the most sediment in the long term) (e.g., Carling 1988; Andrews and Nankervis 1995; Emmett and Wolman 2001). A bank-full threshold for significant sediment transport assumes a low bed load supply (Buffington and Montgomery 1999*a*). As bed load supply increases, surface grain sizes fine, reducing the threshold for sediment transport to values less than bank-full (e.g., Dietrich et al. 1989; Buffington and Montgomery 1999*b*; Lisle et al. 2000). The assumption of a low bed load supply may not be valid for areas that have been recently disturbed by fire or logging or areas with chronically high sediment inputs (e.g., weak lithologies or persistent mass wasting).

Using field data, we express τ_{bf}^* as a power function of mean bank-full shear stress (τ), with separate functions for different channel types (Fig. 2). Although τ appears in both variables of the plot (τ_{bf}^* is calculated from τ (eq. 1)), it is nonetheless useful to express τ_{bf}^* as a function of τ as part of our model development. The stratification of these data represents channel response to hydraulic roughness similar to that of Fig. 1 (Buffington and Montgomery 2001). Hence, we use τ_{bf}^* as a roughness correction factor (i.e., τ_{bf}^* is an apparent value of τ_c^* that incorporates channel roughness; greater roughness reduces channel competence and observed bed-surface grain size, resulting in apparently larger values of τ_{bf}^*). Textural response to local bed load supply (as discussed above) is also implicitly included in τ_{bf}^*.

The relationships shown in Fig. 2 can be mathematically represented as

$$\tau_{bf}^* = k \tau^n = k(\rho g h S)^n \qquad (3)$$

where k and n are empirical values that vary with channel type and local catchment conditions.

Channel type and selection of appropriate values for k and n are predicted from stream gradient (Fig. 3). Previous studies demonstrate that different reach-scale channel types preferentially occur over different ranges of channel gradient (Montgomery and Buffington 1997, 1998; Buffington et al. 2003). Although the observed gradient ranges of different channel types overlap, they nonetheless have nonoverlapping central tendencies (25th–75th percentiles of slope) that allow first-order prediction of channel type based on reach-average channel gradient. A continuous range of slopes is developed

© 2004 NRC Canada

Fig. 2. Bank-full Shields stress (τ^*_{bf}) as a function of total bank-full shear stress (τ) and channel type in Pacific Northwest rivers (morphologic definitions of Montgomery and Buffington 1997, 1998; Buffington et al. 2003). PR, pool–riffle (circles); PB, plane-bed (open triangles); wfPR, wood-forced pool–riffle (squares); SP, step–pool (diamonds); CA, cascade (solid triangles). PR, PB, and wfPR data are from Buffington and Montgomery (1999*a*, 2001); SP and CA data are from Montgomery and Buffington (1997).

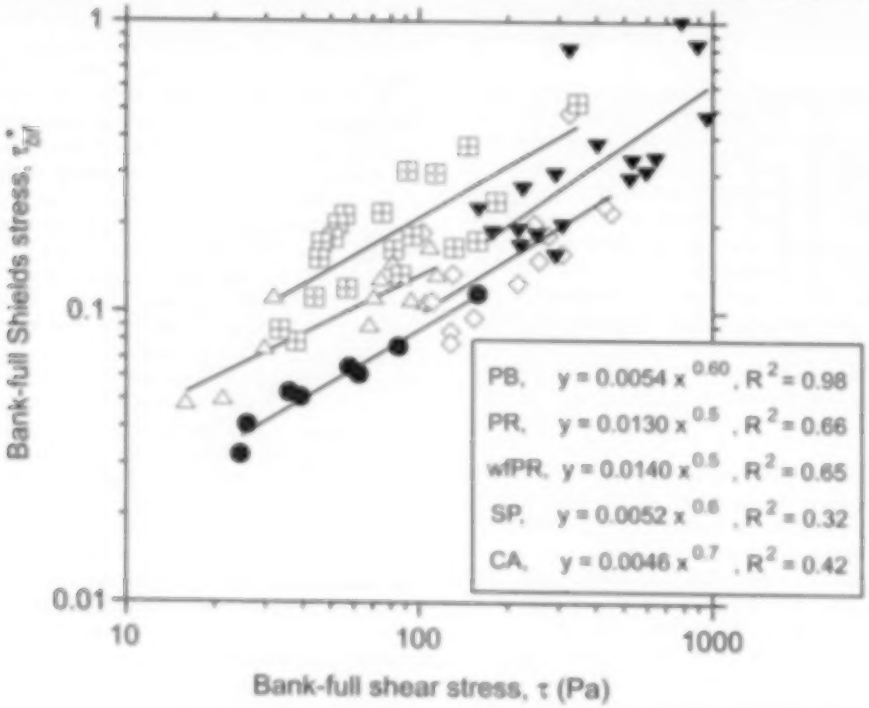
Bank-full Shields stress, τ^*_{bf}
1
0.1
0.01
10
100
1000
Bank-full shear stress, τ (Pa)
PB, y = 0.0054 x^0.60, R^2 = 0.98
PR, y = 0.0130 x^0.5, R^2 = 0.66
wfPR, y = 0.0140 x^0.5, R^2 = 0.65
SP, y = 0.0052 x^0.6, R^2 = 0.32
CA, y = 0.0046 x^0.7, R^2 = 0.42

Fig. 3. Box plots of channel gradient for different reach-scale channel types. The horizontal line within each box indicates the median value, box ends are quartiles, and whiskers are tenths. PR, pool–riffle; PB, plane-bed; wfPR, wood-forced pool–riffle; SP, step–pool; CA, cascade. See Buffington et al. (2002, 2003) for data sources. Broken lines define typical slope ranges for each channel type.

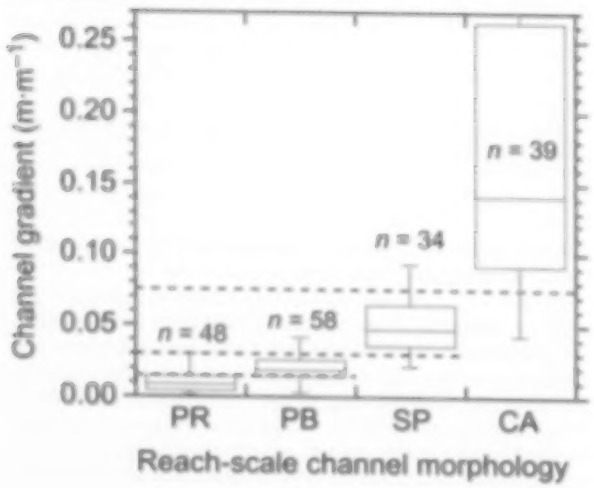

for predicting channel type by selecting range boundaries as the approximate midpoint between successive box ends. The resulting characteristic slope ranges are as follows: <1.5% for pool–riffle channels, >1.5%–3% for plane-bed channels, >3%–7.5% for step–pool channels, and >7.5% for cascade channels (Fig. 3). Characteristic slopes for each channel type are statistically different for both their central tendencies (box ranges) and the above continuous ranges (*t* test, $p < 0.05$, Bonferroni correction). However, channel morphologies different from those expected for a given slope range can occur, particularly where due to external forcing. For example, in forested basins wood debris can force a pool–riffle or step–pool morphology in channels that might otherwise have a plane-bed morphology (Montgomery et al. 1995; Montgomery and Buffington 1998). Moreover, reach-scale channel morphology can be influenced by the local sediment supply. Channels with high transport capacities and low sediment supplies may scour to bedrock and not produce the alluvial channel type expected from the above channel gradient ranges. In some settings with relatively uniform sediment supplies, the occurrence of bedrock versus alluvial channel types can be predicted by considering drainage area (a surrogate for both discharge and basin sediment supply) in addition to channel slope (Montgomery et al. 1996*a*; Massong and Montgomery 2000). Finally, recent debris-flow scour or deposition also can alter the expected channel type.

In general, alluvial channel type can be predicted from slope and combined with empirical τ^*_{bf} functions to correct

© 2004 NRC Canada

grain-size predictions for channel type and associated roughness. However, predictions of channel type based on stream gradient should be viewed as first-order approximations that require field validation and empirical adjustment for local catchment conditions.

Inserting eqs. 2 and 3, eq. 1 can be rewritten as

$$D_{50} = \frac{(\rho \alpha A^{\beta} S)^{1-n}}{(\rho_s - \rho) k g^n} \quad (4)$$

Equation (4) indicates that for a given channel type and for a given physiographic region (i.e., for specific values of k, n, α, and β), surface grain size can be predicted as a function of drainage area and slope, values readily determined from a DEM. Reach-average values of D_{50} predicted from eq. 4 are then compared with preferred spawning-gravel sizes (e.g., Kondolf and Wolman 1993) to assess the availability and spatial distribution of suitable spawning reaches. To demonstrate the model and explore the significance of hydraulic roughness, we present a sample application using data from Pacific Northwest catchments and channel types.

Methods

Study sites and analysis

We examined three mountain catchments in western Washington, USA (Fig. 4). The Boulder River (a tributary to the North Fork Stillaguamish River) and Finney Creek (a tributary to the Skagit River) are located in the Northern Cascades north of Seattle. The Willapa River is located along the Pacific coast south of Seattle. The drainage networks of the Boulder River and Finney Creek basins are characterized by a variety of alluvial channel types, ranging from low-gradient plane-bed and pool–riffle channels to steep-gradient step–pool and cascade channels (morphologic definitions of Montgomery and Buffington 1997, 1998; Buffington et al. 2003). In contrast, the channels of the Willapa basin are a mixture of alluvial and bedrock reaches, with many of the alluvial channels forced by large wood jams on slopes that otherwise would not support alluvial deposits (Massong and Montgomery 2000).

These three basins were chosen because of the availability of hydraulic geometry data and because the basins represent a broad range of lithology, geologic history, and physical size. The Boulder River and Finney Creek are underlain by Cretaceous metamorphic rocks (folded and foliated phyllite, greenschist, and argillitic mélanges) and glacial sediments derived from Pleistocene ice-sheet advances (Tabor et al. 2002). In contrast, the Willapa River is incised into Tertiary marine sediments (sandstones, siltstones, and mudstones) and Eocene marine basalts (Massong and Montgomery 2000). The glacial histories of the basins also differ. Both the Boulder River catchment and the Finney Creek basin contain abundant ice-sheet deposits from Pleistocene glaciation, while the Willapa basin escaped glaciation because of its position south of the Pleistocene ice-sheet advance. The physical size of the study basins also differs. The drainage area of the Boulder River catchment (63 km^2) is roughly half the size the Finney Creek basin (128 km^2), which is in turn about one-fifth the size of the Willapa River basin (680 km^2).

Ten-metre DEMs (based on 40-ft contour lines; 1 foot = 0.3048 m) were used for each study basin. For the Finney Creek basin, the drainage network was determined from the DEM in terms of critical values of slope and drainage area needed to support channel incision and maintenance of a stream network (Montgomery and Dietrich 1992). Following the approach suggested by Montgomery and Foufoula-Georgiou (1993), cells were classified as streams if the product of drainage area and slope squared exceeded 50 000 m^2 (a value the produces good agreement between predicted and observed stream networks in the study area). For both the Boulder and Willapa catchments, the drainage networks were defined from the Washington State Department of Natural Resources hydrology coverage, which is based on channels occurring on the US Geological Survey 7.5′ topographic maps and supplementary interpretation of aerial photographs. For all basins, individual channel segments were defined between the intersection of blue lines and 40-ft contours depicted on 7.5′ quadrangles. These segments were further divided at tributary confluences that occurred between contour intervals.

Hydraulic geometry relationships for predicting bank-full depth were obtained from field studies (Fig. 5). τ^*_{bf} values were predicted as a function of channel type (from Figs. 2 and 3). Based on salmonid preference for gravel- and cobble-bed rivers (Montgomery et al. 1999), we focused our analysis on channels with slopes <3% (typical of plane-bed, pool–riffle, and forced pool–riffle morphologies having gravel–cobble beds (Montgomery and Buffington 1998; Buffington et al. 2003). In contrast, alluvial channels with slopes greater than 3% tend to be composed of boulder-sized substrate (step–pool and cascade morphologies) that are generally inhospitable for spawning salmonids. Although salmonids (particularly resident species) do spawn in gravel and cobble patches that occur in local backwater areas and low shear-stress environments in these steep channels (Kondolf et al. 1991), salmonids typically prefer lower-gradient, plane-bed and pool–riffle channels (Inoue et al. 1997; Montgomery et al. 1999).

We conducted three sets of analyses to illustrate our approach and to systematically evaluate the potential effects of hydraulic roughness on spawning-gravel availability in channels with gradients <3%. Scenario 1 examines an idealized case in which all channels have a plane-bed morphology. This is an end-member case, representing low hydraulic roughness (Montgomery et al. 1998; Buffington and Montgomery 1999*a*). Scenario 2 predicts spawning-gravel availability in a network composed of both plane-bed and pool–riffle channels. This case represents the addition of bar roughness and predicts channel type based on characteristic gradients (i.e., <1.5% for pool–riffle, >1.5%–3% for plane-bed; Fig. 3). Hence, this scenario describes the effects of self-formed plane-bed and pool–riffle morphologies and their associated roughness. Scenario 3 adds wood roughness and optimizes the occurrence of plane-bed, pool–riffle, and wood-forced pool–riffle channels to maximize spawning-gravel availability. Where surface grain size is predicted to be too coarse for spawning with a plane-bed morphology, a pool–riffle morphology is selected to add bar roughness and reduce substrate size. If the predicted grain size is still too coarse to be suitable for spawning, a wood-forced pool–riffle morphology is selected

© 2004 NRC Canada

Fig. 4. Study site locations in Washington, USA.

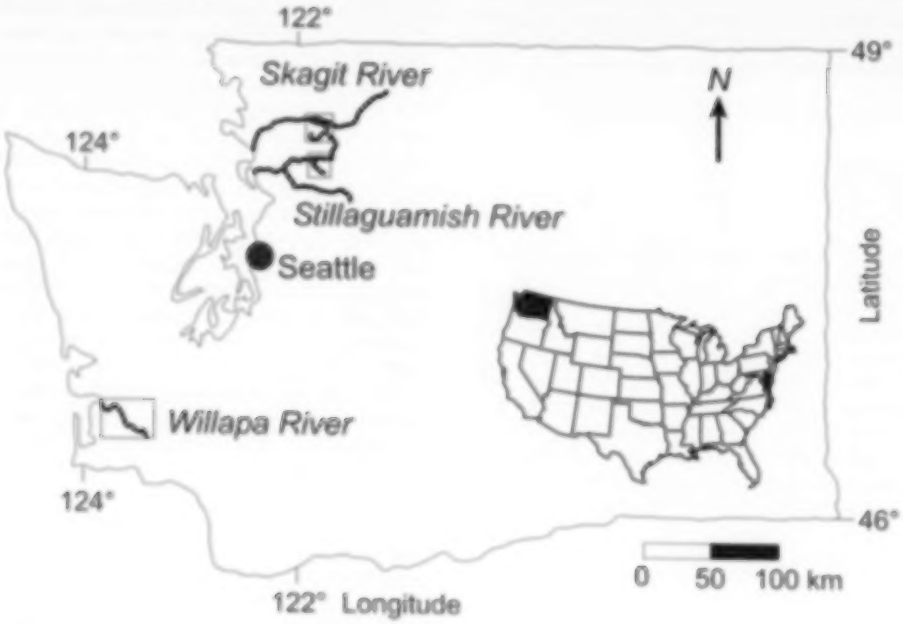

Fig. 5. Bank-full depth (h) versus drainage area (A) for the Willapa River (open circles; data from Massong and Montgomery 2000) and the Boulder River and Finney Creek (solid circles; data from Montgomery et al. 1998).

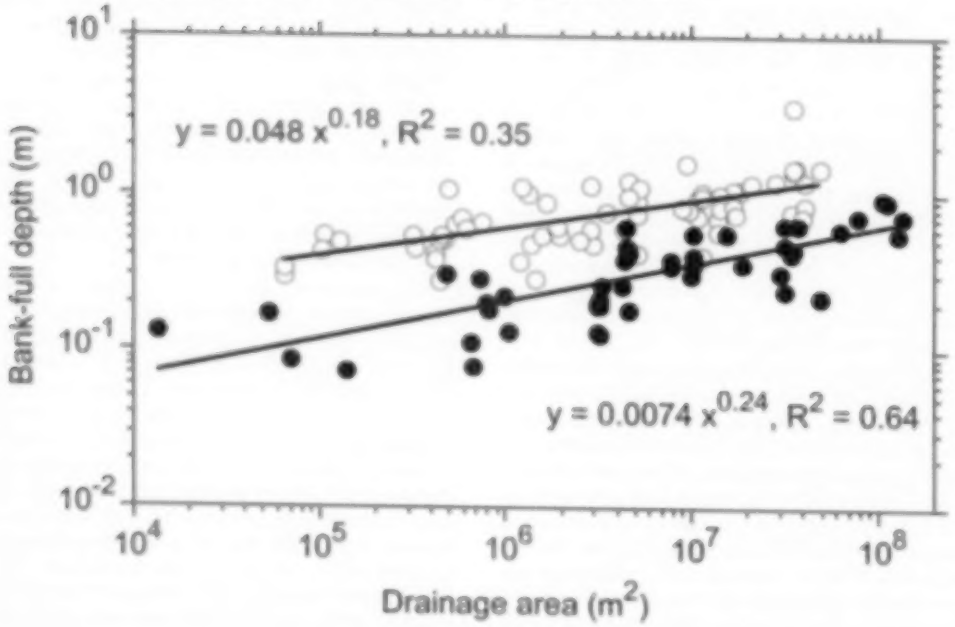

to add wood roughness and further reduce bed-surface grain size. Consequently, bar and wood roughness is added wherever the shear stress is otherwise too great to permit sufficiently fine gravel for spawning (i.e., in areas designated as too coarse plane-bed or pool–riffle under Scenario 2). Scenario 3 is intended to be a "what-if" scenario for assessing potential watershed productivity as a function of spawning-gravel availability (one of several limiting factors affecting potential productivity of a region).

Finally, we compare reach-average values of D_{50} predicted from eq. 4 to preferred spawning-gravel sizes to assess the availability of suitable spawning reaches. A general range of suitable spawning substrate is defined from Kondolf and Wolman's (1993) data as D_{50} = 7–47 mm (Fig. 1). This

© 2004 NRC Canada

range of values is based on the quartile ranges (25th and 75th percentiles) of their reported median grain-size distributions (see Fig. 1). Although salmonids can spawn in both smaller and larger median grain sizes than the selected range, these values represent a central tendency of sizes used by salmonids as a whole.

Results

In these mountain drainage basins, the largest proportion of channel segments is those with slopes greater than 3% (Figs. 6–8). These steep segments comprise almost 90% of the total stream length in each basin and are generally inhospitable to spawning salmonids because of boulder-bed channel morphologies (Table 1). These results are the same for each scenario, with differences between scenarios occurring within channel segments with slopes <3%.

Scenario 1: minimal roughness (plane-bed channels)

Predicted reach-average D_{50} values are divided into three categories in channel segments with slopes <3%: <7 mm (too small for spawning), 7–47 mm (just right), and >47 mm (too coarse). Results indicate that 21%–34% of the stream length with slopes <3% could host suitable spawning gravels with minimal roughness and a plane-bed morphology (Figs. 6*a*–8*a*; Table 1). However, most of the stream length with slopes <3% would have substrate too coarse for salmonid spawning if characterized by a plane-bed morphology and minimal hydraulic roughness; predictions indicate that 66%–79% of this stream length would be unsuitable for spawning.

Scenario 2: self-formed roughness (plane-bed and pool–riffle channels)

When we include the potential occurrence of pool–riffle channels and consequent textural fining due to bar form drag, the predicted availability of spawning sites increases (Figs. 6*b*–8*b*). Suitable pool–riffle channels are predicted to comprise 43%–64% of the stream length with slopes <3% (Table 1), and they make up 86%–100% of the total available spawning habitat. This represents a 27%–32% increase in spawning-gravel availability over the plane-bed case (Scenario 1). Moreover, our results indicate that plane-bed channels with suitable spawning gravels are relatively rare (no more than 7% of the stream length with slopes <3%).

Scenario 3: optimal conditions

By optimizing channel type and hydraulic roughness, 98%–100% of the stream length with slopes <3% is potentially available for salmonid spawning (Figs. 6*c*–8*c*). 21%–34% of the stream length is predicted to require minimal hydraulic roughness (plane-bed morphology), 39%–51% of the stream length would require textural fining due to bar roughness (pool–riffle morphology), and 15%–31% of the stream length would require the combined effects of bar and wood roughness (wood-forced pool–riffle morphology) to produce suitable spawning gravels (Table 1). In these steep basins, no more than 2% of the stream length with slopes <3% is predicted to have grain sizes too small for spawning.

This scenario highlights potential effects on grain size and spawning habitat caused by differences in channel roughness

Fig. 6. Maps showing the predicted extent and distribution of salmonid spawning gravels for (*a*) Scenario 1, (*b*) Scenario 2, and (*c*) Scenario 3 in the Boulder River basin. PR, pool–riffle; PB, plane-bed; wfPR, wood-forced pool–riffle; SP, step–pool; CA, cascade.

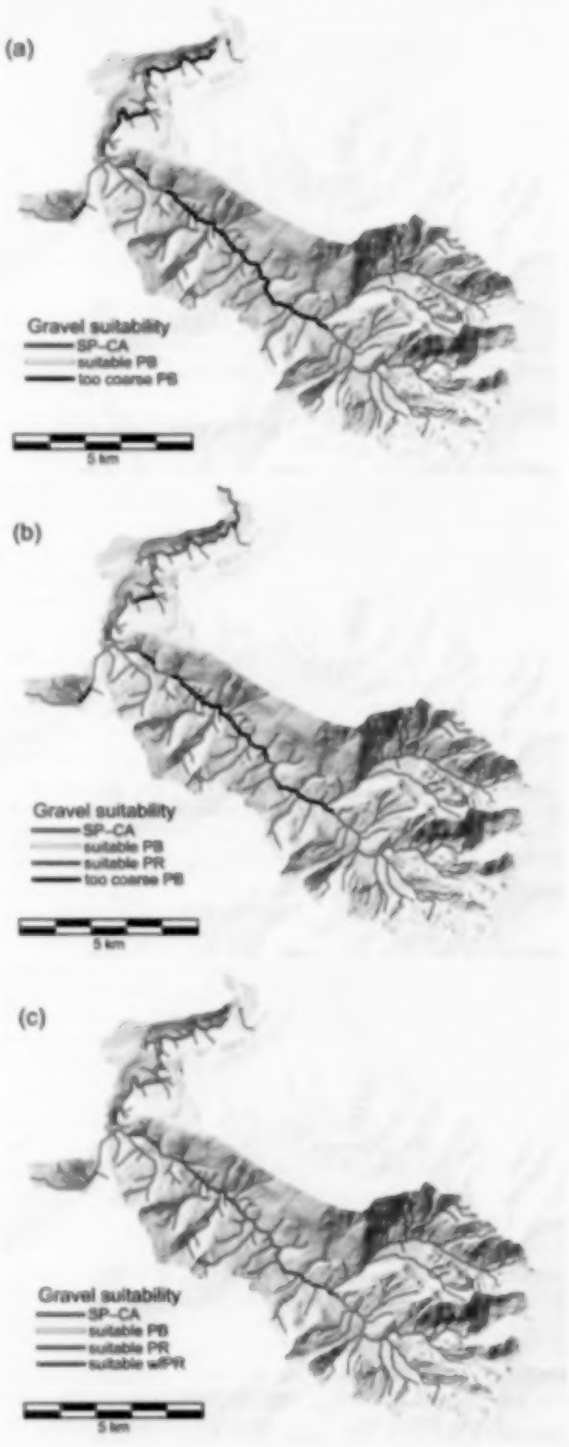

© 2004 NRC Canada

Fig. 7. Maps showing the predicted extent and distribution of salmonid spawning gravels for (*a*) Scenario 1, (*b*) Scenario 2, and (*c*) Scenario 3 in the Finney Creek basin. PR, pool–riffle; PB, plane-bed; wfPR, wood-forced pool–riffle; SP, step–pool; CA, cascade.

Fig. 8. Maps showing the predicted extent and distribution of salmonid spawning gravels for (*a*) Scenario 1, (*b*) Scenario 2, and (*c*) Scenario 3 in the Willapa River basin. PR, pool–riffle; PB, plane-bed; wfPR, wood-forced pool–riffle; SP, step–pool; CA, cascade.

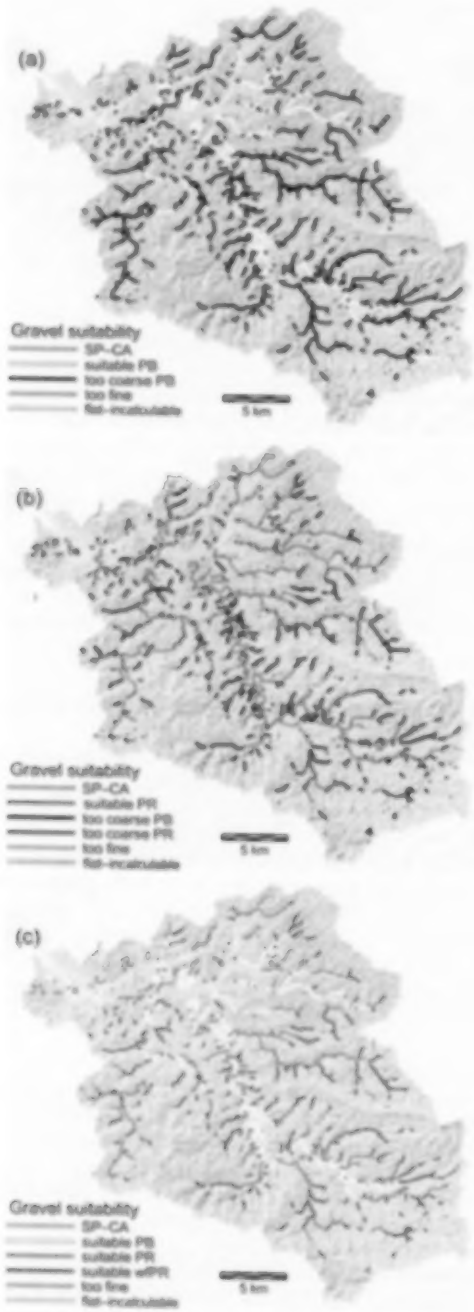

(changing k and n values in eq. 4), rather than slope-related changes in typical channel type and competence (Scenario 2). In particular, wood loading is an external factor that forces changes in roughness and channel morphology independent of channel gradient (Montgomery et al. 1995; Montgomery and Buffington 1998; Buffington and Montgomery 1999*a*). For example, slopes of wood-forced pool–riffle channels commonly span those of pool–riffle and plane-bed

© 2004 NRC Canada

Table 1. Stream-segment statistics by D_{50} class (mm).

Segment types		Boulder			Finney			Willapa		
Slope	Morphology	<7	7–47*	>47	<7	7–47*	>47	<7	7–47*	>47
% of total stream length										
>3%	Step–pool, cascade	—	—	89	—	—	87	—	—	87
% of stream length with S <3%										
Scenario 1: minimal roughness										
<3%	Plane-bed	0	21	79	0	34	66	2	29	69
Scenario 2: self-formed roughness										
>1.5%–3%	Plane-bed	0	7	50	0	2	34	0	0	36
<1.5%	Pool–riffle	0	43	0	0	64	0	4	56	4
Scenario 3: optimal roughness										
<3%	Plane-bed	0	21	0	0	34	0	2	29	0
<3%	Pool–riffle	0	48	0	0	51	0	0	39	0
<3%	Wood-forced pool–riffle	0	31	0	0	15	0	0	30	0

*Suitable spawning reaches (D_{50} = 7–47 mm). D_{50}, median surface grain size.

channels (Montgomery et al. 1995; Montgomery and Buffington 1997).

Discussion

The results obtained for each catchment are strikingly similar, despite differences in basin lithology, geomorphic history, and physical size. In each basin, nearly 90% of the total stream length is predicted to be unsuitable for spawning because of steep slopes (>3%) and associated boulder-bed morphologies (step–pool and cascade channels). Moreover, in each catchment hydraulic roughness due to bars and wood could potentially control more than 65% of the available spawning habitat (Scenario 1 vs. 3). Although 35% of the potential spawning habitat requires only minimal roughness (plane-bed morphology) (Scenarios 1 and 3), the occurrence of suitable plane-bed reaches is likely rare (no more than 7% of the stream length with slopes <3%; Scenario 2).

The predicted locations of each channel type also are quite similar within each basin. Channel segments with suitable spawning gravels tend to be confined to mainstem reaches within each basin, with bar roughness important for spawning-gravel maintenance in lower-mainstem reaches and wood roughness important for maintaining spawning gravels in the steeper, upper-mainstem channels (Scenario 3).

However, it is important to note that our predictions are based on region-specific functions. While these functions are appropriate for the basins used in our sample predictions, they may not apply to other locations. Consequently, we recommend construction of local relationships for bank-full depth, channel type, and roughness before applying our analysis framework to other catchments.

In particular, channel type and hydraulic roughness may depend on a variety of site-specific characteristics, such as (*i*) the size, frequency, and effectiveness of roughness elements, (*ii*) the size and volume of sediment supplied to a channel, (*iii*) valley confinement (and its effect on channel width and depth), and (*iv*) the local basin physiography, hydrologic regime, and geomorphic processes. For example, plane-bed channels are rare in many forest environments because of the preponderance of in-channel wood debris that forces pool-and-bar morphology (Montgomery et al. 1995; Buffington et al. 2002). Moreover, differences in either the tree species or the style and rate of wood input to channels may cause differences in the effectiveness of wood, despite similar wood loadings (Buffington et al. 2003). Similarly, other types of flow obstructions (e.g., bedrock projections and boulders, rather than bars and wood) may create different relationships among roughness, channel type, and grain size.

We also recommend that predictions be ground-truthed (i.e., field verification of predicted values of channel slope, channel type, reach-average grain size, etc.). For example, channel gradients obtained from DEMs may differ substantially from observed field values (Massong and Montgomery 2000), causing errors to cascade through predictions of channel type, roughness correction, and surface grain size (eq. 4). High bed load supply can also cause observed surface grain sizes to be finer than predicted (as discussed in the Analysis framework section). Consequently, the predicted grain size could be used as a reference value against which to explore departures due to sediment supply and other geomorphic processes not specified in the analysis (e.g., Dietrich et al. 1996; Montgomery et al. 1998; Buffington and Montgomery 1999*a*, 1999*b*). However, empirical τ^*_{sc} functions will include regional sediment-supply effects, which may preclude this reference state approach.

Although we focus on the potential availability of salmonid spawning sites as influenced by hydraulic roughness, the rate and caliber of sediment supply also is an important control on surface grain size (Buffington and Montgomery 1999*b*). In particular, increased sediment supply can cause textural fining through size-selective deposition of fine-grained particles. While supply-related textural fining has the potential to increase spawning-gravel extent in channels that otherwise would be too coarse, it may induce higher embryo mortality, offsetting any potential gains in spawning-habitat availability. Increased sediment supply can cause bed mobility at stages lower than bank-full and thus more frequent scour and a higher probability of egg excavation (Montgomery et al. 1996*b*). Furthermore, increased sediment loading may lead to greater interstitial filling of bed material, resulting in

© 2004 NRC Canada

reduced intragravel flow of oxygen to buried salmonid embryos, as well as creating a physical barrier to emergence (Everest et al. 1987; Chapman 1988; Bjornn and Reiser 1991).

Sediment inputs typically are neither uniform nor random, but rather are structured by basin topology, geology, and associated geomorphic processes. For example, the style, magnitude, and frequency of sediment inputs can exhibit systematic downstream variations in mountain basins as one moves from steep, confined headwater regions to low-gradient alluvial valleys (Benda and Dunne 1997*a*, 1997*b*; Montgomery 1999; Buffington et al. 2003). Moreover, network structure and the location of tributary inputs can influence the spatial distribution of sediment size, quantity, and consequent aquatic habitat (Rice et al. 2001*a*, 2001*b*; Martin et al. 2004). Thus, broad-scale geomorphic controls on sediment supply should be considered in addition to channel type and competence.

Results of our analyses indicate that textural fining due to bar and wood resistance has the potential to dramatically affect the extent of salmonid spawning habitat in mountain drainage basins. In particular, wood roughness can be a first-order control on the availability of spawning gravel in steep, upper-mainstem reaches (slopes of <1.5%–3%).

Land management practices of splash damming, riparian clear-cutting, and stream cleaning have decreased the amount of wood debris in many channels throughout North America. Our results suggest that consequent textural coarsening in response to wood loss decreased salmonid spawning habitat availability and may be a factor in historic declines of fish populations (Nehlsen et al. 1991; Montgomery 2003). The impact of wood loss can range from significant textural coarsening that may destroy spawning habitat for salmonids in general to less severe changes in grain size that may alter the species-specific appeal of a given channel reach (i.e., textural coarsening may stimulate a shift in the type of salmonids that use a given portion of the channel network). Wood loss can further compound impacts on fish populations by decreasing pool frequency and area and thus the availability of potential rearing habitat (Montgomery et al. 1995, 1999; Buffington et al. 2002).

Our analysis is intended to predict potential availability of spawning habitat based on general hydraulic controls on surface grain size. It is a first-order assessment of basin conditions that is not species specific. Nor does our analysis consider catchment-specific controls on access to various portions of the drainage network. For example, both the Boulder River and Finney Creek have waterfalls that limit anadromous fish to the lower reaches of each basin. However, because our analysis is purposefully general, basin-specific or species-specific issues can be overlain on our approach. For example, our current analysis could be tailored to spawning-gravel availability for a particular species of concern, such as coho salmon habitat in coastal basins of the Pacific Northwest.

Our analysis has several potential land management applications. It allows rapid prediction of the extent and distribution of potential salmonid spawning sites at basin scales. It can also be used to identify unrealized spawning sites (i.e., suitable locations that are not currently used but are part of the potential habitat range). Moreover, the approach can be used to prioritize locations for salmonid habitat conservation or restoration. Finally, our approach can be used to explore what-if scenarios for assessing potential habitat response to natural or anthropogenic disturbances. For example, the analyses presented in this paper could be used as part of a proactive land management plan for optimizing spawning habitat availability by managing channel type in locations where spawning gravels are limited. Based on model results of this sort and field verification, one might plan riparian growth that would supply wood debris and associated roughness where shear stresses and grain sizes are too large. Similarly, channel dimensions (width and depth) might be altered to encourage development of pool–riffle versus plane-bed morphologies (Buffington et al. 2003).

However, it is important to note that our approach is not a dynamic process–response model. Our analysis does not include specific predictions of channel response and is not intended for that use. While our predictions can be used to identify potential locations that might benefit from altered roughness (such as the addition of wood debris), a channel may respond in many different ways to this change in roughness. For example, addition of roughness elements may cause changes in channel width, depth, or slope in addition to, or in place of, the intended effect of textural fining (Buffington and Montgomery 2001).

Because our analysis focuses on reach-scale predictions of surface grain size, it should be viewed as a coarse-level quantification of potential spawning habitat. In particular, subreach-scale grain size patches and textural variability are not captured by this analysis, but may be important factors in spawning-site selection and overall reach suitability (Buffington and Montgomery 1999*a*). Nevertheless, there is a general association between reach-level channel types and textural-patch complexity. Both the number and frequency of textural patches within a reach increase across plane-bed, pool–riffle, and wood-forced pool–riffle channel types because of increasing spatial variability of shear stress and sediment supply forced by subreach-scale roughness elements (Buffington and Montgomery 1999*a*). Consequently, reach-level predictions provide a first-order assessment of habitat quality that has implications for subreach usage. Inoue et al. (1997) found that reach-scale channel morphology provides a dominant control on subreach habitat availability and is a better predictor of salmonid abundance than that obtained from reach-specific channel-unit characteristics.

The results presented here illustrate our analysis framework and demonstrate the potential effects of channel type and hydraulic roughness. Companion investigations comparing predicted versus observed spawning locations are currently being conducted.

Acknowledgements

Financial support was provided by the Pacific Northwest Research Station of the USDA Forest Service (cooperative agreement PNW-94-0617). Tom Lisle and Steve Rice provided valuable comments on an earlier draft of this paper.

References

Andrews, E.D. 1984. Bed-material entrainment and hydraulic geometry of gravel-bed rivers in Colorado. Geol. Soc. Am. Bull. **95**: 371–378.

© 2004 NRC Canada

Andrews, E.D., and Nankervis, J.M. 1995. Effective discharge and the design of channel maintenance flows for gravel-bed rivers. *In* Natural and anthropogenic influences in fluvial geomorphology. *Edited by* J.E. Costa, A.J. Miller, K.W. Potter, and P.R. Wilcock. Geophys. Monogr. No. 89. American Geophysical Union, Washington, D.C. pp. 151–164.

Benda, L., and Dunne, T. 1997*a*. Stochastic forcing of sediment supply to channel networks from landsliding and debris flow. Water Resour. Res. **33**: 2849–2863.

Benda, L., and Dunne, T. 1997*b*. Stochastic forcing of sediment routing and storage in channel networks. Water Resour. Res. **33**: 2865–2880.

Bjornn, T.C., and Reiser, D.W. 1991. Habitat requirements of salmonids in streams. *In* Influence of forest and rangeland management on salmonid fishes and their habitats. *Edited by* W.R. Meehan. Am. Fish. Soc. Spec. Publ. 19. Bethesda, Md. pp. 83–138.

Bradley, W.C. 1970. Effect of weathering on abrasion of granitic gravel, Colorado River (Texas). Geol. Soc. Am. Bull. **81**: 61–80.

Brummer, C.J., and Montgomery, D.R. 2003. Downstream coarsening in headwater channels. Water Resour. Res. **39**. doi: 10.1029/2003WR001981.

Buffington, J.M., and Montgomery, D.R. 1997. A systematic analysis of eight decades of incipient motion studies, with special reference to gravel-bedded rivers. Water Resour. Res. **33**: 1993–2029.

Buffington, J.M., and Montgomery, D.R. 1999*a*. Effects of hydraulic roughness on surface textures of gravel-bed rivers. Water Resour. Res. **35**: 3507–3522.

Buffington, J.M., and Montgomery, D.R. 1999*b*. Effects of sediment supply on surface textures of gravel-bed rivers. Water Resour. Res. **35**: 3523–3530.

Buffington, J.M., and Montgomery, D.R. 2001. Reply to comments on "Effects of hydraulic roughness on surface textures of gravel-bed rivers" and "Effects of sediment supply on surface textures of gravel-bed rivers" by John M. Buffington and David R. Montgomery. Water Resour. Res. **37**: 1529–1533.

Buffington, J.M., Lisle, T.E., Woodsmith, R.D., and Hilton, S. 2002. Controls on the size and occurrence of pools in coarse-grained forest rivers. River Res. Appl. **18**: 507–531.

Buffington, J.M., Woodsmith, R.D., Booth, D.B., and Montgomery, D.R. 2003. Fluvial processes in Puget Sound rivers and the Pacific Northwest. *In* Restoration of Puget Sound rivers. *Edited by* D.R. Montgomery, S. Bolton, D.B. Booth, and L. Wall. University of Washington Press, Seattle, Wash. pp. 46–78.

Carling, P. 1988. The concept of dominant discharge applied to two gravel-bed streams in relation to channel stability thresholds. Earth Surf. Processes Landforms, **13**: 355–367.

Chapman, D.W. 1988. Critical review of variables used to define effects of fines in redds of large salmonids. Trans. Am. Fish. Soc. **117**: 1–21.

Constantine, C.R., Mount, J.F, and Florsheim, J.L. 2003. The effects of longitudinal differences in gravel mobility on the downstream fining pattern in the Cosumnes River, California. J. Geol. **111**: 233–241.

Cui, Y., and Parker, G. 2005. Numerical model of sediment pulses and sediment supply disturbances in mountain rivers. J. Hydraul. Eng. In press.

Dietrich, W.E., and Dunne, T. 1978. Sediment budget for a small catchment in mountainous terrain. *Z.* Geomorphol. Supp. Band. **29**: 191–206.

Dietrich, W.E., Kirchner, J.W., Ikeda, H., and Iseya, F. 1989. Sediment supply and the development of the coarse surface layer in gravel-bedded rivers. Nature (London), **340**: 215–217.

Dietrich, W.E., Power, M.E., Sullivan, K.O., and Montgomery, D.R. 1996. The use of an analytical reference state in watershed analysis. *In* Abstracts with programs. Geological Society of America, Boulder, Colo. **28**(5): 27906A. (Abstr.)

Dunne, T., and Leopold, L.B. 1978. Water in environmental planning. W.H. Freeman & Co., San Francisco, Calif.

Emmett, W.W., and Wolman, M.G. 2001. Effective discharge and gravel-bed rivers. Earth Surf. Processes Landforms, **26**: 1369–1380.

Everest, F.H., Beschta, R.L., Scrivener, J.C., Koski, K.V., Sedell, J.R., and Cederholm, C.J. 1987. Fine sediment and salmonid production: a paradox. *In* Streamside management: forestry and fishery interactions. *Edited by* E.O. Salo and T.W. Cundy. University of Washington Institute of Forest Resources, Seattle, Wash. pp. 98–142.

Henderson, F.M. 1963. Stability of alluvial channels. Trans. Am. Soc. Civil Eng. **128**: 657–720.

Inoue, M., Nakano, S., and Nakamura, F. 1997. Juvenile masu salmon (*Oncorhynchus masou*) abundance and stream habitat relationships in northern Japan. Can. J. Fish. Aquat. Sci. **54**: 1331–1341.

Kondolf, G.M., and Wolman, M.G. 1993. The sizes of salmonid spawning gravels. Water Resour. Res. **29**: 2275–2285.

Kondolf, G.M., Cada, G.F., Sale, M.J., and Felando, T. 1991. Distribution and stability of potential salmonid spawning gravels in steep boulder-bed streams in the eastern Sierra Nevada. Trans. Am. Fish. Soc. **120**:177–186.

Leopold, L.B., Wolman, M.G., and Miller, J.P. 1964. Fluvial processes in geomorphology. W.H. Freeman, San Francisco, Calif.

Lisle, T.E., Nelson, J.M., Pitlick, J., Madej, M.A., and Barkett, B.L. 2000. Variability of bed mobility in natural, gravel-bed channels and adjustments to sediment load at local and reach scales. Water Resour. Res. **36**: 3743–3755.

Martin, D., Benda, L., and Shreffler, D. 2004. Core areas: a framework for identifying critical habitat for salmon. King County, Department of Natural Resources and Parks, Water and Land Resources Division, Seattle, Wash.

Massong, T.M., and Montgomery, D.R. 2000. Influence of lithology, sediment supply, and wood debris on the distribution of bedrock and alluvial channels. Geol. Soc. Am. Bull. **112**: 591–599.

Montgomery, D.R. 1999. Process domains and the river continuum. J. Am. Water Resour. Assoc. **35**:397–410.

Montgomery, D.R. 2003. King of fish: the thousand-year run of salmon. Westview Press, Boulder, Colo.

Montgomery, D.R., and Buffington, J.M. 1997. Channel-reach morphology in mountain drainage basins. Geol. Soc. Am. Bull. **109**: 596–611.

Montgomery, D.R., and Buffington, J.M. 1998. Channel processes, classification, and response. *In* River ecology and management. *Edited by* R. Naiman and R. Bilby. Springer-Verlag, New York. pp. 13–42.

Montgomery, D.R., and Dietrich, W.E. 1992. Channel initiation and the problem of landscape scale. Science (Washington, D.C.), **255**: 826–830.

Montgomery, D.R., and Foufoula-Georgiou, E. 1993. Channel network source representation using digital elevation models. Water Resour. Res. **29**: 3925–3934.

Montgomery, D.R., Buffington, J.M., Smith, R.D., Schmidt, K.M., and Pess, G. 1995. Pool spacing in forest channels. Water Resour. Res. **31**: 1097–1105.

Montgomery, D.R., Abbe, T.B., Buffington, J.M., Peterson, N.P., Schmidt, K.M., and Stock, J.D. 1996*a*. Distribution of bedrock and alluvial channels in forested mountain drainage basins. Nature (London), **381**: 587–589.

Montgomery, D.R., Buffington, J.M., Peterson, N.P., Schuett-Hames,

© 2004 NRC Canada

D., and Quinn, T.P. 1996*b*. Streambed scour, egg burial depths, and the influence of salmonid spawning on bed surface mobility and embryo survival. Can. J. Fish. Aquat. Sci. **53**: 1061–1070.

Montgomery, D.R., Dietrich, W.E., and Sullivan, K. 1998. The role of GIS in watershed analysis. *In* Landform monitoring, modelling, and analysis. *Edited by* S.N. Lane, K.S. Richards and J.H. Chandler. John Wiley & Sons, Chichester, UK. pp. 241–261.

Montgomery, D.R., Beamer, E.M., Pess, G.R., and Quinn, T.P. 1999. Channel type and salmonid spawning distribution and abundance. Can. J. Fish. Aquat. Sci. **56**: 377–387.

Mueller, E., and Pitlick, J. 2005. Downstream changes in channel geometry and sediment texture in a headwater stream. J. Geophys. Res. (Earth Surf.) In press.

Nehlsen, W., Williams, J.E., and Lichatowich, J.A. 1991. Pacific salmon at the crossroads: stocks at risk from California, Oregon, Idaho, and Washington. Fisheries, **16**: 4–21.

Parker, G. 1978. Self-formed straight rivers with equilibrium banks and mobile bed. Part 2. The gravel river. J. Fluid Mech. **89**: 127–146.

Parker, G. 1991. Selective sorting and abrasion of river gravel. I. Theory. J. Hydraul. Eng. **117**: 131–149.

Rice, S. 1998. Which tributaries disrupt downstream fining along gravel-bed rivers? Geomorphology, **22**: 39–56.

Rice, S., and Church, M. 1996. Bed material texture in low order streams on the Queen Charlotte Islands, British Columbia. Earth Surf. Processes Landforms, **21**:1–18.

Rice, S.P., Greenwood, M.T., and Joyce, C.B. 2001*a*. Macroinvertebrate community changes at course sediment recruitment points along two gravel bed rivers. Water Resour. Res. **37**: 2793–2803.

Rice, S.P., Greenwood, M.T., and Joyce, C.B. 2001*b*. Tributaries, sediment sources, and the longitudinal organisation of macroinvertebrate fauna along river systems. Can. J. Fish. Aquat. Sci. **58**: 824–840.

Shields, A. 1936. Anwendung der Aehnlichkeitsmechanik und der Turbulenzforschung auf die Geschiebebewegung. Mitteilungen der Preussischen Versuchsanstalt für Wasserbau und Schiffbau, Heft 26, Berlin, Germany.

Tabor, R.W., Booth, D.B., Vance, J.A., and Ford, A.B. 2002. Geologic map of the Sauk River 30- by 60-minute quadrangle, Washington. U.S. Geol. Surv. Geol. Invest. Ser. Map I-2592.

Wolman, M.G., and Miller, J.P. 1960. Magnitude and frequency of forces in geomorphic processes. J. Geol. **68**: 54–74.

© 2004 NRC Canada

Maternal and seasonal differences in egg sizes and spawning activity of northwest Atlantic haddock (*Melanogrammus aeglefinus*) in relation to body size and condition

Edward A. Trippel and Steven R.E. Neil

Abstract: Egg and larval production of 22 captive spawning pairs of northwest Atlantic haddock (*Melanogrammus aeglefinus*) were monitored. Females spawned an average of nine egg batches (range 3–16) with a mean batch fecundity of 60 000 eggs and mean total fecundity of 535 000 eggs. Mean spawning duration was 37 days with a mean batch interval of 5.4 days. In multiple linear regression, male Fulton's condition factor (range 1.10–1.55) and mean batch interval explained 56% of variation in fertilization rate (33% and 23%, respectively). Seasonal composite egg diameter spanned 1.37–1.53 mm among females. Mean egg diameter within females declined seasonally by an average of 10.4% (37% by volume). Females produced 46 larvae per gram body weight. Body weight was the single best predictor of fecundity (r^2 = 0.57), with Fulton's condition factor (range 1.04–1.76) explaining no significant additional variation over length or weight. Length and condition explained 39% of variation in seasonal composite egg diameter (22% and 17%, respectively) and body weight independently explained 32%. Sex-specific parental condition and body size acted through large egg size and elevated fertility to enhance reproductive output. Male spawning success was more sensitive than egg production to changes in condition.

Résumé : Nous avons suivi la production d'oeufs et de larves de 22 couples d'aiglefins (*Melanogrammus aeglefinus*) en fraye et gardés en captivité. Les femelles déposent en moyenne 9 masses d'oeufs (étendue 3–16) avec une fécondité moyenne par masse de 60 000 oeufs et une fécondité moyenne totale de 535 000 oeufs. La durée moyenne de la fraye est de 37 j et l'intervalle moyen entre les pontes de 5,4 j. Dans une régression multiple linéaire, le facteur de condition de Fulton des mâles (étendue 1,10–1,55) et l'intervalle moyen entre les pontes expliquent 56 % de la variation du taux de fertilisation (respectivement 33 % et 23 %). D'une femelle à une autre, le diamètre saisonnier global des oeufs varie de 1,37–1,53. Chez une même femelle, le diamètre moyen des oeufs décline en moyenne de 10,4 % (37 % en volume) durant la saison. Les femelles produisent 46 larves par gramme de masse corporelle. La masse corporelle est le meilleur facteur unique pour prédire la fécondité (r^2 = 0,57); le facteur de condition de Fulton (étendue 1,04–1,76) n'explique pas de variation significative supplémentaire que ne le fait la longueur ou la masse. La longueur et la condition expliquent 39 % de la variation du diamètre global saisonnier des oeufs (respectivement 22 % et 17 %) et, de façon indépendante, la masse corporelle explique 32 %. C'est par la grande taille des oeufs et la fertilité élevée que la condition et la taille spécifique au sexe des parents favorisent le rendement de la reproduction. Le succès de la reproduction des mâles est plus sensible aux changements de condition que ne l'est la production d'oeufs.

[Traduit par la Rédaction]

Introduction

Allocation of energy to reproduction comprises a substantial investment in teleost fishes (Calow 1979; Van Winkle et al. 1997). Seasonal pattern and extent of energy allocation are a function of nutritional condition and body weight and vary among species (LeCren 1951; Lambert and Dutil 2000). Individuals of many fish species release their annual reproductive investment in a single spawning event, and others, particularly marine teleosts, exhibit protracted seasonal spawning behaviour (Breder and Rosen 1966; Chambers 1997). Multiple egg batches are released such that an individual's spawning period may span weeks or months (Hislop et al. 1978; McEvoy and McEvoy 1991; Kjesbu et al. 1996). Protracted spawning often occurs in highly fecund species and acts to release eggs into variable environmental conditions during the spawning period.

Large eggs tend to produce large larvae, and hence, variation in egg size influences larval quality and fitness (Hutchings 1991; Marteinsdottir and Steinarsson 1998; Trippel 1998).

Received 22 September 2003. Accepted 14 May 2004. Published on the NRC Research Press Web site at http://cjfas.nrc.ca on 25 January 2005.
J17742

E.A. Trippel[1] and S.R.E. Neil. Fisheries and Oceans Canada, St. Andrews Biological Station, 531 Brandy Cove Road, St. Andrews, NB E5B 2L9, Canada.

[1]Corresponding author (e-mail: trippele@mar.dfo-mpo.gc.ca).

 doi: 10.1139/F04-125 © 2004 NRC Canada

Variation in egg size can have a direct influence on larval energy stores, resistance to starvation, and initial feeding success (Knutsen and Tilseth 1985; Brooks et al. 1997; Keckeis et al. 2000). Egg production and their size, viability, and seasonal pattern of release are therefore important to understanding several key processes that shape early life growth, survival, and recruitment of marine fish species.

Marked reductions in the size and condition of gadoids have occurred over the past decade in the northwest Atlantic and elsewhere that have impaired reproductive potential and thereby contributed to repressed recruitment and failed population recovery for these fish stocks (Lambert and Dutil 1997; Trippel et al. 1997*a*; Rätz and Lloret 2003). As well, interest in cultivating a variety of gadoids has intensified as the harvested landings of groundfish decline globally (Baskerville-Bridges and Kling 2000; Hansen et al. 2001; Trippel and Neil 2003). Despite the current wide interest in the depleted status of demersal fish stocks and the associated significance of stock reproductive potential and recruitment (Marshall et al. 1999; Trippel 1999; Katsukawa et al. 2002), little is known of the manner in which annual reproductive investment is seasonally allocated for individual northwest Atlantic haddock (*Melanogrammus aeglefinus*). Presently, data on haddock reproductive potential are primarily limited to estimates of annual fecundity based on oocytes of preserved ovaries (Grand Bank (Hodder 1963), northeast Arctic (Sonina 1973), North Sea (Raitt 1933; Hislop and Shanks 1981), southwestern Scotian Shelf (Waiwood and Buzeta 1989), and eastern Scotian Shelf (Blanchard et al. 2003*b*)). Knowledge of seasonal changes in the production and sizes of eggs and spawning activity of individuals of varying body metrics of the northwest Atlantic are unknown, yet are important to more fully understand haddock early life recruitment mechanisms (Marshall and Frank 1999; Fogarty et al. 2001). Only a single study has examined the egg production of individual captive haddock (Hislop et al. 1978), which evaluated the effect of ration size on fecundity, egg batch production, and egg size of North Sea haddock.

The objectives of our study using captive Atlantic haddock of the Bay of Fundy were to (*i*) evaluate the synchrony of seasonal egg batch production and its relationship with fertilization and hatching rates, (*ii*) examine the associations of parental body attributes and fertilization success, and (*iii*) evaluate how egg production and egg size covary with body length, weight, and condition factor as well as estimate the relative contribution of each body metric in explaining variation in these reproductive traits.

Methods

Atlantic haddock were captured as juveniles or young adults from the lower Bay of Fundy during 1995 and 1997 and transported to outdoor holding tanks (diameter 3.9 m, volume 15 m^3) at the Biological Station in St. Andrews, New Brunswick, Canada. Fish were in the size range of 30–45 cm, suggesting that they were juvenile or young adults approximately 2–4 years old (Hurley et al. 1999). Fish were fed to satiation every 3–4 days on a diet of Atlantic herring (*Clupea harengus*), Atlantic mackerel (*Scomber scombrus*), northern shortfin squid (*Illex illecebrosus*), and Aesop shrimp (*Pandalus montagui*); because of depression in appetite, reduced rations were given during the spawning period (Fordham and Trippel 1999). Individuals were tagged near the dorsal fin with uniquely numbered Petersen "spaghetti-type" tags and monitored for sex and reproductive state prior to spawning by applying gentle pressure to the abdomen and watching closely for the release of gametes. Prior to the spring spawning periods of 1997–1999, adult pairs were relocated to smaller outdoor circular tanks (diameter 1.8 m, volume 3.5 m^3). Over 3 years, the spawning performance of 22 adult pairs was monitored. Haddock monitored in 1997 were held in captivity since autumn 1995. Those monitored in 1998 and 1999 were held in captivity since autumn 1997. Extrapolation of results of captive fish experiments to wild fish has been recognized as a valuable tool (Tyler and Dunn 1976; Hislop et al. 1978; Lambert and Dutil 2000) and the procedures followed were those recommended by Lambert and Thorsen (2003).

Fork length (FL) (±0.5 cm), body weight (±10 g), and Fulton's condition factor ($K = 100$(body weight/FL^3)) were recorded approximately 2–3 weeks prior to and after spawning (referred to as pre- and postspawning). Fulton's condition factor has been widely used to represent nutritional condition in spawning experiments with live fish (e.g., Chambers and Waiwood 1996; Kjesbu et al. 1996). Individuals were 3–6 years old based on the approximate age at capture and holding times. Length at first maturity of female haddock of the Bay of Fundy and western Scotian Shelf (North Atlantic Fisheries Organisation Division 4X) commonly spans 30–45 cm (Trippel et al. 1997*b*), and thus, several of the females could have been first-time spawners. During spawning, water temperature was maintained at 5–6 °C (flow 26 L·min^{-1}), equivalent to temperatures of local spawning grounds such as Browns Bank (Waiwood and Buzeta 1989). Egg collectors were fitted to each tank and checked daily (Thorsen et al. 2003). Spawned eggs were removed and the collective volume (±1 mL) was adjusted for packing among eggs (Kjesbu 1989). The number of eggs of each batch was estimated from a mean egg volume based on the diameters of 60 individual eggs (±0.01 mm); diameters were calculated as the mean of two estimates for each egg made using an image analysis system (BioScan Optimas V6.0; BioScan Inc., Edmunds, Washington). Sixty individual eggs from each batch were used to calculate mean egg diameter for a batch.

Fertilization rate of each egg batch was estimated as the mean proportion of eggs exhibiting cell division in three sets of 200–350 eggs (magnification × 40). Egg samples not showing signs of cell division upon collection were maintained an additional 12 h at 6 °C to ensure ample time for cell division to commence before fertilization rate was assessed.

For each batch, the three groups of eggs used to estimate fertilization rate were incubated separately in 250-mL glass beakers at 6 °C in a refrigerated room. Filtered and ultraviolet-treated seawater used for incubation was changed every 1–2 days, and any opaque eggs on the incubator bottom were assumed to be dead and were removed. Eggs typically hatched in 16–19 days, and the date of hatching of an egg batch was represented by the day of peak hatch. For each batch, hatching rate was estimated by the mean proportion of eggs that hatched in the three incubators. Seasonal com-

© 2004 NRC Canada

posite values per female for egg diameter, fertilization, and hatching rates were obtained by weighting batch-specific values by batch fecundity. The numbers of eggs and day 0 larvae produced per maternal gram (equivalent to viable eggs per gram) were determined for each female. Four females from 1998 were also monitored in 1999, which allowed egg and larval production to be monitored over 2 consecutive years.

Single classification ANOVA was used to test for significant differences among body size in 1997–1999 (SPSS, version 11.5). Homogeneity and normality of variances (including percent data) were achieved without data transformation (Levene test and Shapiro-Wilks test, respectively). A posteriori comparisons of body size were made using Duncan's multiple range test ($\alpha = 0.05$). A log link was used for fecundity – body size relationships. The equations were of the form $Y = aX^b$, where Y is fecundity; X is length, weight, or condition factor; and a and b are parameters estimated from the regression coefficients. Simple linear regression was used to examine for significant relationships between several body size characteristics and reproductive traits other than fecundity. Since weight is considered to reflect two aspects of growth (length and condition) and each of these has a separate effect on individual fecundity and egg size, it was considered useful to partition these effects. Hence, condition factor was incorporated into multiple regression models with length or weight as the first predictor (e.g., Blanchard et al. 2003). As reproductive parameters commonly covaried with body length, ANCOVA with fork length as a covariate was used to further test for among-year differences in reproductive characteristics (Sokal and Rohlf 1995).

Results

Variability among individuals

Prespawning females ranged in length from 46 to 60 cm, in body weight from 1.14 to 3.10 kg, and in Fulton's condition factor from 1.04 to 1.76 (Table 1). Spawning began in late March and ended by mid-June. Female weight loss averaged 24.1% ± 1.9% (mean ± SE) and males 13.0% ± 1.3% (final body weights were not measured of all fish). Females released an average of nine egg batches (ranging from 3–16) with a mean batch fecundity of 60 175 ± 6821 eggs (Table 1). Mean female fecundity was 535 817 ± 65 757, which equated to 234 ± 20.3 eggs per gram of female. Average duration of spawning was 37 ± 3.0 days and eggs were released once every 5.4 ± 0.8 days. Adult pairs exhibited considerable variability in fertilization and egg hatching success (Figs. 1 and 2). Seasonal composite fertilization rate was 57% ± 7.1% (Table 1). Seven females achieved >80% composite fertilization among all batches. Fifty-five of the 202 batches (27%) released by all females failed to be fertilized. Two of the females did not achieve fertilization of any spawned eggs; 147 of 187 batches (79%) were partly or completely fertilized when excluding these two females. Hatching rates were evaluated for fertilized and total eggs spawned. The seasonal composite hatching rate of fertilized eggs was 31% ± 4.9% and for spawned eggs was 20% ± 4.0%.

Seasonal composite egg diameter was 1.46 ± 0.01 mm (Figs. 1 and 2). For some individuals, egg diameter declined successively between egg batches; for others, egg diameter either increased slightly or stayed at initial levels for several batches before declining (Figs. 1 and 2). Percent decline in egg diameter between initial and terminal batches ranged from 2% to 17% (mean 10.4% ± 0.9%) (Table 1).

Relationships among parental attributes and reproductive traits

Significant ($P < 0.05$) relationships existed between fecundity and fork length, prespawning body weight, and condition factor (Table 2; Fig. 3). For batch-specific fecundity, significant relationships existed with fork length and prespawning body weight but not condition factor (Table 2). Condition did not explain a significant amount of variation in fecundity (total or batch) beyond that explained by length alone ($r^2 = 0.056$, $P = 0.126$ and $r^2 = 0.001$, $P = 0.888$, respectively). Significant positive linear relationships existed between egg diameter (initial and seasonal composite) and fork length, prespawning body weight, and condition factor (Table 2). In addition to length, condition explained a further 23.1% and 17.1% ($P < 0.05$) of the variation of initial and seasonal composite egg diameter, respectively (Table 3). Condition did not explain more of the variability in the fecundity – body weight relationships or the composite egg size – body weight relationships ($r^2 = 0.001$, $P = 0.817$ and $r^2 = 0.042$, $P = 0.278$, respectively). Regression of condition and length was not significant ($P = 0.220$), whereas regression of condition and body weight was significant ($P < 0.001$).

For fertilization success, a significant positive relationship existed with prespawning male condition (range 1.10–1.55) (Fig. 4) ($r^2 = 0.463$, $P = 0.003$ when pair 97-3 was omitted), and significant negative relationships existed with mean batch interval and the coefficient of variation of batch interval (Table 2). In addition to male condition, mean batch interval explained a further 23.7% ($P < 0.05$) in variation in fertilization success (Table 3). Females that exhibited short interbatch intervals (2.8–3.8 days on average) and were accompanied by high-condition males ($K > 1.24$) achieved >80% composite fertilization rates. Regression of male condition was not significant with mean batch interval ($r^2 = 0.125$, $P = 0.149$) or the coefficient of variation of batch interval ($r^2 = 0.052$, $P = 0.363$).

Fork length, prespawning body weight, and condition factor of females did not explain a significant amount of variation in linear regression with fertilization rate ($r^2 = 0.028$, $P = 0.457$, $r^2 = 0.027$, $P = 0.462$, and $r^2 = 0.011$, $P = 0.637$, respectively) or hatching rate ($r^2 = 0.009$, $P = 0.675$, $r^2 = 0.012$, $P = 0.634$, and $r^2 = 0$, $P = 0.976$, respectively). The male to female body length ratio of spawning pairs (range 0.87–1.10) did not explain a significant amount of variation in fertilization rate ($r^2 = 0.052$, $P = 0.305$). For hatching rate, no significant relationships existed with male condition ($r^2 = 0.045$, $P = 0.399$), mean batch interval ($r^2 = 0.049$, $P = 0.323$), and coefficient of variation of batch interval ($r^2 = 0.002$, $P = 0.825$).

Variability among years

Females monitored in 1998 were in captivity for approximately 6 months before onset of spawning and were shorter (8.6%), weighed less (31%), and had a lower condition fac-

© 2004 NRC Canada

Table 1. Body size and reproductive parameters of 22 spawning pairs of Bay of Fundy haddock maintained at water temperatures of

Female No.	Fish pair	Sex	Fork length (cm)	Body weight (kg)			Condition factor		Egg batches	Date span of spawning	Days spawning	Fecundity	Mean batch fecundity
				Initial	Final	% change	Initial	Final					
1	97-1	F	55.5	2.55			1.49		8	5 Mar. – 16 May	78	965 436	120 680
		M	57.0	2.20			1.19						
2	97-2	F	59.0	2.92			1.42		8	25 Apr. – 29 May	35	1 015 970	126 996
		M	57.0	2.06			1.11						
3	97-3	F	54.5	2.70			1.67		7	11 Apr. – 21 May	41	490 712	70 102
		M	48.0	1.60			1.45						
4	97-4	F	59.5	3.10			1.47		5	13 Apr. – 12 May	29	550 908	110 182
		M	65.0	3.50			1.27						
5	97-5	F	53.0	2.10			1.41		8	4 Apr. – 24 May	50	595 960	74 495
		M	51.0	1.80			1.36						
6	97-6	F	52.0	2.15			1.53		10	11 Apr. – 6 May	25	510 440	51 044
		M	48.0	1.90			1.58						
7	98-1	F	54.5	2.84	2.15	–24.5	1.76	1.33	9	8 Apr. – 11 May	22	459 437	51 049
		M	47.5	1.18	1.06	–10.0	1.10	0.99					
8	98-2	F	48.0	1.23			1.10		3	16 Apr. – 26 May	40	228 254	76 085
		M	53.0	1.66			1.12						
9	98-3	F	52.5	1.86	1.64	–11.8	1.29	1.14	12	11 Apr. – 22 May	41	525 387	43 782
		M	46.2		1.43								
10	98-4	F	46.0	1.36	0.99	–27.6	1.4	1.01	11	11 Apr. – 9 May	28	198 525	18 048
		M	46.5	1.23	1.13	–8.1	1.22	1.12					
11	98-5	F	53.0	2.01	1.82	–9.1	1.35	1.22	7	15 Apr. – 27 May	42	193 745	27 678
		M	52.0		1.76								
12	99-1	F	53.0	1.88	1.33	–29.3	1.27	0.89	16	27 Mar. – 21 May	55	679 204	42 450
		M	53.0	2.04	1.74	–14.7	1.37	1.16					
13	99-2	F	55.0	2.88	2.09	–24.4	1.73	1.26	13	24 Mar. – 7 May	44	812 291	62 484
		M	51.0	1.99	1.76	–11.6	1.5	1.33					
14	99-3	F	58.5	2.83	2.01	–28.9	1.42	1.05	12	25 Mar. – 3 May	39	1 169 779	97 482
		M	51.0	1.91	1.59	–16.8	1.44	1.2					
15 (1)	98-6	F	50.0	1.52	1.23	–19.1	1.21	0.98	6	14 Apr. – 2 May	18	108 852	18 142
		M	49.0	1.41	1.24	–12.1	1.2	1.05					
15 (2)	99-4	F	58.0	3.12	2.2	–29.5	1.6	1.12	12	29 Mar. – 12 May	45	1 077 134	89 761
		M	54.0	2.26	1.79	–20.8	1.44	1.14					
16 (1)	98-7	F	47.0	1.14			1.1		7	2 May – 22 May	21	229 162	32 737
		M	44.0		0.92			1.08					
16 (2)	99-5	F	50.5	1.97	1.36	–31.0	1.53	1.06	13	19 Apr. – 30 May	41	565 062	43 466
		M	48.2	1.47	1.21	–17.5	1.31	1.08					
17 (1)	98-8	F	50.0	1.65			1.32		12	15 May – 2 July	48	349 916	29 160
		M	44.5		0.98			1.11					
17 (2)	99-6	F	53.0	2.01			1.35		6	9 May – 31 May	23	232 766	38 794
		M	52.5	1.85			1.28						
18 (1)	98-9	F	56.0	2.40	1.77	–26.5	1.37	1.01	11	9 Apr. – 13 May	34	513 911	46 719
		M	46.0	1.23	1.14	–7.3	1.26	1.17					
18 (2)	99-7	F	56.5	1.87	1.35	–27.8	1.04	0.75	6	18 Apr. – 7 May	19	315 125	52 521
		M	49.0	1.82	1.62	–11.0	1.55	1.38					
Mean	1997	F	55.6	2.59			1.50		7.7		43.0	688 238	92 250
		SE	1.26	0.16			0.04		0.67		7.88	96 997	12 703
		n	6				6		6		6	6	6
		M	54.3	2.08			1.26						
		SE	2.47	0.29			0.05						
		n	6				6						
	1998	F	50.8	1.78			1.32	1.12	8.7		32.7	311 910	38 156
		SE	1.15	0.19			0.07	0.05	1.04		3.60	51 570	6 163
		n	9				9	6	9		9	9	9
		M	52.5	1.32			1.18	1.09					
		SE	4.56	0.09			0.03	0.02					
		n	5				5	6					

© 2004 NRC Canada

5–6 °C between 1997 and 1999.

	% batch		Egg diameter (mm)							
% fertilized	Fertilized eggs	Total	Initial	Terminal	% decline	Composite	Larval production	No. of larvae·g female^{-1}	No. of eggs·g female^{-1}	Mean batch interval (days)
20.1	32.4	6.7	1.62	1.4	–13.5	1.54	64 531	25.3	379	10.3±4.3
48.5	71.5	34.9	1.56	1.42	–9	1.47	354 899	121.5	347	5.1±1.5
59.9	47.5	28.5	1.59	1.4	–11.9	1.54	139 641	51.7	182	6.7±1.9
76.3	49.1	37.5	1.5	1.41	–6	1.47	206 488	66.6	177	7.3±5.7
6.2	41.4	3.6	1.55	1.3	–16.1	1.45	21 328	10.2	283	7.1±3.8
24.1	30.4	6.2	1.45	1.34	–7.6	1.42	31 835	14.8	237	4.9±2.2
38.6	27.8	10.7	1.55	1.51	–2.6	1.53	49 226	17.3	162	4.1±1.4
0	0	0	1.37	1.34	–2.2	1.32	0	0	186	20.0±11.0
80.3	6.9	5.6	1.51	1.29	–14.6	1.42	29 286	15.7	282	3.6±1.8
96.8	64.7	62.6	1.48	1.36	–12	1.4	124 289	91.4	146	2.8±0.6
28.6	28.2	8.0	1.51	1.25	–17.2	1.37	15 583	7.8	96	6.3±4.0
93.1	47.2	44.0	1.55	1.35	–12.9	1.46	298 724	158.9	361	3.6±0.9
90.9	4.2	3.9	1.63	1.47	–9.8	1.54	32 146	11.2	282	3.7±0.6
81.9	16.8	13.8	1.59	1.37	–13.8	1.46	160 929	56.9	413	3.6 + 0.6
44.5	25.5	11.3	1.50	1.36	–9.3	1.44	12 342	8.1	72	3.6±1.2
76.5	38.4	29.4	1.57	1.35	–14.0	1.46	314 128	100.7	345	4.0±2.3
70.6	73.2	51.7	1.44	1.32	–8.3	1.41	118 434	103.9	201	3.3±2.1
95.6	13.5	12.9	1.62	1.44	–11.1	1.53	82 337	41.8	286	3.4±1.5
0	0	0	1.47	1.30	–11.6	1.35	0	0	212	4.4±2.9
40.8	0	0	1.57	1.45	–7.6	1.53	0	0	116	4.4±0.8
80.8	53.0	42.8	1.47	1.28	–14.8	1.40	219 999	91.6	214	3.4±1.4
97.7	15.3	14.9	1.50	1.45	–3.3	1.50	49 336	26.4	169	3.8±1.5
39.2	45.4	19.6	1.54	1.38	–10.6	1.48	136 447	48.4	268	6.9
10.9	6.1	6.4	0.02	0.02	1.38	0.02	52 277	17.1	34.4	0.80
6	6	6	6	6	6	6	6	6	6	6
48.9	31	21.4	1.48	1.33	–10.2	1.4	63 240	37.3	175	5.7
11.8	9.1	8.0	0.02	0.02	1.65	0.02	25 154	14.8	21.4	1.82
9	9	9	9	9	9	9	9	9	9	9

© 2004 NRC Canada

Table 1 (*concluded*).

Female No.	Fish pair	Sex	Fork length (cm)	Body weight (kg) Initial	Final	% change	Condition factor Initial	Final	Egg batches	Date span of spawning	Days spawning	Fecundity	Mean batch fecundity
	1999	F	54.9	2.37			1.42	1.02	11.1		38.0	693 052	60 994
		SE	1.08	0.21			0.07	0.06	1.42		4.81	134 542	8 967
		n	7				7	6	7		7	7	7
		M	51.2	1.91			1.41	1.22					
		SE	0.74	0.08			0.03	0.04					
		n	7				7	6					
	1997–1999	F	53.4	2.19		–24.1	1.42	1.02	9.2		37.2	535 817	60 175
		SE	0.79	0.13		1.9	0.04	0.04	0.69		3.00	65 757	6 821
		n	22			12	22	12	22		22	22	22
		M	50.6	1.75		–13.0	1.30	1.15					
		SE	1.00	0.14		1.3	0.03	0.03					
		n	18			10	18	12					

Note: Fertilization, hatching rate, and egg diameter were weighted by batch fecundity to determine seasonal composite values per female. Females unavailable for some individuals. *n* is the number of fish.

tor (12%) than females in 1997 and 1999, which were in captivity for >1.5 years (Table 1) (ANOVA, Duncan's multiple range test, $\alpha = 0.05$; significant for length and weight). Slopes of length-based relationships among the three years were not significantly different for fecundity ($P = 0.183$), number of batches ($P = 0.534$), duration of spawning ($P = 0.882$), batch interval ($P = 0.789$), initial egg diameter ($P = 0.633$), seasonal composite egg diameter ($P = 0.285$), fertilization rate ($P = 0.449$), and hatching rate ($P = 0.438$), yet batch fecundity was significantly different among years ($P = 0.034$). For parameters having homogeneous slopes, we tested for significant differences among y-intercepts among the three years and found fecundity ($P = 0.278$), number of batches ($P = 0.143$), duration of spawning ($P = 0.596$), batch interval ($P = 0.318$), and hatching rate ($P = 0.144$) to be not significantly different, whereas initial egg diameter ($P = 0.044$), seasonal composite egg diameter ($P = 0.031$), and fertilization rate ($P = 0.046$) were significantly different (ANCOVA). Hence, smaller egg sizes were evident in females that were more recently captured from the wild, even after accounting for their smaller body size. The high fertilization rate in 1999 was associated with high male condition factor (Table 1).

Variability within individuals

Four females were monitored over two breeding years, i.e., 1998 and 1999 (Fig. 2). Two females (15 and 16) underwent substantial gains in weight and condition, which were accompanied by increased number of egg batches, spawning duration, seasonal composite egg diameter, and fertilization rate (Table 2). Hatching rate of all eggs spawned increased for female 15 and declined for female 16 even though fertilization rate was high. Total egg production increased for both females (4.8-fold and 1.4-fold higher per equated weight, respectively).

For the other two females monitored over 2 years, female 17 underwent a minor change in condition and female 18 a substantial reduction in condition (Table 2). Both females released a lower number of egg batches between years and their respective spawning durations decreased (Fig. 2). Fertilization rates for the two females increased from first to second monitored breeding year. Hatching rate of all eggs spawned remained nil for female 17 and, because of a decrease in hatching rate of fertilized eggs, declined for female 18. Total egg production decreased for both females (45% and 21% lower per equated weight, respectively).

Discussion

Egg size

Seasonal declines in egg size for temperate marine teleosts have been observed for many spring-spawning populations (see reviews by Bagenal (1971) and Chambers (1997)). After a slight rise, egg diameter declined successively between egg batches in Bay of Fundy haddock. Seasonal declines in egg size for individual haddock were similar to those of North Sea haddock (Hislop et al. 1978) and averaged 10.4% (37% by volume). Haddock collected off the eastern United States and maintained as a group under advanced photoperiod exhibited seasonal declines in egg size of approximately 6%–15% (Buckley et al. 2000).

The seasonal declines in egg size of haddock and its close correlate larval size likely play a role in influencing early life survivorship (Chambers et al. 1989; Trippel 1998; Marteinsdottir and Begg 2002). Large larvae generated early in the spring season will have different feeding capabilities and energy stores available than those originating from small eggs of late batches. For gadoids, seasonal declines in egg size have a physiological basis. As a female successively releases eggs, the body's protein and lipid reserves become depleted. As a result, near completion of spawning, the ability to mobilize material from somatic tissue to the ovary for final oocyte development is considerably reduced (Kjesbu et al. 1991). In Atlantic cod (*Gadus morhua*), a difference in egg diameter of 1.30–1.60 mm resulted in an 80% heavier larva at hatch and double the ratio of yolk to total larval dry weight (Trippel 1998).

Maternal effects on variation in egg size of captive haddock have been evaluated for North Sea haddock (Hislop et al. 1978). They maintained 11 fish (34–42 cm total length,

© 2004 NRC Canada

	% hatch		Egg diameter (mm)							
% fertilized	Fertilized eggs	Total	Initial	Terminal	% decline	Composite	Larval production	No. of larvae·g female^{-1}	No. of eggs·g female^{-1}	Mean batch interval (days)
82.4	19.3	17.0	1.58	1.41	−10.4	1.5	133 943	56.6	282	3.8
7.5	6.5	5.7	0.02	0.02	1.35	0.01	48 421	21.2	40.2	0.12
7	7	7	7	7	7	7	7	7	7	7
56.9	31.2	19.5	1.53	1.37	−10.4	1.46	105 702	46.4	234	5.4
7.1	4.9	4.0	0.01	0.01	0.89	0.01	23 424	9.8	20.3	0.79
22	22	22	22	22	22	22	22	22	22	22

15–18 were monitored in 2 successive years. Means ± SE are presented for each year and for all years combined. Seasonal changes in body weight are

375–730 g, K = 0.86–1.16 initial or 0.97–1.31 when adjusted for fork length) at different feeding levels from November to the completion of spawning in March. Dry weight of the eggs (high ration: 42.8 mg for 500 eggs; low ration: 35.2 mg for 500 eggs) was lighter in fish kept on low ration. In our study, separating the effect of condition factor from length in regression analysis further supports the significance of the former variable in governing egg size. Body weight was also an important predictor of egg size. Consequently, declines in egg size have likely accompanied the reductions in body size, condition, and fecundity of haddock stocks of the northwest Atlantic. It was shown that the size and weight of the eggs of wild North Sea haddock, as well as their relative fecundity, were influenced by maternal size and age (Hislop 1988). Our observations on captive female haddock (body weight 1.14–3.10 kg, K = 1.04–1.76) provide some underlying biological evidence to support the positive correlation reported between female condition (weight at 50 cm) and recruitment for southwestern Scotian Shelf haddock over a three-decade period (Marshall and Frank 1999). It would be of interest to conduct data simulations on predicted seasonal production and sizes of eggs (based on various adult population structures and nutritional status), size at hatch, hatching period, and seasonal prey availability to model individual larval haddock performance under variable environments (Laurence et al. 1991; Mertz and Myers 1994). Among eight regions in the north Atlantic, haddock consistently exhibited higher recruitment variability and lower resilience than Atlantic cod (Fogarty et al. 2001). A modelling approach with these parent–progeny components may assist in elucidating the recruitment mechanisms characteristic of this species relative to Atlantic cod.

Fecundity

In the present study, body weight had the greatest influence on fecundity (r^2 = 0.57). The effect of condition factor was not significant, beyond that of length or weight alone. Blanchard et al. (2003) showed relative condition (LeCren 1951) to have variable effects on fecundity of eastern Scotian Shelf haddock (for three years, the explained variation in fecundity by condition in addition to length was 1%, 9.8%, and 22.7%). For our captive haddock, the absence of low values of prespawning condition (none <1.0) may partly explain why condition failed to have a significant effect on fecundity. Similarly, in Baltic cod, condition only explained 1% additional variation in the fecundity–length relationship, a stock not considered to be food limited (Kraus et al. 2000). For further examination of the utility of condition in predicting fecundity, refer to Koops et al. (2004).

Realized fecundity estimates observed in our study for Bay of Fundy haddock were within the broad range of potential fecundities observed for similar-sized wild haddock of the same area (Waiwood and Buzeta 1989; Blanchard 2000). Thus, although atresia of oocytes is known to reduce realized fecundity and result in potential overestimation of fecundity from oocyte counts from preserved ovaries, further experimental research is required to establish appropriate correction factors for atresia for Bay of Fundy haddock (e.g., Kjesbu et al. 1991; Witthames and Greer Walker 1995). Our findings revealed that feeding of captive haddock for >1 year did not significantly elevate their egg production over haddock maintained in captivity for approximately 6 months before spawning (after adjusting for length); however, initial and seasonal egg size were significantly elevated (i.e., 1997 and 1999 versus 1998).

Fertilization and hatching success

Fertilization and hatching success averaged 56% and 31%, respectively, and were highly variable among females. Variable fertilization success among haddock adult pairs and hatching of fertilized eggs are presumably related to a number of parental attributes, including milt volume and sperm concentration (Trippel et al. 1998), and egg quality (Trippel et al. 2000). Eggs with high ash content (≥20% dry matter) released by haddock during paired mating were characterized by lower fertilization (33% versus 59%) and hatching rates (0% versus 24%) than eggs with low ash (<20% ash) (Trippel et al. 2000). In addition to maternal factors (Brooks et al. 1997; Rideout et al. 2004), variation in hatching success of fertilized eggs may have been influenced by pater-

© 2004 NRC Canada

Fig. 1. Egg batch, fertilized eggs, and larval production (bars) and egg diameter (●) of 14 spawning pairs of captive Bay of Fundy haddock (*Melanogrammus aeglefinus*). Numbers 1–14 refer to females 1–14 in Table 1. Open bars, unfertilized; hatched bars, fertilized but did not hatch; solid bars, fertilized and hatched.

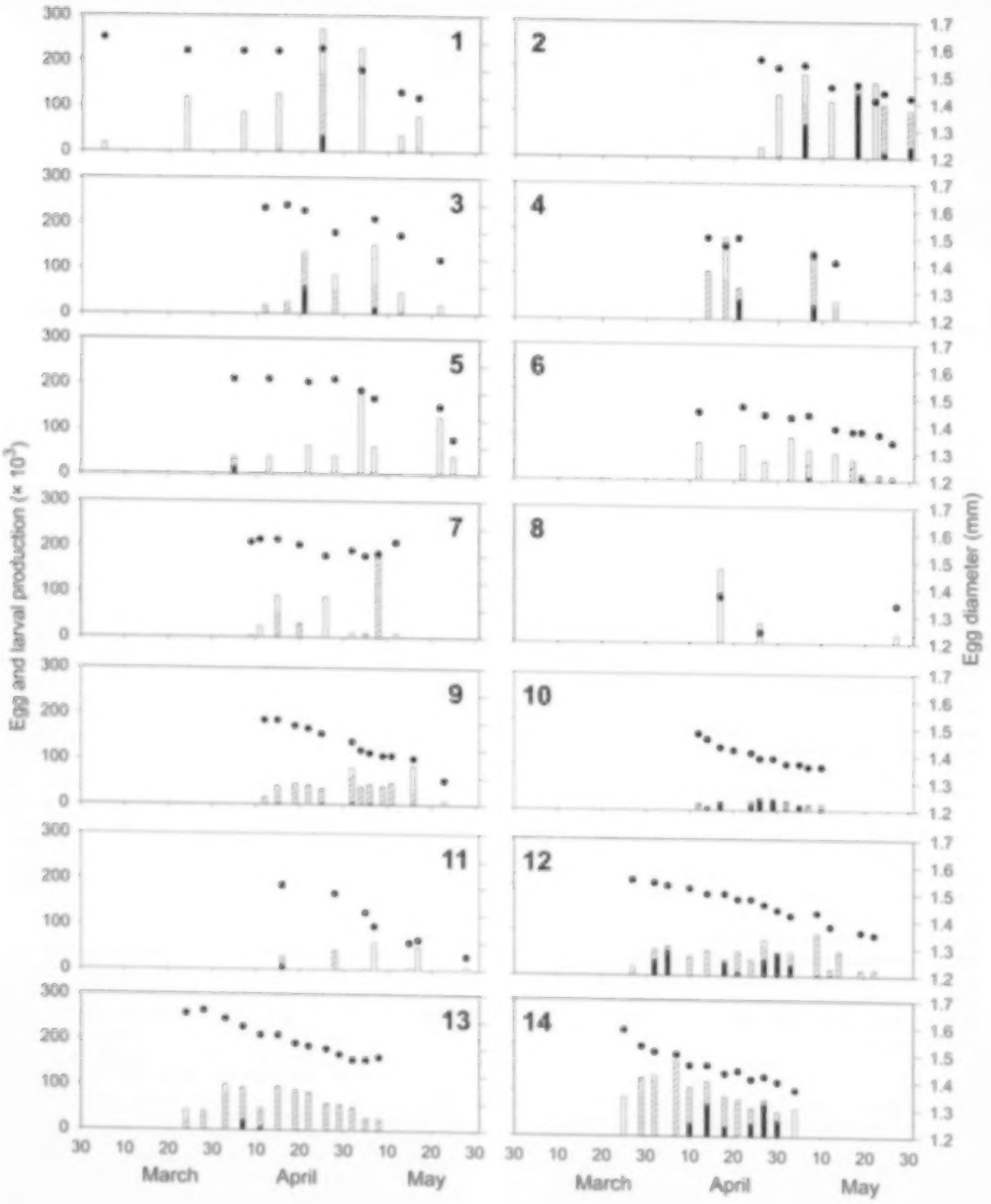

© 2004 NRC Canada

Fig. 2. Egg batch, fertilized eggs, and larval production (bars) and egg diameter (●) of four spawning pairs of captive Bay of Fundy haddock (*Melanogrammus aeglefinus*) each maintained for 2 successive years. Fork length (FL), body weight (BW), and Fulton's condition factor (*K*) are presented. Numbers 15–18 refer to females 15–18 in Table 1. Open bars, unfertilized; hatched bars, fertilized but did not hatch; solid bars, fertilized and hatched.

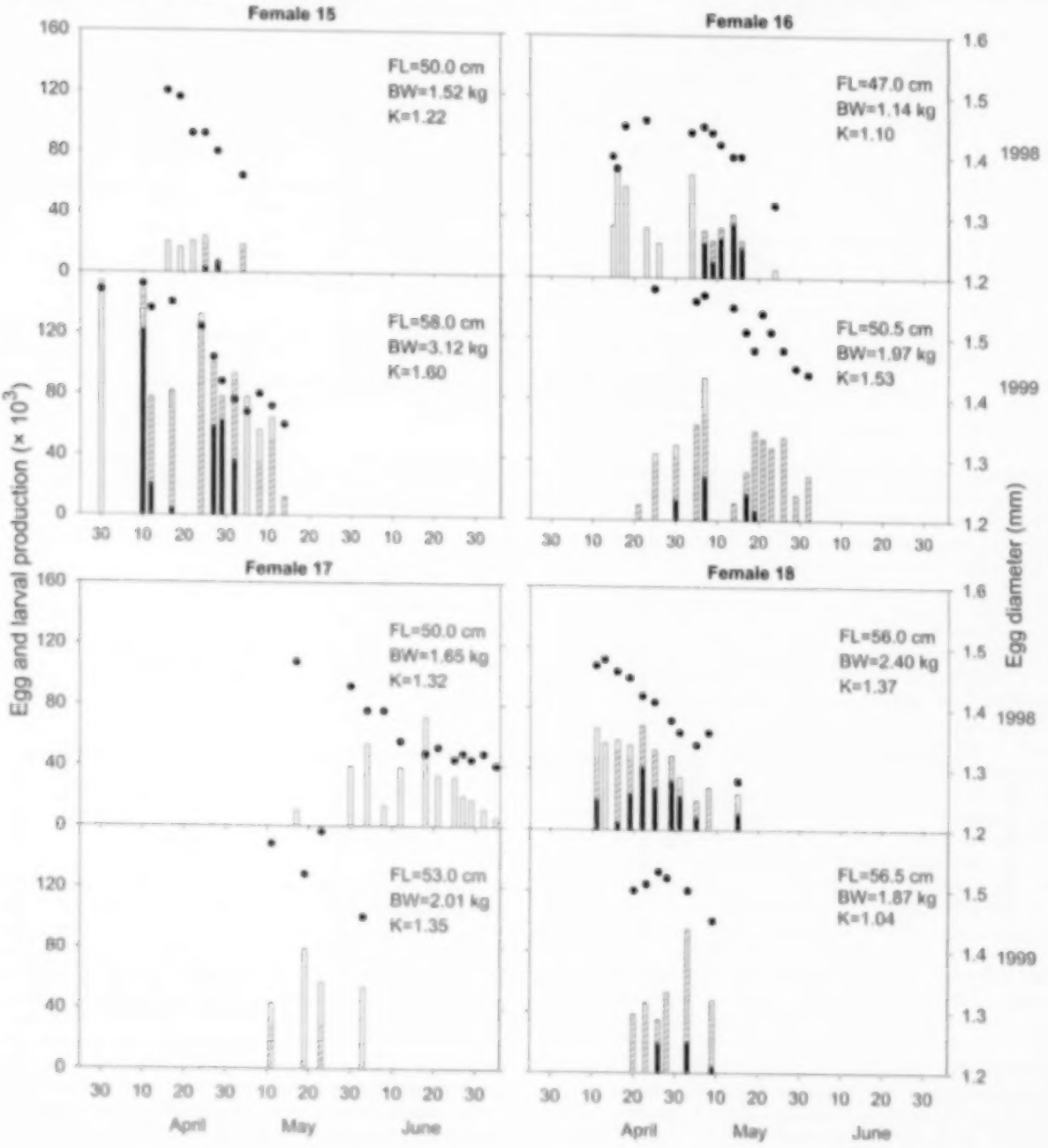

nity (Trippel and Morgan 1994; Wedekind et al. 2001) and male–female interactions (Saillant et al. 2001).

The ability of male condition to predict fertilization rates of haddock is presumably a function of ejaculate volume (Stockley et al. 1997; Trippel et al. 1998) and possibly sperm motility. In in vitro sperm competitions of Atlantic cod involving low- and high-condition males, the latter achieved greater fertilization success (Rakitin et al. 1999*a*). High-condition males might also aid in attracting and inducing females to enter into synchronous ovulation through superior courtship behaviour and associated acoustic stimuli, as during the spawning period, an attribute of increased condition

© 2004 NRC Canada

Table 2. Simple linear regression equations among prespawning body size of haddock (fork length (cm), body weight (kg), and Fulton's condition factor) with fecundity, egg diameter (mm), and fertilization rate for pooled data from 1997 to 1999.

Regression equation	n	r^2	P
Fecundity = 7.538×10^{-6}(fork length)$^{6.241}$	22	0.489	<0.001
= 134 913(body weight)$^{1.621}$	22	0.572	<0.001
= 199 039(condition factor)$^{2.478}$	22	0.296	0.009
Mean batch fecundity = 8.096×10^{-6}(fork length)$^{6.682}$	22	0.535	<0.001
= 20 406(body weight)$^{1.269}$	22	0.462	<0.001
= 34 380(condition factor)$^{1.277}$	22	0.104	0.144
Initial egg diameter = 0.009(fork length) + 1.062	22	0.249	0.018
= 0.068(body weight) + 1.379	22	0.393	0.002
= 0.217(condition factor) + 1.223	22	0.403	0.001
Composite egg diameter = 0.008(fork length) + 1.028	22	0.218	0.028
= 0.060(body weight) + 1.323	22	0.324	0.006
= 0.188(condition factor) + 1.192	22	0.314	0.007
Fertilization rate = 134.5(condition factor) – 114.841	18	0.326	0.013
= –5.193(mean batch interval) + 85.098	22	0.34	0.004
= –48.602(log$_e$(mean batch interval)) + 132.987	22	0.445	0.001
= –73.657(CV batch interval) + 91.528	22	0.182	0.048

Note: Condition factor for fecundity and egg size relationships is based on females and for fertilization rate on males; n is the number of fish and CV is the coefficient of variation.

Fig. 3. Relationships of fecundity and seasonal composite egg diameter with fork length, prespawning body weight, and Fulton's condition factor for captive Bay of Fundy haddock (*Melanogrammus aeglefinus*). Data are shown for 1997 (●), 1998 (▼), and 1999 (■); fitted lines are for pooled data with the equations given in Table 2.

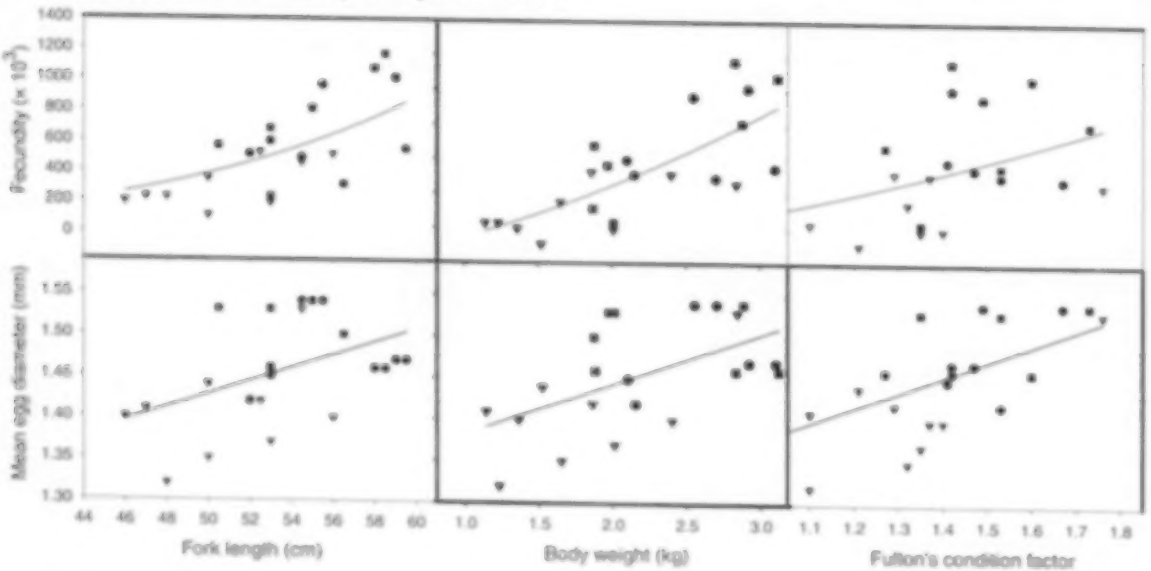

is the swelling of the paired drumming muscles attached to the swim bladder (Templeman and Hodder 1958; Hawkins et al. 1967; Hawkins and Amorim 2000). Evidence from our analysis, however, suggests that females are able to spawn regularly independent of the condition of the courting male (female haddock also have been observed to undergo rhythmic ovulation and spawning without a male present; E.A. Trippel, unpublished data). Even so, the behavioural and physical actions associated with the breeding embrace (ability to grasp the female and align the genital pores during the ventral mount) and the enticement of the female to join in the spawning act once she ovulates may be better achieved by high-condition males. Therefore, sire condition-based mating success may be a function of a number of physiological and behavioural attributes that infer heightened fitness to their prospective female partner (Reynolds and Gross 1992).

We found that the male to female length ratio did not explain a significant amount of variability in haddock fertilization success. This is in part due to the similarity in the size of fish within each pair (male to female length range 0.87–1.10). In experiments on other fish species using a broader

© 2004 NRC Canada

Table 3. Results and significance levels of multiple linear regressions for egg diameter and fertilization rate of haddock using pooled data from 1997 to 1999.

Variable	Independent variable	Regression coefficient	Variance explained (%)	*P*	*n*
Initial egg diameter	Intercept	0.998			
	Fork length	0.005	24.9	0.018	
	Condition factor	0.178	23.1	0.015	
			$r^2 = 0.480$	0.002	22
Composite egg diameter	Intercept	0.974			
	Fork length	0.005	21.8	0.028	
	Condition factor	0.15	17.1	0.044	
			$r^2 = 0.389$	0.009	22
Fertilization rate	Intercept	–34.921			
	Condition factor	91.118	32.6	0.013	
	Mean batch interval	–4.189	23.7	0.017	
			$r^2 = 0.563$	0.002	18

Note: Fulton's condition factor for egg size relationships is based on females and for fertilization rate on males; *n* is the number of fish.

Fig. 4. Relationship of prespawning male Fulton's condition factor and fertilization rate (seasonal composite) for captive Bay of Fundy haddock (*Melanogrammus aeglefinus*). Data are shown for 1997 (●), 1998 (▼), and 1999 (■); the fitted line is for pooled data with the equation given in Table 2.

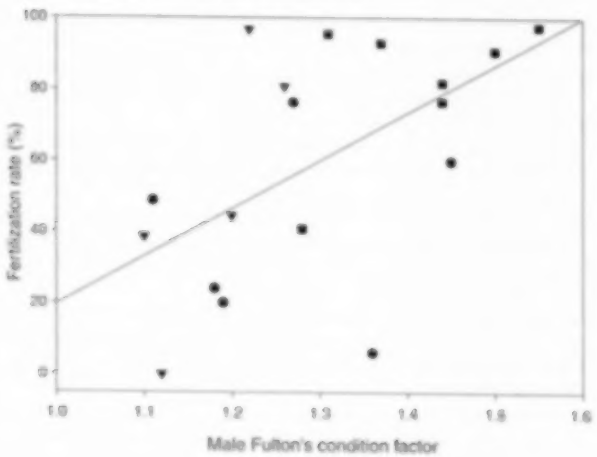

size range of males, it was shown that females tended to mate with males of similar body size to themselves, i.e., size-assortative mating (Foote 1988; Rakitin et al. 2001 (range 0.80–1.37); Bekkevold et al. 2002 (range 0.54–2.40)). Nonetheless, female preference for another partner may not be solely dependent on male size (Sargent et al. 1986; Semsar et al. 2001). Research on female choice in brook trout (*Salvelinus fontinalis*) found that females delay mating if a preferred male is not present (Blanchfield and Ridgway 1999). In our study, it is not clear whether reduced fertilization success was an expression of a female's preference for a different male, as there was no provision for female mate choice. The analysis presented on fertilization success does not account for the variability in sperm characteristics among males and the variability in the influence of female ovarian fluid on sperm motility (Litvak and Trippel 1998) or female choice at the gamete level (Rakitin et al. 1999*a*). Presumably, these gamete interactions also influenced fertilization rates in our study.

Little is known of the fertilization processes of wild gadoids (Markle and Waiwood 1986; Westin and Nissling 1991). Female fertilization dynamics in wild haddock spawning assemblages may involve promiscuous breeding with multiple males during release of a single egg batch, which could in turn elevate fertilization rates beyond those observed when isolated with a single male. Tank sizes used for paired mating were comparable in volume with the 3-m^3 glass-fronted concrete tanks used by Hislop et al. (1978) (two males were maintained with each female) and were the same as those used in Atlantic cod spawning studies (Trippel 1998; Fordham and Trippel 1999). In another study on paired mating, captive male haddock in these tanks produced daily courtship sounds (Bremner et al. 2002). Individuals monitored in our study did not exhibit stress symptoms such as inactivity and darkened markings (Thorsen et al. 2003). Further research is required to more fully understand the underlying factors leading to differences in haddock fertilization success and embryo viability. However, male condition and uniform time intervals between frequent egg batches (i.e., synchronous spawning) to date appear to be the best predictors of fertility. Patterns of female mate choice, sire dominance, and role of peripheral males in this species should be explored by determining the parentage of offspring generated by captive spawning aggregations (Hutchings et al. 1999; Hawkins and Amorim 2000; Trippel 2003). Peripheral males may elevate fertilization rates beyond those possible by a lone, low-condition male (in our study, 0% fertilization was predicted at prespawning male $K = 0.85$). However, given that haddock, like Atlantic cod, are determinate spawners (Rideout and Burton 2000), individuals participating in group spawns may jeopardize future matings because of sperm depletion (Nakatsuru and Kramer 1982). In protogynous hermaphrodites (e.g., serranids), when large males were heavily harvested, some females changed sex to maintain the operational sex ratio and avoid sperm limitation (Adams et al. 2000).

It is often assumed that female processes are responsible for the positive correlations between condition and recruitment that have been reported in the fisheries literature (Marshall and Frank 1999; Lambert et al. 2003). Our study is among the first to demonstrate that sire condition can have a profound limiting effect on total fertilized egg production of gadoids (Rakitin et al. 1999*a*; Trippel 2003). Adult gadoids

© 2004 NRC Canada

have been reported to size segregate during spawning (Hutchings and Myers 1993; Trippel and Morgan 1994), and consequently, male condition may play a greater role in female mate choice and spawning success than previously believed.

Individual monitoring in successive years

The monitoring of four females over 2 years in the present study generally confirmed the trends in reproductive traits and other life history attributes recorded on fish of various sizes monitored only once. Females that increased substantially in weight and condition exhibited an increase in fecundity, egg size, egg batches, and spawning duration, whereas females that maintained or lost body weight exhibited depressed reproductive output. In our study, it is interesting that the two female haddock that maintained or declined in condition spawned larger eggs (fewer batches were released), yet in the complete data set the overall pattern was a positive relationship between Fulton's condition factor and seasonal egg size ($r^2 = 0.314$). Of the females monitored, two of them had the same male partner in successive years (females 16 and 18). Thus, genetic factors would not have affected fertilization and hatching success of these pairs between years, and consequently, the key factors influencing early life history success for these fish would have been phenotypic changes in parental body characteristics and gamete quality (Rakitin et al. 1999*b*). Despite the limitations posed by small sample sizes, long-term monitoring of individual females (genotype unchanged) provides new insight into phenotypic variation in egg production of this long-lived teleost, although one must be cognizant of the paternal effect whether the sire remains unchanged or not (Evans and Gieffen 1998; Trippel 2003).

It is plausible, based on length at maturity (Trippel et al. 1997*b*), that three of the 18 monitored females were first-time spawners. Small 30- to 40-cm gravid females were captured from Browns Bank in 1998 and 1999 (Blanchard 2000) and the smallest fish in our experiments were approximately 45 cm (females 8, 10, and 16). Significant relationships with body length, weight, and Fulton's condition factor alone are of great utility in predicting haddock reproductive output among our group of fish that either all or a large majority were repeat spawners. Further evaluation of the reproductive potential of first-time spawning haddock, however, is warranted (Hislop 1988; Wigley 1999).

The predictive equations developed in this study are of potential use to estimate haddock reproductive potential and calculation of related biological reference points for fisheries management, although caution should be taken if extrapolating to other stocks or to body sizes and condition ranges not investigated (Lambert et al. 2003). We observed condition and body weight to act through gender-specific effects on haddock reproductive potential. In contrast with the negative effect of low sire condition on zygote formation that occurs during the brief fertilization process, the effect of low maternal condition and body weight via reduced egg size on progeny fitness is inevitably prolonged through various early life history stages. Sex-specific sensitivity in reproductive success to changes in fish condition has not been intensively studied. As condition declines in both sexes, synergistic interactions may begin that act via gamete quantity, quality, and spawning performance to influence recruitment in a depensatory mode. Further research is warranted to investigate this possibility as condition declines to severely low levels.

Acknowledgements

We thank the crew of the RV *J.L. Hart* for assistance in collecting haddock from the Bay of Fundy. Technical support involved in broodstock husbandry and egg collections was given by C.M. Doherty, P.R. Harmon, J.C. Reid, and J. Wade, for which the authors are grateful. J.L. Blanchard, R.G. Halliday, J.R.G. Hislop, R.M. Rideout, T.D. Shepherd, and two anonymous reviewers provided helpful comments on earlier drafts of the manuscript. The study was funded by Fisheries and Oceans Canada and the Canada/New Brunswick Cooperative Agreement on Economic Diversification.

References

Adams, A., Mapstone, B.D., Russ, G.R., and Davies, C.R. 2000. Geographic variation in the sex ratio, sex specific size, and age structure of *Plectropomus leopardus* (Serranidae) between reefs open and closed to fishing on the Great Barrier Reef. Can. J. Fish. Aquat. Sci. **57**: 1448–1458.

Bagenal, T.B. 1971. The interrelation of the size of fish eggs, the date of spawning and the production cycle. J. Fish Biol. **3**: 207–219.

Baskerville-Bridges, B., and Kling, L.J. 2000. Larval culture of Atlantic cod (*Gadus morhua*) at high stocking densities. Aquaculture, **181**: 61–69.

Bekkevold, D., Hansen, M.M., and Loeschcke, V. 2002. Male reproductive competition in spawning aggregations of cod (*Gadus morhua* L.). Mol. Ecol. **11**: 91–102.

Blanchard, J.L. 2000. Maternal contribution to the reproductive potential of a recovering fish stock: variability in the fecundity and condition of haddock (*Melanogrammus aeglefinus*). M.Sc. thesis, Dalhousie University, Halifax, N.S.

Blanchard, J.L., Frank, K.T., and Simon, J.E. 2003. Effects of condition on fecundity and total egg production of eastern Scotian Shelf haddock (*Melanogrammus aeglefinus*). Can. J. Fish. Aquat. Sci. **60**: 321–332.

Blanchfield, P.J., and Ridgway, M.S. 1999. The cost of peripheral males in a brook trout mating system. Anim. Behav. **57**: 537–544.

Breder, C.M., Jr., and Rosen, D.E. 1966. Modes of reproduction in fishes. Natural History Press, Garden City, N.Y.

Bremner, A.A., Trippel, E.A., and Terhune, J.M. 2002. Sound production by adult haddock, *Melanogrammus aeglefinus*, in isolation, pairs and trios. Environ. Biol. Fishes, **65**: 359–362.

Brooks, S., Tyler, C.R., and Sumpter, P. 1997. Egg quality in fish: what makes a good egg? Rev. Fish Biol. Fish. **7**: 321–330.

Buckley, L.J., Bradley, T.M., and Allen-Guilmette, J. 2000. Production, quality, and low temperature incubation of eggs of Atlantic cod *Gadus morhua* and haddock *Melanogrammus aeglefinus* in captivity. J. World Aquacult. Soc. **31**: 22–29.

Calow, P. 1979. The cost of reproduction — a physiological approach. Biol. Rev. **54**: 23–40.

Chambers, R.C. 1997. Environmental influences on egg and propagule sizes in marine fishes. *In* Early life history and recruitment in fish populations. *Edited by* R.C. Chambers and E.A. Trippel. Chapman and Hall, New York. pp. 63–102.

Chambers, R.C., and Waiwood, K.G. 1996. Maternal and seasonal differences in egg sizes and spawning characteristics of captive Atlantic cod, *Gadus morhua*. Can. J. Fish. Aquat. Sci. **53**: 1986–2003.

© 2004 NRC Canada

Chambers, R.C., Leggett, W.C., and Brown, J.A. 1989. Egg size, female effects and the correlation between early life history traits of capelin (*Mallotus villosus*): an appraisal at the individual level. Fish. Bull. **87**: 515–523.

Evans, J.P., and Geffen, A.J. 1998. Male characteristics, sperm traits, and reproductive success in winter-spawning Celtic Sea Atlantic herring, *Clupea harengus*. Mar. Biol. **132**: 179–186.

Fogarty, M.J., Myers, R.A., and Bowen, K.G. 2001. Recruitment of cod and haddock in the North Atlantic: a comparative analysis. ICES J. Mar. Sci. **58**: 952–961.

Foote, C.J. 1988. Male mate choice dependent on male size in salmon. Behaviour, **106**: 63–80.

Fordham, S.E., and Trippel, E.A. 1999. Feeding behaviour of cod (*Gadus morhua*) in relation to spawning. J. Appl. Ichthyol. **15**: 1–9.

Hansen, T., Karlsen, Ø., Taranger, G.L., Hemre, G.I., Holm, J.C., and Kjesbu, O.S. 2001. Growth, gonadal development and spawning time of Atlantic cod (*Gadus morhua*) reared under different photoperiods. Aquaculture, **203**: 51–67.

Hawkins, A.D., and Amorim, M.C. 2000. Spawning sounds of the male haddock, *Melanogrammus aeglefinus*. Environ. Biol. Fishes, **59**: 29–41.

Hawkins, A.D., Chapman, C.J., and Symonds, D.Y. 1967. Spawning of haddock in captivity. Nature (Lond.), **215**: 923–925.

Hislop, J.R.G. 1988. The influence of maternal length and age on the size and weight of the eggs and the relative fecundity of the haddock, *Melanogrammus aeglefinus*, in British waters. J. Fish Biol. **13**: 85–98.

Hislop, J.R.G., and Shanks, A.M. 1981. Recent investigations on the biology of the haddock, *Melanogrammus aeglefinus*, of the northern North Sea and the effects on fecundity of infection with copepod parasite *Lernaeocera branchialis*. J. Cons. Int. Explor. Mer, **39**: 244–251.

Hislop, J.R.G., Robb, A.P., and Gauld, J.A. 1978. Observations on the effects of feeding level on growth and reproduction in haddock, *Melanogrammus aeglefinus* (L.), in captivity. J. Fish Biol. **13**: 85–98.

Hodder, V.A. 1963. Fecundity of Grand Bank haddock. J. Fish. Res. Board Can. **20**: 1465–1487.

Hurley, P., Black, G., Comeau, P., and Mohn, R.K. 1999. Assessment of 4X haddock in 1998 and the first half of 1999. Can. Sci. Advisory Secretariat Res. Doc. 99/147.

Hutchings, J.A. 1991. Fitness consequences of variation in egg size and food abundance in brook trout, *Salvelinus fontinalis*. Evolution, **45**: 1162–1168.

Hutchings, J.A., and Myers, R.A. 1993. Effect of age on the seasonality of maturation and spawning of Atlantic cod, *Gadus morhua*, in the Northwest Atlantic. Can. J. Fish. Aquat. Sci. **50**: 2468–2474.

Hutchings, J.A., Bishop, T.D., and McGregor-Shaw, C.R. 1999. Spawning behaviour of Atlantic cod, *Gadus morhua*: evidence of mate competition, mate choice, and a negative effect of fishing. Can. J. Fish. Aquat. Sci. **56**: 97–104.

Katsukawa, T., Matsuda, H., and Matsumiya, Y.I. 2002. Population reproductive potential: evaluation of long-term stock productivity. Fish. Sci. **68**: 1106–1112.

Keckeis, H., Bauer-Nemeschkal, E., Menshutkin, V.V., Nemeschkal, H.L., and Kamler, E. 2000. Effects of female attributes and egg properties on offspring viability in a rheophilic cyprinid, *Chondrostoma nasus*. Can. J. Fish Aquat. Sci. **57**: 789–796.

Kjesbu, O.S. 1989. The spawning activity of cod, *Gadus morhua* L. J. Fish Biol. **34**: 195–206.

Kjesbu, O.S., Klungsøyr, J., Kryvi, H., Witthames, P.R., and Greer Walker, M. 1991. Fecundity, atresia, and egg size of captive Atlantic cod (*Gadus morhua*) in relation to proximate body composition. Can. J. Fish. Aquat. Sci. **48**: 2333–2343.

Kjesbu, O.S., Solemdal, P., Bratland, P., and Fonn, M. 1996. Variation in annual egg production in individual captive Atlantic cod (*Gadus morhua*). Can. J. Fish. Aquat. Sci. **53**: 610–620.

Knutsen, G.M., and Tilseth, S. 1985. Growth, development, and feeding success of Atlantic cod larvae *Gadus morhua* related to egg size. Trans. Am. Fish. Soc. **114**: 507–511.

Koops, M.A., Hutchings, J.A., and McIntyre, T.M. 2004. Testing hypotheses about fecundity, body size and maternal condition in fishes. Fish Fish. **5**: 1–11.

Kraus, G., Müller, A., Trella, K., and Köster, F.W. 2000. Fecundity of Baltic cod: temporal and spatial variation. J. Fish Biol. **56**: 1327–1341.

Lambert, Y., and Dutil, J.-D. 1997. Can simple condition indices be used to monitor and quantify seasonal changes in the energy reserves of Atlantic cod (*Gadus morhua*)? Can. J. Fish. Aquat. Sci. **54**(Suppl. 1): 104–112.

Lambert, Y., and Dutil, J.-D. 2000. Energetic consequences of reproduction in Atlantic cod (*Gadus morhua*) in relation to spawning level of somatic energy reserves. Can. J. Fish. Aquat. Sci. **57**: 815–825.

Lambert, Y., and Thorsen, A. 2003. Integration of captive and wild studies to estimate egg and larval production of fish stocks. J. Northwest Atl. Fish. Sci. **33**: 71–79.

Lambert, Y., Yaragina, N.A., Kraus, G., Marteinsdottir, G., and Wright, P.J. 2003. Using environmental and biological indices as proxies of egg and larval production of fish stocks. J. Northwest Atl. Fish. Sci. **33**: 115–159.

Laurence, G.C., Smiglielski, A.S., Halavik, T.A., and Burns, B.R. 1991. Implications of direct competition between larval cod (*Gadus morhua*) and haddock (*Melanogrammus aeglefinus* L.) in laboratory and growth studies at different food densities. Rapp. P.-v. Réun. Cons. Int. Explor. Mer, **178**: 304–311.

LeCren, E.D. 1951. The length–weight relationship and seasonal cycle in gonad weight and condition in the perch *Perca fluviatilis*. J. Anim. Ecol. **20**: 201–219.

Litvak, M.K., and Trippel, E.A. 1998. Sperm motility patterns of Atlantic cod (*Gadus morhua*) in relation to salinity: effects of ovarian fluid and egg presence. Can. J. Fish. Aquat. Sci. **55**: 1871–1877.

Markle, D.F., and Waiwood, K.G. 1986. Fertilization failure in gadids: aspects of its measurements. J. Northwest Atl. Fish. Sci. **6**: 89–93.

Marshall, C.T., and Frank, K.T. 1999. The effect of interannual variation in growth and condition on haddock recruitment. Can. J. Fish. Aquat. Sci. **56**: 347–355.

Marshall, C.T., Yaragina, N.A., Lambert, Y., and Kjesbu, O.S. 1999. Total lipid energy as a proxy for total egg production by fish stocks. Nature (Lond.), **402**: 288–290.

Marteinsdottir, G., and Begg, G.A. 2002. Essential relationships incorporating the influence of age, size, and condition on variables required for estimation of reproductive potential in Atlantic cod, *Gadus morhua*. Mar. Ecol. Prog. Ser. **235**: 235–256.

Marteinsdottir, G., and Steinarsson, A. 1998. Maternal influence on the size and viability of Icelandic cod (*Gadus morhua* L.) eggs and larvae. J. Fish Biol. **52**: 1241–1258.

McEvoy, L.A., and McEvoy, J. 1991. Size fluctuation in the eggs and newly hatched larvae of captive turbot (*Scophthalmus maximus*). J. Mar. Biol. Assoc. U.K. **71**: 679–690.

Mertz, G., and Myers, R.A. 1994. Match/mismatch predictions of spawning duration versus recruitment variability. Fish. Oceanogr. **3**: 236–245.

© 2004 NRC Canada

Nakatsuru, K., and Kramer, D.L. 1982. Is sperm cheap? Limited male fertility and female choice in the lemon tetra (Pisces, Characidae). Science (Wash., DC), **216**: 753–755.

Raitt, D.S. 1933. The fecundity of the haddock. Fish. Board Scot. Sci. Invest. 1932(1).

Rakitin, A., Ferguson, M.M., and Trippel, E.A. 1999*a*. Sperm competition and fertilization success in Atlantic cod (*Gadus morhua*): effects of size and condition factor on gamete quality. Can. J. Fish. Aquat. Sci. **56**: 2315–2323.

Rakitin, A., Ferguson, M.M., and Trippel, E.A. 1999*b*. Spermatocrit, spermatozoa density and size in Atlantic cod (*Gadus morhua*): correlation and variation during the spawning season. Aquaculture, **170**: 349–358.

Rakitin, A., Ferguson, M.M., and Trippel, E.A. 2001. Male reproductive success and body size in Atlantic cod *Gadus morhua* L. Mar. Biol. **138**: 1077–1085.

Rätz, H.-J., and Lloret, J. 2003. Variation in fish condition between Atlantic cod (*Gadus morhua*) stocks, the effect on their productivity and management implications. Fish. Res. **60**: 369–380.

Reynolds, J.D., and Gross, M.R. 1992. Female mate preference enhances offspring growth and reproduction in a fish, *Poecilia reticulata*. Proc. R. Soc. Lond. B Biol. Sci. **250**: 57–62.

Rideout, R.M., and Burton, M.P.M. 2000. The reproductive cycle of male Atlantic cod (*Gadus morhua* L.) from Placentia Bay, Newfoundland. Can. J. Zool. **78**: 1017–1025.

Rideout, R.M., Trippel, E.A., and Litvak, M.K. 2004. Predicting haddock embryo viability based on early cleavage patterns. Aquaculture, **230**: 215–228.

Saillant, E., Chatain, B., Fostier, A., and Przybyla, C. 2001. Parental influence on early development in the European sea bass. J. Fish Biol. **58**: 1585–1600.

Sargent, R.C., Gross, M.R., and van den Berghe, E.P. 1986. Male mate choice in fishes. Anim. Behav. **34**: 545–550.

Semsar, K., Kandel, F.L., and Godwin, J. 2001. Manipulations of the AVT system shift social status and related courtship and aggressive behavior in the bluehead wrasse. Horm. Behav. **40**: 21–31.

Sokal, R.R., and Rohlf, F.J. 1995. Biometry: the principles and practice of statistics in biological research. 3rd ed. W.H. Freeman and Company, New York.

Sonina, M.A. 1973. Peculiarities of the fecundity dynamics of the Arcto-Norwegian haddock (*Melanogrammus aeglefinus* (Linné)). ICES C.M. 1973/F:13.

Stockley, P., Gage, M.J.G., Parker, G.A., and Møller, A.P. 1997. Sperm competition in fishes: the evolution of testis size and ejaculate characteristics. Am. Nat. **149**: 933–954.

Templeman, W., and Hodder, V.M. 1958. Variation with fish length, sex, stage of sexual maturity, and season in the appearance and volume of the drumming muscles of the swim-bladder in the haddock, *Melanogrammus aeglefinus* (L.). J. Fish. Res. Board Can. **15**: 355–390.

Thorsen, A., Trippel, E.A., and Lambert, Y. 2003. Experimental methods to monitor the production and quality of eggs of captive marine fish. J. Northwest Atl. Fish. Sci. **33**: 55–70.

Trippel, E.A. 1998. Egg size and viability and seasonal offspring production of young Atlantic cod. Trans. Am. Fish. Soc. **127**: 339–359.

Trippel, E.A. 1999. Estimation of stock reproductive potential: history and challenges for Canadian Atlantic gadoid stock assessments. J. Northwest Atl. Fish. Sci. **25**: 61–81.

Trippel, E.A. 2003. Estimation of male reproductive success of marine fishes. J. Northwest Atl. Fish. Sci. **33**: 81–113.

Trippel, E.A., and Morgan, M.J. 1994. Age-specific paternal influences on reproductive success in Atlantic cod (*Gadus morhua*) of the Grand Banks. ICES Mar. Sci. Symp. **198**: 414–422.

Trippel, E.A., and Neil, S.R.E. 2003. Effects of photoperiod and light intensity on growth and activity of juvenile haddock (*Melanogrammus aeglefinus*). Aquaculture, **217**: 633–645.

Trippel, E.A., Kjesbu, O.S., and Solemdal, P. 1997*a*. Effects of adult age and size structure on reproductive output of marine fishes. *In* Early life history and recruitment in fish populations. *Edited by* R.C. Chambers and E.A. Trippel. Chapman and Hall, New York. pp. 31–62.

Trippel, E.A., Morgan, M.J., Fréchet, A., Rollet, C., Sinclair, A., Annand, C., Beanlands, D., and Brown, L. 1997*b*. Changes in age and length at sexual maturity of Northwest Atlantic cod, haddock and pollock stocks, 1972–1995. Can. Tech. Rep. Fish. Aquat. Sci. No. 2157.

Trippel, E.A., Doherty, C.M., Wade, J., and Harmon, P.R. 1998. Controlled breeding technology for haddock (*Melanogrammus aeglefinus*) in mated pairs. Bull. Aquat. Assoc. Can. **98-3**: 30–35.

Trippel, E.A., Castell, J.D., Neil, S.R.E., and Blair, T.J. 2000. Assessment of egg quality of haddock (*Melanogrammus aeglefinus*) in paired matings. *In* Reproductive physiology of fish. *Edited by* B. Norberg, O.S. Kjesbu, G.L. Taranger, E. Andersson, and S.O. Stefansson. Proceedings of the 6th International Symposium on the Reproductive Physiology of Fishes, 4–9 July 1999, Bergen, Norway. Institute of Marine Research and University of Bergen, Bergen, Norway. pp. 405–407.

Tyler, A.V., and Dunn, R.S. 1976. Ration, growth, measures of somatic and organ condition in relation to meal frequency in winter flounder (*Pseudopleuronectes americanus*), with hypotheses regarding population homeostasis. J. Fish. Res. Board Can. **33**: 63–75.

Van Winkle, W., Shuter, B.J., Holcomb, B.D., Jager, H.I., Tyler, J.A., and Whitaker, S.Y. 1997. Regulation of energy acquisition and allocation to respiration, growth and reproduction: simulation model and example using rainbow trout. *In* Early life history and recruitment in fish populations. *Edited by* R.C. Chambers and E.A. Trippel. Chapman and Hall, New York. pp. 103–137.

Waiwood, K.G., and Beamish, M.-I. 1989. Reproductive biology of Southwest Scotian Shelf haddock (*Melanogrammus aeglefinus*). Can. J. Fish. Aquat. Sci. **46**(Suppl. 1): 153–170.

Wedekind, C., Müller, R., and Spicher, H. 2001. Potential genetic benefits of mate selection in whitefish. J. Evol. Biol. **14**: 980–986.

Westin, L., and Nissling, A. 1991. Effects of salinity on spermatozoa motility, percentage of fertilized eggs and egg development of Baltic cod (*Gadus morhua*), and implications for cod stock fluctuations. Mar. Biol. **108**: 5–9.

Wigley, S.E. 1999. Effects of first-time spawners on stock–recruitment relationships for two groundfish species. J. Northwest Atl. Fish. Sci. **25**: 215–218.

Witthames, P.R., and Greer Walker, M. 1995. Determinacy of fecundity and oocyte atresia in sole (*Solea solea*) from the Channel, North Sea and the Irish Sea. Aquat. Living Resour. **8**: 91–109.

© 2004 NRC Canada

Changes in the crustacean communities of Lakes Michigan, Huron, and Erie following the invasion of the predatory cladoceran *Bythotrephes longimanus*

Richard P. Barbiero and Marc L. Tuchman

Abstract: The crustacean zooplankton communities in Lakes Michigan and Huron and the central and eastern basins of Lake Erie have shown substantial, persistent changes since the invasion of the predatory cladoceran *Bythotrephes* in the mid-1980s. A number of cladoceran species have declined dramatically since the invasion, including *Eubosmina coregoni*, *Holopedium gibberum*, *Daphnia retrocurva*, *Daphnia pulicaria*, and *Leptodora kindti*, and overall species richness has decreased as a result. Copepods have been relatively unaffected, with the notable exception of *Mesocyclops edax*, which has virtually disappeared from the lakes. These species shifts have for the most part been consistent and equally pronounced across all three lakes. Responses of crustacean species to the *Bythotrephes* invasion do not appear to be solely a consequence of size, and it is likely that other factors, e.g., morphology, vertical distribution, or escape responses, are important determinants of vulnerability to predation. Our results indicate that invertebrate predators in general, and invasive ones in particular, can have pronounced, lasting effects on zooplankton community structure.

Résumé : Les communautés de crustacés zooplanctoniques des lacs Michigan et Huron et des cuvettes centrale et orientale du lac Érié ont subi des changements importants et durables depuis l'invasion du cladocère prédateur *Bythotrephes* au milieu des années 1980. Plusieurs espèces de cladocères ont vu leur abondance décliner de façon spectaculaire depuis l'invasion, en particulier, *Eubosmina coregoni*, *Holopedium gibberum*, *Daphnia retrocurva*, *Daphnia pulicaria* et *Leptodora kindti*, ce qui a fait baisser la richesse globale en espèces. Les copépodes ont été peu affectés, avec l'exception notable de *Mesocyclops edax* qui est pratiquement disparu des lacs. Ces changements spécifiques se sont produits en général de façon semblable et avec la même intensité dans les trois lacs. Les réactions des espèces de crustacés à l'invasion de *Bythotrephes* ne semblent pas se faire seulement en fonction de la taille; il est donc probable que d'autres facteurs, tels que la morphologie, la répartition verticale et les comportements d'évitement, jouent un rôle important dans leur vulnérabilité à la prédation. Nos résultats indiquent que les invertébrés prédateurs en général, et les prédateurs envahisseurs en particulier, peuvent avoir un effet considérable et durable sur la structure de la communauté zooplanctonique.

[Traduit par la Rédaction]

Introduction

The ability of selective predation by vertebrates to substantially alter the size and composition of zooplankton communities has long been recognized (Hrbáček 1960; Hrbáček et al. 1961; Brooks and Dodson 1965); however, substantially less is known about the role of invertebrate predators in shaping zooplankton community structure. Numerous studies have documented the ability of invertebrate predation to mediate shifts in the size of zooplankton populations, particularly in the absence of strong vertebrate predation pressure (McQueen 1969; Dodson 1974; de Bernardi and Giussani 1975), but its importance in structuring zooplankton communities in the presence of vertebrate planktivores is generally considered to be low (Zaret 1980; de Bernardi et al. 1987; Hansson and Tranvik 1996).

The invasion of new predatory invertebrates into aquatic systems offers an opportunity to assess the effects of invertebrate predation on zooplankton community structure. Such an opportunity presented itself during the mid-1980s when *Bythotrephes longimanus* (initially referred to as *B. cederstroemi*), a large predatory cladoceran native to northern Europe and Asia, invaded the Laurentian Great Lakes. This species was first found in Lake Ontario in 1982 (Johannsson et al. 1991) and subsequently spread to all five Great Lakes (Bur et al. 1986; Evans 1988; Cullis and Johnson 1988), es-

Received 28 April 2003. Accepted 16 March 2004. Published on the NRC Research Press Web site at http://cjfas.nrc.ca on 22 January 2005.
J17493

R.P. Barbiero.[1] DynCorp Science and Engineering Group, 1359 W Elmdale Ave., Suite 2, Chicago, IL 60660, USA.
M.L. Tuchman. US Environmental Protection Agency, Great Lakes National Program Office, 77 W Jackson Boulevard, Chicago, IL 60604, USA.

[1]Corresponding author (e-mail: gloeotri@sbcglobal.net).

 doi: 10.1139/F04-149 © 2004 NRC Canada

tablishing persistent populations in all but Lake Ontario and the western basin of Lake Erie. It has since spread to 50 inland Ontario lakes (Therriault et al. 2002), as well as several inland lakes in the United States (Yan and Pawson 1998). The effects of *B. longimanus* on the zooplankton community in Lake Michigan were particularly well documented during the initial years of the invasion (Lehman 1987, 1988). These studies indicated a pronounced shift in cladoceran community composition coincident with the appearance of *Bythotrephes* (Lehman 1988; Branstrator and Lehman 1991; Lehman and Cáceres 1993), as well as changes in the abundances of several rotifer species (Sandgren and Lehman 1990). To date, however, there have been no long-term assessments of the potential impacts of *Bythotrephes* on the Great Lakes. Elucidation of such impacts and their persistence requires long-term, internally consistent data sets. Although the importance of exploiting long-term data sets to elucidate impacts of freshwater invaders has been stressed (Yan et al. 2001), to date only one such data set has come to light: that of Harp Lake, Ontario (Yan and Pawson 1997; Yan et al. 2001, 2002). The Great Lakes National Program Office (GLNPO) of the US Environmental Protection Agency has been monitoring the Laurentian Great Lakes since 1983. Thus, a detailed, internally consistent and spatially extensive data set exists of zooplankton community composition during both the pre- and post-invasion periods. Here we make use of this unique data set to examine the impacts that *B. longimanus* has had on the crustacean zooplankton communities of Lakes Huron, Michigan, and Erie (monitoring of Lake Superior did not begin until after the appearance of *Bythotrephes* in that lake). Specifically, we were interested in determining whether changes have occurred in zooplankton community structure since the invasion of *B. longimanus*, how persistent any such changes have been, and how consistent these have been across the three lakes.

Methods

Lakes Erie, Michigan, and Huron were sampled annually during late summer (1 August – 4 September), a period that likely coincided with peak cladoceran abundances in Lakes Michigan and Huron (Wells 1960; Watson and Carpenter 1974), but not in Lake Erie where maximum populations occur in late June and July (Johannsson et al. 1999). Sampling was conducted between 1983 and 1999 with the following exceptions: Lakes Huron and Erie were not sampled in 1992, 1994, and 1995, and data from 1997 are not available for any of the three lakes. Because *Bythotrephes* has failed to establish substantial populations in the western basin of Lake Erie, results from that lake will be restricted to the central and eastern basins. The two basins of Lake Erie are morphometrically distinct; most of the central basin is 20 to 24 m deep, whereas depths in the smaller eastern basin exceed 60 m. Therefore they are treated separately in all analyses. Sampling was spatially extensive throughout the offshore waters of all lakes (Fig. 1). Zooplankton samples were collected with vertical net tows taken at each station from either 20 m deep or 1 m above the bottom, whichever was shallower, with a 0.5-m-diameter, 64-μm-mesh conical net (diameter:length = 1:3). The net was equipped with a flow meter and appropriate corrections were made for filtering efficiency. Since 1997, additional zooplankton tows have been taken from a depth of 100 m or 2 m from the bottom, whichever is shallower, using a 153-μm-mesh conical net. Data from these tows were used for comparisons of crustacean lengths but were not used in the assessment of changes in historical densities.

Fig. 1. Map of sampling stations in Lakes Michigan, Huron, and Erie. Not all stations were sampled in all years.

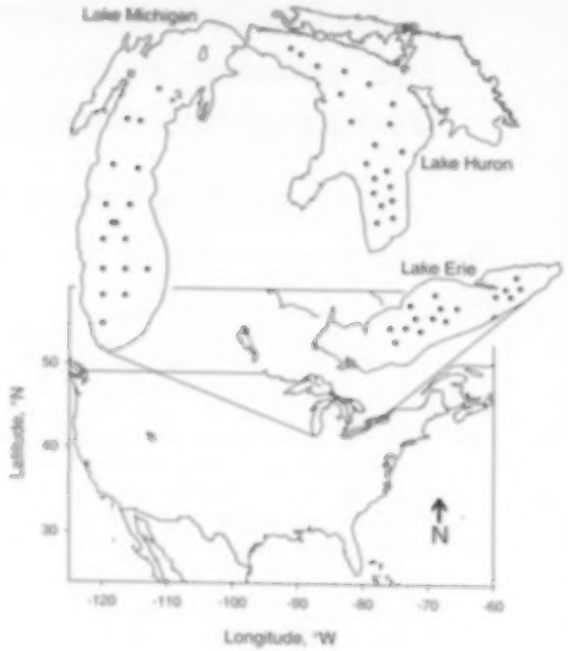

Shipboard operations are conducted on a 24-h basis, and it is recognized that species undergoing diurnal vertical migration (DVM) could have been underestimated at stations sampled during the daytime. Because sampling times for zooplankton tows were not recorded for cruises before 1997, no corrections could be made for differences in time of day of collection. However, sampling runs on each lake typically take more than 24 h, and this should result in a mix of daytime and nighttime samples being taken for each lake in each year. Therefore, the main impact of using 20-m tows should be to increase intra-annual variability in density estimates, rather than to introduce any systematic interannual bias. We therefore feel that these data are representative of temporal trends in community composition and species densities. Populations of the deep-living species *Mysis relicta*, *Limnocalanus macrurus*, and *Leptodiaptomus sicilis*, however, cannot be accurately assessed with data from 20-m tows and will not be considered here.

After collection, samples were immediately narcotized with soda water and preserved with sucrose formalin solution (Haney and Hall 1973) approximately 20 min later. Samples were split in the laboratory using a Folsom plankton splitter, and four stratified aliquots were examined per sample using a stereoscopic microscope such that rare species were enumerated from the less dilute aliquots. On average, about 600 individuals were identified per sample. Crustacean taxonomy generally followed Balcer et al. (1984); other sources

© 2004 NRC Canada

Table 1. Lake-wide late summer densities (number·m^{-3}) of common crustacean zooplankton species in Lakes Michigan (MI), Huron (HU), and Erie (ER C, central basin; ER E, eastern basin) averaged over all years of study (1983–1999).

	Lake			
Species	MI	HU	ER C	ER E
Bythotrephes longimanus	11	10	32	23
Leptodora kindti	18	10	30	41
Diaphanosoma birgei	9	1	774	388
Holopedium gibberum	19	129	28	70
Daphnia mendotae	3 418	1 413	4 091	3 203
Daphnia longiremis	6	15	97	126
Daphnia pulicaria	164	74	171	154
Daphnia retrocurva	93	75	687	1 162
Eubosmina coregoni	28	118	663	618
Bosmina longirostris	1 762	945	2 748	1 597
Total cladocerans	5 531	2 936	9 345	7 408
Leptodiaptomus ashlandi	1 917	507	197	44
Leptodiaptomus minutus	1 009	1 151	335	306
Leptodiaptomus siciloides	0	0	57	179
Skistodiaptomus oregonensis	101	110	3 326	2 280
Diaptomid copepodites	6 657	11 832	8 176	10 050
Epischura lacustris	71	57	187	246
Epischura copepodites	154	562	1 146	1 894
Total calanoids	10 038	14 336	13 464	15 011
Acanthocyclops vernalis	1	5	67	130
Diacyclops thomasi	1 525	814	911	399
Cyclopoid copepodites[a]	4 106	4 572	4 222	3 942
Mesocyclops edax	23	38	1 196	762
Mesocyclops copepodites	16	110	1 510	619
T. extensus copepodites	313	41	393	1 209
Total cyclopoids	6 367	5 659	8 587	7 990

Note: Group totals include all species, including those not shown.
[a]Mostly *Diacyclops thomasi*.

consulted included Brooks (1959), Evans (1985), and Hudson et al. (1998). Immature calanoids and cyclopoids were identified to the lowest taxonomic level possible, usually suborder or genus. Length measurements were made on the first 20 individuals of each species encountered per sample. *Bythotrephes* was measured from the anterior margin of the eye to the insertion point of the first pair of spines on the caudal process; corrections were not made for shrinkage in formalin. Differences in *Bythotrephes* lengths among the four lake areas were assessed using a generalized linear model (GLM) with stations (n = 8–26) as a random factor nested within lake areas and individual length measurements from each station constituting within-station replicates. Between 120 and 384 individual length measurements were used per lake area. Specific differences between pairs of lake areas were assessed using Tukey–Kramer pairwise comparisons. Only measurements from 100-m tows taken in 1999 were used for this analysis.

Changes in densities of major groups and individual species before and after the *Bythotrephes* invasion were assessed using either a t test or, where assumptions of normality and homoscedasticity were not met, the Mann–Whitney rank sum test. Because trends were assessed using annual lake-wide averages, we defined the initial year of invasion as the first year in which *Bythotrephes* appeared at a majority of sites in each lake. Thus, post-invasion years began in 1986 for Lakes Huron and Erie and in 1987 for Lake Michigan. While referred to for brevity as pre- and post-invasion periods, these more properly correspond to pre- and post-lake-wide colonization periods. The conservative approach of using annual lake-wide average values rather than individual station values was adopted, as in the latter case, extremely high sample sizes would have permitted the detection of minor differences unlikely to be of ecological importance. Temporal autocorrelation was tested for using a lag of one time period; no significant effects were found for any species–lake combination. Significance was assessed at $\alpha = 0.05$. Although we recognize that a large number of tests using similar null hypotheses were conducted in our analyses, we were not testing a universal null hypothesis, i.e., a significant effect in any of the comparisons would not have implied a significant effect overall, nor would it have lessened interest in the results of subsequent tests. Therefore, no Bonferroni-type corrections were deemed necessary, and significance was assessed in all cases at $\alpha = 0.05$. The reader is advised to interpret the results accordingly.

Patterns in zooplankton community composition across the lakes were explored with the use of detrended correspondence analysis (DCA), using the program CANOCO version 4.0. This is an ordination technique that extracts axis scores

© 2004 NRC Canada

Fig. 2. Average lake-wide (basin-wide in the case of Lake Erie) late summer densities of *Bythotrephes* in (*a*) Lake Michigan, (*b*) Lake Huron, and (*c*) central and (*d*) eastern basins of Lake Erie. Note differences in scale between graphs. Bars represent one standard error.

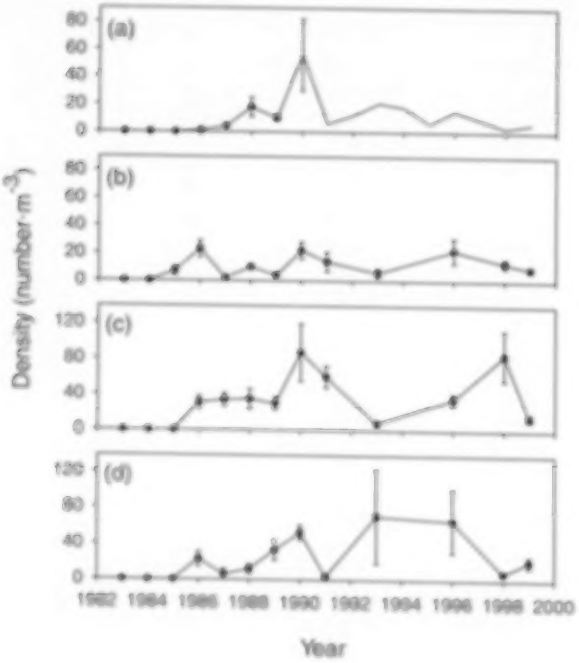

from samples on the basis of species composition such that samples with similar species composition are close by, and those with dissimilar species composition are far apart. Only those species constituting more than 1% of total abundances in any sample were included in the analysis. Densities were converted to natural logarithms before analysis to reduce the undue influence of dominant species.

Results

When averaged over all years of the study (1983–1999), diaptomid copepodites were numerically dominant in all lakes during late summer (Table 1). Adult calanoids were represented mostly by *Leptodiaptomus minutus* and *Leptodiaptomus ashlandi* in Lakes Michigan and Huron, whereas *Skistodiaptomus oregonensis* and *Epischura lacustris* were most prevalent in Lake Erie. Cyclopoids were represented almost exclusively by *Diacyclops thomasi* in Lakes Huron and Michigan, with *Mesocyclops edax* co-dominant in Lake Erie. *Daphnia mendotae* was the dominant cladoceran across all lakes, although several other daphnids, including *Daphnia retrocurva*, *Daphnia pulicaria*, and *Daphnia longiremis*, were also found, along with the smaller cladocerans *Bosmina longirostris* and *Eubosmina coregoni*.

Bythotrephes longimanus was first found in North America in Lake Ontario in 1982 (Johannsson et al. 1991), although substantial populations have never become established in the lake. *Bythotrephes* was subsequently found at two stations in southern Lake Huron during a GLNPO cruise in December 1984 (Barr et al. 1986). In August 1985, populations of this

Fig. 3. Size-frequency distributions of *Bythotrephes* lengths in (*a*) Lake Michigan, (*b*) Lake Huron, and (*c*) central and (*d*) eastern basins of Lake Erie in 1999. Vertical reference lines indicate mean lengths; shaded areas indicate interquartile ranges.

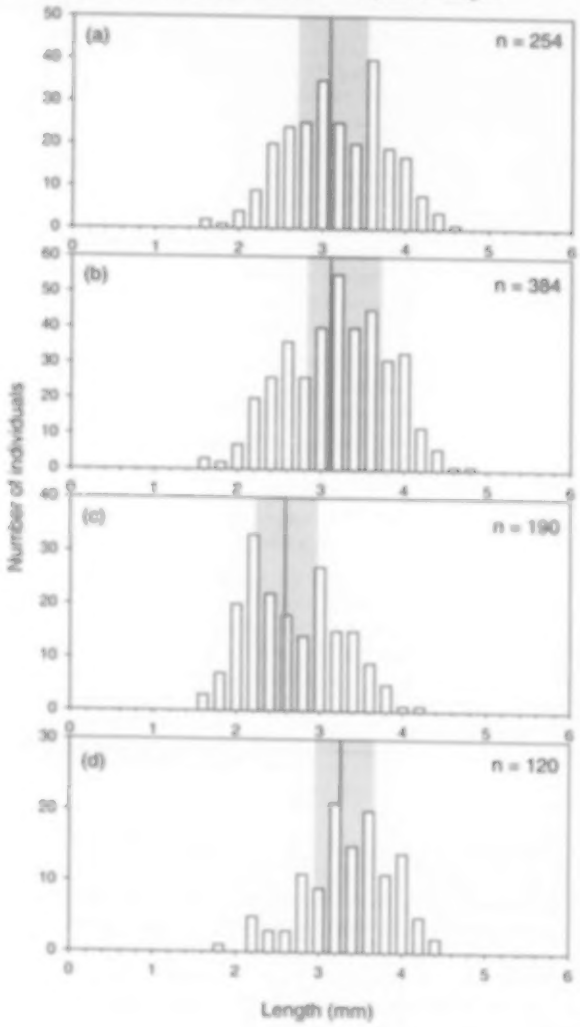

organism were still fairly small and largely restricted to the southern portion of the lake. By 1986 it was seen in sizeable numbers at most stations. *Bythotrephes* was first found in Lake Erie during a GLNPO cruise in mid-November 1985. At that time, individuals were found in vertical net tows in the western and central basins and in the western-most portion of the eastern basin. By August of 1986, populations were firmly established in the central and eastern basins, where this organism has been seen consistently during GLNPO's annual August cruises. In contrast, *Bythotrephes* has been virtually absent from the western basin. *Bythotrephes* was first found in Lake Michigan at two offshore sites in the central and northern area of the lake during a GLNPO cruise on 21–22 August 1986. By August 1987, the organism was distributed throughout the lake and has since maintained a

© 2004 NRC Canada

Fig. 4. Average late summer species richness (including *Bythotrephes*) per sample observed in (*a*) Lake Michigan, (*b*) Lake Huron, and (*c*) central and (*d*) eastern basins of Lake Erie. Bars represent one standard error; arrows indicate first post-invasion year; broken reference lines indicate average pre-invasion species richness.

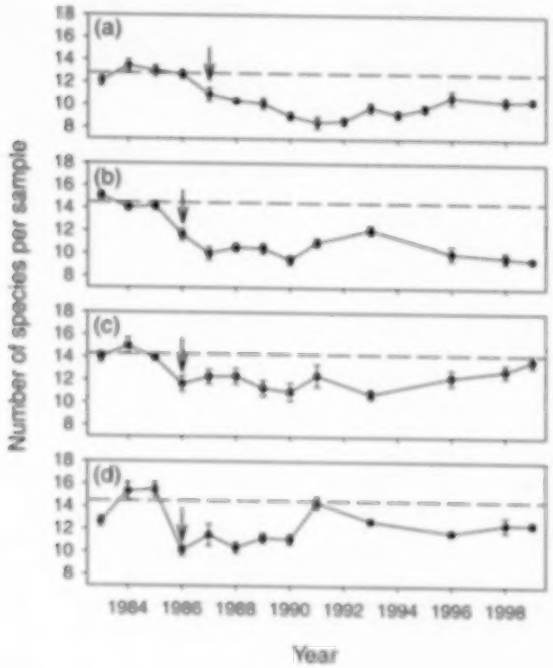

Fig. 5. Average lake-wide (basin-wide in the case of Lake Erie) late summer densities of cladocerans (excluding *Bythotrephes*) in (*a*) Lake Michigan, (*b*) Lake Huron, and (*c*) central and (*d*) eastern basins of Lake Erie. Note differences in scale between graphs. Bars represent one standard error; arrows indicate first post-invasion year.

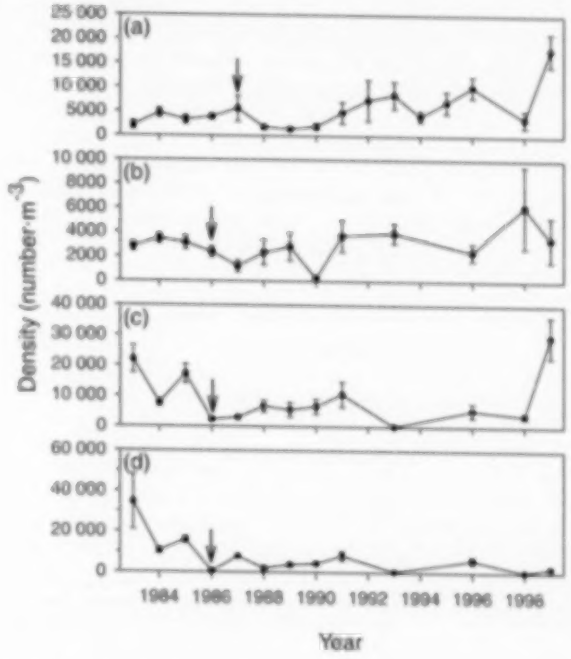

persistent, if somewhat variable, presence in the offshore waters.

Population densities of *Bythotrephes* have been highest in the central basin of Lake Erie, where the overall late summer average since the establishment of the population in 1986 has been 41 m^{-3} (Fig. 2). Densities have been nearly as high in the eastern basin (mean = 32 m^{-3}), although somewhat more variable. Densities in Lakes Huron and Michigan have been much lower (13 and 10 m^{-3}, respectively) and have only occasionally approached the levels seen in Lake Erie. Although populations have shown some fluctuations over the years, the species is firmly established in all three lakes.

Bythotrephes lengths in 1999 were highest in the eastern basin of Lake Erie (mean = 3.26 mm), intermediate for Lakes Michigan and Huron (mean = 3.09 and 3.11 mm, respectively), and lowest in the central basin of Lake Erie (mean = 2.58; Fig. 3). The GLM procedure indicated that statistical differences in lengths existed between the different lake areas ($F = 9.198$, $p = 0.0001$). Pair-wise comparisons showed statistically significant differences in mean lengths between all lakes except Lakes Michigan and Huron.

Crustacean species richness in August fell in all lakes immediately following the *Bythotrephes* invasion (Fig. 4). Pre-invasion species richness averaged approximately 14 species·sample^{-1}, except in Lake Michigan where richness was slightly lower (12.8). Since the invasion, average richness has fallen between 16% (Erie, central basin) and 28% (Michigan), with all decreases determined to be statistically significant by the Mann–Whitney rank sum test ($P < 0.001$). Richness values during the 1990s were slightly higher than those recorded immediately after the invasion in the eastern basin of Lake Erie and, to a lesser extent, in Lake Michigan. However, lake-wide late summer averages after the invasion have remained below the pre-invasion average for all years of the study in all lakes.

Dramatic effects on abundances of major groups by and large were not seen. Total cladoceran abundances did decline notably in Lake Erie in the first year of invasion and remained relatively suppressed in both basins (Fig. 5). The difference between pre- and post-invasion abundances was statistically significant for the eastern basin (Table 2), but not the central basin, owing to unusually high cladoceran abundances in 1999. Excluding this year, the difference between the two periods was highly significant ($t = 3.802$, $P = 0.003$). A slight decrease in cladoceran abundance was seen in the years immediately following the invasion in Lake Michigan, although in neither Lake Michigan nor Lake Huron were statistically significant differences between the two periods seen. No clear patterns were evident in calanoid abundance, and no statistically significant differences were found between the pre- and post-invasion periods. Similarly, no clear patterns were apparent in cyclopoid abundances, and no statistically significant differences were found between the pre- and post-invasion periods.

A number of crustacean species exhibited distinct changes in density coincident with the appearance of *Bythotrephes*. In many cases these changes were quite abrupt and consis-

© 2004 NRC Canada

Table 2. Results of *t* test (*t*), or Mann–Whitney rank sum test (*T*) where assumptions of normality and homoscedasticity are not met, of differences in late summer densities of crustacean species during the pre- and post-invasion periods in Lakes Michigan and Huron and the central and eastern basins of Lake Erie.

	Lake			
Species	Michigan	Huron	Central Erie	Eastern Erie
Leptodora kindti	$T = 58$	$t = 5.372$	$t = 2.228$	$T = 25$
	$P =$ **0.004**	$P =$ **<0.001**	$P =$ **0.048**	$P = 0.554$
Daphnia pulicaria	$T = 58$	$T = 36$	$T = 30$	$T = 30.5$
	$P =$ **0.004**	$P =$ **0.014**	$P = 0.146$	$P = 0.122$
Daphnia retrocurva	$T = 58$	$T = 30$	$t = 3.564$	$T = 35$
	$P =$ **0.004**	$P = 0.15$	$P =$ **0.004**	$P =$ **0.022**
Daphnia mendotae	$t = -1.216$	$T = 25$	$t = 2.822$	$T = 36$
	$P = 0.244$	$P = 0.554$	$P =$ **0.017**	$P =$ **0.014**
Daphnia longiremis			$T = 8$	$t = -1.048$
			$P =$ **0.035**	$P = 0.317$
Diaphanosoma birgei			$t = 2.592$	$T = 34$
			$P =$ **0.025**	$P =$ **0.034**
Eubosmina coregoni	$T = 58$	$T = 35$	$T = 35$	$T = 36$
	$P =$ **0.004**	$P =$ **0.022**	$P =$ **0.022**	$P =$ **0.014**
Bosmina longirostris	$T = 18$	$t = -1.205$	$T = 14$	$T = 21$
	$P = 0.06$	$P = 0.253$	$P = 0.272$	$P = 0.933$
Holopedium gibberum	$T = 50$	$t = 3.351$	$T = 34$	$T = 34$
	$P = 0.06$	$P =$ **0.006**	$P =$ **0.034**	$P =$ **0.034**
Total cladocerans	$t = -1.130$	$t = 0.274$	$t = 1.549$	$T = 36$
	$P = 0.277$	$P = 0.789$	$P = 0.150$	$P =$ **0.014**
Mesocyclops edax	$T = 53$	$T = 36$	$t = 3.476$	$T = 36$
	$P =$ **0.025**	$P =$ **0.014**	$P =$ **0.005**	$P =$ **0.014**

Note: In all cases, a two-tailed null hypothesis was used. Probabilities significant at $\alpha = 0.05$ are shown in bold.

tent across all three lakes. Densities of the native predatory cladoceran *Leptodora kindti* declined markedly in both Lakes Michigan and Huron immediately after the invasion of *Bythotrephes* (Fig. 6). In both lakes, *Leptodora* was virtually absent from the open waters through the early 1990s, and although occasionally found in somewhat greater numbers since then, densities have consistently remained below pre-invasion levels. The situation was similar in the central basin of Lake Erie, although a particularly large *Leptodora* population was seen in 1988. In all three cases, post-invasion declines were statistically significant (Table 2). *Leptodora* populations have been more variable in the eastern basin of Lake Erie, and there has not been a clear reduction in densities since the appearance of *Bythotrephes*.

The large daphnid *D. pulicaria* was a sizeable component of the immediate pre-invasion communities of Lakes Michigan and Huron and has virtually disappeared from each lake since the invasion (Fig. 7). This species was only seen in sizeable numbers in 1984 in Lake Erie, so its subsequent absence from that lake is harder to ascribe to *Bythotrephes*. The smaller *D. retrocurva* declined immediately after the arrival of *Bythotrephes* in all three lakes (Fig. 7). This species seemed to recover in Lake Huron in the mid-1990s, exhibiting large but highly variable populations in 1991 and 1993. As with *D. pulicaria*, pre-invasion numbers were quite variable in Lake Erie, although population decreases were significant in all lakes but Huron (Table 2). In contrast to these daphnids, the dominant cladoceran in the lakes, *D. mendotae*, did not show a clear response to the appearance of *Bythotrephes* (Fig. 8). Populations have changed during the period of record, in particular, declining in Lake Erie and increasing in Lake Michigan during the 1990s. There is some suggestion of decreased densities during the initial year of invasion in Lake Erie, and overall *D. mendotae* populations have been statistically significantly lower in that lake in post-invasion compared with pre-invasion years. However, the major declines appear to have taken place 5 or more years after the invasion, suggesting causes other than *Bythotrephes*.

Two cladocerans that were found in significant numbers only in Lake Erie exhibited opposite responses to *Bythotrephes*. Post-invasion populations of *Diaphanosoma birgei* were statistically significantly lower in both basins of Lake Erie (Fig. 9), whereas *D. longiremis* appeared to increase during the post-invasion period, although this increase was only statistically significant in the central basin.

Among the smaller cladocerans, *E. coregoni* had been a relatively minor component of the crustacean communities in Lakes Michigan and Huron but was more prominent in Lake Erie. In all three lakes, this species declined precipitously immediately following the appearance of *Bythotrephes* (Fig. 10) and has since remained at very low levels. These changes were statistically significant in all lakes (Table 2). Populations of the closely related *B. longirostris* have generally increased during the post-invasion period (Fig. 10), although the timing of these increases has varied widely in the three lakes and, with the exception of the eastern basin

© 2004 NRC Canada

Fig. 6. Average lake-wide (basin-wide in the case of Lake Erie) late summer densities of *Leptodora kindti* in (*a*) Lake Michigan, (*b*) Lake Huron, and (*c*) central and (*d*) eastern basins of Lake Erie. Note differences in scale between graphs. Bars represent one standard error; arrows indicate first post-invasion year.

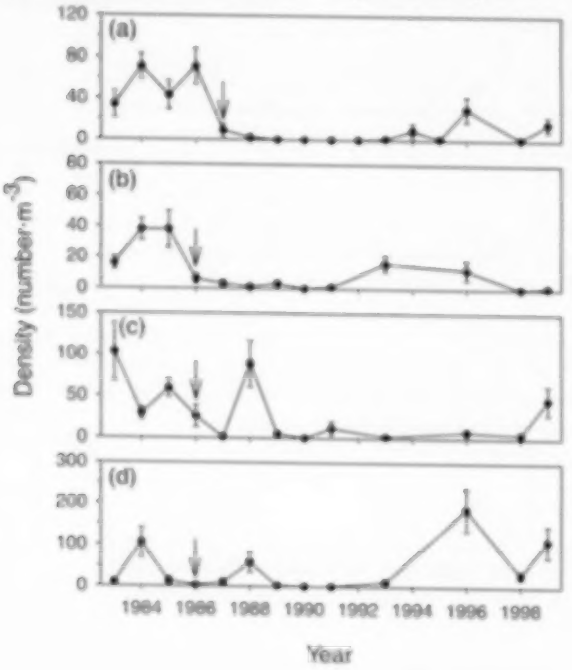

of Lake Erie, appear for the most part to have occurred substantially after the arrival of *Bythotrephes*. Another relatively minor component of the crustacean community, *Holopedium gibberum*, experienced dramatic and relatively sustained declines immediately following the arrival of *Bythotrephes* in all three lakes (Fig. 11), although its suppression has not been as complete as that of *E. coregoni*. The large population of *H. gibberum* seen in Lake Michigan in 1996 was due to an anomalously high count at a single station in that year. With the exception of this lake, the declines in *H. gibberum* have been statistically significant (Table 2).

By and large consistent, sustained changes in calanoid populations were not seen in any of the lakes coincident with the arrival of *Bythotrephes*. However, the cyclopoid copepod *M. edax* exhibited a very clear, statistically significant decline in all three lakes following the invasion, and populations have since remained extremely low (Fig. 11).

DCA ordination of crustacean communities indicated marked differences between pre- and post-invasion crustacean communities in all three lakes (Fig. 12). Although crustacean communities in Lakes Huron and Michigan were clearly differentiated from those in Lake Erie in the ordination, the trajectory of change between pre- and post-invasion communities was similar in all lakes: post-invasion samples exhibited an increase in axis 1 scores and a decrease in axis 2 scores relative to pre-invasion samples. The location of species in ordination space provides an indication of the relative importance of different taxa in differentiating between pre- and post-invasion communities; those with lower axis 1 scores and higher axis 2 scores should be most prominent in pre-invasion communities (Fig. 12). Most notable among such species were *D. retrocurva*, *D. pulicaria*, *H. gibberum*, *E. coregoni*, and *L. kindti*, which agrees with the observations made above. In addition, *D. birgei* and *M. edax* exhibited particularly low axis 1 scores, indicating their greater dominance in pre-invasion communities, although their position on axis 2 indicates that these taxa were more important in Lake Erie than in the other lakes.

Median lengths of cladoceran species from 1994 to 1999 (excluding the eastern basin of Lake Erie) showing post-*Bythotrephes* declines ranged from 0.5 to 1.08 mm and exhibited substantial overlap with those species whose populations were apparently unaffected by the invasion (Fig. 13). *Eubosmina coregoni* was the smallest of the impacted species, with a lower interquartile length of 0.4 mm and a median length of 0.5 mm. Three species with very similar size distributions, *H. gibberum* (interquartile range, 0.58–0.95 mm; median, 0.7 mm), *D. birgei* (interquartile range, 0.58–0.85 mm; median, 0.74 mm), and *D. longiremis* (interquartile range, 0.6–0.95 mm; median, 0.75 mm) showed differing responses to *Bythotrephes*, the first two declining and the latter species generally increasing. The two largest daphnids in the lakes, *D. mendotae* and *D. pulicaria*, also showed opposite responses, the former unaffected and the latter virtually eliminated. Lengths of these two species overlapped considerably, although *D. pulicaria* was extremely rare, so it is unclear how representative the few data available for it are.

Discussion

The crustacean communities in Lakes Michigan and Huron and the central and eastern basins of Lake Erie exhibited dramatic reductions in the populations of a number of mostly cladoceran species and a decline in species richness following the appearance of *Bythotrephes*. Direct predation by *Bythotrephes* offers the most parsimonious explanation for the restructuring of the cladoceran communities in Lakes Michigan, Huron, and Erie. Cladocerans are known to be a favored prey of this genus (Mordukhai-Boltovskaya 1958; Vanderploeg et al. 1993; Schulz and Yurista 1999), and nearly all of the species that exhibited declines in our study have been shown to be vulnerable to *Bythotrephes* predation through either field or laboratory studies. Our results also show strong agreement with those from Harp Lake, a Precambrian Shield lake in south-central Ontario invaded by *Bythotrephes* in the early 1990s that has been the subject of the most extensive studies of *Bythotrephes* effects in North America to date (Yan and Pawson 1997; Yan et al. 2001, 2002).

The lakes examined here have been subject to various forcings over the course of this study. However, the timing and abruptness of the changes seen in this study, and their consistency across the three lakes, argue strongly for *Bythotrephes* as the main causative factor in the restructuring of the crustacean communities. Nutrient levels in both Lakes Michigan and Erie have declined during the period under

© 2004 NRC Canada

Fig. 7. Average lake-wide (basin-wide in the case of Lake Erie) late summer densities of *Daphnia pulicaria* and *Daphnia retrocurva* in Lake Michigan, Lake Huron, and the central (Erie C) and eastern (Erie E) basins of Lake Erie. Note differences in scale between graphs. Bars represent one standard error; arrows indicate first post-invasion year.

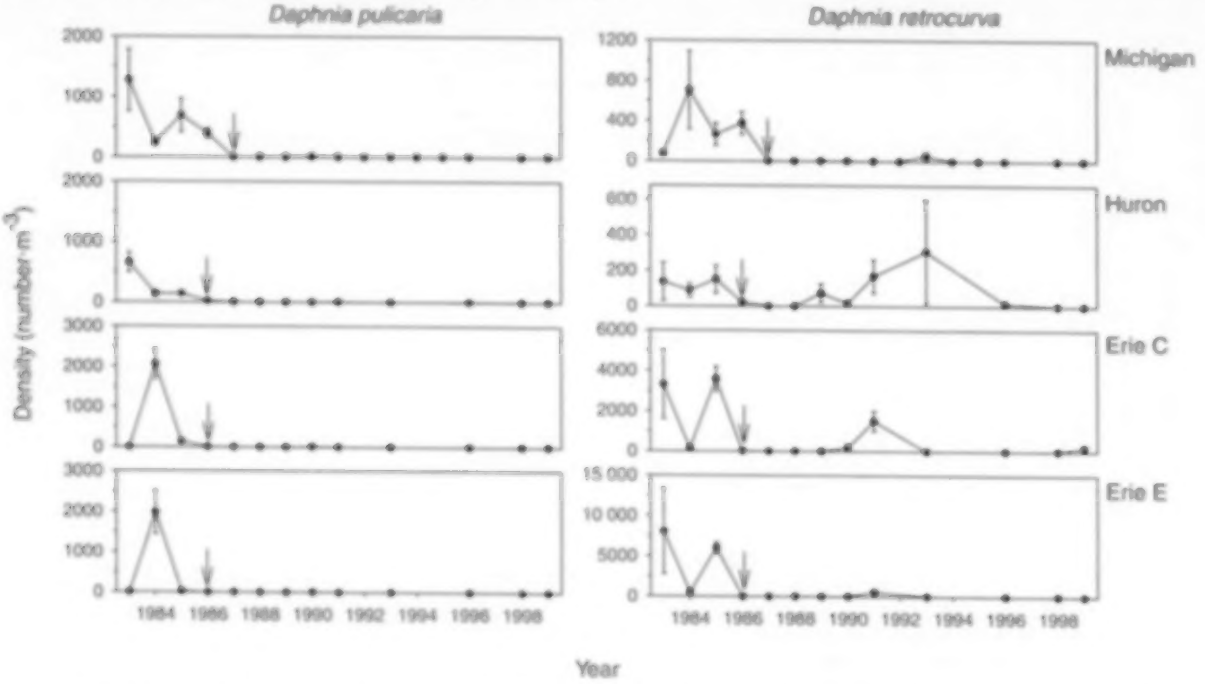

Fig. 8. Average lake-wide (basin-wide in the case of Lake Erie) late summer densities of *Daphnia mendotae* in (*a*) Lake Michigan, (*b*) Lake Huron, and (*c*) central and (*d*) eastern basins of Lake Erie. Note differences in scale between graphs. Bars represent one standard error; arrows indicate first post-invasion year.

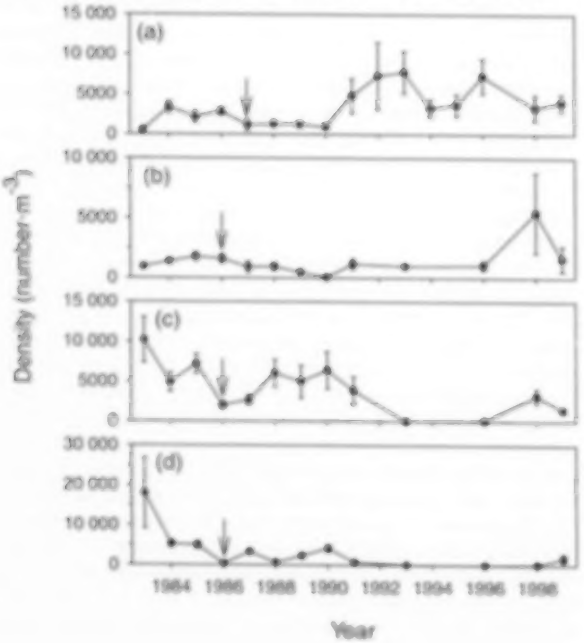

consideration here (Charlton et al. 1999; Barbiero et al. 2002), but these changes have been gradual and are unlikely to have produced the sudden shifts in crustacean community composition seen. Also, the lack of nutrient reductions in Lake Huron would argue against this as a causative mechanism. All three lakes have been invaded by the zebra mussel, *Dreissena polymorpha* (Griffiths et al. 1991), an organism thought to have had pronounced impacts on community structure and trophic relations in parts of the Great Lakes (Leach 1993; Fahnenstiel et al. 1995; Holland et al. 1995). However, the chronology of the *Dreissena* invasion is not consistent with the timing of changes seen in this study. Colonization of the central basin of Lake Erie did not occur until 1988, with the eastern basin colonized the following year (Griffiths et al. 1991). Isolated nearshore populations only became established in Lakes Michigan and Huron in 1990. Most of the major shifts in crustacean populations in our study occurred before these colonization dates. It is harder to assess what role variations in fish stocks might have had on the shifts in crustacean communities seen in our study, although the notable declines in both large and small cladoceran species is inconsistent with the selective reduction in larger individuals that typically results from intense vertebrate planktivory (Brooks and Dodson 1965; Mills et al. 1987).

Our results indicate that the dramatic alterations in the daphnid community observed during the early post-invasion period in Lake Michigan (Lehman 1988, 1991) have persisted and that these changes have not been confined to Lake Michigan, but have occurred in Lake Huron and in the eastern and central basins of Lake Erie as well. These include

© 2004 NRC Canada

Fig. 9. Average basin-wide late summer densities of *Diaphanosoma birgei* and *Daphnia longiremis* in the central (Erie C) and eastern (Erie E) basins of Lake Erie. Bars represent one standard error; arrows indicate first post-invasion year.

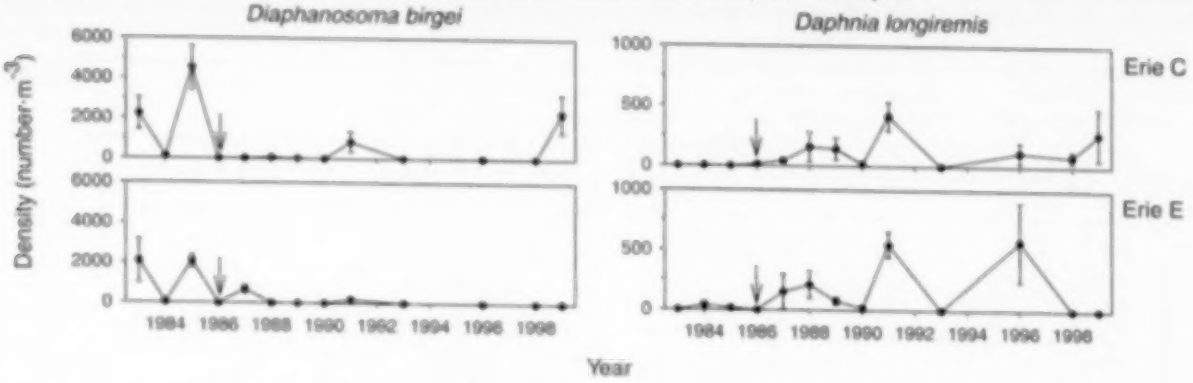

Fig. 10. Average lake-wide (basin-wide in the case of Lake Erie) late summer densities of *Eubosmina coregoni* and *Bosmina longirostris* in Lake Michigan, Lake Huron, and the central (Erie C) and eastern (Erie E) basins of Lake Erie. Note differences in scale between graphs. Bars represent one standard error; arrows indicate first post-invasion year.

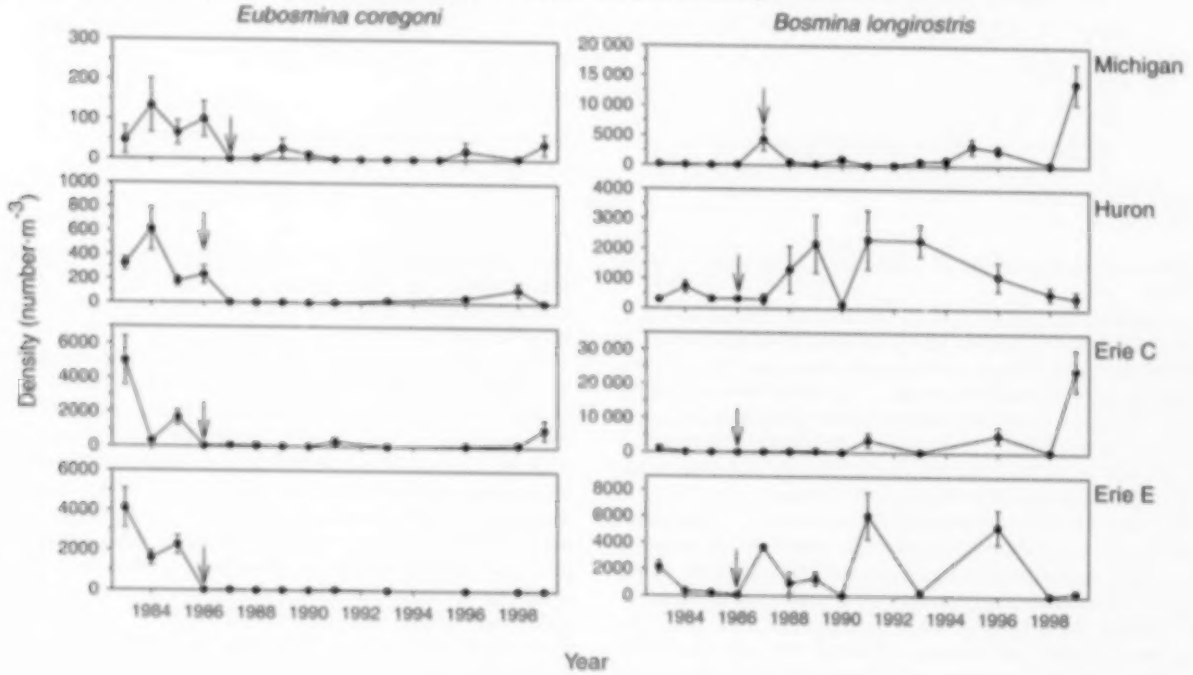

the disappearance of *D. retrocurva* and *D. pulicaria* from the offshore waters and the subsequent sole dominance of the daphnid community by *D. mendotae* (Lehman 1991). The suppression of *D. pulicaria* has been the most complete of any species in our study, and *Bythotrephes* has been shown to prey upon *D. pulicaria* in the laboratory (Burkhardt and Lehman 1994; Schulz and Yurista 1999). However, the short history of *D. pulicaria* in Lake Michigan (Evans and Jude 1986) and the lack of substantial pre-invasion populations in Lake Erie (Davis 1968; Watson and Carpenter 1974) raises the possibility that other factors might have contributed to its absence from these lakes. *Daphnia retrocurva* has historically been co-dominant with *D. mendotae* in the offshore waters of Lake Michigan (Wells 1960; Evans and Jude 1986) and was also reported as a co-dominant daphnid with *D. mendotae* in Lake Erie in early studies (Chandler 1940; Bradshaw 1964; Watson and Carpenter 1974). Its post-invasion disappearance from both of these lakes has been pronounced. Although quantitative data are sparse, it does not appear to have been an important component of the crustacean community of Lake Huron (Watson and Carpenter 1974; Evans 1986). Yan and Pawson (1997) have also reported dramatic decreases in *D. retrocurva* abundance in Harp Lake following the *Bythotrephes* invasion, with no declines seen in *D. mendotae* abundance. Feeding experiments have shown the ability of

© 2004 NRC Canada

Fig. 11. Average lake-wide (basin-wide in the case of Lake Erie) late summer densities of *Holopedium gibberum* and *Mesocyclops edax* in Lake Michigan, Lake Huron, and the central (Erie C) and eastern (Erie E) basins of Lake Erie. Note differences in scale between graphs. Bars represent one standard error; arrows indicate first post-invasion year.

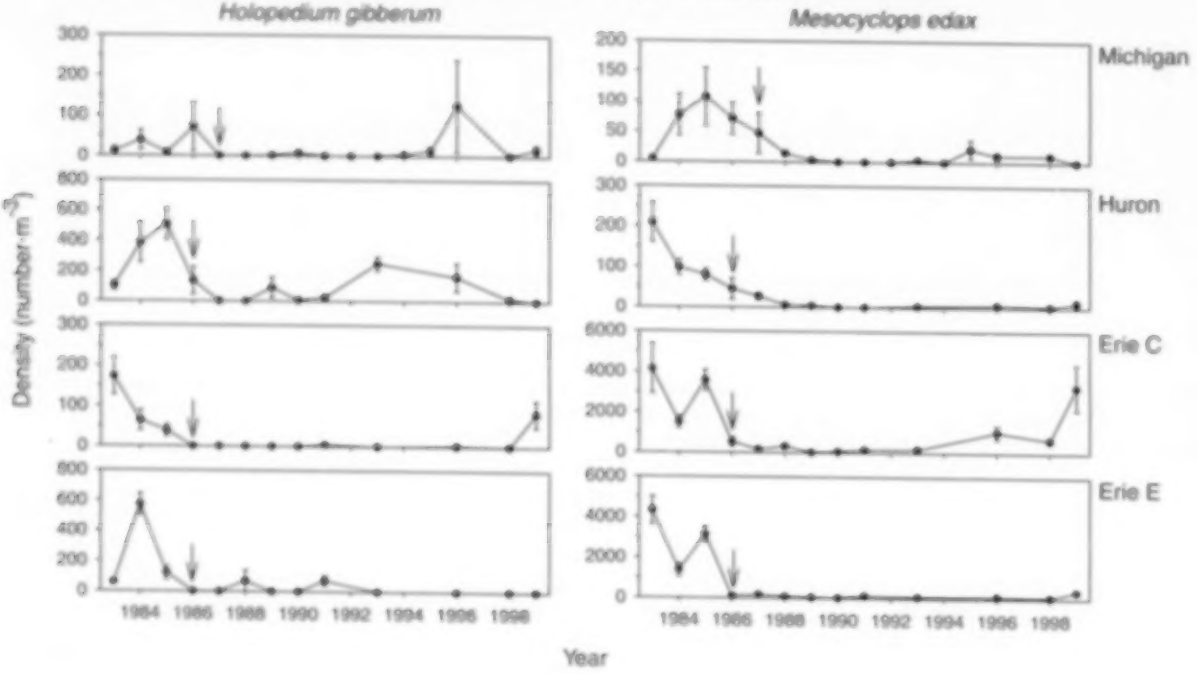

Bythotrephes to prey on *D. retrocurva* (Vanderploeg et al. 1993).

Another response seen in the initial studies on Lake Michigan and corroborated by the present study is the reduction in offshore populations of *Leptodora* (Lehman 1988, 1991). *Leptodora* populations have not been completely eliminated from the lakes, however, and substantial post-invasion populations were occasionally seen in our study. This species continues to be successful in the nearshore waters of Lake Michigan (Lehman and Cáceres 1993) and in the western basin of Lake Erie where *Bythotrephes* has never established substantial populations (Garton et al. 1990). Expansion into the open waters from these sources during periods of reduced *Bythotrephes* abundance could explain in part the occasionally large post-invasion populations that we saw. Lehman (1991) has shown a pronounced lack of spatial overlap between *Leptodora* and *Bythotrephes* in Lake Michigan, and temporal segregation has also been seen in Harp Lake (Yan and Pawson 1997), Lago Maggiore (Manca et al. 1992), and Lake Erie (Berg and Garton 1988; Johannsson et al. 1999).

The mechanism behind the negative association between these two predatory species is unclear. Initially it was thought that the decline in *L. kindti* seen in Lake Michigan was due to exploitation competition by *B. longimanus* (Branstrator and Lehman 1991; Lehman 1991; Yurista and Schulz 1995), although increases in its preferred prey *Conochilus unicornis* seen in both Lakes Huron and Michigan since its decline (M.L. Tuchman, unpublished data) argue against this. An alternate explanation is direct predation by *Bythotrephes* on *Leptodora*. There is some laboratory evidence that *B. longimanus* can capture and consume *L. kindti* (Branstrator 1995), and predation by this species has been implicated in the summer declines of *L. kindti* in Lago Maggiore (Manca and Comoli 2000).

Late summer (August and September) populations of *B. longirostris* were reported to have increased in Lake Michigan in the two years following the establishment of *Bythotrephes*, and this was attributed to the collapse of the offshore *Leptodora* population and a subsequent easing of predation pressure (Branstrator and Lehman 1991). Although post-invasion densities of *B. longirostris* in our study were not consistently higher, they showed no evidence of decline in any of the lakes, whereas the closely related *E. coregoni* exhibited sustained decreases. These results contrast with a number of studies showing that *Bosmina* is vulnerable to *Bythotrephes* predation. Allozymes of both *Bosmina* and *Eubosmina* have been found in *Bythotrephes* from Lake Michigan (Schulz and Yurista 1999), and both *B. longirostris* and *Bosmina tubicen* have declined catastrophically in Harp Lake since the *Bythotrephes* invasion (Yan and Pawson 1997; Yan et al. 2001). Mesocosm experiments have also demonstrated the susceptibility of *Bosmina* to *Bythotrephes* (Wahlström and Westman 1999), and feeding experiments on natural offshore zooplankton communities from Lake Huron have shown no substantial difference in selectivity between *E. coregoni* and *B. longirostris* (Vanderploeg et al. 1993). At present, therefore, it is hard to explain the contrasting responses of *E. coregoni* and *B. longirostris* to the arrival of *Bythotrephes*.

Holopedium gibberum, which decreased in all lakes in our study, has also been shown to be consumed by *Bythotrephes*

© 2004 NRC Canada

Fig. 12. Results of detrended correspondence analysis of (*a*) samples and (*b*) species for 1983–1999 late summer zooplankton densities in Lakes Michigan (□), Huron (○), and the central (△) and eastern (▽) basins of Lake Erie. Open symbols, pre-invasion years; solid symbols, post-invasion years. Species abbreviations are as follows: Dpul, *Daphnia pulicaria*; Hgib, *Holopedium gibberum*; Ecor, *Eubosmina coregoni*; Dret, *Daphnia retrocurva*; Lkin, *Leptodora kindti*; Dtho, *Diacyclops thomasi*; Lash, *Leptodiaptomus ashlandi*; Lmin, *Leptodiaptomus minutus*; Ccop, cyclopoid copepodites; Dmen, *Daphnia mendotae*; Blon, *Bosmina longirostris*; Dcop, diaptomid copepodites; Meda, *Mesocyclops edax*; Sore, *Skistodiaptomus oregonensis*; Text, *Tropocyclops extensus*; Elac, *Epischura lacustris*; Dbir, *Diaphanosoma birgei*; Mcop, *Mesocyclops edax*; Tcop, *Tropocyclops* copepodites; Ecop, *Epischura* copepodites. Taxa whose position in ordination space suggest a greater importance in pre-invasion communities are circled.

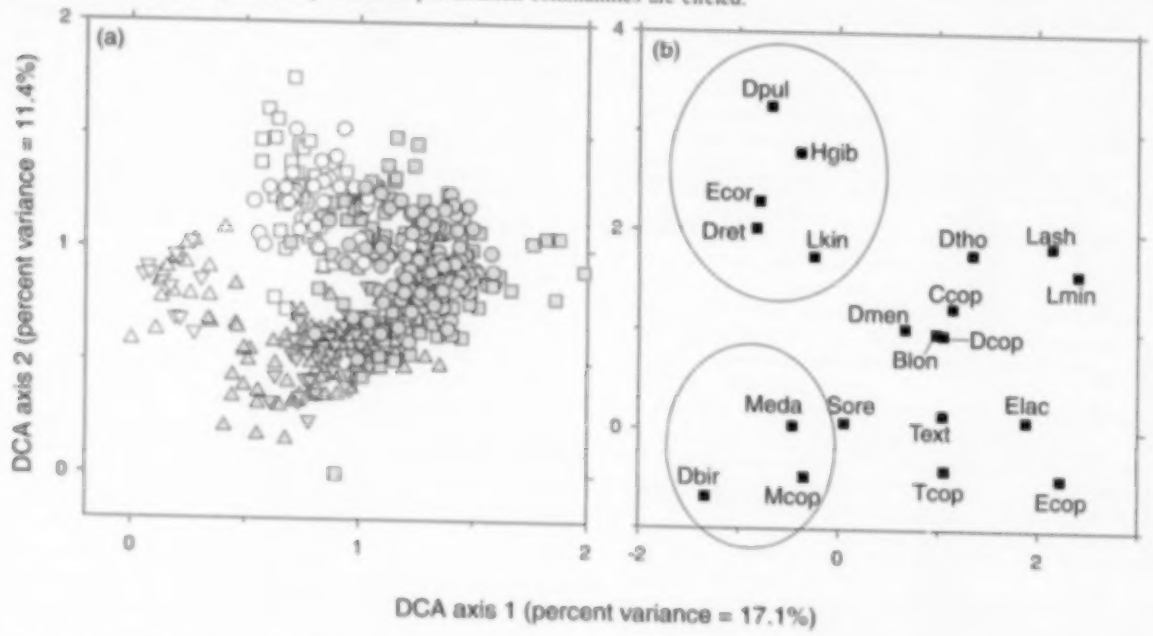

on the basis of both allozyme (Schulz and Yurista 1999) and mesocosm (Wahlström and Westman 1999) studies. In Harp Lake, however, there has been no decline in *H. gibberum* after the *Bythotrephes* invasion (Yan et al. 2001). *Diaphanosoma birgei*, which declined in our study, has also decreased in Harp Lake (Yan et al. 2001).

In our study, size, and particularly small size, did not appear to be a good predictor of population decline subsequent to *Bythotrephes* invasion. Although Yan et al. (2001) documented an overall increase in cladoceran size since the *Bythotrephes* invasion of Harp Lake, this did not appear to be the case in the Great Lakes, where the largest cladoceran, *D. pulicaria*, was apparently eliminated while the smallest, *B. longirostris*, suffered no negative effects. Makarawicz et al. (1995), examining data from Lake Michigan between 1984 and 1992, showed a marked decline in mean cladoceran length between 1986 and 1987, although this was not sustained. Species with contrasting responses to *Bythotrephes* showed a high degree of overlap in lengths, as was the case with *D. birgei* and *D. longiremis*, for example. It seems likely, therefore, that characteristics other than size play a role in determining the vulnerability to *Bythotrephes* predation. These could include morphological defenses, behaviors that reduce spatial overlap, or escape responses.

The development of diurnal vertical migration (DVM) by *D. mendotae* has been offered as a possible mechanism accounting for its reduced susceptibility to the visually feeding *Bythotrephes* (Schulz and Yurista 1999). An earlier report (Wells 1960) had indicated that the depth of migration for both *D. retrocurva* and *D. mendotae* in 1954 did not exceed 20 m, and Lehman and Cáceres (1993) reported a shift to more extreme DVM in *D. mendotae* after the introduction of *Bythotrephes*. *Daphnia mendotae* currently undergoes very pronounced DVM in Lake Michigan (Barbiero et al. 2004). Why only *D. mendotae* should have developed enhanced DVM and why this should have happened in at least three different lakes, however, remains unclear.

A consistent, but somewhat unexpected, consequence of the *Bythotrephes* invasion was the precipitous decline in densities of *M. edax* in all three lakes. *Mesocyclops edax* was also reported to have disappeared from Harp Lake after the arrival of *Bythotrephes* (Yan and Pawson 1997). *Mesocyclops edax* preys upon smaller crustaceans (Brandl and Fernando 1975; Williamson and Magnien 1982) and a variety of rotifer genera including *Asplanchna*, *Keratella*, *Polyarthra*, *Conochilus*, *Kellicottia*, and *Synchaeta* (Gilbert and Williamson 1978; Williamson and Gilbert 1980; Williamson and Magnien 1982). Feeding experiments have consistently shown that adult copepods are not preferred food items of *Bythotrephes* (Vanderploeg et al. 1993; Schulz and Yurista 1999; Wahlström and Westman 1999). This, coupled with the lack of declines seen in *B. longirostris* and total rotifer numbers (M.L. Tuchman, unpublished data) after the *Bythotrephes* invasion, makes it hard to explain the response of *M. edax*. However, ample evidence exists that nauplii are utilized by *Bythotrephes* and that these might in fact be pre-

© 2004 NRC Canada

Fig. 13. *Size–frequency distributions of Bosmina longirostris, Eubosmina coregoni, Daphnia retrocurva, Holopedium gibberum, Diaphanosoma birgei, Daphnia longiremis, Daphnia mendotae,* and *Daphnia pulicaria* for Lakes Michigan and Huron and the eastern basin of Lake Erie during late summer, 1994–1999. Vertical reference lines indicate median lengths, shaded areas indicate interquartile ranges, and arrows indicate species showing distinct declines in post-invasion years.

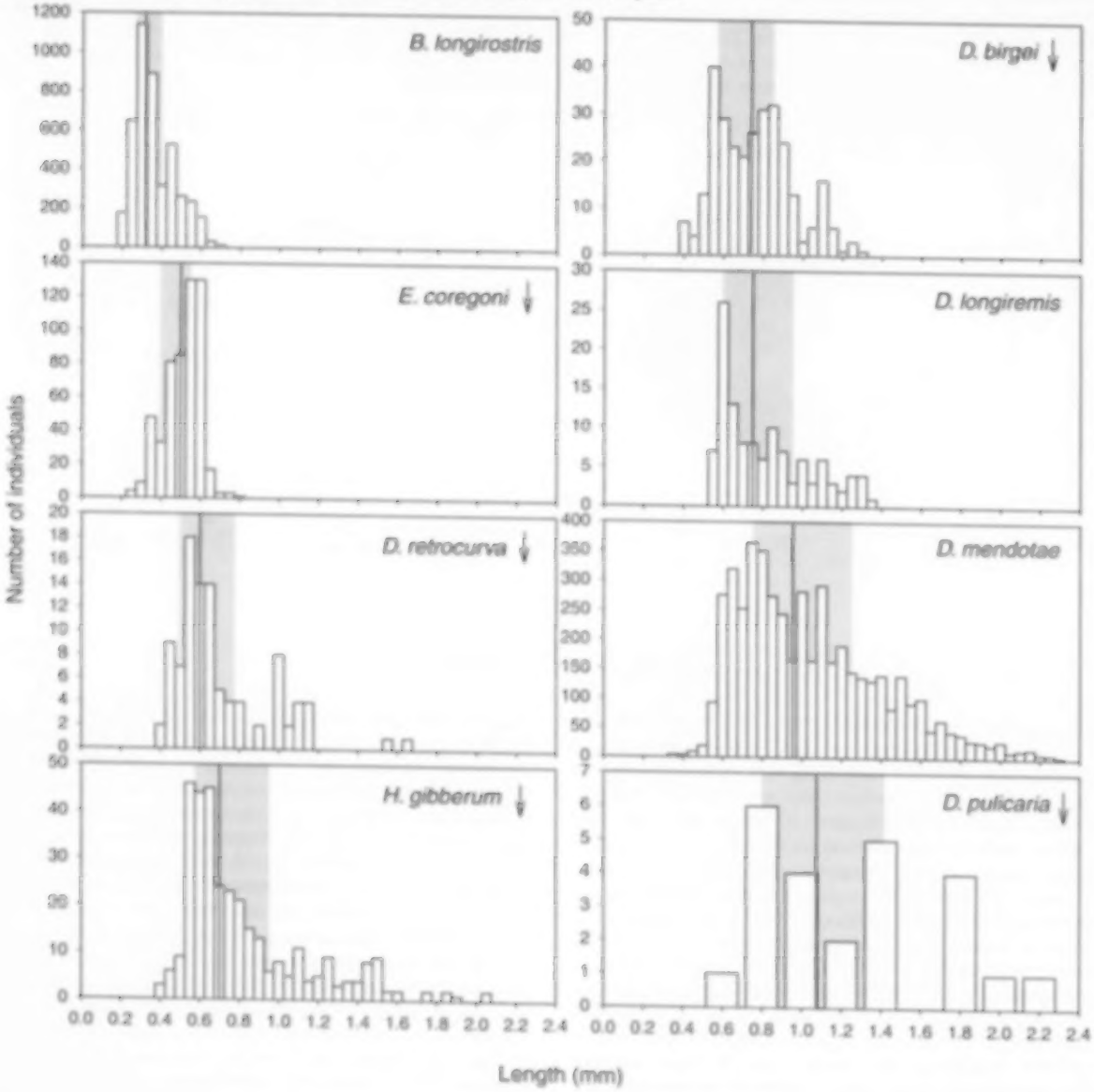

ferred prey of juveniles (Nauwerk 1993; Vanderploeg et al. 1993; Schulz and Yurista 1999). It is possible that *M. edax* naupliі are particularly vulnerable to *Bythotrephes* predation and that the declines in its populations are due to losses incurred during the naupliar stage. Predation by juvenile *Bythotrephes* has been estimated to constitute 44% of total lifetime consumption (Yurista and Schulz 1995), so these losses could be substantial.

It has been suggested that *Bythotrephes* predation should have less impact on the Lakes Erie and Huron zooplankton communities than on those of Lake Michigan (Yurista and Schulz 1995) because of the smaller sizes of *Bythotrephes* in Lakes Erie and Huron and the higher reported abundances in Lake Michigan. Information on lake-specific sizes of *Bythotrephes* derives largely from reports by Berg and Garton (1988) and Garton et al. (1990) for Lake Erie, Vanderploeg et al. (1993) for Lake Huron, and Yurista and Schulz (1995) for Lake Michigan. Our results show that the changes in zooplankton communities across the four regions examined after the *Bythotrephes* invasion were surprisingly uniform

© 2004 NRC Canada

and that lengths of *Bythotrephes* in Lake Michigan were not greater than those in the other regions examined, with the exception of the central basin of Lake Erie, although volumetric densities were actually higher in Lake Erie than in the other two lakes considered here. Areal densities calculated from deep tows collected by our program for the two years that are currently available (1998 and 1999) generally confirm the differences in volumetric densities reported here and indicate lowest densities in Lake Michigan, highest densities in Lake Erie, and intermediate densities in Lake Huron (Barbiero et al. 2001; Barbiero and Tuchman 2002). Bilkovic and Lehman (1997) appears to be the only other report to compare sizes of *Bythotrephes* among these three lakes using data derived from a single study, and their results largely agree with our own, i.e., smaller individuals in the central basin of Lake Erie compared with Lakes Huron and Michigan. These authors noted that, in spite of differences in dry weight, lipid concentrations of *Bythotrephes* in the central basin were equal to, or higher than, those for the other lakes, suggesting that food limitation was not responsible for their smaller size. Instead, they suggested that a smaller deep-water refuge from visually feeding planktivores might explain the smaller size of *Bythotrephes* in that region of Lake Erie. Our results are not inconsistent with their hypothesis. The perception that *Bythotrephes* has had minimal impact in Lake Erie is probably due to the fact that most studies of it have been restricted to the western basin, where large populations have never become established (Berg and Garton 1988; Garton et al. 1990).

Our results indicate that *Bythotrephes* has had dramatic, sustained effects on the zooplankton communities of Lakes Michigan, Huron, and Erie. Impacts on the crustacean communities have been consistent across the lakes, in spite of differences in lake morphometry and trophic state, and have also agreed in large part with findings from the only other North American lake for which detailed information is available (Yan and Pawson 1997; Yan et al. 2001). These results indicate that invertebrate predators in general, and invasive ones in particular, can have profound effects on zooplankton community structure, even in systems that have served as models for the role of vertebrate planktivory fish on zooplankton populations (Wells 1970).

Acknowledgements

We would like to thank L.A. Kuhns, L.L. Schacht, and R.E. Little for sample analysis and fruitful discussions. Statistical assistance was provided by K.M. Miller of CSC. N. Yan provided useful comments on this manuscript. The information in this document has been funded by the US Environmental Protection Agency under contract number 68-C-01-091 to DynCorp I&ET. It has been subjected to Agency review and approved for publication.

References

Balcer, M.D., Korda, N.L., and Dodson, S.I. 1984. Zooplankton of the Great Lakes. A guide to the identification and ecology of the common crustacean species. The University of Wisconsin Press, Madison, Wis.

Barbiero, R.P., and Tuchman, M.L. 2002. Results from GLNPO's biological open water surveillance program of the Laurentian Great Lakes 1999. US Environmental Protection Agency, Great Lakes National Program Office, Chicago, Ill., EPA-905-R-02-001.

Barbiero, R.P., Little, R.E., and Tuchman, M.L. 2001. Results from the U.S. EPA's biological open water surveillance program of the Laurentian Great Lakes: III. Crustacean zooplankton. J. Gt. Lakes Res. **27**: 167–184.

Barbiero, R.P., Tuchman, M.L., Warren, G.J., and Rockwell, D.C. 2002. Evidence of recovery from phosphorus enrichment in Lake Michigan. Can. J. Fish. Aquat. Sci. **59**: 1639–1647.

Barbiero, R.P., Schacht, L.L., Little, R.E., and Tuchman, M.L. 2004. Crustacean zooplankton communities in Lake Michigan. *In* The Lake Michigan ecosystem: ecology, health and management. *Edited by* T. Edsall and M. Munawar. Ecovision World Monograph Series. SBP Academic Publishing, Amsterdam, the Netherlands. In press.

Berg, D.J., and Garton, D.W. 1988. Seasonal abundance of the exotic predatory cladoceran *Bythotrephes cederstroemi* in Western Lake Erie. J. Gt. Lakes Res. **14**: 497–488.

de Bernardi, R., and Giussani, G. 1975. Population dynamics of three cladocerans of Lago Maggiore related to predation pressure by a planktophagous fish. Int. Ver. Theor. Angew. Limnol. Verh. **19**: 2906–2912.

de Bernardi, R., Giussani, G., and Manca, M. 1987. Cladocera: predators and prey. Hydrobiologia, **145**: 225–243.

Bilkovic, D.M., and Lehman, J.T. 1997. Lipid concentration and size variation of *Bythotrephes* (Cladocera: Cercopagidae) from Lakes Erie, Huron and Michigan. J. Gt. Lakes Res. **23**: 149–159.

Bradshaw, A.S. 1964. The crustacean zooplankton picture: Lake Erie, 1939–49–59: Cayuga 1910–51–61. Int. Ver. Theor. Angew. Limnol. Verh. **15**: 700–708.

Brandl, Z., and Fernando, C.H. 1975. Investigations on the feeding of carnivorous cyclopoids. Verh. Int. Ver. Theor. Angew. Limnol. **19**: 2959–2965.

Branstrator, D.K. 1995. Ecological interactions between *Bythotrephes cederstroemi* and *Leptodora kindti* and the implications for species replacement in Lake Michigan. J. Gt. Lakes Res. **21**: 670–679.

Branstrator, D.K., and Lehman, J.T. 1991. Invertebrate predation in offshore Lake Michigan: regulation of *Bosmina longirostris* by *Leptodora kindtii*. Limnol. Oceanogr. **36**: 483–495.

Brooks, J.L. 1959. Cladocera. *In* Freshwater biology. 2nd ed. *Edited by* W.T. Edmondson. Wiley, New York. pp. 587–656.

Brooks, J.L., and Dodson, S.I. 1965. Predation, body size and the composition of the plankton. Science (Wash., D.C.), **150**: 28–35.

Bur, M.T., Klarer, D.M., and Krieger, K.A. 1986. First records of a European cladoceran, *Bythotrephes cederstroemi*, in Lakes Erie and Huron. J. Gt. Lakes Res. **12**: 144–146.

Burkhardt, S., and Lehman, J.T. 1994. Prey consumption and predatory effects of an invertebrate predator (*Bythotrephes*: Cladocera, Cercopagidae) based on a phosphorus budget. Limnol. Oceanogr. **39**: 1007–1019.

Chandler, D.C. 1940. Limnological studies of Western Lake Erie. I. Plankton and certain physical-chemical data of the Bass Islands region from September 1938 to November 1939. Ohio J. Sci. **40**(6): 261–336.

Charlton, M.N., Le Sage, R., and Milne, J.E. 1999. Lake Erie in transition: the 1990's. *In* State of Lake Erie (SOLE) — past, present and future. *Edited by* M. Munawar, T. Edsall, and I.F. Munawar. Ecovision World Monograph Series, Backhuys Publishers, Leiden, the Netherlands. pp. 97–123.

Cullis, K.I., and Johnson, G.E. 1988. First evidence of the cladoceran *Bythotrephes cederstroemi* Schoedler in Lake Superior. J. Gt. Lakes Res. **14**: 524–525.

© 2004 NRC Canada

Davis, C.C. 1968. The July 1967 zooplankton of Lake Erie. Proc. Conf. Great Lakes. Res. **11**: 61–75.

Dodson, S.I. 1974. Adaptive changes in plankton morphology in response to size-selective predation. A new hypothesis of cyclomorphosis. Limnol. Oceanogr. **19**: 721–729.

Evans, M.S. 1985. The morphology of *Daphnia pulicaria*, a species newly dominating the offshore southeastern lake Michigan summer *Daphnia* community. Trans. Am. Microsc. Soc. **104**: 223–231.

Evans, M.S. 1986. Lake Huron rotifer and crustacean zooplankton, April–July 1980. J. Gt. Lakes Res. **12**: 281–292.

Evans, M.S. 1988. *Bythotrephes cederstroemi*: its new appearance in Lake Michigan. J. Gt. Lakes. Res. **14**: 234–240.

Evans, M.S., and Jude, D.J. 1986. Recent shifts in *Daphnia* community in southeastern Lake Michigan: a comparison of the inshore and offshore regions. Limnol. Oceanogr. **31**: 56–67.

Fahnenstiel, G.L., Bridgeman, T.B., Lang, G.L., McCormick, M.J., and Nalepa, T.F. 1995. Phytoplankton productivity in Saginaw Bay, Lake Huron: effects of zebra mussel (*Dreissenas polymorpha*). J. Gt. Lakes Res. **21**: 465–475.

Garton, D.W., Berg, D.J., and Fletcher, R.J. 1990. Thermal tolerances of the predatory cladocerans *Bythotrephes cederstroemi* and *Leptodora kindti*. Relationship to seasonal abundance in Western Lake Erie. Can. J. Fish. Aquat. Sci. **47**: 731–738.

Gilbert, J.J., and Williamson, C.E. 1978. Predator–prey behavior and its effects on rotifer survival in associations of *Mesocyclops edax*, *Asplanchna girodi*, *Polyarthra vulgaris* and *Keratella cochlearis*. Oecologia, **37**: 13–22.

Griffiths, R.W., Schloesser, D.W., Leach, J.H., and Kovalak, W.P. 1991. Distribution and dispersal of the zebra mussel (*Dreissena polymorpha*) in the Great Lakes region. Can. J. Fish. Aquat. Sci. **48**: 1381–1388.

Haney, J.F., and Hall, J.D. 1973. Sugar coated *Daphnia*: a preservation technique for Cladocera. Limnol. Oceanogr. **18**: 331–333.

Hansson, L.-A., and Tranvik, L.J. 1996. Quantification of invertebrate predation and herbivory in food chains of low complexity. Oecologia, **108**: 542–551.

Holland, R.E., Johengen, T.H., and Beeton, A.M. 1995. Trends in nutrient concentrations in Hatchery Bay, western Lake Erie, before and after *Dreissena polymorpha*. Can. J. Fish. Aquat. Sci. **52**: 1202–1209.

Hrbáček, J. 1960. Density of the fish population as a factor influencing the distribution and speciation of the species in the genus *Daphnia*. XVth International Congress of Zoology, London, 1958, Sect. X, No. 27, pp. 794–795.

Hrbáček, J., Dvořáková, M., Kořínek, V., and Procházková, L. 1961. Demonstration of the effect of the fish stock on the species of plankton and the intensity of metabolism of the whole plankton association. Verh. Int. Ver. Limnol. **14**: 192–195.

Hudson, P.L., Reid, J.W., Lesko, L.T., and Selgeby, J.H. 1998. Cyclopoid and harpacticoid copepods of the Laurentian Great Lakes. Ohio Biol. Surv. Bull. NS, **12**(2).

Johannsson, O.E., Mills, E.L., and O'Gorman, R. 1991. Changes in the nearshore and offshore zooplankton communities in Lake Ontario. Can. J. Fish. Aquat. Sci. **48**: 1546–1557.

Johannsson, O.E., Graham, D.M., Einhouse, D.W.E., and Mills, E.L. 1999. Historical and recent changes in the Lake Erie zooplankton community and their relationship to ecosystem function. *In* State of Lake Erie (SOLE) — past, present and future. *Edited by* M. Munawar, T. Edsall, and I.F. Munawar. Ecovision World Monograph Series, Backhuys Publishers, Leiden, the Netherlands. pp. 169–196.

Leach, J.H. 1993. Impacts of the zebra mussel (*Dreissena polymorpha*) on water quality and spawning reefs in western Lake Erie. *In* Zebra mussels: biology, impacts and control. *Edited by* T. Nalepa and D. Schloesser. Lewis Publishers, Boca Raton, Fla. pp. 381–397.

Lehman, J.T. 1987. Palearctic predator invades North American Great Lakes. Oecologia (Berlin), **74**: 478–480.

Lehman, J.T. 1988. Algal biomass unaffected by food-web changes in Lake Michigan. Nature (Lond.), **332**: 537–538.

Lehman, J.T. 1991. Causes and consequences of cladoceran dynamics in Lake Michigan: implications of species invasion by *Bythotrephes*. J. Gt. Lakes Res. **17**: 437–445.

Lehman, J.T., and Cáceres, C.E. 1993. Food-web responses to species invasion by a predatory invertebrate *Bythotrephes* in Lake Michigan. Limnol. Oceanogr. **38**: 879–891.

Makarawicz, J.C., Bertram, P., Lewis, T., and Brown, E.H., Jr. 1995. A decade of predatory control of zooplankton species composition of Lake Michigan. J. Gt. Lakes Res. **21**: 620–640.

Manca, M., and Comoli, P. 2000. Biomass estimates of freshwater zooplankton from length–carbon regression equations. J. Limnol. **59**: 15–18.

Manca, M., Calderoni, A., and Mosello, R. 1992. Limnological research in Lago Maggiore: studies on hydrochemistry and plankton. Mem. Ist. Ital. Idrobiol. **50**: 171–200.

McQueen, D.J. 1969. Reduction of zooplankton standing stocks by predaceous *Cyclops bicuspidatus thomasi* in Marion Lake, British Columbia. J. Fish. Res. Board Can. **26**: 1605–1618.

Mills, E.L., Green, D.M., and Schiavone, A., Jr. 1987. Use of zooplankton size to assess the community structure of fish populations in freshwater lakes. North Am. J. Fish. Manag. **7**: 369–378.

Mordukhai-Boltvskaya, E.D. 1958. Preliminary notes on feeding of the carnivorous cladocerans *Leptodora kindti* and *Bythotrephes*. Dokl. Acad. Nauk. SSSR, **122**: 820–830.

Nauwerk, A. 1993. Migration strategies of crustacean zooplankton in Lake Mondsee. Arch. Hydrobiol. **39**: 123–136.

Sandgren, C.D., and Lehman, J.T. 1990. Response of chlorophyll *a*, phytoplankton and microzooplankton to the invasion of Lake Michigan by *Bythotrephes*. Verh. Int. Ver. Limnol. **24**: 386–392.

Schulz, K.L., and Yurista, P.M. 1999. Implications of an invertebrate predator's (*Bythotrephes cederstroemi*) atypical effects on a pelagic zooplankton community. Hydrobiologia, **380**: 179–193.

Therriault, T.W., Grigorovich, I.A., Cristescu, M.E., Ketelaars, H.A.M., Viljanen, M., Heath, D.D., and MacIsaac, H.J. 2002. Taxonomic resolution of the genus *Bythotrephes* Leydig using molecular markers and a re-evaluation of its global distribution, with notes on factors affecting dispersal, establishment and abundance. Divers. Distrib. **8**: 67–84.

Vanderploeg, H.A., Liebig, J.R., and Omair, M. 1993. *Bythotrephes* predation on Great Lakes' zooplankton measured by an *in situ* method: implications for zooplankton community structure. Arch. Hydrobiol. **127**: 1–8.

Wahlström, E., and Westman, E.1999. Planktivory by the predacious cladoceran *Bythotrephes longimanus*: effects on zooplankton size structure and abundance. Can. J. Fish. Aquat. Sci. **56**: 1865–1872.

Watson, N.H.F., and Carpenter, G.F. 1974. Seasonal abundance of crustacean zooplankton and net plankton biomass of Lakes Huron, Erie and Ontario. J. Fish. Res. Board Can. **31**: 309–317.

Wells, L. 1960. Seasonal abundance and vertical movements of planktonic crustacea in Lake Michigan. U.S. Fish. Wildl. Serv. Bull. **60**(172): 343–369.

Wells, L. 1970. Effects of alewife predation on zooplankton populations in Lake Michigan. Limnol. Oceanogr. **15**: 556–565.

Williamson, C.E., and Gilbert, J.J. 1980. Variation among zooplankton predators: the potential of *Asplanchna*, *Mesocyclops*,

© 2004 NRC Canada

and *Cyclops* to attack, capture and eat various rotifer prey. *In* Evolution and ecology of zooplankton communities. *Edited by* W.C. Kerfoot. University Press of New England, Hanover, New Hampshire. pp. 509–517.

Williamson, C.E., and Magnien, R.E. 1982. Diel vertical migration in *Mesocyclops edax*. Implications for predation rate estimates. J. Plankton Res. **4**: 329–339.

Yan, N.D., and Pawson, T.W. 1997. Changes in the crustacean zooplankton community of Harp Lake, Canada, following invasion by *Bythotrephes cederstroemi*. Freshw. Biol. **37**: 409–425.

Yan, N.D., and Pawson, T.W. 1998. Seasonal variation in the size and abundance of the invading *Bythotrephes cederstroemi* in Harp Lake, Ontario, Canada. Hydrobiologia, **361**: 157–168.

Yan, N.D., Blukacz, A., Sprules, W.G., Kindy, P.K., Hackett, D., Girard, R.E., and Clark, B.J. 2001. Changes in zooplankton and the phenology of the spiny water flea, *Bythotrephes*, following its invasion of Harp Lake, Ontario, Canada. Can. J. Fish. Aquat. Sci. **58**: 2341–2350.

Yan, N., Girard, R., and Boudreau, S. 2002. An introduced invertebrate predator (*Bythotrephes*) reduces zooplankton species richness. Ecol. Lett. **5**: 481–485.

Yurista, P.M., and Schulz, K.L. 1995. Bioenergetic analysis of prey consumption by *Bythotrephes cederstroemi* in Lake Michigan. Can. J. Fish. Aquat. Sci. **52**: 141–150.

Zaret, T.M. 1980. Predation and freshwater communities. Yale University Press, New Haven, Conn.

© 2004 NRC Canada

Use of length-based models to estimate biological parameters and conduct yield analyses for male Dungeness crab (*Cancer magister*)

Z. Zhang, W. Hajas, A. Phillips, and J.A. Boutillier

Abstract: Length-based models were developed for the male Dungeness crab (*Cancer magister*) population on the Fraser delta near Vancouver, British Columbia. The models incorporate the probability of moulting, moult increments, natural mortality during moulting and non-moulting periods, direct fishing mortality, and handling mortality that occurs when sublegal-sized crabs are caught and released. The models were used to investigate how long-term yield might be affected by the combination of handling mortality and an intensive fishery. The models were calibrated to survey data, and key biological parameters were estimated. The probability of moulting is near one for male crabs in the 130- to 150-mm carapace width range and decreases as crabs get larger. There is a 70.1% probability a crab will survive the 1-month period beginning with a moult. The non-moulting natural mortality rate is 0.97 year^{-1}. When handling mortality is incorporated into the model, yield per recruit increases with the exploitation rate until it reaches approximately 94%. $F_{0.1}$ is equivalent to 70%. An approach was developed to calculate the threshold ratio of discarded to retained crabs beyond which fishing would reduce the long-term yield.

Résumé : Nous avons mis au point des modèles basés sur la longueur que nous avons appliqués à une population de crabes dormeurs mâles (*Cancer magister*) du delta du Fraser, près de Vancouver. Les modèles tiennent compte de la probabilité de la mue, de la croissance à la mue, de la mortalité naturelle durant les périodes de mue et en dehors de ces périodes, de la mortalité directe due à la pêche et de la mortalité due à la manipulation, lorsque des crabes de taille inférieure à la taille réglementaire sont capturés et relâchés. Les modèles ont servi à déterminer comment le rendement à long terme peut être affecté par la combinaison de la mortalité due à la manipulation et d'une intensité de pêche élevée. Nous avons calibré les modèles aux données d'inventaire et nous avons estimé les paramètres biologiques. La probabilité de la mue chez les crabes de largeur de carapace 130–150 mm est près de 1 et elle diminue en fonction de la taille chez les crabes plus grands. La probabilité qu'un crabe survive à la période d'un mois qui suit la mue est de 70,1 %. La mortalité naturelle est de 0,97·année^{-1} en l'absence de mue. Si la mortalité due à la manipulation est ajoutée au modèle, le rendement par recrue augmente en fonction du taux d'exploitation jusqu'à atteindre approximativement 94 %. $F_{0,1}$ équivaut à 70 %. Nous avons développé une méthodologie pour calculer le seuil du rapport des crabes rejetés sur les crabes retenus au-dessus duquel la pêche réduit le rendement à long terme.

[Traduit par la Rédaction]

Introduction

This study was motivated by concerns about the very intensive Dungeness crab (*Cancer magister*) fishery in the Fraser delta near Vancouver, British Columbia. Dungeness crabs are commercially harvested using traps. Only male crabs of carapace width excluding spines (CW) ≥ 155 mm may be retained.

On the Fraser delta, mature male moulting crabs primarily moult in the spring (Jamieson et al. 1998). The commercial fishery is opened when the crabs are sufficiently hard, usually by late June or mid-July on the Fraser delta. Legal-sized male crabs are rapidly fished down over a period of about 6 weeks from the fishery opening. Nearly all legal-sized male crabs have been removed from the stock by the end of the fishing season at the end of November. Despite escape rings in the traps, sublegal-sized crabs are also captured and then discarded back into the water. As the season progresses, the ratio of sublegal- to legal-sized crabs appearing in the traps increases, and by the end of the season the ratio is often greater than 10.

The expected rate of handling mortality is largely unknown. A higher rate of injured crabs has been observed in areas where there is an intensive harvest (our unpublished data). Tegelberg (1971) did some experiments to try to determine handling rates. The lowest value was 5%. The highest value of 57% was achieved by dropping soft-shell crabs on the deck of a ship.

Received 29 May 2003. Accepted 2 July 2004. Published on the NRC Research Press Web site at http://cjfas.nrc.ca on 26 January 2005.
J17551

Z. Zhang,[1] W. Hajas, A. Phillips, and J.A. Boutillier. Shellfish Stock Assessment Section, Pacific Biological Station, 3190 Hammond Bay Road, Nanaimo, BC V9T 6N7, Canada.

[1]Corresponding author (e-mail: zhangz@pac.dfo-mpo.gc.ca).

 doi: 10.1139/F04-155 © 2004 NRC Canada

Some of the sublegal-sized crabs that suffer handling mortality would otherwise survive, grow into legal-sized crabs, be harvested by the fishery, and contribute to future yields. There is an optimum fishing effort where the long-term yield is a maximum. We evaluate changes in yield per recruit with various exploitation rates, and we estimate the amount of gain or loss in long-term yield for continuing fishing at various ratios of discarded to retained crabs. The goal of these analyses is to determine the impact of such an intensive fishery and how the handling mortality affects the optimum fishing effort.

These analyses require models to describe the growth and mortality of male Dungeness crabs. Crabs grow by moulting, so it is necessary to model both the probability of moulting and the size increments. The resulting growth model is more complex and difficult to implement than the length-at-age models commonly used for fin-fish. The mortality of crabs is complicated by the period immediately after moulting when the mortality rate is presumably high.

The models require parameter values. Natural mortality rates (M) have been estimated for Dungeness crabs. For example, Butler and Hankin (1992) review the literature and conclude that M for male Dungeness crabs may lie in the range of 0.8–1.2 year^{-1}, although lower values are quite plausible. Morado et al. (1999) found that natural mortality is especially high immediately after moulting. However, moulting and non-moulting periods are generally not considered when natural mortality rates are estimated. We not only estimate the natural mortality rate during the non-moulting period but developed, for the first time, a method for estimating the moulting survival fraction.

Smith and Jamieson (1989) provide suitable parameter values for moult increments, but the probability of moulting is a more difficult issue. Previously, probabilities of moulting have been estimated from tagging studies (Hancock and Edwards 1967; Bennett 1974; McCaughran and Powell 1977) or based on analyses of size–frequency distributions and moult increments (Weber and Miyahara 1962; Hankin et al. 1989; Mohr and Hankin 1989). However, the results for both of these methods are confounded with moulting-related mortality. To overcome this problem, we develop a new method that is not affected by moulting-related mortality.

With suitable models and corresponding parameter values, we evaluate the impact of fishing intensity and handling mortality on long-term yield.

Materials and methods

The models for these analyses were calibrated to data collected from Vancouver Harbour. The harbour is part of the Fraser Delta, but because of navigational concerns, it is closed to the crab fishery. The traps used for the scientific surveys are similar to commercial traps except that the escape ports are wired shut. We assume that Vancouver Harbour is representative of the entire delta. The assumption that crabs do not migrate into or out of the harbour is supported by our unpublished tagging data and a study by Smith and Jamieson (1991), who reported that male Dungeness crabs undergo only limited net migration.

The data used in these analyses were collected from 1994 to 2000. Surveys were performed in June and October of each year. It is convenient to consider the October surveys as "pre-moult" and the June surveys as "post-moult". There was also a survey done in February 2001 to investigate the impact of soak time on crab catch rates.

Traps were set in strings of 3–22 traps. Entire strings were deployed or retrieved at the same time. We assume that traps of the same string do not interfere with each other. Traps were retained after spending 1–24 h in the water in the June and October surveys. In the February 2001 survey, soak time ranged from 1 to 46 h. Each time a set was pulled, the number of traps and the soak time were recorded. For each captured crab, the sex, size, shell condition, and sometimes weight were recorded. The shell condition was used to determine if the crab was new shell or old shell (moulted or not moulted during the latest moulting season).

Size was measured by the interspine carapace width excluding spines (CW). The minimum size limit for the crab fishery corresponds to a size of 155 mm. It is rare for a female crab to reach the minimum size limit. Male crabs reach maturity at approximately 130 mm. Immature males are rarely observed in the traps (Fig. 1). Neither females nor immature males were considered in the analyses.

In this study, we use catch-per-unit-effort (CPUE) as a measure of abundance. We standardize CPUE using the data collected in February 2001. We estimate natural mortality rates based on the changes in standardized CPUE between the post- and pre-moult surveys. We estimate proportions of moulting based on the estimated relative abundances of new and old shell crabs at the beginning of the moulting season. After estimating size-dependent vulnerability to the traps, we estimate the survival fraction for newly moulted crabs through the moulting season. These estimated parameters are used in models to assess the impact of fishing intensity and handling mortality of sublegal-sized crabs on long-term yield.

Standardisation of fishing effort

For trap fisheries, fishing effort is usually measured in trap hours. There is a saturation effect for Dungeness crabs caught in the traps (Fig. 2). To better measure the abundance of crabs, catch per trap (CPT) was modelled as

$$(1) \qquad CPT = CPT_{\infty}(1 - \exp(-k\,\tau_{soak}))$$

where CPT_{∞} is the maximum number of crabs likely to appear in a trap, k measures the rate at which the catch-rate declines, and τ_{soak} is the soak time. CPT_{∞} and k were estimated from February 2001 survey data by minimizing the sum of squares of error.

The standardized soak time, τ^{*}_{soak}, is the time required to catch the same number of crabs if every hour was as effective as the first:

$$(2) \qquad \tau^{*}_{soak} = \frac{CPT(\tau_{soak})}{CPT(1)}$$

or

$$\tau^{*}_{soak} = \frac{1 - \exp(-k\,\tau_{soak})}{1 - \exp(-k)}$$

The standardized effort is

$$(3) \qquad E^{*} = \tau^{*}_{soak}\,NT$$

© 2004 NRC Canada

Fig. 1. Size–frequency distribution for male Dungeness crabs (*Cancer magister*) caught in all the scientific surveys from Vancouver Harbour.

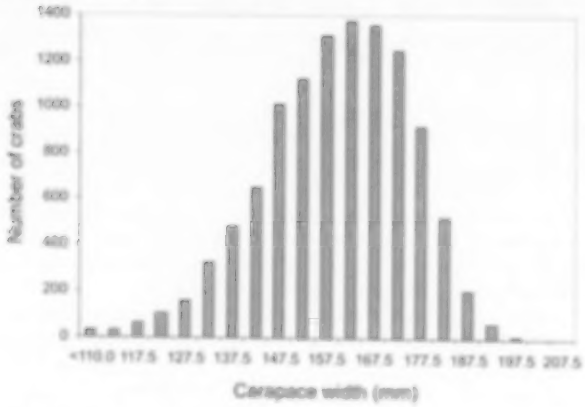

where NT is the number of traps in a string. The standardized CPUE is

$$\text{(4)} \qquad \text{CPUE}^* = C/E^*$$

where C is the number of crabs caught in a string of traps. CPUE* is assumed to be proportional to the density of the crab population.

Natural mortality rate during non-moulting period

The natural mortality rate was estimated by comparing CPUE* from two different surveys taken during the same intermoult period in Vancouver Harbour. The expected relationship between the survey results and the natural mortality rate is

$$\text{(5)} \qquad M = \frac{-1}{t_\beta - t_\alpha} \ln\left(\frac{\text{CPUE}^*(t_\beta)}{\text{CPUE}^*(t_\alpha)}\right)$$

where t_α and t_β are the times at which the surveys occurred and CPUE*(t) is the standardized CPUE at time t. M is the non-moulting, natural, instantaneous mortality rate. There is the assumption that catchability is the same during both surveys. Only legal-sized crabs (CW > 155 mm) were used to estimate natural mortality.

M was estimated for the June–October period from 1994 to 2000. The survey in June 1994 was conducted with only six trap hauls in contrast to 20 or more trap hauls in the other survey occasions, and the estimated value for 1994 is much higher than for other years (Table 1). Therefore, 1994 was excluded from the estimate of the mean value of M. The mean natural mortality rate was calculated with the values weighted according to fishing effort in the surveys:

$$\text{(6)} \qquad \overline{M} = \frac{\sum_{y=1995}^{2000} M_y E_y^*}{\sum_{y=1995}^{2000} E_y^*}$$

where M_y is the estimated natural mortality rate for the year and E_y^* is the smaller of E^* for June and October of that year. The standard error (SE) for $\overline{M}$

Fig. 2. Catch per trap (CPT) with soak hours (t) for male Dungeness crabs (*Cancer magister*): CPT = 14.62(1 – exp(–0.19t)); ●, observed data.

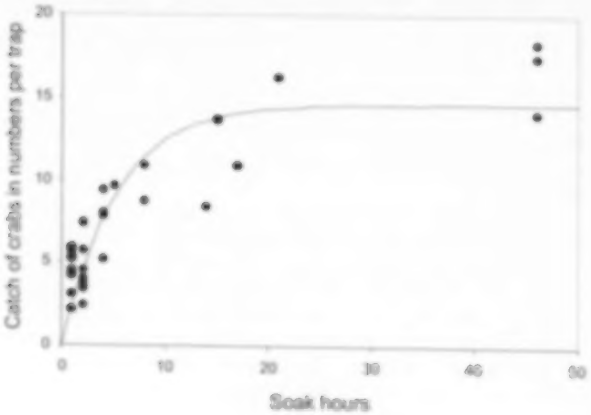

$$\text{(7)} \qquad \text{SE}(\overline{M}) = \sqrt{\frac{\sum_{y=1995}^{2000} f_y (M_y - \overline{M})^2}{n(n-1)}}$$

where n is the number of years where data were used and

$$f_y = \frac{nE_y^*}{\sum_{y=1995}^{2000} E_y^*}$$

The estimated value of $\overline{M}$ is applied all year except for the 1-month period beginning when a crab moults. M is termed the non-moulting natural mortality rate in this paper.

Probability of moulting

The probability of moulting is an important aspect of growth for Dungeness crabs. On the Fraser delta, soft-shell crabs are primarily observed during a brief period in the spring. To simplify calculations, all moulting is assumed to occur at the same time t_0. During a post-moult survey, shell condition can be used to identify old-shell crabs that did not moult during the previous moulting season. The probability of moulting can be determined by estimating the number of crabs (old-shell crabs + new-shell crabs) just before t_0 and the number of old-shell crabs just after t_0.

Let t_{-1} and t_1 be the times of the pre- and post-moult surveys. Variations of eq. 5 were used to estimate abundances immediately before and after moulting. The relative abundance of crabs immediately before moulting is

$$\text{CPUE}^*(t_0) = \text{CPUE}^*(t_{-1}) \exp(-M(t_0 - t_{-1}))$$

The relative abundance of old-shell crabs immediately after moulting is

$$\text{CPUE}_o^*(t_0) = \text{CPUE}_o^*(t_1) \exp(-M(t_0 - t_1))$$

where $\text{CPUE}_o^*(t)$ is the CPUE* of old-shell crabs at time t. The fraction of crabs that moult is

© 2004 NRC Canada

Table 1. Fishing effort and catch-per-unit-effort (CPUE) in June and October surveys and estimated instantaneous annual natural mortality (M) for the legal-sized male crabs in Vancouver Harbour in years 1994–2000.

	Number of traps		Standardised effort		Standardised CPUE		M
Year	June	October	June	October	June	October	
1994	6	20	34.14	111.80	3.75	0.75	4.83
1995	27	21	153.09	120.09	0.88	0.62	1.05
1996	33	41	183.64	229.19	1.14	0.94	0.58
1997	30	29	168.30	162.40	1.42	0.57	2.74
1998	60	52	336.13	293.84	1.07	1.11	–0.11
1999	62	69	308.73	219.84	1.89	1.21	1.34
2000	60	69	275.37	221.42	1.78	1.27	1.01
Weighted mean[a]							0.97 ± 0.39

[a]Weighted mean of estimated natural mortality rates in 1995–2000 ± standard error.

$$p = \frac{\mathrm{CPUE}^*(t_0) - \mathrm{CPUE}^*_1(t_0)}{\mathrm{CPUE}^*(t_0)} \tag{8}$$

or

$$p = 1 - \frac{\mathrm{CPUE}^*_1(t_1)}{\mathrm{CPUE}^*(t_{-1})} \exp(M(t_1 - t_{-1}))$$

For the Vancouver Harbour surveys, the probability of moulting was estimated for 5-mm size intervals from 130- to 195-mm CW. Mean probabilities were calculated with values weighted as they were for the mean natural mortality rate.

There appears to be a discontinuity at CW ≈ 150 mm (Fig. 3). One regression line was fitted for the 130- to 150-mm size range and another for the 150- to 185-mm size range. Crabs larger than 185-mm CW were not considered because the corresponding sample size was too small to achieve reliable estimates.

Fig. 3. Size-specific moulting probability for male Dungeness crabs (*Cancer magister*): ●, estimated proportions of moulting; ◇, weighted mean proportion of moulting.

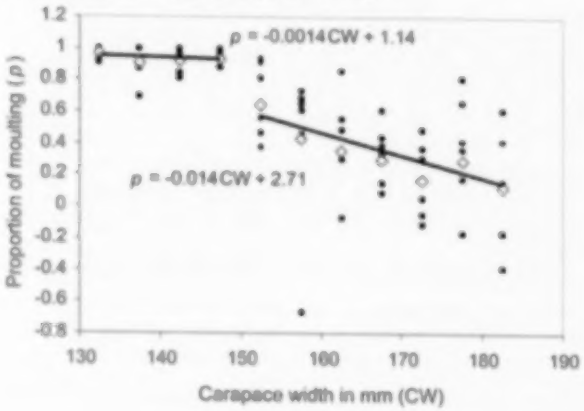

Moult increment

The moult increment is another aspect of growth that could affect the impact of fishing intensity and handling mortality on yield. Previous studies indicate that moult increment is correlated with pre-moult size of crabs (Butler 1961; Collier 1983; Warner 1987). Combining the data collected from British Columbia and California, Smith and Jamieson (1989) formulated the following equation for the post-moult carapace width, PW, based on the pre-moult carapace width, MW:

$$\mathrm{PW} = 1.069\mathrm{MW} + 18.07 + \varepsilon_{\mathrm{SD}} \tag{9}$$

where $\varepsilon_{\mathrm{SD}}$ is a normally distributed random variable with a mean of zero and a standard deviation of 3.29 mm. The equation is applicable when the pre-moult size is in the range $80 \le \mathrm{MW} \le 174$ mm.

Equation 9 can be rewritten to express the probability distribution of the post-moult size. When a crab of the ith size class moults, the probability that it ends up in the jth size class is

$$r_{i,j} = \int_{L_j}^{U_j} \frac{1}{\sqrt{2\pi \cdot 3.29}} \times \exp\left(-\frac{(x - 1.069\mathrm{MW}_i - 18.07)^2}{2 \cdot 3.29^2}\right) \mathrm{d}x \tag{10}$$

where MW_i is the mid-width of the ith size and L_j and U_j are the lower and upper bounds of the jth size class, respectively. They are defined as

$$\begin{cases} L_j = 130 + 5(j-1) \\ \mathrm{MW}_j = L_j + 2.5 \\ U_j = L_j + 5 \end{cases} \tag{11}$$

With the parameter values used in these analyses, there is a negligible probability of negative growth.

Size-dependent vulnerability

Size-dependent vulnerability is important in two ways. Firstly, it is a further refinement in establishing the relationship between abundance and CPUE. Also, low vulnerability will protect a size class from the traps and fishing-related mortality. An approximation of size-dependent vulnerability

© 2004 NRC Canada

is derived from the size–frequency distribution of crabs appearing in the surveys.

The size–frequency distribution for male Dungeness crabs caught in the scientific traps exhibits a peak at approximately 157.5 mm CW (Fig. 1). Few crabs in the traps are larger than 200 mm or less than 130 mm CW. The lack of large crabs likely reflects issues of mortality. The lack of smaller crabs likely reflects lower vulnerabilities. We assume that all legal-sized crabs are fully vulnerable. For sublegal-sized crabs, we assume vulnerability declines exponentially with size. The equation used for vulnerability is

$$(12)\quad \begin{cases} v_i = 1 & (i \geq 6) \\ v_i = \exp(-a(157.5 - \mathrm{MW}_i)) & (1 \leq i \leq 5) \end{cases}$$

where v_i and MW_i are the vulnerability and mid-width size class for the ith size class, respectively, and a is the model parameter to be estimated.

To estimate a, the vulnerability model (eq. 12) was combined with the probability of moulting (eq. 8) and the growth increments (eq. 10) and applied to pre-moult data to predict the size–frequency distribution of new-shell crabs during the post-moult surveys. The value of a was chosen to give the most accurate size–frequency distribution for crabs in the 165- to 195-mm CW range ($8 \leq i \leq 13$). Crabs below this range are not considered because they may have been smaller than the minimum size (130-mm CW) considered in the analysis. Crabs larger than this range are just not commonly observed.

Survey results were adjusted for size-specific vulnerability:

$$(13)\quad N_i(t) = \frac{\mathrm{CPUE}_i^*(t)}{v_i}$$

where $N_i(t)$ and $\mathrm{CPUE}_i^*(t)$ are the corrected (or absolute) abundance and CPUE* for the ith size class at time t, respectively. At the time of the post-moult survey, the predicted size frequency of new-shell crabs in the 8th to 13th size ranges is predicted to be

$$(14)\quad \hat{\Gamma}_{\mathrm{N},j}(t_1) = \frac{\sum_{i=1}^{j-1} v_j N_i(t_{-1}) p_i r_{i,j}}{\sum_{k=8}^{13} \sum_{i=1}^{k-1} v_k N_i(t_{-1}) p_i r_{i,k}} \qquad (8 \leq j \leq 13)$$

$\hat{\Gamma}_{\mathrm{N},j}(t_1)$ was calculated on a year-specific basis with year-specific values of p_i. The expected catches of new-shell crabs in the jth ($8 \leq j \leq 13$) size classes are

$$(15)\quad \hat{C}_{\mathrm{N},j} = \hat{\Gamma}_{\mathrm{N},j}(t_1) \sum_{i=8}^{13} C_{\mathrm{N},i}(t_1)$$

where $C_{\mathrm{N},i}(t_1)$ is the year-specific actual catch of new-shell crabs in the ith size class in the post-moult survey. The expected catches were then compared against the actual catches using a χ^2 statistic:

$$(16)\quad \chi^2 = \sum_{\text{year}} \sum_{j=8}^{13} \frac{(\hat{C}_{\mathrm{N},j}(t_1) - C_{\mathrm{N},j}(t_1))^2}{\hat{C}_{\mathrm{N},j}(t_1)}$$

A grid search was used to find the value of a that minimized χ^2.

Moulting survival fraction

Dungeness crabs are believed to suffer high mortality during and shortly after they moult. This is modelled by replacing M by a survival fraction, S, that applies for a time period, τ_{moult}, that begins with moulting.

As was the case for a, S was estimated by using pre-moult surveys to predict the results of the post-moult surveys. In order to estimate S, we consider absolute abundances instead of just a normalized size–frequency distribution. The amount of time between the pre- and post-moult surveys is $t_1 - t_{-1}$. If the crab moults, the moulting survival fraction, S, applies for a period of τ_{moult} and the natural mortality rate, M, applies for a period of $t_1 - t_{-1} - \tau_{\mathrm{moult}}$. Therefore, the probability that a crab in the ith size class in the pre-moult survey becomes a new-shell crab in the post-moult survey is $p_i \cdot S \cdot \exp(-M(t_1 - t_{-1} - \tau_{\mathrm{moult}}))$. Equation 10 gives the size distribution in the post-moult survey. The predicted abundance of new-shell crabs of the jth size class ($8 \leq j \leq 13$) predicted for the post-moult survey is

$$(17)\quad \hat{N}_{\mathrm{N},j}(t_1) = \sum_{i=1}^{j} N_i(t_{-1}) \exp(-M(t_1 - t_{-1} - \tau_{\mathrm{moult}})) \times S\, p_i\, r_{i,j}$$

Year-specific values of $\hat{N}_{\mathrm{N},j}(t_1)$ were calculated using year-specific values of p_i, and τ_{moult} was given a value of 1 month. The predicted values were compared with survey values on the basis of

$$(18)\quad \mathrm{SSD} = \sum_{\text{year}} \sum_{j=8}^{13} \left(\hat{N}_{\mathrm{N},j}(t_1) - \frac{\mathrm{CPUE}_{\mathrm{N},j}^*(t_1)}{v_j} \right)^2$$

where $\mathrm{CPUE}_{\mathrm{N},j}^*(t_1)$ is CPUE* for new-shell crabs in the jth size class in the post-moult survey. As when the vulnerability coefficient was estimated, only crabs with a post-moult size in the 165- to 195-mm size range ($8 \leq j \leq 13$)) were considered. A value of S was chosen to minimize the value of SSD.

Yield-per-recruit analysis

The growth and mortality models can be used to estimate yield per recruit for crabs on the Fraser delta. When handling mortality is included in the models, we can estimate its effect on yield per recruit and determine which levels of fishing effort result in the maximum yield per recruit.

For these analyses, a recruit is defined to be a male crab with $130 \leq \mathrm{CW} < 155$ mm. Smaller crabs have very low vulnerability to the traps. Most of the recruits will be of legal harvest size after their next moult.

The recruit represents a size range. At year 0, the beginning of the simulation, the size frequency corresponding to a recruit is based on survey data and the following vulnerability equation:

© 2004 NRC Canada

$$(19)\quad \begin{cases} N_{0,i} = \dfrac{C_i / v_i}{\sum_{j=1}^{5} C_j / v_j} & (1 \le i \le 5) \\ N_{0,i} = 0 & (i \ge 6) \end{cases}$$

where $N_{y,i}$ is the number of crabs of the ith size class in the yth year, C_i is the total catch of crabs of the ith size class in all the surveys, and v_i is the vulnerability coefficient for the ith size class (eq. 12).

The simulation begins just before harvest in year 0. The size frequency from one year is used to generate the size frequency for the next:

$$(20)\quad N_{y,j} = N_{y-1,j} \exp(-Z_j \tau_{\text{harvest}}) \exp(-M(1 - \tau_{\text{harvest}}) \times (1 - p_j) + \sum_{i=1}^{j-1} N_{y-1,i} \exp(-Z_i \tau_{\text{harvest}}) \times \exp(-M(1 - \tau_{\text{harvest}} - \tau_{\text{moult}})) S p_i r_{i,j} \quad (y = 1, 2, 3, \ldots)$$

where Z_i is the size-specific instantaneous mortality rate during harvest, and τ_{harvest} is the length of the harvest in years. The first term in eq. 20 represents old-shell crabs and the summation represents new-shell crabs.

Because crabs greater than 210-mm CW are rarely observed in Vancouver Harbour, we set $1 \le j \le 16$. Any crabs destined to grow larger than 210-mm CW are assumed to suffer senescent mortality instead. Equation 20 is applied until mortality has reduced the original recruit to a very small (<0.0001) fraction of a crab.

To use eq. 20, size-specific mortality rates are required for the fishing season. They are as follows:

$$(21)\quad \begin{cases} Z_i = M + F h v_i & (i \le 5) \\ Z_i = M + F h(1 - RT) v_i + F \,\text{RT}\, v_i & (i = 6) \\ Z_i = M + F v_i & (i \ge 7) \end{cases}$$

where h is the handling mortality rate, F is the fishing mortality rate, and RT is the retention rate for crabs that are just barely of legal size. The handling mortality rate is assumed to be 5% for the yield-per-recruit analysis.

The number of crabs contributing to the yield is

$$(22)\quad \begin{cases} C_{y,i} = 0 & (i \le 5) \\ C_{y,i} = N_{y,i} \dfrac{F\,\text{RT}}{Z_i}(1 - \exp(-Z_i \tau_{\text{harvest}})) & (i = 6) \\ C_{y,i} = N_{y,i} \dfrac{F}{Z_i}(1 - \exp(-Z_i \tau_{\text{harvest}})) & (i \ge 7) \end{cases}$$

The corresponding exploitation rate, E_i, for legal-sized crabs larger than or equal to 160-mm CW is

$$(23)\quad E_i = \frac{F}{Z_i}(1 - \exp(-Z_i \tau_{\text{harvest}})) \quad (i \ge 7)$$

Equation 22 gives the number of crabs caught per recruit. The corresponding yield per recruit (YPR) is simply

$$(24)\quad \text{YPR} = \sum_{y} \sum_{i=6}^{16} C_{y,i} W_i$$

where W_i is the estimated weight of a crab of the ith size class. The relationship between carapace width and weight has been established on the basis of a sample of 180 crabs from the Vancouver Harbour surveys.

$$(25)\quad W_i = 0.000102\,\text{MW}_i^{3.10}$$

YPR can be calculated as a function of the fishing mortality rate. From this function, we determine $F_{0.1}$, the instantaneous fishing mortality rate at which the slope of the yield-per-recruit function is 0.1 times the slope near $F = 0$. Then eq. 23 is used to get $E_{0.1}$, the exploitation rate corresponding to $F_{0.1}$. The crab season is assumed to be 2 months long in the YPR calculations.

Impact of fishing at a high ratio of sublegal- to legal-sized crabs on long-term yield

To assess the impact of fishing at a high ratio of sublegal- to legal-sized crabs in the catch on long-term yield, we consider what happens when the last crab of the season is harvested. The current harvest increases by one crab. We assume the crab has a CW of 157.5 mm and therefore its contribution to yield can be calculated from eq. 25.

However, to harvest the last legal-sized crab, N_s sublegal-sized crabs will be captured and discarded back into the water. The number of sublegal-sized crabs to die as a result of the harvest of the last legal-sized crab is $h \cdot N_s$. We assume the size distribution of the crabs that suffer handling mortality is similar to that of sublegal-sized crabs appearing in the scientific surveys. Therefore, on a size-specific basis, the number of crabs that die as a result of the last-harvested legal-sized crab is

$$(26)\quad \begin{cases} H_{0,i} = N_s h C_i \Big/ \sum_{j=1}^{5} C_j & (i \le 5) \\ H_{0,i} = 1 & (i = 6) \\ H_{0,i} = 0 & (i \ge 7) \end{cases}$$

where $H_{0,i}$ is the number of the ith size class in year 0, the beginning of the simulation. To determine the contribution that these crabs could have eventually made to future harvests, we use a model that is very similar to the one used in the yield-per-recruit analysis. The only difference is that the yield-per-recruit analysis starts with $N_{0,i}$, which represents a number of crabs just before harvest, and the current analysis starts with $H_{0,i}$, which represents a number at the end of harvest. At the beginning of the next harvest, the number of crabs lost owing to the harvest of the last crab in year 0 would have been

$$(27)\quad N_{1,j} = H_{0,j} \exp(-M(1 - \tau_{\text{harvest}}))(1 - p_j) + \sum_{i=1}^{j-1} H_{0,i} \exp(-M(1 - \tau_{\text{harvest}} - \tau_{\text{moult}})) S p_i r_{i,j}$$

For the 2nd year onwards, the model is identical to that used in the yield-per-recruit analysis (eq. 20).

© 2004 NRC Canada

Table 2. Proportion of moulting for different size classes.

	Mid-carapace width (mm) of a size class												
Year	132.5	137.5	142.5	147.5	152.5	157.5	162.5	167.5	172.5	177.5	182.5	187.5	192.5
1995	1.00	1.00	1.00	1.00	0.56	0.65	0.49	0.39	–0.12	0.81	0.16	N/A	1.00
1996	1.00	1.00	1.00	0.89	0.92	–0.66	0.30	0.33	0.38	0.41	0.42	–0.25	N/A
1997	1.00	1.00	0.97	1.00	0.81	0.69	0.86	0.61	0.05	0.66	0.13	1.00	N/A
1998	0.91	1.00	1.00	0.98	0.94	0.46	0.56	0.45	0.49	0.18	–0.38	–0.38	1.00
1999	1.00	0.87	0.81	0.94	0.38	0.73	–0.07	0.09	–0.05	–0.17	–0.17	–0.96	–0.51
2000	0.93	0.70	0.85	0.88	0.47	0.61	0.35	0.15	0.31	0.36	0.61	0.71	0.66
$\bar{P}^a$	0.97	0.91	0.92	0.94	0.65	0.43	0.35	0.30	0.17	0.30	0.12	–0.06	0.24

Note: N/A, no catch of crabs in this size class in the October survey, so the proportion cannot be calculated.
[a]Weighted mean proportion of moulting.

Fig. 4. Yield per recruit and exploitation rate ($E_{0.1}$) at three different retention rates (RS) for male Dungeness crabs (*Cancer magister*) of 155- to 160-mm carapace width: ●, $E_{0.1}$; bolded line, RS = 100%; broken line, RS = 50%; shaded line, RS = 0%.

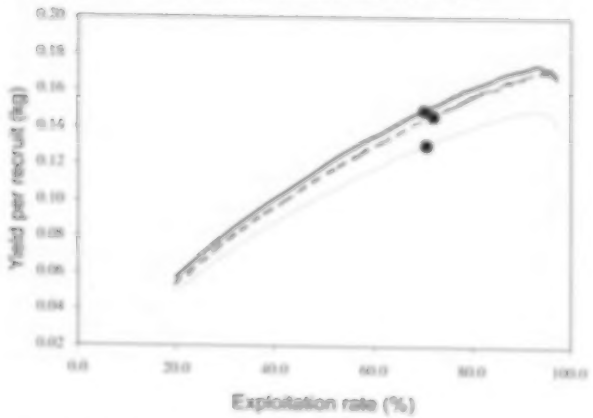

Fig. 5. Gain in yield in the long term for catching one more legal-sized crab at different ratio of sublegal- to legal-sized crabs in the catch and with different handling mortality rate (h): shaded line, h = 5%; solid line, h = 10%; broken line, h = 15%; bolded line, h = 20%.

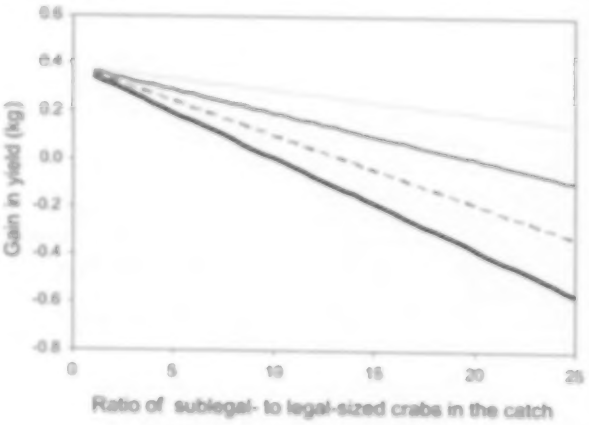

From the model results, we can calculate the contribution that these sublegal-sized crabs and the last-harvested crab in year 0 would have made to harvests in years 1, 2, 3,... if they had not suffered handling mortality during year 0. We assume the instantaneous fishing mortality rate is 8.2 year^{-1}, which corresponds to an exploitation rate of 0.7 when the fishing season is 2 months long. The retention rate for the 6th size class, RT, was set to one. Handling mortality rates of 5%, 10%, 15%, and 20% were evaluated.

Results

The average level of saturation (CPT_∞) was estimated to be 14.62 crabs per trap with a coefficient of variation of 6.5%. The instantaneous rate of decrease in catch rate (k) was estimated to be 0.19 with a coefficient of variation of 16.1%. The coefficient of determination for the regression (eq. 1) is 0.76. An examination of the residuals from Fig. 2 showed that the residuals have an approximately normal distribution. Catch rate decreases with soak time (Fig. 2). A trap catches approximately 2.5 crabs the 1st hour after setting but only 0.032 crabs in the 24th hour.

The estimated non-moulting annual natural mortality rates varied from approximately 0 to 3 year^{-1} in 1995–2000 (Table 1). The weighted average rate was estimated to be 0.97 year^{-1} with a standard error of 0.39 year^{-1}. The survival fraction for the month beginning with a moult, S, is 70.1%, which is equivalent to an instantaneous annual mortality rate of 4.27 year^{-1} for the 1-month moulting period. The survival fraction for the moulting crabs is 0.76 times that for non-moulting crabs during the moulting season. Without harvest, the probability of a crab surviving a whole year is approximately 28.8% if it moults and 37.9% if it does not.

For large crabs (CW > 150 mm), there is a highly significant (p = 0.01) linear trend between size and the probability of moulting (Fig. 3). The estimated average probability of moulting decreases from 54.7% to 11.5% when the size of crabs increases from 152.5-mm to 182.5-mm CW. For crabs in the 185- to 195-mm CW range, estimated proportions of moulting have large variations and do not appear to be reliable, probably because of the relatively small size of catch data for these crabs (Table 2). For smaller crabs, the linear relationship is not statistically significant (p = 0.65). Almost all of these smaller crabs would moult in the spring (Fig. 3). The estimated coefficients are given in Fig. 3.

The parameter a for the vulnerability model (eq. 12) was estimated to be 0.076. The estimated vulnerability coeffi-

© 2004 NRC Canada

cient decreases exponentially from 1.0 for legal-sized crabs to 0.15 for crabs of 130- to 135-mm CW.

When the handling mortality rate is 5%, yield per recruit increases with the exploitation rate until it reaches 94%. An exploitation rate greater than 94% would result in a decline in yield per recruit (Fig. 4). $F_{0.1}$ was estimated to be equivalent to approximately 70%. Although the retention rate for barely legal-sized crabs has very little influence on this trend, a higher retention rate results in higher yield for a given exploitation rate (Fig. 4).

As the ratio of sublegal- to legal-sized crabs in the traps increases, the gain in long-term yield decreases at an approximately linear trend (Fig. 5). At handling mortality rates of 5%, 10%, 15%, or 20%, the net gain is zero when the ratio of sublegal- to legal-sized crabs in the catch reaches approximately 40:1, 20:1, 13.5:1, or 10:1, respectively. Fishing above these threshold ratios would result in a net loss in long-term yield.

Discussion

These analyses comprise the development of suitable models for the growth and mortality of Dungeness crabs, the estimate of model parameters for the models, and the application of the models to address concerns of a fishery. The experience gained from working with these models suggests further research that could be done.

The growth models developed in these analyses are size-dependent. The probability of moulting and the distribution of the moult increments depend on the size of the crab. Numerically, size-dependent growth models such as eq. 20 are generally more complex to implement than length-at-age models such as the von Bertalanffy growth equation as described in Quinn and Deriso (1999).

The parameter values necessary to predict moult increments were taken from the literature, but a new approach was used to estimate the probability of moulting. These analyses have contributed a method for estimating the probability of moulting that is unaffected by circumvents of moult-related mortality. The two common methods for estimating the probability of moulting are based on the analysis of mark–recapture data (Bennett 1974; McCaughran and Powell 1977; Hankin et al. 1985) or size–frequency data (Weber and Miyahara 1962; Hankin et al. 1989; Mohr and Hankin 1989). The weakness of these methods is that they either ignore moult-related mortality completely or have had to guess at its extent.

Because of variations in natural mortality rates and possible year-to-year variations in the vulnerability of crabs to the traps and in the accuracy of using CPUE* as a measure of abundance, the estimated moulting proportion for individual years could be under- or over-estimated. However, the mean proportions of moulting would be more accurate, as under- and over-estimates of individual moulting proportions would cancel each other out to some extent.

As in Koeneman (1985), the probability of moulting is found to be size-dependent. Smaller crabs (CW < 150 mm) are almost certain to moult during the season. The probability of moulting declines as crabs get larger. Generally, our analyses show a higher probability of moulting for large crabs than those reported by Koeneman (1985).

Both moulting-related and non-moulting-related natural mortality are considered. It is important to differentiate between these two natural mortalities as Morado et al. (1999) concluded that newly moulted crabs are more susceptible to disease-related infections. The non-moulting natural mortality rate was estimated from estimates of abundance and standard methodology. The estimated mean non-moulting natural mortality rate is 0.97 year^{-1}. When the moulting and non-moulting mortalities are pooled, the effective instantaneous rate becomes 1.25 year^{-1}. This mortality rate is lower than the natural mortality rates for male Dungeness crabs reported by Gotshall (1978) and Smith and Jamieson (1991). Gotshall (1978) estimated that the natural mortality rate varied from 1.08 to 3.56 year^{-1} in Northern California using commercial CPUE data. Smith and Jamieson (1991) found that the natural mortality rate was around 2.5 year^{-1} near Tofino on the west coast of Vancouver Island using tagging information. However, our estimated rate is more consistent with the mortality range of 0.8 to 1.2 year^{-1} proposed by Butler and Hankin (1992). Moulting-related mortality was estimated by fitting models to survey data. Our result quantitatively confirms that newly moulted crabs have a lower survival fraction than non-moulted crabs through the moulting season.

Moulting-related mortality has been incorporated through the moulting-survival fraction, S, which is used instead of the M during the moulting season. Handling mortality of sublegal-sized crabs is a concern for the fishery that is addressed through the model parameter, h, which is used in eq. 21.

The analyses also used a model for the time dependence of CPUE. This model makes it possible to combine data where a range of soak times has been used.

The vulnerability model used in the analyses is useful to make estimated abundances comparable among different size ranges. The size-specific vulnerabilities estimated in these analyses are consistent with the observation that relatively few small crabs appear in the traps.

The yield-per-recruit analysis shows that long-term yield peaks when the exploitation rate reaches 94%. Handling mortality does reduce the potential long-term yield. With 5% handling mortality, long-term yield will eventually start to decrease as fishing effort increases further.

Although the yield-per-recruit analysis seems to show that such a high exploitation rate is needed to produce the maximum amount of yield, $F_{0.1}$ was estimated to be equivalent to 70%, suggesting that this high fishing level should be reduced. Deriso (1987) showed that for a broad range of models of stock dynamics, $F_{0.1}$ policy does not unduly reduce the spawning abundance. The $F_{0.1}$ measure is also, in a sense, a bioeconomic criterion in that a marginal yield of less than 10% was felt to be close to the point at which most fisheries administrators would consider further increases in fishing mortality or effort to be no longer economically worthwhile (FAO 1993).

Fishing with a high intensity would also increase the mortality on sublegal-sized crabs, as they are frequently caught and released in search for legal-sized crabs, especially after a large fraction of legal-sized crabs have been removed. Continuing to fish would result in a net loss in the long-term yield, when the ratio of discarded to retained crabs is higher

© 2004 NRC Canada

than the threshold level. Determination of the threshold ratio relies on the handling mortality rate, which is yet to be investigated for the Dungeness crab fishery. This analysis provides the fishery managers another measure for regulating the fishery, once the handling mortality rate is known. The fishing season should be closed when the threshold level is reached.

These analyses suggest further work that could be done. One of the most useful things to do would be to consider the impact of uncertainty on our conclusions. For example, there was much uncertainty in our estimate of the non-moulting mortality rate and that will have direct impact on the estimated value of the probability of moulting, the moulting survival fraction, and the application of the models. An integrated approach to parameter estimation would give more confidence in the estimated parameter values. The results of these analyses depend heavily on CPUE* as an indicator of abundance. Any investigation of this assumption would be beneficial.

In short, the paper describes a new way of estimating size-specific moulting probability and a methodology for determining the survival fraction for newly moulted crustaceans through the moulting season. The methods should be applicable to any crustaceans having a well-defined moulting season and a reliable postmoult indicator. A length-based yield-per-recruit model was developed to assess the impact of fishing intensity on yield. The paper also presents an approach for calculating the amount of gain or loss in long-term yield for fishing at various ratios of discarded to retained crabs. This approach can be applied to other fisheries where sublegal-sized animals can be released and the ratio of discarded and retained animals is known.

Acknowledgements

We thank two anonymous reviewers and an Associate Editor, Dr. G.T. Evans, for constructive comments, which greatly improved the quality of the paper.

References

Bennett, D.B. 1974. Growth of the edible crab (*Cancer pagurus* L.) off southwest England. J. Mar. Biol. Assoc. U.K. **54**: 803–823.

Butler, T.H. 1961. Growth and age determination of the Pacific edible crab *Cancer magister* Dana. J. Fish. Res. Board Can. **18**: 873–889.

Butler, T.H., and Hankin, D.G. 1992. Comment on mortality rates of Dungeness crabs (*Cancer magister*). Can. J. Fish. Aquat. Sci. **49**: 1518–1525.

Collier, P.C. 1983. Movement and growth of post-larval Dungeness crabs, *Cancer magister*, in the San Francisco area. Calif. Dep. Fish Game Fish Bull. **172**: 125–133.

Deriso, R.B. 1987. Optimal $F_{0.1}$ criteria and their relationship to maximum sustainable yield. Can. J. Fish. Aquat. Sci. **44**(Suppl. 2): 339–348.

Food and Agriculture Organization. 1993. Reference points for fisheries management: their potential application to stradling and highly migratory resources. FAO Fish. Circ. No. 864.

Gotshall, D.W. 1978. Catch-per-unit-effort studies of northern California Dungeness crabs, *Cancer magister*. Calif. Fish Game, **64**: 189–199.

Hancock, D.A., and Edwards, E. 1967. Estimation of annual growth in the edible crab (*Cancer pagurus*). J. Cons. Int. Explor. Mer, **31**: 246–264.

Hankin, D.G., Diamond, N., Mohr, M., and Ianelli, J. 1985. Molt increments, annual molting probabilities, fecundity and survival rates of adult female Dungeness crabs in northern California. *In* Proceedings of the Symposium on Dungeness Crab Biology and Management. Alaska Sea Grant Rep. No. 85-3. pp. 189–206.

Hankin, D.G., Diamond, N., Mohr, M., and Ianelli, J. 1989. Growth and reproductive dynamics of adult female Dungeness crabs (*Cancer magister*) in northern California. J. Cons. Int. Explor. Mer, **46**: 94–108.

Jamieson, G.S., Phillips, A., and Smith, B.D. 1998. Implications of selective harvests in Dungeness crab (*Cancer magister*) fisheries. *In* North Pacific Symposium on Invertebrate Stock Assessment and Management. *Edited by* G.S. Jamieson and A. Campbell. Can. Spec. Publ. Fish. Aquat. Sci. No. 125. pp. 309–321.

Koeneman, T.M. 1985. A brief review of the commercial fisheries for *Cancer magister* in southeast Alaska and Yakutat waters, with emphasis on recent seasons. *In* Proceedings of the Symposium on Dungeness Crab Biology and Management. Alaska Sea Grant Rep. No. 85-3. pp. 61–76.

McCaughran, D.A., and Powell, G.C. 1977. Growth model for Alaska king crab (*Paralithodes camtschatica*). J. Fish. Res. Board Can. **34**: 989–995.

Mohr, M.S., and Hankin, D.G. 1989. Estimation of size-specific molting probabilities in adult decapod crustaceans based on postmolt indicator data. Can. J. Fish. Aquat. Sci. **46**: 1819–1830.

Morado, J.F., Giesecke, R.H., and Syrjala, S.E. 1999. Molt related mortalities of the Dungeness crab *Cancer magister* caused by a marine facultative ciliate *Mesanophrys pugettensis*. Dis. Aquat. Org. **38**: 143–150.

Quinn, T.J., and Deriso, R.B. 1999. Quantitative fish dynamics. Oxford University Press, New York.

Smith B.D., and Jamieson, G.S. 1989. Growth of male and female Dungeness crabs near Tofino, British Columbia. Trans. Am. Fish. Soc. **118**: 556–563.

Smith, B.D., and Jamieson, G.S. 1991. Movement, spatial distribution, and mortality of male and female Dungeness crabs (*Cancer magister*) near Tofino, British Columbia. Fish. Bull. U.S. **89**: 137–148.

Tegelberg, H.C. 1971. Condition, yield, and handling mortality studies on Dungeness crabs during the 1969 and 1970 seasons. *In* 23rd Annual Report of the Pacific Marine Commission for the Year 1970. Pacific Marine Commission, Portland, Oregon. pp. 42–47.

Warner, R.W. 1987. Age and growth of male Dungeness crabs, *Cancer magister*, in northern California. Cal. Fish Game, **73**: 4–20.

Weber, D.D., and Miyahara, T. 1962. Growth of the adult male king crab *Paralithodes camtschatica* (Tilesius). U.S. Fish. Wild. Ser. Fish. Bull. **200**: 53–75.

© 2004 NRC Canada

Effects of a native crayfish (*Orconectes virilis*) on the reproductive success and nesting behavior of sunfish (*Lepomis* spp.)

Nathan J. Dorn and Gary G. Mittelbach

Abstract: While crayfish are traditionally considered fish prey, they are capable of feeding on substrate-bound fish eggs and their introductions have been blamed for the decline in fish populations in Europe and North America. To investigate their potential effects on fish reproductive success we measured the effects of a native crayfish (*Orconectes virilis*) on the reproductive success of two substrate-nesting sunfish, pumpkinseed (*Lepomis gibbosus*) and bluegill (*Lepomis macrochirus*), in replicated pond experiments. Crayfish were observed feeding on eggs in both experiments. Crayfish presence delayed successful reproduction by pumpkinseeds in densely vegetated ponds, resulting in lower young-of-the-year biomass in ponds with crayfish. In the second experiment, with bluegills in less-vegetated ponds, crayfish prevented successful reproduction entirely. However, when we added crayfish-proof exclosures to the crayfish ponds late in the summer, bluegills located the crayfish-free habitat and successfully reproduced inside the exclosures (1 month after first successful reproduction in control ponds). The results of these experiments demonstrate the potential strong negative effects of crayfish on sunfish reproduction and suggest that the spatial distribution of crayfish and other egg predators may influence fish nesting behaviors and habitat choices. Further studies are needed to determine the magnitude of crayfish effects in natural lakes and ponds where sunfish and crayfish co-occur.

Résumé : Bien que les écrevisses soient considérées comme des proies des poissons, elles peuvent s'alimenter d'oeufs de poissons fixés au substrat; leur introduction a été blâmée pour le déclin de populations de poissons, tant en Europe qu'en Amérique du Nord. Afin de déterminer les effets potentiels des écrevisses sur le succès de la reproduction des poissons, nous avons mesuré les effets d'écrevisses indigènes (*Orconectes virilis*) sur le succès reproductif de deux crapets qui nichent sur le substrat, le crapet-soleil (*Lepomis gibbosus*) et le crapet arlequin (*Lepomis macrochirus*), dans des expériences répétées en étang. La présence d'écrevisses retarde les reproductions réussies chez les crapets-soleils dans les étangs à végétation dense; il y a donc une biomasse réduite de jeunes de l'année dans les étangs contenant des écrevisses. Dans une deuxième expérience impliquant des crapets arlequins dans des étangs avec moins de végétation, les écrevisses enraient entièrement lee succès de la reproduction. Cependant, l'addition d'enclos à l'épreuve des écrevisses en fin d'été permet aux crapets arlequins d'identifier les zones sans écrevisses et de se reproduire avec succès dans les enclos (avec un mois de retard par rapport à la première reproduction réussie dans les étangs témoins). Ces expériences démontrent les effets potentiels très négatifs que peuvent avoir les écrevisses sur la reproduction des crapets et elles indiquent que la répartition spatiale des écrevisses et des autres prédateurs des oeufs peut influencer les comportements de nidification des poissons et leur choix d'habitat. D'autres études seront nécessaires pour déterminer l'ampleur des effets des écrevisses dans les lacs et les étangs naturels dans lesquels les écrevisses et les crapets coexistent.

[Traduit par la Rédaction]

Introduction

The early life stages of species are especially vulnerable to predators, and high mortality during these stages can have strong effects on the recruitment dynamics of populations (Werner and Gilliam 1984). For many species of fish, the earliest egg and fry stages are closely associated with benthic substrates or vegetation for days to months (Breder and Rosen 1966). In these substrate-bound habitats the eggs and fry are vulnerable to a suite of predators that pose little or no threat to larger and more mobile life stages. A variety of vertebrate and invertebrate species are known to feed on the early life stages of fish (e.g., Gross and MacMillan 1981; Mol 1996; Selgeby 1998) and some observations suggest that fish select breeding sites based on relative predation risk to their eggs (Knapp 1993; Takemon and Nakanishi 1998; Östlund-Nilsson 2000). Interestingly, direct experimental tests of the effects of egg predators on the reproductive success and spawning habitats of fish populations are lacking. This is in contrast to the well-studied effects of piscivores on fish feeding behaviors and foraging-habitat choice (e.g., Werner et al. 1983; Mittelbach 2002).

Crayfish (Decapoda) have historically been considered detritivores and herbivores (Momot 1995) and have been com-

Received 31 July 2003. Accepted 21 July 2004. Published on the NRC Research Press Web site at http://cjfas.nrc.ca on 25 January 2005.
J17681

N.J. Dorn[1,2] and G.G. Mittelbach. W.K. Kellogg Biological Station and Department of Zoology, Michigan State University, Hickory Corners, MI 49060, USA.

[1]Corresponding author (e-mail: dornn@fiu.edu).

[2]Present address: Department of Biological Sciences, Florida International University, Miami, FL 33199, USA.

 doi: 10.1139/F04-158 © 2004 NRC Canada

monly introduced to lakes and streams as forage for fish, to reduce unwanted macrophytes (Hanson and Chambers 1995), or to provide human food (Gherardi and Holdich 1999). Studies of interactions between crayfish and fish have focused primarily on the value of crayfish as dietary items for large predatory fish even though crayfish and fish potentially interact in a variety of ways (Carpenter and Lodge 1986; Dorn and Mittelbach 1999). Being relatively large invertebrates with omnivorous feeding habits, crayfish could be important predators of benthic fish eggs (Carpenter and Lodge 1986; Hanson and Chambers 1995), but good data are limited and inconclusive (see Horns and Magnuson 1981; Savino and Miller 1991). Recent studies from Europe and North America implicate introduced crayfish in the decline of fish populations in rivers (Guan and Wiles 1997), lakes (Covich et al. 1999; Wilson 2002), and streams (Bryan et al. 2002). The mechanisms causing the negative effects of crayfish on fish are largely unknown, but predation on substrate-bound eggs or fry is one oft-cited hypothesis. The introduced crayfish species of greatest concern in the midwestern United States is *Orconectes rusticus* (the rusty crayfish) (Covich et al. 1999), which displaces *Orconectes virilis* (the northern crayfish) — the species we examined in these experiments. *Orconectes rusticus* and *O. virilis* have similar adult sizes and diets (Hill et al. 1993), but *O. rusticus* is more aggressive and less vulnerable to fish predators (Capelli and Munjal 1982; Garvey et al. 1994).

In this paper we report the results from two field experiments designed to examine the potential impacts of crayfish on the reproductive success and nesting behavior of two species of North American sunfish: pumpkinseed (*Lepomis gibbosus*) and bluegill (*Lepomis macrochirus*). These species are common sportfish that reside in littoral habitats but do not feed extensively on crayfish. Both species concentrate their eggs in nests, but the bluegill is a colony-nesting species, while the pumpkinseed is a solitary-nesting species. Specifically, we sought to determine the potential for crayfish to suppress successful reproduction (of either species). In the bluegill study we also examined the ability of reproducing fish to modify nest-site selection and to find crayfish-free nesting habitat.

Materials and methods

These experiments were conducted at the experimental-pond facility at the W.K. Kellogg Biological Station (KBS) in southwestern Michigan. The ponds are bowl-shaped, having a maximum depth of 2 m and a diameter of 29 m. The biota of these ponds is representative of that that found in nearby natural lakes and ponds, and the ponds contain a diverse assemblage of macrophytes, plankton, and benthic invertebrates (e.g., Crowder and Cooper 1982; Rettig and Mittelbach 2002; Dorn and Wojdak 2004). Water levels fluctuate little year-round and the ponds can support permanent populations of sunfish unless purposefully drained. Nutrient levels are in the mesotrophic range (total phosphorus 22–30 $\mu g \cdot L^{-1}$), with a relatively high calcium concentration (80 $mg \cdot L^{-1}$, S. Hamilton, KBS, Michigan State University, Hickory Corners, MI 49060, USA, unpublished data). Prior to these experiments the ponds had never contained crayfish, being isolated (800 m) and uphill from the nearest known population of crayfish. The crayfish *O. virilis* (Hagen) was added to the treatment ponds in 1999 and 2001. *Orconectes virilis* is widely distributed throughout the eastern United States and Canada and is considered native to the upper Midwest. *Orconectes virilis* can be found in several lakes around KBS, including the lake from which we collected the fish. For the experiments, we collected crayfish in large numbers from ponds at the Michigan Department of Natural Resources research station in Saline. The source ponds in Saline had high densities of crayfish (5–10 $\cdot m^{-2}$), few macrophytes, and small populations of fish (largemouth bass (*Micropterus salmoides*) and bluegill). The 1999 experiment examined the effects of crayfish on pumpkinseed reproductive success, while the 2001 experiment examined the effects of crayfish on bluegill reproductive success and nesting behavior.

Sunfish (Centrarchidae) are distributed throughout much of eastern North America. The pumpkinseed and bluegill are two of the most common species; both are medium-sized fish (adults 10–20 cm standard length (SL)) and in southern Michigan they often account for >75% of total fish biomass in small lakes and ponds (Werner et al. 1977). Pumpkinseeds and bluegills reproduce repeatedly over several weeks in the late spring – early summer after water temperatures reach 18–20 °C. Large adult males construct depressions (nests) by fanning the substrate with their caudal fins. Males solicit eggs from females and guard the brood until the young swim off the nest (6–10 days after egg deposition). Male pumpkinseeds tend to nest in a solitary manner, while bluegills usually aggregate their nests into colonies (commonly 5–50 individuals per colony in Michigan Lakes; N. Dorn, unpublished data). Colony nesting is thought to have evolved as a defense against egg predators (Gross and MacMillan 1981).

Pumpkinseed experiment in 1999

Six 30-year-old ponds (each 26 m in diameter) were used for the 1999 experiment. These ponds had organic sediments and a heavy cover of macrophytes that reached to the pond surface by midsummer, and were ringed by a border of cattails (*Typha* sp.). The shallow margins of the ponds had two types of firmer substrate for nesting: the extensive cattail root systems and small areas of gravel that had been added to each pond. In sum the sunfish had three options for nesting substrates — organic sediments, cattail roots, and gravel. The ponds were drained in March 1999 to remove fish and were allowed to sit empty for approximately 2 months, after which they were refilled to 1.6 m depth in May. Invertebrate communities recolonized from nearby ponds, from the water source (a permanent on-site reservoir), and from the pond sediments, which had only partially dried. Large populations of zooplankton (*Daphnia* sp.) and benthic invertebrates were found in all six ponds at the beginning of the experiment. In June, 12 adult pumpkinseeds (6 of each sex) were collected from a local lake and added to each pond (average SLs were 112–122 mm for males and 104–114 mm for females). Three of the six ponds were stocked with crayfish (mean carapace length 38.5 mm, range 24–53 mm) at 1.5 individuals $\cdot m^{-2}$ (800 crayfish per pond) and a biomass density of 26 g wet mass $\cdot m^{-2}$, prior to fish addition. Three ponds served as no-crayfish controls (hereinafter "crayfish" or "no-crayfish" ponds). Crayfish reproduction in the ponds was extremely

© 2004 NRC Canada

low in both experiments, as most females had already dropped their young in the source ponds prior to stocking. To compare crayfish activity-density (a combination of behavior and density) in both of our experiments with natural systems, we used standardized trapping techniques (Lodge et al. 1986) on 3 or 4 dates throughout each summer to quantify crayfish activity-density. Crayfish were trapped overnight (15- to 18-h sets) using 2–4 Gee minnow traps (Nylon Net Company, Memphis, Tennessee) per pond with openings adjusted to 4 cm diameter. Traps were baited with 120 g of beef liver and set in the ponds (at least 5 m apart) between 1700 and 1800 on each trap date.

While our experimental ponds are small relative to most natural lakes, the stocking densities and average activity-densities of crayfish in our experiments were well within the ranges observed for *Orconectes* spp. in Midwest (USA) lakes, ponds, and streams. For example, Momot et al. (1978) report *Orconectes* spp. densities of 1.2–21.2 individuals·m^{-2} from a variety of systems, and *O. virilis* in particular was found at densities of 1.9–6.1·m^{-2} (4.6–21.2 g·m^{-2}) for several consecutive years in oligotrophic marl-bottom lakes in Michigan (see also Momot and Gowing 1977). Activity-densities of various *Orconectes* species from Midwest lakes are commonly 2–10 per trap (Capelli and Magnuson 1983; Collins et al. 1983), but can occasionally be up to 20 or more crayfish per trap, even in the presence of predatory fish (Olsen et al. 1991; Lodge and Hill 1994). In our experiments activity-densities were 1.9 and 9.4·trap^{-1}.

Nighttime observations of active nests and crayfish predation were made from the shoreline with a flashlight at 2- to 4-day intervals from the beginning of the experiment (12 June) through 14 July. In both experiments an active nest was defined as any unmolested nest containing eggs or fry. Nesting observations (number of nests per pond) were analyzed using repeated-measures analysis of variance (rmANOVA, SAS® version 6.0; SAS Institute Inc. 1989).

In this experiment, we measured pumpkinseed recruitment success as the biomass of young-of-the-year (YOY) fish produced per pond. YOY fish were sampled in July and September 1999. In July (when fish were very small) we sampled with a window-screen seine (2.3 m × 2.9 m with 1.8 mm mesh) attached to two wooden poles and operated by two swimmers (as in Rettig and Mittelbach 2002). The seine was placed in the middle of the pond and swum through the water towards shore, seining one radius of the pond. In September, when YOY fish were larger, the ponds were sampled with a bag seine (23 m long with 3.2 mm mesh), capturing approximately 15% of the pond in one seine haul. All collected fish were euthanized with MS 222 and preserved in 10% formalin or 95% ethanol. As a measure of reproductive success we calculated total biomass sampled for each pond after converting average length (N = 35 fish) to mass for each pond with pond-specific length – wet mass regressions. Biomass, calculated as the product of average size and total number of fish collected, was compared using one-way ANOVA. For each sampling date we also compared mean individual mass and numbers of YOY fish to evaluate how each factor contributed to observed differences in total YOY biomass.

We examined YOY otoliths to determine the effects of crayfish on the timing of successful larval production. Otoliths were removed from a random sample of at least 35 individuals collected from each pond in September, and were prepared using standard methods (Stevenson and Campana 1992). Briefly, sagittal otoliths were extracted and placed in clear glue (Crystalbond Adhesive 509, Aremco Products Inc., Cottage Valley, New York) on a microscope slide. The otoliths were polished when necessary and viewed under a compound microscope at 10–40× magnification. Daily rings (Taubert and Coble 1977) on the right otolith were counted twice and averaged to determine fish age. If the two counts differed by >2 days, we made a third count and used the average of the two most similar counts. Four fish were discarded because it was not possible to clearly read the daily rings. YOY ages were analyzed using both a non-parametric test of the summed distributions and ANOVA comparing the six pond averages.

We also checked for differences in YOY growth rates between treatments by regressing fish mass against fish age in each pond, and then using ANOVA to compare the fitted slopes of the regression lines (estimates of the increase in mass per day).

Bluegill experiment in 2001

The six ponds used in the 1999 experiment were renovated during the summer of 2000 as part of an overall pond renovation at the experimental-pond facility. Sediments and plastic liners were removed and replaced, with each pond receiving ~25 cm of a homogeneous sand and clay mixture. Ponds were filled to 2 m depth (29 m diameter) in November 2000 from the permanent reservoir and were allowed to colonize naturally with algae, macrophytes, and invertebrates from nearby ponds. At the beginning of the experiment the ponds had substantial populations of plankton, benthic invertebrates, and filamentous metaphytic green algae (*Zygnema* sp. and *Cladophora* sp.), as well as sparse macrophytes (Dorn and Wojdak 2004). Because these ponds were younger, the benthic communities were admittedly less mature than those in the 1999 ponds or other natural ponds; however, structurally and biologically they resembled a sandy-bottom littoral habitat with abundant filamentous algae. Forty-five reproductively mature bluegills were stocked into each pond in June 2001. The populations stocked into each pond included 15 females (range of pond mean lengths 129–131 mm SL), 15 large males (129–131 mm SL), and 15 small males (67–69 mm SL). The two male sizes correspond to the two commonly observed reproductive strategies described by Gross (1982) as parentals (larger nest-builders and -guarders) and sneakers. Crayfish were stocked at a similar density as in the 1999 experiment (1.44·m^{-2}, 950 animals in total); however, the crayfish were smaller (average CL 29 mm, range 24–46 mm) and therefore the biomass density was lower (9.5 g·m^{-2}).

A complete census of nesting activity in each pond was conducted every 2–3 days from 12 June to 3 August by divers using mask and snorkel or SCUBA. On each sampling date the entire pond bottom was censused for active nests as well as evidence of nesting attempts. In this experiment, recruitment was measured at the larval stage and was quantified through time as the number of YOY bluegills produced per pond. We wanted to quantify YOY fish production as early as possible (immediately after swim-up) and to sample

© 2004 NRC Canada

more frequently than in the 1999 experiment, to better document the dynamics of YOY production. Repeated seining of the ponds would have disturbed bluegill nesting. However, because the ponds contained few macrophytes, we were able to sample YOY weekly with nighttime (2200) ichthyoplankton net tows pulled across the surface of the pond (equal sampling effort was applied to each pond). Nighttime tows were employed to reduce net avoidance. The ichthyoplankton net (0.5 mm mesh with an opening of 68 cm diameter) was towed 27 m at 0.75 $m \cdot s^{-1}$ and captured larval fish <8–10 mm SL in the upper 68 cm of the water column. Larvae were preserved in 10% formalin and enumerated, and a random sample was measured for SL.

During the first 4 weeks of the 2001 experiment, no successful nesting or recruitment of larval fish occurred in the crayfish ponds. On 5 July, one crayfish-proof exclosure was added to each of the three crayfish ponds to evaluate whether bluegills could reproduce successfully if a small amount of predator-free nesting habitat was available. The exclosures measured 1.9 m^2 in area with walls made of 50 cm tall aluminum flashing and bottoms of fiberglass screen (1.2 mm mesh). Each exclosure was filled with approximately 5 cm of substrate taken from the pond bottom. Exclosures were placed approximately 4 m from the center of the pond (away from the area of previously attempted nesting).

Results

Pumpkinseed experiment in 1999

Pumpkinseeds nested on cattail roots and gravel around the margins of the ponds (up to 0.5 m deep) in 1999. Crayfish did not have a significant effect on the number of active nests (i.e., those with eggs or larvae) observed in the ponds through time (number·pond^{-1}·night^{-1}) (rmANOVA, treatment and treatment × time effect P values > 0.36). On several nights in June and early July, crayfish were observed feeding on pumpkinseed eggs or fry inside nests. Pumpkinseeds attempted to defend their nests by rushing at the crayfish with open mouths, and occasionally striking the crayfish on top of the carapace. In response, crayfish would either raise their chelae in defense or back away from the nest. Crayfish activity-density over the summer averaged 1.9 crayfish·trap^{-1} (standard error = 0.2 crayfish·trap^{-1}, N = 3 dates).

Total YOY biomass was significantly lower in the crayfish ponds than in the no-crayfish ponds on the 2 sampling dates (one-way ANOVA, uncorrected P values; July, $F_{[1,4]} = 11.76$, $P = 0.026$; September, $F_{[1,4]} = 10.39$, $P = 0.032$; Fig. 1*a*). One crayfish pond failed to produce any YOY by the July sampling date. Nest destruction was observed several times in that pond and the first successful reproduction occurred in late July. Although not statistically different, YOY numbers averaged 39% and 27% fewer in samples from crayfish ponds (Fig. 1*b*; July, $F_{[1,4]} = 1.43$, $P = 0.3$; September, $F_{[1,4]} = 1.1$, $P = 0.35$). YOY from crayfish ponds averaged less than half the mass of the YOY from the no-crayfish ponds on both dates and were statistically smaller in July (Fig. 1*c*; July, $F_{[1,4]} = 21.06$, $P = 0.01$; September, $F_{[1,4]} = 3.68$, $P = 0.13$).

Examination of otoliths indicated that YOY were born later in the crayfish ponds (Fig. 2). The distribution of YOY

Fig. 1. Production of young-of-the-year (YOY) pumpkinseed sunfish (*Lepomis gibbosus*) in ponds with (shaded bars) and without (open bars) crayfish (*Orconectes virilis*) during summer 1999. (*a*) Mean total biomass (numbers × mean size) of YOY sampled with standardized seining. (*b*) Mean number of YOY captured in seines. (*c*) Mean wet mass (g) of sampled YOY. Error bars represent 1 standard error and P values are from one-way analysis of variance (N = 3).

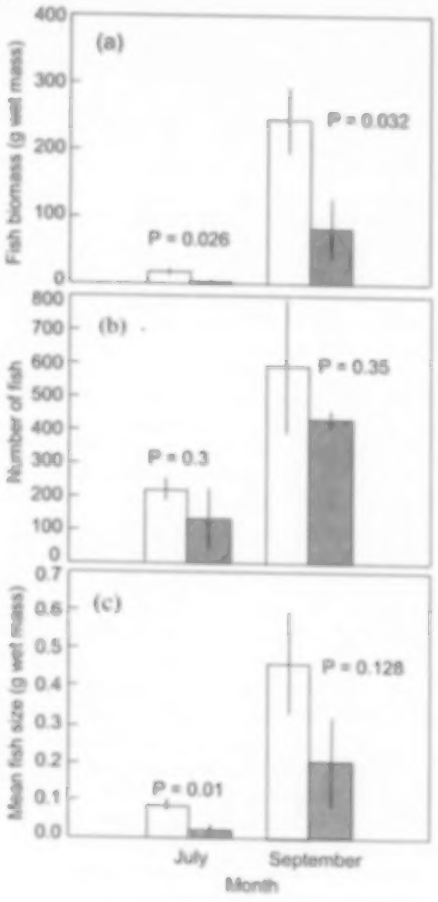

birth dates was significantly different when analyzed with a non-parametric Komolgorov–Smirnov two-tailed test of distributions (maximum difference = 0.575, two-sided P < 0.001), and the median birth dates differed by 12 days ($F_{[1,4]} = 7.175$, $P = 0.055$). The birth date frequency distributions calculated from YOY collected in September may reflect both variation in the distribution of birth dates between treatments and differences in cohort survival to September. We are unable to directly address the question of potential variation in cohort survival between treatments. However, we observed no differences in YOY growth with or without crayfish, which suggests that size-dependent effects on survival were not prominent. YOY mass correlated positively with age in all six of the ponds, and there was no significant difference between the slopes of the regressions for the two treatments ($F_{[1,5]} = 0.401$, $P = 0.56$), indicating

© 2004 NRC Canada

Fig. 2. Distribution of birth dates of YOY pumpkinseeds collected from ponds with (solid bars) and without (open bars) crayfish in 1999. Birth dates were estimated by enumerating otolith daily growth rings. The distributions differed significantly ($P < 0.001$) as determined by a non-parametric Kolmogorov–Smirnov test.

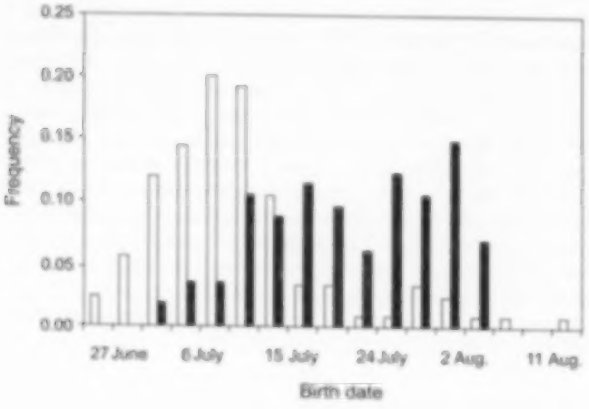

that the YOY grew at similar rates in the crayfish and no-crayfish ponds.

Bluegill experiment in 2001

In the no-crayfish ponds, active nests were first discovered on 14 June (2 days after addition of females), and bluegills in those ponds continued to nest actively until 3 July (3–4 bouts of reproduction) (Fig. 3*a*). In crayfish ponds, bluegill nesting attempts started on 14 June and male bluegills kept a group of nest spots swept clean through mid-July. However, no active nests (with eggs or fry but unmolested by crayfish) were observed in the crayfish ponds during the first 4 weeks of the experiment (Fig. 3*a*). On 14 and 29 June we observed crayfish destroying groups of 5–6 nests that still contained a few remaining eggs in two of the ponds. Overall crayfish activity-density was higher in 2001 than in 1999 (average activity-density in 2001was 9.4 crayfish·trap^{-1} (standard error = 0.92 crayfish·trap^{-1}, $N = 4$ dates), but was still easily within the range of natural activity-densities.

On 5 July we added one crayfish-proof exclosure to each crayfish pond to determine whether adult bluegills would be able to reproduce when given a crayfish-free nesting habitat. Eleven days later (16 July), active nests were observed inside the exclosure in one pond. Within a few more days, male bluegills in the other ponds were observed nesting inside their respective exclosures; active nesting continued until 3 August (Fig. 3*a*). No crayfish were observed inside the exclosures and active nests were never found outside the exclosures. After nesting commenced in the exclosures, male bluegills stopped sweeping off nests at the sites of previous nesting attempts.

Bluegill larvae were first collected in the no-crayfish ponds 14 days after the start of the experiment (26 June), and abundant larvae were caught in tow samples for the following 3 weeks (Fig. 3*b*). After 16 July, most larval fish in the no-crayfish ponds had grown to a size (>10 mm SL) at which they were able to avoid capture by our towed ichthyoplankton net. However, divers in the no-crayfish ponds continued to observe YOY throughout the remainder of the experiment. In the crayfish ponds, no larval fish were captured prior to the addition of the exclosures (Fig. 3*b*). However, bluegill larvae were caught in the crayfish ponds 18 days after the exclosures were added (23 July), and larval densities were especially high on 30 July.

Fig. 3. Timeline of bluegill sunfish (*Lepomis macrochirus*) nest activity and larval recruitment in ponds with (●) and without (○) crayfish during summer 2001 ($N = 3$). (*a*) Mean number of active bluegill nests (nests with eggs or fry) per pond. (*b*) Mean number (+1) of free-swimming YOY bluegills caught per standardized ichthyoplankton tow per pond. Error bars denote 1 standard error. Crayfish exclosures were added to crayfish ponds on 5 July.

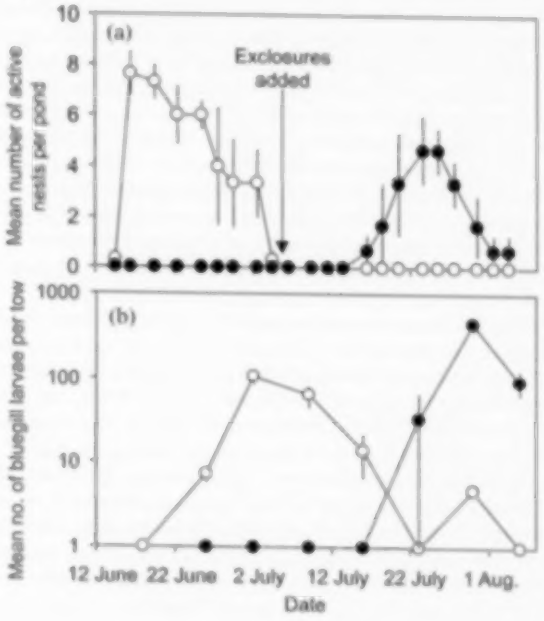

Discussion

Although a host of freshwater animals, including many species recently introduced to the Great Lakes region (Selgeby 1998; Chotkowski and Marsden 1999; Lodge et al. 2000), are known to eat the early life stages of fish, little is known about the impacts or potential impacts of any of these organisms on fish reproductive success, spawning behavior, or population size. Some attempts have been made to quantify the impact of egg predators by extrapolating estimates of predator feeding rates (e.g., Mol 1996; Fitzsimons et al. 2002); however, no experimental studies have measured reproductive success of populations in the presence and absence of putative egg/fry predators. Our results indicate that the presence of crayfish can have strong impacts on the reproductive success of freshwater sunfish in ponds. Our observations suggest that direct egg predation was responsible for the effects; however, other types of fish/crayfish interactions may also reduce reproductive success and we consider

© 2004 NRC Canada

some of these interactions below. The difference in YOY biomass between the crayfish and no-crayfish ponds in the 1999 pumpkinseed experiment was caused by a combination of YOY size and density. The smaller average size of YOY pumpkinseeds in the presence of crayfish was consistent with differences in age; YOY were born later, on average, in the ponds with crayfish. There was no evidence of differential YOY growth between the pond types. The observed later YOY birth dates may be a result of pumpkinseeds becoming more successful over time in the presence of crayfish, either by adjusting their spawning behaviors or by changing nest-site selection. Although crayfish destroyed some of their nests, male pumpkinseeds were persistent in their reproductive attempts and variable in their use of nest sites. In some cases we found nests in extremely shallow water (<20 cm), against the bank, or in small aggregated groups. These nesting behaviors may have led to the eventual successful production of larvae in the presence of crayfish and suggest that pumpkinseeds may adjust their nest-site selection or behavioral strategies in response to egg predation by crayfish.

Other food-web interactions could have led to lower YOY pumpkinseed biomass in the presence of crayfish. For example, pumpkinseeds feed extensively on benthic invertebrate prey (Werner and Hall 1976; Osenberg et al. 1992) and competition between adult pumpkinseeds and crayfish for benthic invertebrates may have lowered the energy available for sunfish reproduction. However, there were no significant differences in the abundance of benthic invertebrates between treatments (rmANOVA P values >0.18); invertebrate biomass was measured with D-net sweeps through the vegetation in June, July, and August (N. Dorn, unpublished data).

It is also possible that reproductive success in crayfish exclosures (both experiments) was lower because of repeated harassment by crayfish and increased costs of nest defense (which may have led to nest abandonment). However, whether crayfish lowered sunfish reproductive output by feeding on eggs, by increasing the cost of nest defense, or by a combination of the two, we view this interaction as part of the overall impact of crayfish as potential nest-stage predators.

In the 2001 bluegill experiment, no YOY were produced in the crayfish ponds before the addition of crayfish exclosures. Active nests were never found in the crayfish ponds before the addition of crayfish exclosures, and crayfish were observed eating fish eggs on two separate occasions. In the no-crayfish ponds bluegill reproduction followed the normal course of reproduction observed in local lakes: most nesting occurs during 3–4 weeks in June and ceases early in July. First successful reproduction in the crayfish ponds occurred a month later than in the no-crayfish ponds, and only after we added the crayfish exclosures. As in the pumpkinseed experiment, YOY recruitment was delayed in the bluegill study, but in striking contrast to the pumpkinseed experiment, production of larval fish failed completely for almost 5 weeks (note that male bluegills kept their nest spots swept clean). Successful recruitment was perfectly correlated with the addition of crayfish-proof exclosures and the concomitant shifts in nesting sites. In addition, Dorn and Wojdak (2004) report that zooplankton biomass (bluegill prey) was significantly greater in the crayfish ponds than in the no-crayfish ponds. These observations strongly indicate that bluegills had abundant resources for reproduction but simply lacked a safe spawning habitat.

Colony nesting by bluegills is thought to provide increased protection from nest predators, the nests in the interior of the colony being safer (Gross and MacMillan 1981). The size of our ponds limited the total number of adult bluegills we could stock at a reasonable density (i.e., 15 parental males and 15 females). Therefore, it is possible that larger bluegill colonies would experience less of an impact of crayfish predation than we found in our experiments. We cannot evaluate this hypothesis, as no studies have directly tested the effect of colony size on bluegill nesting success. In lakes we have surveyed in Michigan, bluegill colonies typically range from 5 to 50 nesting males (N. Dorn, unpublished data). Therefore, our experimental set-up, while limited in the number of bluegills per pond, is not out of line for many natural systems. Again, we emphasize that our results demonstrate the potential impacts of crayfish on sunfish reproductive success, but not necessarily the magnitude of these effects in other systems.

Interactions between crayfish and fish populations

Crayfish have been introduced to water bodies throughout the globe for purposes of augmenting fish forage or controlling macrophytes (Hobbs et al. 1989; Hanson and Chambers 1995). In addition to purposeful introductions, crayfish have also been inadvertently introduced to water bodies through vectors like the bait trade (Lodge et al. 2000). While past work indicates strong direct impacts of crayfish on macrophyte and macroinvertebrate populations (Chambers et al. 1990; Lodge et al. 1994), there have been relatively few studies examining the effects of crayfish on fish populations (Dorn and Mittelbach 1999).

The results of previous cage and aquarium studies of crayfish egg predation are suggestive but inconclusive (Horns and Magunson 1981; Savino and Miller 1991). However, a recent study combining crayfish feeding rates, crayfish densities, and egg densities indicates that crayfish (*Orconectes* spp.) are potentially important egg predators of lake trout (*Salvelinus namaycush*), a cold-water broadcast-spawning fish (Fitzsimons et al. 2002). Although egg predation by crayfish has been occasionally observed in the field (e.g., Magnuson et al. 1975), our experimental results provide the most direct evidence to date indicating that crayfish may reduce fish reproductive success.

Introduced species of crayfish have been implicated in the demise of fish populations in European rivers (Guan and Wiles 1997; Nyström 1999) and North American lakes (Lodge et al. 1985; Covich et al. 1999; Wilson 2002) and streams (Bryan et al. 2002). In the Midwest, *O. virilis* is being replaced by the invasive *O. rusticus*, and invasions by *O. rusticus* have been blamed for declines in fish populations (Magnuson et al. 1975; Covich et al. 1999; Wilson 2002). *Orconectes virilis* and *O. rusticus* have similar adult sizes and feeding habits (Olsen et al. 1991; Hill et al. 1993) but *O. rusticus* is more aggressive (Capelli and Munjal 1982), has greater defensive armor, is less vulnerable to predation by bass (*Micropterus* spp.) in open habitats, and attains higher densities (Capelli and Magnuson 1983; Olsen et al. 1991; Garvey et al. 1994). Therefore, we believe that the potential impact of *O. rusticus* on sunfish nesting success

© 2004 NRC Canada

would be even greater than that we have observed for *O. virilis*.

Predators and fish nesting habitats

Nest predators may affect species' reproductive strategies or breeding-site selection. For sunfish, nest-site selection is traditionally thought to be a response to habitat structure; sunfish nest preferentially on relatively open (Colgan and Ealey 1973), hard-bottom substrates (i.e., sandy gravel) when available (Breder and Rosen 1966; Bietz 1981; Popiel et al. 1996). A survey by Popiel et al. (1996) showed that pumpkinseeds favored nesting on mixed sand–gravel habitats and avoided soft-organic and cobble habitats. If egg predators have significant effects on egg survival, and fish are able to recognize areas of high and low egg-predation risk, then nest-habitat selection may occur as a response to spatial variation in predation risk as well as habitat structure (also noted in Gross and MacMillan 1981). In lakes with multiple habitats, crayfish are heterogeneously distributed and most abundant in structured environments like cobble, which provide a refuge from predaceous fish (Lodge and Hill 1994). Likewise, small fish (various species) and bullheads (*Ictalurus* spp.), which are known egg predators of sunfish (Gross and MacMillan 1981; Popiel et al. 1996), are most abundant in vegetated habitats (Gross and MacMillan 1981; Werner et al. 1983). In lakes or other water bodies with multiple habitat types, bluegills and pumpkinseeds would reduce exposure to both types of predators if they nested in relatively open habitats, which is where they often breed (Breder and Rosen 1966; Colgan and Ealey 1973; Gross and MacMillan 1981).

The results of our 2001 experiment suggest that bluegills can discriminate between safe and risky nesting habitats. No crayfish were observed inside the exclosures in the crayfish ponds, and active nests were never found outside the exclosures. There also was no evidence of fish attempting to nest in any other areas of the pond (except for the original, abandoned, nest sites), suggesting that bluegills selected nesting locations inside the exclosures (which occupied <1% of the pond bottom) to avoid egg predation by crayfish. Other aspects of the exclosure besides the absence of crayfish may have stimulated nesting, and we cannot rule this out directly because we did not have a crayfish-permeable control structure. However, if bluegills were attracted to some physical feature of the exclosure then we might have expected nesting attempts on both sides of the exclosure walls (inside and out), which did not occur.

Other researchers have observed correlations between fish spawning sites and lower levels of egg-predation risk (e.g., Beauchamp et al. 1992; Knapp 1993; Östlund-Nilsson 2000). However, our study is the first to experimentally manipulate the presence of egg predators, offering fish an environment with variable predation risk. More experimental work is needed to fully evaluate the relative roles of brood predators, environmental structure, and other factors in determining the breeding-site choices of fish.

Viewing and managing the spawning landscape

Observational studies based on extrapolation of egg and fry survival rates or predator feeding rates (e.g., Wisenden 1994; Mol 1996; Fitzsimons et al. 2002), along with our experimental results, suggest that egg and fry predators may strongly influence reproductive success and population size of some fish species. If introduced predator species have different patterns of habitat use or higher overall densities than native egg predators, they may change the spawning landscape in ways that become more hazardous for early life stages of fish.

The impacts of crayfish on sunfish reproductive success may be limited in lakes where crayfish activity-densities are low or spatially variable, allowing sunfish to find safe nesting habitats. However, in many midwestern lakes, the aggressive and introduced crayfish *O. rusticus* is displacing the native *O. virilis* (Lodge et al. 2000). In one particularly well-studied system (Trout Lake, Wisconsin, USA), the invasion by *O. rusticus* has been correlated with declines in bluegill and pumpkinseed populations (Wilson 2002). *Orconectes rusticus* is thought to utilize open non-cobble habitats to a greater degree than the crayfish species they replace (Capelli and Magnuson 1983; Lodge et al. 1985), and activity-densities of *O. rusticus* on open sand and muck habitats (in the presence of fish predators) exceed 20·trap^{-1} in some invaded lakes (K. Wilson, Department of Zoology, University of Toronto, Toronto, ON M5S 3G5, Canada, personal communication). This activity-density is more than twice the activity-density we measured in our 2001 experiment with bluegills.

Future considerations of available or appropriate spawning habitat should consider a "fish-eye view" of both the physical habitat structure and the distribution of early-life-stage predators. Because fish breed consistently in particular habitats types, spawning habitat has been generally identified and quantified using metrics of physical structure or other abiotic variables (e.g., Takemon and Nakanishi 1998; Bernier-Bourgault and Magnan 2002). However, densities of egg and fry predators can vary from site to site as well (Wisenden 1994; Fitzsimons et al. 2002), and natural selection may produce inverse correlations between breeding activity and egg-predator abundance. In the Great Lakes, lake trout spawn on reefs and other rocky areas and are believed to respond to appropriate structural and abiotic features of the habitat (Marsden et al. 1995*a*). While egg predators like crayfish and benthic fish were historically considered unimportant (Wagner 1981), there has been increasing interest in determining their impacts on egg survival (Marsden et al. 1995*b*; Fitzsimons et al. 2002). Beauchamp et al. (1992) reported that the self-sustaining population of lake trout in Lake Tahoe (California, USA) spawned in a non-traditional habitat — over macroalgae (*Chara delicatula*) located on deep-water mounds surrounded by even deeper (>100 m) water. Egg predators were uncommon on the mounds (few sculpins (*Cottus* spp.) and no crayfish) and it was postulated that trout spawned in these sites, rather than in other deep rocky areas, in response to the paucity of egg predators (Beauchamp et al. 1992). Spawning-habitat use by lake trout, sunfish (this study), cichlids (Wisenden 1994; Takemon and Nakanishi 1998), and other species of fish in other contexts may be a reflection of their behavioral and (or) selected responses to variable densities of important egg predators as well as physical habitat variables.

Adding artificial structures to lakes and other systems to enhance fisheries, restore degraded habitats, or meet a variety of other types of goals is common practice (e.g., D'Itri

© 2004 NRC Canada

1985; Jude and Deboe 1996). It has also been a goal in some cases to introduce these structures as breeding habitats for fish (Peck 1986). However, some benthic organisms, including crayfish and fish (e.g., gobies (*Neogobius* spp.) and sculpins), that inhabit these structures may act as both fish prey (Janssen and Quinn 1985; Jude and Deboe 1996) and fish-egg predators (Chotkowski and Marsden 1999; Fitzsimmons et al. 2002). If artificial structures (e.g., reefs, docks, riprap, and breakwalls) allow crayfish or other egg-predator populations to colonize new habitats or increase overall densities (owing to increased juvenile survival), then rates of predation on fish eggs and fry may also increase. Biologists and resource managers must weigh the potential costs and benefits of these structures to fish breeding success and population dynamics. Likewise, any assessment of crayfish introductions must consider their multiple consequences, including potential negative effects on fish populations through egg predation or other mechanisms (Carpenter and Lodge 1986).

Acknowledgements

We thank T. Darcy, K. Dorn, M.L. Dorn, E. Garcia, J. Rettig, J. Smedes, C. Steiner, E. Thobaben, M. Watson, A. Wilson, J. Wojdak, and P. Wykoff for advice and help with the experiments, and T. Darcy, E. Garcia, K. Gross, S. Hamilton, T. Kreps, D. Lodge, A. Sarnelle, J. Wojdak, and anonymous reviewers for valuable comments and suggestions on the manuscript. The Zoology Department of Michigan State University, the G.H. Lauff Fund, and the W.K. Kellogg Biological Station (KBS) Graduate Research Training Grant funded by National Science Foundation (NSF) grants DIR-09113598 and DBI-9602252 provided financial support. G.G.M. acknowledges support during manuscript preparation from the National Center for Ecological Analysis and Synthesis, a Center funded by the NSF (DEB-0072909), the University of California, and the Santa Barbara campus. This is KBS contribution number 974.

References

Beauchamp, D.A., Allen, B.C., Richards, R.C., Wurtsbaugh, W.A., and Goldman, C.R. 1992. Lake trout spawning in Lake Tahoe: egg incubation in deepwater macrophyte beds. N. Am. J. Fish. Manag. **12**: 442–449.

Bernier-Bourgault, I., and Magnan, P. 2002. Factors affecting redd site selection, hatching, and emergence of brook charr, *Salvelinus fontinalis*, in an artificially enhanced site. Environ. Biol. Fishes, **64**: 333–341.

Bietz, B.F. 1981. Habitat availability, social attraction and nest distribution patterns in longear sunfish (*Lepomis megalotis peltastes*). Environ. Biol. Fishes, **6**: 193–200.

Breder, C.M., Jr., and Rosen, D.E. 1966. Modes of reproduction in fishes. Natural History Press, Garden City, N.Y.

Bryan, S.D., Robinson, A.T., and Sweester, M.G. 2002. Behavioral responses of a small native fish to multiple introduced predators. Environ. Biol. Fishes, **63**: 49–56.

Capelli, G.M., and Magnuson, J.J. 1983. Morphoedaphic and biogeographic analysis of crayfish distribution in Northern Wisconsin. J. Crustacean Biol. **3**: 548–564.

Capelli, G.M., and Munjal, B.J. 1982. Aggressive interactions and resource competition in relation to species displacement among crayfish of the genus *Orconectes*. J. Crustacean Biol. **2**: 486–492.

Carpenter, S.R., and Lodge, D.M. 1986. Effects of submersed macrophytes on ecosystem processes. Aquat. Bot. **26**: 341–370.

Chambers, P.A., Hanson, J.M., Burke, J.M., and Prepas, E.E. 1990. The impact of the crayfish *Orconectes virilis* on aquatic macrophytes. Freshw. Biol. **24**: 81–91.

Chotkowski, M.A., and Marsden, J.E. 1999. Round goby and mottled sculpin predation on lake trout eggs and fry: field predictions from laboratory experiments. J. Gt. Lakes Res. **25**: 26–35.

Colgan, P., and Ealey, D. 1973. Role of woody debris in nest site selection by pumpkinseed sunfish, *Lepomis gibbosus*. J. Fish. Res. Board Can. **30**: 853–856.

Collins, N.C., Harvey, H.H., Tierney, A.J., and Dunham, D.W. 1983. Influence of predatory fish density on trapability of crayfish in Ontario lakes. Can. J. Fish. Aquat. Sci. **40**: 1820–1828.

Covich, A.P., Palmer, M.A., and Crowl, T.A. 1999. The role of benthic invertebrate species in freshwater ecosystems. Bioscience, **49**: 119–127.

Crowder, L.B., and Cooper, W.E. 1982. Habitat structural complexity and the interaction between bluegill and their prey. Ecology, **63**: 1802–1813.

D'Itri, F.M. 1985. Artificial reefs: marine and freshwater applications. Lewis Publishers, Chelsea, Mich.

Dorn, N.J., and Mittelbach, G.G. 1999. More than predator and prey: a review of interactions between fish and crayfish. Vie Milieu, **49**: 229–237.

Dorn, N.J., and Wojdak, J.M. 2004. The role of omnivorous crayfish in littoral communities. Oecologia, **140**: 150–159.

Fitzsimons, J.D., Perkins, D.L., and Krueger, C.C. 2002. Sculpins and crayfish in lake trout spawning areas in Lake Ontario: estimates of abundance and egg predation on lake trout eggs. J. Gt. Lakes Res. **28**: 421–436.

Garvey, J.E., Stein, R.A., and Thomas, H.M. 1994. Assessing how fish predation and interspecific competition influence a crayfish assemblage. Ecology, **75**: 532–547.

Gherardi, F., and Holdich, D.M. 1999. Crayfish in Europe as alien species. A.A. Balkema, Rotterdam, the Netherlands.

Gross, M.R. 1982. Sneakers, satellites and parentals: polymorphic mating strategies in North American sunfishes. Z. Tierpsychol. **60**: 1–26.

Gross, M.R., and MacMillan, A.M. 1981. Predation and the evolution of colonial nesting in bluegill sunfish (*Lepomis macrochirus*). Behav. Ecol. Sociobiol. **8**: 163–174.

Guan, R., and Wiles, R. 1997. Ecological impact of introduced crayfish on benthic fishes in a British lowland river. Conserv. Biol. **11**: 641–647.

Hanson, J.M., and Chambers, P.A. 1995. Review of effects of variation in crayfish abundance on macrophyte and macroinvertebrate communities of lakes. ICES Mar. Sci. Symp. **199**: 175–182.

Hill, A.M., Sinars, D.M., and Lodge, D.M. 1993. Invasion of an occupied niche by the crayfish *Orconectes rusticus*: potential importance of growth and mortality. Oecologia, **94**: 303–306.

Hobbs, H.H., III, Jass, J.P., and Huner, J.V. 1989. A review of global crayfish introductions with particular emphasis on two North American species (Decapoda: Cambaridae). Crustaceana, **56**: 299–316.

Horns, W.H., and Magnuson, J.J. 1981. Crayfish predation on lake trout eggs in Trout Lake, Wisconsin. Rapp. P.-V. Réun. Cons. Int. Explor. Mer, **178**: 299–303.

Janssen, J., and Quinn, J. 1985. Biota of the naturally rocky area of southwestern Lake Michigan with emphasis on potential prey fish. *In* Artificial reefs: marine and freshwater applications.

© 2004 NRC Canada

Edited by F.M. D'Itri. Lewis Publishers, Chelsea, Mich. pp. 431–442.

Jude, D.J., and Deboe, S.F. 1996. Possible impacts of gobies and other introduced species on habitat restoration efforts. Can. J. Fish. Aquat. Sci. **53**: 136–141.

Knapp, R.A. 1993. The influence of egg survivorship on the subsequent nest fidelity of female bicolour damselfish, *Stegastes partitus*. Anim. Behav. **46**: 111–121.

Lodge, D.M., and Hill, A.M. 1994. Factors governing species composition, population size, and productivity of cool-water crayfishes. Nord. J. Freshw. Res. **69**: 111–136.

Lodge, D.M., Beckel, A.L., and Magnuson, J.J. 1985. Lake-bottom tyrant. Nat. Hist. **8**: 33–37.

Lodge, D.M., Kratz, T.K., and Capelli, G.M. 1986. Long-term dynamics of three crayfish species in Trout Lake, Wisconsin. Can. J. Fish. Aquat. Sci. **44**: 591–597.

Lodge, D.M., Kershner, M.W., Aloi, J.E., and Covich, A.P. 1994. Effects of an omnivorous crayfish (*Orconectes rusticus*) on a freshwater littoral food web. Ecology, **75**: 1265–1281.

Lodge, D.M., Taylor, C.A., Holdich, D.M., and Skurdal, J. 2000. Nonindigenous crayfishes threaten North American freshwater biodiversity: lessons from Europe. Fisheries (Bethesda), **25**: 7–19.

Magnuson, J.J., Capelli, G.M., Lorman, J.G., and Stein, R.A. 1975. Consideration of crayfish for macrophyte control. *In* Proceedings of a Symposium on Water Quality Management Through Biological Control. Rep. No. ENV 07-75-1. *Edited by* P.L. Brezonik and J.L. Fox. University of Florida, Gainesville. pp. 66–74.

Marsden, J.E., Perkins, D.L., and Krueger, C.C. 1995*a*. Recognition of spawning areas by lake trout: deposition and survival of eggs on small, man-made rock piles. J. Gt. Lakes Res. **21**: 330–336.

Marsden, J.E., Casselman, J.M., Edsall, T.A., Elliot, R.F., Fitzsimons, J.D., Horns, W.H., et al. 1995*b*. Lake trout spawning habitat in the Great Lakes — a review of current knowledge. J. Gt. Lakes Res. **21**: 487–497.

Mittelbach, G.G. 2002. Fish foraging and habitat choice: a theoretical perspective. *In* Handbook of fish and fisheries. *Edited by* P.J.B. Hart and J.D. Reynolds. Blackwell Science Ltd., Oxford. pp. 251–266.

Mol, J.H. 1996. Impact of predation on early life stages of the armoured catfish *Hoplosternum thoracatum* (Silurformes–Callychthyidae) and implications for the syntopic occurrence with other related catfishes. Oecologia, **107**: 395–410.

Momot, W.T. 1995. Redefining the role of crayfish in aquatic ecosystems. Rev. Fish. Sci. **3**: 33–63.

Momot, W.T., and Gowing, H. 1977. Production and population dynamics of the crayfish *Orconectes virilis* in three Michigan lakes. J. Fish. Res. Board Can. **34**: 2041–2055.

Momot, W.T., Gowing, H., and Jones, P.D. 1978. The dynamics of crayfish and their role in ecosystems. Am. Midl. Nat. **99**: 10–35.

Nyström, P. 1999. Ecological impact of introduced and native crayfish on freshwater communities. *In* Crayfish in Europe as alien species. *Edited by* F. Gherardi and D. M. Holdich. A.A. Balkema, Rotterdam, the Netherlands. pp. 63–85.

Olsen, T.M., Lodge, D.M., Capelli, G.M., and Houlihan, R. 1991. Impact of the introduced crayfish *Orconectes rusticus* in northern Wisconsin lakes: laboratory, and long-term field studies. Can. J. Fish. Aquat. Sci. **48**: 1853–1861.

Osenberg, C.W., Mittelbach, G.G., and Wainwright, P.C. 1992. Two-stage life histories in fish: the interaction between juvenile competition and adult performance. Ecology, **73**: 255–267.

Östlund-Nilsson, S. 2000. Are nest characters of importance when choosing a male in the fifteen-spined stickleback (*Spinachia spinachia*)? Behav. Ecol. Sociobiol. **48**: 229–235.

Peck, J.W. 1986. Dynamics of reproduction by hatchery trout on a man-made spawning reef. J. Gt. Lakes Res. **12**: 293–303.

Popiel, S.A., Pérez-Fuentetaja, A., McQueen, D.J., and Collins, N.C. 1996. Determinants of nesting success in the pumpkinseed (*Lepomis gibbosus*): a comparison of two populations under different risks from predation. Copeia, 1996: 649–656.

Rettig, J.E., and Mittelbach, G.G. 2002. Interactions between adult and larval bluegill sunfish: positive and negative effects. Oecologia, **130**: 222–230.

SAS Institute Inc. 1989. SAS®. Version 6.0. 4th ed. SAS Institute Inc., Cary, N.C.

Savino, J.F., and Miller, J.E. 1991. Crayfish (*Orconectes virilis*) feeding on young lake trout (*Salvelinus namaycush*): effect of rock size. J. Freshw. Ecol. **6**: 161–170.

Selgeby, J. 1998. Predation by ruffe (*Gymnocephalus cernuus*) on fish eggs in Lake Superior. J. Gt. Lakes Res. **24**: 304–308.

Stevenson, D.K., and Campana, S.E. 1992. Otolith microstructure examination and analysis. Can. Spec. Publ. Fish. Aquat. Sci. No. 117.

Takemon, Y., and Nakanishi, K. 1998. Reproductive success in female *Neolamprologus mondabu* (Cichlidae): influence of substrate types. Environ. Biol. Fishes, **52**: 261–269.

Taubert, B.D., and Coble, D.W. 1977. Daily rings in otoliths of three species of *Lepomis* and *Tilapia mossambica*. J. Fish. Res. Board Can. **34**: 332–340.

Wagner, W.C. 1981. Reproduction of planted lake trout in Lake Michigan. N. Am. J. Fish. Manag. **1**: 159–164.

Werner, E.E., and Gilliam, J.F. 1984. The ontogenetic niche and species interactions in size-structured populations. Annu. Rev. Ecol. Syst. **15**: 393–425.

Werner, E.E., and Hall, D.J. 1976. Niche shifts in sunfishes: experimental evidence and significance. Science (Wash., D.C.), **191**: 404–406.

Werner, E.E., Hall, D.J., Laughlin, D.R., Wagner, D.J., Wilsmann, L.A., and Funk, F.C. 1977. Habitat partitioning in a freshwater community. J. Fish. Res. Board Can. **34**: 360–370.

Werner, E.E., Gilliam, J.F., Hall, D.J., and Mittelbach, G.G. 1983. An experimental test of the effects of predation risk on habitat use in fish. Ecology, **64**: 1540–1548.

Wilson, K.A. 2002. Impacts of the invasive rusty crayfish (*Orconectes rusticus*) in northern Wisconsin lakes. Ph.D. dissertation, University of Wisconsin, Madison.

Wisenden, B.D. 1994. Factors affecting reproductive success in free-ranging convict cichlids (*Cichlasoma nigrofasciatum*). Can. J. Zool. **72**: 2177–2185.

© 2004 NRC Canada

Predator-recognition training of hatchery-reared walleye (*Stizostedion vitreum*) and a field test of a training method using yellow perch (*Perca flavescens*)

Brian D. Wisenden, Josh Klitzke, Ryan Nelson, David Friedl, and Peter C. Jacobson

Abstract: Fishes reared in captivity are predator-naive and suffer large predation mortality when stocked into lakes with a full complement of predators. We tested the potential of predator training to enhance post-stocking survival of hatchery-reared walleye (*Stizostedion vitreum*). In the first part of the study, we found that walleye (*i*) use chemical cues for assessing predation risk, (*ii*) do not have innate recognition of the odor of northern pike (*Esox lucius*) as an indicator of predation, and (*iii*) associate predation risk with pike odor after a single simultaneous encounter with pike odor and chemical alarm cues from walleye skin. In the second part of the study, we attempted to mass-train yellow perch, *Perca flavescens* (as a surrogate for walleye), to fear pike odor. Perch response to pike odor was not changed by placing sponge blocks containing pike odor and perch alarm cues around the perimeter of a pond. On pre- and post-training assays, perch avoided traps scented with perch alarm cues, but did not avoid traps labeled with pike odor or water. We conclude that recognition training offers potential as a management tool for walleye, but significant logistic challenges must be solved before it can be implemented.

Résumé : Les poissons élevés en captivité n'ont pas l'expérience de la prédation et ils subissent une forte mortalité due à la prédation lorsqu'ils sont introduits dans des lacs qui contiennent une gamme complète de prédateurs. Nous évaluons ici le potentiel d'un entrainement aux prédateurs pour augmenter la survie après l'empoissonnement chez des dorés jaunes (*Stizostedion vitreum*) élevés en pisciculture. Dans la première partie de l'étude, nous avons trouvé (*i*) que les dorés utilisent des signaux chimiques pour évaluer les risques de prédation, (*ii*) qu'ils ne reconnaissent pas de façon innée l'odeur du grand brochet (*Esox lucius*) comme indicateur du risque de prédation et (*iii*) qu'il suffit d'une seule exposition simultanée à l'odeur de brochet et aux substances d'alerte de peau de dorés pour qu'ils associent l'odeur de brochet au risque de prédation. Dans la seconde partie de l'étude, nous avons essayé d'entrainer des groupes de perchaudes, *Perca flavescens* (en remplacement des dorés) à craindre l'odeur des brochets. La réaction des perchaudes à l'odeur de brochets ne change pas lorsqu'on place des blocs d'éponges contenant l'odeur de brochet et les signaux d'alerte de la perchaude sur le périmètre d'un étang. Dans les tests avant et après l'entrainement, les perchaudes évitent les pièges marqués de signaux d'alerte de perchaudes, mais pas ceux marqués d'odeur de brochet ou d'eau. Nous concluons que l'entrainement à la reconnaissance d'odeurs peut avoir un potentiel comme outil d'aménagement des dorés, mais qu'il y a des problèmes logistiques importants à résoudre avant son utilisation.

[Traduit par la Rédaction]

Introduction

Chemical cues are ubiquitous in aquatic environments (Wisenden 2003). Olfaction is the most ancient of the senses and provides information for such critical activities as finding food, avoiding predators, and cueing reproductive behavior (Hara 1993; Kats and Dill 1998; Stacey and Sorensen 2002). Several classes of chemical cues are used for detecting predation risk. Alarm cues are chemicals released when tissue is damaged by a predatory attack (Chivers and Smith 1998). These cues are released only in this context and thereby reliably indicate risk to conspecifics and ecologically similar heterospecific prey (Mathis and Smith 1993*c*; Chivers and Smith 1998). Behavioral responses to these cues reduce the probability of predation (Mathis and Smith 1993*a*; Mirza and Chivers 2000; Gadzewich and Chivers 2002).

Because of the steep selection gradient imposed by predation, a significant fitness benefit accrues from recognition of risk from indirect indicators. Many prey species use the presence of conspecific chemical alarm cues to extend the range of stimuli that indicate risk (Chivers and Smith 1998). When alarm cues are released, chemical and visual stimuli correlated with the event, such as predator odor, diet of the

Received 6 May 2004. Accepted 2 July 2004. Published on the NRC Research Press Web site at http://cjfas.nrc.ca on 1 February 2005.
J18112

B.D. Wisenden,[1] J. Klitzke, and R. Nelson. Biology Department, Minnesota State University Moorhead, Moorhead, MN 56563, USA.
D. Friedl and P.C. Jacobson. Minnesota Department of Natural Resources, 14583 County Road 19, Detroit Lakes, MN 56501, USA.

[1]Corresponding author (e-mail: wisenden@mnstate.edu).

 doi: 10.1139/F04-164 © 2004 NRC Canada

predator, smell of the habitat, and appearance of the predator, become associated with predation risk (Suboski 1990; Chivers and Smith 1998). As testimony to the extreme importance of predator recognition, a single simultaneous exposure to alarm cues and a novel stimulus is sufficient for learned recognition to occur, persisting for at least 4 months in fathead minnows (*Pimephales promelas*; Chivers and Smith 1994), at least 10 days in brook char (*Salvelinus fontinalis*; Mirza and Chivers 2000), and 21 days in rainbow trout (*Oncorhynchus mykiss*; Brown and Smith 1998). By attending to correlates of alarm-cue release, prey species quickly track temporal and spatial shifts in predator identity and abundance.

This learning paradigm has application to fisheries management in instances where fish are reared in predator-free environments and subsequently released into natural waters that contain predators (Suboski and Templeton 1989). Mortality of stocked fish due to predators is a perennial problem for stocking programs (Santucci and Wahl 1993; Szendrey and Wahl 1996). Recognition training could improve the survival rate of stocked fish and thereby improve the cost-effectiveness of hatchery programs, enhance fishery quality, and contribute to the economic benefits associated with the recreational sport fishery and related tourism industry. Recognition training has been shown to be effective for several species of hatchery-reared salmonids (Brown and Smith 1998; Berejikian et al. 1999; Mirza and Chivers 2000).

To successfully apply predator-recognition training to hatchery-based stocking programs, four conditions must be met. The first three are (1) that the game species use chemical cues for assessing predation risk, (2) that they do not already have internal cognitive recognition of the predator odor (or sight) as an indicator of danger, and (3) that they associate predation risk with predator odor (or sight) after a single simultaneous exposure to conspecific chemical alarm cues and stimuli from predators. The fourth condition is feasibility of implementation (see below).

In the first part of this study we explore the potential application of predator-recognition training to hatchery-reared walleye (*Stizostedion vitreum*). The Minnesota Department of Natural Resources intercept spawning walleye in the spring spawning run, strip their gametes, incubate fertilized eggs in a hatchery, and transfer the resulting larvae to small prairie pothole lakes that serve as rearing ponds. The combination of shallow water (mean depth 2.8 m) and frequent low winter concentrations of dissolved oxygen ensure that large piscivorous fish usually do not survive over winter ("carryover") to prey upon the next crop of walleye the following year. In the fall, as temperatures begin to cool, walleye fingerlings, by now approximately 15–20 cm in length, are harvested from the rearing ponds and transferred to area lakes for fishery enhancement. Although walleye are efficient predators as adults, as juveniles they are subject to the same predation pressures as other similar-sized fish. Mortality over the first 2 weeks after stocking can be high, and a large proportion is thought to be due to predation, northern pike (*Esox lucius*) being the dominant predator. Here we test if walleye fall fingerlings can be trained to recognize pike odor, thereby satisfying the first three conditions outlined above.

Following the establishment of the potential for recognition training, there remains the significant logistical problem of developing a mechanism of training walleye on a scale typical of fisheries stocking programs. Whereas laboratory studies typically train fish on an individual-by-individual basis, the state of Minnesota alone stocks 1.2 million walleye fingerlings annually. To be a practical tool for fisheries management, the method of recognition training must be simple and rapid, and not demand additional facilities or personnel (i.e., inexpensive). This is the fourth condition for the successful implementation of predator-recognition training in fisheries management.

In the second part of this study, we attempted to train a whole population of yellow perch, *Perca flavescens* (as a surrogate for walleye), by applying alarm cues and pike odor directly to the small lake in which they lived. Perch are an appropriate surrogate for walleye because both possess percid club cells in the epidermis (darters, Smith 1982; walleye, Wisenden 2003; perch, Shireen Alemadi and Brian Wisenden, Minnesota State University Moorhead, unpublished data), which are a likely component of alarm cues in the Percidae.

Materials and methods

Walleye training experiment

Approximately 200 juvenile walleye were obtained from Axberg Pond, a walleye rearing pond located in western Minnesota near Moorhead (46°50′N, 96°10′W). Fish were transferred to the aquatic research facilities at Minnesota State University Moorhead (MSUM) and held in four 570-L holding tanks (88 cm × 75 cm × 82 cm high) at 21 °C. Each tank was fitted with two biological filtration columns, and partial water changes (about 15% of tank volume) were conducted weekly. Walleye were fed fathead minnows purchased from a bait dealer.

Ten test aquaria were set up in two rows along one wall in a room in the MSUM aquatic-research facility. Test aquaria were 190 L in volume (91 cm × 46 cm × 48 cm high) with a thin layer of naturally colored gravel and a large-capacity power filter hanging on the outside of the short pane. A sponge filter in the center of the tank received two tubes of airline tubing; one delivered compressed air, while the other served as a means by which chemical stimuli could be injected surreptitiously. A grid with cell dimensions of 10 cm × 10 cm was drawn on the front (long) viewing pane to be used for scoring vertical distribution and activity (described below). The outer surfaces of the back and sides were painted blue to preclude visual contact among fish in the test aquaria. The solid appearance of painted glass seemed to promote a sense of security in walleye and help them adjust to captivity. Dim ambient lighting also helped walleye adjust to captivity. Room lighting was limited to two partially shaded 25-W floor lamps. We placed three juvenile walleye in each test aquarium. We found that social interactions among a group of three stimulated activity and normal foraging behavior. Normal feeding on fathead minnows commenced almost immediately after the walleye were netted and transferred from the holding tanks to test aquaria, but resumption of normal swimming activity required about a week of acclimation to the test tank.

Chemical alarm cues were collected from 17 juvenile

© 2004 NRC Canada

walleye (total length (TL) = 18.7 ± 0.62 cm (mean ± SE). Each fish was killed humanely by cervical dislocation with a knife blade and measured, and skin fillets were removed from each side. The skin fillets were measured (length and average width) to calculate the area of skin removed, and placed in a beaker of chilled dechlorinated tap water. A total of 1006.06 cm^2 of walleye skin was collected from the 17 walleye. The fillet area collected per fish was 59.1 ± 4.8 cm^2. A kitchen hand blender was used to rupture percid epidermal club cells and simulate the release of chemical cues during a predatory attack. The resulting solution was filtered through a loose wad of polyester wool to remove scales and connective tissue and diluted to a final volume of 1200 mL. Aliquots of 60 mL were frozen at –20 °C until needed. At the same time, we froze 60-mL aliquots of blank dechlorinated tap water that had been passed through a wad of polyester fiber. Each 60-mL dose contained 50 cm^2 of walleye skin, approximately equivalent to one donor fish.

Predator odor was collected from a northern pike (TL = 50.6 cm) collected from Boyer Lake, Minnesota (46°52′N, 96°03′W). The pike was held for 7 days in a 75-L aquarium containing dechlorinated tap water. Tank water was removed in 120-mL aliquots and frozen at –20 °C until needed.

Each group of three fish was tested twice. On the first (conditioning) day, walleye were given 120 mL of pike odor + 60 mL of water (control treatment) or 120 mL of pike odor + 60 mL walleye skin extract (experimental treatment). These trials served to (*i*) test for preexisting recognition of pike odor as dangerous (control treatment) and (*ii*) determine if walleye respond to injury-released alarm cues with antipredator behavior (experimental treatment). Ultimately, the first trial provided walleye the opportunity to associate alarm cues with pike odor. After each batch of conditioning trials was completed (several hours), tank water was siphoned out of each tank until just the backs of the walleye were exposed (a depth of about 5 cm). Each test tank was immediately refilled with fresh dechlorinated tap water. Thus, test stimuli were mostly removed from the test tank, and any cues that remained were greatly diluted. We did not capture the walleye and move them to a new tank to completely exchange the water because walleye become highly stressed when handled. This stress may have inadvertently caused walleye in control trials (pike odor + water) to associate pike odor with the stress of handling. On the second (test) day, about 2–5 days later, each group of three walleye was retested with 120 mL of pike odor alone. This trial tested for a learned association between pike odor and predation risk. We predicted that walleye previously exposed to walleye skin and pike odor would now recognize pike odor as an indicator of predation risk, whereas control walleye would continue to be indifferent to pike odor.

Most trials were conducted in the morning (0700–1100), when walleye were most active. Activity was scored as the total number of grid lines crossed by the three walleye. Vertical distribution was recorded by noting which of the four horizontal zones each fish occupied at 10-s intervals over the 10-min observation period. Vertidal distribution ranged from a maximum value of 720 (all fish on the bottom for the entire observation period) to a minimum of 180 (all fish at the surface for the entire observation period). We recorded activity and vertical distribution for 10 min (prestimulus observation period). Then, for 90 s, we injected test stimuli. Behavioral recording resumed for another 10 min (post-stimulus observation period). After a batch of test trials was finished, the fish were killed by cervical dislocation with a knife blade and measured. To clean test tanks, we stirred the gravel to suspend fecal pellets and drained all of the water by siphon.

We used Wilcoxon–Mann–Whitney tests (Siegel and Castellan 1988) to compare the magnitude of behavioral change between the treatments, followed by Wilcoxon's matched-pairs signed-ranks tests to test for deviation from zero for individual treatments (Siegel and Castellan 1988). We used one-tailed probability distributions because dozens of previous studies had indicated that antipredator behavior in response to chemical alarm cues is manifested as a reduction in activity and movement to the bottom (for reviews see Lima and Dill 1990; Chivers and Smith 1998; Wisenden 2003).

Field population training of yellow perch

This experiment was conducted in Deming Lake, Minnesota (47°10′N, 95°10′W), within the boundaries of Itasca State Park. This lake is 5.5 ha in area and contains yellow perch, pumpkinseed sunfish (*Lepomis gibbosus*), fathead minnows, northern redbelly dace (*Phoxinus eos*), golden shiners (*Notemigonus crysoleucus*), blacknose shiners (*Notropis heterolepis*), brook stickleback (*Culaea inconstans*), Iowa darters (*Etheostoma exile*), and black bullhead (*Ameiurus melas*). Large piscivorous species are not known to occur in this lake.

Alarm cues of perch were prepared by killing 28 perch (TL = 7.98 ± 0.81 cm) by decapitation and removing skin fillets from each flank. A total of 271.25 cm^2 of perch skin was collected and placed in well water resting on a bed of ice. A conventional kitchen hand blender was used to rupture percid club cells and simulate the release of chemical cues due to a predatory attack. The solution was diluted to 2700 mL and filtered through a wad of polyester wool. The concentration of perch skin extract was 0.1 cm^2 of skin per 1 mL of solution.

We prepared pike odor from a northern pike (TL = 38.6 cm) seined from Lake Itasca, Minnesota (47°13′N, 95°12′W). The pike was placed in a 75-L aquarium for 3 days to allow dietary cues to pass out of the pike's gut (Mathis and Smith 1993*b*). The water was replaced with 37 L of fresh lake water and another 3 days were allowed to pass. We used this aquarium water as pike odor.

The experiment compared the numbers of fish captured in minnow traps scented by sponge blocks soaked in either water (control), pike odor (predator odor), or perch skin extract (chemical alarm cues). We used conventional cellulose kitchen sponge (unscented) cut into cubes (2 cm × 2 cm × 3 cm) that could hold 5 mL of test stimulus. Thus, each sponge holding perch skin extract contained the equivalent 0.5 cm^2 of skin. On the first day of the experiment we set 45 traps around the perimeter of Deming Lake. We set the traps in groups of three, each trio containing one of each stimulus type. The three traps in each group were placed in the water simultaneously, then we waited 5 min before setting the next trio. Traps were left in the water for 2 h, after which we pulled trios individually at 5-min intervals. This protocol main-

© 2004 NRC Canada

Fig. 1. Median (± quartiles) walleye (*Stizostedion vitreum*) activity before (open bars) and after (hatched bars) the introduction of test stimuli. On the training day, walleye received pike (*Esox lucius*) odor plus either water (control) or walleye skin extract (alarm cues). On testing day, the same walleye were retested with pike odor only (*, $P < 0.05$; ns, nonsignificant, $P > 0.05$.)

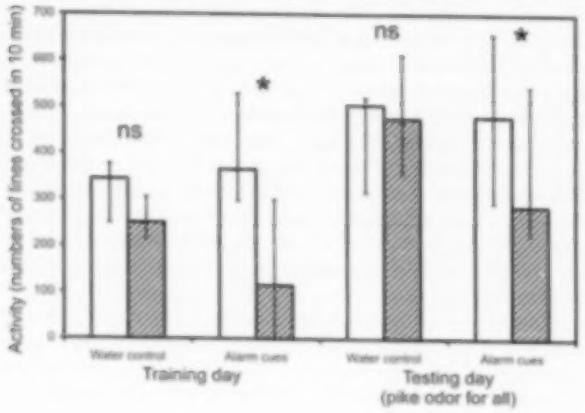

tained a constant fishing time of 2 h for every trap and provided 5 min per trio to process the catch.

We waited 3 days and then placed 60 pairs of scented sponges around the perimeter of the lake at intervals of about 5 m. Sponges were attached together in pike odor – perch alarm cue pairs. Sponges were larger for the second day of the experiment. Sponge blocks (2.6 cm × 2.6 cm × 3.9 cm) were each infused with 15 mL of skin extract, thus holding the equivalent of 1.5 cm^2 of perch skin area. Sponge blocks holding pike odor were 3.5 cm × 3.5 cm × 3.8 cm and each held 30 mL of pike odor. These sponges were left in the lake for 2 h. After another 4 days (7 days since the first trapping experiment), we reset 45 traps in trios as before, with sponge blocks of the same dimensions as on the first day. Trap trios, as before, contained either water, pike odor, or perch skin extract.

We used Kruskal–Wallis one-way analyses of variance (KW) to test for differences among sponge treatments followed by post-hoc α-adjusted pairwise comparisons among treatments (Siegel and Castellan 1988).

Results

Walleye training experiment

Upon first exposure to pike odor, walleye given pike odor + walleye skin extract (alarm cue) decreased activity significantly more than walleye given pike odor + water (Wilcoxon–Mann–Whitney test, $z = 2.821$, $P = 0.002$; Fig. 1). A comparison of activity before and after introduction of stimuli showed no change for walleye given pike odor + water (Wilcoxon's matched-pairs signed-ranks test, $T^+ = 78$, $n = 15$, $P = 0.165$) but a significant decrease for walleye given pike odor + walleye skin extract ($T^- = 119$, $n = 15$, $P < 0.001$; Fig. 1). Walleye in both treatments increased vertical distribution (time near bottom) (pike odor + water: $T^+ = 96$, $n = 14$, $P = 0.002$; pike odor + walleye skin extract: $T^+ = 80$, $n = 13$, $P = 0.007$; Fig. 2), suggesting a general apprehensiveness in response to novel stimuli. Vertical distribution did not differ between treatments ($z = 0.29$, $P = 0.386$).

Fig. 2. Median (± quartiles) walleye vertical distribution (i.e., which of the four horizontal zones each fish occupied at 10-s intervals over the 10-min observation period) before (open bars) and after (hatched bars) the introduction of test stimuli. On the training day, walleye received pike odor plus either water (control) or walleye skin extract (alarm cues). On testing day, the same walleye were retested with pike odor only (*, $P < 0.05$; ns, nonsignificant, $P > 0.05$).

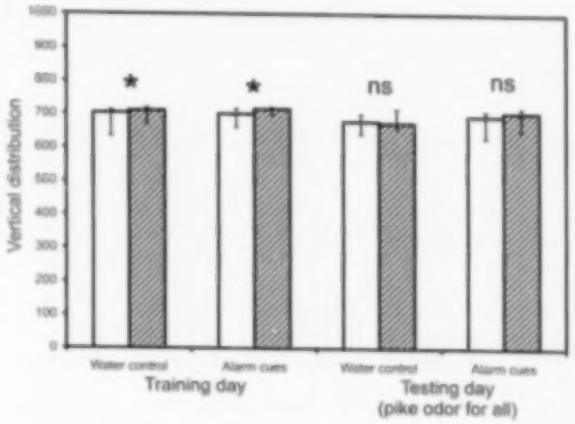

Overall, walleye did not respond strongly on first exposure to pike odor alone, but did respond to the combination of pike odor and walleye skin extract.

When retested with pike odor, walleye previously given pike odor + water did not change activity ($T^- = 58$, $n = 15$, $P = 0.467$); however, walleye previously given pike odor + walleye skin extract significantly decreased activity ($T^- = 113$, $n = 15$, $P < 0.001$; Fig. 1). The change in activity differed significantly between the treatments ($z = 1.91$, $P = 0.028$). Thus, after a single, simultaneous exposure to pike odor and conspecific alarm cues, walleye later responded to pike odor alone in the same way as to walleye skin extract on the first day — with the antipredator response of reduced activity. Although vertical distribution shifted in the predicted direction, there were no statistically significant changes in vertical distribution for either treatment on the second day (pike odor + water: $T^+ = 78$, $n = 15$, $P = 0.165$; pike odor + walleye skin extract: $T^+ = 55$, $n = 13$, $P = 0.271$; Fig. 2). There was no significant difference between treatments in vertical distribution ($z = 0.145$, $P = 0.444$).

Perch population training in Deming Lake

Upon first exposure to test cues, perch avoided traps labeled with perch skin extract but gave no indication that they recognized pike odor as dangerous (KW = 8.59, $P < 0.020$; Fig. 3*a*). The numbers of perch captured in the three trap types were 127, 125, and 57 for pike odor, water, and perch skin extract, respectively. Alpha-adjusted post-hoc pairwise comparisons showed that traps labeled with perch alarm cues caught significantly fewer perch than traps labeled with either pike odor or water. Pike-odor- and water-labeled traps did not differ in perch catches (Fig. 3*a*). Following seeding of Deming Lake with sponges of perch skin and pike odor, the response of perch to the test stimuli remained virtually unchanged from the first day of trapping

© 2004 NRC Canada

Fig. 3. Median (± quartiles) number of yellow perch (*Perca flavescens*) and pumpkinseed (PK) sunfish (*Lepomis gibbosus*) caught per trap in Deming Lake, Minnesota, on the first day (*a*) and the second day (*b*) of the experiment. Traps were scented with either perch skin extract (hatched bars), water (open bars), or pike odor (stippled bars) (ns, nonsignificant, $P > 0.05$). The letters above the bars denote statistical significance in pairwise comparisons at $P < 0.05$.

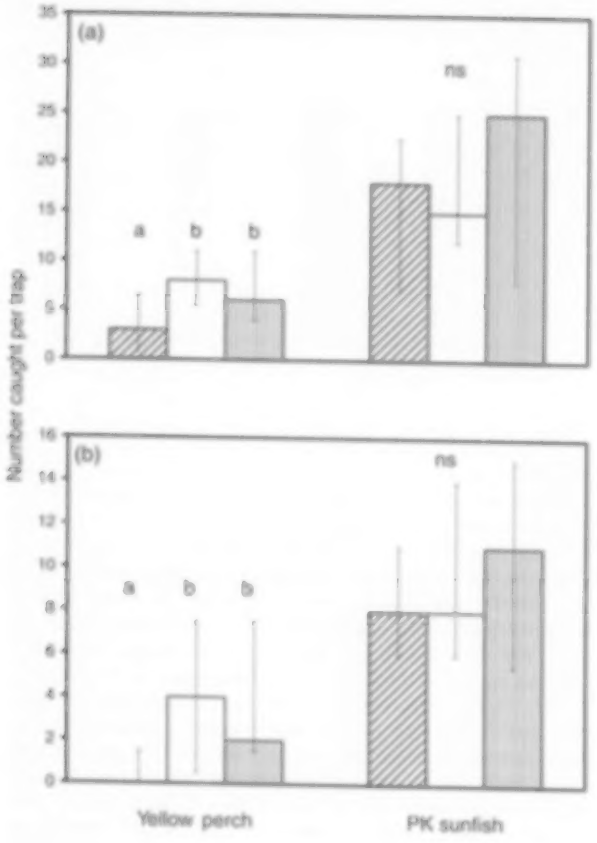

(KW = 8.16, $P = 0.02$), with 88, 84, and 16 perch caught in traps scented with pike odor, water, and perch alarm cues, respectively (Fig. 3*b*). Simultaneous addition of alarm cues and novel predator odor did not result in demonstrable acquired recognition by perch of pike odor as an indicator of risk.

Density of pumpkinseed sunfish was sufficient to test for a cross-species reaction to perch alarm cues (Chivers and Smith 1998; Pollock et al. 2003) and the potential of a learned association of predation risk with pike odor via a cross-species alarm cue. On first exposure, pumpkinseed sunfish did not show differential catch numbers based on chemical stimuli in each trap (KW = 1.43, $P = 0.488$). On the first day, 316, 320, and 229 sunfish were captured in traps labeled with pike odor, water, and perch skin, respectively (Fig. 3*a*). After the lake was seeded with pike odor and perch alarm cues, sunfish on the second exposure continued to ignore both perch alarm cues and pike odor (KW = 0.74, $P = 0.691$). We caught 162, 176, and 129 pumpkinseed sunfish for pike odor, water, and perch alarm cue treatments, respectively (Fig. 3*b*).

Discussion

We succeeded in establishing the potential for predator-recognition training of hatchery-reared walleye (conditions 1–3 above), but we did not succeed in demonstrating a method for implementing it on a large scale (condition 4 above). Juvenile walleye in our study used chemical cues for assessing predation risk, did not have a preexisting genetic template for recognizing pike odor, and used alarm cues to acquire recognition of pike odor as an indicator of predation risk. Therefore, there exists the potential to train hatchery-reared walleye to recognize significant sources of predation risk before they are stocked into established fish communities. Through predator-recognition training, predator-naïve hatchery-reared fish gain some of the survival skills normally acquired in the wild. This, in turn, could lead to better post-stocking survival of walleye, improve the cost-efficiency of stocking programs, enhance fishery quality, and stimulate economic benefits associated with it.

Several hatchery-reared salmonid species are able to acquire predator recognition through releaser-induced training (rainbow trout, Brown and Smith 1998; chinook salmon (*Oncorhynchus tshawytscha*), Berejikian et al. 1999; brook char, Mirza and Chivers 2000). Antipredator behavioral response to predator odors translates into survival benefits when trained hatchery-reared fish encounter predators (Berejikian et al. 1999; Mirza and Chivers 2000). Our study is the first to apply recognition training to a hatchery-reared percid game species.

To our knowledge, our data represent the first field demonstration of perch avoidance of conspecific alarm cues; thus, this study provides an important field verification of earlier laboratory results (Mirza et al. 2003). This is also the first field test for a response to predator kairomones. Because we were able to detect avoidance of perch alarm cues, it seems likely that we would have detected avoidance of pike odor if acquired recognition had occurred. We cannot say from our data whether our inability to detect an effect was caused by inadequacies in the method of training (seeding), in the method of testing (scented traps), or both. We can only speculate whether predator recognition may have been achieved with a more intensive seeding of alarm and predator cues. We added a total of 1.8 L of pike odor and 75 cm^2 of perch skin (equivalent to slightly more than eight perch) distributed along about 300 m of shoreline.

Pumpkinseed sunfish in Deming Lake have never shown any response to chemical alarm cues from either conspecific sunfish (Jennifer Dehn, University of Minnesota, and Brian Wisenden, Minnesota State University Moorhead, unpublished data), heterospecific fathead minnows (Wisenden et al. 2003), or perch (this study). Centrarchid populations in other locations exhibit alarm reactions to alarm cues (e.g., Brown and Brennan 2000). We do not know why Deming Lake pumpkinseed sunfish appear to be unresponsive to these cues.

An alternative mechanism for recognition training is to seed the holding tanks used to transport walleye from the rearing ponds (or hatchery) to the destination lake. Holding

© 2004 NRC Canada

tanks have a relatively small volume and would require less alarm cue and less effort to achieve predator-recognition training. We are currently testing this method.

Another possible mechanism for mass training is to release a predator into the rearing pond a few weeks before harvest of the fingerlings. Previous work has shown that predator introduction causes chemical and visual recognition of the predator by entire populations of minnows in 1 week to a few weeks (Chivers and Smith 1995; Brown et al. 1997). Assuming that a large pike would not survive over winter in a small pond, predator stocking a week or two before walleye harvest might be an effective approach to transfer predator recognition to juvenile walleye. The loss of fingerling walleye to a single pike over a few weeks would be small compared with the potential increase in survival of remaining walleye once they were stocked into a large lake with a large pike population. There is inherent risk in this approach in that mild winters allow large fish in rearing ponds to survive to the following season. The resulting carry-over significantly reduces rates of harvesting walleye fingerlings.

Releaser-induced predator-recognition learning is a widely occurring phenomenon among taxa ranging from Platyhelminthes (Wisenden and Millard 2001) to Arthropoda (Wisenden et al. 1997), fishes (Göz 1941; Magurran 1989; Chivers and Smith 1994), birds (McLean et al. 1999), and mammals (McLean et al. 2000). The flexibility of this learning paradigm allows prey to adapt to predation landscapes that shift over ecological time and space. The application of this powerful ecologically selected learning mechanism to enhance resource management holds much promise for any species reared in a predator-free environment and later released into the wild. The outstanding challenge to this method is streamlining the logistics of the training process to accommodate the large numbers of animals typically involved in resource-enhancement programs.

Acknowledgements

Mariya Rzaszutak, Travis Thiel, and Tonya Overbo spent 2 years helping to develop the walleye training protocol. A Learning by Doing grant to B.D.W. from the Minnesota State Colleges and Universities Center for Teaching and Learning and a grant from the MSUM College of Social and Natural Sciences funded the expansion of the aquatic-research facility at MSUM that allowed us to accommodate this project. A research grant from the MSUM Biology Department to M. Rzaszutak helped fund the project in 2001, and grants from the MSUM Alumni Foundation bought the thousands of minnows needed to feed walleye during the final "data year" of the project. We thank Gary Huberty (Fisheries Specialist) and Mike Livingood (Fisheries Technician) of the Minnesota Department of Natural Resources at Detroit Lakes for field assistance in collecting juvenile walleye. The 2002 Animal Behavior class of the University of Minnesota Itasca Biological Field Station helped collect data for the perch training experiment. They are Annie Bakken, Sarah Compton, Trevor Estabrooks, Nate Foster, Erica Hansen, Nguyen Hoang, Nathan Hollenbeck, Jennifer McClain, David Pass, Kristen Seitz, Sopheak Srun, and Nicole Untener. This research was conducted under MSUM's Institutional Animal Care and Use Committee protocol No. 99-T-BIOL-015-N-N-01 and University of Minnesota (Itasca Biological Field Station) Institutional Animal Care and Use Committee protocol No. 0005A51841.

References

Berejikian, B.A., Smith, R.J.F., Tezak, E.P., Schroder, S.L., and Knudsen, C.M. 1999. Chemical alarm signals and complex hatchery rearing habitats affect antipredator behavior and survival of chinook salmon (*Onchorhynchus tshawytcha*) juveniles. Can. J. Fish. Aquat. Sci. **56**: 830–838.

Brown, G.E., and Brennan, S. 2000. Chemical alarm signals in juvenile green sunfish (*Lepomis cyanellus*, Centrarchidae). Copeia, 2000: 1079–1082.

Brown, G.E., and Smith, R.J.F. 1998. Acquired predator recognition in juvenile rainbow trout (*Oncorhynchus mykiss*): conditioning hatchery-reared fish to recognize chemical cues of a predator. Can. J. Fish. Aquat. Sci. **55**: 611–617.

Brown, G.E., Chivers, D.P., and Smith, R.J.F. 1997. Differential learning rates of chemical versus visual cues of a northern pike by fathead minnows in a natural habitat. Environ. Biol. Fishes, **49**: 89–96.

Chivers, D.P., and Smith, R.J.F. 1994. Fathead minnows, *Pimephales promelas*, acquire predator recognition when alarm substance is associated with the sight of unfamiliar fish. Anim. Behav. **48**: 597–605.

Chivers, D.P., and Smith, R.J.F. 1995. Free-living fathead minnows rapidly learn to recognize pike as predators. J. Fish Biol. **46**: 949–954.

Chivers, D.P., and Smith, R.J.F. 1998. Chemical alarm signalling in aquatic predator–prey systems: a review and prospectus. Ecoscience, **5**: 338–352.

Gadzewich, K.J., and Chivers, D.P. 2002. Acquired recognition by fathead minnows: influence of habitat characteristics on survival. J. Chem. Ecol. **28**: 439–445.

Göz, H. 1941. Über den Art- und Individualgeruch bei Fischen. Z. Vergl. Physiol. **29**: 1–45.

Hara, T.J. 1993. Role of olfaction in fish behaviour. *In* Behaviour of teleost fishes. 2nd ed. *Edited by* T.J. Pitcher. Chapman and Hall, New York. pp. 171–199.

Kats, L.B., and Dill, L.M. 1998. The scent of death: chemosensory assessment of predation risk by prey animals. Ecoscience, **5**: 361–394.

Lima, S.L., and Dill, L.M. 1990. Behavioral decisions made under the risk of predation: a review and prospectus. Can. J. Zool. **68**: 619–540.

Magurran, A.E. 1989. Acquired recognition of predator odour in the European minnow (*Phoxinus phoxinus*). Ethology, **82**: 216–223.

Mathis, A., and Smith, R.J.F. 1993*a*. Chemical alarm signals increase the survival time of fathead minnows (*Pimephales promelas*) during encounters with northern pike (*Esox lucius*). Behav. Ecol. **4**: 260–265.

Mathis, A., and Smith, R.J.F. 1993*b*. Chemical labeling of northern pike (*Esox lucius*) by the alarm pheromone of fathead minnows (*Pimephales promelas*). J. Chem. Ecol. **19**: 1967–1979.

Mathis, A., and Smith, R.J.F. 1993*c*. Intraspecific and cross-superorder responses to chemical alarm signals by brood stickleback. Ecology, **74**: 2395–2404.

McLean, I.G., Hoelzer, C., and Studholme, B.J.S. 1999. Teaching predator-recognition to a naïve bird: implications for management. Biol. Conserv. **87**: 123–130.

© 2004 NRC Canada

McLean, I.G., Schmitt, N.T., Jarman, P.J., Duncan, C., and Wynne, C.D.L. 2000. Learning for life: training marsupials to recognise introduced predators. Behaviour, **137**: 1361–1376.

Mirza, R.S., and Chivers, D.P. 2000. Predator-recognition training enhances survival of brook trout: evidence from laboratory and field enclosures. Can. J. Zool. **78**: 2198–2208.

Mirza, R.S., Fisher, S.A., and Chivers, D.P. 2003. Assessment of predation risk by juvenile yellow perch (*Perca flavescens*): responses to alarm cues from conspecifics and prey guild members. Environ. Biol. Fishes, **66**: 321–327.

Pollock, M.S., Chivers, D.P., Mirza, R.S., and Wisenden, B.D. 2003. Fathead minnows learn to recognize chemical alarm cues of introduced brook stickleback, *Culaea inconstans*. Environ. Biol. Fishes, **66**: 313–319.

Santucci, V.J., and Wahl, D.H. 1993. Factors influencing survival and growth of stocked walleye (*Stizostedion vitreum*) in a centrarchid-dominated impoundment. Can. J. Fish. Aquat. Sci. **50**: 1548–1558.

Siegel, S., and Castellan, N.J., Jr. 1988. Nonparametric statistics for the behavioral sciences. McGraw-Hill, New York.

Smith, R.J.F. 1982. Reaction of *Percina nigrofasciata*, *Ammocrypta beani*, and *Etheostoma swaini* (Percidae, Pisces) to conspecific and intergeneric skin extracts. Can. J. Zool. **17**: 2253–2259.

Stacey, N.E., and Sorensen, P.W. 2002. Hormonal pheromones in fish. *In* Hormones, brain, and behavior. Vol. 2. *Edited by* D. Pfaff, D. Arnold, A. Etgen, S. Fahrbach, and R. Rubin. Academic Press, New York. pp. 375–435.

Suboski, M.D. 1990. Releaser-induced recognition learning. Psychol. Rev. **97**: 271–284.

Suboski, M.D., and Templeton, J.J. 1989. Life skills training for hatchery fish: social learning and survival. Fish. Res. (Amst.), **7**: 343–352.

Szendrey, T.A., and Wahl, D.H. 1996. Size-specific survival and growth of stocked muskellunge: effects of predation and prey availability. N. Am. J. Fish. Manag. **16**: 395–402.

Wisenden, B.D. 2003. Chemically-mediated strategies to counter predation. *In* Sensory processing in the aquatic environment. *Edited by* S.P. Collin and N.J. Marshall. Springer-Verlag, New York. pp. 236–251.

Wisenden, B.D., and Millard, M.C. 2001. Aquatic flatworms use chemical cues from injured conspecifics to assess predation risk and to associate risk with novel cues. Anim. Behav. **62**: 761–766.

Wisenden, B.D., Chivers, D.P., and Smith, R.J.F. 1997. Learned recognition of predation risk by *Enallagma* damselfly larvae (Odonata, Zygoptera) on the basis of chemical cues. J. Chem. Ecol. **23**: 137–151.

Wisenden, B.D., Pollock, M.S., Tremaine, R.J., Webb, J.M., Wismer, M.E., and Chivers, D.P. 2003. Synergistic interactions between chemical alarm cues and the presence of conspecific and heterospecific fish shoals. Behav. Ecol. Sociobiol. **54**: 485–490.

© 2004 NRC Canada

Bimodal population size distributions and biased gillnet sampling

Anders Gravbrøt Finstad and Ole Kristian Berg

Abstract: Bimodal size distributions have been commonly observed in Arctic char (*Salvelinus alpinus*). We document an example of such bimodality caused solely by biased gillnet sampling. The observed bimodality was a direct artefact of the sampling method resulting from an abrupt increase in gillnet catchability of fish larger in total length than between 25 and 30 cm. Mean gillnet selectivity (catchability) of char in the upper mode of the observed bimodal size distribution was about 40 times higher than the corresponding value for char in the observed lower mode. Fish of intermediate size, lacking in the gillnet samples, were present in the population and readily obtainable by electrofishing. The observed size difference in gillnet vulnerability is likely to result from behavioural changes following ontogenetic niche shifts.

Résumé : On a souvent observé des distributions de taille bimodales chez l'omble chevalier (*Salvelinus alpinus*). Nous présentons un exemple d'une telle bimodalité qui est causée uniquement par un échantillonnage faussé au filet maillant. La bimodalité observée est un artefact direct de la méthode d'échantillonnage qui résulte d'une augmentation abrupte de la probabilité de capture dans le filet des poissons plus grands que 25 à 30 cm de longueur totale. La sélectivité moyenne (probabilité de capture) du filet maillant pour la capture des ombles du mode supérieur de la distribution bimodale des tailles est environ 40 fois plus élevée que pour celle des ombles du mode inférieur de la distribution bimodale observée. Les poissons intermédiaires, absents des échantillons récoltés au filet maillant, sont présents dans la population et facilement capturés par pêche électrique. La différence de probabilité de capture au filet maillant observée en fonction de taille est vraisemblablement due à des modifications de comportement consécutives à des changements ontogéniques de niche.

[Traduit par la Rédaction]

Introduction

Among northern hemisphere freshwater fishes, population size distributions with two distinct size modes (population bimodality) have commonly been observed (e.g., Power 1978). Particular focus has been centred on the common observations of bimodal population size structures in the circumpolar salmonid Arctic char (*Salvelinus alpinus*). Theories describing ecological and evolutionary factors generating the lack or scarcity of intermediate-sized fish in this species have been proposed (e.g., Griffiths 1994; Hammar 2000; Parker et al. 2001). Suggested mechanisms have included cannibalism and parasitism (Hammar 2000), trophic specialisation (Parker and Johnson 1991), or life history variation (Parker et al. 2001), whereas Power (1978) speculated whether the observed bimodality could be an effect of bias in the gillnet sampling. Population bimodality (sensu Finstad et al. 2003) can be generated in a population with stable age structure by within-population differences in growth, or alternatively, by differences in year-class strength (Griffiths 1994; Finstad et al. 2003). Bimodal size and age distributions in gillnet samples have been reported to persist over long periods of time in some Arctic char populations (e.g., Johnson 1983; Svenning and Borgstrøm 1995).

We propose an alternative explanation for the occurrence of bimodal size distributions of Arctic char in gillnet samples. Gillnet sampling is a common methodology used in fish stock assessment. In many stock assessment studies, series of nets containing different mesh sizes are employed with the assumption of targeting different-sized individuals with equal efficiency (Kurkilahti et al. 2002). However, even the most advanced combination of mesh sizes in gillnet series may show size-dependent selectivity and therefore produce biased estimates of the true population size structure (e.g., Jensen and Hesthagen 1996; Finstad et al. 2000). Finstad et al. (2000) demonstrated that smaller and younger Arctic char could be underrepresented in gillnet catches. Further, an abrupt increase in gillnet selectivity for large char was observed and related to a niche shift to cannibalism. Although the particular population studied by Finstad et al. (2000) did not exhibit a bimodal size distribution, Finstad et al. (2000) presented a model that could explain bimodal size distributions in gillnet catches as a result of ontogenetic behavioural change.

More recently, Finstad et al. (2003) examined published data sets reporting bimodal size distributions in gillnet samples of Arctic char. By simulating population structure re-

Received 29 December 2003. Accepted 31 August 2004. Published on the NRC Research Press Web site at http://cjfas.nrc.ca on 25 January 2005.
J17891

A.G. Finstad[1,2] and O.K. Berg. Department of Biology, Norwegian University of Science and Technology, N-7491 Trondheim, Norway.

[1]Corresponding author (e-mail: anders.finstad@nina.no).
[2]Present address: Norwegian Institute for Nature Research, Tungasletta 2, N-7485 Trondheim, Norway.

 doi: 10.1139/F04-157 © 2004 NRC Canada

Fig. 1. The study area, Lake Trestikkelen at Bear Island (74.5°N, 19.0°E), in the Arctic Ocean. Solid lines indicate 2-m depth contours; broken lines indicate the 1.5- and 5.5-m depth contours.

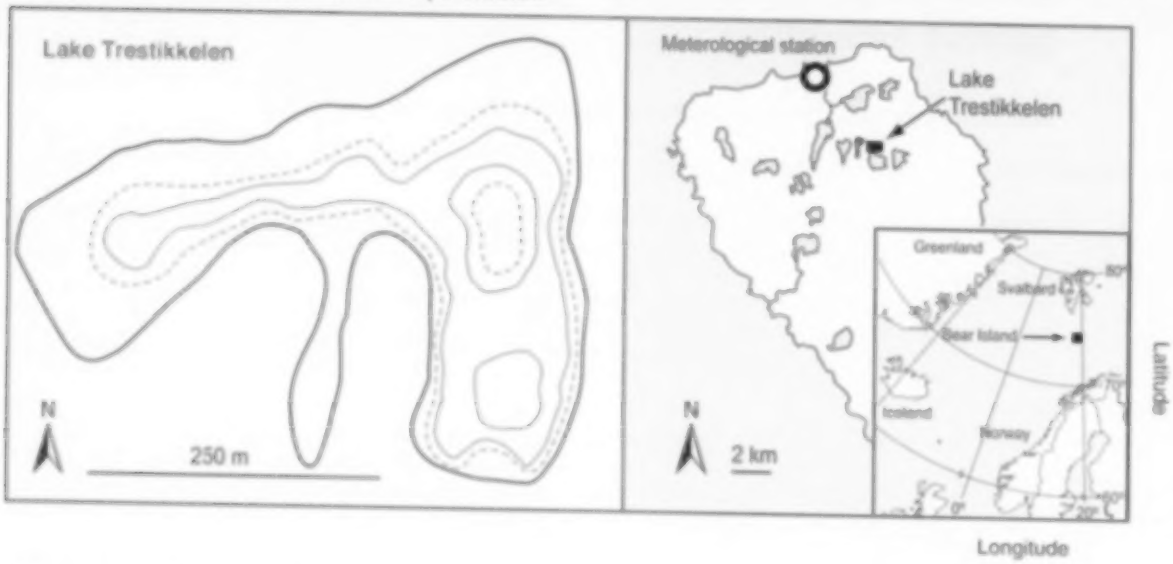

sulting from empirical growth patterns, it was demonstrated that the observed bimodal population size distribution could not be generated under assumptions of a stable age structure.

In our previous work (Finstad et al. 2000, 2003), we have relied on indirect, model-based logic to support our arguments. In this paper, we provide direct empirical evidence to demonstrate how bimodal size distributions can result from biased gillnet sampling. We use size-stratified mark–recapture methods in a small, arctic lake to get unbiased estimates of abundance of Arctic char by size categories. We then compare the resulting size distribution with the raw catches from multimesh gillnet samples from the same lake

Material and methods

Study site

The study was conducted in the relatively small (11.3 ha) and shallow (mean depth 1.8 m) monomictic arctic lake Trestikkelen (Fig. 1) situated at Bear Island (74.5°N, 19.0°E) in the Arctic Ocean. The ice-free period normally starts in mid-July and lasts for 2.5 to 3.5 months. Bottom substrate consists of gravel, stone, and fine sand with the only macrovegetation being submerged mosses. The shoreline consists of gravel and stone boulders. The lake holds a single-species population of resident Arctic char, and piscivory is frequent among the largest fish. Because of the remote geographical location, fishing activity is negligible.

Estimating the population size distribution

We estimated the size–frequency structure of the Arctic char population of Lake Trestikkelen by mark–recapture. Char ranging in length from 80 to 499 mm were divided into 10 size groups, and the abundance of fish within each size group was estimated independently using a single-census Petersen estimate (Ricker 1975, section 3.2.2). In accordance with Ricker (1975), we attempted to use different sampling gears when catching fish for marking and in the recapture fishing effort. The majority (95%) of fish captured for marking were caught with electrofishing gear (pulsed DC backpacker, current output 650 V at 1000 Ω, pulse length 1.8 ms at 70 Hz) in the shallow areas of the lake (<1.5 m). In addition, we captured fish for marking in the deeper areas of the lake using gillnets. Most of the fish (73%) checked for marks were caught using gillnets, with sampling effort distributed evenly throughout the lake. In addition, we used electrofishing gear in the shallow parts of the lake that were less accessible to gillnets. This procedure led to a slightly unevenly spatially distributed effort in capturing fish for marking but a more evenly distributed recapture effort.

Marking of fish was conducted in the period from 17 to 21 July 2002. Size was measured as total length (mm), and the fish were marked by removing the adipose fin or a small part of the pelvic fin. To minimise unaccounted mortality caused by capture and handling, gillnetted fish were observed for a minimum of 48 h before being evenly distributed throughout the lake. Individuals that were wounded during the marking process were killed and only char in apparent good physical condition were released. To retain the original size distribution of the population, individuals killed in the marking process were replaced by similar-sized individuals from immediate down- or up-stream systems. Fish introduced into the system in this way were marked with separate combinations of fin removal.

We used logistic regression to test for differences in recapture probability between marked native or introduced fish (origin). Fish size (total length, mm) was included in the model as a covariate to adjust for size differences in recapture probability. Because we could not identify individual fish from our marks, the model describes recapture probability of a fish with a given origin and size. Logistic regression was also used to test for differences in recapture probability

© 2004 NRC Canada

Table 1. Basic numbers in the size-stratified mark–recapture estimation of population structure and gillnet selectivity in size classes from 80 to 499 mm in Lake Trestikkelen, Bear Island, 2002.

Size class (mm)	*M*	*C*	*R*	*N* (±95% CI)
80–99	692 (80)	322	24	8954 (6116–13566)
100–119	350 (92)	203	17	3978 (2539–6569)
120–149	137 (65)	46	8	721 (386–1474)
150–199	54 (14)	9	3	138 (56–344)
200–249	14 (7)	4	3	19 (8–47)
250–299	18 (11)	3	3	19 (8–48)
300–349	7 (3)	3	3	8 (3–20)
350–399	4 (2)	2	2	6 (2–13)
400–449	6 (3)	5	5	7 (3–16)
450–499	5 (3)	2	2	6 (2–15)

Note: *M*, total numbers of fish marked (fish introduced into the lake given in parentheses); *C*, numbers of fish captured and checked for marks; *R*, numbers of recaptured fish; *N*, estimated number in population (±95% confidence interval, CI).

of marked fish during the recapture period, where marked or unmarked was used as a binary dependent variable, recapture date as an independent variable, and fish size as a covariate.

To allow marked fish to recover and resume natural behaviour, no fishing was conducted for 1 week before the second capture event. Recapture was conducted from 29 July to 8 August 2002; fish caught and checked for marks were not reintroduced into the lake. The number of fish in each of the 10 length classes (Table 1) was estimated (±95% confidence interval, CI) according to the adjusted Petersen estimate (Ricker 1975, section 3.2.2) yielding a direct estimate of the population size distribution.

Gillnet sampling

To illustrate the size structure as observed in gillnet catches, we employed multimesh gillnets (30 m × 1.5 m) of a type proposed for monitoring use in the Nordic countries (referred to as NORDIC gillnets; Appelberg 1995). The nets were a slight modification of the original NORDIC series as the two lower mesh sizes (5 and 6.25 mm) had been removed. The series consisted of 12 mesh sizes (monofilament thickness, mm): 8 (0.10), 10 (0.13), 12.5 (0.13), 15.5 (0.15), 19.5 (0.15), 24 (0.15), 29 (0.15), 35 (0.16), 43 (0.20), and 55 mm (0.23) (bar mesh size). This combination of mesh sizes has previously been suggested to target different-sized individuals with approximately equal efficiency (Kurkilahti et al. 2002).

In the mark–recapture experiment, we additionally employed single-mesh-size bottom gillnets 1.5 m × 10 m, with mesh sizes 8, 10, and 12.5 mm, and 1.5 m × 30 m, with mesh sizes 19.5, 24, 29, and 35 mm. A total of 16 NORDIC gillnets and a variable amount of single-mesh-size gillnets nets were evenly distributed throughout the lake during the recapture effort. The nets covered most habitats except a small pelagic area over the deepest parts (maximum depth 5.5 m) of the study lake. However, we did not observe any indication of pelagic behaviour of the char, and most of the fish caught in gillnets were caught in the lower section of the net. The nets were hauled approximately every 20 h.

The size structure of the population estimated by mark–recapture was compared with the apparent size structure as observed in the NORDIC multimesh gillnet catches from the recapture of marked fish, as well as in the NORDIC multimesh gillnet catches obtained in a 12-h preliminary test fishing of the lake before starting the mark–recapture experiment on 16 July. Because of the limited number of larger fish in the lake, our gillnet catches severely altered the population size structure with respect to larger fish. Therefore, to interpret an observed initial size distribution, as appearing in gillnet catches, we only used the first 62 h of gillnet fishing for this purpose.

Mean gillnet capture probability for each size class was inferred for the whole net series combined and represents the proportion of the estimated number in a given size class caught in NORDIC gillnets during the test fishing subsequent to the start of the mark–recapture experiment, excluding 18 fish caught during the initial test fishing of the lake before this. These fish were added to the final population estimate, however, to obtain an estimate of the original population structure before we started fishing. Confidence intervals for the mean gillnet catchability of each size class were calculated by substituting the estimated abundance by the upper and lower 95% CI of the abundance estimate.

Size-dependent capture probabilities

A size-dependent capture probability model for the NORDIC multimesh gillnet was developed using the capture of marked fish in NORDIC catches. The model is based on recaptures of Arctic char of given sizes and not of individual fish. The event of recapturing a marked fish of a given size on the NORDIC gillnet series was treated as a binary response variable in logistic regression where total length (T_L, in mm) was entered as a covariate (predictor). The probability of capturing a fish of size i on NORDIC gill nets (p_i) was estimated as

$$(1) \qquad p_i = (1 + e^{-\beta})^{-1}$$

where $\beta = b_0 + b_1 (T_L)$, and b_0 and b_1 are estimated constants.

Results

In total, 86 fish were captured on the NORDIC multimesh gillnet during the first 62 h of gillnet fishing. The length distribution (Fig. 2*b*) of these gillnet captures revealed a distinct bimodal size–frequency distribution. Most of the fish

© 2004 NRC Canada

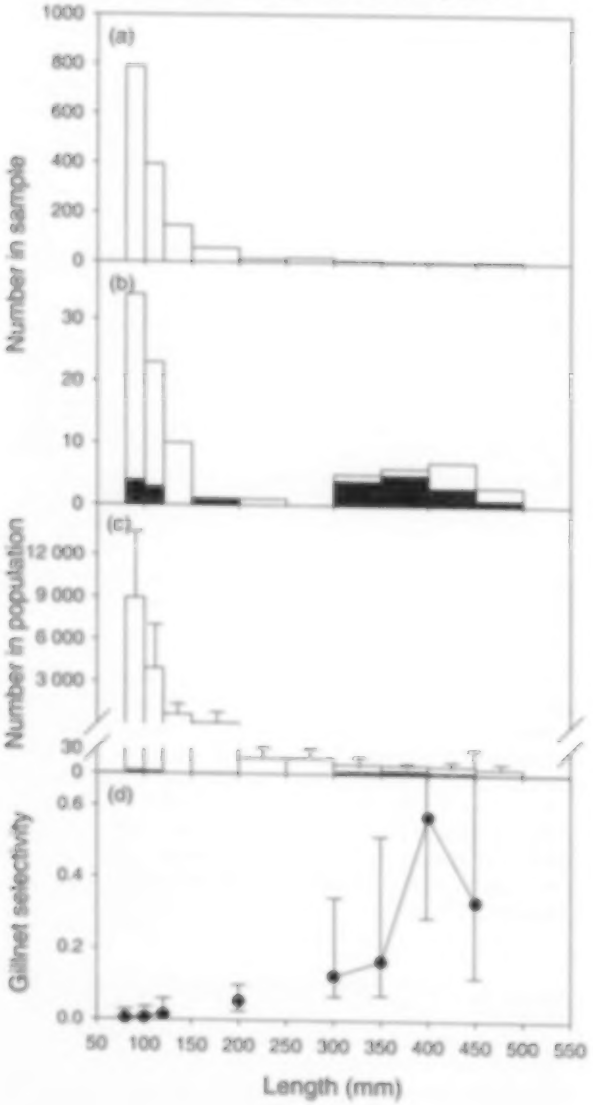

Fig. 2. Observed size distribution in (*a*) electrofished catches and (*b*) NORDIC multimesh gillnet catches of (*c*) estimated size structure (±95% confidence interval, CI) obtained by size-stratified mark–recapture and (*c*) estimated gillnet selectivity (±95% CI) from Lake Trestikkelen, Bear Island, 2001. As the size structure of the population changed rapidly with increasing number of large char caught, only the catch from the first 62 h of gillnet sampling are shown in *b*, and solid bars indicate fish caught during the initial test fishing ($N = 18$). For illustration, these fish are also included in *c*, as they would have been part of the estimated population if not killed in the test fishing. (*d*) Relative selectivity of the different size classes are calculated as the number of fish caught on NORDIC gillnet during the first 62 h of test fishing divided by estimated number in population (±95% CI of estimates). Note the break in scaling in *c*.

captured were in size classes 80–150 mm ($N = 63$) and 300–500 mm ($N = 21$). Notable was the almost total lack of fish between 150 and 300 mm in the gillnet captures. Only two fish in this last size range were captured by the multimesh gillnet sampling. However, fish in this size interval were readily caught by electrofishing gear when hiding between large boulders in the shallow areas of the lake (Fig. 2*a*). The size structure of the gillnet samples changed with a decrease in the number of large fish (>300 mm) during the test fishing period. The initial 20 h of test fishing consisted almost solely of large fish (>300 mm), and the frequency of large fish then subsequently decreased with time (Fig. 2*b*).

A total of 1287 fish were marked, 1213 of which were captured with electrofishing gear. Subsequently, a total of 599 fish were captured and checked for marks, 161 of which were captured with electrofishing gear. For all size classes combined, 70 marked individuals were recaptured (Table 1). We were unable to detect differences in recapture probability between introduced fish and fish originating from the studied population (model summary: –2 log likelihood = 658.71, $\chi^2 = 66.10$, $P < 0.001$; parameters: total length, Wald $\chi^2 = 68.69$, $p < 0.001$; origin, Wald $\chi^2 = 1.85$, $p = 0.173$). Accordingly, the individuals introduced into the population to retain the original size configuration were included in the population size distribution estimate. Neither was there any change in the frequency of marked individuals in the catches with the time of recapture (model summary: –2 log likelihood = 474.70, $\chi^2 = 69.97$, $p < 0.001$; total length, Wald $\chi^2 = 28.90$, $p < 0.001$; recapture time, Wald $\chi^2 = 2.37$, $p < 0.124$). The total Arctic char population in Lake Trestikkelen was estimated to be 13 854 individuals greater than 80 mm in length (Fig. 2*c*). The estimated population size distribution could be described as approximately lognormal, with most of the population consisting of small char less than 120 mm in total length ($N = 13\,600$), with only a minor number ($N = 50$) larger than 250 mm.

The estimated population structure was fundamentally different from the population structure observed in gillnet catches. This was reflected in the estimates of gillnet selectivity where the total probability of capture, given as the number of fish in each size class from the NORDIC gillnet catches divided by the estimated number in the population of each size class, increased from an average of 0.7% for the size classes 80–149 mm to an average of 30% for the size classes 300–450 mm (Fig. 2*d*). Only one fish in the size range 149–300 mm was captured in the test fishing subsequent to the mark–recapture estimation (Fig. 2*b*). Mean gillnet catchability of char in the upper mode of the observed size distribution (>300 mm) was 39 times higher than the corresponding value for all char in the lower mode (<149 mm) (Fig. 2*d*). This yielded a corresponding overrepresentation of large char in the gillnet samples. It is evident that the observed upper mode in the size–frequency distribution of the gillnet catches (Fig. 2*b*) was generated by a rapid increase in gillnet catchability starting at total lengths of approximately 300 mm (Fig. 2*d*).

The marked fish ($N = 1287$) released into the lake constituted a group of fish with known length–frequency composition (Fig. 3*a*), and 26 of these were recaptured on the NORDIC multimesh gillnet. Although only 54

© 2004 NRC Canada

Fig. 3. Size–frequency distribution of marked fish (*a*) released in Lake Trestikkelen and (*b*) captured in NORDIC multimesh gillnet catches. (*c*) The resulting size-dependent capture probability model, estimated by logistic regression (eq. 1, $b_0 = -5.64$ (±0.370 standard error, SE), $b_1 = 0.013$ (±0.002 SE)), is illustrated with 95% confidence interval (dotted lines).

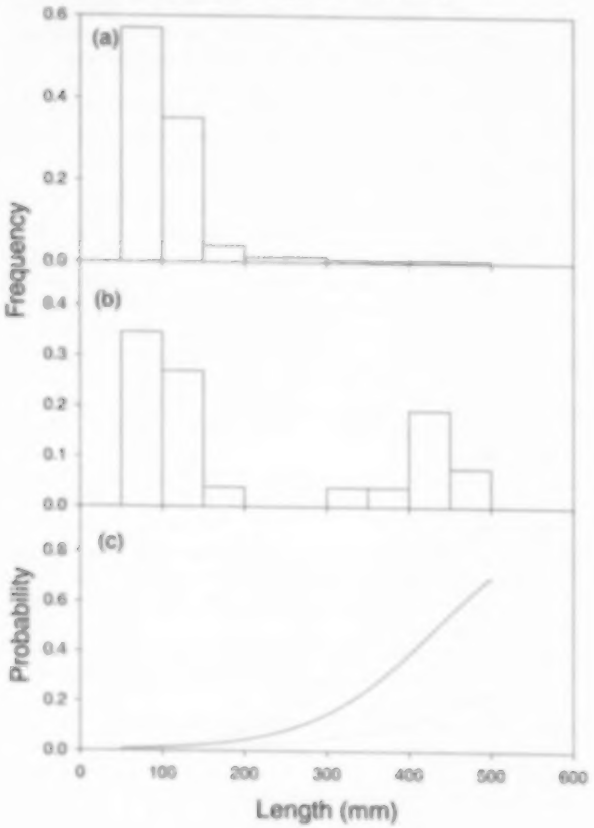

(4%) of the marked fish released into the lake were >250 mm, 9 out of 26 (35%) of the marked fish recaptured on the NORDIC multimesh gillnet belonged to this size group (Fig. 3*b*). The size distribution of marked fish in the lake was approximately lognormal, with the number of marked fish decreasing with size (Fig. 3*a*). However, the size–frequency distribution of the marked fish captured on NORDIC multimesh gillnets was distinctively bimodal and the intermediate size classes were lacking (Fig. 3*b*). There was a highly significant relation between size and capture probability of marked fish on the NORDIC multimesh gillnet (model summary: −2 log likelihood = 208.71, $\chi^2 = 43.84$, $p < 0.001$; T_L, Wald $\chi^2 = 55.22$, $p < 0.001$; constant, Wald $\chi^2 = 224.39$, $p < 0.001$). The resulting size-dependent capture probability remained low for fishes <250 mm and then rapidly increased (Fig. 3*c*). A more complex model (square or cubic) may be expected upon visual inspection of the mean capture probabilities for each size class (Fig. 2*d*). Probably as a result of low sample size, the fit of these higher-order terms did not prove significant and were therefore excluded from the model.

Discussion

Both statistical and methodological uncertainties are involved in estimates obtained by mark–recapture methods (see Ricker 1975), and the assumptions of mark–recapture experiments are seldom met in natural populations (e.g., Gatz and Loar 1988). However, none of the basic assumptions was significantly violated in the present experiments. Marking fish with fin removal has not been found to induce significant increases in mortality in short-term studies (Mears and Hatch 1976; O'Grady 1984; Johnsen and Ugedal 1988), and because of the short time span (1–3 weeks) between marking and recapture, recruitment into length classes owing to growth is negligible. Different sampling tools were employed for the majority of fish for marking and recaptures, making the estimates more robust to sampling bias (Ricker 1975). Furthermore, during the study period, all drainage to and from the study lake occurred through groundwater seepage. Concordantly, no immigration or emigration of fish to and from the lake was possible, making the present experiment a true closed mark–recapture estimate. Additionally, bias in the mark–recapture estimates cannot explain the observed changes in size-dependent capture probability as this is estimated directly by sampling fish from a known size distribution (marked individuals released into the lake). Furthermore, as the study lake is shallow (mean depth 1.8 m, maximum depth 5.5 m), size-dependent differences in habitat use are unlikely to explain the observed bias in gillnet catches.

The numbers of recaptures are small in the larger size classes, making the uncertainties in the estimates relatively large. However, the differences between the estimated proportions of fish larger than 200 mm in population and the observed proportion in gillnet samples are far too large to be explained by stochastic uncertainties in the number of recaptures. Also, that all fish larger than 250 mm checked for marks were recaptures supports the low estimate of fish from the observed upper mode in the population. That we were unable to recapture all of the fish in these size classes may, rather counterintuitively, be a result of the relatively intensive gillnet fishing and the small size of the study lake. We suggest that a number of fish had been in contact with the net, were wounded, and subsequently became inactive, making them invulnerable to gillnet sampling in the relatively short and intensive period of recaptures.

The original size distribution obtained by gillnets rendered the same basic properties as previously reported from other Arctic char populations showing bimodal size distributions in population samples with a lack or scarcity of intermediate-sized individuals (e.g., Parker and Johnson 1991; Hammar 2000). It is clear that the observed bimodal population structure in Lake Trestikkelen was a direct artefact of a profound bias when using gillnets as the sampling method. This is also supported by the observation of a distinct bimodal size–frequency distribution of marked fish in the NORDIC multimesh gillnet samples, despite the fact that the size–frequency distribution of marked fish in the lake re-

© 2004 NRC Canada

sembled lognormal with a decreasing number of fish with increasing size. The profound increase in gillnet selectivity with increasing size corresponds with findings from previous studies of gillnet selectivity in Arctic char by Finstad et al. (2000), pointing to a generality of our findings. This conclusion is further emphasised by the distribution obtained with electrofishing gear, which yielded an apparent size–frequency distribution completely different from that obtained by multimesh gillnet.

The inherent effect of increased body size on swimming speed will only give rise to a gradual increase in gillnet catchability with increasing size (Rudstam et al. 1984). The observed abrupt increase in the gillnet catchability of large char must therefore be related to other factors generating a sudden increase in activity of the fish above a certain size. Such factors may be size-dependent behavioural differences or diet shifts. In the present study, marked differences in diet between the two size modes of the observed size distribution were apparent. Whereas fish in the larger mode almost solely preyed on conspecifics, the corresponding diet of lower-mode fish was restricted to small invertebrates. Similar ontogenetic niche shifts have also been observed between the observed size modes of Arctic char in previous studies reporting bimodal size distributions (Parker and Johnson 1991; Svenning and Borgstrøm 1995; Hammar 2000). Similar but opposite-directed differences in motion pattern with size could also be triggered by antipredator behaviour of fish in the observed lower mode (L'Abée-Lund et al. 1993). As previously noted for arctic populations of Arctic char (e.g., Svenning and Borgstrøm 1995; Hammar 2000), the intermediate-sized individuals were lacking in the gillnet samples from Lake Trestikkelen. These fish were readily obtainable when we used electrofishing gear, indicating that their absence from gillnet samples results directly from behavioural restraints. Behavioural influence on gillnet selectivity is discussed in length by Finstad et al. (2000).

Population bimodality in Arctic char may provide an example of how erroneous interpretation of sampling can give rise to scientific theories elaborated to explain a nonexistent phenomenon. This emphasises the importance of methodological verification when obtaining population measures by passive sampling gear. Large alterations in sampling vulnerability can radically deceive the observer, particularly in animals with ontogenetic niche or habitat shifts or other nonrandom physiological or behavioural changes. This is especially important for the widely applied and economically important field of fisheries research, where information on population structure and abundance relies on catch-per-unit-effort methods. Limitations of stock assessment are known to have large applied consequences (e.g., Hutchings and Myers 1994; Shelton and Lilly 2000; Harley et al. 2001; Myers and Worm 2003).

Acknowledgments

We are grateful for the comments and corrections made by two anonymous referees. Per Harald Olsen is acknowledged for technical assistance in the field and Anne Cooper for comments on previous drafts of the manuscript. The staff at the Bjørnøya Meterological Station and the Norwegian Coast Guard provided logistic support. The fieldwork received financial support from the Norwegian National Committee on Polar Research.

References

Appelberg, M., Berger, H.M., Hesthagen, T., Kleiven, E., Kurkilahti, M., Raitaniemi, J., and Rask, M. 1995. Development and intercalibration of methods in Nordic freshwater fish monitoring. Water Air Soil Pollut. **85**: 401–406.

Finstad, A.G., Jansen, P.A., and Langeland, A. 2000. Gillnet selectivity and size and age structure of an alpine Arctic char (*Salvelinus alpinus*) population. Can. J. Fish. Aquat. Sci. **57**: 1718–1727.

Finstad, A.G., Jansen, P.A., and Hirvonen, H. 2003. Bimodal size distributions in Arctic char, *Salvelinus alpinus* (L.): artefacts of biased sampling. Can. J. Fishes. Aquat. Sci. **60**: 1104–1110.

Gatz, A.J., and Loar, J.M. 1988. Petersen and removal population size estimates: combining methods to adjust and interpret results when assumptions are violated. Environ. Biol. Fishes, **21**: 239–307.

Griffiths, D. 1994. The size structure of lacustrine Arctic charr (Pisces: Salmonidae) population. Biol. J. Linn. Soc. **51**: 337–357.

Hammar, J. 2000. Cannibals and parasites: conflicting regulators of bimodality in high latitude Arctic char, *Salvelinus alpinus*. Oikos, **88**: 33–47.

Harley, S.J., Myers, R.A., and Dunn, A. 2001. Is catch-per-unit-effort proportional to abundance? Can. J. Fish. Aquat. Sci. **58**: 1760–1772.

Hutchings, J.A., and Myers, R.A. 1994. What can be learned from the collapse of a renewable resource? Atlantic cod, *Gadus morhua*, of Newfoundland and Labrador. Can. J. Fish. Aquat. Sci. **51**: 2123–2146.

Jensen, J.W., and Hesthagen, T. 1996. Direct estimates of the selectivity of a multimesh and a series of single gillnets for brown trout. J. Fish Biol. **46**: 862–871.

Johnsen, B.O., and Ugedal, O. 1988. Effects of different kinds of fin-clipping on over-winter survival and growth of fingerling brown trout, *Salmo trutta* L., stocked in small streams in Norway. Aquacult. Fish. Manag. **19**: 305–311.

Johnson, L. 1983. Homeostatic characteristics of single-species fish stocks in Arctic lakes. Can. J. Fish. Aquat. Sci. **40**: 987–1024.

Kurkilahti, M., Appelberg, M., Hesthagen, T., and Rask, M. 2002. The effect of fish shape on gillnet selectivity: a study with Fulton's condition factor. Fish. Res. **54**: 153–170.

L'Abée-Lund, J.H., Langeland, A. Johnson, B., and Ugedal, O. 1993. Spatial segregation by age and size in Arctic char — a trade off between feeding possibilities and risk of predation. J. Anim. Ecol. **62**: 160–168.

Mears, H.C., and Hatch, R.W. 1976. Overwinter survival of fingerling brook trout with single and multiple fin clips. Trans. Am. Fish. Soc. **6**: 669–674.

Myers, R.A., and Worm, B. 2003. Rapid worldwide depletion of predatory fish communities. Nature (Lond.), **423**: 280–283.

O'Grady, M.F. 1984. The effects of fin-clipping, floyd-tagging and fin-damage on the survival and growth of brown trout (*Salmo trutta* L.) stocked in Irish lakes. Fish. Manag. **15**: 49–58.

Parker, H.H., and Johnson, L. 1991. Population structure, ecological segregation and reproduction in non-anadromous Arctic char, *Salvelinus alpinus* (L.), in four unexploited lakes in the Canadian High Arctic. J. Fish Biol. **38**: 123–147.

Parker, H.H., Noonburg, E.G., and Nisbet, R.M. 2001. Models of alternative life-history strategies, population structure and potential speciation in salmonid fish stocks. J. Anim. Ecol. **70**: 260–272.

© 2004 NRC Canada

Power, G. 1978. Fish population structure in arctic lakes. J. Fish. Res. Board Can. **35**: 53–59.

Ricker, W.E. 1975. Computation and interpretation of biological statistics of fish populations. Bull. Fish. Res. Board Can. No. 191.

Rudstam, G.L., Magnuson, J.J., and William, M.T. 1984. Size selectivity of passive fishing gear: a correction for encounter probability applied to gillnet. Can. J. Fish. Aquat. Sci. **41**: 1252–1255.

Shelton, P.A., and Lilly, G.R. 2000. Interpreting the collapse of the northern cod stock from survey and catch data. Can. J. Fish. Aquat. Sci. **57**: 2230–2239.

Svenning, M., and Borgstrøm, R. 1995. Population structure in landlocked Spitsbergen Arctic char. Sustained by cannibalism? Nord. J. Freshw. Res. **71**: 424–431.

© 2004 NRC Canada

Widespread consumption-dependent systematic error in fish bioenergetics models and its implications

Przemyslaw G. Bajer, Gregory W. Whitledge, and Robert S. Hayward

Abstract: Data from laboratory evaluations of seven fish bioenergetics models (BEMs) were used to investigate possible associations between BEM prediction error in relative growth rate (RGR_{error}) and levels of model input variables: mean daily food-consumption rate and fish body weight. Correlation between RGR_{error} and fish body weight was found in three BEMs applied under submaintenance feeding conditions. A strong correlation between RGR_{error} and mean daily consumption level was observed in all models over full consumption ranges; consumption level explained 70%–96% of variation in RGR_{error}. All BEMs underestimated (by 2- to 5-fold) growth at lower consumption levels and overestimated (by 2- to 3-fold) growth at higher consumption levels. RGR_{error} values associated with higher consumption levels were greater (up to 22 cal·g^{-1}·day^{-1}) than those at lower consumption levels (up to 10 cal·g^{-1}·day^{-1}). Correlation between consumption rate and RGR_{error} in all seven models indicates widespread systematic error among BEMs that likely arises from deficiencies in consumption-dependent model parameters. Results indicate that many BEMs are substantially inaccurate when predicting fish growth from higher feeding rates or estimating consumption from higher growth rates, even when higher consumption levels or growth episodes are of short duration. Findings obtained under submaintenance feeding conditions indicate that additional body-weight- and consumption-dependent terms should be added to BEM subequations for routine metabolism to account for metabolic reduction.

Résumé : Les données des évaluations en laboratoire de sept modèles bioénergétiques (BEM) de poissons nous ont servi à étudier les associations possibles entre l'erreur de prédiction par les BEM du taux relatif de croissance (RGR_{erreur}), d'une part, et la valeur des variables d'entrée des modèles, soit le taux journalier moyen de consommation de nourriture et la masse corporelle des poissons, d'autre part. Il existe une corrélation entre RGR_{erreur} et la masse corporelle des poissons dans trois des BEM utilisés dans des conditions d'alimentation inférieures au niveau de maintien (SMFC). Il y a aussi une forte corrélation entre RGR_{erreur} et le taux journalier moyen de consommation dans tous les modèles sur toute l'étendue des taux de consommation; le taux de consommation explique 70–96 % de la variation de RGR_{erreur}. Tous les BEM sous-estiment la croissance (par un facteur de 2–5) aux faibles taux de consommation et la surestiment (par un facteur de 2–3) aux taux de consommation plus élevés. Les RGR_{erreur} associées aux taux plus élevés de consommation sont plus grandes (pouvant atteindre 22 cal·g^{-1}·jour^{-1}) que celles liées aux taux de consommation plus faibles (atteignant 10 cal·g^{-1}·jour^{-1}). La corrélation entre le taux de consommation et RGR_{erreur} dans les sept modèles indique qu'il y a une erreur systématique générale dans les BEM qui provient vraisemblablement d'imprécisions des paramètres des modèles reliés à la consommation. Nos résultats montrent que plusieurs BEM sont erronés dans la prédiction de la croissance des poissons à partir des taux d'alimentation élevés et dans l'estimation de la consommation à partir de taux de croissance élevés, même lorsque les épisodes de forte consommation ou de forte croissance sont de courte durée. Dans les conditions SMFC, nos résultats indiquent qu'on doit ajouter aux sous-équations du métabolisme ordinaire des BEM des termes additionnels pour la masse corporelle et la consommation, afin de tenir compte de la réduction du métabolisme.

[Traduit par la Rédaction]

Introduction

Construction and application of fish bioenergetics models (BEMs) have increased substantially in the last decade (Hewett and Johnson 1987; Hanson et al. 1997; Bajer et al. 2004). Models for almost 40 fish species are now readily available through user-friendly software (Hanson et al. 1997) while many others exist in various formats. BEMs are appealing because they are based on balanced, energy-fate equations that have been thought to promote reasonable predictive behavior. These models have been widely used to evaluate factors that constrain fish growth (Hayward and

Received 6 August 2003. Accepted 27 July 2004. Published on the NRC Research Press Web site at http://cjfas.nrc.ca on 26 January 2005.
J17692

P.G. Bajer, G.W. Whitledge, and R.S. Hayward.[1] Department of Fisheries and Wildlife Sciences, 302 Anheuser–Busch Natural Resources Building, University of Missouri–Columbia, Columbia, MO 65211-7240, USA.

[1]Corresponding author (e-mail: HaywardR@missouri.edu).

 doi: 10.1139/F04-159 © 2004 NRC Canada

Margraf 1987; Hill and Magnuson 1990), impacts of fish predation on prey populations (Jones et al. 1993; Rand et al. 1995; Kershner et al. 1999), contaminant bioaccumulation in fishes (Jackson 1996), and waste loads from aquaculture (Axler et al. 1994). They have also been applied to enhance understanding of basic ecological processes such as the role of fish in lake nutrient cycling (Schindler and Eby 1997), and commonly serve as subcomponents of individual-based models of fish life history and population dynamics (Trebitz 1991; Rose and Cowan 1993) and other model types (Hayes et al. 2000; Burke and Rice 2002). Unquestionably, BEMs are contributing significantly to current perceptions of what is true in many of the less directly observable aspects of aquatic ecology, fisheries management, and aquaculture.

In fact, however, most BEMs have not been well evaluated over the ranges of conditions to which they have been applied. Rigorous, independent evaluations of BEMs under controlled laboratory conditions are disproportionately rare relative to the high and increasing number of times they have been applied. Laboratory-based tests of BEMs can greatly reduce the uncertainty inherent in field-based evaluations, because model input and output variables, including daily food consumption, growth rate, diet composition, predator and prey caloric densities, and fish thermal experience can be determined with much greater accuracy. Because laboratory evaluations are more likely to correctly identify errors in BEMs, they are essential for assuring model accuracy and for facilitating model improvement (Ney 1993; Bajer et al. 2003). Despite their limited number relative to field-based evaluations, laboratory evaluations of fish BEMs have provided valuable insights into model strengths and weaknesses. Such evaluations have indicated that BEM predictions may not be equally accurate over the ranges of conditions to which they are applied. For example, BEMs have exhibited varying degrees of performance associated with different ration levels (Cui and Wootton 1989; Whitledge and Hayward 1997), fish body weights (Bajer et al. 2004), and temperatures (Hartman and Brandt 1993; Chipps et al. 2000). However, experimental designs and analytical approaches used in laboratory evaluations have tended not to facilitate identification of error sources in BEMs, so model-improvement efforts have been rare.

A recent evaluation of two BEMs based on laboratory-derived consumption and growth data for yellow perch (*Perca flavescens*) (Bajer et al. 2003) showed that growth-prediction error was strongly correlated with mean daily food consumption (a BEM input variable) in both models. Both BEMs underestimated growth rate at lower consumption levels and overestimated growth rate at higher consumption levels, albeit to differing degrees. Madenjian and O'Connor (1999) found similar error in a lake trout (*Salvelinus namaycush*) BEM. Identification of consumption-dependent prediction error in these three BEMs suggests that their internal subequations for calculating energy costs of egestion, excretion, and specific dynamic action are likely error sources, because each involves consumption dependence (Bajer et al. 2003). In a yet more recent laboratory evaluation (Bajer et al. 2004), mean daily consumption level was again found to be correlated with growth-prediction error in a white crappie (*Pomoxis annularis*) BEM, explaining approximately 80% of total model prediction error. In this BEM, fish body weight was also found to be correlated with growth-prediction error, particularly for fish feeding at submaintenance levels.

Finding a similar correlation between growth-prediction error and consumption level in four BEMs suggested that consumption-dependent systematic error may be widespread among BEMs. To further substantiate this, we reevaluated data from published laboratory evaluations of three additional BEMs for the presence of consumption-dependent error. The presence of body-weight-dependent error, as was observed in the white crappie model, was also further explored in six BEMs. We show the frequency of occurrence of consumption- and body-weight-dependent error across a total of seven BEMs, and portray the range of magnitude of consumption-dependent error that exists among these models. Through modeling we also demonstrate the importance of consumption-dependent error in BEMs and show why its presence may often be overlooked in model evaluations. Types of BEM applications that may be most prone to this error are suggested, and insights are given into potential error sources within BEMs. Our findings demonstrate a critical need to evaluate and improve predictive accuracies of fish BEMs.

Materials and methods

We reevaluated data from published laboratory evaluations of three BEMs that provided sufficient information to explore possible consumption-dependent growth-prediction error. These include evaluations of BEMs for largemouth bass (*Micropterus salmoides*) (Whitledge and Hayward 1997), smallmouth bass (*Micropterus dolomieu*) (Whitledge et al. 2003), and bluegill (*Lepomis macrochirus*) (Whitledge et al. 1998). Data from laboratory evaluations of four additional BEMs for which consumption-dependent growth-prediction error has previously been identified were included so that the nature of this type of error could be broadly portrayed across a total of seven BEMs. These four evaluations involved BEMs for lake trout (Madenjian and O'Connor 1999), yellow perch and Eurasian perch (*Perca fluviatilis*) (Bajer et al. 2003), and white crappie (Bajer et al. (2004) this issue). Body-weight dependence of growth-prediction error, previously detected only in the white crappie BEM (Bajer et al. 2004), was explored in the six other BEMs identified above. We did not assess temperature influences (another primary BEM input variable) on prediction errors in the seven BEMs because, for the most part, laboratory evaluations of these models were performed over narrow temperature ranges (but see Bajer et al. 2004).

For each model, observed (RGR_O; cal·g^{-1}·day^{-1}, 1 cal = 4.184 J) and predicted (RGR_P; cal·g^{-1}·day^{-1}) relative growth rates were determined as

$$(1) \qquad RGR_O = \frac{O_f - O_i}{n\bar{O}} \cdot ED_{predator}$$

and

$$(2) \qquad RGR_P = \frac{P_f - O_i}{n\bar{O}} \cdot ED_{predator}$$

where O_f, P_f, and O_i are the observed and predicted final weights and observed initial fish weight for each modeling interval, respectively; $\bar{O}$ is the mean observed fish weight

© 2004 NRC Canada

Table 1. Experiment durations, total number of modeling intervals (number of fish × number of experimental intervals), and ranges of fish body weight, daily consumption level, and temperature for laboratory evaluations of bioenergetics models (BEMs).

BEM	Duration of exp. (days)	Total modeling interval	Fish body weight (g)	Daily consumption (% body weight·day^{-1}; cal·g^{-1}·day^{-1})[†]	Temp. (°C)	Model source
Largemouth bass	63*	24	141–292	1.4 –3.8 (17–46)	22, 27	Hanson et al. 1997
Smallmouth bass	63*	21	121–262	1.7–5.2 (16–48)	22, 27	Whitledge et al. 2003
Bluegill	105–112	42	9–52	0.6–2.2 (15–56)	24	Hanson et al. 1997
Lake trout	320–407	12	713–3240	0.2–1.2 (3.5–18)	3.1–10.2	Hanson et al. 1997
Yellow perch	125–144*	347	18–35	0–3.5 (0–77)	21	Hanson et al. 1997
Eurasian perch	125–144*	347	18–35	0–3.5 (0–77)	21	Karås and Thoresson 1992
White crappie	63–70*	39	72–341	0.5–7.3 (4.3–91)	23–30	Bajer et al. 2004

*Study for which values of relative growth rate error (RGR_{error}; cal·g^{-1}·day^{-1}) were determined separately over multiple 10- to 21-day experiment subintervals for which temperature and applied ration levels were constant. For other studies RGR_{error} values were determined over the full modeled growth trajectories. In such cases the number of modeled intervals equals the number of fish used in experiments. References containing details on each BEM are provided.

†1 cal = 4.184 J.

during the interval; n is the number of days in the modeling interval; and $ED_{predator}$ is fish energy density (cal·g^{-1}). The relative growth-rate-prediction error (RGR_{error}; cal·g^{-1}·day^{-1}) was calculated as the difference between predicted and observed relative growth rates ($RGR_{error} = RGR_P - RGR_O$) for each model.

For all but the lake trout model, values of RGR_O, RGR_P, and RGR_{error} were determined from multiple model-predicted and laboratory-observed growth trajectories of individual fish. For the lake trout model these values were calculated from group means of initial and final fish body weights reported in Madenjian and O'Connor (1999, their tables 3 and 4). Durations of modeling intervals used for calculating RGR_O, RGR_P, and RGR_{error} were the same as those used in the original evaluation studies (Table 1); some studies (lake trout, Madenjian and O'Connor 1999; hybrid bluegill, Whitledge et al. 1998) used single modeling intervals that spanned the full durations of experiments, while others involved multiple subintervals for which temperature and fish feeding levels were consistent (Table 1).

To permit direct comparisons of error among models, RGR_{error} values were expressed in cal·g^{-1}·day^{-1} (converted from g·g^{-1}·day^{-1}) to standardize for differences in fish energy densities across the seven model-evaluation data sets. Values of fish energy density were determined as in the original BEM-evaluation studies. Fish energy densities were modeled as constant values in published laboratory evaluations of the bluegill, largemouth bass, and smallmouth bass BEMs. Various values of fish energy density were used in the published evaluations of BEMs for lake trout, yellow perch, Eurasian perch, and white crappie.

For each BEM, RGR_{error} values were regressed against corresponding mean observed daily consumption rates (cal·g^{-1}·day^{-1}) across all modeling intervals. Regressions of RGR_O and RGR_P values against corresponding mean observed daily consumption rates were also performed for each BEM so that both proportional and absolute BEM prediction error could be determined across consumption levels. A third set of regressions was performed to explore possible relationships between RGR_{error} values and corresponding mean observed fish body weights for each model. For each BEM, regressions involving fish body weight were run over full ranges of consumption level and separately over submaintenance feeding conditions when these were present.

Errors for BEM estimates of consumption were not evaluated because these have consistently been of similar magnitude as RGR_{error} values over broad ranges of conditions, but in the opposite direction (Bajer et al. 2003; Bajer et al. 2004). When significant relationships have been observed between RGR_{error} and consumption level or fish body weight, corresponding relationships between consumption-prediction error and these two input variables have been likewise significant but with slopes of opposite sign (Bajer et al. 2004).

We demonstrate the effect that even short periods of relatively high consumption level can have on growth-prediction error when a BEM containing consumption-dependent error is used. We used the bluegill BEM (Hanson et al. 1997) to predict observed 22-day growth trajectories for two groups of hybrid bluegill (F_1 female *Lepomis cyanellus* × male *L. macrochirus*), one in which fish fed consistently at low to moderate rates (control group) and a second in which fish fed at relatively high rates over an early portion of the 22-day interval (treatment group). Daily food-consumption and growth data for the hybrid bluegill were obtained from a selected 22-day segment of a 105-day laboratory experiment (Whitledge et al. 1998). Control fish that had been fed continually ad libitum before and during the 22-day period consumed only 1.0%–1.9% body weight·day^{-1}, on average, throughout the 22 days. In contrast, the treatment group that was food-deprived for 14 days just prior to the 22-day period consumed, on average, 8.0% body weight·day^{-1} on the first day of refeeding, whereupon consumption rates declined to 3.5% and 1.6% (moderate feeding levels) by days 12 and 22, respectively. Mean body weights of control and treatment fish were similar (15.9 and 17.3 g, respectively), and both groups experienced a constant temperature of 24 °C. A mean body weight trajectory (g) was predicted by the bluegill BEM for each group based on known temperature and directly determined group-specific mean daily food consumption (g). The accuracy of growth predictions was evaluated by comparing predicted and observed mean growth trajectories for each group. Predictive error was presented as the percent difference between predicted and observed mean

© 2004 NRC Canada

Table 2. Coefficients and statistics for regression relationships between RGR_{error} (cal·g^{-1}·day^{-1}; 1 cal = 4.184 J) and mean daily consumption rate (MCON; cal·g^{-1}·day^{-1}) for each of the seven BEMs evaluated.

BEM	β_0	β_1	F	df	r^2
Largemouth bass	–7.58	0.42	104.9	1, 22	0.82
Smallmouth bass	–6.87	0.28	56.2	1, 19	0.74
Bluegill	–21.1 (–5.65)	6.11 (0.17)	561.5	1, 40	0.93
Lake trout	–3.43 (–1.60)	1.76 (0.19)	235.1	1, 10	0.96
Yellow perch	–11.5	0.45	1808.9	1, 345	0.83
Eurasian perch	–8.32	0.26	815.2	1, 345	0.70
White crappie	–5.99	0.32	180.3	1, 37	0.83

Note: All regression relationships were highly significant ($p < 0.0001$). Regression relationships for all BEMs were linear ($RGR_{error} = \beta_0 + \beta_1 \cdot MCON$), except for the lake trout and bluegill models, which were of the form $RGR_{error} = \beta_0 + \beta_1 \cdot \ln(MCON)$. To facilitate comparisons of coefficient values among all seven models, β_0 and β_1 values for linear regression models are also shown parenthetically for the bluegill and lake trout models (linear models fit the data reasonably well for these two BEMs).

body weights (g) on each day of the 22-day modeling interval for both groups.

Results

Significant positive regression relationships were observed between RGR_{error} values and corresponding mean daily consumption levels for all seven BEMs (Table 2). Mean daily consumption level accounted for between 70% (Eurasian perch BEM) and 96% (lake trout BEM) of the total variation in RGR_{error} across all models. All BEMs underestimated growth rates at lower ration levels and overestimated growth at higher ration levels (Fig. 1), clearly demonstrating the widespread presence of systematic model error. Models exhibited zero RGR_{error} at intermediate consumption levels, which varied among the models for different species, and ranged from 8 cal·g^{-1}·day^{-1} for the lake trout model to about 35 cal·g^{-1}·day^{-1} for the bluegill and yellow perch models. Slopes of regression models relating RGR_{error} to mean daily consumption level varied more than 2-fold across the seven BEMs (Table 2); higher slope values indicated a greater tendency for a BEM to over- and under-estimate growth rates at higher and lower consumption levels, respectively. Regression slopes were lowest for the bluegill (0.17) and lake trout (0.19) models and highest for the yellow perch (0.45) and largemouth bass (0.42) models.

Over- and under-estimation of growth rates at high and low ration levels were substantial. At higher consumption levels (35–80 cal·g^{-1}·day^{-1}) the most-error-prone yellow perch model overestimated observed relative growth rates by 2- to 3-fold (5–21 cal·g^{-1}·day^{-1}), while the least-error-prone bluegill model overestimated growth rates by 15%–50% (0.7–5 cal·g^{-1}·day^{-1}; Fig. 2). At lower consumption levels (<12 cal·g^{-1}·day^{-1}) RGR_{error} values expressed on proportional bases were even greater; the yellow perch and bluegill BEMs underestimated observed growth rates by 5- and 2.5-fold, respectively. However, these higher proportional errors at low consumption levels arose mainly from the effect of lower observed growth rates in denominators; absolute errors associated with low consumption levels were generally lower (approximately 6 cal·g^{-1}·day^{-1}) than those associated with higher consumption levels (Fig. 2). RGR_{error} values observed for the other five models were intermediate to those determined for the yellow perch and bluegill models.

The white crappie BEM had exhibited a significant positive relationship ($p \leq 0.0001$) between RGR_{error} and observed mean body weight, but only under conditions where fish were feeding at submaintenance levels (see Bajer et al. 2004). Likewise, no significant body-weight dependence of RGR_{error} was found for any of the six other BEMs ($p > 0.05$) when evaluation data sets included broad ranges of consumption levels. However, the yellow perch and Eurasian perch models, whose evaluations also included fish fed at submaintenance levels, both also showed significant positive linear relationships ($p < 0.05$) between RGR_{error} and mean body weight under submaintenance feeding conditions. For both models, as for the white crappie model, weight loss was more substantially overpredicted for smaller fish than for larger fish. Hence, all three of the BEMs whose evaluations included submaintenance feeding showed similar body-weight dependencies under these conditions.

When applied to the control hybrid bluegill group that fed continually at low to moderate levels (1.0%–1.9% body weight·day^{-1}), the least-error-prone bluegill BEM accurately predicted mean growth rate over the 22-day period. The growth prediction error remained below 2.5% of observed mean body weight (Fig. 3*a*). However, the same model severely overestimated growth of the treatment hybrid bluegills, whose consumption level was initially high (8% body weight·day^{-1}) but then declined over the 22-day period to levels similar to those of control fish. The growth prediction error for this group reached 29% of observed mean body weight by the end of the 22-day simulation (Fig. 3*b*). Of the total growth-prediction error that had accumulated by the end of the 22-day model run for treatment fish, 66% and 93% developed within the first 7 and 14 days of the simulation, when daily consumption levels averaged 5.75% and 3.39% body weight·day^{-1}, respectively (Fig. 4). Relatively little additional error accumulated during the final 8 days of simulation, when consumption levels were mostly moderate (between 1.64% and 2.77% body weight·day^{-1}), indicating that model predictions were essentially in agreement with the observed growth pattern during this time. The substantial error that accumulated during simulation days 1–14 under higher consumption levels was not diminished by the lower

© 2004 NRC Canada

Fig. 1. Relationships between relative growth rate prediction error (RGR_{error}; the difference between predicted and observed relative growth rates (cal·g^{-1}·day^{-1}; 1 cal = 4.184 J)) and mean daily consumption rate (also cal·g^{-1}·day^{-1}) determined from laboratory evaluations of seven bioenergetics models (BEMs). (*a*) Bluegill, *Lepomis macrochirus* (Whitledge et al. 1998). (*b*) Lake trout, *Salvelinus namaycush* (Madenjian and O'Connor 1999). (*c*) Largemouth bass, *Micropterus salmoides* (Whitledge and Hayward 1997). (*d*) Smallmouth bass, *Micropterus dolomieu* (Whitledge et al. 2003). (*e*) Yellow perch, *Perca flavescens* (●), and Eurasian perch, *Perca fluviatilis* (○) (Bajer et al. 2003). (*f*) White crappie, *Pomoxis annularis* (Bajer et al. 2004).

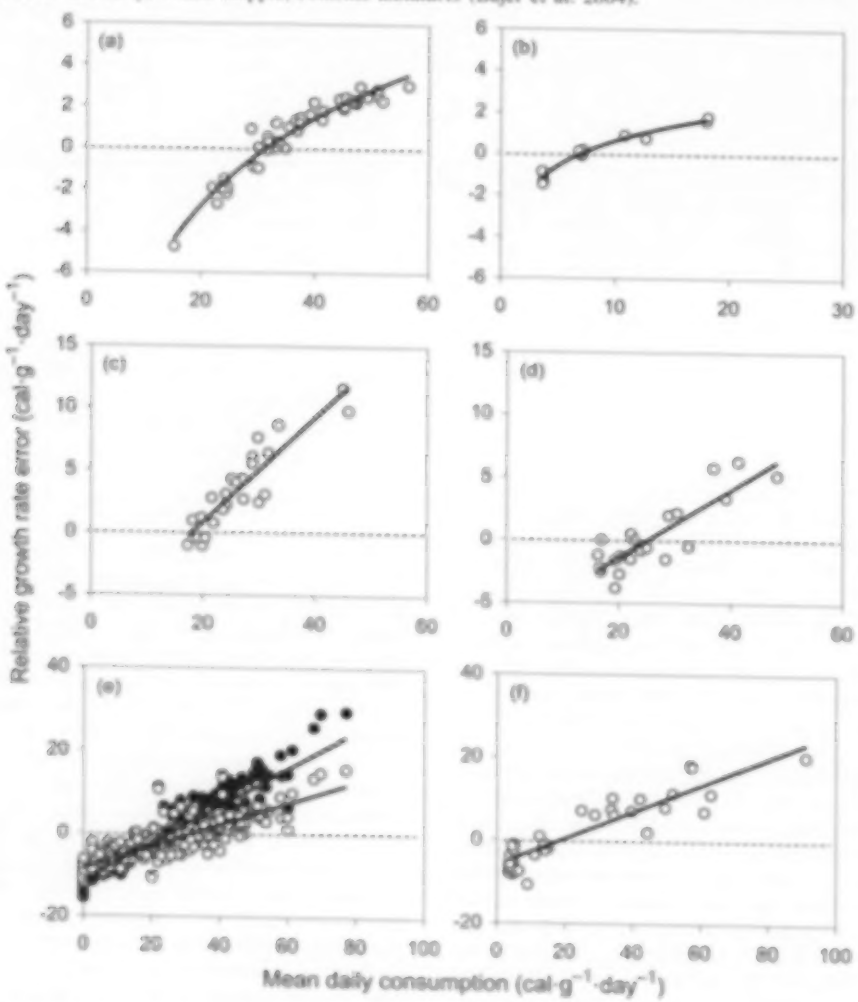

consumption levels that followed in the final 8 days of the modeling interval.

Discussion

Results showed that all seven of the examined BEMs contained systematic error that was associated with consumption rate. Finding significant positive relationships between food-consumption level and RGR_{error} that transected zero-error reference lines in all seven models indicates that consumption-dependent error is common among BEMs. This apparently widespread error can be substantial, resulting in over- or under-estimation of growth rates by as much as 2- to 5-fold when these models are applied under conditions involving relatively high or low consumption levels. Less, but potentially important error can occur at intermediate consumption levels as well. We expect that the errors in predicting fish growth rates that we observed will be of similar magnitude when BEMs are used to estimate consumption levels from high or low growth rates, except in the opposite direction, as demonstrated for the white crappie model by Bajer et al. (2004). Symmetry of consumption- and growth-prediction error (relative to the zero-error axis) tends to result under a given set of growth conditions because growth and consumption variables occur on opposite sides of the energy-balance equation at the core of BEMs; for example, underestimation of a fish's energy costs by a BEM will lead to overestimation of its growth and underestimation of its energy consumption.

Although our findings showed that BEM predictions of growth rate became substantially inaccurate at both high and low consumption levels, predictive inaccuracy was greatest

© 2004 NRC Canada

Fig. 2. Comparisons of observed (●) and BEM-predicted (○) relative growth rates (cal·g^{-1}·day^{-1}; 1 cal = 4.184 J) in relation to mean daily consumption rates (also cal·g^{-1}·day^{-1}) determined from laboratory evaluations of BEMs for bluegill, *Lepomis macrochirus* (Whitledge et al. 1998) (*a*), and yellow perch (Bajer et al. 2003) (*b*). Among all seven BEMs considered, the accuracy of growth predictions versus consumption level was greatest (the least difference between observed and predicted regression lines) for the bluegill model and lowest for the yellow perch model.

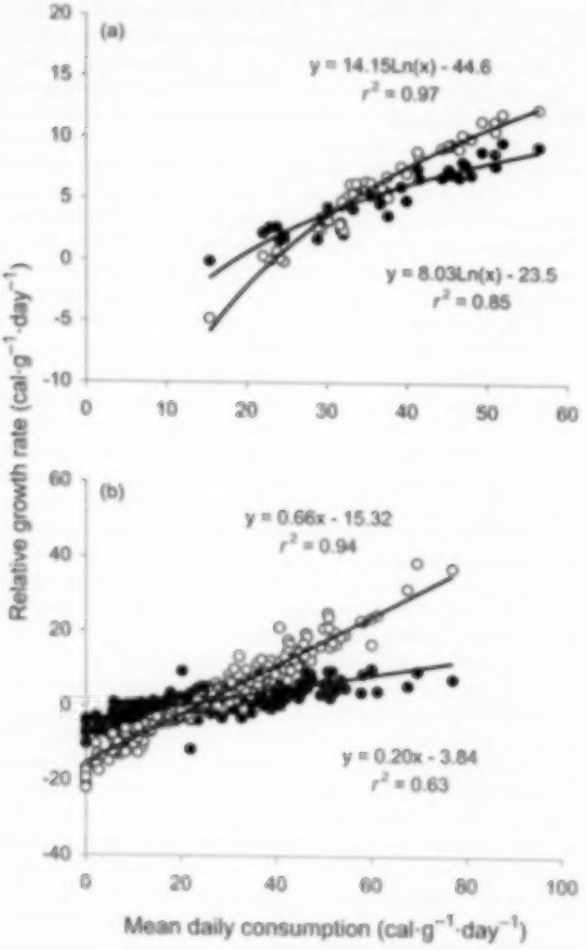

Fig. 3. Observed 22-day mean body weight trajectories for hybrid bluegill (F_1; female *Lepomis cyanellus* × male *L. macrochirus*) (solid lines) and corresponding predicted trajectories from a bluegill (*L. macrochirus*) BEM (broken lines) for the control group (*a*) and treatment group (*b*). Control fish consumed food at uniform low to moderate rates (1.0%–1.9% body weight·day^{-1}) over the 22 days; treatment fish were caused to become hyperphagic and initially consumed food at high rates over days 1–7 (8.0%–3.8% body weight·day^{-1}), after which their consumption rates gradually declined to those of the control fish.

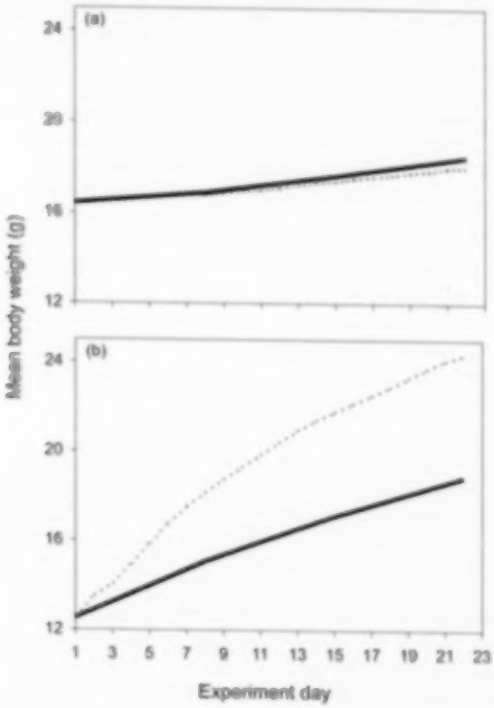

under conditions of higher consumption because here, absolute error rates were highest even though relative error was often greater under low-consumption conditions. For example, the yellow perch BEM under- and over-estimated observed growth rates by the same relative magnitude (2.9-fold) at consumption levels of 21 and 60 cal·g^{-1}·day^{-1}, respectively. However, in absolute terms (in cal·g^{-1}·day^{-1}), predictive error was nearly 20 times greater at the higher versus the lower consumption level (16 and 0.9 cal·g^{-1}·day^{-1}, respectively). Likewise, we expect that predictions of consumption will be most severely underestimated when high growth rates are entered into BEMs.

Because of the high magnitude of BEM prediction errors under conditions of high growth or consumption rates, even relatively short episodes of these conditions within a modeling interval can result in substantial overall predictive inaccuracy. Moreover, such error effects of high growth or consumption conditions, once incurred, are not likely to diminish even if lower growth rates and consumption levels follow in the modeling interval, because of their lesser opposing effects. When the bluegill BEM was applied to the treatment-group hybrid bluegill, growth of these fish, which fed at high rates (4.0%–8.0% body weight·day^{-1}) over the initial 7 days of the 22-day modeling interval, was substantially overestimated. Despite subsequent declining consumption rates that ultimately reached lower levels over the remaining 15 days, the prediction error that had mostly accumulated early on, persisted throughout the entire modeling interval. Hence, initially accumulated error was not offset by the subsequent improvement of model performance. In contrast, model predictions for the control group of hybrid bluegills that did not experience initially high consumption rates were very accurate. These results also demonstrate that a restricted period of high consumption can lead to substantial and sustained inaccuracy of BEM predictions, even for models that are otherwise capable of producing accurate growth

© 2004 NRC Canada

Fig. 4. Cumulative error (percentage of observed body weight) for bluegill (*Lepomis macrochirus*) BEM predictions of the observed 22-day mean weight trajectory of treatment-group hybrid bluegill (F_1; female *Lepomis cyanellus* × male *L. macrochirus*). Hybrid bluegill were fed at high levels (8.0%–3.8% body weight·day^{-1}) during days 1–7, moderate levels (4.25%–2.11%) during days 8–14, and lower levels (2.77%–1.64%) throughout the remaining 8 days.

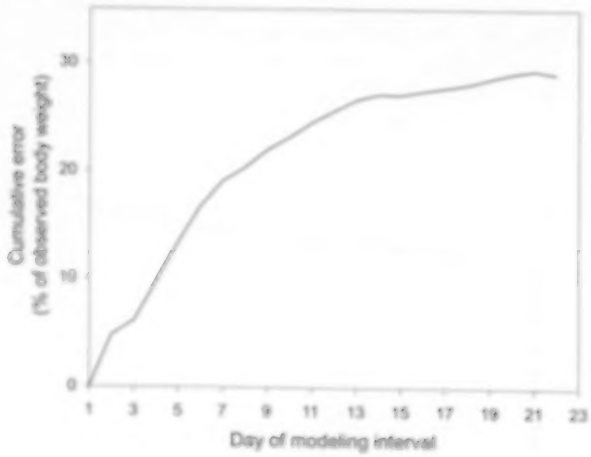

predictions under more moderate consumption levels. The same would be expected for estimates of a fish's cumulative consumption over modeling intervals that include short episodes of rapid growth. The observations highlight the importance of evaluating BEMs over the full ranges of growth conditions under which they may be applied, to avoid the misperceptions of overall BEM predictive accuracy that can result if models are tested only under conditions of moderate growth and consumption.

Modeling of hybrid bluegill growth also demonstrated that even the BEM containing the least systematic error among the seven evaluated, the bluegill BEM, was capable of producing substantially erroneous predictions when applied to a relatively short episode of high consumption rate. Prediction errors from the six other BEMs would have been greater if they had been applied under comparable conditions. In general, users should not assume that BEMs will yield equally accurate predictions across all consumption levels and should be cautious about applying them beyond the ranges of conditions under which their performance has been rigorously evaluated.

That many BEMs may be substantially inaccurate, particularly when applied under high or low consumption and growth conditions, suggests a number of common application settings where important predictive error would be expected. First, however, in-situ estimates of the consumption rates of fish (i.e., not from BEMs) indicate that episodes of both high and low consumption levels may commonly occur in a variety of natural aquatic environments (e.g., Hayward and Margraf 1987; Weiland and Hayward 1997; Whitledge and Hayward 2000). Consequently, applications of BEMs to natural fish populations in general are likely to involve episodes of high and low consumption levels, particularly during growing seasons, when water temperatures permit fish consumption levels to range broadly.

BEMs used to estimate the predatory demand of fish populations would appear to be particularly vulnerable to substantial inaccuracy. Predatory demand is the amount of food required by individual fish, and ultimately whole populations, to achieve maximum growth rates. This metric is used to estimate the prey biomass that a population would consume over a time period if sufficient prey were available (Ney 1993). The inference from our results is that BEMs could yield substantial underestimates of predatory demand because when growth rates are high, corresponding consumption rates would be severely underestimated. Consequently, BEM-based estimates of predator population biomasses that could be supported by local prey populations would be substantially overestimated. Management policies based on such results could pose a serious risk of overexploiting local prey populations and destabilizing existing predator–prey balances. The ecological and economic implications of such modeling errors could be serious, particularly for large systems such as the Great Lakes, where large-scale BEM-based predictions of predatory demand have been applied to ecologically and commercially important fish species.

The accuracy of spatially explicit modeling of fish growth rate potentials could also be impacted by BEM error trends observed in our evaluations. Such modeling combines the results of BEMs and foraging models implemented with spatially (the environment is divided into grid cells) and temporally varying inputs of temperature, prey abundance, and prey size to produce maps of spatial growth potentials. Our results indicate that modeled growth potentials for environmental cells offering very good and poor consumption conditions could be substantially over- and under-estimated, respectively, leading to overrepresentation of the extent to which growth conditions vary over space and time.

Applications of BEMs in aquaculture settings, where fish are typically fed and grown at high rates, may also be particularly error-prone. Uses of BEMs not only to predict fish growth and consumption rates but also to assess the impacts of aquaculture on, for example, water quality according to modeled fish egestion and excretion rates may be affected. Also, BEMs are being used increasingly as components of broader models relating to fisheries management, aquatic ecology, and aquaculture. The impacts of the systematic error that we have observed in BEMs on the accuracy of predictions and the insights generated by models that incorporate BEMs are likely variable and currently unknown. Potential effects of widespread systematic error in BEMs should be carefully considered when either constructing or applying models that contain BEMs as subcomponents.

If the subequation that calculates energy cost or loss for a given parameter within a BEM is erroneous, the overall prediction error of the BEM will tend to be correlated with the input variable that drives the erroneous subequation. Consequently, the consumption-dependent prediction error observed in the seven BEMs likely emanates from inaccuracies in subequations for calculating egestion (F), excretion (U), or specific dynamic action (SDA), because these are consumption-dependent parameters in the seven models, and in most other BEMs. Brett and Groves (1979) provided labo-

© 2004 NRC Canada

ratory evidence that fish fed at near-maximum rates have SDA costs that approach those of resting routine metabolism. That such levels of SDA were observed under high-consumption conditions in the seven models that we evaluated, including the most-error-prone yellow perch model (Bajer et al. 2003, their Figs. 4*b* and 4*d*), suggests that SDA was appropriately calculated under conditions where BEM errors were greatest. However, Beamish and Trippel (1990) advised that SDA could represent substantial portions of fish energy budgets and vary widely (3%–41%) in response to a number of variables including energy intake, fish body weight, composition of the diet, and environmental factors such as temperature. They suggested that the practice of calculating SDA costs as constant proportions of gross or digestible energy intake in BEMs may be inappropriate oversimplification. Given the substantial role that SDA can play in energy budgets and the uncertainty with which it is accurately determined in BEMs, its potential involvement in the consumption-dependent error in BEMs cannot be dismissed.

BEM outputs have been reported as being relatively insensitive to modest percent changes in parameter values for determining F and U (Kitchell et al. 1977; Bartell et al. 1986; Adams and Breck 1990). This view has fostered a tendency to not put forth new efforts to develop best possible species-specific estimators of F and U when new BEMs have been constructed (to a certain extent this applies to SDA as well). Instead, equation forms and even coefficient values for determining F and U have been liberally "borrowed" (sensu Ney 1993) across BEMs. All of the BEMs that we evaluated, with the exception of the Eurasian perch model (Karås and Thoresson 1992), estimate F and U largely from equations developed by Elliott (1976) for brown trout (*Salmo trutta*) or from a simplified version of these (Kitchell et al. 1977). We suspect that BEM inaccuracies due to errors in calculating F and U may not always be negligible as has been suggested. The relatively minor effects of inaccurate determinations of F and U at low to moderate consumption levels may become more pronounced if these parameters sometimes reach much higher levels. Recently, Bajer et al. (2003) found indirect evidence that energy losses associated with F and U constituted substantial portions of yellow perch energy budgets (being higher than both routine metabolism and SDA) at higher consumption levels (3% body weight·day^{-1}), indicating a setting for potentially greater impacts when these parameters are inaccurately determined. Perhaps most insightful, however, is an observation from a recent reexamination of the methods of Elliott (1976), the source study for most F and U calculations in BEMs. It was observed that test fish were food-deprived for up to 3 days prior to feeding, an experimental condition that may have resulted in the determination of anomalously low egestion rates, including at higher consumption levels (James Breck, Michigan Department of Natural Resources, 1109 North University Avenue, Ann Arbor, MI 48109-1084, USA, personal communication).

Unaccounted-for activity costs that may increase with food-consumption level and declining relative prey size (e.g., Kerr 1971; Brett and Groves 1979; Sherwood et al. 2002) cannot be totally dismissed as potential contributors to the consumption-dependent error that we observed in the seven BEMs. However, we consider these unlikely sources of this error. Consumption-dependent prediction error was observed when BEMs were applied to fish consuming evasive (other fish) as well as non-evasive (mealworms) prey types; the magnitudes of model prediction errors were in some cases higher when applied to fish consuming non-evasive prey. We also found no relationship between the magnitude of BEM error (slope of error regressions) and the relative size of prey used in experiments. Such a relationship might be expected if increased feeding-activity cost was incurred as fish were forced to eat prey of progressively smaller relative size, owing to the need to consume more prey items (Sherwood et al. 2002). Moreover, we note that increases in fish activity costs would have had to be very substantial to account for observed growth-prediction errors at high consumption levels. For example, we determined that white crappie metabolic rates would have had to increase substantially (activity multiplier >2) relative to routine resting metabolism to account for the observed growth-prediction errors at high consumption levels. This amount of activity-cost increase seems highly unlikely considering that the fish used to evaluate the white crappie BEM were held individually (without costs of aggression) in relatively small experimental chambers (where movement was limited), and had ready access to their prey. We routinely observed these fish and saw little evidence of substantial activity. Fish used to evaluate five of the six other BEMs (largemouth bass, smallmouth bass, bluegill, yellow perch, and Eurasian perch) were also held individually in chambers that limited their movement during evaluation experiments. Consequently, we believe that efforts to fundamentally improve BEMs should focus first on laboratory studies to develop better estimators of F and U that are applicable over broad ranges of consumption level, fish body weight, temperature, and prey type.

Growth-rate underestimation by BEMs occurred when fish were provided substantially restricted rations. Under low-consumption conditions, BEM errors associated with F, U, and SDA should be low because each of these parameters is calculated as a fraction of consumption level. We suspect that model error under these conditions is related to the general inability of BEMs to accommodate the reductions in resting routine metabolism that are known to occur in many fish species during periods of submaintenance feeding in order to conserve energy (Beamish 1964; Glass 1968; Mehner and Wieser 1994). Our finding of consistent body-weight-dependent overprediction of weight loss under submaintenance conditions also indicates that smaller fish reduce their metabolic rates more substantially under weight-loss conditions than do their larger counterparts. Development of consumption- and body-weight-dependent subequations that describe reductions in routine metabolic costs under submaintenance feeding conditions would improve predictions of growth and consumption by BEMs under these conditions.

An efficient approach for reducing systematic error in BEMs that is associated with consumption level or other input variables (e.g., fish body weight and temperature) may be to develop correction equations as was done for the white crappie model (Bajer et al. 2004). Regression-based error-correcting equations were developed for the white crappie BEM from model prediction errors determined from comparisons of predicted and observed growth responses when

© 2004 NRC Canada

white crappie of a range of sizes were reared at different feeding levels and temperatures. The correction approach is efficient because (*i*) a model's overall error is reduced without the need to consider specific error sources, and (*ii*) the data set used to initially evaluate a BEM can also provide the information required to develop correction equations. In contrast, efforts to fundamentally improve BEMs will likely require one data set to evaluate a model's prediction error and distinct data sets to improve the subequations for each erroneous parameter.

Finally, we note that the experimental designs in the published laboratory studies used to evaluate most of the BEMs were incomplete, as they did not encompass the full arrays of conditions under which these models may be applied. Most notably, analyses of possible temperature effects on model performance were not possible in most cases. In addition, testing of models under conditions where fish fed at submaintenance levels was restricted to a few models, all of which showed body-weight dependence of growth-prediction error under these conditions. Laboratory evaluations of BEMs should include conditions of weight loss. Also, possible effects of food type on model performance could not be fully evaluated because single prey types were used during each of the model evaluations. Further work is needed to evaluate temperature, submaintenance-feeding, and prey-type effects on the performance of BEMs, as well as possible influences of activity level. More optimal experimental designs for BEM evaluation are described by Bajer et al. (2004).

Acknowledgements

Funding for this work was provided in part by research grants to R.S. Hayward from the Missouri Department of Conservation and the North Central Regional Aquaculture Center. We thank James Breck for helpful insights and suggestions relating to this study, and Marc Trudel for providing a thorough review of the manuscript.

References

Adams, S.M., and Breck, J.E. 1990. Bioenergetics. *In* Methods for fish biology. *Edited by* C.B. Schreck and P.B Moyle. American Fisheries Society, Bethesda, Md. pp. 389–415.

Axler, R., Owe, C., Ameel, J., Ruzycki, E., and Henneck, J. 1994. Water quality issues associated with aquaculture: a case study in Minnesota mine pit lakes. Lake Reservoir Manag. **9**: 53.

Bajer, P.G., Whitledge, G.W., Hayward, R.S., and Zweifel, R.D. 2003. Laboratory evaluation of two bioenergetics models applied to yellow perch (*Perca flaviatilis*): identification of a major source of systematic error. J. Fish Biol. **62**: 436–454.

Bajer, P.G., Hayward, R.S., Whitledge, G.W., and Zweifel, R.D. 2004. Simultaneous evaluation and improvement of a bioenergetics model for white crappie (*Pomoxis annularis*). Can. J. Fish. Aquat. Sci. **61**: xxxx–xxxx. This issue.

Bartell, S.M, Breck, J.E., Gardner, R.H., and Brenkert, A.L. 1986. Individual parameter perturbation and error analysis of fish bioenergetics models. Can. J. Fish. Aquat. Sci. **43**: 160–168.

Beamish, F.W.H. 1964. Influence of starvation on standard and routine oxygen consumption. Trans. Am. Fish. Soc. **93**: 103–107.

Beamish, F.W.H., and Trippel, E.A. 1990. Heat increment: a static or dynamic dimension in bioenergetics models? Trans. Am. Fish. Soc. **119**: 649–661.

Brett, J.R., and Groves, D.D. 1979. Feeding metabolism. *In* Fish physiology. Vol. 8. Bioenergetics and Growth. *Edited by* W.S. Hour, D.J. Randall, and J.R. Brett. Academic Press, New York. pp. 298–305.

Burke, B.J. and Rice, J.A. 2002. A linked foraging and bioenergetics model for southern flounder. Trans. Am. Fish. Soc. **131**: 120–131.

Chipps, S.R., Einfalt, L.M., and Wahl, D.H. 2000. Growth and food consumption by tiger muskellunge: effects of temperature and ration level on bioenergetic model predictions. Trans. Am. Fish. Soc. **129**: 186–193.

Cui, Y., and Wootton, R.J. 1989. Bioenergetics and growth of a cyprinid, *Phoxinus phoxinus* (L.): development and testing of a growth model. J. Fish Biol. **34**: 47–64.

Elliott, J.M. 1976. Energy losses in waste products of brown trout (*Salmo trutta* L.). J. Anim. Ecol. **45**: 561–580.

Glass, N.R. 1968. The effect of time of food deprivation on the routine oxygen consumption of largemouth black bass (*Micropterus salmoides*). Ecology, **49**: 340–343.

Hanson, P.C., Johnson, T.B., Schindler, D.E., and Kitchell, J.F. 1997. Fish bioenergetics 3.0. University of Wisconsin Sea Grant Institute, Madison.

Hartman, K.J., and Brandt, S.B. 1993. Systematic sources of bias in a bioenergetics model: examples for age-0 striped bass. Trans. Am. Fish. Soc. **122**: 912–926.

Hayes, J.W., Stark, J.D., and Shearer, K.A. 2000. Development and test of a whole-lifetime foraging and bioenergetics growth model for drift-feeding brown trout. Trans. Am. Fish. Soc. **129**: 315–332.

Hayward, R.S., and Margraf, F.J. 1987. Eutrophication effects on prey size and food available to yellow perch in Lake Erie. Trans. Am. Fish. Soc. **116**: 210–223.

Hewett, S.W., and Johnson, B.L. 1987. A generalized bioenergetics model of fish growth for microcomputers. Sea Grant Tech. Rep. No. WISCG-87-245, University of Wisconsin, Madison.

Hill, D.K., and Magnuson, J.J. 1990. Potential effects of global climate warming on the growth and prey consumption of Great Lakes fishes. Trans. Am. Fish. Soc. **119**: 265–275.

Jackson, L.J. 1996. How will decreased alewife growth rates and salmonid stocking affect sport fish PCB concentrations in Lake Ontario. Environ. Sci. Technol. **30**: 701–705.

Jones, M.L., Koonce, J.F., and O'Gorman, R. 1993. Sustainability of hatchery-dependent salmonine fisheries in Lake Ontario: the conflict between predatory demand and prey supply. Trans. Am. Fish. Soc. **122**: 1002–1018.

Karås, P., and Thoresson, G. 1992. An application of a bioenergetics model to Eurasian perch (*Perca fluviatilis* L.). J. Fish Biol. **41**: 217–230.

Kerr, S.R. 1971. Analysis of laboratory experiments on growth efficiency of fishes. J. Fish. Res. Board Can. **28**: 801–808.

Kershner, M.W., Schael, D.M., Knight, R.L., Stein, R.A., and Marschall, E.A. 1999. Modeling sources of variation for growth and predatory demand of Lake Erie walleye (*Stizostedion vitreum*), 1986–1995. Can. J. Fish. Aquat. Sci. **56**: 527–538.

Kitchell, J.F., Stewart, D.J., and Weininger, D. 1977. Applications of a bioenergetics model to yellow perch (*Perca flavescens*) and walleye (*Stizostedion vitreum*). J. Fish. Res. Board Can. **34**: 1922–1935.

Madenjian, C.P., and O'Connor, D.V. 1999. Laboratory evaluation of a lake trout bioenergetics model. Trans. Am. Fish. Soc. **128**: 802–814.

Mehner, T., and Wieser, W. 1994. Energetics and metabolic correlates of starvation in juvenile perch (*Perca fluviatilis*). J. Fish Biol. **45**: 325–333.

Ney, J.J. 1993. Bioenergetics modeling today: growing pains on the cutting age. Trans. Am. Fish. Soc. **122**: 736–748.

© 2004 NRC Canada

Rand, P.S., Stewart, D.J., Lantry, B.F., Rudstam, L.G., Johannsson, O.E., Goyke, E.P. et al. 1995. Effect of lake-wide planktivory by the pelagic prey fish communities in Lakes Michigan and Ontario. Can. J. Fish. Aquat. Sci. **57**: 1546–1563.

Rose, K.A., and Cowan, J.H., Jr. 1993. Individual-based model of young-of-the-year striped bass population dynamics. I. Model description and baseline simulations. Trans. Am. Fish. Soc. **122**: 415–438.

Schindler, D.E., and Eby, L.A. 1997. Stoichiometry of fishes and their prey: implications for nutrient recycling. Ecology, **78**: 1816–1831.

Sherwood, G.D., Pazzia, I., Moeser, A., Hontela, A., and Rasmussen, J.B. 2002. Shifting gears: enzymatic evidence for the energetic advantage of switching diet in wild-living fish. Can. J. Fish. Aquat. Sci. **59**: 229–241.

Trebitz, A.S. 1991. Timing of spawning in largemouth bass: implications of an individual-based model. Ecol. Modell. **59**: 203–227.

Weiland, M.A., and Hayward, R.S. 1997. Cause for the decline of large rainbow trout in a tailwater fishery: Too much putting or too much taking? Trans. Am. Fish. Soc. **126**: 758–773.

Whitledge, G.W., and Hayward, R.S. 1997. Laboratory evaluation of a bioenergetics model for largemouth bass at two temperatures and feeding levels. Trans. Am. Fish. Soc. **126**: 1030–1035.

Whitledge, G.W., and Hayward, R.S. 2000. Determining sampling date interval for precise in situ estimates of cumulative food consumption by fishes. Can. J. Fish. Aquat. Sci. **57**: 1131–1138.

Whitledge, G.W., Hayward, R.S., Noltie, D.B., and Wang, N. 1998. Testing bioenergetics models under feeding regimes that elicit compensatory growth. Trans. Am. Fish. Soc. **127**: 740–746.

Whitledge, G.W., Hayward, R.S., Zweifel, R.D., and Rabeni, C.F. 2003. Development and laboratory evaluation of a bioenergetics model for sub-adult and adult smallmouth bass. Trans. Am. Fish. Soc. **132**: 316–325.

© 2004 NRC Canada

Simultaneous identification and correction of systematic error in bioenergetics models: demonstration with a white crappie (*Pomoxis annularis*) model

Przemyslaw G. Bajer, Robert S. Hayward, Gregory W. Whitledge, and Richard D. Zweifel

Abstract: Recent evidence indicates that important systematic error exists in many fish bioenergetics models (BEMs). An approach for identifying and correcting this error is demonstrated with a white crappie (*Pomoxis annularis*) BEM. Model-predicted trajectories of growth and cumulative consumption for 39 individual white crappie obtained from six 60-day laboratory experiments diverged from observed values by up to 42.5% and 227%, respectively, indicating systematic error in the BEM. To evaluate correlates of the systematic error, model prediction errors were regressed against three major input/output variables of BEMs that were covered by the laboratory experiments: fish body weight (80–341 g), temperature (23–30 °C), and consumption level (0.5%–6.2% daily). Consumption level explained >80% of the prediction error for growth and consumption. Two multiple regression equations containing body weight, temperature, and consumption variables were developed to estimate growth prediction error (R^2 = 0.96) and consumption prediction error (R^2 = 0.86), and incorporated into the white crappie BEM to correct its predictions. Cross-validation indicated that growth and consumption prediction error was reduced 2- to 4-fold by correction. Given recent evidence of widespread systematic error and increasing application rates of BEMs, the efficient error-identification and -correction approach described appears broadly applicable and timely.

Résumé : Des études récentes indiquent qu'il existe une erreur systématique importante dans plusieurs modèles bioénergétiques (BEM)de poissons. Nous faisons la démonstration d'une méthode pour identifier et corriger cette erreur à l'aide d'un BEM de la marigabe blanche (*Pomoxis annularis*). Les trajectoires de croissance et de consommation cumulative de 39 individus obtenues dans six expériences de 60 jours diffèrent des valeurs observées par autant que 42,5 % et 227 %, respectivement; il y a donc une erreur systématique dans le BEM. Afin d'évaluer les facteurs qui sont en corrélation avec l'erreur systématique, nous avons fait des régressions entre les erreurs de prédiction du modèle et trois variables d'entrée ou de sortie des BEM obtenues dans les expériences de laboratoire, soit la masse corporelle des poissons (80–341 g), la température (23–30 °C) et le niveau de consommation (0,5–6,2 % par jour). Le niveau de consommation explique >80 % de l'erreur de prédiction de la croissance et de la consommation. Nous avons mis au point deux équations de régression multiple qui incluent comme variables la masse corporelle, la température et la consommation, afin d'estimer l'erreur de prédiction de la croissance (R^2 = 0,96) et de la consommation (R^2 = 0,86); nous les avons incorporées au BEM de la marigane blanche pour corriger les prédictions. Une validation croisée indique que la correction réduit par un facteur de 2–4 les erreurs dans les prédictions de croissance et de consommation. Étant donné la démonstration récente d'une erreur systématique générale dans les BEM et compte tenu de l'utilisation de plus en plus fréquente des BEM, la méthode efficace d'identification et de correction des erreurs que nous décrivons arrive à point et semble devoir s'appliquer sur une grande échelle.

[Traduit par la Rédaction]

Introduction

Fish bioenergetics models (BEMs) have been developed for a substantial and increasing number of species and life stages (Hewett and Johnson 1987; Hanson et al. 1997) and evidence indicates rapidly increasing application rates of these models. A primary literature search (*Biological Abstracts*) revealed that of a total of 114 studies that used BEMs from 1980 to 2003, more than two-thirds were published in the last 7 years of the 23-year period. We suspect that numerous additional

Received 6 August 2003. Accepted 27 July 2004. Published on the NRC Research Press Web site at http://cjfas.nrc.ca on 26 January 2005.
J17693

P.G. Bajer, R.S. Hayward,[1] G.W. Whitledge, and R.D. Zweifel.[2] Department of Fisheries and Wildlife Sciences, 302 Anheuser–Busch Natural Resources Building, University of Missouri–Columbia, Columbia, MO 65211-7240, USA.

[1]Corresponding author (e-mail: HaywardR@missouri.edu).
[2]Present address: Department of Wildlife and Fish Science, South Dakota State University, Brookings, SD 57007, USA.

 doi: 10.1139/F04-160 © 2004 NRC Canada

Table 1. Applied ration levels, temperatures, body-weight ranges, and total and subperiod durations for six laboratory experiments in which consumption and growth rates for white crappie (*Pomoxis annularis*) were determined.

Exp. No.	*n*	Range of mean fish body weights (g)	Growth condition	Subperiod	Duration (days)	Ration level (% body weight·day^{-1})[a]	Temp. (°C)
1	9	156–173	Moderate gain	1	21	1.0	30
				2	21	2.0	26
				3	21	1.0	23
2	8	131–143	Loss	1	20	0.5	27
				2	22	0.5	27
				3	23	0.5	27
3	6	261–288	Loss	1	20	0.5	27
				2	22	0.5	27
				3	23	0.5	27
4	6	72–122	Rapid gain	1	24	6.2	24
				2	23	4.3	27
				3	23	3.2	30
5	5	179–215	Rapid gain	1	24	3.9	24
				2	23	2.8	27
				3	23	2.4	30
6	5	268–324	Rapid gain	1	24	4.0	24
				2	23	2.6	27
				3	23	2.3	30

Note: Applied conditions produced weight loss or moderate or rapid weight gain. Experiments 2 and 3 involved constant conditions of applied ration level and temperature across the three subperiods, while all other experiments involved distinct combinations of ration level and temperature within subperiods (*n* is the number of fish in each experiment).

[a]Fish were fed rations ad libitum during subperiods 1, 2, and 3 of experiments 4–6.

BEM applications were performed during 1980–2003 at a similar increasing rate, to facilitate decisions relating to fisheries management, aquatic ecology, and aquaculture, but were either not published or placed in the grey literature.

Recent studies have identified the presence of strong systematic error in BEMs (Madenjian and O'Connor 1999; Bajer et al. 2003), while another study has shown this type of error to be widespread among these models and to have potentially important consequences relating to predictions of consumption and growth rates (Bajer et al. 2004). That many BEMs apparently contain important systematic error, while being applied at increasing rates, heightens the need for actions to improve them.

Bajer et al. (2003), and to a further extent Bajer et al. (2004), discuss likely sources of the systematic error found within BEMs. These insights should facilitate efforts to fundamentally improve BEMs by identifying specific internal subequations that warrant reevaluation and possible improvement. However, fundamental improvement of BEMs will require substantial research efforts without the guarantee of success. The present study introduces an efficient alternative approach for reducing systematic error in BEMs, leading to improved accuracy of growth and consumption predictions. Through this approach, systematic error is both identified and corrected from a single set of laboratory data that can be developed with reasonable effort. The approach that we describe appears valuable and timely, as it could expedite needed improvements to these frequently used models.

Methods

Laboratory data sets

White crappie (*Pomoxis annularis*) were grown in six laboratory experiments each of approximately 60 days' duration to provide test data for evaluating the accuracy of growth and consumption predictions by means of a modified version of the white crappie BEM of Zweifel (2000). Collectively, the experiments permitted model evaluation under conditions where white crappie of various sizes were gaining weight (experiments 1, 4, 5, and 6) as well as losing weight (experiments 2 and 3) at temperatures from just below the growth optimum (23 °C) to incipient upper lethal levels for older juvenile and adult fish (30 °C). Model performance under these higher temperatures was of particular interest because of plans to eventually use it to evaluate white crappie growth responses under summer thermal conditions for wide ranges of consumption level. Fish were held individually in each experiment and each fish's daily consumption was directly determined under known temperature. Changes in fish body weight were determined every 7–20 days. Fish weights in experiments ranged from about 70 to 325 g and applied ration levels ranged from 0.5% (submaintenance feeding) to about 6% of body weight per day (ad libitum feeding).

Experiment 1 consisted of three successive 21-day subperiods, each with distinct combinations of constant temperature and ration level (Table 1). Planned temperature changes during this experiment were made at rates not exceeding 1 °C·day^{-1}, while changes in ration level between subperiods were performed immediately. Experiments 2 and 3 each involved continuous submaintenance feeding at 27 °C; the two experiments differed in the sizes of fish that were tested (Table 1). Experiments 4–6 also consisted of three subperiods, each offering distinct growth conditions. In each of these experiments, fish were provided rations ad libitum, while the temperature was incremented from 24 to 27 to 30 °C over

© 2004 NRC Canada

the three 15-day subperiods. Subperiods were separated by 10 days for acclimation to temperature changes; during these 10-day periods fish were fed at half-maximum rations, achieved by feeding ad libitum every other day. The three experiments varied primarily in the sizes of fish that were grown (Table 1). All laboratory experiments were conducted between June and August during 1997, 2000, and 2002. All white crappie used in experiments were collected from Little Dixie Lake, Callaway County, Missouri. No fish was used in more than one experiment.

White crappie were acclimated to experimental conditions for at least 1 month prior to each experiment. During the first 2 weeks of acclimation, fish were provided fathead minnows (*Pimephales promelas*) and allowed to swim freely in groups in 1000-L laboratory tanks equipped with temperature-regulation, biofiltration, water-recirculation, and aeration capacities. After 2 weeks, fish were placed individually in 70-L perforated plastic chambers submerged within the 1000-L experimental tanks and each fish was fed a half-maximum ration. Temperature and dissolved oxygen concentrations were monitored daily during acclimation and experimentation, while ammonia, nitrite, and nitrate concentrations were measured weekly. Temperatures remained within 0.5 °C of desired levels and dissolved oxygen concentrations remained above 7 mg·L^{-1}. Ammonia, nitrite, and nitrate concentrations did not exceed 0.003, 0.25, and 30.0 mg·L^{-1}, respectively.

During experiments, individual white crappie were weighed weekly (experiment 1) or every 10–20 days (experiments 2–6), including at the beginning and end of each experiment. Fish were starved for 24 h prior to weighing, held in a soft dip net to allow excess water to drain in a consistent manner, placed in a plastic container, and weighed to the nearest 0.1 g. Fish total lengths (to the nearest 1.0 mm) were measured whenever they were weighed.

Daily consumption was determined to the nearest 0.1 g for individual white crappie. Combined weights of blotted live fathead minnows were determined before providing them to each white crappie. Any uneaten minnows were removed from experimental chambers after 24 h and their combined weight was subtracted from that of minnows provided 24 h earlier. During submaximum feeding (experiments 1–3), weights of minnows provided daily were adjusted as the white crappie grew, to maintain constant consumption on a percent body weight basis.

Caloric densities of individual white crappie ($ED_{predator}$; cal·g wet weight^{-1}·day^{-1}; 1 cal = 4.184 J), which were required for bioenergetics modeling, were estimated throughout laboratory experiments from relative weights (W_r) (Ney 1999) as

$$(1) \qquad ED_{predator} = 541.3 + 7.42W_r$$

$$(n = 22, p < 0.01, r^2 = 0.46)$$

To construct this relationship, we selected white crappie experiencing conditions similar to experimental fish at the beginning, during, and upon completion of experiments. Wet and dry weights (to the nearest 0.1 g), total length (to the nearest 1.0 mm), and W_r were determined for each fish. Two 1-g samples from each fish were separately dried and pulverized, and the caloric density was determined by means of bomb calorimetry; the results were averaged to determine the mean caloric density. Fish caloric densities were regressed against corresponding wet and dry weights, total lengths, and W_r values. The relationship between caloric density and W_r alone was selected for estimating these values for experimental fish.

Energy densities of prey fish were also determined by bomb calorimetry. Five 50-g samples of fathead minnows (approximately 50 fish per sample) were taken throughout each experiment and bombed. Because the caloric densities of fathead minnows varied little within experiments, mean experiment-specific values (964–1244 cal·g wet weight^{-1}) were used in BEM simulations.

Description of the BEM

We modified an existing white crappie BEM (Zweifel 2000). Then, using data from the six laboratory experiments, we evaluated the modified model's ability to accurately predict observed white crappie consumption and growth. Ultimately, we corrected the modified model to reduce inherent systematic error and improve its predictive accuracy.

The modified white crappie BEM (Table 2) is based on the balanced energy equation used by Kitchell et al. (1977)

$$(2) \qquad G = C - (M + F + U)$$

where growth (G) over a time period is the difference between energy gained through food consumption (C) and the sum of energy costs and losses through metabolism (M), egestion (F), and excretion (U). All model variables are expressed in common units (cal·g^{-1}·day^{-1}).

Metabolic costs are represented by standard metabolism (R_s), hereinafter called resting routine metabolism (Jobling 1994), which is increased by activity cost (ACT) and by the costs of processing and assimilating consumed food, or specific dynamic action (SDA), as

$$(3) \qquad M = R_s \text{ ACT} + \text{SDA}$$

as in Hanson et al. (1997). Resting routine metabolism is determined from the general body-weight- and temperature-dependent equation

$$(4) \qquad R_s = (\beta_0 W^{\beta_1}) e^{\beta_2 T}$$

where W is fish body weight (g wet weight), T is temperature (°C), β_0 and β_1 are intercept and slope values for the allometric function, respectively, and β_2 is the slope of temperature dependence of R_s. Equation 4 differs from the equations used in the original white crappie BEM (Zweifel 2000) to determine R_s. The original white crappie BEM determined R_s values from laboratory-derived resting routine metabolic rates of individually held white crappie ranging from 50 to 300 g at 18, 21, 24, 27, and 30 °C. Whereas R_s values are typically calculated from a single body-weight- and temperature-dependent equation (Kitchell et al. 1977; Hanson et al. 1997), Zweifel (2000) derived three such equations for distinct ranges of fish weight. However, subsequent evaluation revealed that unreasonable R_s values were produced by these three equations for certain conditions (fish body weight >100 g under temperatures of 28–30 °C). To ameliorate this problem, we fitted eq. 4 to the full range of white crappie metabolism data (Zweifel 2000) through multiple regression analysis. Although the resulting model explained only 35% of the variability in the data, overall it

© 2004 NRC Canada

Table 2. Parameter values (and units) for the modified white crappie bioenergetics model (BEM) (uncorrected).

Parameter	Description	Value	Units
Consumption (*C*)			
a	Intercept for body-weight dependence of C_{max}	1389.9	cal·g wet weight^{-1}
b	Slope for body-weight dependence of C_{max}	–0.661	
Q_{10}	Slope for temperature dependence of consumption	2.945	
T_m	Temperature above which consumption ceases	32	°C
T_o	Temperature at which consumption is maximal	24	°C
Respiration (*M*)			
Resting routine metabolism (R_s)			
β_0	Intercept for body-weight and temperature dependence of R_s	76.66	cal·g wet weight^{-1}
β_1	Slope for body-weight dependence of R_s	–0.623	
β_2	Slope for temperature dependence of R_s	0.0237	
Specific dynamic action and activity costs			
SDA	Specific dynamic action coefficient	0.160	cal·g wet weight^{-1}
ACT	Activity multiplier of R_s	1.0	
Egestion (*F*) and excretion (*U*)			
F	Egestion coefficient	0.104	cal·g wet weight^{-1}
U	Excretion coefficient	0.068	cal·g wet weight^{-1}

Note: The modified model is identical with the original model of Zweifel (2000) except that resting routine metabolism (R_s) is determined from a multiple regression equation. Associated equations (or citations for them) are given in the text. 1 cal = 4.184 J.

provided more reasonable R_s values (0.4%–2% body weight·day^{-1}) than were given by the set of three equations.

The activity multiplier (ACT) in eq. 3 accounts for metabolic costs in excess of resting routine metabolism relating to, for example, swimming, prey pursuit, and activity and stress from social interaction. For fish in our laboratory experiments, activity costs were assumed to be negligible (ACT = 1) because fish were held in relatively small, 70-L chambers that allowed very limited opportunity for swimming. When fed, fish were observed to slowly approach and readily capture their prey with little rapid movement. During nonfeeding periods, only minor spontaneous movement was observed. Moreover, holding fish individually eliminated activity due to social interaction.

Relationships among consumption (C), maximum daily consumption (C_{max}), proportion of maximum consumption ingested (P), and the influences of body weight and temperature on C_{max} and C are as defined in consumption equation 2 of Hanson et al. (1997).

F, U, and SDA values in both the original and modified model were determined as

$$F = 0.104C \quad (5)$$

$$U = 0.068(C - F) \quad (6)$$

and

$$\text{SDA} = 0.160(C - F) \quad (7)$$

The general forms of eqs. 5–7 are commonly used in fish BEMs (Hanson et al. 1997).

Predicting growth and consumption

The modified white crappie BEM was run to predict absolute (g·day^{-1}) and relative daily growth rates (cal·g^{-1}·day^{-1}) of individual white crappie throughout each of the six laboratory experiments. On the first day of a model run, predicted body weight was set at a fish's observed initial body weight. For each daily time step, an observed daily consumption value (g) was entered and converted to caloric intake according to prey caloric density. The model then calculated a daily value for resting routine metabolism (R_s; cal·g wet weight^{-1}) from predicted body weight and observed temperature. Consumption losses through F and U and metabolic cost of SDA (all in cal·g wet weight^{-1}) were calculated as fractions of either daily caloric consumption (C) or digested energy ($C - F$). Total energy costs and losses were then subtracted from daily consumption, yielding daily growth in cal·g wet weight^{-1}, which was converted to body mass using a daily caloric density value for white crappie. Caloric densities of individual white crappie were estimated from the mean of observed W_t values over 20-day experiment subperiods (eq. 1). Daily growth was accumulated over time to produce a predicted growth trajectory.

The modified BEM was also run to estimate daily consumption rates (cal·g^{-1}·day^{-1}, and also % body weight·day^{-1}) and, ultimately, cumulative consumption (g prey) for each fish in each of the six laboratory experiments. Consumption estimates were made using the P-fit approach (Kitchell et al. 1977; Hewett and Johnson 1992). Through an iterative process this determines the fixed proportion (P) of maximum daily consumption (C_{max}) that causes the model to grow a fish from its observed initial weight to its observed final weight over the total number of days in a modeling interval under the observed thermal conditions. Fitted P values were converted to daily consumption rates using predicted daily weights of individual fish and observed temperatures. Estimated daily consumption rates (cal·g^{-1}) were then converted to grams of food consumed using prey caloric density and white crappie weight and summed over days in the modeling interval to estimate cumulative consumption (g prey).

When estimating consumption for individual fish using the modified BEM, laboratory experiments were first di-

© 2004 NRC Canada

vided into three subperiods of 15–25 days each during which combinations of ration level, temperature, and white crappie body weight remained similar (Table 1). This measure was taken so that measured levels of predictive error for the BEM could be linked to specific levels of consumption, temperature, and fish weight. Such subperiods were formed even for experiments 2 and 3, throughout which applied temperatures and ration levels remained constant. A single *P*-fit procedure was conducted for each fish within each subperiod of each experiment. Predicted cumulative consumption values for individual fish over whole experiments were calculated by summing predicted cumulative consumption over the component subperiods.

Representing the accuracy of model predictions

The accuracy of white crappie growth and consumption predictions by the modified BEM was described for each of the six laboratory experiments that collectively represented growth conditions ranging from highly favorable to poor (Table 1). Growth-prediction accuracy was determined by comparing predicted with observed growth trajectories for each fish in each experiment. The accuracy of growth predictions was represented as (*i*) the mean of absolute daily growth errors (MGE) and also as (*ii*) the maximum of absolute daily growth errors (MaxGE), each expressed as a percentage of observed mean body weight (or single-day body weight for MaxGE) (Bajer et al. 2003). MGE represents the average departure of a predicted growth trajectory from the corresponding observed trajectory

$$\text{MGE} = \frac{\sum_{i=1}^{n} \left| \frac{(P_i - O_i)}{O_i} \right|}{n} \times 100 \quad (8)$$

where P_i and O_i are predicted and observed body weights on day i of a growth trajectory, respectively, and n is the total number of days in the trajectory. Absolute values of relative daily differences between predicted and observed values were used because modeled trajectories can cross over observed trajectories; if absolute values are not used, negative errors will be subtracted from positive errors, causing underrepresentation of overall mean error. Maximum daily errors were determined as

$$\text{MaxGE} = \max \left| \frac{(P_i - O_i)}{O_i} \right| \times 100 \quad (9)$$

MaxGE values indicate volatility of model predictions that may not be evident from MGE. For example, a high MaxGE value relative to the MGE value for a pair of predicted and observed growth trajectories would highlight a situation where predicted and observed values agree well over much of a modeling interval, but predicted values depart substantially from observed values near the interval's end.

The accuracy of consumption predictions by the modified white crappie BEM was likewise determined from individual fish responses and considered differences between predicted and observed cumulative consumption over whole experiments. The accuracy of model predictions of cumulative consumption for each fish was expressed as cumulative consumption error (CCE), calculated as the difference between predicted and observed cumulative consumption values on the final day of a modeled trajectory, expressed as a percentage of observed final-day cumulative consumption

$$\text{CCE} = (P_t - O_t)/O_t \times 100 \quad (10)$$

where P_t and O_t are predicted and observed cumulative consumption values on the final day of a modeled trajectory, respectively.

Identifying systematic error and its sources

Three primary input/output variables for BEMs (hereinafter PIO variables), fish body weight (g), daily consumption (cal·g^{-1}·day^{-1}), and temperature (°C), were used to explore possible systematic error in the modified white crappie model. It was reasonable to use the PIO variables to search for systematic error because each influences values of one or more of the internal energy cost/loss variables (R_a, SDA, F, and U) within the BEM with the exception of activity (ACT). Inadequacies in the internal relationships between the energy cost/loss variables and their associated PIO variables (e.g., eqs. 5–7) would promote systematic error in the BEM. Ideally, the BEM prediction error rate will remain close to zero across all levels of fish body weight, daily consumption, or temperature. The presence of correlation between model prediction error rates and levels of any of the PIO variables would indicate inadequacies in the BEM's internal equations and the presence of systematic error. Regression analysis can provide a quantitative description of any such relationships between PIO variables and model prediction error rates that result from systematic error. Such correlation will also indicate likely sources of systematic model error because each PIO variable has known linkages to particular energy cost/loss variables within the model.

To explore possible systematic error in the modified white crappie BEM, we looked for correlation between the three PIO variables and the magnitude of model prediction error. A growth rate prediction error (GRE) value and a consumption rate prediction error (CRE) value were determined for each fish within each of the three subperiods of each laboratory experiment. Individual GRE and CRE values were determined within experiment subperiods (Table 1) instead of over whole experiments so that each model prediction error value would be associated with relatively static levels of daily consumption, temperature, and fish body weight (the PIO variables). A total of 117 GRE values (three subperiods times the total number of fish per experiment, summed over the six experiments) were produced, and likewise for CRE values, each being associated with a mean daily consumption, temperature, and body-weight value for an individual fish from a subperiod.

For each of the 18 experiment subperiods, a GRE value (cal·g^{-1}·day^{-1}) was determined for each fish as

$$\text{GRE} = \frac{(P_t - O_t)}{n\bar{O}} \cdot \text{ED}_{\text{predator}} \quad (11)$$

where P_t and O_t are predicted and observed fish weights at the end of a subperiod, respectively, $\bar{O}$ is mean observed fish weight during the subperiod, n is the number of days in the subperiod, and $\text{ED}_{\text{predator}}$ is predator energy density (cal·g^{-1})

© 2004 NRC Canada

during the subperiod. A CRE value (cal·g^{-1}·day^{-1}) was also determined for each fish in each experiment subperiods as

$$\text{(12)} \quad \text{CRE} = \frac{(P_t - O_t)}{n\,\overline{O}} \cdot \text{ED}_{\text{prey}}$$

where P_t and O_t are predicted and observed cumulative consumption values on the final day of a subperiod, respectively, n and $\overline{O}$ are as previously defined, and ED_{prey} is prey energy density.

Before conducting simple regressions of GRE and CRE values on corresponding values of each of the three PIO variables, potential non-independence within the regression data sets was eliminated. The potential for non-independence existed because an individual fish's responses were measured 3 times, once in each of the three subperiods within an experiment. To eliminate this, we randomly selected and retained only one of the three sets of error data per fish. This reduced the total number of observations in each simple regression analysis by two-thirds, resulting in 39 observations for each. We evaluated similarity among regressions of GRE and CRE values on each of the three PIO variables (six simple regressions) that arose from 10 distinct random selections of one of the three possible sets of data per fish. The slopes and intercepts of the 10 randomly selected versions of each of the six regressions did not differ (heterogeneity of slopes analysis followed by analysis of covariance, $p > 0.05$), indicating good stability among the relationships between PIO variables and both GRE and CRE values.

Correcting the BEM for systematic error

Following examination of simple regression results, all three PIO variables (daily consumption, body weight, and temperature) were included in various linear combinations as predictor variables in multiple regression analyses aimed at developing a best GRE prediction equation for the modified white crappie BEM. A separate equation was similarly constructed for predicting CRE values. These two equations would ultimately be incorporated into the BEM to correct prediction error on a daily time-step basis. The effectiveness of incorporating these correction equations to improve BEM predictions was subsequently evaluated via a cross-validation procedure. Parameter-selection criteria for the best multiple regression models included Akaike's information criterion (AIC) scores and, to a lesser degree, improvement in R^2 values. In general, we selected models with the fewest parameters whose AIC scores were within seven points of the lowest AIC values observed (Burnham and Anderson 2001). Selected multiple regression models were evaluated for goodness of fit to the GRE and CRE data and for the need to include interaction terms based on examination of residual plots.

When constructing the correction equation for CRE values, we used the observed white crappie growth rate (GRATE; cal·g^{-1}·day^{-1}) as a surrogate predictor variable for daily consumption. For BEM applications aimed at estimating food consumption, observed daily consumption data will clearly not be available for CRE correction, unlike in our laboratory experiments designed specifically for model evaluation. GRATE is an appropriate surrogate variable for daily consumption when predicting CRE values, because it tends to be well correlated with daily consumption level both in laboratory and natural settings (Davis and Warren 1971; Carline and Hall 1973; Allen and Wootton 1982).

Evaluation of the corrected BEM

Cross-validation (Neter et al. 1996) was used to independently evaluate whether white crappie BEM predictions were improved by including error-correction equations. For this evaluation, error-correction equations for both consumption and growth predictions developed from the full data set were redeveloped using halves of the data set. The two half data sets each included information from three laboratory experiments that were randomly selected without replacement, with one of the two weight-loss experiments (experiments 2 and 3) being forced at random into each half data set. As was done for the full data set, multiple regression analyses were used to develop BEM correction equations for consumption and growth predictions for each half data set. (Hereinafter, correction equations developed from halves of the data set are correction "subequations", while those based on all six experiments are "full" correction equations.) Correction subequations were forced to include the same predictor variables (PIO variables) that had been selected for the full correction equations. First, GRE, CRE, and associated PIO values were generated by using the uncorrected BEM (the modified BEM without correction equations) to predict growth and consumption rates for one half of the data (experiments 1, 3, and 5). Two correction subequations (one predicting GRE values and the other, CRE values) were then developed from this half data set and incorporated into the BEM. This corrected model was then used to predict growth and consumption for fish in the other half data set (experiments 2, 4, and 6). This procedure was then run in the opposite direction so that data from experiments 2, 4, and 6 were used to develop correction subequations, and the corrected BEM containing these equations was tested on experiments 1, 3, and 5. Results from the two procedures were then combined. Whereas full correction equations were derived from 39 sets of GRE and CRE values and associated PIO values, correction subequations were derived from 20 (experiments 1, 3, and 5) and 19 (experiments 2, 4, and 6) sets. When running corrected models, growth and consumption predictions were modified in each daily time step in accordance with the amount of predictive error estimated by the correction subequations in response to daily values of the PIO variables.

Improvement of the white crappie BEM's predictive accuracy from inclusion of correction subequations was assessed by comparing uncorrected model predictions with those from the independently corrected models. Absolute (body weight (g) and cumulative consumption (g)) as well as relative model predictions (growth rates (cal·g^{-1}·day^{-1}) and consumption rates (cal·g^{-1}·day^{-1})) were evaluated. To visually assess improvements, plots of predicted mean growth trajectories from uncorrected and corrected models were compared with observed mean growth trajectories for each of the six laboratory experiments. For each experiment, differences between mean values of MGE, MaxGE, and CCE for the corrected versus uncorrected models were evaluated by means of paired t tests ($p < 0.025$, one-tailed tests), with pairing based on modeling error for an individual fish's trajectories of growth and consumption. Heterogeneity of slopes tests

© 2004 NRC Canada

Fig. 1. Observed mean growth trajectories ±1 standard error (SE) for white crappie (*Pomoxis annularis*) in laboratory experiments 1–6 (*a–f*, respectively) compared with means of predicted growth trajectories by the uncorrected (solid line) and corrected (broken line) white crappie bioenergetics models (BEMs). Fish continually lost weight, owing to the imposition of submaintenance rations in experiments 2 and 3, but gained weight under moderate to high ration levels in all other experiments. Note that *y*-axis scales vary among the six panels.

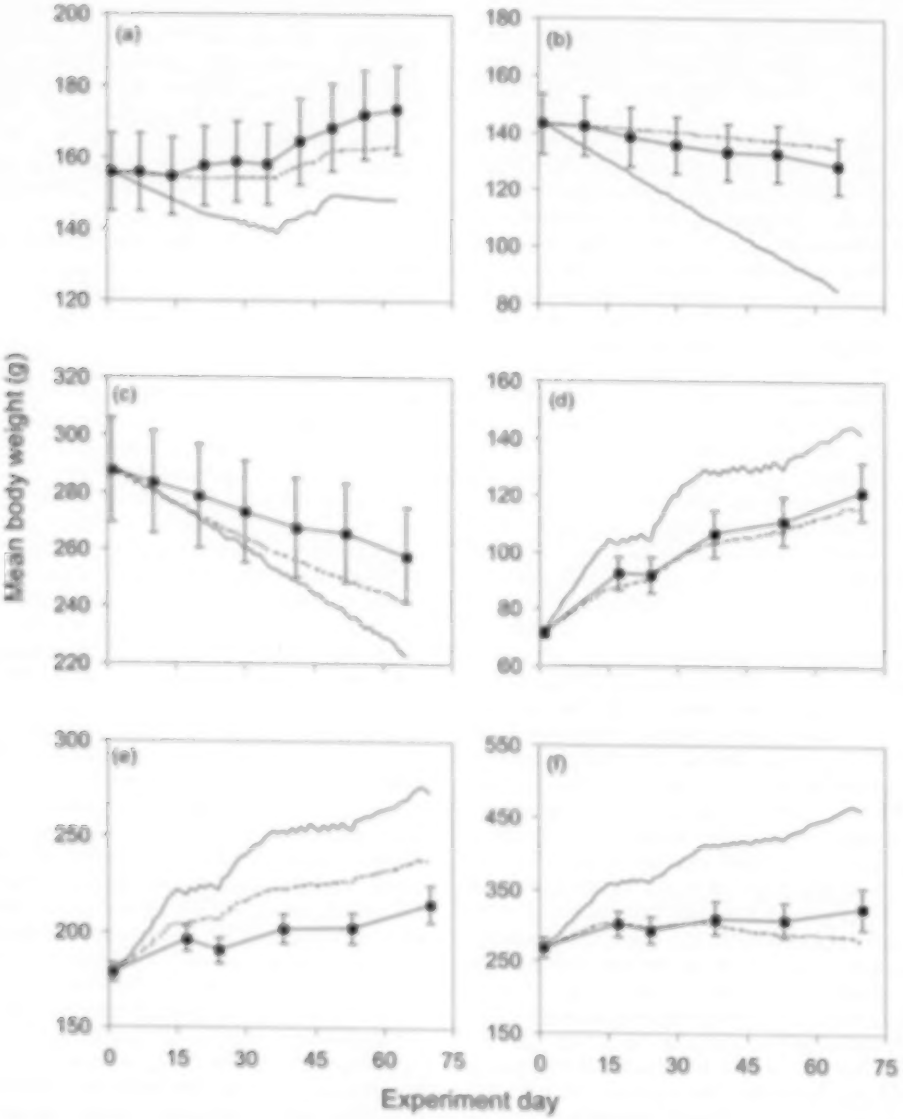

($p < 0.025$, one-tailed tests) were also applied to determine whether the inclusion of independently derived correction subequations diminished the slopes of originally observed relationships between GRE and CRE values and the PIO variables, which portrayed systematic model error. Changes in intercept values for the same relationships were considered significant if the pre- and post-correction intercepts ±2 standard errors (SEs) did not overlap. Observed improvements in BEM predictive accuracy based on cross-validation are considered indicative of improvement that will result when the white crappie model with full correction equations is applied over conditions encompassed by the six laboratory experiments.

Results

Accuracy of the BEM before correction

Overall, predicted growth trajectories by the uncorrected white crappie BEM were reasonably accurate (Fig. 1), but the accuracy varied considerably across the six experiments. MGE ranged from about 7% (experiment 3: 275-g fish fed at 0.5% body weight daily at 27 °C) to 28% (experiment 6:

© 2004 NRC Canada

Table 3. Mean (MGE) and maximum (MaxGE) errors for predictions of fish growth in the six laboratory experiments by the uncorrected and corrected white crappie BEMs.

Exp. No.	Growth condition	MGE		MaxGE	
		Uncorrected	Corrected	Uncorrected	Corrected
1	Moderate gain	10.0 (1.8)	3.3* (0.8)	16.5 (2.7)	6.7* (1.1)
2	Loss	17.1 (1.5)	3.2* (0.8)	35.2 (2.6)	5.7* (1.2)
3	Loss	6.5 (0.7)	3.7 (0.8)	14.9 (1.6)	7.5* (1.8)
4	Rapid gain	15.7 (3.7)	2.7* (0.3)	24.0 (3.9)	6.5* (1.3)
5	Rapid gain	20.1 (3.2)	9.1* (1.4)	29.5 (4.5)	14.3* (1.9)
6	Rapid gain	27.7 (3.9)	6.6* (1.3)	42.5 (6.9)	14.5* (4.4)

Note: Applied conditions produced weight loss or moderate or rapid weight gain. MGE and MaxGE values (both as % body weight·day^{-1}) represent mean and maximum daily departures of model-predicted from observed growth trajectories, respectively. Differences between MGE values for the corrected versus uncorrected model were evaluated using paired t tests for each experiment (an asterisk indicates significantly lower error (one-tailed test) for the uncorrected model at $p \leq 0.05$ and likewise for MaxGE; $p = 0.06$ for the decline in MGE for experiment 3). Values in parentheses are standard errors.

Table 4. Mean values of observed cumulative consumption by white crappie in each laboratory experiment, predicted cumulative consumption by the uncorrected and corrected BEMs and consumption prediction errors (CCE) for each model.

Exp. No.	Cumulative consumption (g)			CCE (%)	
	Observed	Model-predicted			
		Uncorrected	Corrected	Uncorrected model	Corrected model
1	117 (10)	160 (7)	141 (9)	42.3 (9.1)	25.7* (9.3)
2	39 (3)	124 (4)	25 (6)	224.0 (17.9)	−36.1* (12.7)
3	78 (4)	142 (3)	117 (17)	84.5 (9.5)	46.1 (15.4)
4	188 (24)	152 (16)	174 (27)	−17.6 (2.9)	−8.95 (3.29)
5	246 (31)	169 (19)	216 (42)	−30.4 (2.9)	−14.9 (7.0)
6	400 (70)	223 (32)	376 (84)	−42.6 (2.6)	−10.31* (7.7)

Note: Differences in mean CCE values for the uncorrected and corrected models were evaluated by using paired t tests for each experiment (an asterisk indicates significantly lower error (one-tailed test) for the uncorrected model at $p \leq 0.05$; $p = 0.075$, 0.060, and 0.053 for experiments 3, 4, and 5, respectively). Values in parentheses are standard errors.

300-g fish fed ad libitum at 24–30 °C), while MaxGE ranged from 15% (experiment 3) to 43% (experiment 6) (Table 3). Predicted mean body weight trajectories exceeded 1 SE of observed trajectories for all six experiments, and exceeded 2 SEs for four experiments (Fig. 1).

Prediction error for cumulative consumption by the uncorrected model was more variable across experiments than for growth predictions. Lower CCE values (17%–43%) were observed for fish gaining weight (experiments 1 and 4–6), while substantially higher CCE values (84%–224%) were observed for fish undergoing weight loss due to submaintenance feeding (experiments 2 and 3) (Table 4).

Evaluating sources of systematic error in the model

Simple linear regression analyses showed that the uncorrected model's predictive error for both growth and consumption rates during subperiods of the six laboratory experiments was strongly correlated with observed mean daily consumption levels (C; cal·g^{-1}·day^{-1}). Consumption level was positively correlated with GRE and negatively correlated with CRE. Daily consumption level accounted for 81% and 82% of the total variation associated with GRE and CRE, respectively (Table 5). The uncorrected model increasingly overestimated growth rate (Fig. 2*a*) and underestimated consumption rate (Fig. 2*c*) as daily consumption levels increased above 20 cal·g^{-1}·day^{-1} (approximately 1.5% body weight·day^{-1}), while the opposite was true for consumption levels below 20 cal·g^{-1}·day^{-1}.

Temperature was negatively correlated with GRE and positively correlated with CRE for the uncorrected model (Table 5), but these correlations were substantially weaker than those between predictive error and consumption level. The PIO variables temperature and consumption level were intercorrelated ($r^2 = 0.44$, $p = 0.004$), and this may have accounted for some of temperature's association with GRE and CRE.

Overall, fish body weight was not correlated with GRE or CRE (Table 5). However, closer investigation revealed that body weight was strongly correlated with GRE (positively) and CRE (negatively) for fish that were losing weight (experiments 2 and 3) but not for fish gaining weight (Figs. 3*a* and 3*b*). For fish losing weight, body weight explained 94% ($F_{[1,12]} = 204.5$, $p < 0.0001$) of the variation in GRE and 96% ($F_{[1,12]} = 246.1$, $p < 0.0001$) of that in CRE. For white crappie <350 g that were losing weight, the uncorrected BEM increasingly underestimated relative growth rate and overestimated relative consumption rate as fish size decreased. Body weight was not correlated with consumption ($F_{[1,37]} = 1.1$, $p = 0.29$) or temperature ($F_{[1,37]} = 0.3$, $p = 0.58$).

As expected, the observed GRATE value (cal·g^{-1}·day^{-1}) for white crappie was strongly correlated with observed daily

© 2004 NRC Canada

Table 5. Simple linear regressions of BEM-predicted growth-rate errors (GRE values) and consumption-rate errors (CRE values) (both in cal·g^{-1}·day^{-1}; 1 cal = 4.184 J) versus mean daily consumption (C; cal·g^{-1}·day^{-1}), fish body weight (W; g), and temperature (T; °C) across all six laboratory experiments.

Response variable	Predictor variable	β_0	β_1	$F_{[1,37]}$	r^2	p
Uncorrected BEM						
GRE	C	–5.99	0.32	180.7	0.81	0.0001
GRE	T	43.8	–1.61	8.64	0.18	0.005
GRE	W	–2.24	0.019	1.72	0.05	0.19
CRE	C	9.53	–0.51	193.3	0.82	0.0001
CRE	T	–80.5	2.96	11.97	0.24	0.001
CRE	W	2.93	–0.028	1.46	0.04	0.23
CRE	GRATE	3.87	–1.52	94.8	0.72	0.0001
Corrected BEM						
GRE	C	0.045*	–0.034*	4.68	0.11	0.04
GRE	T	3.65	–0.16	1.28	0.03	0.46
GRE	W	–0.23	–0.0028	0.49	0.01	0.47
CRE	C	1.61*	–0.10*	9.1	0.19	0.004
CRE	T	–22.9	0.84	5.11	0.11	0.03
CRE	W	–3.80	0.016	2.7	0.07	0.11
CRE	GRATE	0.16	–0.21*	3.58	0.08	0.07

Note: Separate regressions are shown for the uncorrected and corrected BEMs. Regression results for the predictor variable growth rate (GRATE; cal·g^{-1}·day^{-1}) were applicable to CRE values only. An asterisk indicates significantly reduced values of β_0 (intercept) and β_1 (slope). Decreases in slope were determined by means of heterogeneity of slopes tests at $p \leq 0.05$ (one-tailed test). The intercept was considered to be lower for the corrected BEM if the intercept mean ± 2 SEs was lower than and did not overlap that of the uncorrected model.

consumption ($F_{[1,37]} = 833$, $r^2 = 0.97$, $p < 0.0001$; Fig. 4*a*) over the range of growth conditions provided in experiments 1–6. Ultimately, GRATE was used as the necessary surrogate variable for observed daily consumption in the process of building a multiple regression equation for predicting CRE values and correcting consumption predictions by the BEM. GRATE was negatively correlated with CRE and explained 72% of its total variation (Table 5; Fig. 4*b*). Although daily consumption was a better predictor of CRE, its applicability beyond laboratory evaluations is limited. In most cases it should be possible to use GRATE in place of consumption level when forming correction equations.

Development of error-correction equations

A multiple regression model containing three predictor variables, body weight (W), body weight interacting with temperature ($W{\cdot}T$), and consumption interacting with temperature ($C{\cdot}T$), was selected as the best model for predicting GRE values in the white crappie BEM based on AIC and adjusted R^2 values ($F_{[2,35]} = 357.9$, $R^2 = 0.96$, $p < 0.0001$; Table 6). The resulting equation for correcting growth predictions by the BEM was

$$\text{GRE} = -13.54 + 0.108W - 0.0026(WT) + 0.013(CT) \quad (13)$$

A two-predictor-variable model containing relative growth rate (GRATE, the surrogate variable for consumption) and body weight was selected for predicting CRE values ($F_{[2,36]} = 122.3$, $R^2 = 0.86$, $p < 0.0001$; Table 6). The resulting equation for correcting consumption predictions was

$$\text{CRE} = 15.81 - 1.67\text{GRATE} - 0.061W \quad (14)$$

Equations 13 and 14 could ultimately be incorporated into the uncorrected white crappie BEM to form a corrected model if cross-validation assessments indicated that their inclusion would lead to significantly more accurate predictions of growth and consumption.

Evaluation of the corrected BEM

Growth and consumption predictions were generated by the two corrected versions of the white crappie BEM. Each version included correction subequations with the same predictor variables as in eqs. 13 and 14, but with distinct coefficient values that were derived by applying multiple regression analysis to the data from experiments 1, 3, and 5, and separately to the data from experiments 2, 4, and 6. A corrected model incorporating correction subequations from the data from experiments 1, 3, and 5 was used to predict observed growth and consumption of individual fish in experiments 2, 4, and 6, and vice versa.

Predicted mean growth trajectories resulting from inclusion of correction subequations in the cross-validation procedure consistently tracked much closer to observed trajectories than those predicted by the uncorrected model (Fig. 1). Across all six experiments, MGE and MaxGE values for corrected models were 2–4 times lower than corresponding values for the uncorrected model. MGE and MaxGE values remained below 10% and 15%, respectively, versus 28% and 43% for the uncorrected model (Table 3). Observed decreases in MGE and MaxGE were statistically significant or marginally so (paired t tests, $p < 0.025$, 0.05, one-tailed tests) except for MGE in experiment 3, the only experiment in which prediction error for the uncorrected model was <10%.

Predictions of cumulative consumption likewise improved from incorporation of correction subequations into the white crappie BEM (Table 4). For fish gaining weight (experiments 1 and 4–6), CCE remained below 26%, whereas the highest CCE value approached 43% for the uncorrected model. For fish losing weight (experiments 2 and 3), origi-

© 2004 NRC Canada

Fig. 2. (*a*) Regression relationships of uncorrected BEM growth prediction error (GRE) for individual fish versus the observed mean daily consumption rate of fish over corresponding modeling intervals. (*b*) Similarly for the GRE of the corrected BEM (derived by cross-validation; ○ and ● represent independent predictions by each of the corrected half-models). (*c*) Uncorrected BEM prediction error for consumption rate (CRE) versus each fish's observed mean daily consumption rate over corresponding modeling intervals. (*d*) Similarly for the CRE from the corrected BEM. All four regression relationships were significant ($p < 0.05$). Slopes and intercepts for regressions related to corrected models (*b* and *d*) were significantly closer to zero than for corresponding regression relationships for the uncorrected model (*a* and *c*) (slope differences were evaluated by means of heterogeneity of slopes tests at $p \leq 0.025$, one-tailed test; intercepts were considered to differ if the intercept means ±2 SEs did not overlap). 1 cal = 4.184 J.

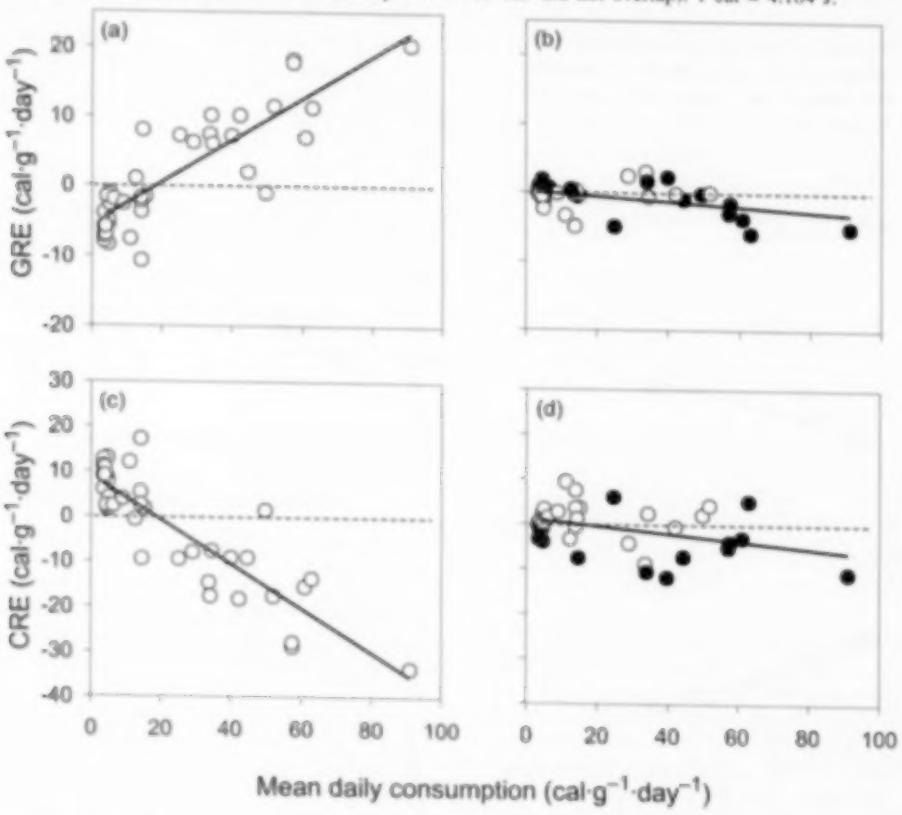

nally high errors of 224% and 84% decreased to 36% and 46%, respectively. Observed declines in CCE values were significant (or marginally so) for three of the six experiments (paired *t* test, $p \leq 0.025$, 0.05, one-tailed tests; Table 4). For experiments 3, 4, and 5, where declines in CCE were nonsignificant, mean CCE values declined 45%, 49%, and 51%, respectively, when correction equations were included.

Systematic error after model correction

Errors associated with predictions of growth rates (GRE values) and consumption rates (CRE values) were reevaluated for the corrected model through the cross-validation procedure. The previously observed strong influence of mean daily consumption on GRE in the uncorrected BEM (Fig. 2*a*) was markedly reduced (Fig. 2*b*). A significant relationship between daily consumption and GRE remained after correction (Table 5), but the previous high positive regression slope decreased to a slight negative value and the intercept was significantly reduced to near zero. A slight tendency to underestimate growth rate as consumption level increased was indicated for the corrected model over the entire range of consumption levels evaluated (0–90 cal·g^{-1}·day^{-1}, equivalent to 0%–8% body weight·day^{-1}; Fig. 2*b*). The previously significant negative relationship between GRE and temperature became nonsignificant after correction (Table 5), indicating a lack of systematic error associated with temperature in the corrected model. Overall, fish body weight was not correlated with GRE either before or after model correction. However, the highly significant influence of body weight on GRE exclusively for fish losing weight was much reduced after model correction (Fig. 5*a*). Although a significant relationship between GRE and fish body weight remained after correction, the indicated biasing effect was minor.

An improved capacity to predict consumption rates after model correction was likewise indicated by the cross-validation procedure. The previous strong effect of daily consumption level on CRE (Fig. 2*c*) was much reduced (Fig. 2*d*). Although the relationship between CRE and daily consumption remained significant after correction, as for GRE, regression slope and intercept values were altered significantly to val-

© 2004 NRC Canada

Fig. 3. (*a*) Regression relationships for growth rate prediction errors (GRE; cal·g^{-1}·day^{-1}; 1 cal = 4.184 J) of the uncorrected BEM versus mean body weights of individual white crappie over modeling intervals; the regression analysis based on all observations (○ plus ●) was nonsignificant ($p > 0.05$); however, the regression based exclusively on fish that were losing weight (●) was highly significant (GRE = –10.48 + 0.0308*W*; $F_{[1,12]} = 204.5$, $r^2 = 0.95$, $p < 0.0001$). (*b*) Similarly for the consumption rate prediction errors of the uncorrected model (CRE; cal·g^{-1}·day^{-1}); again, the regression analysis based on all observations (○ plus ●) was nonsignificant ($p > 0.05$), while that based exclusively on fish that were losing weight was highly significant (CRE = 16.64 – 0.0483*W*; $F_{[1,12]} = 246.1$, $r^2 = 0.93$, $p < 0.0001$).

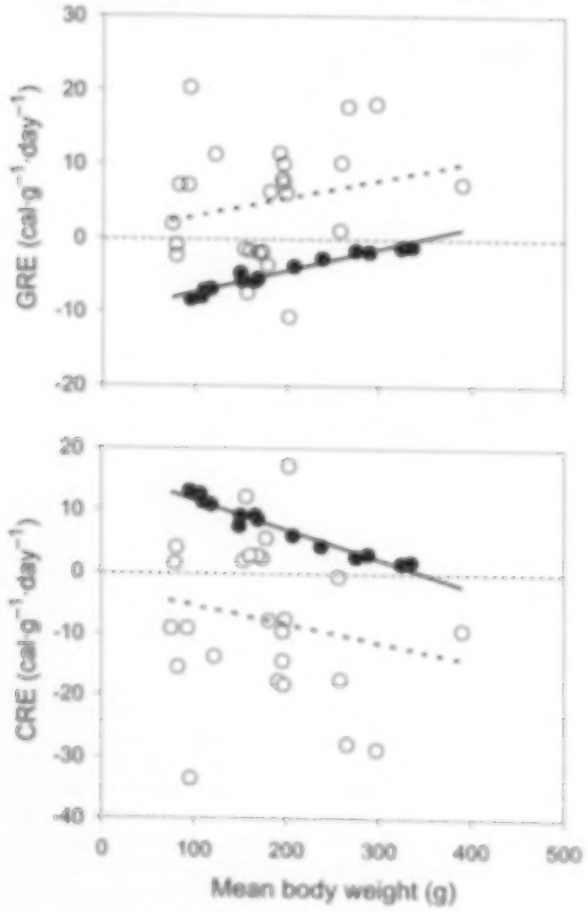

Fig. 4. (*a*) Regression relationships of observed individual white crappie growth rates (GRATE; cal·g^{-1}·day^{-1}; 1 cal = 4.184 J) from all laboratory experiments and corresponding mean observed daily consumption rate (*C*; cal·g^{-1}·day^{-1}) (GRATE = –2.96 + 0.305*C*; $F_{[1,37]} = 833.9$, $r_2 = 0.95$, $p < 0.0001$). (*b*) Consumption rate prediction error (CRE; cal·g^{-1}·day^{-1}) of the uncorrected BEM (for individual white crappie) versus corresponding observed growth rates (GRATE; cal·g^{-1}·day^{-1}) (CRE = 3.87 – 1.52GRATE; $F_{[1,37]} = 94.8$, $r^2 = 0.71$, $p < 0.0001$).

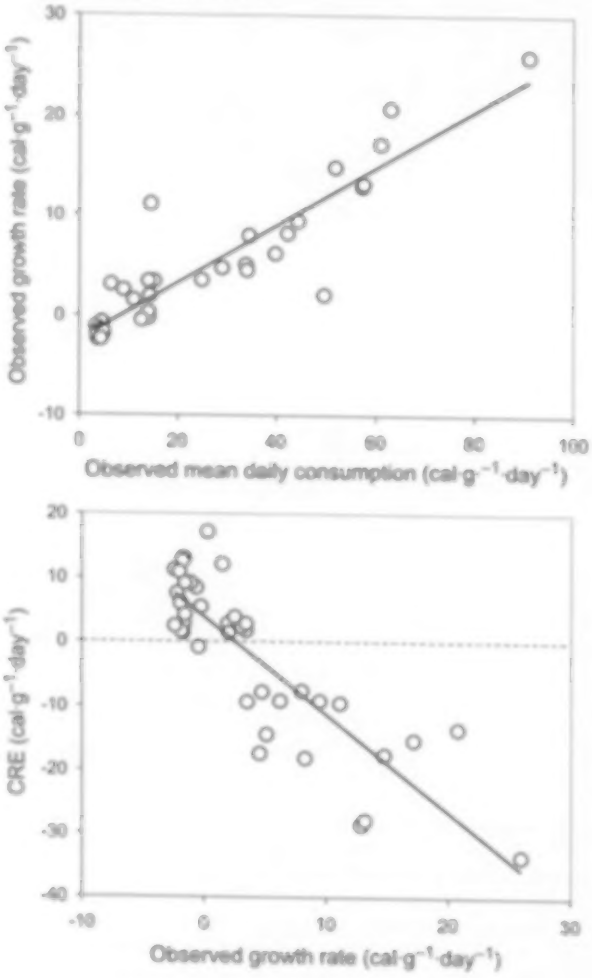

ties close to zero (Table 5). A slight tendency to overestimate consumption at very low ration levels (<10 cal·g^{-1}·day^{-1}, equivalent to <1% body weight·day^{-1}) and to underestimate consumption at high ration levels (>30 cal·g^{-1}·day^{-1}, equivalent to >3% body weight·day^{-1}) was indicated for the corrected model (Fig. 2*d*). Prediction error was indicated to be approximately 6 times lower than for the uncorrected model at corresponding ration levels, and did not exceed 5 cal·g^{-1}·day^{-1} (equivalent to 0.5% body weight·day^{-1}).

After correction, the relationship between CRE and temperature also remained significant (Table 5). There was an indication that the corrected model would slightly underestimate consumption at the lower end of the tested temperatures (23 °C) and overestimate at the upper end (30 °C). However, the overall error in predicting consumption rate was small and did not exceed 0.2% body weight·day^{-1} over the range of temperatures evaluated. The overall relationship between CRE and fish body weight, which was nonsignificant in the uncorrected model, remained so following model correction (Table 5). As for GRE, an indicated strong relationship between CRE and body weight exclusively for fish undergoing weight loss (Fig. 3*b*) was substantially reduced following correction (Fig. 5*b*). Although a significant CRE versus body weight

© 2004 NRC Canada

Table 6. Multiple regression results for response variables growth rate errors (GRE values) and consumption rate errors (CRE values) (both in cal·g^{-1}·day^{-1}; 1 cal = 4.184 J) versus mean levels of three predictor variables: consumption level (*C*; cal·g^{-1}·day^{-1}), fish body weight (*W*, g), and temperature (*T*, °C).

Response variable	Predictor variables in model	R^2	AIC
GRE	*C*, *T*, *T*·*C*, *T*·*W*, *C*·*W*, *C*·*T*·*W*	0.97	–518.8
GRE	*W*, *C*, *T*, *T*·*C*, *C*·*W*, *C*·*T*·*W*	0.97	–517.6
GRE*	*W*, *T*·*C*, *T*·*W*	0.96	–517.0
GRE	*C*, *W*, *T*	0.95	–506.3
GRE	*C*, *T*	0.80	–453.0
CRE	*W*, GRATE, *T*	0.88	–431.6
CRE	*W*, GRATE, *T*, *W*·GRATE	0.89	–430.2
CRE	*W*, GRATE, *T*, *T*·GRATE	0.88	–430.1
CRE*	GRATE, *W*	0.86	–426.8
CRE	GRATE, *T*	0.72	–399.9

Note: Regression results for the predictor variable growth rate (GRATE; cal·g^{-1}·day^{-1}) were applicable to CRE values only. Values of GRE and CRE and associated mean predictor variables were derived from individual fish for each of the three subperiods of the six laboratory experiments. All possible two- and three-way interactions among the three predictor variables were also considered. The best multiple regression models for GRE and CRE (*) were selected according to Akaike's information criterion (AIC) scores, adjusted R^2 values, and the number of predictor variables in the model, with more parsimonious models being favored. Selected multiple regression models represent full correction equations that could be incorporated into the uncorrected BEM to improve predictive accuracy.

relationship remained, the biasing effect was relatively minor.

Discussion

Significance of approach

Relatively few BEMs have been rigorously evaluated in laboratory settings; however, awareness of the potential to accurately identify model error through laboratory evaluations is growing (e.g., Madenjian and O'Connor 1999; Bajer et al. 2003; Whitledge et al. 2003). Despite findings that internal error exists within BEMs, seemingly logical post-evaluation efforts to reduce this error have been rare. We believe that the lack of efforts to improve BEMs is due to to the fact that error sources within these models have remained largely unknown. However, even if likely error sources in these models could be identified, the envisioned set of studies required to improve BEMs' internal subequations may be daunting and without guarantee of success. Recent laboratory evaluations (Madenjian and O'Connor 1999; Bajer et al. 2003) and the present study have identified at least two forms of systematic error within BEMs. Evidence that this systematic error is widespread among BEMs and can cause substantial over- and under-estimation of fish growth and consumption rates (Bajer et al. 2004) heightens the need to improve the predictive accuracy of BEMs, particularly given that rates of application of these models are rapidly increasing.

We have presented a novel and efficient approach for both identifying and correcting systematic error in BEMs that should substantially improve these models' abilities to accurately predict growth and consumption. Correction of systematic error in BEMs is possible, owing to the identification of significant relationships between model prediction error and levels of certain PIO variables (consumption rate, temperature, and fish body weight) for several BEMs (Bajer et al. 2003, 2004; present study). The correction approach that we present is considered efficient because model error evaluation and correction can be accomplished for a broad array of application conditions from a single laboratory data set that can be generated as a result of a reasonable level of effort.

Model correction versus fundamental improvement

Although we believe that development of correction equations offers an efficient and effective means for reducing potentially important systematic error in individual BEMs, model correction is not intended to fully substitute for the development of sound BEMs. Models that are fundamentally sound should perform better than those that incorporate correction equations. Accordingly, our error-correction approach is not intended to promote "rough-cut" construction of new BEMs, where developers might plan to counter expected inaccuracies by subsequently applying correction equations. Nor should our correction approach discourage in-depth efforts to fundamentally improve existing BEMs, such as by developing more complete and accurate internal equations for calculating energy costs and losses.

The findings of Bajer et al. (2004) indicate that all BEMs should be assumed to contain systematic error that could result in important inaccuracies whenever they are applied. Consequently, we suggest that error correction should be considered for any BEM when there are near-term plans for its application and the model has not been either fundamentally improved (e.g., via reevaluation and improvement of internal subequations) or corrected under the ranges of consumption level, fish body weight, and temperature to which it will be applied. Although prediction error in BEMs may be greatest under conditions where fish experience high consumption and growth rates (Bajer et al. 2004), we caution against using unimproved or uncorrected BEMs when high consumption and growth conditions are not anticipated in

© 2004 NRC Canada

Fig. 5. (*a*) Before- (●) and after-correction (○) regression relationships of BEM growth rate prediction errors (GRE) versus mean body weights of individual white crappie over modeled intervals. (*b*) Similarly for consumption rate prediction error (CRE) versus mean body weights. For both GRE and CRE, regression slopes and intercepts were significantly closer to zero following correction of the BEM (slope differences were determined by heterogeneity of slopes tests at $p \leq 0.05$, one-tailed test; intercepts were considered to differ if intercept means ±2 SEs did not overlap). 1 cal = 4.184 J.

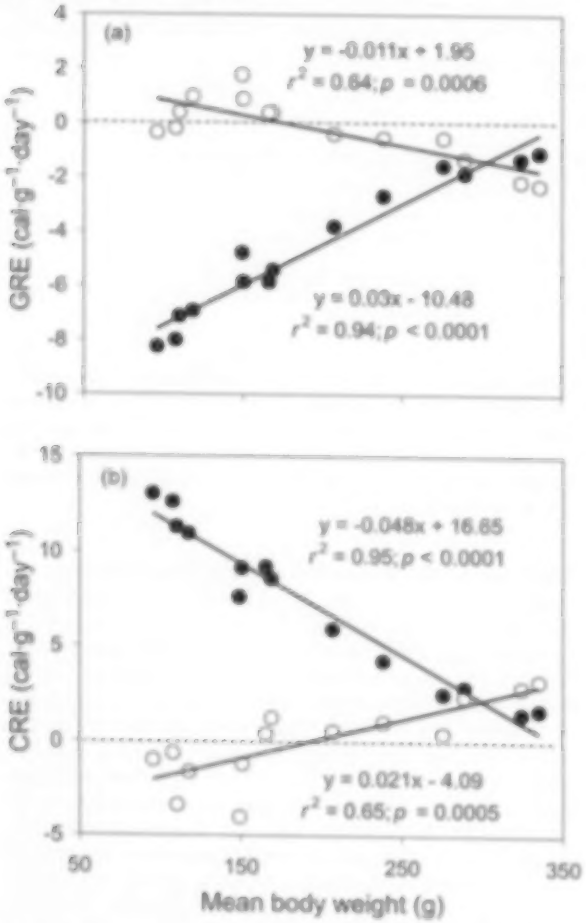

the application setting. Such conditions are difficult to anticipate, particularly in field settings, and it has been demonstrated that even short episodes of higher consumption or growth rates can lead to substantial prediction error.

Facilitating fundamental improvement of BEMs

The initial steps of developing correction equations for BEMs can also facilitate efforts to fundamentally improve these models. Defined correlations between model prediction error and certain PIO variables (necessary for model correction) indicate which energy cost/loss parameters within a BEM (R_s, ACT, SDA, F, and U) are likely sources of systematic error. Consumption level was highly correlated with prediction error in the uncorrected white crappie model, and it follows that one or more of the consumption-dependent cost/loss parameters in the uncorrected white crappie model (SDA, F, and U; eqs. 5–7) were likely sources of the observed systematic error. That a strong correlation has been found between consumption level and prediction error in a substantial number of BEMs (Madenjian and O'Connor 1999; Bajer et al. 2003, 2004) suggests inaccuracies in the equations for calculating SDA, F, or U in many BEMs. Another potential source of the observed consumption-dependent systematic error in BEMs could be unaccounted-for feeding-activity costs that are independent of SDA, and may involve feeding and foraging activity (Brett and Groves 1979; Cui and Wootton 1989) that increases with consumption level. A more detailed consideration of likely sources of the consumption-dependent systematic error within BEMs is provided by Bajer et al. (2004).

Although an overall relationship between model prediction error and fish body weight was not observed for the uncorrected white crappie model, a strong correlation was found when the analysis was restricted to fish from experiments 2 and 3 that were losing weight. Under these conditions, the uncorrected model underestimated growth rates of white crappie and overestimated their consumption rates. Growth and consumption prediction error increased with decreasing fish weight, accounting for the correlation between model prediction error rate and fish body weight. Inadequacy of the equation for routine standard metabolism (R_s) was indicated as the source of this error because it is the only energy cost/loss term in the uncorrected model with body-weight dependence. Hence, the correlation between model prediction error rate and fish body weight indicates that calculated R_s values were generally too high for fish undergoing weight loss and that overcalculation of metabolic cost increased for fish of lesser body weight. Reduction of metabolic rates in fish experiencing submaintenance feeding conditions is reasonably well documented (Beamish 1964; Glass 1968; O'Connor et al. 2000). However, this energy-conserving metabolic response is not included in most BEMs even though these models are sometimes applied to fish losing weight.

The uncorrected white crappie BEM was not originally designed to accommodate fish undergoing weight loss, and rigorous evaluation using data from experiments 2 and 3 revealed that it estimated consumption rates particularly poorly under these conditions. However, correction of the model using a data set that included some fish subjected to submaintenance feeding caused it to perform quite well under weight-loss conditions. Hence, a capacity was demonstrated for the correction procedure to extend a BEM's predictive ability beyond the bounds within which it was originally constructed.

Applying the corrected model

Cross-validation results indicated that the corrected BEM would provide substantially better predictions of white crappie growth and consumption than the uncorrected model when applied within the bounds of consumption level, body weight, and temperature covered by our six laboratory experiments. However, the set of error-correction equations that we developed were derived under all conditions present in our laboratory growth experiments, not only those of the three PIO variables. Consequently, even when white crappie experience consumption levels, temperatures, and body weights in other application settings that are within those bounded by our six laboratory ex-

© 2004 NRC Canada

periments, the correction equations that we present could be suboptimal, a possibility not fully reflected by our cross-validation results. In particular, substantial differences in white crappie activity levels or prey types, relative to those of the underlying laboratory experiments, could conceivably affect the extent to which our correction equations are optimal.

Through modeling, however, we were able to gain insight into the extent to which differences in fish activity level over time and locations would affect the applicability of the correction equations that we developed for the white crappie BEM through laboratory evaluations. First, using the uncorrected white crappie model, we entered the same initial fish weight (100 g), temperature (27 °C), and activity level (ACT = 1) in five single-time-step model runs, each run differing only in consumption level (0, 20, 40, 60, and 80 cal·g^{-1}); the resulting five model outputs of relative growth rate (RGR) increased linearly with consumption level (Fig. 6). We repeated these five simulations but with the corrected model. As expected, the resulting line of RGR values from the corrected model transected the corresponding line from the uncorrected model, the RGR values from the corrected model being lower at high consumption and higher at low consumption, reflecting correction of consumption-dependent model error (Fig. 6). The area between these two lines represented the estimated growth prediction error from the uncorrected model. The critical result was that when we ran the same simulations again with the two models, but using a substantially increased activity level (ACT = 3), the relationship between the RGR lines versus consumption level from the two models remained identical, even though both lines were shifted substantially downward because of the tripling of activity cost. Thus, prediction error (the area between the two lines) was uninfluenced by the marked change in activity level, so the same correction equation developed under one activity level will be appropriate at other activity levels. It is assumed, of course, that appropriate activity levels will be entered for all BEM simulations.

When developing the multiple regression equation for correcting the white crappie model's estimates of consumption, we used GRATE as a necessary surrogate for the input variable, consumption level. However, in BEM application settings where fish activity cost is substantially greater than that assumed in our laboratory experiments (zero activity cost), the relationship that we derived to estimate CRE values and correct consumption estimate error will be less appropriate. This relates to the fact that fish growth rates will decline with increasing activity (Fig. 6), causing the relationship between GRATE and CRE to be different from that which we originally observed across the laboratory experiments. However, in these other settings the relationship between total energy allocated to growth and activity (EGA = growth rate + activity, both in cal·g^{-1}·day^{-1}) versus CRE will remain the same as we determined in the laboratory. Thus, in application settings with substantially different fish activity costs, our correction equation for consumption (eq. 14) will be appropriate if GRATE is replaced by EGA. Again, this will require that fish activity cost be known over modeling intervals, but rightfully, activity levels should be determined even when uncorrected models are used.

We were unable to assess the extent to which differences in prey types would influence the appropriateness of the correction equations that we developed for the white crappie BEM, because only one prey type (fathead minnow) was used in the six laboratory experiments. However, we do feel that potential influences of differing prey types on the appropriateness of the presented set of BEM correction equations should be investigated. Although small fish often represent major portions of white crappie diets, this is not always so. We urge prospective users of the white crappie BEM to conduct what should be simple laboratory experiments to determine whether the corrected BEM performs as well for white crappie consuming an alternative prey type of interest as it does for white crappie consuming fathead minnows. We have presented a novel approach for reducing recently identified important error in BEMs. Efforts from other users of BEMs will be required to evaluate and further develop this approach

Fig. 6. Relative growth rates predicted by the uncorrected (broken lines) and corrected (solid lines) white crappie BEM for a 100-g fish at 27 °C and five different consumption levels. Predictions were generated for two levels of fish activity: ACT = 1 represents no activity cost above resting routine metabolism; ACT = 3 represents an activity cost that is three times resting routine metabolism. The areas between the solid and broken lines represent the prediction error, which does not change over the two activity levels. 1 cal = 4.184 J.

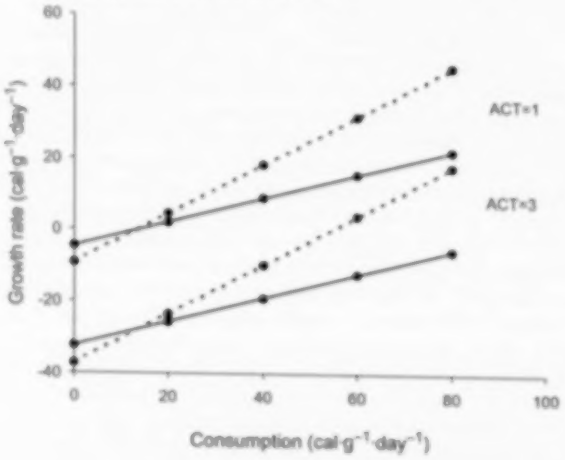

Designing laboratory experiments for correcting BEMs

The process of collecting data for evaluating BEMs has been considered difficult, and may account for the fact that rigorous evaluations have lagged well behind model application rates (Hewett and Johnson 1987). This view could apply to the process of constructing correction equations for BEMs, because development of a model-evaluation data set is the initial step. However, we believe that data sets for BEM evaluations, including those covering broad ranges of growth conditions, can be developed with reasonable effort if certain efficiency measures are incorporated into experimental designs. Fundamentally, a data set for evaluating a BEM will consist of observed growth rates for fish of a range of body weights experiencing known ranges of daily consumption level and temperature. Also needed are known or reasonably estimated values of activity cost and caloric density for test

© 2004 NRC Canada

fish and their prey. We recommend laboratory over field experiments for developing correction equations because the conditions that fish must experience to produce observed growth can be more accurately determined. Using individually held fish versus fish groups as the sample unit (as in the present study) allows substantially more observations per area of laboratory space and tends to improve statistical power. Holding fish individually also eliminates social interaction among them, which can be problematic in terms of its effects on food consumption and activity.

The use of full factorial experimental designs is desirable and may be feasible, particularly when using individually held fish. If possible, each of the three BEM input/output variables (consumption level, body weight, and temperature) should be represented at a minimum of three levels that span the full ranges of these conditions in anticipated BEM application settings. A full factorial design with three factors represented at three levels would involve 27 treatments, each with a distinct combination of consumption level, body weight, and temperature. We suggest that at least four fish be assigned to each treatment to reduce within-treatment variance. Full factorial designs promote a clearer interpretation of the determined predictive error because the applied variables are uncorrelated and allow for the subsequent construction of robust correction equations. Alternatively, less space-demanding fractional factorial designs, such as the one used in the present study, can provide good descriptions of systematic error in BEMs if sufficient portions of the array of consumption levels, body weights, and temperatures are covered.

Growth experiments need only be run long enough to establish a fish's growth pattern under a given set of conditions; 20-day experiments are recommended, where body weights are measured at the start and finish of this interval, consumption is measured daily, and temperature is constant. Longer experiments contribute no additional information in evaluation and correction data sets while substantially increasing costs. Short experiment periods also tend to involve more constant sets of growth conditions, which is desirable when analyzing associations between model error rate and associated consumption levels, body weights, and temperatures.

Acknowledgements

Funding for this work was provided in part by research grants to R.S. Hayward from the Missouri Department of Conservation. These grants provided graduate research assistantship (GRA) funding for P.G. Bajer and R.D. Zweifel. We thank James Breck for insights and helpful suggestions relating to many aspects of this study, and Marc Trudel for a thorough review of the manuscript.

References

Allen, J.R.M., and Wootton, R.J. 1982. The effect of ration and temperature on the growth rates of the three-spined stickleback (*Gasterosteus aculeatus* L.). J. Fish Biol. **20**: 409–422.

Bajer, P.G., Whitledge, G.W., Hayward, R.S., and Zweifel, R.D. 2003. Laboratory evaluation of two bioenergetics models applied to yellow perch (*Perca flavitilis*): identification of a major source of systematic error. J. Fish Biol. **62**: 436–454.

Bajer, P.G., Whitledge, G.W., and Hayward, R.S. 2004. Widespread consumption-dependent systematic error in fish bioenergetics models and its implications. Can. J. Fish. Aquat. Sci. **61**. This issue.

Beamish, F.W.H. 1964. Influence of starvation on standard and routine oxygen consumption. Trans. Am. Fish Soc. **93**: 103–107.

Brett, J.R., and Groves, D.D. 1979. Feeding metabolism. *In* Fish physiology. Vol. 8. Bioenergetics and growth. *Edited by* W.S. Hoar, D.J. Randall, and J.R. Brett. Academic Press, New York. pp. 298–305.

Burnham, K.P., and Anderson, D.R. 2001. Kullback–Leibler information as a basis for strong inference in ecological studies. Wildl. Res. **28**: 111–119.

Carline, R.F., and Hall, D.J. 1973. Evaluation of a method for estimating food consumption rates of fish. J. Fish. Res. Board Can. **30**: 623–629.

Cui, Y., and Wootton, R.J. 1989. Bioenergetics of growth of a cyprinid, *Phoxinus phoxinus* (L.): development and testing of a growth model. J. Fish Biol. **34**: 47–64.

Davis, G.E., and Warren, C.E. 1971. Estimation of food consumption rates. *In* Methods for assessment of fish production in fresh waters. *Edited by* W.E. Ricker. Blackwell Scientific Publications, Oxford. pp. 227–248.

Glass, N.R. 1968. The effect of time of food deprivation on the routine oxygen consumption of largemouth bass (*Micropterus salmoides*). Ecology, **49**: 340–343.

Hanson, P.C., Johnson, T.B., Schindler, D.E., and Kitchell, J.F. 1997. Fish bioenergetics 3.0. University of Wisconsin Sea Grant Institute, Madison.

Hewett, S.W., and Johnson, B.L. 1987. A generalized bioenergetics model of fish growth for microcomputers. Sea Grant Tech. Rep. No. WISCG-87-245, University of Wisconsin, Madison.

Hewett, S.W., and Johnson, B.L. 1992. Fish bioenergetics model 2: an upgrade of a generalized bioenergetics model of fish growth for microcomputers. University of Wisconsin Sea Grant Institute, Madison.

Jobling, M. 1994. Fish bioenergetics. Chapman and Hall, London.

Kitchell, J.F., Stewart, D.J., and Weininger, D. 1977. Applications of a bioenergetics model to yellow perch (*Perca flavescens*) and walleye (*Stizostedion vitreum*). J. Fish. Res. Board Can. **34**: 1922–1935.

Madenjian, C.P., and O'Connor, D.V. 1999. Laboratory evaluation of a lake trout bioenergetics model. Trans. Am. Fish. Soc. **128**: 802–814.

Neter, J., Kutner, M.H., Nachtsheim, C.J., and Wasserman, W. 1996. Applied linear statistical models. 4th ed. The McGraw–Hill Companies Inc., New York.

Ney, J.J. 1999. Pratical use of biological statistics. *In* Inland fisheries management in North America. *Edited by* C.C. Kohler and W.A. Hubert. American Fisheries Society, Bethesda, Md. pp. 167–191.

O'Connor, K.I., Taylor, A.C., and Metcalfe, N.B. 2000. The stability of standard metabolic rate during a period of food deprivation in juvenile Atlantic salmon. J. Fish Biol. **57**: 41–51.

Whitledge, G.W., Hayward, R.S., Zweifel, R.D., and Rabeni, C.F. 2003. Development and laboratory evaluation of a bioenergetics model for sub-adult and adult smallmouth bass. Trans. Am. Fish. Soc. **132**: 316–325.

Zweifel, R.D. 2000. Development and evaluation of a bioenergetics model for white crappie. M.Sc. thesis, University of Missouri, Columbia.

© 2004 NRC Canada

Movements associated with home-range establishment by two species of lowland river fish

David A. Crook

Abstract: Individuals that occupy restricted home ranges for long periods have little chance to sample surrounding habitats and may only be able to respond to changes in the distribution of resources at very local scales. Processes leading to the selection of a home range, therefore, potentially have an important bearing on individual fitness and, ultimately, on population structure. In this study, movements associated with the establishment of home ranges by golden perch (*Macquaria ambigua*) and common carp (*Cyprinus carpio*) in an Australian lowland river were examined using radiotelemetry. To examine behaviour associated with exploration and settlement into new home ranges, fish were artificially translocated into an unfamiliar river section. Although there was substantial intraspecific variation in patterns of movement, all fish tracked over the entire study period eventually settled into restricted home ranges. Several fish of both species either moved away from established home ranges and settled in new areas, or undertook large-scale movements and subsequently returned to the original home range. It is suggested that such movements may provide a mechanism by which fish can reap the benefits of home-range occupation whilst still being able to respond to changes in the distributions of spatially and temporally dynamic resources.

Résumé : Les individus qui occupent des aires vitales restreintes durant de longues périodes ont peu d'occasions d'évaluer les habitats environnants et ils sont peut-être réduits à réagir aux changements de répartition des ressources à des échelles très locales. Les mécanismes qui mènent à la sélection d'une aire vitale ont donc potentiellement une forte influence sur le fitness individuel et, en fin de compte, sur la structure de la population. La radiotélémétrie a servi à étudier les déplacements associés à l'établissement de l'aire vitale chez la perche dorée (*Macquaria ambigua*) et la carpe (*Cyprinus carpio*) dans une rivière de plaine d'Australie. Le déplacement artificiel de poissons vers une section non familière de rivière a permis de suivre les comportements reliés à l'exploration et à l'établissement dans une nouvelle aire vitale. Bien qu'il y ait une importante variation intraspécifique des patterns de déplacement, tous les poissons suivis pendant toute la période d'étude se sont éventuellement établis dans des aires vitales restreintes. Plusieurs poissons des deux espèces ont quitté des aires vitales établies et se sont installés dans de nouveaux milieux; d'autres ont entrepris de longs déplacements pour revenir ensuite dans leur aire vitale d'origine. Il apparaît donc que de tels déplacements fournissent un mécanisme qui permet aux poissons de tirer les bénéfices de l'occupation d'une aire vitale, tout en étant capables de réagir aux changements de répartition de ressources qui varient de façon dynamique dans l'espace et le temps.

[Traduit par la Rédaction]

Introduction

A tenet of theoretical models that link individual levels of fitness to patterns of space utilization is that animals have the ability to acquire knowledge of the quality of habitats potentially available to them (MacArthur and Pianka 1966; Fretwell and Lucas 1970; Brown 1990). However, individuals that occupy restricted home ranges for long periods may have little chance to sample surrounding habitats and, as a consequence, may only be able to respond to changes in the distribution of resources at very local scales (Armstrong et al. 1997). The processes leading to the initial selection of a restricted home range, therefore, are likely to have an important bearing on the relative fitness of an individual and, ultimately, on the structure of populations (Morris 1992; Switzer 1993; Armstrong et al. 1997).

A large number of studies of riverine fish populations have shown that most individuals occupy restricted home ranges (see review by Rodríguez 2002). This body of research forms the central tenets of what has become known as the restricted-movement paradigm (sensu Gowan et al. 1994). Although many previous studies have examined the home-range movements of riverine fish, apart from the study of Armstrong et al. (1997), there has been little detailed

Received 24 September 2003. Accepted 18 June 2004. Published on the NRC Research Press Web site at http://cjfas.nrc.ca on 26 January 2005.
J17759

D.A. Crook.[1] The Johnstone Centre, School of Science and Technology, Charles Sturt University, Wagga Wagga, New South Wales, Australia, and the Cooperative Research Centre for Freshwater Ecology, Murray–Darling Freshwater Research Centre, Albury, New South Wales, Australia.

[1]Present address: Department of Sustainability and Environment, Arthur Rylah Institute for Environmental Research, 123 Brown Street, Heidelberg, 3084, Victoria, Australia (e-mail: David.Crook@dse.vic.gov.au).

 doi: 10.1139/F04-151 © 2004 NRC Canada

Fig. 1. Map showing the location of the study site on the Broken River in southeastern Australia.

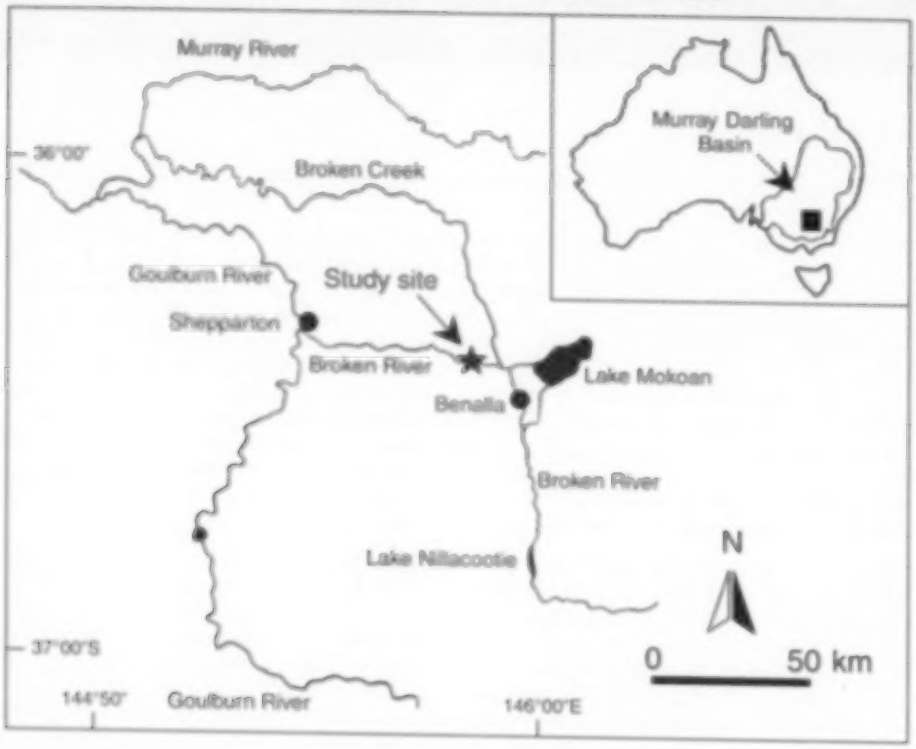

study of the behaviour associated with the establishment of new home ranges by fish in rivers. Armstrong et al. (1997) transplanted Atlantic salmon parr (*Salmo salar*), collected from a natural stream, into an adjoining 80 m long stream enclosure to examine exploratory and settlement behaviour. Most of the transplanted fish exhibited mobile exploratory behaviour for only a short period (<2.5 days) before settling into restricted home ranges, and some individuals did not sample alternative habitats at all before settlement. Armstrong et al. (1997) also found that, once settled into home ranges, Atlantic salmon parr rarely exhibited exploratory behaviour outside the home range (see also Armstrong et al. 1994, 1998).

The aim of the current study was to examine movements associated with the establishment of home ranges by golden perch (*Macquaria ambigua*) and common carp (*Cyprinus carpio*) in an Australian lowland river. Golden perch are native to lowland rivers in southeastern Australia, whilst carp were introduced from southeast Asia and have become widespread in Australian lowland rivers since the early 1970s (Shearer and Mulley 1978). In a previous study (Crook 2004*b*), both of these species were found to exhibit strong site fidelity and occupy restricted home ranges. Although the home ranges of individuals of the species may overlap (Crook 2002), little information relating to competition or other behavioural interactions between the species is currently available. Crook (2004*b*) found that the home ranges of both species were not always spatially constant, with some individuals changing the locations of their home ranges during the study. Based on these findings, a "home-range shift" (HRS) conceptual model was proposed to describe the movements of golden perch and carp (Crook 2004*b*). In the model, it is suggested that fish exhibit fidelity to restricted home ranges for extended periods that are interspersed by relatively short periods of mobility associated with HRS behaviour. The process of HRS includes an emigration phase, an exploratory mobile phase, and a home range establishment phase. Under the tenets of the model, behaviour associated with exploration and home-range establishment is particularly important because it determines the location of the new home range and, therefore, the quality and quantity of resources available to an individual once it has settled. In the current study, an artificial HRS is imposed upon individual fish to examine behaviour associated with exploration and settlement into new home ranges.

Materials and methods

Study site and habitat description

The study was conducted between February and May 2001 in a low-gradient region of the Broken River in southeastern Australia (Fig. 1). The Broken River has a mean annual discharge of 2×10^8 m^3 and the dominant habitat types within the study region are relatively shallow, fast-flowing runs interspersed by deep, slow-flowing pools. As the aim of the study was to examine the movements of displaced fish within a well-characterized environment, a 4000 m long section of the river was treated as a large experimental enclosure. Fish movement in the study section was blocked at the upstream end by an existing barrier consisting of a concrete

© 2004 NRC Canada

Fig. 2. Mean daily temperature (dotted line) and discharge (solid line) in the Broken River during the study period. Floodplain inundation occurs at a discharge of ~21 400 ML·day^{-1}.

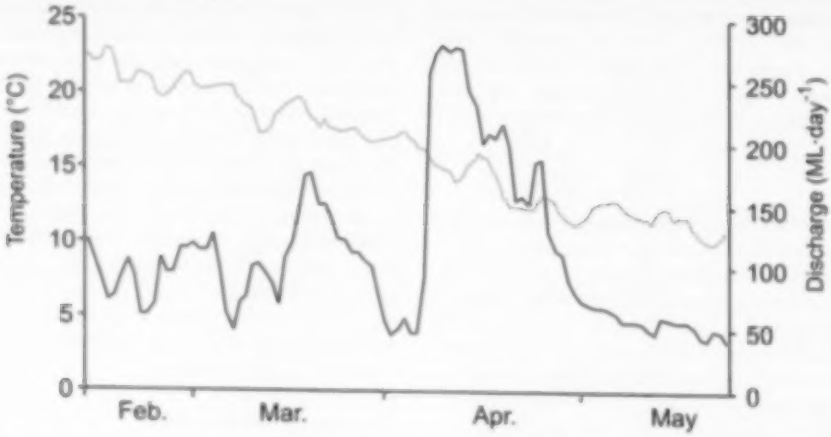

roadway. To block the downstream end of the study section, a fence made of 50 mm mesh plastic fencing material was constructed 4000 m downstream of the upstream river crossing. This fence was cut to fit the shape of the riverbed and was held in place using metal pickets. A 500 mm wide skirt attached along the bottom of the fence, made of the fencing material and facing upstream, was weighed down with sand bags to ensure that fish could not pass underneath the fence.

Depth and current velocity (at 0.4 of total depth from riverbed) measurements were taken at 20-m intervals along the river channel thalweg using a weighted measuring line and a submersible flow meter (General Oceanics, Miami, Florida, USA) from a canoe on 24 January 2001. A global positioning system (GPS) unit and a detailed map of the study section were used to determine the location of each set of habitat measurements. The study section was divided into two mesohabitat types (pools, runs) based on a combination of visual classification and an assessment of the depth and velocity measurements. Habitats defined as pools and runs represented 51% and 49%, respectively, of the study-section length. Water temperatures during the study period ranged from 10 to 23 °C, with a gradual decline associated with the change in seasons from summer to autumn (Fig. 2). River flow was generally low during the study period, although a rapid rise in water level occurred on 8 April 2001 (day 48). This rise in level caused the water to breach the downstream fence so that it no longer presented a complete barrier to fish movement. The fence was subsequently removed on 15 April (day 55) and the study continued without a downstream barrier.

Fish collection and radio-tagging

Fifteen golden perch and 15 carp were collected for radio-tagging on 16–19 February 2001 by angling, backpack electrofishing, and fyke-netting. All of the golden perch and seven of the carp were collected from the main channel of the Broken River, and eight of the carp were collected from a billabong (small floodplain lake) beside the main river channel. The fish-collection sites were well upstream and downstream of major barriers to fish movement, so that the fish would be highly unlikely to have prior knowledge of the study section. All golden perch were collected from the upstream collection site, which was situated above Casey weir and was ~25 km by river from the study section. All of the carp were from the downstream collection site, which was situated below Gowangardie weir and was ~50 km by river from the study section.

Table 1. Identifying codes (ID), lengths, and wet weights of radio-tagged golden perch (*Macquaria ambigua*) and carp (*Cyprinus carpio*).

Golden perch			Carp		
ID	Total length (mm)	Weight (g)	ID	Fork length (mm)	Weight (g)
G1	360	675	C1[a]	280	450
G2	320	475	C2	430	1475
G3	320	450	C3[a]	380	1225
G4	300	350	C4[a]	320	675
G5	280	300	C5[a]	370	1050
G6	300	350	C6	470	1800
G7	350	675	C7[a]	290	575
G8	300	375	C8	430	1575
G9	380	750	C9	430	1525
G10	330	525	C10	400	1300
G11	280	325	C11	420	1475
G12	310	400	C12	440	1525
G13	300	375	C13[a]	290	525
G14	360	650	C14[a]	540	2750
G15	370	700	C15[a]	470	1750
Mean	320	490	Mean	400	1310

[a]Collected from a billabong beside the main river channel.

Collected fish were held in two 6400-L holding pools (one for each species) beside the study section for up to 4 days before release. Following removal from the holding pools, each fish was anaesthetized in a 100 mg·L^{-1} solution of MS 222 and then weighed and measured (Table 1). Single-stage 151-MHz transmitters (Titley Electronics, Ballina, New South Wales, Australia) were attached externally using the method described by Crook (2004*a*). The transmitters weighed 3.4 g in air and had estimated battery lives of

© 2004 NRC Canada

4 months. The release locations were 200 m apart along the river channel, with one individual of each species released at each location. The most upstream and downstream release points were each located ~600 m from the upstream and downstream barriers, respectively. Releases began at the most downstream location and proceeded upstream, with the first fish released at 0915 and the last fish released at 1550 on 20 February 2001.

Fish tracking

Tracking began 2 h after the last radio-tagged fish was released. Tracking surveys were conducted every day for the first 10 days and were then conducted every 5 days for the remainder of the 3-month study period. In the first 10 days, surveys were conducted in the early morning and late afternoon of each day so that the net distances moved during the day and night could be estimated separately. When the tracking frequency was reduced, three surveys were conducted on each trip (late afternoon, early morning, late afternoon) to allow estimation of net movements for both day and night. The tracking surveys took 2–3 h and were conducted by walking with a scanning radio receiver from the upstream barrier to the downstream fence and then returning upstream. Upon locating a radio-tagged fish, geographic coordinates were assigned using a GPS unit and a detailed reference map of the study section. The habitat type in which each fish was located was also noted. If any of the fish were not located during a survey, the river was scanned for ~3 km downstream of the study section to determine whether the fence barrier had been breached. In addition to the regular ground surveys, an aerial survey consisting of six passes over the 35 km long stretch of river between the study section and the downstream Gowangardie weir was conducted on 2 May 2001 to determine whether any fish had moved farther downstream.

Analysis of movement data

To determine whether fish showed an initial homing tendency, the data were examined visually and χ^2 tests performed for each species to establish if there were net displacements in either upstream or downstream directions after days 1, 5, and 10. The distances (m) between fish locations along the river channel were then calculated using the geographic coordinates and aerial photographs of the study section scanned in Arcview 3.2™. As the aim of the study was to determine whether the fish exhibited an initial mobile phase followed by a more sedentary phase, the study period was arbitrarily divided into two distinct phases for the purposes of the analysis. Days 1–10, which included the first 18 estimated distances, were defined as the initial period of the study. Days 50–90, which included the last 18 estimated distances, were defined as the final period of the study. The distance between successive observations was measured to examine variation in the amount of movement between the two species, between day and night, and between the initial and final phases of the study period. As the time between successive observations varied slightly, the distance data were standardized by dividing the distance travelled by the time (h) elapsed in travelling between locations. It should be noted, however, that fish did not move at a constant rate or in a constant direction and that the distance data do not represent a measure of the speed of movement. The distance data were $\log_{10}(x + 1)$-transformed to meet the assumptions of normality and homogeneity of variance required for parametric analyses. A three-way analysis of variance (ANOVA) was then conducted using the mean distance moved by each individual fish over the initial and final phases as the dependant variable, with species (golden perch, carp), time of day (day, night), and survey period (initial, final) as factors. Fish that were not located during the final survey period because of transmitter failure were removed from this analysis. In describing the results of the study, movements associated with home-range occupation were defined on the basis of the home-range and site-fidelity analyses conducted by Crook (2004*b*). Golden perch and carp were deemed to be occupying home ranges when their locations were restricted to within approximately 100 and 500 m, respectively, over periods of 15 days or more.

Analysis of habitat data

The minimum numbers of habitats visited by each fish during the entire tracking period, the initial phase of the study (days 1–10), and the final stage of the study (days 50–90) were estimated by determining the number of separate pool and run habitats between the most upstream and downstream locations of the fish during each of the three periods. For fish tracked over the whole 90-day study period, a two-way ANOVA using $\log_{10}$-transformed data was performed to determine whether the number of habitats visited differed between the two species and (or) between the initial and final phases of the study. The relative overall use of pools and runs by golden perch and carp over the study period was examined by calculating a selectivity index (D) (Jacobs 1974):

$$(1) \qquad D = r - p/(r + p - 2rp)$$

where p is the proportion of pool habitat available (i.e., 0.51) and r is the proportion of the pool habitat used (i.e., number of locations in pools / total number of locations). When D is calculated in this manner, positive values indicate a preference for pool habitats and negative values indicate a preference for run habitats. Mann–Whitney U tests were performed to examine separately any differences in habitat-preference values between the species, at different times of day, and between the initial and final phases of the study. The habitat-preference values for the third survey of each trip in the final phase of the study (i.e., the second afternoon survey) were not included in this analysis to maintain equality between the numbers of observations at each time of day.

Results

Movement patterns

Of the 30 fish fitted with radio transmitters, 17 were tracked for the entire 90-day study period and 25 were tracked for more than 50 days. The tracking surveys demonstrated that the fence at the downstream end of the study section acted as an effective barrier to fish movement until the high-flow event on day 48. Prior to day 48, five fish (G1, G9, G15, C5, C13) made rapid downstream movements to <30 m of the fence, but did not proceed farther downstream (Figs. 3 and 4). During the ground and aerial tracking surveys, only one fish (G14) was ever located outside the study section. This

© 2004 NRC Canada

Fig. 3. Locations of radio-tagged golden perch (*Macquaria ambigua*) within the study reach over the duration of the study. The locations of the downstream and upstream barriers equal 0 and 4000 m, respectively. Symbols represent radiolocations. The identifying code for each fish is shown in the graph. The arrow indicates a rapid rise in river level. The broken line in the graph for G14 shows the location of the downstream barrier that was breached on day 48.

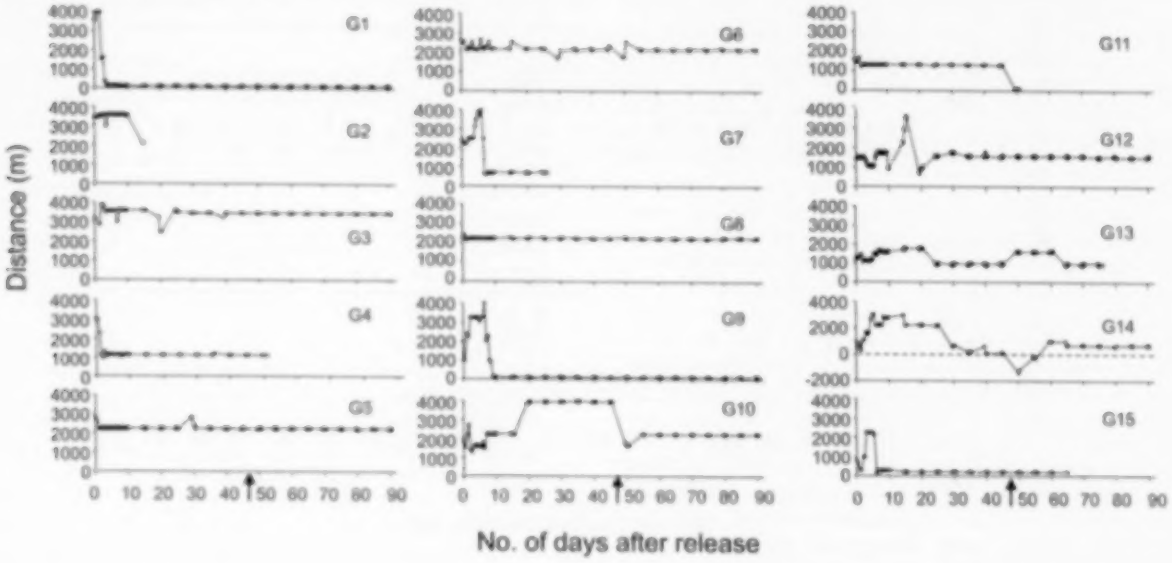

Fig. 4. Locations of radio-tagged carp (*Cyprinus carpio*) within the study reach over the duration of the study. The locations of the downstream and upstream barriers equal 0 and 4000 m, respectively. Symbols represent radiolocations. The identifying code for each fish is shown in the graph. The arrow indicates a rapid rise in river level.

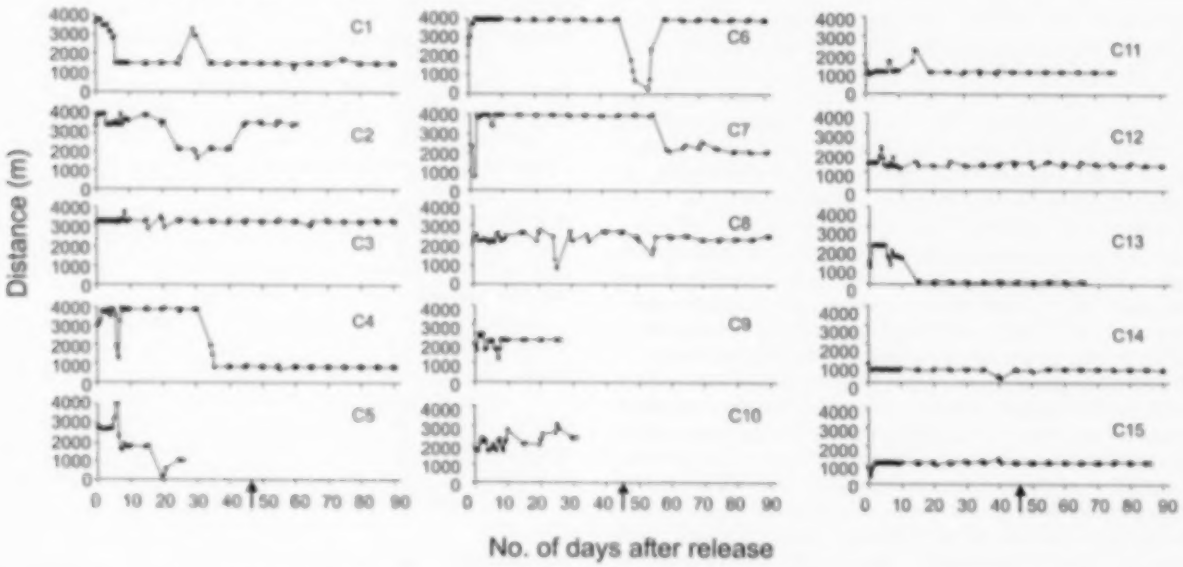

fish moved ~1500 m downstream of the fence barrier after it had been breached and subsequently moved back upstream into the study section (Fig. 3). Failure to locate some of the fish in the later part of the study appeared to be due to transmitter malfunction rather than movement out of the survey area, as a change in the transmitter signal usually preceded failure to locate a particular fish. Transmitter failure, as opposed to movement out of the survey area, was further indicated by the failure to locate missing fish during the aerial surveys between the upstream barrier and Gowangardie weir.

The movements of individuals of both species followed a similar general pattern over the study period. Apart from one fish (G2) whose transmitter failed after day 15, all of the

© 2004 NRC Canada

Fig. 5. Mean distances moved during the day and night by golden perch and carp over the study period. The vertical bars represent ±1 standard error around the mean, and the arbitrarily defined initial and final phases of the study are indicated. (*a*) Golden perch, day. (*b*) Golden perch, night. (*c*) Carp, day. (*d*) Carp, night.

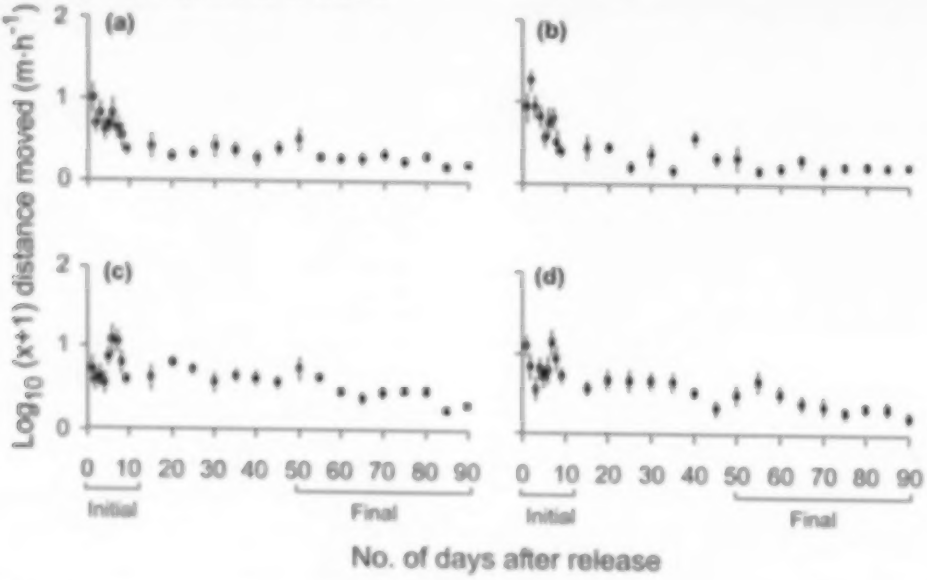

radio-tagged golden perch exhibited relatively high rates of movement during the initial phase, and had settled into restricted home ranges by the end of the final phase (Fig. 3). Of the 15 radio-tagged carp, 13 also exhibited high rates of movement after release, and subsequently established restricted home ranges (Fig. 4). The two carp that did not follow this general pattern (C5, C10) showed relatively high levels of movement until their transmitters failed after days 26 and 31, respectively. There was no evidence of a general tendency by fish to move towards the original site of capture (Figs. 3 and 4), and no significant net displacements occurred in upstream or downstream directions after 1, 5, and 10 days for either species (χ^2 tests: all tests $P > 0.05$).

Although the broad movement patterns of both species were similar, substantial intraspecific variation in the timing and extent of movements was apparent. Three of the golden perch (G5, G8, G11) and two of the carp (C14, C15) exhibited relatively restricted movements over a very short period in the initial phase (Figs. 3 and 4). In contrast, one golden perch (G14) and two carp (C2, C8) exhibited relatively high levels of movement for more than 50 days before settling into restricted home ranges. One of the carp (C3) exhibited very little movement in the initial phase of the study. However, higher levels of movement were exhibited between days 15 and 21, after which time the fish occupied a restricted home range near the original release location (Fig. 3). Two golden perch (G10, G13) and three carp (C2, C4, C7) that exhibited initially high levels of movement followed by lower levels of movement, subsequently exhibited distinct shifts to new home-range locations (Figs. 3 and 4). In three of these cases (G10, G13, C2), the fish later returned to the same home-range locations they had occupied previously. Several fish of both species (G5, G6, C1, C6, C8, C14) also moved relatively large distances from their home ranges, but rather than establishing new home ranges, these fish returned to the original home-range location within a few days.

Many of the large-scale movements undertaken by golden perch after the initial phase of the study appear to have occurred in response to the rapid rise in river level on day 48. Of the 13 golden perch with functional transmitters remaining after day 50, four (G6, G10, G11, G13) moved away from established home ranges between days 45 and 50 (Fig. 3). The single golden perch (G14) that had not established a restricted home range by day 45 also moved ~1500 m downstream between days 45 and 50. As previously mentioned, this fish moved past the breached downstream barrier and subsequently returned upstream into the study section (Fig. 3). Only one (C6) of the remaining 12 carp with functional transmitters moved an unusually large distance between days 45 and 50 (Fig. 4).

Although there was considerable variation in the movements of individual fish, the generality of the transition from mobile to sedentary behaviour is demonstrated by a decline in the distances moved between locations over time for both species (Fig. 5). Movement during the initial phase was significantly higher than during the final phase ($P < 0.001$), and differences between the two survey periods explained most of the variance in the data (Table 2).

Mesohabitat associations

A total of 31 separate mesohabitats (16 pools and 15 runs) were identified within the mapped study section. The minimum number of habitats visited by individual golden perch during the study ranged from 3 to all 31 habitats, whilst individual carp visited between 6 and 30 of the habitats (Table 3). Both golden perch and carp visited significantly more habitats during the initial phase than in the final phase of the study (two-way ANOVA, $P < 0.01$). Overall, there was no

© 2004 NRC Canada

Table 2. Mean squares (MS) and significance levels for the results of a three-way ANOVA on mean $\log_{10}(x + 1)$-transformed distances moved by individual fish, with species (golden perch, carp), time of day (day, night), and survey period (initial phase, final phase) as factors.

Factor	df	MS
Species	1	0.467*
Time of day	1	0.009 ns
Survey period	1	8.185***
Species × time of day	1	0.013 ns
Species × survey period	1	0.519*
Time of day × survey period	1	0.493*
Species × time of day × survey period	1	0.001 ns
Error	92	0.104

Note: *, $P < 0.05$; ***, $P < 0.001$; ns, not significant.

significant difference between the numbers of habitats visited by golden perch and carp ($P > 0.05$). Although four golden perch (G6, G10, G13, G14) made brief excursions through multiple habitats, all golden perch with functional transmitters were observed in a single "home" pool for most of the final phase of the study (Table 3, Fig. 3). Three carp (C11, C13, C15) were observed within single pools in the final phase, although none of these fish was tracked for the full period, owing to transmitter failure (Table 3, Fig. 4). One carp (C6) was observed to have passed through 28 of the 31 habitats during a series of large-scale movements between days 46 and 60, before returning to its previous home pool at the upstream end of the study section (Table 3, Fig. 4). Two carp (C3, C4) were observed in home ranges within single runs during the final phase of the study and six carp (C1, C2, C7, C8, C12, C14) were observed in home ranges that included both pool and run habitats.

In general, both golden perch and carp demonstrated preferences for pool habitats in the initial phase of the study period (Fig. 6). During this period, the habitat-preference values for the two species were not significantly different (Mann–Whitney U test, $P > 0.05$). However, there were significant differences between the two species in the final phase of the study, with golden perch utilizing pool habitats more than carp ($P < 0.001$). Golden perch increased their use of pool habitats over time, with habitat-preference values significantly higher in the final phase than in the initial phase ($P < 0.001$). In contrast, the use of pool habitats by carp decreased over time, with habitat-preference values significantly lower in the final phase than in the initial phase ($P < 0.05$). Neither species showed a significant change in habitat preference between the early-morning and late-afternoon survey times ($P > 0.05$).

Discussion

Following the artificially imposed home-range shift, individuals of both species exhibited an initial period of relative mobility. Levels of mobility then decreased over time as fish settled into discrete home ranges. Under the tenets of the HRS model (Crook 2004*b*), the initial mobile stage consists of exploratory behaviour, where fish sample the environment to assess the suitability of potential residence areas prior to settling into home ranges. Although the results of the current study are consistent with this explanation, there are other potential explanations for the initial mobility that should also be considered. For instance, it is possible that the displaced fish initially attempted to return to their original home ranges, and that the observed mobility simply represents attempted homing by fish. Crook (2004*b*) found that a proportion of artificially displaced golden perch and carp returned to their original home ranges from distances of up to 2.7 km within 5 days of release. In the current study, the golden perch were collected ~25 km upstream of the study site, whilst the carp were collected from ~50 km downstream. If these fish were capable of homing from such distances, one would expect that individuals of each species would tend to move in the direction of the collection site during the initial phase of the study. However, individuals of neither species exhibited a clear tendency to move in the direction of the collection site, and there were no significant net displacements in upstream or downstream directions after days 1, 5, or 10 for golden perch or carp. These observations suggest that neither the golden perch nor the carp were capable of detecting the direction of their original home ranges. However, whilst the fish may not have been capable of homing, having been translocated over such large distances, it is possible that they were attempting to locate their original home ranges during the initial phase of the study.

Another potential explanation for the observed results is that mobility decreased as water temperatures declined with the transition from summer to autumn. Mean daily water temperatures ranged between 19 and 23 °C in the initial phase of the study and between 10 and 16 °C in the final phase. Several previous studies have shown that the mobility of fish decreases at lower water temperatures (e.g., Swanberg 1997; Hilderbrand and Kershner 2000), although the seasonal variations in these studies were usually far greater than in the current study. Swanberg (1997), for example, examined changes in the rates of movement of bull trout (*Salvelinus confluentus*) at water temperatures ranging from 0 °C in winter to 21 °C in summer. Several other studies have shown either no correlation between mobility and water temperature (Allouche et al. 1999) or increased mobility with decreasing water temperatures (Clapp et al. 1990; Moser and Ross 1995). Crook (2004*b*) found that 7% of the daily movements of non-displaced golden perch and 8% of those of carp were greater than 250 m in the first 10 days after release. In contrast, 43% of the daily movements of artificially displaced golden perch and 23% of those of carp were greater than 250 m in the first 10 days. In the current study, 24% of the daily movements of golden perch and 31% of those of carp were greater than 250 m in the first 10 days. Considering that both the current study and the study by Crook (2004*b*) were conducted in the same section of river and under very similar temperature conditions, it appears likely that the higher levels of initial mobility in the current study were due to behaviour associated with artificial displacement rather than to seasonal changes in water temperature.

Although there were consistent broad patterns of movement in the current study, there was a large variation in the more detailed movements of individual fish. Some fish exhibited relatively low levels of movement over only a few

© 2004 NRC Canada

Table 3. Minimum numbers of pool and run mesohabitats visited by individual fish during the entire tracking period (days 1–90), the initial phase of the study (days 1–10), and the final phase of the study (days 50–90).

ID	Tracking period (days)	Pools			Runs		
		Entire	Initial	Final	Entire	Initial	Final
Golden perch							
G1	90	16	16	1	15	15	0
G2	15	5	1	—	4	2	—
G3	90	4	3	1	3	3	0
G4[a]	51	8	8	1	7	7	0
G5	90	2	2	1	2	2	0
G6	90	5	3	4	5	3	5
G7	26	13	13	—	12	12	—
G8	90	1	1	1	2	2	0
G9	90	16	16	1	15	15	0
G10	90	10	6	4	9	6	3
G11[a]	51	8	2	1	7	2	0
G12	90	10	4	1	11	4	0
G13[a]	76	5	3	4	4	2	3
G14[b]	90	13	11	3	13	12	2
G15[a]	65	11	11	1	10	10	0
Mean ± 1 SE	72.8±6.6	8.5±1.2	6.7±1.4	1.9±0.4	7.9±1.2	6.5±1.3	1.0±0.5
Carp							
C1	90	9	8	3	8	8	2
C2[a]	61	9	3	1	8	2	1
C3	90	3	2	0	3	2	1
C4	90	11	9	0	12	9	1
C5	26	15	9	—	15	8	—
C6	90	14	4	14	14	4	14
C7	90	12	12	7	12	12	6
C8	90	7	2	5	8	3	4
C9	26	6	6	—	6	6	—
C10	31	6	5	—	6	5	—
C11[a]	76	6	3	1	7	2	0
C12	90	6	6	1	5	5	1
C13[a]	66	10	6	1	9	5	0
C14	90	5	3	1	4	2	1
C15[a]	86	5	4	1	4	3	0
Mean ± 1 SE	72.8±6.5	8.3±0.9	5.5±0.8	2.9±1.2	8.1±1.0	5.1±0.8	2.6±1.2

Note: The mapped study section contained 31 mesohabitats (16 pools and 15 runs).
[a]Tracked for only part of the final phase, owing to transmitter failure.
[b]Located downstream of the mapped study section between days 50 and 56.

days, before occupying restricted home ranges. In contrast, other fish were relatively mobile for more than 50 days before finally settling into home ranges. There are a variety of factors that may have led to these individual differences in behaviour, including social interactions (e.g., the time taken to establish a position within a dominance hierarchy) or differences in the abilities or motivations of individuals to explore available habitats. However, whilst there was considerable individual variation in the timing and extent of movements, all fish tracked over the entire 90-day study period eventually settled into restricted home ranges.

The results of the study suggest that many golden perch and carp invest a relatively large amount of energy in locating a home range. Of the 15 radio-tracked golden perch, only 3 (20%) settled into home ranges within 2.5 days and 8 (53%) took more than 10 days to establish home-range locations. On average, golden perch visited a minimum of 13.2 (43%) of the 31 available habitats and traversed at least 1620 m (41%) of the 4000 m long study section during the initial phase of the study. Although golden perch visited a relatively large number of different habitats during the initial phase, once they were settled, their home ranges almost invariably consisted of single pool habitats. In general, carp appeared to invest less energy in home-range establishment than golden perch. Of the 15 radio-tracked carp, 6 (40%) settled into home ranges within 2.5 days and only 4 (26%)

© 2004 NRC Canada

Fig. 6. Mesohabitat preferences (D) calculated for all fish of both species on each survey day for (*a*) golden perch and (*b*) carp during the 90-day study period. The arrows represent the direction of increasing preference for either pool or run mesohabitats. The initial and final phases used in the analyses are shown. Open bars denote early morning and solid bars denote late afternoon.

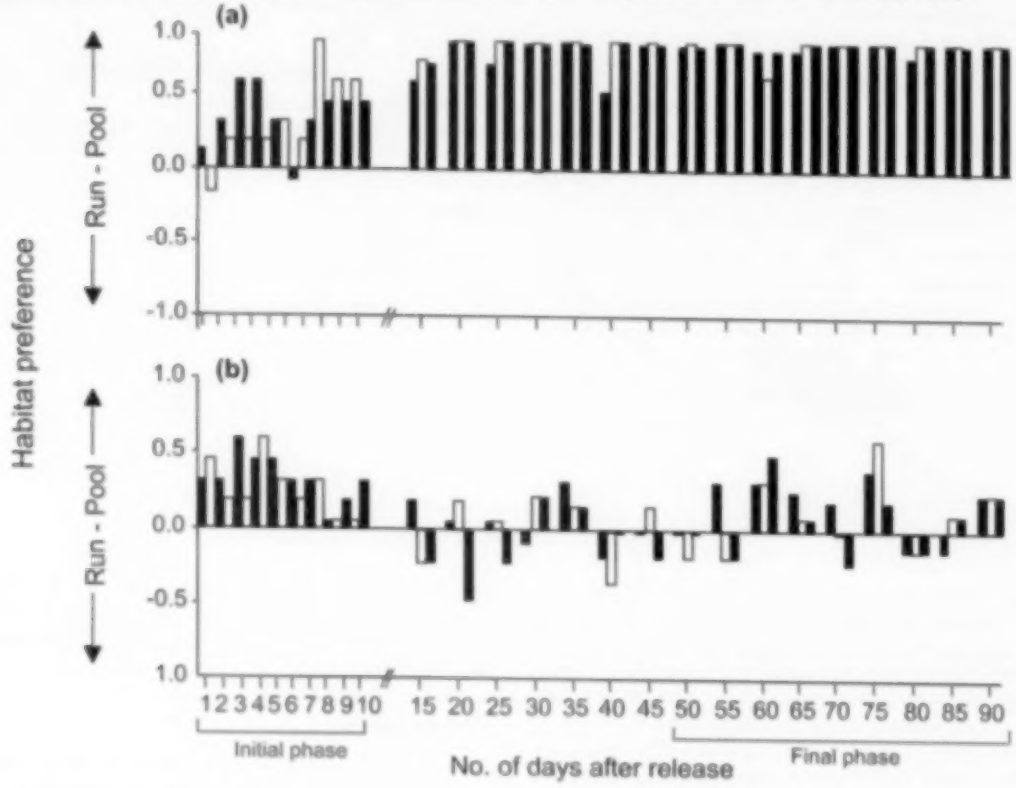

had not established home ranges by day 10. On average, carp visited a minimum of 10.6 (34%) of the 31 available habitats and traversed a minimum of 1323 m (33%) of the 4000 m long study section during the initial phase of the study. In contrast to golden perch, the home ranges occupied by carp were variable with regards to habitat type: some carp occupied single pools, some occupied single runs, and some occupied home ranges that included both types of habitat.

Decisions made during the initial selection of a home range have an important bearing on the resources subsequently available to an individual. However, since many animals change the locations of their home ranges during their lives, the rates at which they change home-range locations are also important in determining access to available resources (Switzer 1993; Gowan and Fausch 2002). In the current study, several fish of both species moved away from established home ranges and settled into home ranges in new areas. Other fish undertook large-scale movements and subsequently returned to the original home range. One possible explanation for these observations is that movement away from the home range allows assessment of the profitability of potentially available habitats outside the home range. An addition to the HRS model is required to incorporate assessment of habitat profitability outside the normal home range (Fig. 7). Like the previous version of the model (Crook 2004*b*), the revised model includes a home range occupation phase, where fish are relatively sedentary and occupy discrete home ranges. However, the HRS phase has been separated into two distinct phases in the revised model. In the mobile phase, fish emigrate from the original home range and explore alternative residence areas. If a more profitable area is not located during exploration, the fish returns to the original home range and resumes sedentary behaviour associated with home-range occupation. If a more profitable residence area is located, the fish enters the HRS phase and will establish a new home range at the more profitable location.

Linking the mobile phase of the HRS model to the assessment of habitat profitability outside the home range has potentially important implications for our understanding of the movements of riverine fish. In particular, it provides a mechanism by which fish can reap the benefits of home-range occupation (e.g., familiarity with the locations of food sources, shelter, potential mates, and predators), whilst still being able to respond to changes in the distributions of spatially and temporally dynamic resources (see Gowan and Fausch 2002). This mechanism could be particularly important in reconciling the predictions of the restricted-movement paradigm with models based on optimisation theory which assume that animals have knowledge of the profitability of habitats outside the normal home range (e.g., Railsback et al. 1999). Incorporation into the HRS model of a decision

© 2004 NRC Canada

Fig. 7. Revised "home range shift" conceptual model for describing the movements of adult riverine fish. The mobile phase of the model incorporates the assessment of habitat profitability outside the normal home range into decisions on whether or not to shift home-range locations. The home range contains core areas that are inhabited frequently, intermediate areas that are used less frequently, and outer areas that are used infrequently.

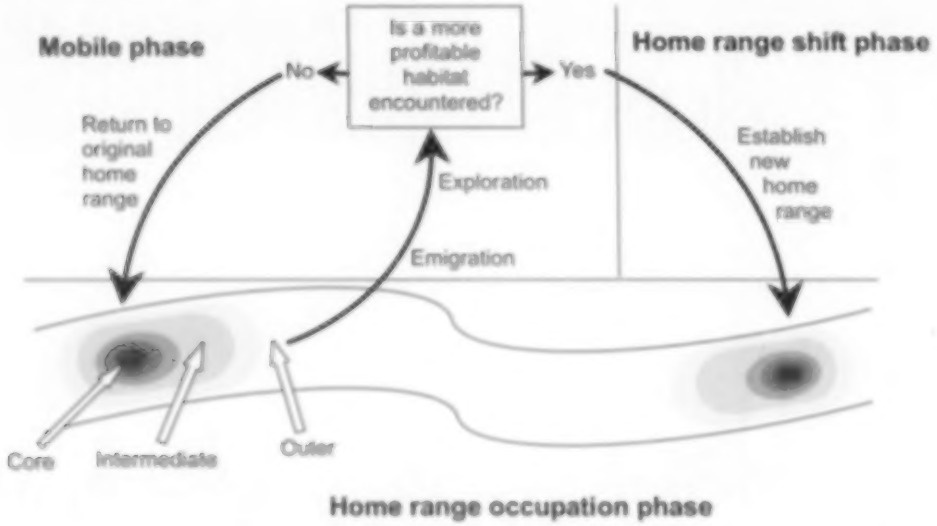

rule relating to the assessment of habitat profitability may also help to explain the adaptive significance of the homing behaviour exhibited by many nonmigratory riverine fish (see Gerking 1959; Quinn and Dittman 1992). In previous studies it has been speculated that homing by nonmigratory fish may be due to behaviour associated with feeding or reproductive movements (Schwartz 1987; Hughes 1997; Hodgson et al. 1998). Under the tenets of the revised HRS model, homing abilities would allow fish to assess the profitability of potentially available habitats without the risk of losing the original home range should they fail to find a more profitable location. Whilst the results of the current study appear consistent with this type of explanation, the utility of both the HRS model and the revised version presented here requires further empirical validation. Behaviours exhibited during the initial selection of a home range appear to have a strong bearing on individual fitness (Morris 1992; Switzer 1993; Armstrong et al. 1997), and although the current study has shed some light on these behaviours for two species, further study is required to improve our understanding of how such behaviours influence the distribution, structure, and stability of home ranges within riverine fish populations.

Acknowledgments

Paul Humphries, Alison King, Alistar Robertson, Robyn Watts, and two anonymous reviewers provided helpful comments on the manuscript. Simon McDonald assisted with the analyses and David Titley designed and manufactured the radio transmitters. Alison King, Paul Humphries, Helen Gigney, and Nigel Anthony assisted with fieldwork. Paul Humphries provided the water-temperature data and Goulburn-Murray Water provided the flow data. I thank Geoff and Lois Heaney, David and Julie Allnut, and Doug Farley for allowing access to the study site and for their generous hospitality. This study was supported by a Charles Sturt University Postgraduate Scholarship and a Cooperative Research Centre for Freshwater Ecology Postgraduate Top-up Scholarship.

References

Allouche, S., Thévenet, A., and Gaudin, P. 1999. Habitat use by chub (*Leuciscus cephalus* L. 1766) in a large river, the French Upper Rhône, as determined by radiotelemetry. Arch. Hydrobiol. **145**: 219–236.

Armstrong, J.D., Shackley, P., and Gardiner, R. 1994. Redistribution of juvenile salmonid fishes after localised catastrophic depletion. J. Fish Biol. **45**: 1027–1039.

Armstrong, J.D., Braithwaite, V.A., and Huntingford, F.A. 1997. Spatial strategies of wild Atlantic salmon parr: exploration and settlement in unfamiliar areas. J. Anim. Ecol. **66**: 203–211.

Armstrong, J.D., Braithwaite, V.A., and Fox, M. 1998. The response of wild Atlantic salmon parr to acute reductions in water flow. J. Anim. Ecol. **67**: 292–297.

Brown, J.S. 1990. Habitat selection as an evolutionary game. Evolution, **44**: 732–746.

Clapp, D.F., Clark, R.D., Jr., and Diana, J.S. 1990. Range, activity and habitat of large, free ranging brown trout in a Michigan stream. Trans. Am. Fish. Soc. **119**: 1022–1034.

Crook, D.A. 2002. Habitat use and movements of golden perch (*Macquaria ambigua*) and common carp (*Cyprinus carpio*) in an Australian lowland river. Ph.D. thesis, Charles Sturt University, New South Wales, Australia.

Crook, D.A. 2004*a*. A method for externally attaching radio-transmitters to minimise dermal irritation. J. Fish Biol. **64**: 258–261.

Crook, D.A. 2004*b*. Is the home range concept compatible with the movements of two species of lowland river fish? J. Anim. Ecol. **73**: 353–366.

Fretwell, S.D., and Lucas, J.H.J. 1970. On territorial behaviour and other factors influencing habitat distribution in birds. Acta Biotheor. **19**: 16–36.

© 2004 NRC Canada

Gerking, S.D. 1959. The restricted movement of fish populations. Biol. Rev. Camb. Philos. Soc. **34**: 221–242.

Gowan, C., and Fausch, K.D. 2002. Why do foraging stream salmonids move during summer? Environ. Biol. Fishes, **64**: 139–153.

Gowan, C., Young, M.K., Fausch, K.D., and Riley, S.C. 1994. Restricted movement in resident stream salmonids: a paradigm lost? Can. J. Fish. Aquat. Sci. **51**: 2626–2637.

Hilderbrand, R.H., and Kershner, J.L. 2000. Movement patterns of stream-resident cutthroat trout in Beaver Creek, Idaho–Utah. Trans. Am. Fish. Soc. **129**: 1160–1170.

Hodgson, J.R., Schindler, D.E., and He, X. 1998. Homing tendency of three piscivorous fishes in a north temperate lake. Trans. Am. Fish. Soc. **127**: 1078–1081.

Hughes, R.N. 1997. Diet selection. *In* Behavioural ecology of teleost fishes. *Edited by* J.-G.J. Godin. Oxford University Press, New York. pp. 134–162.

Jacobs, S. 1974. Quantitative measurement of food selection: a modification of the forage ratio and Ivlev's electivity index. Oecologia, **14**: 413–417.

MacArthur, R.H., and Pianka, E.R. 1966. On optimal use of a patchy environment. Am. Nat. **100**: 603–609.

Morris, D.W. 1992. Scales and costs of habitat selection in heterogeneous landscapes. Evol. Ecol. **6**: 412–432.

Moser, M.L., and Ross, S.W. 1995. Habitat use and movements of shortnose and Atlantic sturgeons in the lower Cape Fear River, North Carolina. Trans. Am. Fish. Soc. **124**: 225–234.

Quinn, T.P., and Dittman, A.H. 1992. Fishes. *In* Animal homing. *Edited by* F. Papi. Chapman Hall, London. pp. 147–211.

Railsback, S.F., Lamberson, R.H., Harvey, B.C., and Duffy, W.E. 1999. Movement rules for individual-based models of stream fish. Ecol. Modell. **123**: 73–89.

Rodríguez, M.A. 2002. Restricted movement in stream fish: the paradigm is incomplete, not lost. Ecology, **83**: 1–13.

Schwartz, F.J. 1987. Homing behaviour of tagged and displaced carp, *Cyprinus carpio*, in Pymatuning Lake, Pennsylvania/Ohio. Ohio J. Sci. **87**: 15–22.

Shearer, K.D., and Mulley, J.C. 1978. The introduction and distribution of the carp, *Cyprinus carpio* Linnaeus, in Australia. Aust. J. Mar. Freshw. Res. **29**: 551–563.

Swanberg, T.R. 1997. Movements of and habitat use by fluvial bull trout in the Blackfoot River, Montana. Trans. Am. Fish. Soc. **126**: 735–746.

Switzer, P.V. 1993. Site fidelity in predictable and unpredictable habitats. Evol. Ecol. **7**: 533–555.

© 2004 NRC Canada

Inverse modelling of trophic flows through an entire ecosystem: the northern Gulf of St. Lawrence in the mid-1980s

Claude Savenkoff, Martin Castonguay, Alain F. Vézina, Simon-Pierre Despatie, Denis Chabot, Lyne Morissette, and Mike O. Hammill

Abstract: Mass-balance models using inverse methodology have been constructed for the northern Gulf of St. Lawrence ecosystem in the mid-1980s, before the groundfish collapse. The results highlight the effects of the major mortality sources (fishing, predation, and other sources of mortality) on the fish and invertebrate communities. Main predators of fish were large cod (*Gadus morhua*) followed by redfish (*Sebastes* spp.), capelin (*Mallotus villosus*), and fisheries. Large cod were the most important predator of small cod, with cannibalism accounting for at least 44% of the mortality of small cod. The main predators of large cod were harp (*Phoca groenlandica*) and grey (*Halichoerus grypus*) seals. However, predation represented only 2% of total mortality on large cod. Mortality other than predation dominated the mortality processes at 52% of the total, while the fishery represented 46%. Tests were performed to identify possible sources of this unexplained mortality. The only way to significantly reduce unexplained mortality on large cod in the model was to increase landings of large cod above those reported. This suggests that fishing mortality was substantially underestimated in the mid-1980s, just before the demise of a cod stock that historically was the second largest in the northwest Atlantic.

Résumé : Des modèles d'équilibre de masse utilisant les méthodes inverses ont été construits pour représenter l'écosystème du nord du Golfe du Saint-Laurent dans le milieu des années 1980, avant l'effondrement des stocks de poissons de fond. Les résultats mettent en évidence les effets des principales causes de mortalité (pêche, prédation et autres causes de mortalité) sur les communautés de poissons et d'invertébrés. Les principaux prédateurs de poissons étaient la grande morue (*Gadus morhua*) suivie par le sébaste (*Sebastes* spp.), le capelan (*Mallotus villosus*) et la pêche. La grande morue était le principal prédateur de la petite morue et ce cannibalisme contribuait à 44 % au moins de la mortalité de la petite morue. Les principaux prédateurs de la grande morue étaient le phoque du Groenland (*Phoca groenlandica*) et le phoque gris (*Halichoerus grypus*). Cependant, cette mortalité par prédation ne représentait que 2 % de la mortalité totale de la grande morue. Les autres causes de mortalité dominaient la mortalité totale avec 52 %, alors que la pêche représentait 46 %. Des tests ont été réalisés pour préciser les causes possibles de cette mortalité inexpliquée. La seule façon de réduire significativement la mortalité inexpliquée dans le modèle a été d'augmenter les prises commerciales de la grande morue au-dessus des valeurs rapportées. Cela suggère que la mortalité par la pêche a été substantiellement sous-estimée dans le milieu des années 1980, juste avant le déclin d'un stock de morues qui était historiquement le deuxième plus grand dans l'Atlantique nord-ouest.

Introduction

From 1992 to 1994, moratoria on fishing for Atlantic cod (*Gadus morhua*) were declared after Canadian east coast stocks collapsed, thus ending one of the largest and longest-running commercial groundfish fisheries in the world (CAFSAC 1994). More than a decade later, in spite of limited fishing, almost all of these stocks show no signs of recovery (Rice and Rivard 2003). The reasons for the failure of these stocks to recover are not well understood. Mass-balance models using Ecopath (Christensen and Pauly 1993; Bundy et al. 2000) and inverse methodology (Vézina and

Received 12 November 2003. Accepted 2 July 2004. Published on the NRC Research Press Web site at http://cjfas.nrc.ca on 27 January 2005.
J17844

C. Savenkoff,[1] M. Castonguay, S.-P. Despatie,[2] D. Chabot, and M.O. Hammill. Pêches et Océans Canada, Institut Maurice-Lamontagne, 850 route de la Mer, Mont-Joli, QC G5H 3Z4, Canada.
A.F. Vézina. Fisheries and Oceans Canada, Bedford Institute of Oceanography, Dartmouth, NS B2Y 4A2, Canada
L. Morissette. Pêches et Océans Canada, Institut Maurice-Lamontagne, 850 route de la Mer, Mont-Joli, QC G5H 3Z4, Canada, and Fisheries Centre, NW Marine Drive Research Station, 6660 NW Marine Drive, Building 022, The University of British Columbia, Vancouver, BC V6T 1Z4, Canada.

[1]Corresponding author (e-mail: savenkoffc@dfo-mpo.gc.ca).
[2]Present address: Environnement Canada, Centre St-Laurent, 105, rue McGill, Montréal, QC H2Y 2E7, Canada.

 doi: 10.1139/F04-154 © 2004 NRC Canada

Platt 1988; Savenkoff et al. 2001) have been constructed for different ecosystems in Atlantic Canada and for different time periods. These models, as opposed to traditional approaches, consider the ecosystem in its whole rather than its components separately and attempt to provide an internally consistent description of trophic interactions between all functional groups of the ecosystem. The models generate a static picture of the ecosystem, taken as representative of a given area and time period, and use mass-balance principles to estimate flows of organic matter or energy among components of an ecosystem.

Ecopath is a widely used software that makes use of biomass and metabolic data to develop flow networks. In most cases, when all of the information to run an Ecopath model is assembled, the model will not balance because of the inconsistencies in the information. In this case, the values of one or more of the terms can be changed iteratively until a balance is obtained. Indeed, there is more than one way to construct an Ecopath model, and there is no unique solution to any model (ecosystem-level information is never complete, i.e., underdetermined system). Arriving at a balanced network with the Ecopath approach is left largely to trial and error, either through user intervention or Monte-Carlo simulations. In contrast, inverse methods directly compute a balanced network, if it exists, subject to constraints posed by the available data and prior knowledge of the system. This is done by finding the solution (all flows) that minimizes the squared imbalances between inputs and outputs through each compartment and between observed/estimated and modelled flows (least-squares criterion) (Vézina and Platt 1988; Savenkoff et al. 2001), although other criteria can be used (Vézina et al. 2004). Inverse methods provide a powerful tool to estimate ecosystem flows using limited data and straightforward mass balance and metabolic constraints. Simulated inverse analyses have shown that the general flow structure of ecosystems can be recovered with these techniques, although some of the detailed interactions can be inaccurate (Vézina and Pahlow 2003). The inverse methodology is also able to generate alternative scenarios (or solutions) that explain the data equally well.

Here, we present results from an inverse model carried out for the first time on an entire ecosystem, the northern Gulf of St. Lawrence (Northwest Atlantic Fisheries Organization (NAFO) divisions 4RS) during the 1985–1987 period. This period is important because it encompasses ecosystem conditions shortly before the large-scale groundfish stock collapses of the late 1980s – early 1990s in the northern Gulf and the first moratorium on cod fishing that was declared in 1994. Three solutions, each based on several random perturbations, were compared to provide an overall view of the ecosystem, identify robust patterns, and show where the uncertainties in food web dynamics lie. Our results enable us to evaluate the combined impact of the main mortality sources (fishing, predation, and natural mortality other than predation) on small and large cod in the northern Gulf of St. Lawrence in the mid-1980s.

Materials and methods

Data used in modelling

The data set covers an area of the northern Gulf of St. Lawrence (NAFO divisions 4RS) equivalent to a total area of 103 812 km^2 (Fig. 1). The nearshore region (depths < 37 m) is not included in the model. This zone was excluded from the model because exchanges between infralittoral and pelagic zones are still poorly understood. Thus, infralittoral species and American lobster (*Homarus americanus*) were not included in this study. The period covered by this analysis is 1985 to 1987, when the groundfish biomass was relatively stable (coefficient of variation (CV) among years for biomass was 29% and 21% for small and large cod, respectively, 20% for redfish, *Sebastes* spp., and 45% and 40% for small and large Greenland halibut, *Reinhardtius hippoglossoides*, respectively), shortly before several groundfish stocks began to collapse. The periods before and after the collapse of many groundfish species were delineated by examining the time series of biomass for the key species in the system.

Based on data availability and the ecological and commercial significance of the species, the trophic food web is depicted by a number of compartments or functional groups representing the main pelagic, demersal, and benthic species present, which are interconnected by mass flows of matter. The whole-system model of the northern Gulf of St. Lawrence was divided into 32 functional groups or compartments (Table 1). We distinguished 5 marine mammal groups, 1 seabird group, 16 fish groups, 8 invertebrate groups, 1 phytoplankton group, and 1 detritus group (Table 1). The groups were chosen to facilitate comparisons with other studies in the northwestern Atlantic (Bundy et al. 2000; Morissette 2001; Savenkoff et al. 2001). Some groups, such as large pelagic feeders and large demersal feeders, are composite groups in which the species were aggregated on the basis of similarity in size and ecological role. The input parameters of the composite groups were weighted by knowledge of the dominant species in these groups in terms of biomass. Cod and Greenland halibut were each separated into two groups based on diet, age/size at first capture, and age/size at maturity. Smaller fish prey mainly on invertebrates, whereas larger fish feed mainly on fish. These changes tend to occur gradually with increasing length, but for this model, it was assumed that the change occurs at 35 cm for cod (Lilly 1991) and 40 cm for Greenland halibut (Bowering and Lilly 1992). Because of a lack of length–frequency data and information on diet compositions of small versus large fish, as well as on the proportions of juvenile and adult fish in the diets of their predators, we could not distinguish juveniles and adults for other fish species. Finally, bacteria were considered part of the detritus compartment (Table 1).

To estimate the magnitude of trophic fluxes, measurements or estimates of major process rates such as consumption, production, and commercial catch are required for each living compartment, as well as quantitative information on the diet composition of the different groups. Input values on species biomass, production, consumption, and export (here equal to commercial catch) are summarized (Tables 2 and 3).

Biomass information was obtained from an annual summer trawl survey for groundfish conducted between 1984 and 1990 in the northern Gulf aboard the M/V *Lady Hammond* with a Western IIA trawl. Trawlable biomass estimates were converted to catchability-adjusted biomass based on catchability coefficients estimated by Harley and Myers

© 2004 NRC Canada

Fig. 1. Northern Gulf of St. Lawrence (Northwest Atlantic Fisheries Organization (NAFO) divisions 4RS) equivalent to a total area of 103 812 km^2.

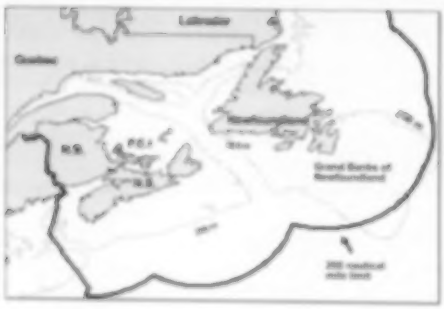

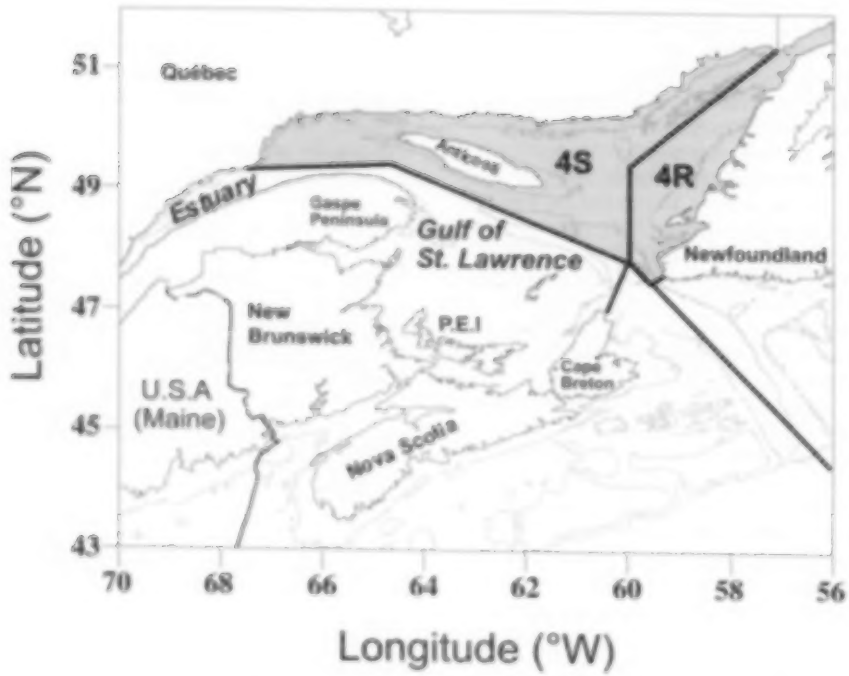

(2001). The method used to apply length-dependent catchability coefficients was described by Savenkoff et al. (2004). Biomass estimates for several other model compartments (seals, seabirds, herring, mackerel, and large crustaceans) were based on data from other surveys or population models. In other cases, biomass was based on densities reported for other ecosystems (sand lance, echinoderms, molluscs, polychaetes, and other benthic invertebrates) or was estimated by initial runs of inverse modelling to meet predator demands (small demersal feeders). Diet composition was based on samples from the northern Gulf where possible. However, these data do not exist for some species. For these species, diet data were taken for the same area but for another time period or from the literature for other areas and (or) time periods (e.g., American plaice, flounders, skates, capelin, and shrimp). Based on these different sources of data (local and literature), we estimated the lower and upper limits of each diet proportion used as inputs in inverse modelling. Means and standard deviations were calculated either directly from the lower and upper limits when there was no information on number of stomachs or from the different diet proportions, which were weighted by the number of stomachs when stomach content analyses were given.

Very little is known about fish and invertebrate production and consumption in the Gulf of St. Lawrence. In those cases, we used a variety of information sources to derive broad limits within which these rates should fall. For fish, in the absence of information on total mortality under the steady-state assumption, the majority of production limits were obtained assuming that production or total mortality is equivalent to biomass multiplied by natural mortality plus the catch. Unfortunately, we had few measures of natural mortality. In many cases, we assumed that natural mortality was equal to a fixed value to get a preliminary production

© 2004 NRC Canada

Table 1. Functional groups used in inverse modelling.

Group name	Code	Main species
Cetaceans	WHA	*Balaenoptera physalus*, *Balaenoptera acutorostrata*, *Megaptera novaeangliae*, *Phocoena phocoena*, *Lagenorhynchus acutus*, *Lagenorhynchus albirostris*
Harp seals	HAS	*Phoca groenlandica*
Hooded seals	HOS	*Cystophora cristata*
Grey seals	GRS	*Halichoerus grypus*
Harbour seals	HSE	*Phoca vitulina*
Seabirds	SEA	*Phalacrocorax carbo*, *Phalacrocorax auritus*, *Larus delawarensis*, *L. argentatus*, *L. marinus*, *Sterna hirundo*, *S. paradisaea*, *Cepphus grylle*, *Oceanodroma leucorhoa*, *Morus bassanus*, *Rissa tridactyla*, *Uria aalge*, *Alca torda*, *Fratercula arctica*
Large Atlantic cod (>35 cm)	LCO	*Gadus morhua*
Small Atlantic cod (≤35 cm)	SCO	*Gadus morhua*
Large Greenland halibut (>40 cm)	LGH	*Reinhardtius hippoglossoides*
Small Greenland halibut (≤40 cm)	SGH	*Reinhardtius hippoglossoides*
American plaice	AMP	*Hippoglossoides platessoides*
Flounders	FLO	*Limanda ferruginea*, *Glyptocephalus cynoglossus*, *Pseudopleuronectes americanus*
Skates	SKA	*Amblyraja radiata*, *Malacoraja senta*, *Leucoraja ocellata*
Redfish	RED	*Sebastes mentella*, *Sebastes fasciatus*
Large demersal feeders	LDF	*Urophycis tenuis*, *Melanogrammus aeglefinus*, *Centroscyllium fabricii*, *Anarhichas* spp., *Cyclopterus lumpus*, *Lycodes* spp., Macrouridae, Zoarcidae, *Lophius americanus*, *Hippoglossus hippoglossus*
Small demersal feeders	SDF	*Myoxocephalus* spp., *Tautogolabrus adspersus*, *Macrozoarces americanus*, juvenile LDF
Capelin	CAP	*Mallotus villosus*
Sand lance	SLA	*Ammodytes* spp.
Arctic cod	ACO	*Boreogadus saida*
Large pelagic feeders	LPF	*Squalus acanthias*, *Pollachius virens*, *Merluccius bilinearis*
Piscivorous small pelagic feeders	PISF	*Scomber scombrus*, piscivorous myctophids and other mesopelagics, *Illex illecebrosus*, piscivorous juvenile LPF
Planktivorous small pelagic feeders	PLSF	*Clupea harengus harengus*, planktivorous myctophids and other mesopelagics, *Scomberesox saurus*, *Gonatus* spp., planktivorous juvenile LPF
Shrimp	SHR	*Pandalus borealis*, *Pandalus montagui*
Large crustaceans	LCRU	*Chionoecetes opilio*, other non-commercial species (*Hyas* spp.)
Echinoderms	ECH	*Echinarachnius parma*, *Strongylocentrotus pallidus*, *Ophiura robusta*
Molluscs	MOL	*Mesodesma deauratum*, *Cyrtodaria siliqua*
Polychaetes	POL	*Exogene hebes*
Other benthic invertebrates	OBI	Miscellaneous crustaceans, nematodes, other meiofauna
Large zooplankton (>5 mm)	LZOO	Euphausiids, chaetognaths, hyperiid amphipods, cnidarians and ctenophores (jellyfish), mysids, tunicates >5 mm, ichthyoplankton
Small zooplankton (<5 mm)	SZOO	Copepods (mainly *Calanus finmarchicus*, *C. hyperboreus*, and *Oithona similis*), tunicates <5 mm, meroplankton
Phytoplankton	PHY	Diatom species such as *Chaetoceros affinis*, *C.* spp., *Leptocylindrus minimus*, *Thalassiosira nordenskioldii*, *Thalassiosira* spp., and *Fragilariopsis* spp., and a mixture of autotrophic and mixotrophic organisms including Cryptophytes, dinoflagellates, Prasinophytes, and Prymnesiophytes
Detritus	DET	Sinking particulate organic matter including both large particles (consisting of animal carcasses and debris of terrigenous and coastal plants) and fine particles (mostly from planktonic organisms, including feces, moults, phytoplankton aggregates, and bacteria)

estimate that was then allowed to vary over a wide range. Direct estimates of total mortality, based on a modified catch curve analysis of the survey data (Sinclair 2001), were available only for large cod. It was also necessary to use empirical data from other areas and (or) time frames (e.g., capelin, sand lance, Arctic cod) or less specific information (e.g., pelagic feeders, benthic invertebrates) for production and consumption estimates. Diet composition and the other input values (biomass, production, consumption, export) for each compartment can be found in Morissette et al. (2003).

Model structure

The general structure of an inverse model includes (*i*) compartmental mass-balance equations, (*ii*) data equations, and (*iii*) constraints. The data equations attempt to fix the value of certain flows or combination of flows (e.g., in-

© 2004 NRC Canada

Table 2. Biomass (B_y^m, in tonnes (t) wet weight·km^{-2}) and export (EX_y^m, in t·km^{-2}·year^{-1}) for each group y used as weight and input parameters for inverse modelling for the 1985–1987 period in the northern Gulf of St. Lawrence.

	Biomass				Export[a]			
Group name	Mean	CV, %	Min	Max	Mean	CV, %	Min	Max
Cetaceans	0.14	66[b]			**3.75×10^{-4}**	6	3.60×10^{-4}	3.90×10^{-4}
Harp seals	0.08	5[c]	0.08	0.09	5.82×10^{-3}	28	**4.20×10^{-3}**	**7.45×10^{-3}**
Hooded seals	0.003	5[c]	0.003	0.004	**1.85×10^{-4}**	141	0	3.68×10^{-4}
Grey seals	0.018	7[c]	0.017	0.019	**6.41×10^{-4}**	63	2.34×10^{-4}	1.04×10^{-3}
Harbour seals	0.003	6[c]	0.002	0.003				
Seabirds	0.004	66[b]			**3.35×10^{-4}**	46[d]		
Large cod	3.93	21	2.99	4.40	**7.63×10^{-1}**	14	6.41×10^{-1}	8.50×10^{-1}
Small cod	1.64	29	1.11	2.02	**8.18×10^{-4}**	81	6.50×10^{-5}	1.33×10^{-3}
Large Greenland halibut	0.27	40	0.08	0.57	**2.54×10^{-2}**	68	1.03×10^{-2}	4.44×10^{-2}
Small Greenland halibut	0.29	45	0.06	0.58				
American plaice	0.67	61	0.22	1.74	**2.04×10^{-2}**	12	1.77×10^{-2}	2.26×10^{-2}
Flounders	0.35	91	0.00	2.13	**7.48×10^{-3}**	14	6.71×10^{-3}	8.71×10^{-3}
Skates	0.17	41	0.10	0.25	**6.42×10^{-5}**	115	0	1.44×10^{-4}
Redfish	12.15	20	10.31	14.95	**2.65×10^{-1}**	10	2.36×10^{-1}	2.85×10^{-1}
Large demersals	0.97	18	0.65	1.39	**9.26×10^{-3}**	16	8.11×10^{-3}	1.09×10^{-2}
Small demersals	1.34	137	0.05	2.64				
Capelin	16.67	141	0.07	33.28	**2.32×10^{-2}**	59	8.74×10^{-3}	3.61×10^{-2}
Sand lance	2.40	17	2.10	2.69				
Arctic cod	0.02	141	0.00	0.05				
Large pelagics	0.06	46	0.02	0.08	**2.49×10^{-3}**	89	1.06×10^{-3}	5.05×10^{-3}
Piscivorous small pelagic feeders	2.46	35	1.67	3.36	**1.25×10^{-2}**	137	1.65×10^{-3}	3.22×10^{-2}
Planktivorous small pelagic feeders	2.53	3	2.43	2.66	**1.76×10^{-1}**	20	1.44×10^{-1}	2.12×10^{-1}
Shrimp	0.83	68	0.58	1.08	**9.40×10^{-2}**	16	8.29×10^{-2}	1.11×10^{-1}
Large crustaceans	0.86	24	0.37	2.14	**4.39×10^{-2}**	8	4.02×10^{-2}	4.67×10^{-2}
Echinoderms	112.30	66[b]						
Molluscs	42.10	66[b]			**3.34×10^{-2}**	12	3.08×10^{-2}	3.81×10^{-2}
Polychaetes	10.50	66[b]						
Other benthic invertebrates	7.80	66[b]						
Large zooplankton	9.64	150	0.01	63.00				
Small zooplankton	50.00	163	5.00	120.00				
Phytoplankton	23.41	70	5.01	45.45				
Detritus	132.61	86	61.63	222.06	5.94×10^{1}	10	**5.35×10^{1}**	**6.53×10^{1}**

Note: CV, coefficient of variation; Min, minimum; Max, maximum. Mean, CV, Min, and Max were based only on the variations in the point estimates for the 3 years. Values used as part of the data equations (right-hand side) or as upper and lower limit constraints are shown in bold.

[a]Export is the sum of the catch and the net migration (emigration out of the system, food intake of predators that are not part of the system, etc.; this term is assumed here to be equal to 0). For detritus, export was loss of detritus buried as sediment.

[b]Calculated as B_y^mCV(B_y^m)$_{\text{mean}}$ with CV(B_y^m)$_{\text{mean}}$ = 66%, the average of all known coefficients of variation for biomass except those estimated for seals.

[c]Estimated from the model of Hammill and Stenson (2000) and not used here in the average of all known coefficients of variation for biomass.

[d]Calculated as EX_y^mCV(EX_y^m)$_{\text{mean}}$ with CV(EX_y^m)$_{\text{mean}}$ = 46%, the average of all known coefficients of variation for export.

corporate the observations into the model that coincide with the period/region for which a solution was derived), whereas the constraints incorporate general knowledge into the model. Under the steady-state assumption, consumption representing the input must balance the sum of the outputs consisting of production, respiration, and egestion (flux of unassimilated food: feces or detrital flow) for individual compartments. In these models, we assumed that there was no year-to-year change in biomass during the studied time period and that net migration was zero (migration out of, or into, the study area, food intake of predators that are not part of the system, etc.). Thus, production was simply the biomass lost to fishing mortality, predation, and natural mortality other than predation (disease, other natural causes of death, and unexplained mortality (unsuspected processes occurring in the ecosystem); hereafter termed "other mortality"). The flows estimated by inverse modelling are described (Table 4), and the general mass-balance equation for individual compartments can be written as (Table 5)

$$\text{(1)}\quad \text{Consumption} - \text{egestion} - \text{respiration} - \text{fishing mortality} - \text{predation} - \text{other mortality} = 0 + \varepsilon$$

The equations calculated for this study were not exactly balanced, that is, the sum of the inputs and outputs for each compartment did not necessarily equal zero and the specified local values (data equations) were not reproduced exactly. These differences are here termed the residuals, which are represented by the error term ε.

Some of the input data were introduced directly into the model as part of the data equations (right-hand side) (Ta-

© 2004 NRC Canada

Table 3. Production (P_y^{im}, in tonnes (t) km^{-2}·year^{-1}) and consumption (Q_y^{im}, in t·km^{-2}·year^{-1}) for each group y used as input parameters for inverse modelling for the 1985–1987 period in the northern Gulf of St. Lawrence.

	Production				Consumption			
Group name	Mean	CV, %	Min	Max	Mean	CV, %	Min	Max
Cetaceans	**0.010**	21	0.008	0.011	0.90	11	**0.82**	**0.97**
Harp seals	**0.007**	63	0.004	0.010	0.51	45	**0.35**	**0.67**
Hooded seals	**0.0003**	45	0.0002	0.0004	0.038	23	**0.032**	**0.044**
Grey seals	**0.0010**	70	0.0005	0.0015	0.06	84	**0.03**	**0.10**
Harbour seals	**0.0001**	43	0.0001	0.0002	0.012	29	**0.010**	**0.015**
Seabirds	**0.0011**	93[a]			0.31	91	**0.11**	**0.51**
Large cod	2.31	47	**1.55**	**3.08**	14.33	58	**5.54**	**23.12**
Small cod	0.99	39	**0.67**	**1.21**	10.46	63	**3.29**	**17.63**
Large Greenland halibut	0.05	111	**0.02**	**0.10**	0.39	38	**0.27**	**0.50**
Small Greenland halibut	0.06	128	**0.01**	**0.12**	0.78	57	**0.29**	**1.27**
American plaice	0.17	144	**0.07**	**0.41**	1.89	61	**0.67**	**3.11**
Flounders	0.08	390	**0.01**	**0.43**	0.60	54	**0.35**	**0.84**
Skates	0.04	65	**0.02**	**0.05**	0.32	47	**0.17**	**0.48**
Redfish	1.78	121	**0.61**	**3.65**	54.49	77	**12.15**	**96.83**
Large demersals	0.11	51	**0.07**	**0.15**	1.99	69	**0.97**	**3.01**
Small demersals	0.44	139	**0.01**	**0.87**	3.82	87	**1.47**	**6.17**
Capelin	10.02	141	**0.04**	**19.99**	132.39	89	**0.56**	**264.22**
Sand lance	**2.76**	93[a]			18.38	71	**9.19**	**27.57**
Arctic cod	0.01	141	**0.00**	**0.02**	0.06	71	**0.03**	**0.09**
Large pelagics	0.01	84	**0.00**	**0.01**	0.37	80	**0.06**	**0.67**
Piscivorous small pelagic feeders	0.48	36	**0.34**	**0.68**	8.63	68	**2.46**	**14.79**
Planktivorous small pelagic feeders	0.68	12	**0.63**	**0.74**	18.61	80	**2.53**	**34.69**
Shrimp	1.20	43	**0.84**	**1.57**	8.03	71	**4.01**	**12.04**
Large crustaceans	0.22	118	**0.11**	**0.48**	1.44	42	**0.72**	**2.16**
Echinoderms	33.67	115	**0.11**	**70.11**	243.15	76	**112.22**	**374.07**
Molluscs	22.95	149	**0.60**	**82.12**	165.74	76	**76.50**	**254.99**
Polychaetes	16.68	147	**0.21**	**74.56**	120.47	76	**55.60**	**185.34**
Other benthic invertebrates	9.17	83	**0.52**	**15.68**	66.25	76	**30.58**	**101.93**
Large zooplankton	29.29	36	**15.43**	**38.57**	169.63	65	**46.37**	**292.89**
Small zooplankton	232.94	69	**120.00**	**345.89**	996.40	79	**438.13**	**1554.67**
Phytoplankton	2459.00	45	**1360.18**	**3557.82**				

Note: CV, coefficient of variation; Min, minimum; Max, maximum. Mean, CV, Min, and Max were calculated on the two extreme values. Values used as part of the data equations (right-hand side) or as upper and lower limit constraints are indicated in bold.

[a]Calculated as P_y^{im}·CV(P_y^{im})$_{mean}$ with CV(P_y^{im})$_{mean}$ = 93%, the average of all known coefficients of variation for production.

ble 5). These included values for exports (catches) from the system, production, and diet proportions locally estimated from field studies (Tables 2–3; see also Morissette et al. (2003) for the diet proportions). We also used data equations for diet proportions available only as point estimates (no variance estimate) or with low observed values (e.g., <0.5%) and low uncertainty (e.g., standard deviation (SD) < 0.6%). This yielded 173 equations (32 mass balances and 141 specified flows; Table 5) that had to be solved for 463 unknown flows (Table 4). This system was strongly underdetermined (e.g., the number of flows to be solved exceeded the number of independent mass-balance relations), so additional constraints that reflected prior knowledge of the system are needed to obtain a meaningful solution.

Model constraints

Each flow was taken to be non-negative, and flows and flow ratios (metabolic efficiencies) were assumed to fall within certain ranges to satisfy basic metabolic requirements (Table 6). Gross growth efficiency (GE) is the ratio of production to consumption and for most groups should have values between 10% and 30% (Christensen and Pauly 1992). Exceptions are top predators, e.g., marine mammals and seabirds, which can have lower GE, and small, fast-growing fish larvae or nauplii or bacteria, which can have higher GE (Christensen and Pauly 1992) (Table 6). Following Winberg (1956), 80% of the consumption was assumed to be physiologically useful for carnivorous fish groups, whereas the non-assimilated food (20%, consisting of urine and feces) was directed to the detritus. For herbivores, the proportion not assimilated could be considerably higher, e.g., up to 40% in zooplankton (Christensen and Pauly 1992). We constrained the assimilation efficiency (AE) to fall between 70% and 90% for all groups except large and small zooplankton (between 50% and 90%; Table 6).

Certain flows have minimal and maximal values imposed (export for detritus, production, consumption, diet composition, etc.). The production and consumption values that were not estimated from local field studies were incorporated as constraints (Table 6). The other diet proportions (e.g., 232 values) with higher values (e.g., >0.5%) were also specified as constraints. To facilitate comparisons with Ecopath

© 2004 NRC Canada

Table 4. Flows (463, in $t{\cdot}km^{-2}{\cdot}year^{-1}$) estimated by inverse modelling and weighting applied during the estimation.

Flows	Description
Respiration (31 unknowns)	
Weight	$\mathrm{Var}(B_y^m)$
Notation	R_y
Respiration of group y. No respiration term for phytoplankton.	
Egestion (30 unknowns)	
Weight	$\mathrm{Var}(B_y^m)$
Notation	D_y
Flow of group y to detritus (detrital flow or non-assimilated food). No egestion term for phytoplankton (including in mortality terms) or detritus.	
Natural mortality other than predation (31 unknowns)	
Weight	$\mathrm{Var}(B_y^m)$
Notation	MO_y
Natural mortality other than predation of group y including disease and other natural causes of death. No mortality term for detritus.	
Predation (349 unknowns)	
Weight	$\mathrm{Var}(\mathrm{Pr}_{x\to y}) = (Q_y^m)^2(\mathrm{CV}(\mathrm{DC}_{x\to y}^m)^2 + \mathrm{CV}(Q_y^m)^2)$
Notation	$\mathrm{Pr}_{x\to y}$
Predation of group x by group y based on the diet composition of each group.	
Export (21 unknowns)	
Weight	$\mathrm{Var}(\mathrm{EX}_y^m)$
Notation	EX_y
Export (including catches) of group y out of the system. No export term for several groups (see Table 2).	
Phytoplankton production (1 unknown)	
Weight	$\mathrm{Var}(P_y^m)$
Notation	P_{Phy}
Net primary production corrected for respiration.	

Note: Var, variance; CV, coefficient of variation; B, biomass; Q, consumption; DC, proportion in diet (by mass). We used the inverse of the variances in the weighting scheme.

models, we added constraints on the ecotrophic efficiency (EE). The ecotrophic efficiency is the fraction of the production that is either passed up the food web or exported. These values should be between 0 and 0.95 (Christensen and Pauly 1992, 1998). Here, a value only slightly above zero indicates that the group is not consumed in noticeable amounts by any other group in the system (e.g., top predators). Conversely, a value near or equal to 0.95 indicates that the group is heavily preyed upon and (or) highly exploited by a fishery, leaving no individuals to die of other causes (small prey organisms). In all, 1230 constraints were added to the 173 mass-balance relations, leading to a system of 1403 equations to be solved for the 463 unknowns.

Model solution

Writing the equations in matrix form

Details of the method of solution for these equations are given in Vézina and Platt (1988) and Savenkoff et al. (2004*b*). The first step was to write out the mass-balance and data equations in matrix form and set up a rectangular matrix (**A**) to represent the connections in the food web. The rows of the matrix are the mass-balance relations; there are as many rows as there are equations (m) (Table 5). The columns of the matrix are the flows; there are as many columns as there are flows (n) in the food web (Table 4).

Once the matrix $\mathbf{A}(m, n)$ is constructed, we specify a vector $\boldsymbol{b}$ that has as many rows as **A** and gives the expected values of the mass-balance relations (zero in the steady-state case; see Table 5) and the values of the flows entered as data equations (input values; see Tables 3 and 5). Vector $\boldsymbol{b}(m \times 1)$ thus contains the right-hand sides of the mass-balance and data equations. Inverse methodology then calculates a vector $\boldsymbol{x}(n \times 1)$ that has as many elements as there are columns in **A**. Vector $\boldsymbol{x}$ represents the flows that, once multiplied by **A**, approximate vector $\boldsymbol{b}$. Finally, after writing eq. 1 in matrix form, the system is

$$\mathbf{A}\boldsymbol{x} = \boldsymbol{b} + \varepsilon \tag{2}$$

The constraints (inequality relations) can also be written in matrix form (matrix **G**) by setting up a matrix with as many rows as there are inequality relations (constraints, c) and the same number of columns (representing the flows) as **A**. We end up with a matrix $\mathbf{G}(c, n)$ and a vector $\boldsymbol{h}(c \times 1)$, with as many elements as there are rows in **G** and corresponding to the right-hand sides of the inequality relations. The other system is

$$\mathbf{G}\boldsymbol{x} > \boldsymbol{h} \tag{3}$$

Solving the equations

In system 2, m, the number of equations, is less than n, the number of flows, and we have an underdetermined or rank-deficient system of equations. We can still find a solution if we reduce the dimensionality of the problem from n (we do not have information for all n) to m (we do have in-

© 2004 NRC Canada

Table 5. Mass balance and data equations (173 equations) and corresponding weights used in this inverse model.

Mass balance for	Description
Consumers (30 eqs.)	
Weight	$\mathrm{Var}(B_y^m)$
Equation	$\sum_x \mathrm{Pr}_{x\to y} - R_y - D_y - \sum_u \mathrm{Pr}_{y\to u} - \mathrm{MO}_y - \mathrm{EX}_y = 0 \pm \varepsilon$
For a consumer y, consumption $\left(\sum_x \mathrm{Pr}_{x\to y}\right)$ representing the input must balance the sum of the outputs consisting of respiration (R_y), egestion (detrital flow, D_y), natural mortality (predation by other groups $\left(\sum_u \mathrm{Pr}_{y\to u}\right)$, and other natural causes of death (MO_y)) and fishing mortality (export, EX_y).	
Phytoplankton (1 eq.)	
Weight	$\mathrm{Var}(B_{\mathrm{Phy}}^m)$
Equation	$P_{\mathrm{Phy}} - \mathrm{MO}_{\mathrm{Phy}} - \sum_y \mathrm{Pr}_{\mathrm{Phy}\to y} = 0 \pm \varepsilon$
Net (corrected for respiration) production (P_{Phy}) must balance the sum of the outputs (phytoplankton mortality including egestion term, $\mathrm{MO}_{\mathrm{Phy}}$, and consumption of phytoplankton by other groups, $\sum_y \mathrm{Pr}_{\mathrm{Phy}\to y}$).	
Detritus (1 eq.)	
Weight	$\mathrm{Var}(B_{\mathrm{Det}}^m)$
Equation	$\sum_x D_x + \sum_x \mathrm{MO}_x - \sum_y \mathrm{Pr}_{\mathrm{Det}\to y} - R_{\mathrm{Det}} - \mathrm{EX}_{\mathrm{Det}} = 0 \pm \varepsilon$
Inputs (egestion $\left(\sum_x D_x\right)$ and other natural causes of death $\left(\sum_x \mathrm{MO}_x\right)$ for other groups) must balance the sum of the outputs (consumption of detritus by other groups, $\sum_y \mathrm{Pr}_{\mathrm{Det}\to y}$, bacterial remineralization of detritus, R_{Det}, and burial, $\mathrm{EX}_{\mathrm{Det}}$). As bacteria were considered part of the detritus, detritus was assumed to respire.	
Export (19 eqs.)	
Weight	$\mathrm{Var}(\mathrm{EX}_y^m)$
Equation	$\mathrm{EX}_y = \mathrm{EX}_y^m \pm \varepsilon$
Export estimated by inverse modelling (EX_y) is equal to input export (EX_y^m) from local field studies (see Table 2).	
Production (7 eqs.)	
Weight	$\mathrm{Var}(P_y^m)$
Equation	$P_y = P_y^m \pm \varepsilon$ with $P_y = \sum_x \mathrm{Pr}_{x\to y} - R_y - D_y$
Production estimated by inverse modelling (P_y) is equal to input production (P_y^m) from local field studies or available only as point estimates (see Table 3).	
Predation[a] (115 eqs.)	
Weight	$\mathrm{Var}(\mathrm{Pr}_{u\to y}) = (Q_y^m)^2 (\mathrm{CV}(\mathrm{DC}_{u\to y}^m)^2 + \mathrm{CV}(Q_y^m)^2)$
Equation	$\frac{\mathrm{Pr}_{u\to y}}{\sum_x \mathrm{Pr}_{x\to y}} = \mathrm{DC}_{u\to y}^m \pm \varepsilon$
Proportion of prey u in diet (by mass) of consumer y estimated by inverse modelling $\left(\frac{\mathrm{Pr}_{u\to y}}{\sum_x \mathrm{Pr}_{x\to y}}\right)$ is equal to input diet proportion ($\mathrm{DC}_{u\to y}^m$) from local field studies or available only as low estimates with low SD (<0.6‰).	

Note: Group codes are in Table 1. Var, variance; CV, coefficient of variation; B, biomass; ε, residual, the difference between observation and model estimate. We used the inverse of the variances in the weighting scheme.

[a]Note that the weight of the additional diet equations (predation) for groups with no information on diet proportion variability (24 of 115) is the average of all known coefficients of variation for diet proportion ($\mathrm{CV}(\mathrm{DC}_{u\to y}^m)_{\mathrm{mean}} = 119\%$). Q_y^m is input consumption from local field studies or literature ($\mathrm{CV}(Q_y^m)_{\mathrm{mean}} = 64\%$) (see Table 3).

© 2004 NRC Canada

Table 6. Constraints (1230 constraints) on food web processes used in the inverse modelling.

Constraint for	Description
Non-negativity (463 constraints)	
Equation	$R_i \geq 0, D_i \geq 0, \mathrm{MO}_i \geq 0, \mathrm{Pr}_{i \to j} \geq 0, \mathrm{EX}_i \geq 0, P_{\mathrm{Prey}} \geq 0$
All of the unknown flows are non-negative.	
Growth efficiency (60 constraints)	
Equation	$\mathrm{GE}_i^{\min} < \frac{\sum_j \mathrm{Pr}_{i \to j} - R_i - D_i}{\sum_j \mathrm{Pr}_{i \to j}} < \mathrm{GE}_i^{\max}$
Growth efficiency (of food conversion; GE = production/consumption) ranges from 0.1% to 1% for marine mammals and seabirds, 10% to 30% for fish, shrimp, large crustaceans, and large zooplankton, 9% to 30% for benthic invertebrates, and 25% to 50% for small zooplankton.	
Assimilation efficiency (60 constraints)	
Equation	$\mathrm{AE}_i^{\min} < \frac{\sum_j \mathrm{Pr}_{i \to j} - D_i}{\sum_j \mathrm{Pr}_{i \to j}} < \mathrm{AE}_i^{\max}$
Assimilation efficiency (AE) ranges between 70% and 90% for all the groups except for large and small zooplankton (50%–90%).	
Ecotrophic efficiency (62 constraints)	
Equation	$\mathrm{EE}_i^{\min} < \frac{\sum_j \mathrm{Pr}_{i \to j} - R_i - D_i - \mathrm{MO}_i}{\sum_j \mathrm{Pr}_{i \to j} - R_i - D_i} < \mathrm{EE}_i^{\max}$
Ecotrophic efficiency (EE; production exported or consumed within the system) ranges between 0 and 0.95 for all groups except for detritus (no constraint).	
Consumption (60 constraints)	
Equation	$Q_i^{\min} < \sum_j \mathrm{Pr}_{i \to j} < Q_i^{\max}$
Predation of group x by group y $\left(\sum_x \mathrm{Pr}_{x \to y}\right)$ ranges between minimum and maximum input consumption values (see Table 3).	
Export (4 constraints)	
Equation	$\mathrm{Exp}_i^{\min} < \mathrm{EX}_i < \mathrm{Exp}_i^{\max}$
Export of group y ranges between minimum and maximum input values (harp seals and detritus; see Table 2).	
Predation (464 constraints)	
Equation	$\mathrm{DC}_{a \to y}^{\min} < \frac{\mathrm{Pr}_{a \to y}}{\sum_x \mathrm{Pr}_{x \to y}} < \mathrm{DC}_{a \to y}^{\max}$
Proportion of prey a in diet (by mass) of consumer y ranges between minimum and maximum input values (see Morissette et al. 2003).	
Predation ratio (8 constraints)	
Equation	$\mathrm{Ratio}^{\min} < \frac{\mathrm{Pr}_{\mathrm{SCO} \to y}}{\mathrm{Pr}_{\mathrm{LCO} \to y}} < \mathrm{Ratio}^{\max}$
Ratio of small cod to large cod (by mass) in the diet composition of seals ranges between 2.50 and 3.50 for harp and harbour seals and 0.75 and 1.25 for hooded and grey seals.	
Production (48 constraints)	
Equation	$P_i^{\min} < \sum_j \mathrm{Pr}_{i \to j} - R_i - D_i < P_i^{\max}$
Production of group y ranges between minimum and maximum input values except for marine mammals and seabirds (see Table 3).	
Bacterial respiration (1 constraint)	
Equation	$R_i^{\min} < R_i$
Bacterial respiration is at least equal to minimum input value (459.21 $t \cdot km^{-2} \cdot year^{-1}$; see Morissette et al. 2003).	

formation for all m; $n - m$ vectors represent the null space of **A**, the part of **A** for which we have no information). The reduction in dimensionality is achieved through a mathematical process called singular value decomposition (SVD). The SVD decomposes the matrix **A** into orthogonal vectors u and v linked by a scale factor (λ), which explain a large proportion of the structure in **A**. Using SVD results, an initial solution is computed to solve system 2 for the x that mini-

© 2004 NRC Canada

mizes the norm of $\mathbf{A}\boldsymbol{x} - \boldsymbol{b}$ ($\|\mathbf{A}\boldsymbol{x} - \boldsymbol{b}\|$, i.e., the sum of squared residual errors) and the norm of $\boldsymbol{x}$ ($\|\boldsymbol{x}\|$; i.e., the sum of squared flows).

Once the problem is reduced to m dimensions using SVD, we have the equivalent of a square system of equations and can solve for a value for $\boldsymbol{x}$, e.g., the solution to the continuity equation can be found. The inequality constraints are then applied to this initial solution to yield a new solution (vector $\boldsymbol{x}$) that satisfies both the mass conservation (system 2) and biological constraints (system 3). The second solution space is searched by the quadratic programming algorithm, which is set up to solve less than or equal inequalities only. Thus, to implement a greater than inequality, we simply multiply the whole row through by –1. The second solution has a higher norm than the first but remains the solution with the smallest norm among the biologically realistic flow networks, e.g., by minimizing both the sum of squared flows and the sum of squared residual errors.

If the procedure failed to provide a reasonable solution (e.g., some flows could be negative), we can use the same technique to further reduce the dimensionality of the problem (to $m - 1$, $m - 2$, etc.) until a solution is found (Vézina and Platt 1988). The solution with m dimensions is called the full-rank solution; the solutions with k dimensions ($m > k$) are the lower-rank solutions. By computing solutions of lower rank, observational noise or errors in the observed data (the data are inconsistent and only an approximate fit to these data) and the interdependencies (some of the equations are co-linear) can be removed. Normally, little is lost in terms of ecosystem flow representations in these lower-rank solutions. The magnitude of the residual error ($\|\mathbf{A}\boldsymbol{x} - \boldsymbol{b}\|$) and the norm of the solution ($\|\boldsymbol{x}\|$) depend on k, the number of dimensions used to represent the observation and parameter spaces of $\mathbf{A}$. A disproportionate increase in the norm of the solution for k close to m is diagnostic of the effect of errors on the inverse solution. On the other hand, rapid increases in the residual norm as k is lowered indicate that information required to approximate a closed mass flow budget is ignored. One criterion for selecting among solutions of different ranks, therefore, would be to select the solution at the turning point in the residual error and solution norm curves. To discount the effect of uncertainties and redundancies in the observational data while preserving the mass balance as much as possible, k is selected. The best solution is the model that produces the smallest sums of squared residuals for the compartmental mass balances (e.g., the solution thus minimizes errors between the assumed and calculated mass balances and between the measured and calculated flows). These different operations were done in Matlab® using the Optimization Toolbox.

Weighting factors

Prior knowledge is crucial in that it allows us to select among a potentially infinite number of solutions to the underdetermined problem. Up to this point, prior knowledge was entered only through the constraints. However, another way to enter prior knowledge in the model is through weighting factors that change the relative weight of the rows and columns of matrix $\mathbf{A}$. The error structure is introduced in the model as

$$\mathbf{S}^{-1/2}\mathbf{A}\mathbf{W}^{1/2}\mathbf{W}^{-1/2}\boldsymbol{x} = \mathbf{S}^{-1/2}\boldsymbol{b} \tag{4}$$

$$\mathbf{G}\mathbf{W}^{1/2}\mathbf{W}^{-1/2}\boldsymbol{x} > \boldsymbol{h} \tag{5}$$

This weighting scheme does two things: (*i*) it introduces a prior hypothesis about the relative sizes of the unknown flows ($\mathbf{W}$), and (*ii*) it limits the influence of large uncertainties on the solution ($\mathbf{S}^{-1}$), e.g., the weighted optimal fits were largely determined by the parts of the ecosystem about which we know the most. The choice of weights for each mass-balance equation (called row weights) and for each unknown flow (column weights) of matrix $\mathbf{A}$ is thus an important part of the solution process. In this study, the variances of the observed data were used as the row weights (which make up the diagonal of matrix $\mathbf{S}$, variance matrix of $\mathbf{A}$) and the variances of the unknown flows as the column weights (which make up the diagonal of matrix $\mathbf{W}$, variance matrix of $\boldsymbol{x}$). We used the inverse of the variances in the weighting scheme.

The variances (Var) of the unknown flows were calculated from the coefficients of variation of the observed data (see Tables 4 and 5). For each predation flow, the variance was

$$\mathrm{Var}(\mathrm{Pr}_{u\to y}) = (Q_y^{\mathrm{in}})^2(\mathrm{CV}(\mathrm{DC}_{u\to y}^{\mathrm{in}})^2 + (\mathrm{CV}(Q_y^{\mathrm{in}})^2) \tag{6}$$

In fact, the real variance for each predation flow should be

$$\mathrm{Var}(\mathrm{Pr}_{u\to y}) = ((Q_y^{\mathrm{in}})^2(\mathrm{DC}_{u\to y}^{\mathrm{in}})^2) \times (\mathrm{CV}(\mathrm{DC}_{u\to y}^{\mathrm{in}})^2 + \mathrm{CV}(Q_y^{\mathrm{in}})^2) \tag{7}$$

where Q_y^{in} was the input consumption of y and $\mathrm{DC}_{u\to y}^{\mathrm{in}}$ was the input proportion of prey u in diet (by mass) of consumer y. However, the large number (68 of 349 flows) of $\mathrm{DC}_{u\to y}^{\mathrm{in}}$ values that were low (<0.1%) or equal to 0% (potential trophic relation in other ecosystems) led to numerical instability and gave more weight to the predation equations compared with other mass-balance equations in the solution. Thus, we removed this term and used a variance mainly influenced by the variance of the consumption for each group (distribution of variance more uniform). This process allowed the model to increase the corresponding residuals of the predation equations. This was motivated by the prior belief that measurements of diets are uncertain, mostly representative of a key species for a functional group, and are not necessarily representative of the period and region investigated. The downweighting process left more room for the measured flows to change from their initially assigned values and thus allowed the model to potentially increase the differences between the initial and final estimates of the diet terms.

Noise in the data: sensitivity studies

To assess the solution's robustness to variations in the data, random perturbations were applied to both input data and right-hand sides of the mass-balance equations (vector $\boldsymbol{b}$) (Tables 2, 3, and 5). Each element (b_i) of vector $\boldsymbol{b}$ was randomly perturbed to a maximum of its standard deviation (SD_i). Each term was thus replaced by $b_i + r_n\mathrm{SD}_i$, where r_n is a randomly chosen real number between –1 and 1. For the model (hereafter termed "normal solution") presented in the next section, the solution is always the mean of 31 balanced inversions corresponding to 31 random perturbations (including a response where $r_n = 0$, i.e., "initial solution") on vector $\boldsymbol{b}$. This number is a compromise between limitations in computing time (1 week for 31 balanced and ecologically realistic random perturbations) and statistical significance. This procedure also allows us to appraise the uncertainty in the

© 2004 NRC Canada

estimated flows given the uncertainties in the input data. The variation in each flow across the 31 perturbations is quantified by its coefficient of variation.

Two sensitivity tests were performed to describe the impact of different mortality processes (fishing, predation, and natural mortality other than predation) on small and large cod: (*i*) a solution with seal predation on cod (hereafter termed "seal solution") constrained to maximum potential values (maximum diet and consumption limits), and (*ii*) a solution including winter misreported catches (hereafter termed "misreporting solution"). In the seal solution, consumption values by seals were set at their maximum limits ±10% (Table 3). The minimum and maximum consumption ranges changed in the seal solution from 0.35–0.67 to 0.60–0.74 t·km^{-2}·year^{-1} for harp seals (*Phoca groenlandica*), from 0.032–0.044 to 0.040–0.048 t·km^{-2}·year^{-1} for hooded seals (*Cystophora cristata*), from 0.03–0.10 to 0.09–0.11 t·km^{-2}·year^{-1} for grey seals (*Halichoerus grypus*), and from 0.010–0.015 to 0.013–0.016 t·km^{-2}·year^{-1} for harbour seals (*Phoca vitulina*) compared with the normal solution. The lower consumption limits in each initial range of the normal solution were obtained from an updated version of the consumption model of Hammill and Stenson (2000). In the seal solution, consumption values estimated by these authors were increased by a factor of 73% for harp seals, 25% for hooded seals, 254% for grey seals, and 37% for harbour seals. In addition, the range of potential proportions of small cod in the seal diets changed in the seal solution from 0.0%–10.7% to 9.6%–11.7% (maximum observed proportion ±10%) for harp seals, from 0.5%–20.8% to 18.7%–22.9% for hooded seals, from 1.9%–23.1% to 20.8%–25.4% for grey seals, and from 2.8%–8.4% to 7.5%–9.2% for harbour seals compared with the normal solution. The range of potential proportions of large cod in the seal diets changed in the seal solution from 0.0%–3.9% to 3.5%–4.3% for harp seals, from 0.5%–21.4% to 19.5%–23.5% for hooded seals, from 2.0%–23.7% to 21.4%–26.1% for grey seals, and from 0.9%–2.8% to 2.5%–3.1% for harbour seals compared with the normal solution.

Even though there is little documented evidence, undeclared catches (non-reported landings and discards at sea) were believed to have been important during the winter otter trawl fishery, which occurred during the 1980s (Fréchet 1991). These would have been mostly age-4 and age-5 fish, and non-reported catches would have been equivalent to those landed during the first 3 months of the year. In the misreporting solution, the catch (1.10 t·km^{-2}·year^{-1}) of large cod represented an increase by 45% of the mean catch value initially used (0.76 t·km^{-2}·year^{-1}) in the normal solution. Finally, all three solutions (normal, seal, and misreporting), which were the means of 31 balanced inversions, were examined for differences in flow patterns.

Properties of the inverse solutions

The least-square mass-balance residuals were normalized in inverse proportion to the weights of the mass-balance equations to eliminate the effect of widely differing values among the parameters. The least-square mass-balance residuals quantify the compatibility (smallest overall sums of squared residuals) between inputs and outputs (Table 7). The lower sums of squared residuals for additional diet equations show a better fit between input data and modelling estimates for that part of the model. For the compartmental mass-balance, export, and production equations, the poorer fit between input data and modelling estimates is related to the estimates for hooded seals. When the estimates for this group are omitted only in the calculation for the normal model, the sums of squared residuals for the compartmental mass-balance, export, and production equations decreased to 1.1×10^{-11}, 9.4×10^{-16}, and 8.1×10^{-16}, respectively. The compartmental mass-balance residuals correspond to annual changes in the biomass for hooded seals of close to –0.06%, –0.03%, and 0.15% for the normal, seal, and misreporting solutions, respectively. The residuals for the export equations correspond to changes between the input and estimated export values for hooded seals of –28%, –12.6%, and –22.5% for the normal, seal, and misreporting solutions, respectively. Finally, the residuals for the production equations correspond to changes between input and estimated values for hooded seals of close to –5.6%, 9.2%, and 1.2% for the normal, seal, and misreporting solutions, respectively. However, these changes are lower than the coefficients of variation for biomass (1%), export (141%), and production (45%) observed for hooded seals. The inverse solutions are consistent with a steady biomass in all compartments but at the expense of the fit to some of the input data. These findings showed that inverse modelling could also find a solution not exactly balanced (not in steady state).

Table 7. Norms of normalized residuals (i.e., sum of squared residual errors divided by weights, diagonal of matrix **S**) for the compartmental mass balances for each model: normal solution, seal solution (predation by each seal group on cod was constrained to maximum potential values (maximum diet and consumption limits)), and misreporting solution (winter misreporting catches of large cod estimated by Fréchet (1991) were added to the mean export input of large cod).

	Normal solution	Seal solution	Misreporting solution
All	8.8×10^{-4}	2.3×10^{-4}	5.4×10^{-3}
Mass balance	1.6×10^{-4}	4.1×10^{-5}	9.5×10^{-4}
Export	6.1×10^{-4}	1.6×10^{-4}	3.7×10^{-3}
Production	1.2×10^{-4}	3.1×10^{-5}	7.1×10^{-4}
Diet	3.7×10^{-5}	5.0×10^{-5}	3.5×10^{-5}

The solution should also not have too many flows that are bound to either their upper or lower limits ("sticky constraints" or active constraints). A large number of active constraints suggests that the optimum may not have been found and, in any case, that the solution was determined by the a priori bounds rather than by patterns in the data. Within our perturbation method, we considered a constraint to be active if it was active in all 31 solutions. The model estimates mainly fell between the upper and lower limits. Overall, only 3% of the constraints were active (Table 8). This shows that the final solution was not overly determined by the bounds that we imposed.

We perturbed the data within their uncertainty range, and the unconstrained part of the solution could move within the a priori bounds. The method as applied here estimated a very large number of parameters, and it is possible that the relatively few data available were insufficient to constrain

© 2004 NRC Canada

these parameters. However, mean CVs of estimated production, consumption, predation, export, and detrital flows decreased significantly by comparison with their a priori CVs (CVs of the observed input data) (Table 9). Also, the a posteriori estimates of respiration flows had smaller variance than those of the a priori estimates. Finally, only the a posteriori CV of other mortality flows was comparable or slightly higher than its a priori CV (parameter insufficiently constrained). The reduction from a priori to a posteriori CV indicates that the model was able to constrain the values that individual flows can take, thus the number of possible flow structures. However, the a posteriori CV of the estimated predation flows was reduced much less than for production or consumption flows. This indicates that the inverse model constrained the partitioning of energy flows among the compartments better than the routes through which this energy reached each compartment (i.e., the trophic structure). This mirrors the findings of Vézina and Pahlow (2003) using simulated inverse analyses where they found that the main features of the flow networks are well recovered but not necessarily the detailed predator–prey relationships.

Finally, 63% of the means of estimated flows had a CV between 0% and 70%. The distribution of parameter estimates is thus different from that of a suite of Poisson variables (where three-quarters of the cases would have a SD ≥ mean, i.e., CV ≥ 100%). The parameterization was different from random, i.e., the results are not simply balances of nearly random numbers.

Results

Main prey groups and predators

Capelin (*Mallotus villosus*) was the major prey among fish, shrimp, and large crustacea in the ecosystem (56% of all matter consumed) in all three solutions (Fig. 2). The three other main prey groups were sand lance (*Ammodytes* spp.), redfish, and shrimp (mostly *Pandalus borealis*). Small demersals (sculpins (*Myoxocephalus* spp.), cunner (*Tautogolabrus adspersus*), ocean pout (*Macrozoarces americanus*)), small cod, and piscivorous small pelagics (mainly Atlantic mackerel (*Scomber scombrus*)) were also heavily consumed in the ecosystem, but they appeared in different order of importance among the solutions.

The mortality imposed on fish by predation and fishing was similar among solutions (between 18.52 and 19.31 t·km^{-2}·year^{-1}). All solutions estimated the same main predators on fish. Large cod were the major predator on fish prey in the system (Fig. 3). After large cod, redfish, capelin, and fishing were the most important predators on fish in each solution. These three main predators accounted for 66% of the mortality imposed on fish by predation and fishing in each solution, whereas the fishery represented close to 7% of the mortality (Fig. 3).

Mortality causes

Except for large cod and large Greenland halibut, predation mortality dominated (close to 77%) total mortality processes (fishing mortality + natural mortality) for fish, shrimp, and large crustaceans (mainly snow crab (*Chionoecetes opilio*)) in each solution (Table 10). For large Greenland halibut, fishing and predation mortality were relu-

Table 8. Summary of the number of estimates that were at the limit set by the constraints for different parameters (active constraints).

	Initial solution			Normal solution			
Flow/efficiency	No. of active constraints	No. of total estimates	Active constraints, %	No. of active constraints	No. of total estimates	Active constraints, %	Description of active constraints
Production	6	24	25	1	24	4	P/B^{Min}_{PUP}
Consumption	17	30	57	0	30	0	
Export	1	2	50	0	2	0	
Proportion of food not assimilated	30	30	100	0	30	0	
Growth efficiency	19	30	63	0	30	0	
Ecotrophic efficiency	19	31	61	1	31	3	EE^{Min}_{SHR}
Diet	130	232	56	10	232	4	$DC^{Min}_{SHR\to LCD}$; $DC^{Min}_{LCD\to LCD}$; $DC^{Min}_{SLA\to SCO}$; $DC^{Min}_{SCO\to SCO}$; $DC^{Min}_{SHR\to SAN}$; $DC^{Min}_{RED\to RED}$; $DC^{Min}_{CAP\to RED}$; $DC^{Min}_{SCO\to RED}$; $DC^{Min}_{SHR\to SHR}$; $DC^{Min}_{LPO\to LPO}$
Respiration	1	1	100	0	1	0	
Total	223	380	59	12	380	3	

Note: Only the estimates based on upper and lower constraint limits are used here (there are no estimates based on data equations). Initial solution, only one inversion before perturbation; normal solution, mean of 31 balanced random perturbations of each element of vector $\mathbf{b}$ (mass-balance and additional equations) by up to its standard deviation.

© 2004 NRC Canada

Table 9. Comparisons between the *a priori* coefficients of variation (CVs of the observed input data) and a posteriori coefficients of variation of the estimated flows.

	Mean input CVs, %	Normal solution mean output CVs, %	Seal solution mean output CVs, %	Misreporting solution mean output CVs, %
Production	93	26	23	23
Consumption	64	36	35	33
Predation	128	78	75	73
Export	46	25	25	25
Respiration	66[a]	56	55	50
Detrital flow	66[a]	46	45	46
Other mortality	66[a]	72	68	69

[a] Because of a lack of information, we used the average of all CVs for biomass. However, these a priori CVs should be considered as minimum values.

Fig. 2. Impacts on prey. Relative contribution of the main vertebrate, shrimp, and crustacean prey to the overall predation mortality in the ecosystem for each solution. The other prey groups include American plaice (*Hippoglossoides platessoides*), large crustaceans, flounders, and large demersals for a 1% contribution each, as well as small Greenland halibut (*Reinhardtius hippoglossoides*), skates, large cod (*Gadus morhua*), large Greenland halibut, Arctic cod, and large pelagics for a contribution <1% each, for each solution. Standard deviation (SD) is shown. Normal solution is shown in solid bars (total: 18.66 ± 3.40 t·km^{-2}·year^{-1}), seal solution in open bars (total: 18.76 ± 2.51 t·km^{-2}·year^{-1}), and misreporting solution in shaded bars (total: 19.09 ± 2.99 t·km^{-2}·year^{-1}). Pisci., piscivorous; Plank., planktivorous.

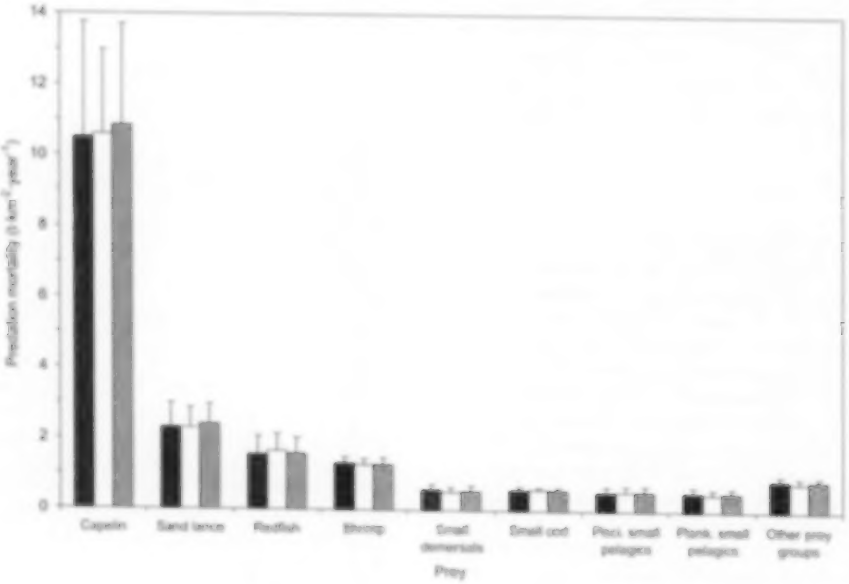

tively similar (close to 40%), whereas natural mortality other than predation accounted for 20% of total mortality. For large cod, natural mortality other than predation (or unexplained mortality) contributed greatly to total mortality in each solution. This is discussed in more detail later.

These results show the importance of predation mortality in the northern Gulf of St. Lawrence ecosystem for the 1985–1987 period. Catch (export) had a large impact on large cod, large Greenland halibut, redfish, large pelagic feeders (*Squalus acanthias*, *Pollachius virens*, and *Merluccius bilinearis*), planktivorous small pelagic feeders (mainly Atlantic herring (*Clupea harengus*)), and large crustaceans (>10% of total mortality).

Trophic links related to forage fish

In the northern Gulf of St. Lawrence during the 1985–1987 period, predation was the dominant source of mortality on fish. The high level of predation was supported by a large pelagic forage base, which included capelin, sand lance, and small pelagic feeders (see Fig. 2). Moreover, biomass was similar between predator and forage fish (21.84 t·km^{-2}·year^{-1} versus 24.09 t·km^{-2}·year^{-1}; Table 2). These forage fish were consumed by many groups (capelin, 20 predators; sand lance, 17 predators; piscivorous small pelagic feeders, 16 predators; planktivorous small pelagic feeders, 17 predators). All three solutions had relatively similar trophic patterns (Fig. 4). Capelin was mainly preyed upon by large cod,

© 2004 NRC Canada

Fig. 3. Impact of predators and fishing. Relative contribution of the main predators and fishing on overall mortality (excluding natural mortality other than predation) in the ecosystem for each solution. The other predators include small Greenland halibut (*Hippoglossoides platessoides*) for a 2% contribution, large Greenland halibut, skates, seabirds, small demersals, and grey seals (*Halichoerus grypus*) for a 1% contribution each, and the other groups for a contribution <1% each, for each solution. Standard deviation (SD) is shown. Normal solution is shown in solid bars (total: 18.51 ± 3.39 t·km^{-2}·year^{-1}), seal solution in open bars (total: 18.61 ± 2.50 t·km^{-2}·year^{-1}), and misreporting solution in shaded bars (total: 19.31 ± 2.99 t·km^{-2}·year^{-1}).

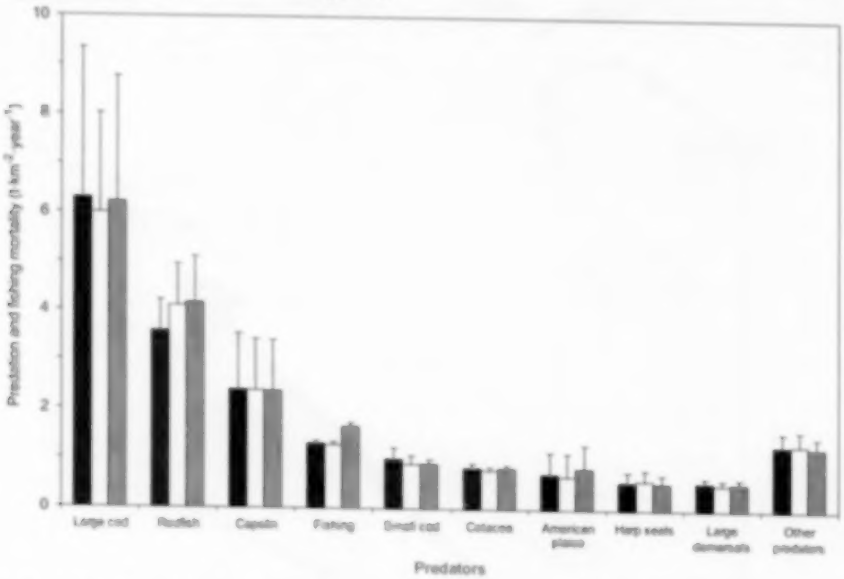

Table 10. Total Mortality (t·km^{-2}·year^{-1}) and details of mortality (%) estimated by each solution.

	Normal solution (seal solution) [misreporting solution]			
Groups	TM_i	$\%EX_i$	$\%\sum_n Pr_{i\to n}$	$\%MO_i$
Large cod	1.65 (1.67) [1.75]	46 (45) [64]	2 (4) [2]	52 (51) [34]
Small cod	0.75 (0.80) [0.79]	0 (0) [0]	75 (73) [71]	25 (27) [29]
Large Greenland halibut	0.06 (0.07) [0.07]	42 (44) [41]	40 (36) [43]	18 (20) [16]
Small Greenland halibut	0.09 (0.09) [0.09]		82 (77) [82]	18 (23) [18]
American plaice	0.30 (0.27) [0.31]	7 (8)[7]	81 (74) [75]	12 (18) [18]
Flounders	0.18 (0.15) [0.19]	4 (5) [4]	86 (80) [83]	10 (15) [13]
Skates	0.05 (0.05) [0.05]	0 (0) [0]	85 (87) [86]	14 (13) [14]
Redfish	2.41 (2.52) [2.48]	11 (10) [11]	64 (65) [63]	25 (25) [27]
Large demersals	0.14 (0.14) [0.14]	7 (7) [7]	74 (72) [74]	19 (22) [19]
Small demersals	0.61 (0.55) [0.59]		94 (93) [93]	6 (7) [7]
Capelin	13.34 (12.82) [13.56]	0 (0) [0]	79 (83) [80]	21 (17) [20]
Sand lance	2.93 (2.89) [3.08]		79 (79) [78]	21 (21) [22]
Arctic cod	0.02 (0.01) [0.02]		93 (93) [93]	7 (7) [7]
Large pelagics	0.01 (0.01) [0.01]	23 (22) [21]	55 (53) [53]	23 (24) [26]
Piscivorous small pelagics	0.65 (0.66) [0.64]	2 (2) [2]	81 (83) [84]	17 (15) [14]
Planktivorous small pelagics	0.74 (0.74) [0.74]	24 (23) [24]	68 (67) [69]	8 (10) [8]
Shrimp	1.45 (1.43) [1.47]	6 (6) [6]	89 (88) [87]	5 (5) [6]
Large crustaceans	0.29 (0.26) [0.28]	15 (17) [15]	58 (66) [56]	27 (17) [29]

Note: TM_i, total mortality ($TM_i = EX_i + \sum_n Pr_{i\to n} + MO_i$); $\%EX_i$, percent of mortality by fishing (= export here); $\%\sum_n Pr_{i\to n}$, percent of mortality by predation; $\%MO_i$, percent of natural mortality other than predation.

small cod, redfish, and whales. Whales, large demersals (*Urophycis tenuis*, *Melanogrammus aeglefinus*, and *Centroscyllium fabricii*), and large cod exerted the main predation pressure on piscivorous small pelagic feeders (Fig. 4). For sand lance, capelin and redfish were the main predators. Also, capelin cannibalism accounted for close to 10% of

© 2004 NRC Canada

Fig. 4. Main predation flows ($t \cdot km^{-2} \cdot year^{-1}$) on piscivorous small pelagic feeders (mainly Atlantic mackerel (*Scomber scombrus*)), capelin (*Mallotus villosus*), and sand lance (*Ammodytes* spp.) estimated by the normal (upper values), seal solutions (middle values in parentheses), and misreporting solution (lower values in square brackets). Note that, for each organism, the predation flows represented (arrows) contribute at least 79% of overall predation mortality. For comparisons, fishing mortality fluxes ($t \cdot km^{-2} \cdot year^{-1}$) are also included. Underlined values have a coefficient of variation >75%. Size of arrows indicates the strength of the flow.

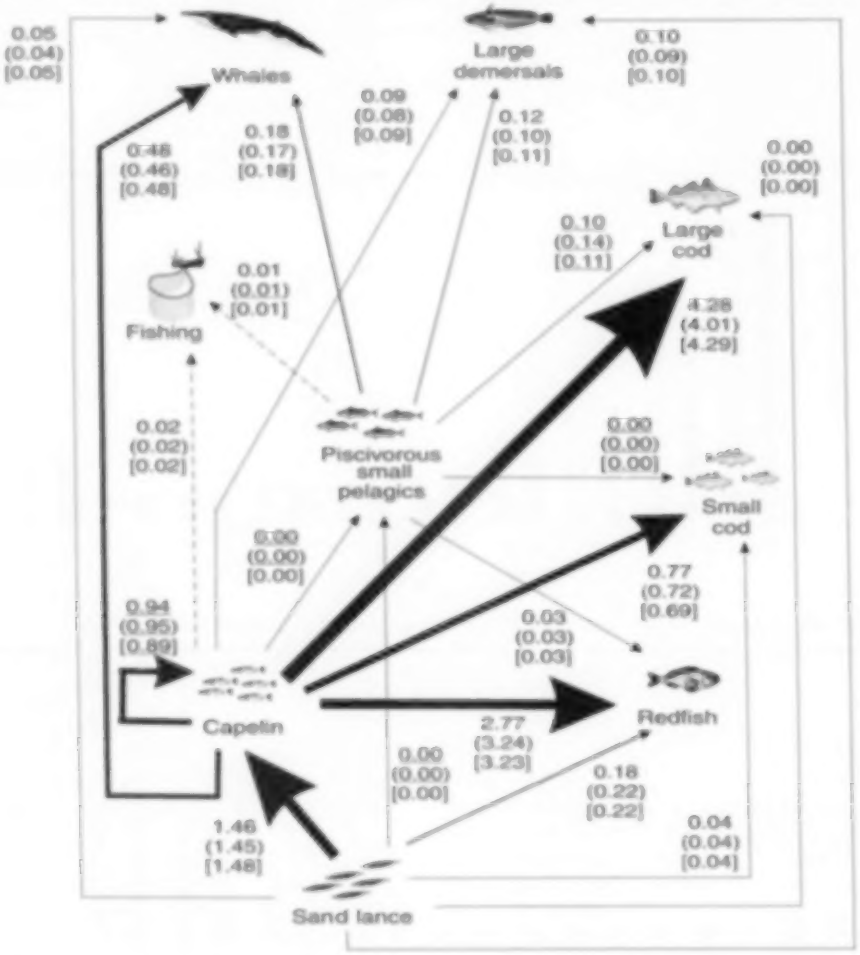

predation mortality in each solution. However, the related predation flow was variable among the final solutions (CV between 94% and 100%).

Trophic links related to shrimp, redfish, and cod

Apart from forage fish, redfish, shrimp, and small cod were also heavily consumed by the other groups (Fig. 2). The major trophic fluxes related to these predation processes show that shrimp were mainly consumed by redfish, whereas the next two important predators (small and large cod) together consumed as much shrimp as redfish did (Fig. 5). Large cod were the main predators of both small cod and redfish and were mainly eaten by harp and grey seals. The impact of the fishery is also shown with high mortality fluxes on large cod and redfish (Fig. 5). The general pattern of shrimp, redfish, and cod interactions was similar among random perturbations and sensitivity tests. This robust feature was not caused by strong constraints. Indeed, based on the coefficients of variation of the input data (diet consumption and consumption data), the a priori coefficients of variation of the predation fluxes of small cod and redfish by large cod were 118% and 303%, respectively. The constraints thus left sufficient room for the estimated flows to change from their initially assigned constraint values. Finally, the a posteriori coefficients of variations of the estimated predation fluxes of large cod on small cod and redfish were 60% and 67%, respectively.

Mortality processes on small and large cod

Predation dominated total mortality of small cod (75% of total mortality; Fig. 6) in the normal solution. Natural mortality other than predation represented about 25% of total mortality, whereas fishing was negligible (Table 10). Large cod followed by large demersal feeders and harp seals were the main predators in the normal solution. We obtained qualitatively the same results with the solution including winter misre-

© 2004 NRC Canada

Fig. 5. Main predation flows (t·km^{-2}·year^{-1}) on shrimp (mainly *Pandalus borealis*), redfish (*Sebastes* spp.), and small and large cod (*Gadus morhua*) estimated by the normal (upper values), seal solutions (middle values in parentheses), and misreporting solution (lower values in square brackets). Note that, for each organism, the predation flows represented (arrows) contribute at least 78% of overall predation mortality. For comparisons, fishing mortality fluxes (t·km^{-2}·year^{-1}) are also included. Underlined values have a coefficient of variation >75%. Size of arrows indicates the strength of the flow.

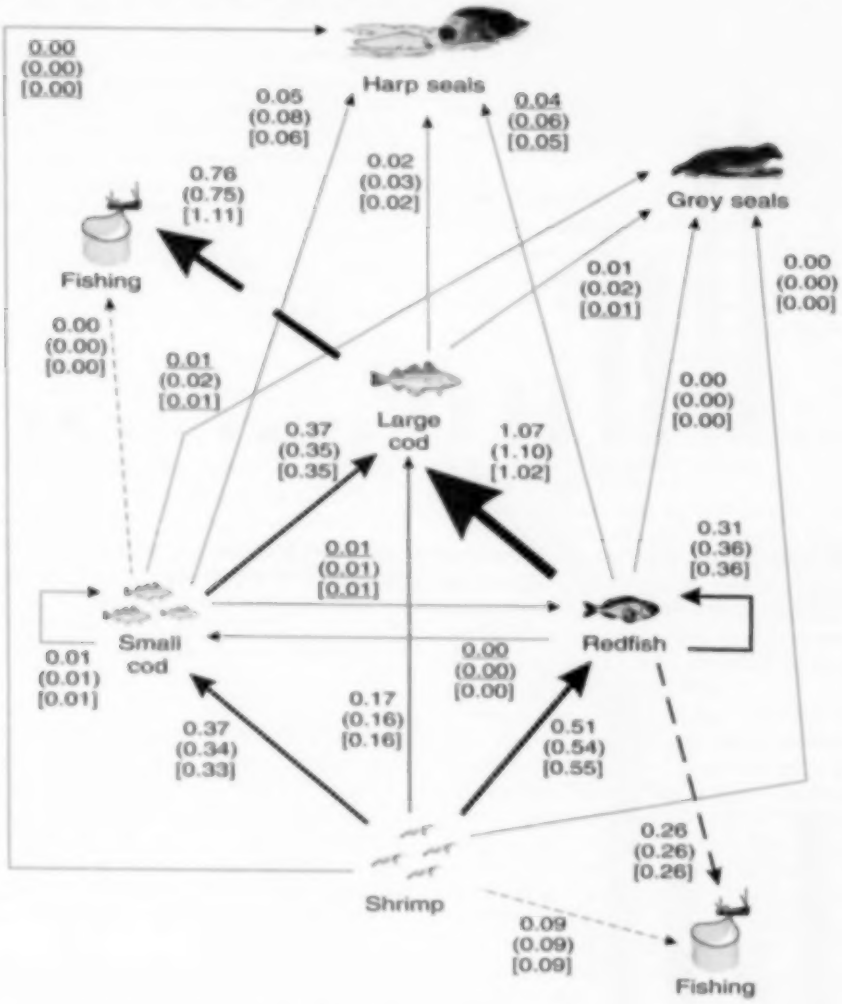

ported catches of large cod (misreporting solution) (Fig. 6). Harp seals contributed to 7% (0.05 ± 0.03 t·km^{-2}·year^{-1}) of the total mortality in the normal and misreporting solutions. This impact increased to 10% (0.08 ± 0.01 t·km^{-2}·year^{-1}) when predation by seals on cod was constrained to maximum values (seal solution) (Fig. 6).

The main predators of large cod were harp and grey seals (Fig. 5). However, when all mortality sources (fishing, predation, and natural mortality other than predation) were considered, predation represented only 2% of total mortality on large cod in the normal solution (Fig. 7). Natural mortality other than predation (unexplained mortality) accounted for 52% of total mortality, whereas the fishery represented 46%. When predation by seals on cod was constrained to maximum values, predation increased to 4% of total mortality (Fig. 7). Fishing accounted for 45% of total mortality, whereas other or unexplained mortality still represented 51%. In the misreporting solution, fishing increased to 64% and dominated total mortality on cod, whereas other or unexplained mortality decreased to 34%. Predation mortality accounted for 2% of total mortality (Fig. 7).

Discussion

Validity of inverse solutions

Uncertainty in the input data

Ecosystem modelling requires the collection of a considerable amount of information. The modelling results described here were influenced by several areas of uncertainty for different groups at the lower and higher trophic levels. A considerable amount of effort has been expended to obtain

© 2004 NRC Canada

Fig. 6. Main mortality causes (predation and natural mortality other than predation, i.e., other causes) on small cod (*Gadus morhua*) estimated by each solution. Normal solution shown in solid bars (total: 0.75 ± 0.13 t·km^{-2}·year^{-1}), seal solution in open bars (total: 0.80 ± 0.10 t·km^{-2}·year^{-1}), and misreporting solution in shaded bars (total: 0.79 ± 0.10 t·km^{-2}·year^{-1}).

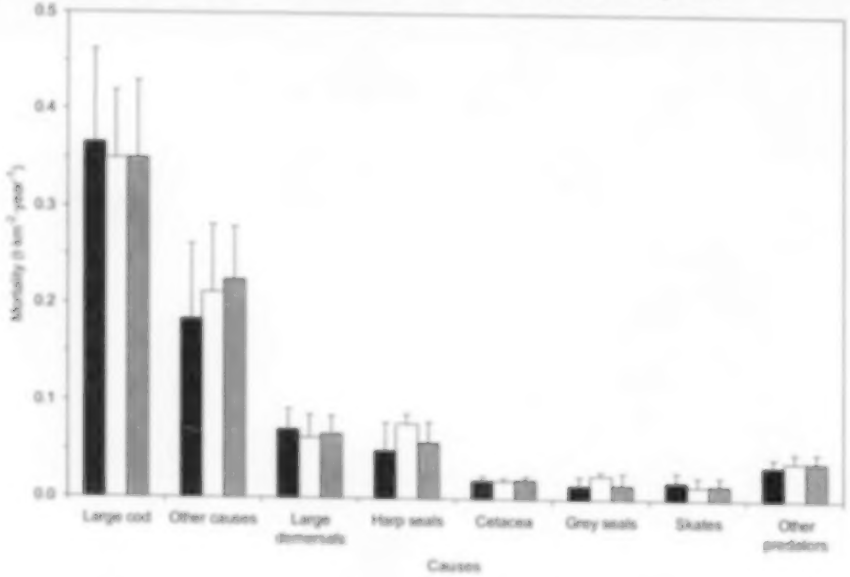

Fig. 7. Main mortality causes (fishing, predation, and natural mortality other than predation, i.e., other causes) on large cod (*Gadus morhua*) estimated by each solution. Normal solution shown in solid bars (total: 1.65 ± 0.10 t·km^{-2}·year^{-1}), seal solution in open bars (total: 1.67 ± 0.11 t·km^{-2}·year^{-1}), and misreporting solution in shaded bars (total: 1.75 ± 0.29 t·km^{-2}·year^{-1}).

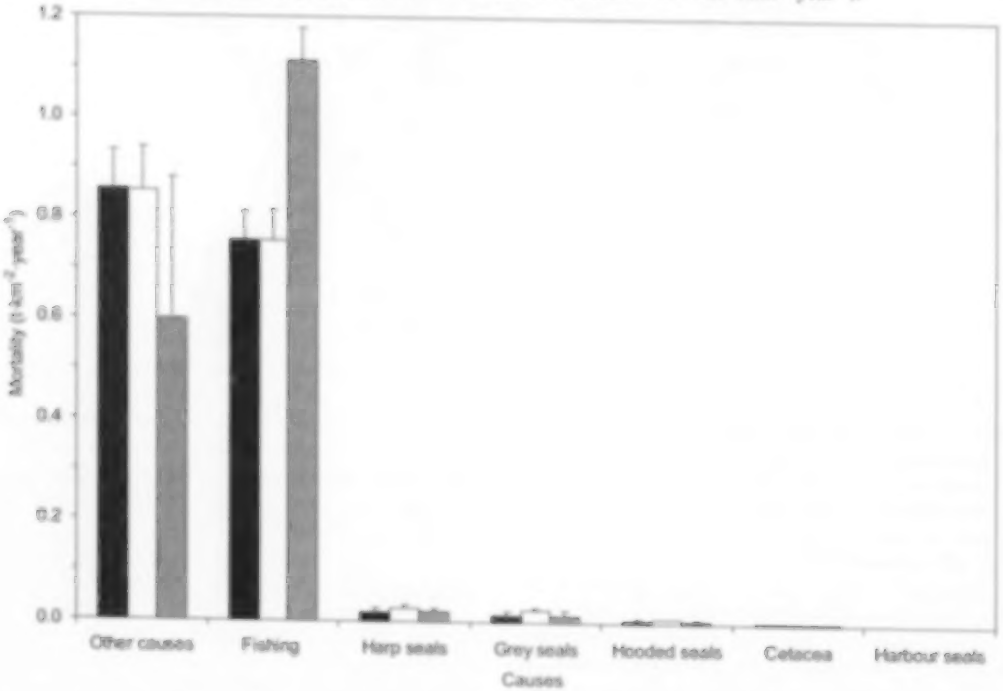

high-quality input data for the study area during the period of interest (Morissette et al. 2003). Catch estimates are considered quite reliable, although there is indirect but reliable evidence for non-negligible misreporting in cod (Fréchet 1991; Hurtubise et al. 1992; Palmer and Sinclair 1997). Good biomass estimates for harp and grey seal, as well as

© 2004 NRC Canada

harvested species, are available, but information on hooded seal and harbour seal biomass is limited, particularly for the mid-1980s. Moreover biomass data for forage species, benthic invertebrates, and zooplankton were sparse or non-existent for the area and period studied and were thus taken from the literature or for the same area but another time period (mid- to late 1990s). For fish, biomass estimates were calculated from sequential population analysis (cod and herring) or from summer scientific trawl surveys carried in the northern Gulf, which provided trawlable biomass estimates that were adjusted for catchability based on Harley and Myers (2001) and Savenkoff et al. (2004). It was necessary to use empirical data from other areas and (or) time frame for fish and invertebrate production and consumption as very little is known about these parameters in the Gulf of St. Lawrence. These different sources of data (local and literature) explain the high coefficients of variations for the production and consumption data (93% and 64%, respectively) compared with that of export (46%).

Further uncertainties with diet data resulted from assuming that the diet for a key species is representative of the functional group to which it belonged or from attributing the proportion of "unidentified" in stomach content analysis in proportion to the different identified groups in the stomachs. The uncertainties remaining in the understanding of the ecosystem may come from incorrect values because no data exist or confidence limits are too large or because of inaccurate aggregation of species within one functional group, as well as from unsuspected processes occurring in the ecosystem. However, such a model provides a useful starting point to frame hypotheses about the ecosystem and to identify data gaps.

Multispecies models and uncertainty in the model estimates

Among the multispecies models, inverse models are static-flow models (Hollowed et al. 2000). The use of upper and lower limits to constrain the majority of input values (production, consumption, export, and diet composition) and the choice of row and column weights make inverse modelling a flexible tool to quantify mass-balanced flow diagrams and trophic transfer efficiencies that are internally consistent.

Because the number of flows to be solved (n = 463 in this case) exceeded the number of independent mass-balance relations (m = 173), the solutions are not unique. Also, because our empirical databases and scientific understanding of ecological processes will never be complete, multiple model configurations have to be used to allow for an explicit implementation and assessment of this uncertainty (Whipple et al. 2000). In this study, by randomly perturbing data inputs, we constructed a set of balanced solutions and used the mean of these 31 random perturbations. This process reduced significantly the number of active constraints (estimates pushed at their preset limits) compared with the initial solution before perturbation. In fact, each perturbed solution had a large number of active constraints (like the initial solution), but the active constraints varied from perturbed solution to perturbed solution. One realization of the data was not sufficient to constrain the model. However, many realizations of the data allowed us to construct a solution that is nearly insensitive to the constraints. This leads to a probabilistic approach to the inverse estimation of mean flows (and not just their variances). The estimated flows fall inside our a priori constraints (once the data are perturbed) and therefore are reasonable "middle ground" descriptions. Also, except for the other mortality flows, the a posteriori estimates are less variable than in our a priori variances, and therefore, the model was useful in constraining observations into a coherent picture. It remains that other equivalent solutions are possible and that information on natural mortality other than predation would improve future inverse models.

Main characteristics of the northern Gulf of St. Lawrence ecosystem during the mid-1980s

Predation was the dominant source of mortality for fish except for large cod and to a lesser extent large Greenland halibut. In all models, large cod, redfish, and capelin represented close to 66% of the mortality imposed on fish by predation and fishing. Large cod (32% of this mortality) were the main predator in this system. The high level of predation was supported by a large pelagic forage base, which included capelin, sand lance, and small pelagic feeders. Capelin was also the major vertebrate prey in the system (near 56% of all vertebrate matter consumed). Capelin plays a key role in the food web by transferring energy from primary and secondary producers (on which it feeds) to higher trophic levels. It is an important prey for other abundant fish species (cod and redfish) and for marine mammals (cetacea and seals) (Piatt and Methven 1992; Lawson et al. 1998; DFO 2001). Our estimates show that predators consumed over a million tonnes of capelin annually in the northern Gulf during the mid-1980s (10.5 t·km^{-2}·year^{-1} or 1.1 × 10^{6} t·year^{-1}). However, the input data for capelin production, consumption, and diet composition were obtained from other areas and (or) time frames (Morissette et al. 2003), resulting in considerable uncertainty in these parameters. Consequently, even though trophic links involving capelin, as well as other forage species, are relatively similar among solutions (owing to local diet compositions for all their predators, e.g., seals, cod, and redfish), significant improvements in our understanding of the Gulf of St. Lawrence ecosystem would require local data pertaining to these species.

Based on a meta-analysis of time series data across nine regions in the North Atlantic, Worm and Myers (2003) calculated strong inverse correlations between shrimp and cod that they interpreted as "top-down" effects. Our results partly support this "top-down" view of species interactions (predators can suppress lower trophic levels) but also suggest that reality is more complex. Even though cod exerted a significant predation pressure on shrimp, redfish consumed as much shrimp as cod did. However, large cod were also the main predators of both small cod and redfish. The strong inverse correlations between shrimp and cod found by Worm and Myers (2003) could thus result from both direct (as predators) and indirect (as main predators of intermediate predators, e.g., small cod and redfish) predation by large cod. The predation by large cod on both small cod and redfish, as well as the decline of cod and redfish stocks in the early 1990s, could explain the negative relationship between cod and shrimp observed by Worm and Myers (2003). The

© 2004 NRC Canada

trophic interactions identified in this study suggest that increases in shrimp biomass in the Gulf in the 1990s are causally related to decreases in cod and redfish biomass.

Mortality processes on small and large cod

The relationship between commercial fish species and their environment has long been of interest to fisheries scientists. Cod stocks in the Northwest Atlantic collapsed in the early 1990s (CAFSAC 1994). Some authors argued that the sole reason for the collapse was overfishing (e.g., Hutchings and Myers 1994; Hutchings 1996; Myers et al. 1996), whereas others proposed that a natural shift to less favourable environmental conditions also made stocks more vulnerable to fishing through processes such as an earlier migration to wintering grounds, which shortened the feeding season (Castonguay et al. 1999), declines in condition (Lambert and Dutil 1997) and in growth and production (Dutil et al. 1999), and an increase in natural mortality (DeYoung and Rose 1993; Dutil and Lambert 2000). The present study enables us to describe the impact of combined mortality processes on small and large cod in the northern Gulf shortly before the onset of the steep population decline.

The model results indicate that predation largely dominated total mortality on small cod. Natural mortality other than predation represented 25% of total mortality, whereas fishing was negligible. Cannibalism generally constitutes a minor component of the diet of cod (Bogstad et al. 1994; Uzars and Plikshs 2000). Our results conform to this pattern, as the proportion of small cod in the diet of large cod was only 4.8% (Morissette et al. 2003). Nonetheless, large cod were the most important predator of small cod, with cannibalism accounting for at least 44% of the mortality of small cod. Stock–recruitment relationships are expected to be compensatory, with higher prerecruit survival at lower spawning stock sizes, when cannibalism occurs (Hilborn and Walters 1992). Thus, cannibalism may have limited recruitment of this commercially valuable stock. Also, during the mid-1980s, cannibalism occurred over the whole year owing to an overlap in the distributions of large and small cod even in the wintertime. Major distribution shifts of adult cod in winter have been observed since the early 1990s (Castonguay et al. 1999). Individual adult fish that previously overwintered in the Gulf have been increasingly distributed deeper and further offshore away from the distribution of juveniles. This partial spatial segregation of juvenile and adult cod may have limited cannibalism in winter since the early 1990s.

Although harp and grey seals were the main predators of large cod, predation represented only 2% of total mortality on large cod when all mortality sources are considered. The commercial fishery represented close to 46% of total mortality, whereas natural mortality other than predation was the main mortality process (52%). Thus, a high proportion of the total mortality of large cod could not be explained by either fishing or predation for the northern Gulf of St. Lawrence between 1985 and 1987. This would amount to about 88 451 t·year^{-1}. The reasons for the large amount of other mortality of large cod in the northern Gulf are not clear. Possible explanations for the high other mortality of large cod in our models include (*i*) overestimation of cod biomass, (*ii*) mortality owing to starvation or disease, (*iii*) underestimation of predation mortality, or (*iv*) underestimation of fishing mortality owing to misreporting.

Biomass estimates for large cod are perhaps the least uncertain of our data inputs for the northern Gulf. Estimates of relative abundance of cod based on the summer bottom-trawl survey are very consistent (e.g., estimates of year-class strength correspond closely between years) with low CVs (21% of the mean for adult ages in 1985–1987).

Death from starvation and poor condition and diseases, which were not monitored, could have also contributed to this unaccounted mortality. One would expect though that this mortality would also affect other fish groups, leading to a high unaccounted mortality term for them too, which it did not (<25%). Moreover, recent work suggests a decline in condition and energy reserves, which may have resulted in increased natural mortality of cod in the northern Gulf of St. Lawrence stock mainly in the early 1990s, after our studied modelling period (Lambert and Dutil 1997; Dutil and Lambert 2000).

The main predators of large cod in our models were harp seals, followed by grey seals. Predation by seals would be underestimated if the biomass of seals, their total energy requirements, their seasonal occurrence in the Gulf, or the proportion of large cod in their diets were underestimated. However, errors in these variables of the order of magnitude required to substantially reduce other mortality seem unlikely. For example, the proportion of cod in seal diets was constrained within the minimum and maximum percentage observed in any single diet sample obtained from different diet studies conducted in the St. Lawrence Estuary, the northern Gulf, and waters of the Northwest Atlantic (Morissette et al. 2003). The proportions of large cod in seal diets in the normal and misreporting solutions were close to the means, whereas they were at the upper limits in the seal solution. These proportions are unrealistically high compared with findings in other areas (Benoit and Bowen 1990; Mohn and Bowen 1996; Hammill and Stenson 2000).

Although it seems unlikely that predation on large cod by seals is underestimated in our models, other unaccounted predation may contribute to the high other mortality of large cod. We have likely underestimated predation or accidental ingestion by cetaceans (e.g., harbour porpoise (*Phocoena phocoena*)). To account for the other mortality (0.86 t·km^{-2}·year^{-1}), however, large cod would have to represent nearly 100% of the biomass eaten by all cetaceans combined (total cetacean consumption: 0.96 t·km^{-2}·year^{-1}), and there is no evidence that baleen whales ever eat large numbers of cod of any size. We may also have omitted other important predators of large cod such as large sharks. Unfortunately, information on large sharks is lacking.

When seal predation on cod was constrained to maximum values, consumption estimates were higher by a factor of 73%, 25%, 254%, and 37% for harp seals, hooded seals, grey seals, and harbour seals, respectively, than the consumption estimates by Hammill and Stenson (2000). However, predation increased only to 4% of total mortality, but other or unexplained mortality still represented 51% of total mortality. Therefore model results show that seal predation had little effect in reducing total mortality of large cod in the northern Gulf before the collapse of the stock. However, seal consumption, particularly of large cod, may be higher than

© 2004 NRC Canada

what we acknowledged from the diet data, owing to methodological weaknesses (failure to detect "belly biting", i.e., consumption of just the abdomen, including the energy-rich liver) and limited spatiotemporal coverage. This would imply that belly biting is an important foraging strategy for seals, which is not consistent with evidence that large cod are consumed whole and large otoliths are recovered from stomach contents (Benoit and Bowen 1990; Hammill and Stenson 2000). Given the very low fishing mortality that cod sustained in the mid-1990s owing to the first moratorium on cod fishing and the concurrent increase in seal biomass (Hammill and Stenson 2000), a comparison with a model developed for the post-collapse period will identify and quantify the impact of different mortality processes on small and large cod and thus the effect of seal predation on cod stocks. However, in light of results from this study, seal predation appears to have contributed little to the cod decline, which is similar to conclusions from other studies for the southern Gulf of St. Lawrence (Sinclair et al. 1995) and the Eastern Scotian Shelf (Mohn and Bowen 1996).

Finally, fishing mortality may have been underestimated owing to misreporting. Note, though, that this cod fishery represented 50% of the total fishery in this ecosystem. In the solution including misreporting of winter catches of large cod (Fréchet 1991), fishing increased to 64% and dominated total mortality, whereas other mortality causes decreased to 34%. Predation mortality accounted for 2% of total mortality. The fishing estimates (1.11 $t{\cdot}km^{-2}{\cdot}year^{-1}$) represented an increase by 45% of the mean catch value initially used (0.76 $t{\cdot}km^{-2}{\cdot}year^{-1}$). This finding agrees with the estimated 20%–40% unreported catch in excess of declared landings for trawlers, as estimated by fishery officers during the mid-1980s in the northern Gulf of St. Lawrence (Palmer and Sinclair 1997). We also tested a solution with catches of large cod constrained to two times its maximum value (1.70 $t{\cdot}km^{-2}{\cdot}year^{-1}$, e.g., extreme scenario) to show how cod unexplained mortality changed with different levels of unreported catch. In this case, other mortality causes were reduced to 12% of total mortality, fishing increased to 87%, and predation represented 1% of total mortality only.

Thus, the only way to significantly reduce unexplained mortality or other mortality causes on large cod in the model is to increase catches of large cod. Fishing, including unaccounted fishing mortality (highgrading, discarding, and underreporting), seems to be a critical source of mortality on large cod in the northern Gulf of St. Lawrence for the 1985–1987 period. Our analysis of various scenarios suggests that direct fishery-related causes are the most likely explanation for a large fraction of the unaccounted mortality on large cod. This suggests that fishing mortality may likely have been substantially underestimated in the mid-1980s, just before the demise of a cod stock that historically was the second largest in the Northwest Atlantic. Furthermore, it is important to remember that reported F was between 0.4 and 0.6 between 1974 and 1990, i.e., over twice $F_{0.1}$, the target fishing mortality level (Fréchet et al. 2003).

Acknowledgements

This study was carried out as a contribution of CDEENA (Comparative Dynamics of Exploited Ecosystems in the Northwest Atlantic), a program supported by the Canadian Department of Fisheries and Oceans (Science Strategic Fund). We are grateful to colleagues who made data available for this manuscript. We thank François Saucier and André Gosselin for giving us access to computing resources (Unix server). We wish to acknowledge Drs. Daniel Duplisea, Jacques A. Gagné, Doug P. Swain, two anonymous referees, and especially Dr. Jake Rice for their thoughtful comments on the manuscript. The CDEENA web site is available at http://www.osl.gc.ca/cdeena/en/accueil.shtml.

References

Benoit, D., and Bowen, W.D. 1990. Summer diet of grey seals (*Halichoerus grypus*) at Anticosti Island, Gulf of St. Lawrence, Canada. *In* Population biology of the sealworm (*Pseudoterranova decipiens*) in relation to its intermediate and seal hosts. *Edited by* W.D. Bowen. Can. Bull. Fish. Aquat. Sci. No. 222. pp. 227–242.

Bogstad, B., Lilly, G.R., Mehl, S., Pálsson, Ó.K., and Stefánsson, G. 1994. Cannibalism and year-class strength in Atlantic cod (*Gadus morhua* L.) in Arcto-boreal ecosystems (Barents Sea, Iceland, and eastern Newfoundland). ICES Mar. Sci. Symp. **198**: 576–599.

Bowering, W.R., and Lilly, G.R. 1992. Greenland halibut (*Reinhardtius hippoglossoides*) off southern Labrador and northeastern Newfoundland (Northwest Atlantic) feed primarily on capelin (*Mallotus villosus*). Neth. J. Sea Res. **29**: 211–222.

Bundy, A., Lilly, G.R., and Shelton, P.A. 2000. A mass-balance model for the Newfoundland–Labrador Shelf. Can. Tech. Rep. Fish. Aquat. Sci. No. 2310.

CAFSAC. 1994. Report on the status of groundfish stocks in the Canadian Northwest Atlantic. DFO Atl. Fish. Stock Status Rep. No. 94/4.

Castonguay, M., Rollet, C., Fréchet, A., Gagnon, P., Gilbert, D., and Bréthes, J.-C. 1999. Distribution changes of Atlantic cod (*Gadus morhua* L.) in the northern Gulf of St. Lawrence in relation to an oceanic cooling. ICES J. Mar. Sci. **56**: 333–344.

Christensen, V., and Pauly, D. 1992. ECOPATH II — a software for balancing steady-state ecosystem models and calculating network characteristics. Ecol. Model. **61**: 169–185.

Christensen, V., and Pauly, D. (*Editors*). 1993. Trophic models of aquatic ecosystems. ICLARM, Manila, Philippines. ICLARM Conf. Proc. **26**.

Christensen, V., and Pauly, D. 1998. Changes in models of aquatic ecosystems approaching carrying capacity. Ecol. Appl. **8** (Suppl.): S104–S109.

Department of Fisheries and Oceans (DFO). 2001. Capelin of the Estuary and Gulf of St. Lawrence. DFO Science, Stock Status Report No. B4-03 (2001).

DeYoung, B., and Rose, G.A. 1993. On recruitment and distribution of Atlantic cod (*Gadus morhua*) off Newfoundland. Can. J. Fish. Aquat. Sci. **50**: 2729–2741.

Dutil, J.-D., and Lambert, Y. 2000. Natural mortality from poor condition in Atlantic cod (*Gadus morhua*). Can. J. Fish. Aquat. Sci. **57**: 826–836.

Dutil, J.-D., Castonguay, M., Gilbert, D., and Gascon, D. 1999. Growth, condition, and environmental relationships in Atlantic cod (*Gadus morhua*) in the northern Gulf of St. Lawrence and implications for management strategies in the Northwest Atlantic. Can. J. Fish. Aquat. Sci. **56**: 1818–1831.

Fréchet, A. 1991. A declining cod stock in the Gulf of St. Lawrence: how can we learn from the past? NAFO (Northwest Atl. Fish. Organ.) Sci. Coun. Stud. **16**: 95–102.

© 2004 NRC Canada

Fréchet, A., Gauthier, J., Schwab, P., Bourdages, H., Chabot, D., Collier, F., Grégoire, F., Lambert, Y., Moreault, G., Pageau, L., and Spingle, J. 2003. The status of cod in the northern Gulf of St. Lawrence (3Pn, 4RS) in 2002. Can. Stock Assess. Sec. No. 2003/065.

Hammill, M.O., and Stenson, G.B. 2000. Estimated prey consumption by harp seals (*Phoca groenlandica*), hooded seals (*Cystophora cristata*), grey seals (*Halichoerus grypus*) and harbour seals (*Phoca vitulina*) in Atlantic Canada. J. Northw. Atl. Fish. Sci. **26**: 1–23.

Harley, S.J., and Myers, R.A. 2001. Hierarchical Bayesian models of length-specific catchability of research trawl surveys. Can. J. Fish. Aquat. Sci. **58**: 1569–1584.

Hilborn, R., and Walters, C.J. 1992. Quantitative fisheries stock assessment: choice, dynamics and uncertainty. Chapman & Hall, New York.

Hollowed, A.B., Bax, N., Beamish, R., Collie, J., Fogarty, M., Livingston, P., Pope, J., and Rice, J.C. 2000. Are multispecies models an improvement on single-species models for measuring fishing impacts on marine ecosystems? ICES J. Mar. Sci. **57**: 707–719.

Hurtubise, S., Fréchet, A., and Savard, L. 1992. Les captures accessoires sur les crevettiers et les sébastiers du Golfe du Saint-Laurent. NAFO Sci. Coun. Res. Doc. No. 92/60.

Hutchings, J.A. 1996. Spatial and temporal variation in the density of northern cod and a review of hypotheses for the stock's collapse. Can. J. Fish. Aquat. Sci. **53**: 943–962.

Hutchings, J.A., and Myers, R.A. 1994. What can be learned from the collapse of a renewable resource, Atlantic cod, *Gadus morhua*, of Newfoundland and Labrador? Can. J. Fish. Aquat. Sci. **51**: 2216–2246.

Lambert, Y., and Dutil, J.-D. 1997. Condition and energy reserves of Atlantic cod (*Gadus morhua*) during the collapse of the northern Gulf of St. Lawrence stock. Can. J. Fish. Aquat. Sci. **54**: 2388–2400.

Lawson, J.W., Anderson, J.T., Dalley, E.L., and Stenson, G.B. 1998. Selective foraging by harp seals, *Phoca groenlandica*, in nearshore and offshore waters of Newfoundland, 1993 and 1994. Mar. Ecol. Prog. Ser. **163**: 1–10.

Lilly, G.R. 1991. Interannual variability in predation by cod (*Gadus morhua*) on capelin (*Mallotus villosus*) and other prey off southern Labrador and northeastern Newfoundland. ICES Mar. Sci. Symp. **193**: 133–146.

Mohn, R., and Bowen, W.D. 1996. Grey seal predation on the eastern Scotian Shelf: modelling the impact on Atlantic cod. Can. J. Fish. Aquat. Sci. **53**: 2722–2738.

Morissette, L. 2001. Modélisation écosystémique du nord du Golfe du Saint-Laurent. M.Sc. thesis, Université du Québec à Rimouski, Que., Canada.

Morissette, L., Despatie, S.-P., Savenkoff, C., Hammill, M.O., Bourdages, H., and Chabot, D. 2003. Data gathering and input parameters to construct ecosystem models for the northern Gulf of St. Lawrence (mid-1980s). Can. Tech. Rep. Fish. Aquat. Sci. No. 2497.

Myers, R.A., Hutchings, J.A., and Barrowman, N.J. 1996. Hypotheses for the decline of cod in the North Atlantic. Mar. Ecol. Prog. Ser. **138**: 293–308.

Palmer, C., and Sinclair, P. 1997. When the fish are gone: ecological disaster and fishers in the northwest Newfoundland. Ferwood Publishing, Halifax, Nova Scotia.

Piatt, J.F., and Methven, D.A. 1992. Threshold foraging behaviour of baleen whales. Mar. Ecol. Prog. Ser. **84**: 205–210.

Rice, J., and Rivard, D. 2003. Proceedings of the zonal assessment meeting — Atlantic cod. Can. Stock Assess. Sec. Proc. Ser. No. 2003/021.

Savenkoff, C., Vézina, A.F., and Bundy, A. 2001. Inverse analysis of the structure and dynamics of the whole Newfoundland–Labrador Shelf ecosystem. Can. Tech. Rep. Fish. Aquat. Sci. No. 2354.

Savenkoff, C., Bourdages, H., Castonguay, M., Morissette, L., Chabot, D., and Hammill, M.O. 2004. Input data and parameter estimates for ecosystem models of the northern Gulf of St. Lawrence (mid-1990s). Can. Tech. Rep. Fish. Aquat. Sci. No. 2531.

Sinclair, A.F. 2001. Natural mortality of cod (*Gadus morhua*) in the Southern Gulf of St. Lawrence. ICES J. Mar. Sci. **58**: 1–10.

Sinclair, A., Chouinard, G., Swain, D., Nielsen, G., Hanson, M., Currie, L., Hurlbut, T., and Hébert, R. 1995. Assessment of the southern Gulf of St. Lawrence cod stock. DFO Atl. Fish. Res. Doc. No. 95/39.

Uzars, D., and Plikshs, M. 2000. Cod (*Gadus morhua* L.) cannibalism in the Central Baltic: interannual variability and influence of recruit abundance and distribution. ICES J. Mar. Sci. **57**: 324–329.

Vézina, A.F., and Pahlow, M. 2003. Reconstruction of ecosystem flows using inverse methods: how well do they work? J. Mar. Sys. **40–41**: 55–77.

Vézina, A.F., and Platt, T. 1988. Food web dynamics in the ocean. I. Best estimates of flow networks using inverse methods. Mar. Ecol. Prog. Ser. **42**: 269–287.

Vézina, A.F., Berreville, F., and Loza, S. 2004. Inverse reconstructions of ecosystem flows in investigating regime shifts: impact of the choice of objective function. Progr. Oceanogr. **60**: 321–341.

Whipple, S.J., Link, J.S., Garrison, L.P., and Fogarty, M.J. 2000. Models of predation and fishing mortality in aquatic ecosystems. Fish Fish. **1**: 22–40.

Winberg, G.G. 1956. Rate of metabolism and food requirements of fish. Fish. Res. Board Can. Trans. Ser. No. 194.

Worm, B., and Myers, R.A. 2003. Meta-analysis of cod–shrimp interactions reveals top-down control in oceanic food webs. Ecology, **84**: 162–173.

© 2004 NRC Canada

Predator-dependent functional responses and interaction strengths in a natural food web

Timothy E. Essington and Sture Hansson

Abstract: Predator-dependent functional responses decouple predation mortality from fluctuations in predator abundance and therefore can prevent strong "top-down" interaction strengths in food webs. We evaluated whether contrasts in the functional response of Baltic Sea cod (*Gadus morhua*) were consistent with the contrasting population dynamics of two prey species, herring (*Clupea harengus*) and sprat (*Sprattus sprattus*): sprat abundance increased nearly threefold following a sharp decline in the cod population (a strong interaction), whereas herring abundance failed to increase (a weak interaction). We found striking differences in the functional response of cod on alternative prey, and these were consistent with the observed patterns in interaction strengths. Cod predation was the dominant source of mortality for age-1 and age-2 sprat but was only important for age-1 herring. Moreover, the magnitude of predation mortality on age-1 and age-2 sprat was highly sensitive to cod biomass, whereas predation mortality on herring was only moderately sensitive to cod biomass. These analyses suggest the possibility that food webs are comprised of linkages that vary with respect to the magnitude and importance of predation mortality and how this mortality varies with changes in predator abundance.

Résumé : Les réponses fonctionnelles qui dépendent des prédateurs peuvent éliminer le lien entre la mortalité due à la prédation et les fluctuations d'abondance des prédateurs et ainsi empêcher le développement d'importantes forces d'interaction de type «descendant» dans les réseaux trophiques. Nous avons vérifié si les différences de réponses fonctionnelles de la morue franche de la Baltique (*Gadus morhua*) étaient compatibles avec les dynamiques de population distinctes de deux de ses proies, le hareng atlantique (*Clupea harengus*) et le sprat (*Sprattus sprattus*) : l'abondance du sprat a augmenté de trois fois après une chute rapide de la population de morues (interaction forte), alors que celle du hareng n'a pas augmenté (interaction faible). Il existe d'importantes différences dans la réponse fonctionnelle de la morue à ces deux proies, différences qui s'accordent aux patterns de forces d'interaction observés. La prédation par les morues est la cause principale de mortalité des sprats d'âges 1 et 2, mais elle n'a d'importance que chez les harengs d'âge 1. De plus, l'intensité de la mortalité due à la prédation chez les sprats d'âges 1 et 2 est très sensible à la biomasse des morues, alors qu'elle ne l'est que moyennement chez les harengs. Nos analyses indiquent qu'il est possible que les réseaux trophiques soient composés de liens qui varient en fonction de l'ampleur et de l'importance de la mortalité due à la prédation et de la variation de cette mortalité en fonction des changements d'abondance des prédateurs.

[Traduit par la Rédaction]

Introduction

The study of food webs has proceeded under three largely divergent pathways (Winemiller and Polis 1996). The topological approach focuses on patterns in food web structure, concentrating on the constraints on connectance and complexity (Dunne et al. 2002). Second, energetic studies depict the flow of energy or biomass through a food web, focusing on the rates and magnitude of material cycling and identifying the trophic source of production (Baird and Ulanowicz 1989). Lastly, interaction webs are used to depict the dynamic behavior of food webs, focusing on the patterns of interaction strength, top-down control, and trophic cascades (Paine 1980) An integration of these disparate approaches is likely to substantially improve our understanding of food web patterns and dynamics (Pickett et al. 1994).

Energetic and interaction webs appear, at least initially, to offer the potential for integration, as a strong energetic link might predispose a strong interaction link. Yet, Paine (1980) recognized that strong energetic links and strong interaction links are largely independent, suggesting that quantifying the rate of energy or biomass flow between trophic groups is not sufficient to predict their dynamics. From a trophodynamic perspective, however, we can posit two conditions required for a strong top-down interaction: (*i*) the mortality rate caused by a predator should represent the dominant component of the prey total mortality rate and (*ii*) the mortality rate imposed by this predator should depend strongly on the abundance of the predator. If these two conditions are met, a strong top-down interaction can arise provided that there are not any strong compensatory responses (e.g., territoriality, space limitation, etc.) that act to maintain constant prey productivity.

One potential avenue to explore these two conditions derives from consideration of the functional response of preda-

Received 7 October 2003. Accepted 2 June 2004. Published on the NRC Research Press Web site at http://cjfas.nrc.ca on 1 February 2005.
J17778

T.E. Essington.[1] School of Aquatic and Fishery Sciences, University of Washington, Box 355020, Seattle, WA 98195, USA.
S. Hansson. Department of Systems Ecology, Stockholm University, S-106 91 Stockholm, Sweden.

[1]Corresponding author (e-mail: essing@u.washington.edu).

 doi: 10.1139/F04-146 © 2004 NRC Canada

tors. The functional response dictates the magnitude of predation because it incorporates key variables such as encounter rates and attack rates. The most commonly used models (Holling 1959) typically assume that per-capita consumption rates of predators are independent of predator abundance, such that predation mortality on prey is linearly dependent of predator abundance. However, elaborations of the classic functional response models provide several mechanisms that can cause predator feeding rates to be dependent on the abundance of other predators. These elaborations represent a significant departure from the classic functional response models and were motivated by growing appreciation (Arditi and Ginzburg 1989; Berryman 1992) and empirical evidence (Hansson et al. 2001; Skalski and Gilliam 2001; Vucetich et al. 2002) that per-capita consumption rates are indeed influenced by predator abundance. The implications of predator-dependent feeding from the perspective of prey species are profound: introducing predator dependence into the feeding rates of predators can decouple the linkage between predator abundance and the total amount of prey consumed. That is, changes in predator abundance might not produce any change in the predation mortality rate experienced by prey. Not surprisingly, recent development of food web models for use in fisheries applications (e.g., Ecopath with Ecosim) has found that model predictions are highly sensitive to the intensity of predator dependence in the functional response (Cox et al. 2002).

A diversity of processes can give rise to functional responses that are predator-dependent and thereby create variable interaction strengths. Theoretical analyses point to the potential contribution of predator interference behavior (Beddington 1975; DeAngelis 1975), prey refuging behavior (Abrams 1994; Abrams and Walters 1996), size-based predation risk (Armstrong 1999), and spatial heterogeneity (Poggiale et al. 1998; Keeling et al. 2000). Despite our improved understanding of the functional response from these theoretical and experimental studies, progress has been hampered by a paucity of studies evaluating the functional response in natural settings (Abrams and Ginzburg 2000). Thus, an improved understanding of the functional response at the organizational scales commensurate with food web analyses offers the prospect of much better understanding of the processes that give rise to variable interaction strengths.

Given that the processes giving rise to predator dependence in the functional response vary depending on prey and predator behaviors, movement rates, and spatial distributions, it follows that linkages within a food web should have varying degrees of interaction strength produced by the functional response of the predators. We assessed this hypothesis by evaluating the functional response of Baltic Sea cod (*Gadus morhua*) on two clupeid prey species. These two species, herring (*Clupea harengus*) and sprat (*Sprattus sprattus*), exhibited markedly different responses to a recent decline in cod abundance, suggesting that the nature of cod's functional response was different for these two species. Through a combination of fishing and poor recruitment, cod biomass dropped nearly 80% from a peak in the early 1980s to their lowest level in 1991 (Fig. 1). During the same period, sprat abundance increased nearly threefold, whereas herring abundance was apparently unaffected by the collapse of cod. This suggests two nonexclusive hypotheses concerning differences in the functional response of cod on alternative prey. Firstly, predation by cod was a more important source of mortality for sprat than for herring. Secondly, predation mortality on sprat depended more strongly on predator abundance, so that sprat was therefore more sensitive to changes in cod abundance.

Fig. 1. Biomasses of cod (*Gadus morhua*; ○), sprat (*Sprattus sprattus*; ●), and herring (*Clupea harengus*; ▲) in the central Baltic, 1975–1995. Estimates are based on a multispecies virtual population analysis using bioenergetics-based food consumption rates for cod. Stock assessment and output were provided by the International Council for the Exploration of the Sea (ICES) and Morten Vinther, Danish Institute for Fisheries Research, personal communication.

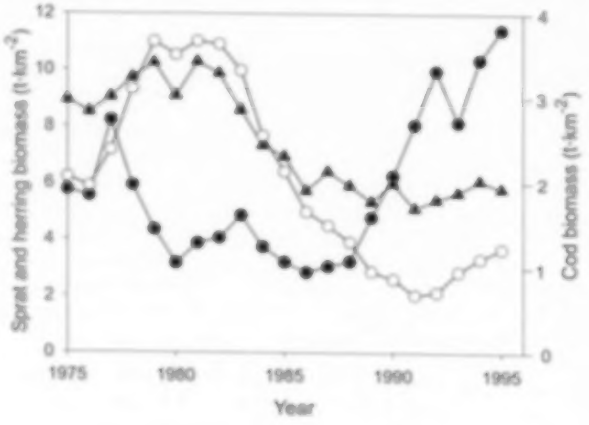

Methods

Description of functional response models

We based all functional response models on predator and prey biomass density (t·km^{-2}). This unit is advantageous over numerical units (number·km^{-2}) because consumption rates are dictated by both body size and population size (Yodzis and Innes 1992). We originally estimated functional response parameters for each cod and prey age-class combination, yet parameterizing the model in this way yielded difficulties owing to observation error: estimates of "shape" parameters are notoriously biased by observation error (Walters and Ludwig 1981). Because initial analyses indicated that there were no consistent differences in the shape parameter among cod age classes, functional response models were parameterized for each prey type by summing mortality rates and cod biomass over all cod age classes. By pooling cod age classes together, we increased the sample size for each data point, thereby improving the precision and reducing bias in these estimates.

Our model development was based on the empirical functional response model of Hassell and Varley (1969) because it allows for a diversity of shapes of the functional response and does not imply any particular mechanism. By replacing their predator-dependent parameter (m) with $1 - \theta$, then the functional response ($f(N, P)$) on prey type j in the absence of handling time or satiation constraints is

© 2004 NRC Canada

$$(1) \qquad f(N,P) = a_j N_j(t) P(t)^{\theta_j - 1}$$

where N_j is biomass of prey type j, P is predator biomass, a_j is the effective search rate, and θ_j describes the degree of predator dependence in the functional response. When $\theta = 1$, the functional response is predator-independent, and when $\theta = 0$, the functional response is strongly density-dependent (ratio-dependent).

The functional response can be manipulated to generate a "predation response" describing how predation mortality rate (M_p; year^{-1}) is affected by prey and predator biomass. The predation response, denoted $g(N, P)$, is

$$(2) \qquad g(N,P) = f(N,P)\frac{P}{N_j} = a_j P(t)^{\theta_j}$$

Thus, the altered parameterization of the Hassell and Varley model (replacing $-m$ with $1 - \theta$) produces an intuitive expression regarding the sensitivity of predation mortality to predator abundance: when θ is near 0, predation mortality is unaffected by predator abundance, when θ is near 1, predation mortality is linearly related to predator abundance, and θ greater than 1 produces accelerating predation mortality with predator abundance. We illustrate the relationship between M_p and P for alternative values of θ (Fig. 2).

The above model does not consider handling time or satiation effects. We can justify the exclusion of the former by recognizing that piscivorous fishes eat few, large prey items a day, so handling time costs are expected to be minimized (Essington et al. 2000). Satiation, on the other hand, could potentially be important. We typically consider satiation as having two effects. First, there is a physiological maximum rate of food intake that acts as an upper limit on consumption rates. Second, we often presume that predator searching rates are related in some way to hunger level, where hunger level itself is related to the amount of remaining stomach capacity. A generalized way of representing the second component of satiation is

$$(3) \qquad T_s = 1 - \left(\frac{\Sigma C_j}{C_{\max}}\right)^h$$

where T_s is time spent searching for prey, ΣC_j is the sum of consumption on all j prey types, $C_{\max}$ is the physiological maximum consumption rate, and h is some unknown constant that describes how searching time declines with reduced hunger level. The functional response is therefore calculated from the product of search time (T_s), rate of effective search per unit search time (a_j), prey abundance (N_j), and some predator-dependent modification of effective search rate:

$$(4) \qquad f(N,P) = C_j(t) = T_s(t) a_j N_j(t) P(t)^{\theta_j}$$

Analytic solutions for $C_j(t)$ are readily obtained under two special cases. The first is the limiting case when h goes to ∞, which describes the functional response when there is no reduction in search rate until consumption rates are very near the maximum rate. In other words, satiation only acts as a limit to the maximum amount of food consumed. We refer to this limiting case as the type-I model to emphasize its similarity to the Holling type-I functional response. The other readily analyzed case is when $h = 1$, which describes the case in which there is a linear decline in search rate with decreasing hunger level. We refer to this special case as the type-II functional response to highlight the mathematical similarity to the Holling type-II model.

Fig. 2. Alternative parameterizations of the Hassell and Varley (1969) predation response model, where predation mortality (M) is a function of predator biomass density (P): $M = aP^{\theta}$. All three of these curves produce the same predation mortality rate (0.5 year^{-1}) on prey when predator biomass equals 2 t·km^{-2} but have different values of the shape parameters (θ) and attack rate parameters (a). Commonly used functional response models are based on an assumption that $\theta = 1$.

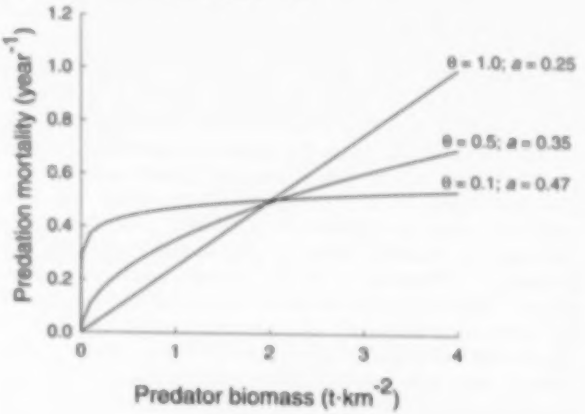

If Baltic Sea cod consumed only herring and sprat, then deriving these two functional response models is straightforward. However, cod also eat known amounts of other food items (C_{other}) whose abundances in the Baltic Sea are unknown (e.g., benthic macroinvertebrates). We therefore need to explicitly consider this consumption of other food types in our functional response models. We begin by reconsidering eq. 3 to account for consumption of other food types:

$$(5) \qquad T_s = 1 - \left(\frac{C_{other} + \Sigma C_j}{C_{\max}}\right)^h$$

When considering the limiting case where h goes to ∞ (type-I models), we can solve for consumption rates on each prey item by substituting eq. 5 for T_s in eq. 4 and rearranging for C_j:

$$(6) \qquad f(N,P) = a_j N_j P^{\theta_j - 1}$$

$$\text{if } C_{\max} > C_{other} + \sum_j a_j N_j P^{\theta_j - 1}$$

$$f(N,P) = (C_{\max} - C_{other})\frac{a_j N_j P^{\theta_j - 1}}{\sum_j a_j N_j P^{\theta_j - 1}}$$

$$\text{if } C_{\max} \le C_{other} + \sum_j a_j N_j P^{\theta_j - 1}$$

Alternatively, for the case when $h = 1$ (type-II model), the same procedure yields the following:

© 2004 NRC Canada

$$(7)\qquad f(N,P)=\frac{(C_{\max}-C_{\text{other}})a_j P(t)^{\theta_j-1}}{C_{\max}+\sum_i a_i N_i(t)P(t)^{\theta_i-1}}$$

Description of data sources

We used estimates of abundance, diet composition, and mean individual sizes for each cod age class provided by the extensive sampling and analysis performed by the International Council for the Exploration of the Sea (ICES). Cod diet composition was based on quarterly stomach content analyses stratified by location and cod age class. Individual herring and sprat in cod stomachs were aged based on size so that we could calculate the percent contribution of each prey age class to cod diets. Age- and quarter-specific consumption rates of cod were calculated using the bioenergetics model of Hansson et al. (1996), which estimates consumption based on observed growth rate, body size, and temperature. Estimates of stock size were based on a multispecies cohort analysis, which accounts for the number of individuals that must have been present in each age class to match observed fisheries catches and predatory losses. These analyses were then tuned to survey data (hydroacoustics and trawling) to match the observed abundance indices. The estimates of stock sizes used in our analyses (presented in Fig. 1) are based on an assessment model that used bioenergetics-based consumption rates for cod (Morten Vinther, Danish Institute for Fisheries Research, Charlottenlund Slot, DK-2920 Charlottenlund, Denmark, personal communication). We show that there is no numerical circularity in assessing functional response relationships from this stock assessment method (Appendix A).

Calculating predation mortality rates

Cod predation on sprat or herring older than age-5 was negligible, so we restricted all analyses to age-1 to age-5 sprat and herring. Thus, there were 10 separate prey categories and 8 different cod age classes. For each prey category, we calculated the predation mortality rate imposed by each cod age class within all 0.25-year time periods between 1977 and 1990, the only period in which all data were available. Instantaneous predation mortality rate imposed by cod age class i on prey type j during each time interval t ($M_{i,j}(t)$; year^{-1}) was calculated from estimates of total consumption of prey type j by age i cod ($C_{i,j}(t)$; kg) and mean biomass of prey j ($\bar{N}_j(t)$; kg) during a specified time interval (Δt):

$$(8)\qquad M_{i,j}(t)=\frac{C_{i,j}(t)}{\bar{N}_j(t)\Delta t}$$

This is equivalent to the well-known Baranov catch equation in fisheries except predation mortality is being calculated instead of fishing mortality.

$C_{i,j}(t)$ was calculated from the product of age-specific individual cod consumption rates (kg·0.25 year^{-1}), abundances, and diet compositions. The mean biomass of prey j in each quarter year is

$$(9)\qquad \bar{N}_j(t)=\frac{N(t)_j[1-\exp(-(Z_j(t)-G_j(t))\Delta t]}{(Z_j(t)-G_j(t))\Delta t}$$

where $Z_j(t)$ is total mortality rate (year^{-1}) during the time interval, $G_j(t)$ is instantaneous growth rate (year^{-1}), Δt is the time period over which biomass was averaged (0.25 year), and $N_j(t)$ is the biomass at the beginning of the quarter. $Z_j(t) - G_j(t)$ was calculated as $\ln(N_j(t)/N_j(t + \Delta t))/0.25$. This calculation assumes that mortality is density-independent, which will not be true if satiation is an important constraint in the functional response. When mortality is density-dependent, eq. 8 will overestimate $M_{i,j}(t)$ if biomass is rapidly increasing and underestimate $M_{i,j}(t)$ if biomass is rapidly decreasing. However, our time scale of analysis (0.25 year) minimized this bias because $(Z_j(t) - G_j(t))\Delta t$ were small. We used an analogous procedure to estimate mean cod biomass during each time period.

We parameterized models to the yearly predation mortality because seasonal fluctuations and random sampling error produced considerable variation in quarterly $M_{i,j}(t)$. Instantaneous mortality rates are additive, so yearly predation mortality is equal to the mean of the quarterly predation mortalities as estimated above.

Our results indicated that incorporating satiation had no positive effect on the goodness of fit, so we therefore focused all subsequent analyses on the simpler model that did not include satiation (eq. 2). Because this model does not require us to consider all predator–prey interactions simultaneously, we derived improved estimates of P for each prey type to better reflect ontogenetic shifts in cod diet composition and consumption rates. To this end, we estimated the relative importance of predation by each cod age class on each prey type based on age-specific consumption rates and diet compositions of cod. Specifically, we calculated a weighted sum of cod age-specific biomasses to substitute for $P(t)$ in the functional response (denoted $\tilde{P}_j(t)$):

$$(10)\qquad \tilde{P}(t)=\sum_i w_{ij}P_i(t)$$

$$w_{ij}=\frac{d_{ij}q_i}{\max_i(d_{ij}q_i)}$$

where $P_i(t)$ is the biomass of age-i cod, d_{ij} is the proportional contribution of prey type j to diets of age-i cod, and q_i is the mass-specific consumption rate of age-i cod.

Parameter estimation and model comparisons

We compared functional response models and parameter values using the information theoretic approach that allows for direct comparison of goodness of fit through the comparison of model likelihoods (Burnham and Anderson 1998). To this end, we fit the following generalized model to the data:

$$(11)\qquad M_j(t)=g[N(t),P(t)]U(t)$$

$$U(t)=\exp(u(t))$$

where $M_j(t)$ is predation mortality on prey type j in year t, $g[N(t),P(t)]$ is the predation response of the predator (i.e., the functional response multiplied by $P(t)/N_j(t)$ (eq. 1)), $N(t)$ is the vector of all prey abundances in year t, and $U(t)$ represents a log-normally distributed error, with $u(t) \sim N(0, \sigma^2)$. Maximum likelihood parameter estimates for each model were determined numerically using a simulated annealing al-

© 2004 NRC Canada

Table 1. Comparison of negative log-likelihood (NLL), number of parameters (n), and Akaike information criteria (AIC).

Model (data type)	NLL	n	AIC[a]
Type-I	257.1	21	556.2
Type-II	264.1	21	570.2
Weighted biomass (reduced)	261.8	11	545.6
Weighted biomass (full)	255.8	20	551.6
Weighted biomass (stepwise)	256.3	14	540.6

Note: The type-I and type-II models used the estimated cod biomass directly, whereas the models indicated by "weighted biomass" were corrected for size-based predation.

[a]By convention, AIC is calculated as $2\text{NLL} + 2n$.

gorithm based on a simplex procedure. We used likelihood profiles to generate approximate 95% confidence intervals of all model parameters (Hilborn and Mangel 1997; Burnham and Anderson 1998).

We performed two types of model comparisons. We compared the goodness of fit of the type-I and type-II satiation models through a direct comparison of the maximum log-likelihoods. These two models have the same number of parameters, so this direct comparison is valid. We constrained C_{max} for both models to be within biologically plausible values. Bioenergetics models predict maximum consumption rates that range from 4% body mass per day for a 100-g cod to 2.6% body mass per day for a 1000-g cod (Hansson et al. 1996). As the bulk of the population biomass was comprised of individuals sized 200–800 g, we used a liberal estimate of 3.5% body mass per day as an upper constraint on the population mass-specific maximum consumption rate.

The second type of model comparison looked in more detail at the parameters of the functional response model that ignores satiation (eq. 2) based on the weighted cod biomass estimates described in the previous section. This comparison sought to determine which prey groups had uniquely different values of the shape parameter (θ). The Akaike information criteria (AIC; Burnham and Anderson 1998) was used to find the most parsimonious model that balanced goodness of fit (as judged from likelihood) and model complexity (as judged from number of parameters). The AIC indicates that the more complicated model offers an improved fit to the data over a simpler model if the difference in the number of parameters is less than the difference in the log-likelihoods.

To this end, we considered the following extension of eq. 2:

$$(12) \qquad M_{p,j}(t) = a_j P(t)^{\theta+\Theta_j}$$

where Θ_j is a deviation from a commonly shared value of the shape parameter (θ) for prey type j. The AIC, which judges the best model as one that minimizes the sum of the negative log-likelihood and the number of parameters, was used to determine the minimum number of Θ_j needed to best describe the dynamics of $M_p(t)$ among all of the j prey groups. This procedure was performed in an analogous manner as forward stepwise regression, where we initially set all Θ_j to zero and then considered the improvements in model fit by sequentially adding Θ_j to the model. At each step, the model that produced the lowest AIC was retained in the model, and the procedure was then repeated until no more parameters were deemed to significantly improve the model fit.

Fig. 3. Maximum likelihood fit of the multispecies functional response model (type II), where satiation constraints are modeled as a linear function of food consumption. This model is based on estimates of the total herring (*Clupea harengus*) and sprat (*Sprattus sprattus*) prey consumed (ΣC_j) and available stomach capacity ($C_{max} - C_{other}$), where C_{max} is the maximum consumption rate and C_{other} is observed consumption of other prey items. Under the type-II model, the sum $\Sigma C_j(t)/(C_{max} - C_{other}(t))$ should be an asymptotic function of the potential consumption rate, calculated as sum of the $a_j N_j(t) P(t)^{\theta-1}$. The observed data show little evidence of an asymptote, producing a relatively poor fit compared with the type-I functional response model. Parameter estimates of C_{max} were constrained to be within biologically plausible values.

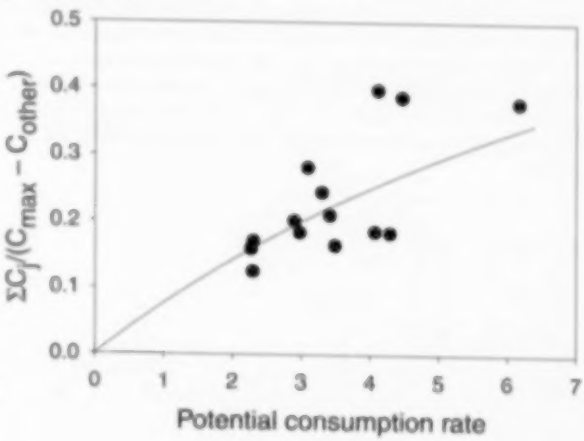

Results

We compared the goodness of fit for the two representations of satiating functional response relationships. The type-I model assumes that search rates are maintained until consumption rates reach C_{max}, whereas the type-II model assumes that effective search rate declines linearly with consumption rate. The type-I model provided a substantially better fit to the data than the type-II model (Table 1). The difference in negative log-likelihoods between these two models was approximately 7, which equals an approximately 1000-fold greater fit of the type-I model over the type-II model.

The poor fit of the type-II model was due to the assumption that effective search rate declines linearly with prey availability with a slope proportional to $1/C_{max}$ and the constraint on C_{max} within biologically plausible values ($C_{max} \leq 3.5\%$ body mass·day^{-1}). The poor fit can be visualized by rearranging eq. 4 and plotting the ratio of total consumption of j prey types ($\Sigma C_j(t)$) to the available consumption rates ($C_{max} - C_{other}(t)$) against the sum of the terms $\Sigma a_j N_j(t) P(t)^{\theta-1}$ (Fig. 3). The independent variable represents the predicted consumption rates in the absence of satiation, so it can be considered a measure of the potential consumption rate. Under the assumptions of the type-II model, there is an asymptotic relationship between the ratio $\Sigma C_j(t)/(C_{max} - C_{other}(t))$ and the potential consumption rate. The data, however, do not asymptote but instead exhibit a steady increase with potential consumption rate (Fig. 3). In other words, consumption rates

© 2004 NRC Canada

Table 2. Relative (per-biomass) consumption rates of cod age classes (w_{ij}) on each prey type.

	Sprat age classes					Herring age classes				
Cod age	1	2	3	4	5+	1	2	3	4	5+
1	0.73	0.61	0.30	0.19	0.25	0.15	0.04	0.01	0.01	0.01
2	1.00	0.79	0.82	0.91	0.62	0.59	0.3	0.12	0.07	0.06
3	0.94	1.00	1.00	1.00	0.91	0.80	0.54	0.30	0.22	0.20
4	0.76	0.97	0.95	0.95	1.00	0.94	0.79	0.60	0.52	0.52
5	0.55	0.82	0.83	0.85	0.94	1.00	0.99	0.92	0.86	0.86
6	0.38	0.64	0.66	0.70	0.77	0.93	1.00	1.00	0.98	0.98
7	0.28	0.49	0.51	0.60	0.64	0.86	0.94	0.97	1.00	1.00
8	0.20	0.35	0.37	0.47	0.50	0.70	0.76	0.81	0.85	0.86

Fig. 4. Maximum likelihood estimates of the attack rate parameter a for cod (*Gadus morhua*) preying on sprat (*Sprattus sprattus*; ●) and herring (*Clupea harengus*; ○). The attack rate parameters indicate the successful encounter and attack rates when the effective cod biomass density equals 1 kg·km^{-2}. Error bars represent approximate 95% confidence intervals calculated from likelihood profiles.

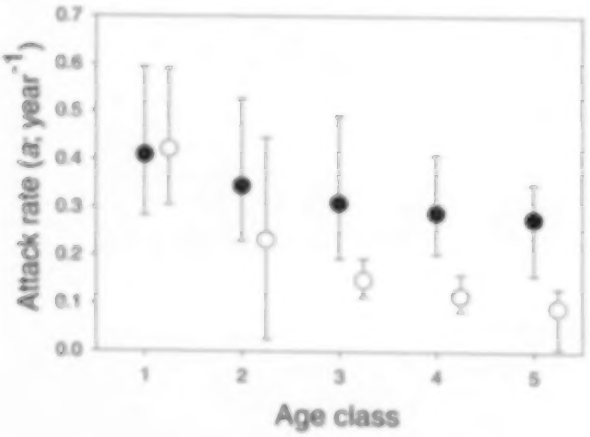

Fig. 5. Maximum likelihood estimates of the predator dependence parameter θ for cod (*Gadus morhua*) preying on sprat (*Sprattus sprattus*; ●) and herring (*Clupea harengus*; ○). The effect of θ on the shape of the predation response curve can be seen in Fig. 2. Error bars represent approximate 95% confidence intervals calculated from likelihood profiles.

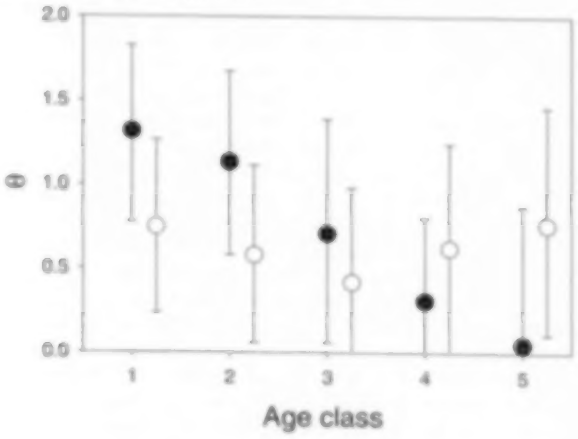

increased approximately linearly with prey abundance within the range of prey abundances experienced by cod throughout this time period. The type-I model predicted that consumption rates were always less than maximum (maximum observed consumption rate = 7.69 kg·kg^{-1}·year^{-1}, or 2% body mass per day). For that reason, the best overall model is one that does not consider satiation at all (e.g., eq. 1) because this model has the same NLL as the type-I model but with one fewer parameter.

The relative (per-biomass) consumption rate of cod age classes on each prey type indicated ontogenetic shifts in diet and consumption rates. Overall, average mass-specific consumption rates of cod declined with age from 1.68 year^{-1} at age-1 to 0.73 year^{-1} at age-8. The relative importance of prey items also shifted with age, with small sprat (age-1 to age-2) comprising 15% of the diet of age-1 cod, 20% of the diet of age-2 to age-4 cod, but less than 10% of the diet of age-5 and older cod. Of the herring age classes, only age-1 contributed substantially to cod diets, with a general pattern of increasing importance with cod age. Taking ontogenetic diet shifts and mass-specific consumption rates together, the per-biomass consumption of sprat by cod was greater for younger cod age classes, whereas the per-biomass consumption of herring tended to be greater for older cod age classes (Table 2).

The estimates of a_j showed considerable variation with prey type and prey age. For cod preying on sprat, a_j declined from a maximum of 0.41 year^{-1} for age-1 sprat to less than 0.3 year^{-1} for age-5 sprat (Fig. 4). The decline in a_j with age was more dramatic for cod preying on herring, where a_j was 0.42 year^{-1} on age-1 herring, declining to 0.09 year^{-1} for age-5 (Fig. 4). Differences in a_j for cod feeding on herring and sprat were most pronounced for older (>3 years old) prey age classes. However, because a_j only represent the attack rate when $P(t) = 1$ kg·km^{-2}, the similarity in a_j for small size classes does not necessarily indicate similar predation rates on younger sprat and herring.

Maximum likelihood estimates of the shape parameter (θ_j) also varied considerably between prey types (Fig. 5). For age-1 and age-2 sprat, maximum likelihood estimates of θ_j were greater than 1, and they declined for older age classes until the maximum likelihood estimate was nearly 0 for age-5 sprat. For herring, θ showed less variation with age class,

© 2004 NRC Canada

Fig. 6. Cod (*Gadus morhua*) predation mortality rate (M; year^{-1}) versus effective cod biomass (t·km^{-2}) for all prey types. Points indicate observed data, and the solid lines indicate the best fitting models. Effective cod biomass was calculated from a weighted average that accounts for ontogenetic shifts in cod diets and consumption rates. Horizontal dotted lines indicate the mortality rate from other sources averaged over 1977–1990.

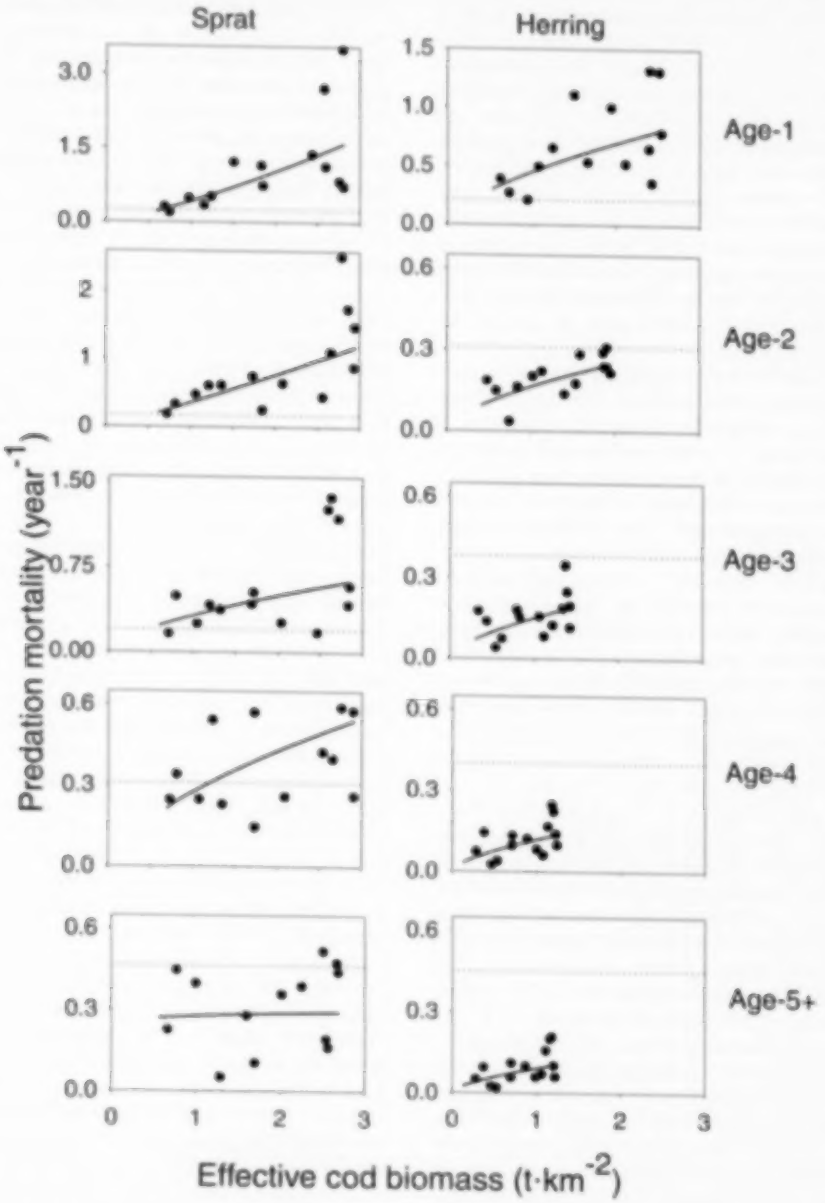

with θ equal to 0.75 at age-1, declining to 0.42 at age-3, and increasing again to 0.76 at age-4.

The most reduced model, in which θ was identical for all prey types, had a maximum likelihood that was 400-fold less than that obtained from the most complex model containing separate θ for each prey type (Table 1). However, the most complex model produced a higher AIC than the most reduced model, because the improvement in goodness of fit was not sufficient to warrant the additional nine parameters.

The stepwise selection procedure indicated that the best model was one of intermediate complexity with three significant values of Θ_j (Table 1): $\theta = 0.64$; age-1 Sprat $\Theta = +0.67$; age-2 Sprat $\Theta = +0.50$; age-5 Sprat $\Theta = -0.58$. Thus, the optimal model was one that grouped the predation response into roughly three categories: highly sensitive predation response (age-1 and age-2 sprat) for which the shape parameter exceeded 1, highly insensitive predation response (age-5 sprat) for which the shape parameter was nearly 0, and moderately

© 2004 NRC Canada

sensitive predation response (remaining prey groups) for which the shape parameter was 0.64.

Differences in the shape parameters can be seen from the observed model fits of $M_p(t)$ vs. $\tilde{P}(t)$ (Fig. 6). Predation mortality on age-1 and age-2 sprat accelerated at high predator biomasses, largely because of high predation rates ($M_p > 2$ year^{-1}) in 2 years with high cod biomass. In contrast, predation mortality on age-5 sprat was largely independent of effective cod biomass. Taking the parameter estimates and the range of effective cod biomasses together, it is possible to compare the reduction in predation mortality that accompanied the decline in cod stocks. Mortality on age-1 sprat ranged from 1.58 to 0.2 year^{-1} during 1977–1990 and mortality on age-2 sprat ranged from 1.18 to 0.1 year^{-1}. In contrast, predation mortality on herring generally exhibited a smaller range of variation. For age-1 herring, the only herring age class that was heavily preyed upon by cod, predation mortality ranged from 0.8 to 0.2 year^{-1}.

We compared the rates of cod predation with other sources of mortality (e.g., fishing, disease, other predators). Other mortality rates were calculated by subtracting estimates of cod predation mortality rate from the total mortality rate (indicated on Fig. 6 as horizontal dotted lines). Cod predation mortality was the dominant component of the total mortality rate of age-1, age-2, and age-3 sprat (Fig. 6). Predation morality rates were as much as 10-fold higher than the average "other" mortality rate for these age classes, particularly for age-1 sprat. Cod predation mortality on age-4 and age-5 sprat was approximately equal to the other sources of mortality (Fig. 6). In contrast, cod predation only dominated total mortality for age-1 herring, and cod predation mortality was always less than the average "other" mortality rate for the remaining age classes (Fig. 6).

Discussion

An analysis of the feeding patterns, relative biomass, and consumption rates of Baltic Sea cod revealed that the predator dependence of the functional response varied markedly among alternative prey and that this variation was consistent with the observed numerical response of these prey. Cod predation was the dominant component of age-1 and age-2 sprat mortality and predation on these age classes was highly sensitive to changes in cod biomass. In contrast, cod predation was only important for one age class of herring (age-1), and this predation mortality was only moderately sensitive to cod biomass. These differences in the relative importance and sensitivity of predation mortality correspond with variation in interaction strengths in the food web. Namely, there was an apparently strong top-down interaction between cod and sprat but a very weak interaction between cod and herring. This study is, to our knowledge, the first to describe differences in the functional response among alternative prey and relate these differences to interaction strengths in food webs.

One of the biggest limitations in attempting to parameterize functional response models at large spatial scales is the lack of precision in the estimates of population biomasses. We used estimates from a recent stock assessment performed by ICES, but most stock assessments have at least 10–20% error. A key feature of the stock assessment procedure is that it attempts to consider variation in predation mortality on sprat and herring. That these models attempt to incorporate cod predation on sprat and herring introduces a potentially troubling tautology in our use of stock assessment output to evaluate alternative functional response parameters. However, we show analytically that there is no numerical circularity in this method (Appendix A). Rather, the emergent parameter estimates are dictated entirely by the estimated terminal fishing mortalities and from the dynamics of predator consumption rate and diet composition (Appendix A). Moreover, this stock assessment procedure results in multispecies assessments that correspond extremely well with single-species stock assessments of cod, sprat, and herring (r^2 between single-species and multispecies predictions ranged from 0.90 to 0.97 for cod cohorts, from 0.75 to 0.82 for herring cohorts, and from 0.72 to 0.83 for sprat cohorts).

We cannot definitively conclude that variation in the functional response was the sole mechanism underlying the contrasting responses of sprat and herring to the cod collapse as other important differences between sprat and herring may have also contributed. For example, fishing likely affected sprat and herring differently. Estimates of fishing mortality rates indicate that fishing rates on sprat declined from 0.3 to 0.1 year^{-1} between 1986 and 1990 (Anonymous 2001), but most of this decline occurred between 1989 and 1990 and would therefore have only modest impacts on the time series during and following the cod crash. Fishing mortality on herring also declined during this period from a peak of 0.3 year^{-1} in 1984 to 0.2 year^{-1} in 1987 and then increasing to 0.25 year^{-1} in 1990 (Anonymous 2001). Thus, fishing mortality on both prey types was generally stable during the majority of the time series, at least compared with the dramatic shift in cod abundance that occurred during the same time period. Another explanation for herring and sprat population dynamics is that declining mesozooplankton abundance and changing species composition during the 1990s may have contributed to reduced growth rates of herring during this period (Flinkman et al. 1998; Möllmann et al. 2000). It is likely that many factors, including the differences in the functional response, were responsible for the contrasting response of sprat and herring.

The contrasts among prey types with respect to the shape parameter of the functional response (θ) lead to some hypotheses concerning how prey behavior and spatial distributions may affect the functional response. A variety of functional response models can be derived that produce a predation response that is asymptotic with predator density, i.e., $\theta < 1$. Commonly invoked mechanisms include predator interference (Beddington 1975; DeAngelis et al. 1975), size-based predation risk (Armstrong 1999), prey refuging behavior (Abrams and Walters 1996), and negative spatial covariance between local predator and prey abundances (Poggiale et al. 1998; Keeling et al. 2000). It is impossible to discern which of these processes contributed to the generally low values of θ observed in most predator–prey interactions. There is, however, some evidence that spatial processes may be important for herring, as herring spawn on shallow bottoms in coastal areas and young fish stay closer to the coast, where cod densities are comparatively low (Ojaveer et al. 1981; Aro 1989). Coastal waters may therefore serve as a refuge for young herring, thereby inducing a negative spatial co-

© 2004 NRC Canada

variance between cod and herring abundance. There may be spatial covariance vertically as well, as evidenced by contrasting dissolved oxygen requirements of herring and cod (Neuenfeldt 2002). Further analyses of the spatial structure of predator–prey interactions in the Baltic will be needed to evaluate these hypotheses.

The positively accelerating predation response for age-1 and age-2 sprat is more difficult to reconcile with theoretical derivations. One explanation for this pattern is enhanced foraging success of cod when cod are more abundant (e.g., positive density-dependent predation rates). Alternatively, prey switching or density-dependent habitat selection of cod (MacCall 1990) might explain this pattern. Indeed, the spatial distribution of cod has changed considerably during the crash, and cod are now concentrated in a smaller part of the Baltic than when the stock was abundant. Meanwhile, the rich population of sprat is not particularly abundant in the Bornholm Basin, where much of the cod is concentrated (Anonymous 2001). Moreover, recent analyses suggest that sprat show little overlap in vertical habitat with cod in this region of the Baltic (Neuenfeldt and Beyer 2003). This shift in spatial distribution may thus have reduced the overlap of cod and sprat, thereby causing a disproportionate drop in predation mortality on sprat. If true, then this explanation suggests that the functional response integrating local interactions over the entire population may have a fundamentally different shape than that occurring at the scales of local interactions. Again, future analyses of the changes in cod and sprat spatial distributions, cod consumption rates, and diet compositions will be important in evaluating this hypothesis.

Values of the attack rate parameters (a_i) and the weightings used to calculate effective cod biomass (w_{ij}) indicate consistent differences between sprat and herring. These differences likely reflect size-dependent predator–prey interactions, which is recognized as a key component of species interactions in aquatic and terrestrial communities (Cohen et al. 1993; Claessen et al. 2002; de Roos and Persson 2002). Moreover, cod show clear patterns of prey selection based on predator–prey size ratios (Juanes 2003). Yet, sized-based relations alone do not predict all of the contrasts in w_{ij} between herring and sprat prey. If size relations alone were responsible for these patterns, then we would expect the variation in w_{ij} to match variation in body sizes. However, the w_{ij} for herring are quite different from those of age-2 and age-3 sprat, despite the fact that herring are intermediate in body size to these two prey groups. Namely, the most important predator on age-1 herring is age-5+ cod, whereas young cod (<3 years) are the most important predators on age-2 and age-3 sprat. Other processes, such as size-specific habitat selection of cod, might be responsible for the differences observed here.

Constraining the functional response model to include satiation led to a poor model fit. In many ways this is not surprising. Bioenergetics-based consumption rates of cod from 1977–1996 indicate that cod fed at 39–73% of their maximum rates (mean = 57%; S. Hansson, unpublished data). These low consumption rates are consistent with recent analyses of consumption rates of other piscivores (Essington et al. 2000). Further, some piscivores have the ability to opportunistically consume prey at rates greatly exceeding their sustained maximum rates, so that even patchy prey encounters might not significantly alter their average feeding rates (Essington et al. 2000). This may be a general result among piscivorous fishes, as Schindler and Eby (1997) found that average piscivore growth rates were only 27% of their maximum rate, even after accounting for environmental constraints (e.g., temperature) on feeding rates.

The food web of the Baltic Sea is more complex than the simple interactions explored here. Cannibalism is common in cod (Uzars and Plikshs 2000), and conspecifics can constitute up to 5% of cod diets (Neuenfeldt and Köster 2000). This feedback may represent an important population regulation mechanism, particularly when cod are very abundant (Neuenfeldt and Köster 2000). Further, sprat and herring predation on cod eggs can account for up to 100% mortality in some locations and has been proposed to significantly impact cod recruitment (Sparholt 1996; Köster and Möllmann 2000*b*; Köster et al. 2001). Sprat can also be an important cannibalistic egg predator (Köster and Möllmann 2000*a*), and large herring can consume considerable quantities of sprat (Feldman et al. 2001). Thus, although the Baltic Sea is a comparatively simple ecosystem containing only three dominant fish species, there is considerable complexity in the food web in the form of cannibalism, omnivory, and intraguild predation. To this, we now add the complication of varying functional response relationships that imply different numerical responses of cod prey to changes in cod abundance.

We agree with Abrams and Ginzburg (2000) that ecologists' understanding of the functional response in field settings is poor and represents a priority for future research. It is now widely acknowledged that phenomena at higher organizational scales are not readily predictable from detailed analysis at smaller scales (O'Neill et al. 1986). Thus, a better perspective on the types of functional responses that emerge at the population scale should provide important new insights into the nature of predator–prey interactions. Arguably, the reason why such questions have been neglected is because evaluating the functional response at a whole-system scale is logistically difficult. This introduces the well-known trade-off between experimentation and analysis of whole-system dynamics. Experimentation allows for precise parameter estimation and elimination of confounding effects but suffers from unknowable scaling artifacts (Weins 2001) that may prevent extrapolation to the system of interest (Naeem 2001). In contrast, post hoc analysis of system dynamics avoids scaling artifacts but suffers from confounding effects and lack of replication and precision.

The question therefore is how to best navigate this trade-off. The answer, of course, depends on how badly the scaling artifacts produce erroneous patterns in experimental data. In the case of estimating functional response parameters, it is worthwhile to note that many of the suggested mechanisms that give rise to predator-dependent functional responses are highly scale-dependent. For example, mathematical derivations of predator-dependent functional response relationships based on spatial covariance and prey refuging behaviors (Abrams and Walters 1996; Poggiale et al. 1998; Keeling et al. 2000) assume that local interactions between predators and prey follow mass-action assumptions ($\theta = 1$) and that predator dependence emerges at larger spatial scales. Similarly, our hypothesized explanation for hypersensitive preda-

© 2004 NRC Canada

tion mortality on young sprat involves cod habitat selection over very large (>100 km) spatial scales. Neither of these processes would be apparent from microcosm or mesocosm experiments. We advocate a diverse approach to the study of functional response patterns that includes appropriately scaled experimentation and the analysis of system dynamics using the model selection and parameter estimation routines presented here and in recent publications (Hilborn and Mangel 1997; Burnham and Anderson 1998).

Acknowledgments

This project was supported by grants from the World Wildlife Fund and the Swedish Foundation for Strategic Environmental Research's Marine Research on Eutrophication Program (MARE/MISTRA) awarded to SH. TEE was supported by New York Sea Grant and the National Science Foundation. We thank Chris Harvey, Steve Martell, and Carl Walters for helpful discussion, Peter Abrams, James Bence, Lev Ginzburg, and Sean Cox for valuable comments on an earlier draft of the manuscript, and several anonymous reductionists for pointing out objections to systems analysis. We thank Morten Vinther and Stefan Neuenfelt for providing critical data for the analysis.

References

Abrams, P.A. 1994. The fallacies of ratio-dependent predation. Ecology, **75**: 1842–1850.

Abrams, P.A., and Ginzburg, L.R. 2000. The nature of predation: prey dependent, ratio dependent or neither? Trends Ecol. Evol. **15**: 337–341.

Abrams, P.A., and Walters, C.J. 1996. Invulnerable prey and the paradox of enrichment. Ecology, **77**: 1125–1133.

Anonymous. 2001. Report of the study group on multispecies predictions in the Baltic ICES ICES CM 2001/H:04.

Arditi, R., and Ginzburg, L.R. 1989. Coupling in predator–prey dynamics: ratio-dependence. J. Theor. Biol. **139**: 311–326.

Armstrong, R.A. 1999. Stable model structures for representing biogeochemical diversity and size spectra in plankton communities. J. Plankton Res. **21**: 445–464.

Aro, E. 1989. A review of fish migration patterns in the Baltic Sea. Rapp. P-V Reun. Cons. Int. Explor. Mer, **190**: 72–96.

Baird, D., and Ulanowicz, R. 1989. The seasonal dynamics of the Chesapeake Bay ecosystem. Ecol. Monogr. **59**: 329–364.

Beddington, J.R. 1975. Mutual interference between parasites and its effect on searching efficiency. J. Anim. Ecol. **44**: 331–340.

Berryman, A.A. 1992. The origins and evolution of predator–prey theory. Ecology, **73**: 1530–1535.

Burnham, K.P., and Anderson, D.R. 1998. Model selection and inference: a practical information-theoretic approach. Springer-Verlag, New York.

Claessen, D., Van Oss, C., de Roos, A.M., and Persson, L. 2002. The impact of size-dependent predation on population dynamics and individual life history. Ecology, **83**: 1660–1675.

Cohen, J.E., Pimm, S.L., Yodzis, P., and Saldaña, J. 1993. Body sizes of animal predators and animal prey in food webs. J. Anim. Ecol. **62**: 67–78.

Cox, S.P., Essington, T.E., Kitchell, J.F., Martell, S.J.D., Walters, C.J., Boggs, C., and Kaplan, I. 2002. Reconstructing ecosystem dynamics in the central Pacific Ocean, 1952–1998. II. The trophic impacts of fishing and effects on tuna dynamics. Can. J. Fish. Aquat. Sci. **59**: 1736–1747.

DeAngelis, D.L. 1975. Stability and connectance in food web models. Ecology, **56**: 238–243.

DeAngelis, D.L., Goldstein, R.A., and O'Neill, R.V. 1975. A model for trophic interaction. Ecology, **56**: 881–892.

de Roos, A.M., and Persson, L. 2002. Size-dependent life-history traits promote catastrophic collapses of top predators. Proc. Nat. Acad. Sci. **99**: 12 907 – 12 912.

Dunne, J.A., Williams, R.J., and Martinez, N.D. 2002. Network structure and biodiversity loss in food webs: robustness increases with connectance. Ecol. Lett. **5**: 558–567.

Essington, T.E., Hodgson, J.R., and Kitchell, J.F. 2000. The role of satiation in the functional response of a piscivore, largemouth bass. Can. J. Fish. Aquat. Sci. **57**: 548–556.

Feldman, V.N., Patokina, F.A., and Kalinina, N.A. 2001. Recent changes in diet composition and daily food intake of the Baltic herring in the Gdansk basin of the Baltic sea. ICES CM 2001/U:02.

Flinkman, J., Aro, E., Vuorinen, I., and Viitasalo, M. 1998. Changes in northern Baltic zooplankton and herring nutrition from 1980's to 1990's: top-down and bottom-up processes at work. Mar. Ecol. Progr. Ser. **165**: 127–136.

Hansson, S., Rudstram, L.G., Kitchell, J.F., Hildén, M., Johnson, B.L., and Peppard, P.E. 1996. Predation rates by North Sea cod (*Gadus morhua*) — predictions from models on gastric evacuation and bioenergetics. ICES J. Mar. Sci. **53**: 107–714.

Hansson, S., DeStasio, B.T., Gorokhova, E., and Mohammadian, M.A. 2001. Ratio-dependent functional responses: tests with the zooplanktivore *Mysis mixta*. Mar. Ecol. Progr. Ser. **216**: 181–189.

Hassell, M.P., and Varley, G.C. 1969. New inductive population model for insect parasites and its bearing on biological control. Nature (Lond.), **223**: 1133–1137.

Hilborn, R., and Mangel, M. 1997. The ecological detective. Princeton University Press, Princeton, N.J.

Holling, C.S. 1959. Some characteristics of simple types of predation and parasitism. Can. Entomol. **41**: 385–398.

Juanes, F. 2003. The allometry of cannibalism in piscivorous fishes. Can. J. Fish. Aquat. Sci. **60**: 594–602.

Keeling, K.J., Wilson, H.B., and Pacala, S.W. 2000. Reinterpreting space, time lags, and functional responses in ecological models. Science (Wash., D.C.), **290**: 1758–1761.

Köster, F.W., and Möllmann, C. 2000*a*. Egg cannibalism in Baltic sprat, *Sprattus sprattus*. Mar. Ecol. Progr. Ser. **196**: 269–277.

Köster, F.W., and Möllmann, C. 2000*b*. Trophodynamic control by clupeid predators on recruitment success of cod? ICES J. Mar. Sci. **57**: 310–323.

Köster, F.W., Hinrichsen, H., St. John, M.A., Schnack, D., MacKenzie, B.R., Tomkiewica, J., and Plikshs, M. 2001. Developing Baltic cod recruitment models. II. Incorporation of environmental variability and species interaction. Can. J. Fish. Aquat. Sci. **58**: 1534–1556.

MacCall, A.D. 1990. Dynamic geography of marine fish populations. University of Washington Press, Seattle, Wash.

Möllmann, C., Kornilovs, G., and Sidrevics, L. 2000. Long-term dynamics of main mesozooplankton species in the central Baltic Sea. J. Plankton Res. **22**: 2015–2038.

Naeem, S. 2001. Experimental validity and ecological scale as criteria for evaluating research programs. *In* Scaling relations in experimental ecology. *Edited by* J.E. Petersen. Columbia University Press, New York. pp. 223–250.

Neuenfeldt, S. 2002. The influence of oxygen saturation on the distributional overlap of predator (cod, *Gadus morhua*) and prey

© 2004 NRC Canada

(herring, *Clupea harengus*) in the Bornholm Basin of the Baltic Sea. Fish. Oceanogr. **11**: 11–17.

Neuenfeldt, S., and Beyer, J.E. 2003. Oxygen and salinity characteristics of predator–prey distributional overlaps shown by predatory Baltic cod during spawning. J. Fish Biol. **62**: 168–183.

Neuenfeldt, S., and Köster, F.W. 2000. Trophodynamic control on recruitment success in Baltic cod: the influence of cannibalism. ICES J. Mar. Sci. **57**: 300–309.

Ojaveer, E., Lindroth, A., Bagge, O., Lehtonen, H., and Toivonen, J. 1981. Fishes and fisheries. *In* The Baltic Sea. *Edited by* A. Voipio. Elsevier Scientific, Amsterdam. pp. 275–350.

O'Neill, R.V., DeAngelis, D.L., Waide, J.B., and Allen, T.F.H. 1986. A hierarchical concept of ecosystems. Princeton University Press, Princeton, N.J.

Paine, R.T. 1980. Food webs — linkage, interaction strength and community infrastructure — the 3rd Tansley Lecture. J. Anim. Ecol. **49**: 667–685.

Pickett, S.T.A., Kolasa, J., and Jones, C.G. 1994. Ecological understanding. Academic Press, San Diego, Calif.

Poggiale, J.C., Michalski, J., and Arditi, R. 1998. Emergence of donor control in patchy predator–prey systems. Bull. Math. Biol. **60**: 1149–1166.

Schindler, D.E., and Eby, L.A. 1997. Stoichiometry of fishes and their prey: implications for nutrient recycling. Ecology, **78**: 1816–1831.

Skalski, G.T., and Gilliam, J.F. 2001. Functional responses with predator interference: viable alternatives to the Holling type II model. Ecology, **82**: 3083–3092.

Sparholt, H. 1996. Causal correlation between recruitment and spawning stock size of central Baltic cod? ICES J. Mar. Sci. **53**: 771–779.

Uzars, E., and Plikshs, M. 2000. Cod (*Gadus morhua* L.) cannibalism in the Central Baltic: interannual variability and influence of recruit abundance and distribution. ICES J. Mar. Sci. **186**: 20–37.

Vucetich, J.A., Peterson, R.O., and Schaefer, C.L. 2002. The effect of prey and predator densities on wolf predation. Ecology, **83**: 3003–3013.

Walters, C.J., and Ludwig, D. 1981. Effects of measurement errors on the assessment of stock–recruitment relationships. Can. J. Fish. Aquat. Sci. **38**: 704–710.

Weins, J.A. 2001. Understanding the problem of scale in experimental ecology. *In* Scaling relations in experimental ecology. *Edited by* J.E. Petersen. Columbia University Press, New York. pp. 61–88.

Winemiller, K.O., and Polis, G.A. 1996. Food webs: what can they tell us about the world? *In* Food webs: integration of patterns and dynamics. *Edited by* K.O. Winemiller. Chapman Hall, New York. pp. 1–22.

Yodzis, P., and Innes, S. 1992. Body size and consumer-resource dynamics. Am. Nat. **139**: 1151–1175.

Appendix A

Predation mortality ($M_p(t)$) in each year was calculated from the consumption of each age class by cod ($C(t)$), divided by the mean prey biomass during each year (eq. 8):

$$\text{(A1)} \quad M_p(t) = \frac{C(t)}{\bar{N}(t)}$$

There is some concern of a numerical circularity in these calculations, because the $N(t)$ are calculated from a multispecies virtual population analysis (MSVPA) based on the estimates of $C(t)$, i.e., $N(t)$ and $C(t)$ are not numerically independent. We fully expand the calculations involved in generating $N(t)$ to show that there is no bias introduced as a consequence of this dependence, but rather that the dynamics of $M_p(t)$ are dictated by changes in observed predator abundance, consumption rate, and diet composition.

To improve the clarity of the derivation, we consider a simple prey population that lives for 2 years, is vulnerable to predation only during age-1, and is vulnerable to fishing only during age-2. Thus, predator consumption only affects the estimate of age-1 abundance. Also, to avoid the need for additional terms to account for fish growth, we show the calculations for parameters expressed in numerical units (e.g., number of fish present or number of fish consumed). These simplifications do not change the conclusion of this mathematical exercise in any way.

The stock assessment is based on an algorithm that reconstructs the abundance of each prey cohort throughout its life based on estimated terminal fishing mortality, fishing yields, predation losses, and losses from other sources of mortality. This procedure requires an estimate of terminal fishing mortality (F_{terminal}) and fishing yield during the final year of life (Y_{terminal}) from which the terminal abundance can be estimated: $N_{\text{terminal}} = Y_{\text{terminal}}/F_{\text{terminal}}$. In this case, the terminal year is age-2 so we refer to this estimate as N_2. The assessment then works backwards to calculate the age-1 abundance ($N_1(t)$) required to produce the observed number of $N_2(t+1)$ by summing all of the mortality terms:

$$\text{(A2)} \quad N_1(t) - N_2(t+1) = C(t) + N_1(t)(1 - \exp(-M_0))$$

where $C(t)$ is the total number of prey items consumed by the predator during year t, and M_0 is the mortality from other agents not explicitly modeled. Thus, $N_1(t)$ can be expressed solely in terms of the input data:

$$\text{(A3)} \quad N_1(t) = \frac{N_2(t+1) + C(t)}{\exp(-M_0)}$$

Mean prey abundance requires an estimate of total mortality (Z; see eq. 8). From eq. A3, we can derive an expression for total mortality as

© 2004 NRC Canada

(A4) $$\bar{Z}_1(t) = \ln\left[\frac{N_2(t+1)\exp(-M_0)}{N_2(t+1)+C(t)}\right]$$

so that mean abundance (eq. 9) equals

(A5) $$\bar{N}_1(t) = \frac{N_2(t+1)[1-\exp(-M_0)]+C(t)}{\exp(-M_0)(\ln(N_2(t+1)) - \ln(N_2(t+1)+C(t)) - M_0)}$$

We also recognize that $C(t)$ is calculated as the product of predator abundance (P), predator consumption rate (Q), and the proportion of predators diet composed of this prey item (p):

(A6) $$C(t) = P(t)Q(t)p(t)$$

Substituting eqs. A6 and A5 into eq. A1, we get a rather complicated expression for $M_p(t)$ that shows the dependence of this estimate solely on the observed data on predator abundance, terminal prey abundance, predator consumption rate, and diet composition:

(A7) $$M_p(t) = \frac{p(t)Q(t)P(t)\exp(-M_0)(\ln[N_2(t+1)] - \ln[N_2(t+1)+p(t)Q(t)P(t)] - M_0)}{N_2(t+1)[1-\exp(-M_0)]+p(t)Q(t)P(t))}$$

The important conclusion is that none of the input parameters on the right-hand side is calculated from the others. In other words, after expanding all calculations, we see that all input parameters used to calculate M_p are numerically independent of each other.

© 2004 NRC Canada

Simulation and experimental measurement of side-aspect target strength of Atlantic salmon (*Salmo salar*) at high frequency

Juha Lilja, Timo J. Marjomäki, Juha Jurvelius, Tuomo Rossi, and Erkki Heikkola

Abstract: Numerical simulations and empirical measurements of swimming Atlantic salmon (*Salmo salar*) were used to describe the effects of fish behavior on side-aspect target strength (TS). Simulation results were based on the numerical solution of the Helmholtz equation with the finite element method (FEM). A three-dimensional geometric model approximated the shape of the swimbladder of an Atlantic salmon. Numerical simulations were used to study the dependence of TS on the fish length, orientation, and swimming behavior. The results showed strong variation in TS, both when the side-aspect angle was changed and when the swimbladder was bent to the direction of the sonar beam. A total of 11 swimming adult Atlantic salmon 62–107 cm long were measured with a horizontally aimed echosounder (200 kHz) and video camera, and the experimental results were compared with the corresponding simulation results. The linear regression between mean TS and the logarithm of fish length (L, cm) was $TS = 24.4\log_{10}(L) - 72.9$ dB. The strong variability of TS owing to the orientation and bending of the fish and large L/λ ratios reduces the usefulness of TS alone for fish size estimation or species discrimination.

Résumé : Des simulations numériques et des mesures empiriques de la nage chez le saumon de l'Atlantique (*Salmo salar*) nous ont servi à décrire les effets du comportement des poissons sur l'intensité de la cible (TS) acoustique en aspect latéral. Les résultats des simulations se basent sur la résolution numérique de l'équation de Helmholtz par la méthode de l'élément fini (FEM). Un modèle géométrique tridimensionnel mime approximativement la forme de la vessie natatoire d'un saumon atlantique. Des simulations numériques ont servi à étudier la dépendance de TS de la longueur, de l'orientation et du comportement de nage du poisson. Les résultats indiquent une forte variation de TS, tant lorsque l'angle de l'aspect latéral est modifié que lorsque la vessie natatoire est repliée dans la direction du faisceau sonar. En tout, nous avons mesuré 11 saumons atlantiques en nage, variant en longueur de 62 à 107 cm, avec un sonar (200 kHz) dirigé horizontalement et avec une caméra vidéo et nous avons comparé les résultats expérimentaux aux résultats simulés correspondants. La régression linéaire entre le TS moyen et le logarithme de la longueur (L, cm) est $TS = 24{,}4\log_{10}(L) - 72{,}9$ dB. La forte variabilité de TS reliée à l'orientation et au repliement du poisson, ainsi qu'aux rapports L/λ élevés, réduit l'utilité des TS seuls pour estimer la taille des poissons ou pour discriminer entre les espèces.

[Traduit par la Rédaction]

Introduction

The ability to assess the wild salmon spawning populations in rivers is a prerequisite for proper management of salmon fisheries, and the use of hydroacoustics has many advantages in this work. Acoustic counting of migrating anadromous fish has increased in rivers because of the decline of many salmonid (*Oncorhynchus* and *Salmo* spp.) populations and the development of the split-beam hydroacoustic technique (Ransom et al. 1998). Rivers with strong, turbulent currents are challenging environments for hydroacoustics. In addition, boundary effects from the surface and bottom may distort fish echoes and impede detection (Mulligan 2000). Many of the early hydroacoustic studies were done with higher frequencies ranging from 120 to 420 kHz, which ensures high spatial resolution of individual fish, owing to both

Received 27 October 2003. Accepted 2 September 2004. Published on the NRC Research Press Web site at http://cjfas.nrc.ca on 29 January 2005.
J17835

J. Lilja.[1] Finnish Game and Fisheries Research Institute, Joensuu Game and Fisheries Research, Yliopistonkatu 6, FIN-80100 Joensuu, Finland.
T.J. Marjomäki. University of Jyväskylä, Department of Biological and Environmental Science, P.O. Box 35, FIN-40014 Jyväskylä, Finland.
J. Jurvelius. Finnish Game and Fisheries Research Institute, FIN-58175 Enonkoski, Finland.
T. Rossi. University of Jyväskylä, Department of Mathematical Information Technology, P.O. Box 35, FIN-40014 Jyväskylä, Finland.
E. Heikkola. VTT Processes, P.O.Box 1603, FIN-40101 Jyväskylä, Finland

[1]Corresponding author (e-mail: juha.lilja@rktl.fi).

 doi: 10.1139/F04-166 © 2004 NRC Canada

narrow beams and short pulse lengths. Conversely, the higher operating frequency is susceptible to interference from drifting debris, suspended sediment, and turbulence. Moreover, the reflected echo amplitudes from fish are more variable and highly dependent on fish behavior. As the ratio of fish length to acoustic wavelength (L/λ) increases, backscattering amplitudes become more dependent on the aspect angle and the bending of the fish (Horne and Clay 1998).

Atlantic salmon (*Salmo salar*) is a commercially and ecologically important species in the River Tornionjoki. Its spawning run has been monitored from 1997 to 1999 by horizontal split-beam echosounding (Romakkaniemi et al. 2000). Anadromous whitefish (*Coregonus lavaretus*) is the other common species migrating to the River Tornionjoki to spawn. Its migration generally occurs later than that of Atlantic salmon (Romakkaniemi et al. 2000). The separation of Atlantic salmon from non-target species was based on the length distribution of captured Atlantic salmon and the relationship between side-aspect target strength (TS) of immobilized fish and their total length (salmon, TS ≥ -29 dB; other fish, TS ≤ -29 dB) (Lilja et al. 2000). The random variability in TS measurements potentially reduces the accuracy of fish size estimation. The standard deviation of the TS measurements with immobilized fish was typically over 2 dB (Lilja et al. 2000). In addition, the variation increases as a result of the change in swimming angle and the bending of the fish. Consequently, the mean TS of upstream migrating fish from detected echoes is potentially different from the mean TS of immobilized fish. Thus, accurate interpretation of acoustic data in the estimation of fish size or population abundance requires an understanding of the scattering properties of fish (MacLennan and Simmonds 1992).

Primary factors affecting the scattering of sound from a fish are the size and shape of the swimbladder and the orientation of the fish in relation to the sound source (Horne and Clay 1998). The effects of these factors on fish TS can be estimated by tethered or caged fish (ex situ) using either direct measurements with dual-beam or split-beam echosounders (in situ) or theoretical backscatter models (Foote 1991; Horne and Clay 1998). Many theoretical models have been proposed, especially for fish with swimbladders (e.g., Foote 1985; Clay 1991; Horne et al. 2000). The swimbladder provides a large acoustic contrast to other fish tissue and is the major source of scattered sound in fish (Foote 1980). For this reason, knowledge of the relationships between TS and changes in swimbladder shape is important.

In this paper, (*i*) the acoustic backscatter from a three-dimensional model of the swimbladder was calculated with the finite element method (FEM), (*ii*) actual swimming behavior of Atlantic salmon in a horizontally aimed acoustic beam was described, and (*iii*) the effect of fish behavior on its TS was identified.

Material and methods

TS simulations and the model for swimbladder

The scattering of acoustic waves from a swimbladder was modeled with the Helmholtz equation, which describes the linear propagation of time-harmonic acoustic waves. The surface of the swimbladder was assumed to be soft, similar to a surface of contact with liquid and air. In this case, the boundary value problem for the scattered acoustic pressure field (p) is of the form

$$(1) \qquad -\nabla^2 p - k^2 p = 0 \text{ in } \Omega$$

$$p = -p_{inc} \text{ on } \partial\Omega$$

where the domain outside the swimbladder is denoted by Ω. The wave number k is defined by $k = \omega c^{-1}$, where ω is the angular frequency and c is the speed of sound. Function p_{inc} denotes the incident pressure wave, which is scattered by the swimbladder. It is assumed to be a plane wave of the form $p_{inc} = \exp(-ik\vec{v} \cdot x)$, where $\vec{v}$ gives the propagation direction (unit vector) and $x = (x_1, x_2, x_3)$. Furthermore, the scattered pressure p satisfies the classical Sommerfeld radiation condition. The finite element solution of this problem requires the unbounded domain surrounding the swimbladder to be truncated at a finite distance, and it becomes necessary to approximate the radiation condition at the truncation boundary. For this purpose, the perfectly matched layer (PML) approach was used to restrict the domain by a finite layer of absorbing medium (Qi and Geers 1998).

The finite element method (FEM) was used for the numerical solution of the Helmholtz equation. The linear system arising from the finite element discretization is solved by an efficient iterative solution procedure known as an algebraic fictitious domain method. For a detailed presentation of the mathematical model and the numerical method, see Heikkola et al. (2003*a*). The formulation of the model with a PML is described in Heikkola et al. (2003*b*). The far-field pattern of the scattered wave can be computed from the finite element solution (Heikkola et al. 2003*a*). The scattering amplitude (F) is the value of the far-field pattern in the direction opposite to the direction of the incident wave. The backscattering cross section (σ) and TS were calculated from the scattering amplitude by the formulas defined in (Urick 1983; Medwin and Clay 1998):

$$(2) \qquad \sigma = |F|^2$$

$$(3) \qquad \text{TS} = 10 \log(\sigma) \text{ dB}$$

The model for the shape of the swimbladder of Atlantic salmon was formulated from X-ray images and was constructed from three parts, defined in Appendix A (eqs. A1–A4). The front (near head) and back (near tail) parts of the swimbladder are formed halves of two ellipsoids. The third part of the model connects the halves of the ellipsoids by a smooth interpolation surface. The intersections of the surface with coordinate planes $x_2 = 0$ and $x_1 = 0$ are illustrated in Figs. 1*a* and 1*b*, respectively.

The effect of the length of the swimbladder on the fish TS was simulated with 11 different lengths, which corresponded to the total lengths of salmon that were used in the ex situ TS measurements (Table 1). For the simulations, the speed of sound was assumed to be $c = 1450$ m·s^{-1} and the frequency of the sonar beam was fixed at 200 kHz ($\omega = 400\pi$ kHz), which was the frequency used in the ex situ measurements. Thus, the wavelength of the acoustic wave field was $\lambda = 0.725$ cm. The propagation direction of the incident wave was $\vec{v} = (0, 1, 0)$, i.e., longitudinal axis of the

© 2004 NRC Canada

Fig. 1. Intersections of the straight swimbladder model with (*a*) the plane $x_2 = 0$ (horizontal view) and (*b*) the plane $x_1 = 0$ (dorsal view). (*c*) Intersection of bent swimbladder (deflection 4.1%) with the plane $x_1 = 0$ (dorsal view).

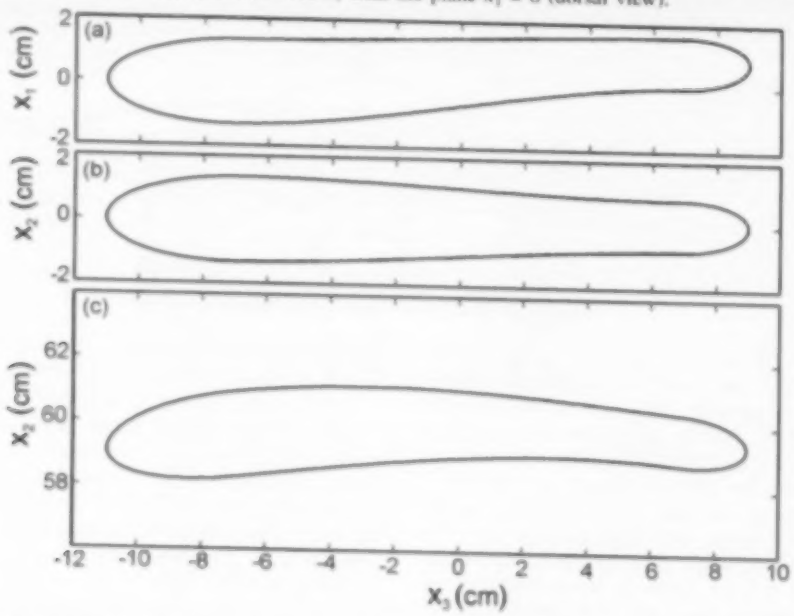

Table 1. Atlantic salmon (*Salmo salar*) total lengths (L_T, cm), weights (W, g), number of measured echoes (N_{echoes}), number of traces (N_{traces}), mean target strength (TS_{mean}, dB), modeled TS (TS_{FEM}, dB) with straight swimbladder, and difference between modeled and measured mean TS ($TS_{FEM} - TS_{mean}$).

L_T (cm)	W (g)	N_{echoes}	N_{traces}	TS_{mean}	TS_{FEM}	$TS_{FEM} - TS_{mean}$
62	2 110	957	20	–28.4	–24.6	3.8
71	2 840	421	12	–27.3	–23.3	4.0
72	3 630	390	15	–27.9	–23.1	4.8
75	3 780	381	14	–27.8	–22.4	5.4
80	4 830	252	6	–26.3	–21.4	4.9
82	5 470	376	10	–28.5	–21.0	7.5
87	5 420	407	8	–25.3	–20.5	4.8
93	7 150	219	10	–25.6	–20.7	4.9
95	7 600	457	13	–23.6	–21.1	2.5
102	10 200	654	28	–23.9	–20.7	3.2
107	11 500	516	17	–23.0	–20.1	2.9

Note: Linear relationship between TS and logarithm of total length is $TS = 24.4\log_{10}(L_T) - 72.9$ dB ($R^2 = 0.79$) and between TS and logarithm of weight is $TS = 7.5\log_{10}(W) - 53.9$ dB ($R^2 = 0.73$).

swimbladder and the direction of the incident wave were perpendicular. The simulated TS was evaluated by calculating the mean value of the scattering cross section (σ) over side-aspect angles 89°–91° and using this mean value in eq. 3 for TS. It is appropriate to take an average over a range of angles when the simulated values are compared with measurements as the measured values also involve several angles.

The effect of the direction of the incident wave was studied using a swimbladder length of 26.8 cm, which is representative of the shortest Atlantic salmon in the ex situ measurements. The propagation direction of the incident wave was of the form $(0, \sin\alpha, \cos\alpha)$ with α (side-aspect angle) varying from 0° (head) to 180° (tail), where α is the angle between vector $\vec{v}$ and the x_3 axis (Fig. 1*b*). Because the surface of the swimbladder is almost perpendicular to the incident beam at approximately 93°, TS is expected to reach maximum around this angle.

When the fish is swimming, its body shape is bending in the horizontal direction, and therefore the shape of the swimbladder also bends during the swimming movement (Fig. 2). A model for a bent swimbladder was obtained indirectly by transforming the straight-swimbladder coordinates to the bent-swimbladder coordinates according to a transformation defined in Appendix A (eq. A5). It was possible to control the bending of the swimbladder geometry by changing its distance from the origin (Fig. 1*c*). The magnitude of the bending depends on the distance of the model from the

© 2004 NRC Canada

Fig. 2. The curves illustrate the movement of the spine of a salmon (*Salmo salar*) (L_T = 87 cm) from neck to adipose fin during 1 s of the swimming motion. The numbers give the chronological order of the curves. This illustration helps to estimate the magnitude of the bending of the fish, e.g., the deflection of line 9 is 11.5% and the sinusoidal curve was defined as a straight spinal.

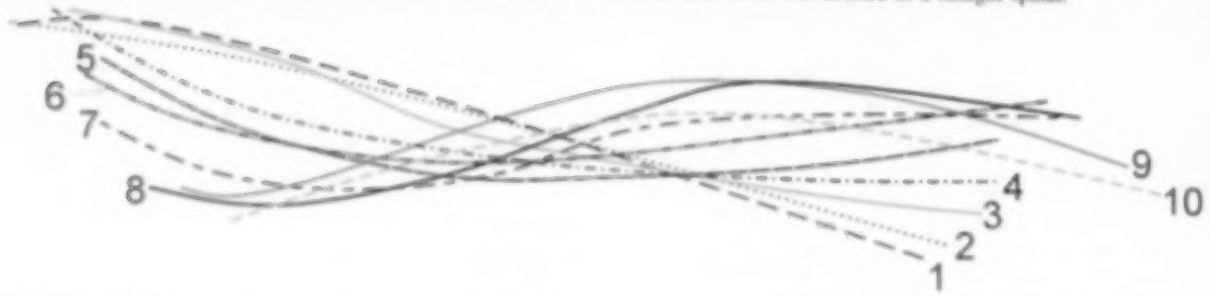

origin such that increased distance reduces the bending. The bending does not change the length of the bladder model, and all parts are bent equally. The deflection from the straight position was measured by calculating the distance d of the middle point of the swimbladder from the line between the head and tail. The value of distance is negative if the middle point is below the line and both halves of the swimbladder (front and back) were bent equally. The distance is then compared with the total length of the swimbladder (s) (deflection % = $d \cdot s^{-1} \cdot 100$). In the simulations, the bending of the swimbladder geometry, with side-aspect angle of 90°, was varied between –10% and 10%. The length of the swimbladder was chosen to be 20 cm. This convenient length of the bladder corresponds with the salmon length of 47 cm. The propagation direction of the incident wave was $\vec{v} = (0,1,0)$.

Ex situ TS measurements

The ex situ side-aspect TS of Atlantic salmon was measured in a large cage (height 1.5 m; length 15 m; width 5 m) in the River Tornionjoki (Fig. 3). Its walls were made of a plastic-covered metallic net (mesh size 1.25 cm × 2.5 cm) and its bottom was made of multifilament net (mesh size 1.0 cm from knot to knot). The cage was anchored to the bottom and to the riverbank. In all, 11 adult Atlantic salmon were used during the TS measurements. The fish were caught with a seine from the River Kemijoki (approximately 20 km from study site), immediately below the lowest hydroelectric dam. The fish were judged to be in excellent condition and were kept for at least 1 day in a large plastic cage before TS measurements.

A split-beam system (Hydroacoustic Technology, Inc. (HTI), Seattle, Wash.) was used throughout the present study. The system consisted of a 200 kHz split-beam echosounder, a digital echo processor, an elliptical-beam transducer, a chart recorder, an oscilloscope, a digital audio tape recorder, and a data analysis computer. The nominal beam widths (measured at –3 dB down from the acoustic axis) were 2.8° (vertical) 10° (horizontal). Echosounder settings were TVG $40\log_{10}R$, ping rate of 10 pings·s^{-1}, and threshold level –46 dB (full beam). In addition to this, an FM slide (chirp) signal (1.25 ms, 10 kHz) was used to increase the signal-to-noise ratio (Ehrenberg and Torkelson 2000). The echosounder system was calibrated before and after TS measurements under the experimental conditions using the standard target method with a tungsten–carbide sphere (38.1 mm diameter) (MacLennan and Simmonds 1992). Acoustic data were analyzed by means of the analysis software HTI EchoScape.

To estimate the movement and swimming angle of the salmon in the acoustic beam, an underwater video camera (Osprey OE 1323 SIT) was used. The camera was placed above the horizontally aimed acoustic beam. The central axis of the visual field of the camera and the acoustic axis of the beam were aimed at the same point, and these axes were perpendicular. The swimming behavior was first recorded on videotape (SVHS), which was digitized afterward. Fish position in the acoustic beam was determined 10 times·s^{-1} (equal to the ping rate) from the video, and swimming angles were measured from these positions with an accuracy of ±2°. It was not possible to do exact synchronizing between echoes and figures from fish position because of the fast ping rate and lack of time synchronization between sounder and video recorder. Nevertheless, the fast ping rate enables one to measure accurately the variation in TS during the swimming behavior.

There was only one Atlantic salmon present in the cage during each set of measurements. This made it possible to measure the TS of an individual fish with known size and avoided the risk of interpreting multiple fish as a single fish. Fish traces were accepted only when the fish swam upstream approximately perpendicular through the acoustic beam. The mean TS of each fish was calculated from the mean backscattering cross section ($\bar{\sigma}$) according to eq. 3.

In addition to calculating the mean TS values for Atlantic salmon, one of the main objectives of this study was to estimate the variation in TS for a single fish in relation to its swimming behavior and angle in the acoustic beam field. The linear relationships between side-aspect TS and the logarithm of total length (L_T, cm) and weight (W, g) of fish were estimated (TS = $A\log_{10}(L_T$ or $W) + B$). Moreover, the relationship between TS and swimming angle was compared with the relationship for immobilized salmon, $TS_{All\ aspect} = 22.2\log_{10}(L_T) + 8.7\cos^3(2(\alpha + 90)) - 75.2$ dB, where L_T represents the total length of fish (cm) and α is the side-aspect angle (°) (Lilja et al. 2000). The relationship between the length of the swimbladder (L_{sb}, cm) and the total length of Atlantic salmon (L_T) was used: $L_{sb} = 0.433L_T$ ($R^2 = 0.98$, n = 22) (J. Lilja, unpublished data). The ratio L_T/λ varied between 85 and 148 and L_{sb}/λ within a range from 36 to 64, respectively, where λ is the wavelength of sound (≈0.7 cm) with sound speed of 1450 m·s^{-1}.

© 2004 NRC Canada

Fig. 3. Overhead schematic of the study site in the River Tornionjoki. The ex situ target strengths of the swimming salmon (*Salmo salar*) were measured in the large cage anchored to the river bottom and bank. A video camera was used to record the swimming behavior of the fish.

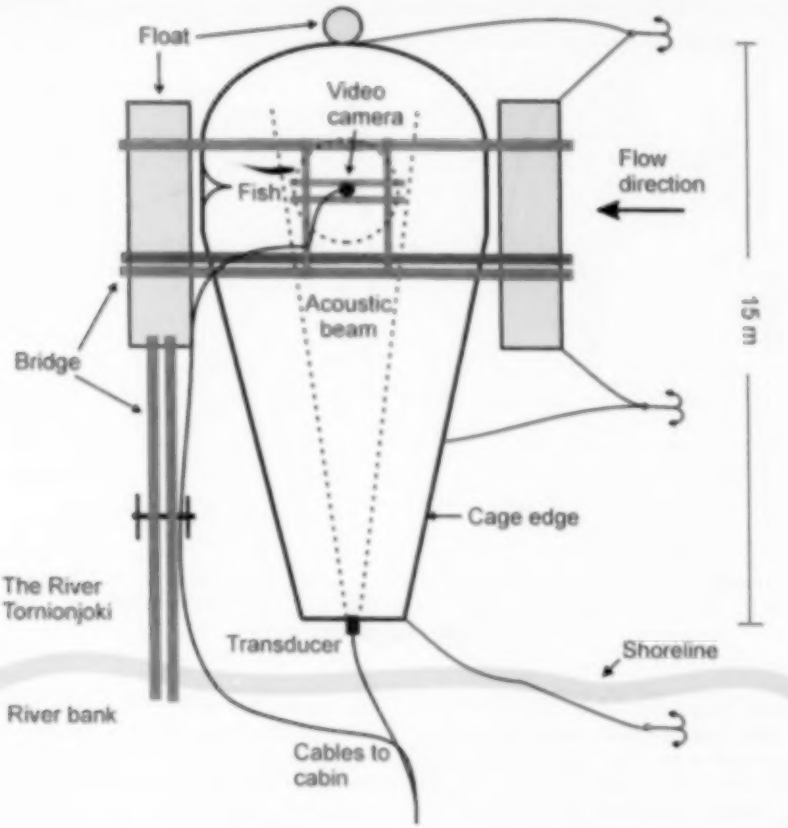

Results

Simulation 1: the effect of swimbladder length on TS

The relationship between simulated TS and swimbladder length at the side-aspect angle of 90° (±1°) was linear (Fig. 4). A comparison between the theoretical (FEM) and experimental results showed that the slope of the simulated regression was approximately the same as the slopes for empirical measurements. The simulated backscattering was, on average, 4.5 dB higher than the mean value of the ex situ measurement but 6 dB lower than the maximum measured value (Table 1). These differences are in accordance with simulation 2, which shows large TS values at certain angles but, on average, lower TS values than at side-aspect angle 90°. The shape of the TS response curve oscillated throughout the measured range of the swimbladder lengths.

Simulation 2: the effect of the direction of the incident wave on TS

The shape of the swimbladder geometry and the measurement frequency (200 kHz) were the same as in the previous simulation, but the length was fixed at 26.8 cm (L_T = 62 cm). The direction of the incident wave was of the form (0, sin α, cos α) with the side-aspect angle α varying from 0° to 180°.

Fig. 4. Relationship between target strength (TS) and length of salmon (*Salmo salar*) at 200 kHz. The lines depict FEM simulation results (dotted line), linear regression for measured mean TS (solid line), and measured maximum TS_{max} (broken line). Plotted points are from simulated model (+), measured mean TS of swimming salmon (●), and measured maximum TS_{max} (○).

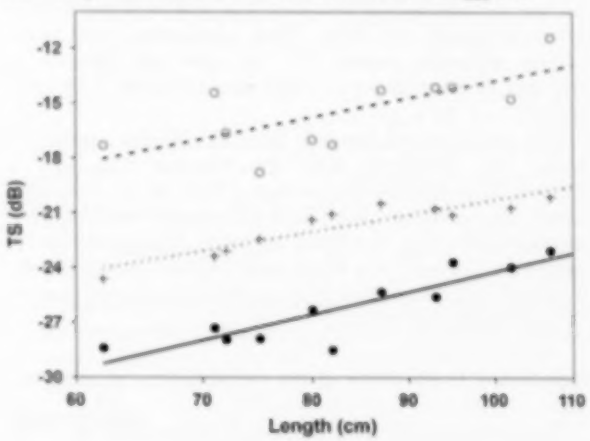

© 2004 NRC Canada

Fig. 5. Simulated relationship between target strength (TS) and side-aspect angle (α) reflected from swimbladder model with frequency of 200 kHz (solid line) and 50 kHz (broken line). The length of the swimbladder was 26.8 cm, which corresponds to a 62-cm total length salmon (*Salmo salar*) (0° = head forward, 180° = tail forward). The dotted line describes the empirically determined relationship TS = $22.2\log_{10}(62\text{ cm}) + 8.7\cos^3(2(\alpha + 90)) - 75.2$ dB (Lilja et al. 2000).

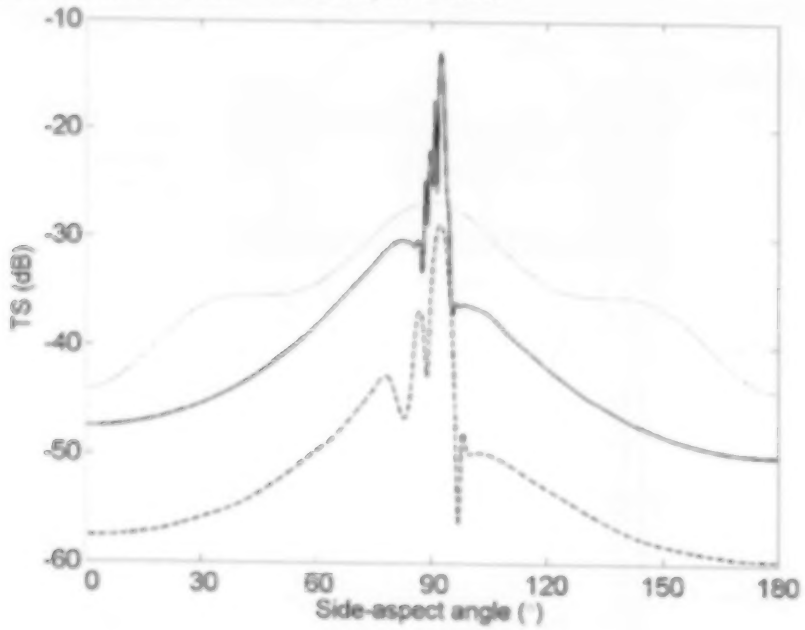

TS was expected to reach maximum value with α between 90° and 95°, because then incident wave meets the surface of the swimbladder at a right angle (see Fig. 1*b*). The relationship between TS and the aspect angle of the swimbladder shows a strong maximum around α = 93° (Fig. 5). The value of TS varies about 25 dB in a narrow angular range from 84° to 97°. Clay and Horne (1994) have reported simulation results (with Kirchoff-ray approximation) also demonstrating strong variation in TS with respect to the side-aspect angle (about 20 dB), but over a wider angular range than here. However, the L/λ ratio was much lower in their tests than here. To demonstrate the effect of frequency on the TS values, the previous test was repeated with a lower frequency (50 kHz). This relationship also has a strong maximum around 93°, but now the variation is smoother and spread over a wider range of angles (79°–99°) (Fig. 5).

The simulated relationship between TS and side-aspect angle was compared with the function $TS_{All\ aspect} = 22.2\log_{10}(L_T) + 8.7\cos^3(2(\alpha + 90)) - 75.2$ dB (L_T = 62 cm), where the coefficients have been determined from empirical measurements (Fig. 5; Lilja et al. 2000). The simulation results were generally at a lower level than the empirically determined function except for the above-mentioned narrow angular range (Fig. 5).

Simulation 3: the effect of the swimbladder bending on TS

The purpose of the third simulation was to study the effect of swimbladder bending on the TS with side-aspect angle of 90°. The length of the swimbladder model was fixed at 20 cm and the side-aspect angle of the incident wave was 90°. In this case, there were no empirical measurements available for comparison. Bending of the swimbladder geometry to the direction of the incident wave (positive deflection) had a significant effect on TS (Fig. 6). Small changes in the deflection led to even 15 dB changes in TS. On the other hand, bending of the geometry away from the sound source (negative deflection) had a small effect on simulated TS, which decreased smoothly approximately 3 dB with the negative deflection. The swimming movement of salmon can produce ±10% deflections from the straight position (Fig. 7*a*). Therefore, bending of the fish is an important factor in the TS measurements.

Ex situ measurements

All 11 salmon could be detected individually with the echosounder as they swam in the cage. From 6 to 28 traces, groups of echoes from individual fish as it swam through the beam, were detected per measured fish, and echoes per trace varied from 10 to 128 (Table 1). Slopes of 24.4 (standard error (SE) = 4.1) and 7.5 (SE = 1.5) and intercepts of –72.9 (SE = 8.0) and –53.9 (SE = 5.7), respectively, were estimated for the linear model between mean TS and logarithm of fish length and weight. The linear relationship between the measured maximum target strength (TS_{max}) and logarithm of the total length (L_T) of salmon was $TS_{max} = 20.6\log_{10}(L_T) - 55$ dB (R^2 = 0.51) (Fig. 4). The maximum value was on average 10.7 dB higher than the measured mean TS.

The spine of the salmon, from the neck to the adipose fin, was detected in 440 freeze-frames. Both swimming angle

© 2004 NRC Canada

Fig. 6. Simulated target strength (TS) as a function of swimbladder bend. The deflection from the straight position was measured by calculating the distance of the middle point of the swimbladder from the line between the head and tail. The vertical broken lines represent mean ± standard deviation limits of the measured deflections on the caged salmon (*Salmo salar*). On the *x* axis, negative values (–) indicate convex deflection and positive values indicate concave deflection.

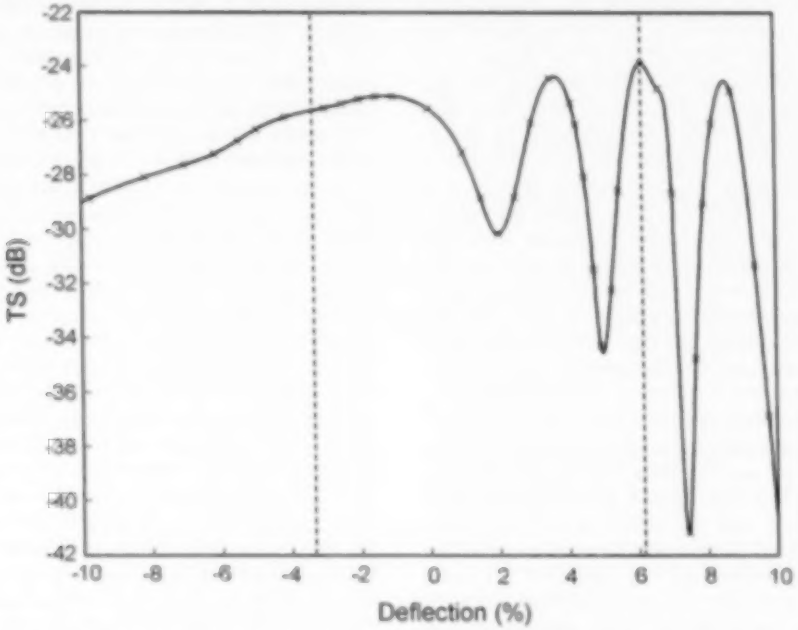

Fig. 7. (*a*) Side-aspect angle and (*b*) fish deflection frequency distributions measured from the freeze frames of the swimming salmon (*Salmo salar*).

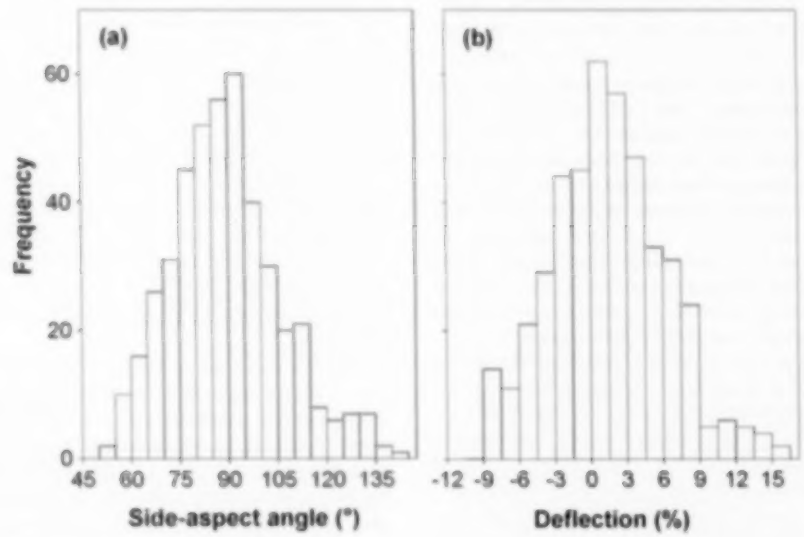

and deflection were measured from these spines. The mean swimming angle was 89° (standard deviation (SD) = 16.7), which was quite near the angle of the full side aspect (90°) (Fig. 7*b*); 95% of the measured angles ranged from 56° to 121°. The deflection from a straight spine varied between –10% and 16%, with an average of 1.4% (SD = 4.7) (Fig. 7*a*). If it was assumed that 0% would be the mean deflection with normal distribution, then 95% of the data would be in the range of the mean ± 9.2%. This range may be used as a typical variation as salmon swim upstream in the river.

Discussion

Furusawa (1991) recommended that a value of $L/\lambda > 2$ provides relatively robust measures of sound scatter by

© 2004 NRC Canada

aquatic organisms, and Horne and Clay (1998) concluded that to avoid bias in acoustic backscatter measures or to aid in species identification of acoustic targets, frequency should be chosen such that L/λ falls within the range of 2 to 10. As the ratio of L/λ increases, scattering length is more dependent on aspect. In this study, the ratio L_1/λ varied between 85 and 148 and L_{10}/λ within the range of 36 to 64, respectively. Therefore, the TS measurements of adult salmon at 200 kHz can be considered as the results of geometric rather than resonant scatter and consequently are more influenced by change in aspect. Additionally, the fish TS is more variable in a horizontally aimed acoustic beam than in a vertical one owing to the swimming behavior of fish. As a fish swims through the horizontally aimed acoustic beam, the swimming angle and the shape of fish and its swimbladder change in relation to the acoustic beam. The conversion of single-frequency acoustic sizes to fish lengths is generally dependent on these two factors at high frequencies (Horne and Clay 1998). Furthermore, both of these factors may increase the proportion of missing echoes in the fish traces, which decreases the detection probability and the size estimation of fish.

Atlantic salmon have a physostomous swimbladder that is elongated; therefore we used a deformed simple ellipsoid model in this study. The dorsal view of the modeled bladder corresponded quite well with the real shape of the swimbladder. On the contrary, there were some differences between the horizontal views of the modeled and real swimbladders. Many fish species have a swimbladder with an irregular geometric form, and the exact quantification is analytically impossible (Foote and Ona 1985; McClatchie et al. 1996*a*). However, the swimbladder of Atlantic salmon has a quite smooth and regular shape, and therefore a three-dimensional model based on analytical functions was used.

The simulation of acoustic scattering by fish swimbladders is often based on various high-frequency models such as the Kirchoff-approximation model (Clay 1992; Jech et al. 1995; Kang and Hwang 2003). Simulation models based directly on the Helmholtz equation give a more accurate representation of the underlying physics than high-frequency approximations, but their numerical solution often requires huge computational work and leads to inaccurate numerical results when the frequency is increased. The simulation of acoustic scattering by the boundary element method (BEM) has been studied by Foote and Francis (2002) and Okumura et al. (2003). In this study, the numerical solution is based on the FEM. The essential difference between BEM and FEM is that the BEM is based on a boundary-integral formulation of the Helmholtz equation, whereas the FEM uses the domain-based formulation presented above. The dimension of the linear system to be solved is therefore an order of magnitude smaller in the BEM than in the FEM. However, it is easier to form the linear system and to develop efficient solution methods for the FEM than for the BEM. With a special discretization mesh and the algebraic fictitious domain method, it is possible to realize a very efficient solution procedure that reduces the memory consumption of the FEM to the level of the BEM (Heikkola et al. 2003*a*).

Many studies have documented a linear relationship between TS and the logarithm of fish length (reviewed by McClatchie et al. 1996*b*). Ex situ measurements of swimming Atlantic salmon showed that the slope of the linear relationship between mean TS and logarithm of fish length is larger than 20, which supports the results for immobilized fish (Lilja et al. 2000). However, these estimated slopes did not statistically differ from the theoretical value of 20. According to Love (1977), the typical slope is 22.8. The simulation of the backscattering amplitude showed approximately the same linear TS–log(length) relationship as the measurements. However, the model did not take into account the reflection from parts of the fish other than the swimbladder. The sound scattering from fish body and bones becomes more important at high frequency (Ye and Farmer 1996).

Earlier studies with anaesthetized fish showed that fish TS decreases when moving away from the side aspect (Love 1977; Dahl and Mathisen 1983; Burwen and Fleischman 1998). Some authors have modeled the effect of the side-aspect angle on TS by the $\cos^3$ function (Kubecka 1994; Lilja et al. 2000). The $\cos^3$ function does not take into account the rapid changes in TS, and it smooths the peaks of TS near the full side-aspect angles. The TS simulations showed a strong peak of TS in a narrow angular range near the full side aspect. The peak became less focused as the frequency of the wave decreased. As the frequency increased, the behavior of acoustic waves began to resemble light waves. This is why ray-tracing techniques are often used to solve acoustic problems. In our study, the L/λ ratio is so high (30–60) that the acoustic scattering problem to be solved can be considered to be of high frequency. It is known that the reflection of sound waves begins to resemble the reflection of light when the frequency grows. Just as reflecting light shows a quick flash in a particular direction (glint), also acoustic waves of sufficiently high frequency exhibit a similar kind of reflection. However, the mathematical model gives an idealized representation from reality and probably magnifies the real behavior of TS in relation to side-aspect angle.

The simulation model for the acoustic scattering does not include many important factors influencing TS values. For example, the fish tissue and skeleton surrounding the swimbladder, transmission of waves through the swimbladder, and various damping mechanisms are completely ignored. Therefore, the simulation results probably magnify some effects such as the variation in TS and cannot be expected to be quantitatively accurate when compared with the measurements. However, with FEM simulations it is possible to study the qualitative effect of side-aspect angle and bending on the TS values.

The TS variation resulting from the change in aspect angle could be split in two groups: first, the slowly varying directivity as smoothed by $\cos^3$ function, and second, the rapid variation in individual TS values as a result of the complex nature of the backscattering process on fish, this variation decreasing with the decrease in frequency (Dahl and Mathisen 1983). However, the strong interference area near the perpendicular angles can cause TS difference or similarity between species with the same length, but this area may vary between species. For example, in the River Tornionjoki, whitefish were clearly smaller than Atlantic salmon, but a whitefish could reflect a much larger echo amplitude compared with a salmon of the same length (Lilja et al. 2000).

As stated earlier, the effect of aspect angle increases with frequency. Consequently, it seems reasonable to assume that

© 2004 NRC Canada

bending affects fish TS more significantly at higher frequencies. During swimming movements, a fish is bending either towards or away from the acoustic source. This horizontal bending of the swimbladder significantly affected the backscattering amplitude, and this effect on fish TS is an unexplored subject in fisheries acoustics. According to Stanton (1989), a minor convex bend of the deformed cylinder decreased approximately 6 dB in TS at 200 kHz. Our results showed that bending of the swimbladder to the direction of the sonic beam causes strong fluctuation of backscattering amplitudes but bending away from the source had no major effect on backscattering amplitudes.

Although the experimental conditions are not natural, the ex situ method allowed us to study the effects of different factors, such as species, swimming angle, and motion of fish, on the TS. According to our results, the side-aspect TS of salmon is highly variable. This is comparable with earlier findings in shallow water horizontal acoustics where it was difficult to discriminate among species or even try to estimate fish size using TS alone (Burwen and Fleischman 1998; Horne 2000; Burwen et al. 2003). During our TS measurements, the salmon usually swam in a circle in the cage, which caused more positive (concave) bends of fish than negative (convex) ones. This is a common behavior demonstrated by caged salmon. Moreover, at short ranges, the acoustic beam is narrow relative to the length of the fish, resulting in some echoes perhaps having an origin from only a portion of the body of the salmon, which also increases bias on the estimate of fish TS, as discussed by Burwen and Fleischman (1998). Nevertheless, the effect of the swimming angle on TS may overestimate the backscattering amplitude because of interference near the angles when the fish is approximately perpendicular to the acoustic wave front. On the other hand, the effect of bending may decrease TS. The interaction of these two factors generally stabilizes the mean TS in a large data set, but the mean TS based on a few echoes may be very biased. Therefore, it is reasonable to use a fast ping rate to detect as many echoes as possible from a swimming salmon or to take advantage of a frequency lower than 200 kHz. Attempts to use TS alone to discriminate among species of similar size magnitude in the horizontal position have been unsuccessful (e.g., Burwen and Fleischman 1998). Moreover, the use of a fixed TS value as the factor of discrimination may also be unrealistic. Therefore, independent estimates of species composition have been required in multispecies communities (e.g., Lilja et al. 2003).

Acknowledgements

We thank Raimo Riikonen for assisting with system setup and logistics during the target strength measurements on the River Tornionjoki. We also thank Juhani Rytilahti from Finnish Game and Fisheries Research Institute for valuable help in handling the live salmon. We are also grateful to Dr Juha Koskela for X-ray pictures. The computer simulations were performed in the SGI Origin 2000 parallel computer located at Center for Scientific Computing in Espoo, Finland.

References

Burwen, D.L., and Fleischman, S.J. 1998. Evaluation of side-aspect target strength and pulse width as potential hydroacoustic discriminators of fish species in rivers. Can. J. Fish. Aquat. Sci. **55**: 2492–2502.

Burwen, D.L., Fleischman, S.J., Miller, J.D., and Jensen, M.E. 2003. Time-based signal characteristics as predictors of fish size and species for a side-looking hydroacoustic applications in a river. ICES J. Mar. Sci. **60**: 662–668.

Clay, C.S. 1991. Low-resolution acoustic scattering models: fluid-filled cylinders and fish with swimbladders. J. Acoust. Soc. Am. **89**: 2168–2179.

Clay, C.S. 1992. Composite ray-mode approximations for backscattering sound from gas-filled cylinders and swimbladders. J. Acoust. Soc. Am. **92**: 2173–2180.

Clay, C.S., and Horne, J.K. 1994. Acoustic models of fish: the Atlantic cod (*Gadus morhua*). J. Acoust. Soc. Am. **96**: 1661–1668.

Dahl, P.H., and Mathisen, O.A. 1983. Measurements of fish target strength and associated directivity at high frequencies. J. Acoust. Soc. Am. **73**: 1205–1211.

Ehrenberg, J.E., and Torkelson, T.C. 2000. FM slide (chirp) signals: technique for significantly improving the signal-to-noise performance in hydroacoustic assessment systems. Fish. Res. **47**: 193–199.

Foote, K.G. 1980. Importance of the swimbladder in acoustic scattering by fish: comparison of gadoid and mackerel target strengths. J. Acoust. Soc. Am. **67**: 2084–2089.

Foote, K.G. 1985. Rather-high-frequency sound scattering by swimbladdered fish. J. Acoust. Soc. Am. **78**: 688–700.

Foote, K.G. 1991. Summary of methods for determining fish target strength at ultrasonic frequencies. ICES J. Mar. Sci. **48**: 211–217.

Foote, K.G., and Francis, D.T.I. 2002. Comparing Kirchhoff-approximation and boundary-element models for computing gadoid target strengths. J. Acoust. Soc. Am. **111**: 1644–1654.

Foote, K.G., and Ona, E. 1985. Swimbladder cross sections and acoustic target strengths of 13 pollack and 2 saithe. Fiskeridir. Skr. Ser. Havunders. **18**: 1–57.

Furusawa, M. 1991. Designing quantitative echo sounders. J. Acoust. Soc. Am. **90**: 26–36.

Heikkola, E., Rossi, T., and Toivanen, J. 2003*a*. A parallel fictitious domain method for the three-dimensional Helmholtz equation. SIAM J. Sci. Comput. **24**: 1567–1588.

Heikkola, E., Rossi, T., and Toivanen, J. 2003*b*. Fast direct solution of the Helmholtz equation with a perfectly matched layer or an absorbing boundary condition. Int. J. Numer. Methods Eng. **57**: 2007–2025.

Horne, J.K. 2000. Acoustic approaches to remote species identification: a review. Fish. Oceanogr. **9**: 356–371.

Horne, J.K., and Clay, C.S. 1998. Sonar system and aquatic organisms: matching equipment and model parameters. Can. J. Fish. Aquat. Sci. **55**: 1296–1306.

Horne, J.K., Walline, P.D., and Jech, J.M. 2000. Comparing acoustic model predictions to *in situ* backscatter measurements of fish with dual-chambered swimbladders. J. Fish Biol. **57**: 1105–1121.

Jech, J.M., Schael, D.M., and Clay, C.S. 1995. Application of three sound scattering models to threadfin shad (*Dorosoma petenense*). J. Acoust. Soc. Am. **98**: 2262–2269.

Kang, D.H., and Hwang, D.J. 2003. *Ex situ* target strength of rockfish (*Sebastes schlegeli*) and red sea bream (*Pagrus major*) in the Northwest Pacific. ICES J. Mar. Sci. **60**: 538–543.

Kubecka, J. 1994. Simple model on the relationship between fish acoustical target strength and aspect for high-frequency sonar in shallow water. J. Appl. Ichthyol. **10**: 75–81.

Lilja, J., Marjomäki, T.J., Riikonen, R., and Jurvelius, J. 2000. Side-aspect target strength of Atlantic salmon (*Salmo salar*), brown trout (*Salmo trutta*), whitefish (*Coregonus lavaretus*) and pike (*Esox lucius*). Aquat. Living Resour. **13**: 355–360.

© 2004 NRC Canada

Lilja, J., Keskinen, T., Marjomäki, T.J., Valkeajärvi, P., and Karjalainen, J. 2003. Upstream migration activity of cyprinids and percids in a channel, monitored by a horizontal split-beam echosounder. Aquat. Living Resour. **16**: 185–190.

Love, R.H. 1977. Target strength of individual fish at any aspect. J. Acoust. Soc. Am. **62**: 1397–1403.

MacLennan, D.N., and Simmonds, E.J. 1992. Fisheries acoustics. Chapman & Hall, London.

McClatchie, S., Alsop, J., Ye, Z., and Coombs, R.F. 1996*a*. Consequence of swimbladder model choice and fish orientation to target strength of three New Zealand fish species. ICES J. Mar. Sci. **53**: 847–862.

McClatchie, S., Alsop, J., Ye, Z., and Coombs, R.F. 1996*b*. A re-evaluation of relationships between fish size, acoustic frequency, and target strength. ICES J. Mar. Sci. **53**: 780–791.

Medwin, H., and Clay, C.S. 1998. Fundamentals of acoustical oceanography. Academic Press, London.

Mulligan, T.J. 2000. Shallow water fisheries sonar: a personal view. Aquat. Living Resour. **13**: 269–273.

Okumura, T., Masuya, T., Takao, Y., and Sawada, K. 2003. Acoustic scattering by an arbitarily shaped body: an application of the boundary-element method. ICES J. Mar. Sci. **60**: 563–570.

Qi, Q., and Geers, T.L. 1998. Evaluation of the perfectly matched layer for computational acoustics. J. Comput. Phys. **139**: 166–183.

Ransom, B.H., Johnston, S.V., and Steig, T.W. 1998. Review on monitoring adult salmonid (*Oncorhynchus* and *Salmo* spp.) escapement using fixed-location split-beam hydroacoustics. Fish. Res. **35**: 33–42.

Romakkaniemi, A., Lilja, J., Nykänen, M., Marjomäki, T.J., and Jurvelius, J. 2000. Spawning run of Atlantic salmon (*Salmo salar*) in the River Tornionjoki monitored by horizontal split beam echosounding. Aquat. Living Resour. **13**: 349–354.

Stanton, T.K. 1989. Sound scattering by cylinders of finite length. III. Deformed cylinders. J. Acoust. Soc. Am. **86**: 691–705.

Urick, R.J. 1983. Principles of underwater sound. McGraw-Hill, New York.

Ye, Z., and Farmer, D.M. 1996. Acoustic scattering by fish in the forward direction. ICES J. Mar. Sci. **53**: 249–252.

Appendix A. Shape of swimbladder and its bending.

The model for the swimbladder consists of three parts. The front and back parts of the bladder are formed by halves of two ellipsoids. The front part is defined by

$$\text{(A1)}\quad \frac{x_1^2}{a_1^2}+\frac{x_2^2}{b_1^2}+\frac{(x_3-z_1)^2}{c_1^2}=1,\quad x_3<z_1$$

and refers to the wider end of the swimbladder, which is nearer to the head of the fish. The back part is defined by

$$\text{(A2)}\quad \frac{(x_1-z_2)^2}{a_2^2}+\frac{x_2^2}{b_2^2}+\frac{(x_3-z_2)^2}{c_2^2}=1,\quad x_3>z_2$$

and is the thin end of the swimbladder nearer to the tail. The constants a_1, b_1, and c_1 are the semi-axes of the ellipsoids, and coordinate planes $x_3 = z_1$ and $x_3 = z_2$ separate the three parts of the swimbladder model. The third part of the model connects the two halves of ellipsoids by a smooth interpolating surface. This is described by defining two interpolating cubic splines $\gamma_1(x_3)$ and $\gamma_2(x_3)$ by the conditions

$$\text{(A3)}\quad \gamma_1(z_1)=a_1,\quad \gamma_1(z_2)=2a_2,\quad \gamma_1'(z_1)=\gamma_1'(z_2)=0$$

$$\gamma_2(z_1)=-a_1,\quad \gamma_2(z_2)=0,\quad \gamma_2'(z_1)=\gamma_2'(z_2)=0$$

and defining the function $d(x_3) = \gamma_1(x_3) - \gamma_2(x_3)$. The intersection of the third part of the model with the coordinate plane $x_3 = z$ is an ellipsoid of the form

$$\text{(A4)}\quad \frac{(x_1-x_z)^2}{a_z^2}+\frac{x_2^2}{b_z^2}=1$$

where

$$x_z=\frac{z-z_1}{z_2-z_1}a_2,\quad a_z=\frac{d(z)}{2}$$

$$b_z=\frac{d(z)-d(z_2)}{d(z_1)-d(z_2)}b_1+\left(1-\frac{d(z)-d(z_2)}{d(z_1)-d(z_2)}\right)b_2$$

For example, the following values were used for the free parameters to determine the shape of the swimbladder model with the length 20 cm:

$$a_1=b_1=\frac{4}{300},\quad c_1=\frac{2}{50},\quad z_1=-\frac{7}{100},$$

$$a_2=b_2=\frac{2}{250},\quad c_2=\frac{1}{50},\quad z_2=\frac{7}{100}$$

Bending of the swimbladder model is performed by a coordinate transformation. This transformation maps the usual space coordinates (x_1, x_2, x_3) to new ones, denoted by (x_1', x_2', x_3'), in the following way:

$$\text{(A5)}\quad x_1'=x_1,\quad x_2'=\sqrt{x_2^2+x_1^2},\quad x_3'=\frac{x_3}{x_2}$$

Thus, each circle with radius r in a plane parallel to the plane $x_1 = 0$ is transformed into a line with $x_2' = r$.

© 2004 NRC Canada

Diurnal variation in acoustic densities: why do we see less in the dark?

Vidar Hjellvik, Olav Rune Godø, and Dag Tjøstheim

Abstract: Diurnal fluctuations in total integrated echo abundance and in vertical density profiles were examined using data from the Norwegian combined acoustic and bottom-trawl survey for demersal fish during winter in the Barents Sea. The total echo abundance was about 40%–50% higher at day than at night. An unknown amount of fish was lost close to the seabed in the acoustic dead zone, but the systematic changes in the near-bottom vertical density profiles did not indicate that migration in and out of the dead zone was the major reason for the large diurnal differences in echo abundance. A more plausible explanation could be that diurnal changes in fish behaviour affect the mean acoustic target strength. Based on the present study, we recommend that the time series of acoustic surveys should be re-analysed, taking the diurnal bias into account. Any comparison of the fish densities indicated by trawl and acoustic surveys will suffer if this bias is not corrected. We believe that model development utilizing this type of information is crucial for future ecosystem-based monitoring.

Résumé : Nous avons examiné les fluctuations journalières des abondances totales intégrées basées sur l'écho et des profils verticaux de densité; nous avons utilisé une combinaison de données norvégiennes provenant d'inventaires acoustiques et d'inventaires au chalut de fond de poissons démersaux durant l'hiver dans la mer de Barents. L'abondance totale déterminée à l'écho est d'environ 40–50 % plus élevée le jour que la nuit. Une quantité inconnue de poissons est perdue près du fond dans la zone acoustique morte; cependant, les changements systématiques qui se produisent dans les profils verticaux de densité près du fond n'indiquent pas que l'immigration ou l'émigration dans la zone morte est la raison majeure des importantes différences journalières dans les abondances déterminées à l'écho. Une explication plus plausible est que les changements diurnes de comportement des poissons affecte la force moyenne des cibles acoustiques. Sur la base de notre étude, nous recommandons une nouvelle analyse des séries chronologiques des inventaires acoustiques qui tienne compte des sources d'erreur journalières. Toute comparaison entre les densités de poissons déterminées par les inventaires au chalut et celles données par les inventaires acoustiques sera affectée si cette erreur n'est pas corrigée. Nous croyons que la mise au point de modèles qui utilisent ce genre d'information est essentielle pour la surveillance future à l'échelle de l'écosystème.

[Traduit par la Rédaction]

Introduction

Light is one of the strongest physical stimuli in biology, affecting both the long-term (seasonal) and short-term (diurnal) behavioural characteristics of fish. Diurnal variations in the results of bottom-trawl surveys (Casey and Myers 1998; Korsbrekke and Nakken 1999; Hjellvik et al. 2002) and acoustic surveys (Engås and Godø 1986; Michalsen et al. 1996; Stensholt et al. 2002) are well known. The causes of these variations and the relationship between them, however, are poorly understood and hence difficult to treat in survey assessments. In particular, poor knowledge of the geographic distribution and behaviour of the targeted stocks is often considered a limitation on the applicability of the acoustic survey method. This is unfortunate, since acoustic surveying is now a standard tool for mapping and assessing commercially exploited fish stocks (MacLennan and Simmonds 1992; Fernö and Olsen 1994). The results are often crucial for the quality of final scientific advice aimed at sustainable management. Thus, any bias reduction in survey assessments is of great importance.

The acoustic dead zones are often considered to be a primary source of bias in acoustic surveys. Fish close to the surface are normally not detectable because the downward-looking transducers on the survey vessel are located at a depth of several metres, and recordings in the near field are unreliable (e.g., MacLennan and Simmonds 1992; Aglen 1994; Demer and Hewitt 1995). Similarly, fish close to the seabed may be lost because of the inaccessibility of targets found in the bottom dead zone. The problem of the bottom dead zone has been widely discussed in the literature (Johannesson and Mitson 1983; Ona and Mitson 1996). It

Received 21 October 2003. Accepted 16 July 2004. Published on the NRC Research Press Web site at http://cjfas.nrc.ca on 1 February 2005.
J17808

V. Hjellvik[1] and O.R. Godø. Institute of Marine Research, P.O. Box 1870, Nordnes, N-5817 Bergen, Norway.
D. Tjøstheim. Department of Mathematics, University of Bergen, Johs. Brunsgt 12, N-5008 Bergen, Norway.

[1]Corresponding author (e-mail: vidarh@imr.no).

 doi: 10.1139/F04-161 © 2004 NRC Canada

Fig. 1. Cruise tracks for 2002. Trawl stations are indicated by circles. Night transects (1800–0600) are drawn in black, day transects (0900–1500) are in red, dawn (0600–0900) and dusk (1500–1800) transects are in green. Times are local.

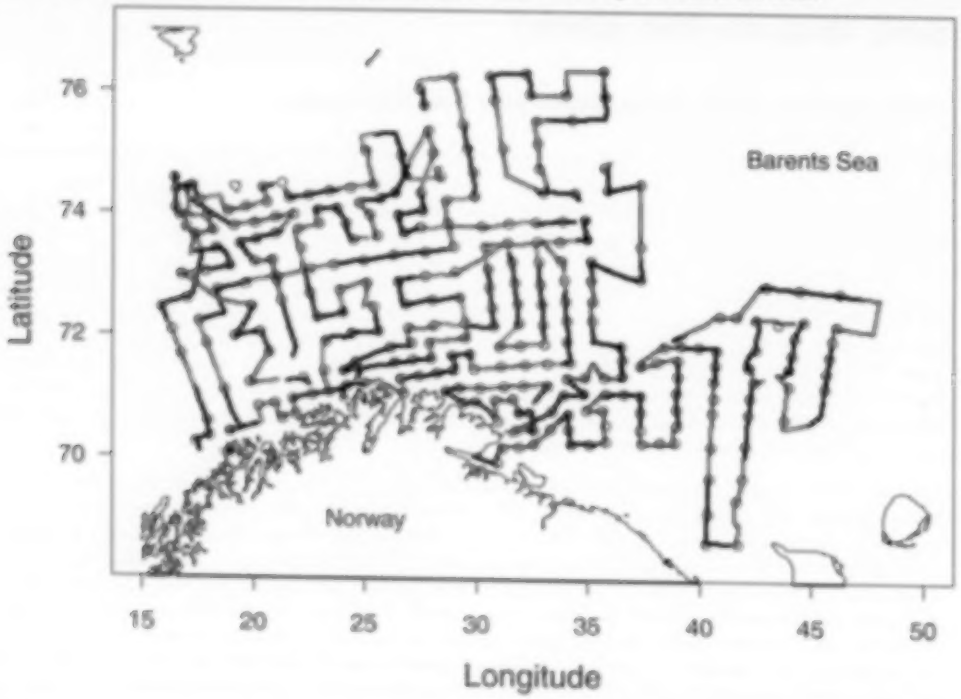

has often been suggested that unexplained variations in the ratio of trawl catches to acoustic recordings arise because an unknown amount of fish is supposed to be hidden in the bottom dead zone (Aglen 1996; Ona and Mitson 1996) or at the surface (Knudsen and Sægrov 2002). Similarly, systematic, large, diurnal variations in the total integrated echo abundance have been ascribed to diurnal migration in and out of the dead zone (e.g., Engås and Godø 1986; Aglen et al. 1999; Lawson and Rose 1999). This kind of migration is, however, not the only possible candidate for explaining diurnal variation in acoustic backscattering. Vertical fish movements higher in the water column may also affect the echo abundance through swim bladder compression and tilt-angle changes (Aglen 1994; Godø and Michalsen 2000; McQuinn and Winger 2003). Thus, assuming the total biomass is constant by day and by night, diurnal variation can be explained by at least three hypotheses: (*i*) fish hide in the bottom or surface dead zones at night; (*ii*) fish target strength (TS) varies because of diurnal variation in the tilt-angle distribution; and (*iii*) fish TS changes because of pressure-related swim bladder changes during vertical migration.

In this study, we have taken a fresh look at diurnal variation in acoustic abundance data, based on a careful and detailed statistical analysis of a large set of combined trawl and acoustic measurements. We have evaluated our results taking into account the above three hypotheses and have tried to determine their relative importance. The analysis of total integrated echo abundance is supported by a systematic investigation of diurnal variation in the acoustic vertical profiles, including a rather detailed study of the layers just above the bottom zone. The main emphasis is on demersal fish, although pelagic fish and plankton are also examined, in so far as their density distributions are relevant to the central argument of this paper. Filtering out large acoustic values that arrive at random time points is important for our analysis. Compared with earlier investigations, it allows us to isolate and present diurnal variation in a more transparent manner, and it makes it easier to discern systematic patterns. Finally, we note that many earlier studies have been qualitative in character, and the results have thus suffered from the lack of any statistical test of significance. In this study, a randomization test is introduced to confirm the statistical significance of the main diurnal changes and also that of any effects observed during the dawn/dusk transition periods.

Materials and methods

The data

Norwegian research vessels undertake a combined acoustic and bottom-trawl survey for demersal fish in the Barents Sea during the winter of each year (Jakobsen et al. 1997; Fig. 1). We have analysed acoustic results from surveys in the period 1997–2002. The data were collected using a 38 kHz SIMRAD EK 500 echo sounder (SIMRAD, Horten, Norway) and interpreted using the Bergen Echo Integrator (BEI) (Foote et al. 1991). The data were recorded in a database with a horizontal resolution of 1 nautical mile (1 n.mi. = 1.852 km) and a vertical resolution of 10 m, referenced to the surface. In addition, near-bottom data were available in 10 bottom-referenced layers each 1 m thick. The bottom

© 2004 NRC Canada

Fig. 2. Bottom layers in a typical case (*a*) and an atypical case (*b*). In (*a*), the bottom offset is 0.3 m; in (*b*), it is 2.2 m. The solid line indicates the corrected bottom. The shaded areas show the first and tenth bottom layers in (*a*) and the third and tenth bottom layers in (*b*). The spikes are drawn manually to avoid bottom signals.

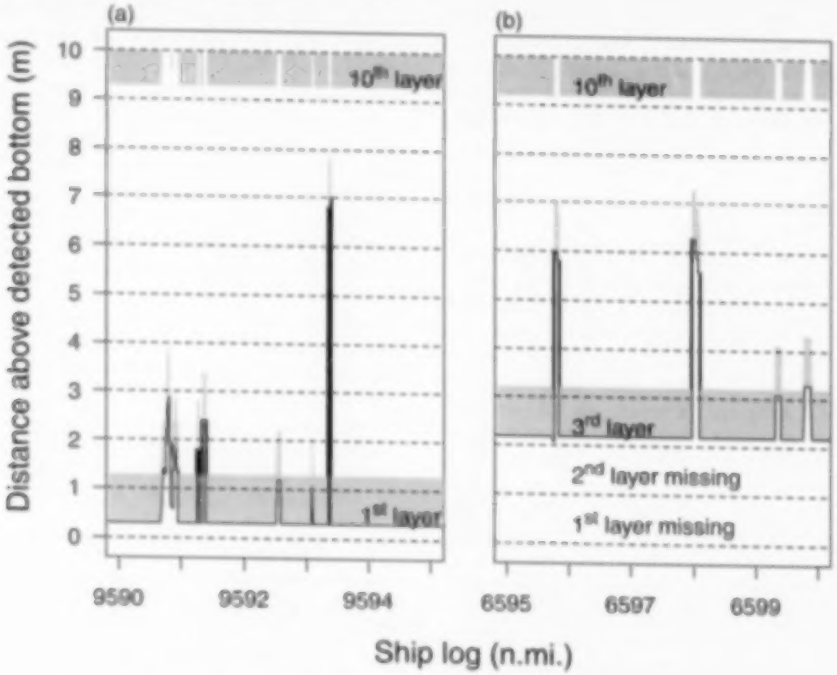

depth is variable, and the vertical distribution of physoclist fish is restricted by pressure more than by depth because of their swim bladder characteristics. Therefore, to obtain a uniform depth scale, we chose to transform the original depth-referenced layers into 30 equally thick layers for each sample, covering the surface–seabed column. For instance, if the bottom depth were 300 m or 600 m, the deepest layer would contain data from the bottom to 10 m or 20 m, respectively. The ten 1-m bottom-referenced layers were used with no such transformation in a separate analysis.

Detailed information on the near-bottom distribution is important for evaluation of the dead zone problem. To avoid interference from the bottom echo, we do not normally end the integration of fish density exactly on the detected bottom (i.e., the depth indicated by the EK500 or BI500). This depth is reduced by an offset, typically 0.5 m, giving a "corrected bottom" at which the integration ends (for details, see Ona and Mitson 1996). However, under good conditions the offset may be less than 0.5 m, and under bad conditions it may be more. The dead zone height in metres for a transducer with beam width 14.2° and pulse duration 1 ms is h_d = bottom offset + 0.375 + 0.00238d, where d is the bottom depth (Ona and Mitson 1996).

Occasionally, the bottom offset is adjusted manually by inspection of the echogram to avoid any automatic bottom detections that are obviously wrong. In the data from BEI, the first bottom-referenced 1-m layer contains data from the corrected bottom to 1 m further up. Sometimes the corrected bottom is more than 1 m above the detected bottom. We have redefined the layers so that the number i bottom-referenced 1-m layer always contains data from $i - 1 + a$ to $i + a$ metres above the detected bottom (except for manually excluded bottom spikes), where $0 \le a < 1$ and $1 \le i \le 9$ (in Fig. 2*a*, $a = 0.3$ and in Fig. 2*b*, $a = 0.2$). If the bottom offset is more than 1 m in a given sample, the first layer is missing (Fig. 2*b*). Unfortunately, this applies to as much as 24% of the samples, and it typically reflects rough ground or rough weather conditions. But importantly, these samples are evenly distributed over day and night. The second layer is missing in only 2% of the cases. The tenth layer is $1 - a$ metres thick (0.7 m in Fig. 2*a* and 0.8 m in Fig. 2*b*). On average it will be 0.5 m, meaning that the echo abundance is reduced by 50% as compared with a full 1-m layer.

Classification

On a daily basis during the surveys, the backscattered acoustic energy was scrutinized mile-by-mile and allocated to species or groups of species using the BEI (Foote et al. 1991). The species and group classifications varied slightly over the years and among vessels (Table 1). The species allocation was done by experienced scientists on the vessel, using visual characteristics while scrutinizing the echograms, as well as information from catches taken at the nearest trawl stations. Typically, 200–300 catches were taken in each survey. Clearly, the classification is not exact. Several sources of error may be involved, for example, the species distribution of the trawl catches does not necessarily reflect that in the whole water column, and vertical migration of fish between day and night may lead to diurnal patterns in the classification error. Objects with target strength below a

© 2004 NRC Canada

Table 1. The species and categories to which acoustic data were allocated on the various vessels the various years.

Year	Vessel	Cod	Had	Red	Sai	Pol	Blw	Oth	Cap	Her	Pla
		Dem	Dem	Dem	Dem	Dem	Dem	Dem	Pel	Pel	Pla
2002	GS	×	×	×	×	×	×	—	×	×	—
2002	JH	×	×	×	×	×	×	×	×	×	×
2001	GS	×	×	×	×	×	—	×	×	×	×
2001	JH	×	×	×	×	×	—	×	×	×	×
2000	GS	×	×	×	×	—	—	×	×	×	×
2000	JH	×	×	×	—	×	—	×	×	×	×
2000	VR	×	×	×	×	×	—	×	×	—	×
1999	GS	×	×	×	×	×	—	×	×	×	×
1999	JH	×	×	×	×	×	—	×	×	×	×
1998	GS	×	×	×	×	×	×	×	×	×	×
1998	JH	×	×	×	×	×	—	×	×	×	×
1998	JM	×	×	×	—	×	—	×	×	×	×
1997	GS	×	×	×	×	—	—	×	×	×	×
1997	JH	×	×	×	×	×	—	×	×	×	×
1997	JM	×	×	×	×	×	—	×	×	×	×
Abundance 100%		650	500	218	56	1545	305	868	3117	383	1120
Abundance 99%		572	394	172	12	309	245	627	843	95	882
% zero samples		7	34	43	93	84	65	66	67	83	4
% at depth >300 m		44	42	62	24	33	74	57	39	30	41

Note: The top row shows categories from left to right as follows: Cod (*Gadus morhua*), haddock (Had; *Melanogrammus aeglefinus*), redfish (Red; *Sebastes marinus*), saithe (Sai; *Pollachius virens*), polar cod (Pol; *Boreogadus saida*), blue whiting (Blw; *Micromesistius poutassou*), others (Oth), capelin (Cap; *Mallotus villosus*), herring (Her; *Clupea harengus*), plankton (Pla). The second row shows the group to which each category belongs: demersal (Dem), pelagic (Pel), and plankton (Pla). The vessels are G.O. Sars (GS), Johan Hjort (JH), and Vædegg (VR). The third and fourth rows from the bottom give for each species average echo abundance multiplied by number of samples (in 1000 m^2 n.mi.$^{-2}$) when (*i*) all samples are included (Abundance 100%) and (*ii*) samples larger than the 99% quantile are excluded (Abundance 99%). The second row from the bottom gives the percentage of zero samples, and the bottom row gives the percentage of nonzero samples that is taken at depths larger than 300 m.

given threshold are generally allocated to the plankton group, which thus may also contain other small organisms (e.g., fish larvae). Small fish of the target species may also be wrongly included in the "other" group.

Large values

The distribution of marine survey data is typically skewed with a few very high values. Large values may dominate distribution statistics and thus obscure any diurnal patterns in the observations. This problem arises with the present data. A log transformation would yield approximately normally distributed echo abundance values, but when analysing vertical density profiles, it is not clear how the log transformation should be done nor how the results should be interpreted. Instead, to discern the general diurnal pattern in the total echo abundance and in the vertical density profiles, we have eliminated a small percentage of the samples with the highest echo abundance values.

Descriptive indicators

To examine the diurnal variation, we calculated the vertical density profiles and the total integrated echo for each 1-h interval. That is, we divided the samples into 24 subgroups, according to the local time t when the samples were taken. Local time was calculated as $t = t_{UTC} + \text{longitude}/15 + \Delta$, where UTC is coordinated universal time, and $\Delta = [-0.4083 \sin[0.0172\ (\text{day} - 80)] - 1.7958 \cos[0.0172\ (\text{day} - 80)] + 2.4875 \sin[0.0344\ (\text{day} - 80)]]/15$, with $1 \le \text{day} \le 365$ being the day of the year is an approximation to the equation of time (Smart 1977, p. 150). If sample i was taken at time t_i, it was allocated to group j if $j - 1 \le t_i < j$, $j = 1, \ldots, 24$. For each subgroup, we calculated the average echo abundance value for each layer and analysed changes over the day in both the total echo abundance and the density profile (i.e., the vertical distribution of acoustic energy). The density profile was described by its 25%, 50%, 75%, and 90% quantiles and the mean.

Randomization

To test whether changes in total echo abundance and in the quantiles of the vertical profile were statistically significant, we performed tests by randomizing the time when the samples were taken. The simplest way to do this would be to perform the following steps m times:

(*i*) allocate a random time, t_i^* where $0 \le t_i^* < 24$, to each sample y_i

(*ii*) allocate the samples into 24 groups as described above, using the new times t_i^* instead of the observed times t_i

(*iii*) calculate the quantiles and the mean for the vertical density profiles and the total echo abundance for each of the 24 groups

This would lead to m observations of each test statistic under the null hypothesis of time independence (i.e., no diurnal fluctuations). For each time group, p values for the observed quantiles, means, and total echo abundance and confidence bands under the null hypothesis would be calculated. However, the samples are strongly correlated in time (autocorrelated), and this is not taken into account in the

© 2004 NRC Canada

procedure outlined above, so the confidence intervals would be too narrow. An adjustment of step (*i*) is needed to take care of the statistical dependence. Instead of allocating a random time to each sample, we allocated a random integer time displacement for each day. For example, if the samples at day $d(i)$ were taken at $t = 0.35, \ldots, 14.53, 15.15, \ldots, 23.78$, and a random displacement of 9 h were drawn for this day, the new times for day $d(i)$ would be $t^* = 9.35, \ldots, 23.53, 0.15, \ldots, 8.78$. Thus, the local correlation structure is preserved, whereas, as an approximation, samples taken on different days were taken to be independent. This intuitive and simple (but somewhat ad hoc) procedure is clearly related to block bootstrapping (Carlstein et al. 1998). Alternatively, a bootstrap based on an autoregressive approximation could have been used.

To better detect differences among day, night, and dawn/dusk, we also grouped the data in these categories, with night defined as 0000–0600 and 1800–2400, dawn/dusk as 0600–0900 and 1500–1800, respectively, and day as 0900–1500. The standard error of, for example, the mean is much smaller for the night data than for a 1-h interval, since the night category contains 12 times as much data, and hence the confidence interval is correspondingly narrower.

Test statistics

In the above scheme, each time period of 1 hour can be tested separately to examine whether the mean, the quantiles, or the total echo abundance for the period differs from the overall average. Owing to random fluctuations, if the null hypothesis of no diurnal variation were true, one would expect, for example, the median to fall outside the 95% confidence interval in 1 of 20 periods on average. However, it is easy to construct global test statistics. We followed the ideas in Hjellvik et al. (2001, 2002) to construct two test statistics, one of which takes a possible symmetric pattern into account. In both cases, we test several null hypotheses: H_0^T, there is no diurnal pattern in the total echo abundance, and H_0^q, there is no diurnal pattern in the quantile q of the vertical density profile. In the general case, the alternative hypotheses are H_1^T and H_1^q: there is a diurnal pattern in the total echo abundance or in the quantile q, respectively. A test statistic for these tests is

$$(1) \qquad \hat{L}_1 = \sum_{j=1}^{24} (\hat{f}_j - \hat{f})$$

where $\hat{f}_j$ is the value of some quantity (e.g., total echo abundance) in time period j, $j = 1, \ldots, 24$, and $\hat{f} = 24^{-1} \sum_{j=1}^{24} \hat{f}_j$. If H_1 is replaced by H_2: there is a diurnal pattern that is symmetric around noon, the following test statistic is appropriate:

$$(2) \qquad \hat{L}_2 = \sum_{j=1}^{12} [(\hat{f}_j - \hat{f}) + (\hat{f}_{25-j} - \hat{f})]^2$$

$$= \sum_{j=1}^{12} (\hat{f}_j + \hat{f}_{25-j} - 2\hat{f})^2$$

If H_2 is true, $\hat{L}_2$ has a higher power for revealing deviations from H_0 than $\hat{L}_1$. This is because under H_0, they have similar distributions, with $\hat{L}_2$ tending to be slightly smaller than $\hat{L}_1$, whereas under H_2, if $\hat{f}_j \approx \hat{f}_{25-j}$, then $\hat{L}_2 \approx 2\hat{L}_1$. The null distributions of $\hat{L}_1$ and $\hat{L}_2$ are estimated from the m randomized samples $\hat{L}_{i,1}^*$ and $\hat{L}_{i,2}^*$, $i = 1, \ldots, m$, and empirical p values of the original observations $\hat{L}_1$ and $\hat{L}_2$ are calculated by relating them to the simulated null distributions.

Results

The impact of large values

The nautical area scattering coefficient (NASC) for the data ranges from 0 to over 70 000 m^2·n.mi.$^{-2}$ (square metres per square nautical mile). The amplitude distribution is rather skewed, with a very high proportion of the total echo abundance deriving from relatively few samples (Table 2). For example, for the demersal category, 13% of the total echo abundance of the demersal category comes from 39 (about 0.1%) of the samples. For the pelagic species, more than 51% of the total echo abundance is from less than 0.5% of the samples. Although a diurnal pattern is seen for the quantiles of the density profiles (Fig. 3*a*), the picture is unclear, mainly because of some large concentrations of pelagic fish encountered around midnight and in the periods 0800–0900 and 1800–1900. There is also a large concentration near the bottom between 1400 and 1600. In particular, for the total echo abundance values in the top part of the figure, no clear pattern emerges because of the unpredictable timing of large echo abundance values. If a more limited comparison of the total night versus total day echo abundance were attempted, based on one survey for instance, the results would again be subject to a few occurrences of extreme concentrations of fish. As the timing of these will in general vary from one year to another, no stable pattern can be expected.

In fact, all the samples with large echo abundance values in the time interval 2300–0200 were recorded by one vessel during 3 successive days (Fig. 4). If these samples were removed, the high pelagic concentrations in the time intervals 2300–2400, 0000–0100, and 0100–0200 would disappear (Fig. 3*a*). This illustrates how sensitive the analysis is to large values. When the 2% of samples that have the largest values are removed (Fig. 3*b*), a very smooth and clear pattern emerges. The 774 samples thus eliminated were evenly distributed between day and night, for both the number of samples and the echo abundance values (Table 3). We consider this filtering of the data to be absolutely essential for a meaningful interpretation of the results.

The diurnal pattern

The general diurnal pattern of the total echo abundance is clear (Fig. 3*b*): the total daytime echo abundance value is about 40% higher than the total nighttime value; the fish are generally more concentrated towards the bottom in daytime; there appears to be a dawn/dusk effect previously unnoticed in the literature, it seems, when the fish are highest in the water column; and the percentage in the bottom segment is somewhat greater during the night.

© 2004 NRC Canada

Table 2. Distribution of echo abundance for the years 1997–2002 for various species and groups.

Echo abundance	Cod	Demersal	Pelagic	All groups
−1	1.000 (38 636)	1.000 (38 636)	1.000 (38 636)	1.000 (38 636)
0	1.000 (35 841)	1.000 (37 664)	1.000 (15 958)	1.000 (38 596)
1	0.998 (32 754)	1.000 (36 389)	1.000 (13 966)	1.000 (38 358)
2	0.992 (30 155)	1.000 (35 399)	0.999 (12 812)	1.000 (38 054)
4	0.972 (25 895)	0.998 (33 900)	0.998 (11 362)	1.000 (37 450)
8	0.914 (19 455)	0.995 (31 400)	0.995 (9 405)	0.999 (36 369)
16	0.781 (11 994)	0.983 (27 244)	0.987 (7 171)	0.996 (34 150)
32	0.558 (5 608)	0.945 (20 609)	0.974 (5 079)	0.982 (29 094)
64	0.294 (1 721)	0.855 (12 506)	0.953 (3 509)	0.936 (20 500)
128	0.117 (375)	0.721 (6 318)	0.924 (2 373)	0.841 (11 386)
256	0.037 (67)	0.574 (2 901)	0.878 (1 485)	0.720 (5 489)
512	0.008 (8)	0.410 (981)	0.821 (921)	0.592 (2 340)
1 024	0.002 (1)	0.307 (343)	0.753 (589)	0.493 (1 079)
2 048	0.000 (0)	0.247 (167)	0.657 (355)	0.411 (567)
4 096	0.000 (0)	0.188 (79)	0.518 (188)	0.317 (282)
8 192	0.000 (0)	0.132 (39)	0.331 (72)	0.213 (122)
16 384	0.000 (0)	0.059 (12)	0.180 (23)	0.105 (36)
32 768	0.000 (0)	0.000 (0)	0.058 (4)	0.024 (4)
65 536	0.000 (0)	0.000 (0)	0.019 (1)	0.008 (1)
Average	16.819	107.209	90.593	226.778
Median	8.125	35.573	0.000	69.922
q_{95}	96.478	578.761	660.991	1 444.023
q_{99}	129.365	927.679	1 822.518	3 141.895

Note: Data are the fraction of total echo abundance contained in samples with echo abundance higher than the value in the leftmost column (m^2 n.mi.$^{-2}$). In parentheses, the number of samples with echo abundance higher than the value in the leftmost column is shown. The last four rows show the average and median echo abundance and the 95% and 99% quantiles. Species and groups are as follows: Cod (*Gadus morhua*); Demersal species (cod, haddock (*Melanogrammus aeglefinus*), redfish (*Sebastes marinus*), saithe (*Pollachius virens*), blue whiting (*Micromesistius poutassou*), others); Pelagic species (capelin (*Mallotus villosus*), herring (*Clupea harengus*)); and All groups (demersal, pelagic, plankton).

When plankton, capelin (*Mallotus villosus*), and herring (*Clupea harengus*) data were removed, the diurnal pattern was the same, but as expected all quantiles were closer to the bottom (Fig. 5*a*). In deep water, the demersal fish generally had a more pelagic distribution (the quantiles were situated higher in the water column), and the diurnal changes in the density profile were more pronounced (Fig. 5*b*). It was sufficient to remove the 1% largest samples to eliminate the irregularities that corrupted the pattern for the demersal fish. However, the removed samples appeared to be less uniformly distributed by time of day, as compared with the case where all species were included (Table 3). In fact, the daytime echo abundance samples we removed were more than twice as large and about twice as many as those removed from the nighttime records. But 39% of the echo abundance within the 1% largest samples was concentrated to 62 samples taken between 1200 and 1800 on 1 day by one vessel. Therefore, the large concentrations of fish might still be randomly distributed over the whole day. If the vessel had arrived 12 h later, there would probably have been a corresponding overweight of nighttime number and echo abundance in the removed samples. Similar arguments can be applied to the dominance of large night recordings for nondemersal fish.

Cod (*Gadus morhua*), the target species in the Barents Sea survey, showed a different pattern (Fig. 6*a*) compared with the complete demersal species group. The pattern in total echo abundance was similar, with 46% higher daytime values, whereas the mean depth of the cod was constant over the 24 h. Generally, the curves do not have the same dip around noon as in Fig. 5. In contrast, plankton density profiles do show this dip at midday (Fig. 6*b*), but the total echo abundance is more constant around the clock, with a slight reduction in daytime.

A summary of the total echo abundance and density profiles for the various species shows similar patterns for all of the demersal fish, although blue whiting (*Micromesistius poutassou*) and the "other" category have a slightly more pelagic distribution than cod, haddock (*Melanogrammus aeglefinus*), redfish (*Sebastes marinus*), and polar cod (*Boreogadus saida*) (Fig. 7). Capelin, herring, and plankton are found higher in the water column than any of the other species.

The demersal group shows good consistency between years, especially regarding total echo abundance, which is about 50% higher in daytime (Fig. 7). 1998 is an exception, however, with a rather low daytime echo abundance value. This temporal stability of the diurnal pattern can easily be missed if large values are not eliminated.

Testing for significance

As a typical illustration, the diurnal patterns seen on Fig. 5*b* are highly significant, for both the total echo abundance and the quantiles of the vertical density profiles (Fig. 8 and Table 4). The observed values clearly exceed the randomized 95% confidence intervals for the respective quantities under the null hypothesis of no diurnal fluctua-

© 2004 NRC Canada

Fig. 3. Vertical density profiles for all species and all years joined together. (*a*) All samples are included. (*b*) Values larger than the 98% quantile are excluded. The area of each segment of a profile is proportional to the average echo abundance over all samples taken in the actual time interval and the actual fraction of the water column. Small circles indicate the 25%, 75%, and 90% quantiles of the profiles; large circles indicate medians; and squares indicate means. The horizontal dotted line indicates the average of the means. The number of samples (*n*) and average echo abundance (nautical area scattering coefficient, NASC) in each time interval are given at the top. The length of the solid bars at the top is proportional to the average echo abundance. The horizontal solid lines in (*b*) indicate the average echo abundance at night, dawn/dusk, and day. The corresponding numbers on the right of (*b*) are the night average and the factors this must be multiplied with to get dawn/dusk and day averages. The number at the bottom of a profile indicates the percentage of the total echo abundance that is contained in the segment closest to bottom.

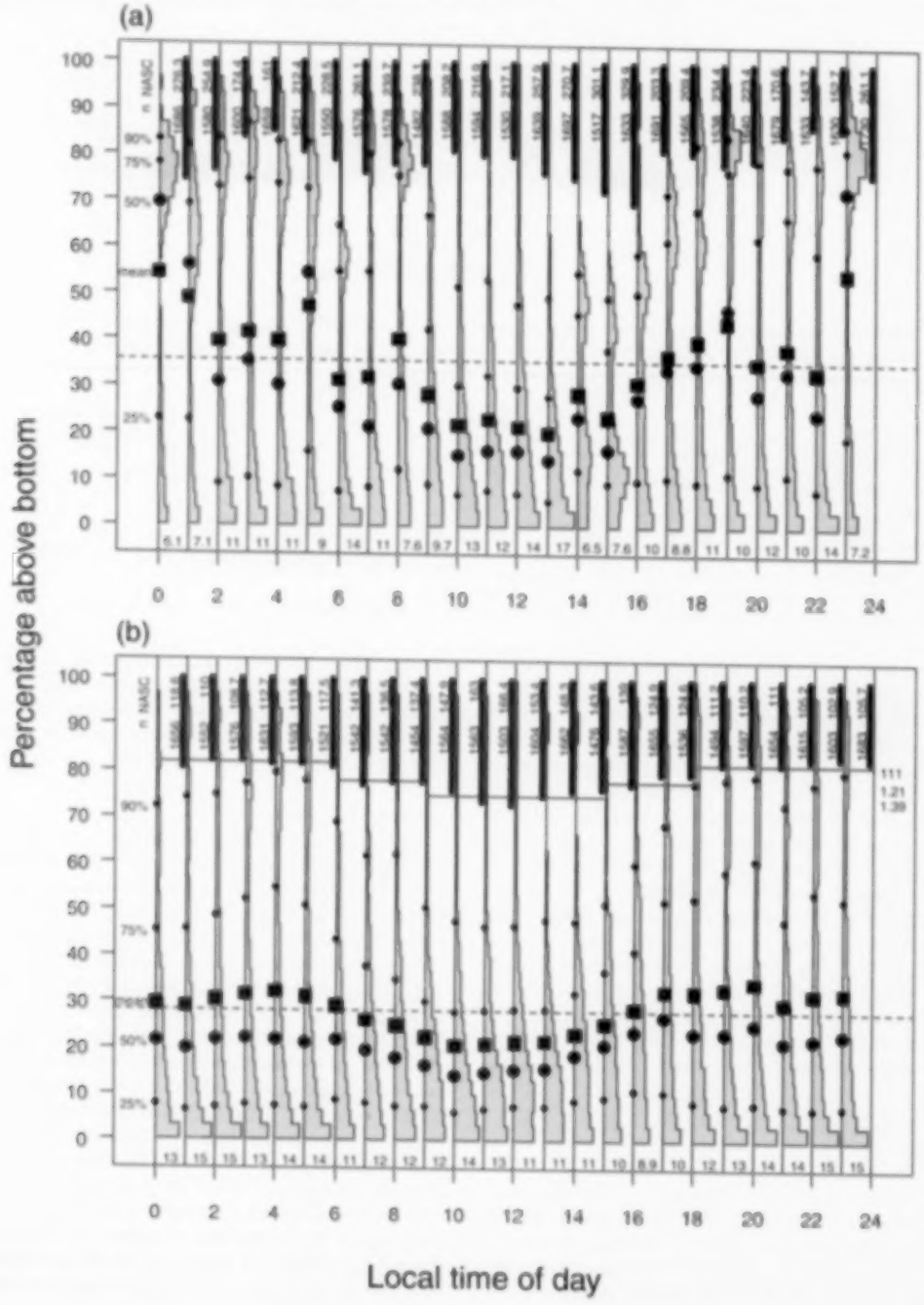

© 2004 NRC Canada

Fig. 4. Total echo abundance (nautical area scattering coefficient, NASC) plotted as a function of local time. Samples taken at the same day are connected with lines. The horizontal dotted line indicates the 98% quantile. Open circles indicate samples taken at 3 successive days by one vessel.

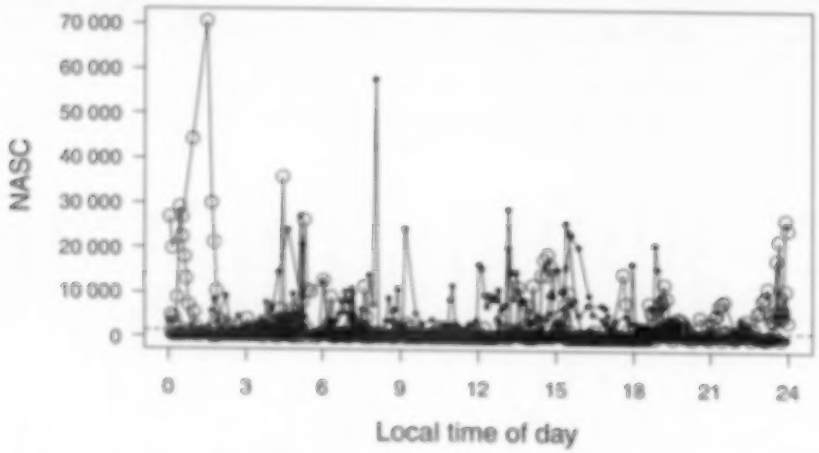

Table 3. Distribution of the samples larger than the 98% (q_{98}) and 99% (q_{99}) quantiles on day (here defined as 0600–1800) and night (1800–2400, 0000–0600) for all species and demersal species.

		Day		Night		
Category	Quant	*n*	Sum	*n*	Sum	% of total*
All species, q_{98}	3141.8	199	1 594 049	188	1 550 629	35.9
All species, q_{99}	1444.0	403	2 012 288	371	1 941 287	45.1
Demersal, q_{98}	927.6	255	919 391	132	393 523	31.7
Demersal, q_{99}	578.7	466	1 068 700	307	518 694	38.3

Note: Quant denotes the echo abundance at the actual quantile, *n* is the number of samples higher than this value, and Sum is the echo abundance summed over these samples.

*Data are the percentage that the echo abundance of the large samples contributes to the total echo abundance.

tions. When the data were allocated to three groups instead of 24 one-hour groups, the confidence intervals were generally narrower because of more observations being in each group. Also, note that the confidence intervals for the dawn/dusk group were narrower than those of the day group, even though the number of observations is about the same. This occurs because the dawn/dusk group is composed of two subgroups, separated in time by 6 hours, while the day group covers a continuous time interval. The lower correlation of the dawn/dusk group is therefore expected.

The results based on the test statistics in eqs. 1 and 2 are given for all species, demersal species, cod, and plankton (Table 4). The diurnal variation was generally most significant in deep waters, and the symmetry-based tests (eq. 2) gave, in most cases, lower p values than the general tests (eq. 1). For cod, the results for the 25% quantile and the median were the most significant (as would be expected from Fig. 6).

Discussion

Acoustic surveys in the Barents Sea show a substantial reduction in the acoustic biomass of all fish categories during the nighttime compared with daytime. In contrast, the plankton category has a relatively constant biomass around the clock, with only a small reduction in daytime. All species or groups of species displayed substantial diurnal vertical migration, although cod showed less variation of the mean depth. Below, we discuss the observed diurnal patterns in distribution and density and evaluate the three hypotheses that were stated in the Introduction.

Diurnal variation

The diurnal pattern of behaviour is a general feature of marine species (Engås and Godø 1986; Neilson and Perry 1990; Abe et al. 1999). Light is normally considered to be the primary trigger of this pattern, but species interactions through predator–prey relationships may provide a causal connection between successive trophic layers of the ecosystem. The variation in light level at high latitudes is dramatically different from that in the tropics. The feeding and survival strategies of species probably vary accordingly. Further, diurnal variations will also relate to area-specific physical and biological features. For example, the opposite diurnal pattern in echo abundance has been observed for pelagic species in the Baltic (Orlowski 2000). Lawson and Rose (1999), using acoustics combined with observations from an underwater vessel for a period of a few days, found daytime densities of Atlantic cod to be an order of magnitude higher than nighttime densities in Placentia Bay, Newfoundland, Canada, at depths of 35–80 m inshore. The reason was that at night, cod were located nearer to the bottom, and

© 2004 NRC Canada

Fig. 5. Vertical density profiles for all species except plankton, capelin (*Mallotus villosus*), and herring (*Clupea harengus*) and all years joined together. Samples larger than the 99% quantile are excluded. (*a*) Samples taken at all bottom depths. (*b*) Samples taken at bottom depths larger than 300 m. The area of each segment of a profile is proportional to the average echo abundance over all samples taken in the actual time interval and the actual fraction of the water column. Small circles indicate the 25%, 75%, and 90% quantiles of the profiles; large circles indicate medians; and squares indicate means. The horizontal dotted line indicates the average of the means. The number of samples (*n*) and average echo abundance (nautical area scattering coefficient, NASC) in each time interval are given at top. The length of the solid bars at the top is proportional to the average echo abundance. The horizontal solid lines indicate the average echo abundance at night, dawn/dusk, and day. The corresponding numbers on the far right of the figure are the night average and the factors this must be multiplied with to get dawn/dusk and day averages. The number at the bottom of a profile indicates the percentage of the total echo abundance that is contained in the segment closest to bottom.

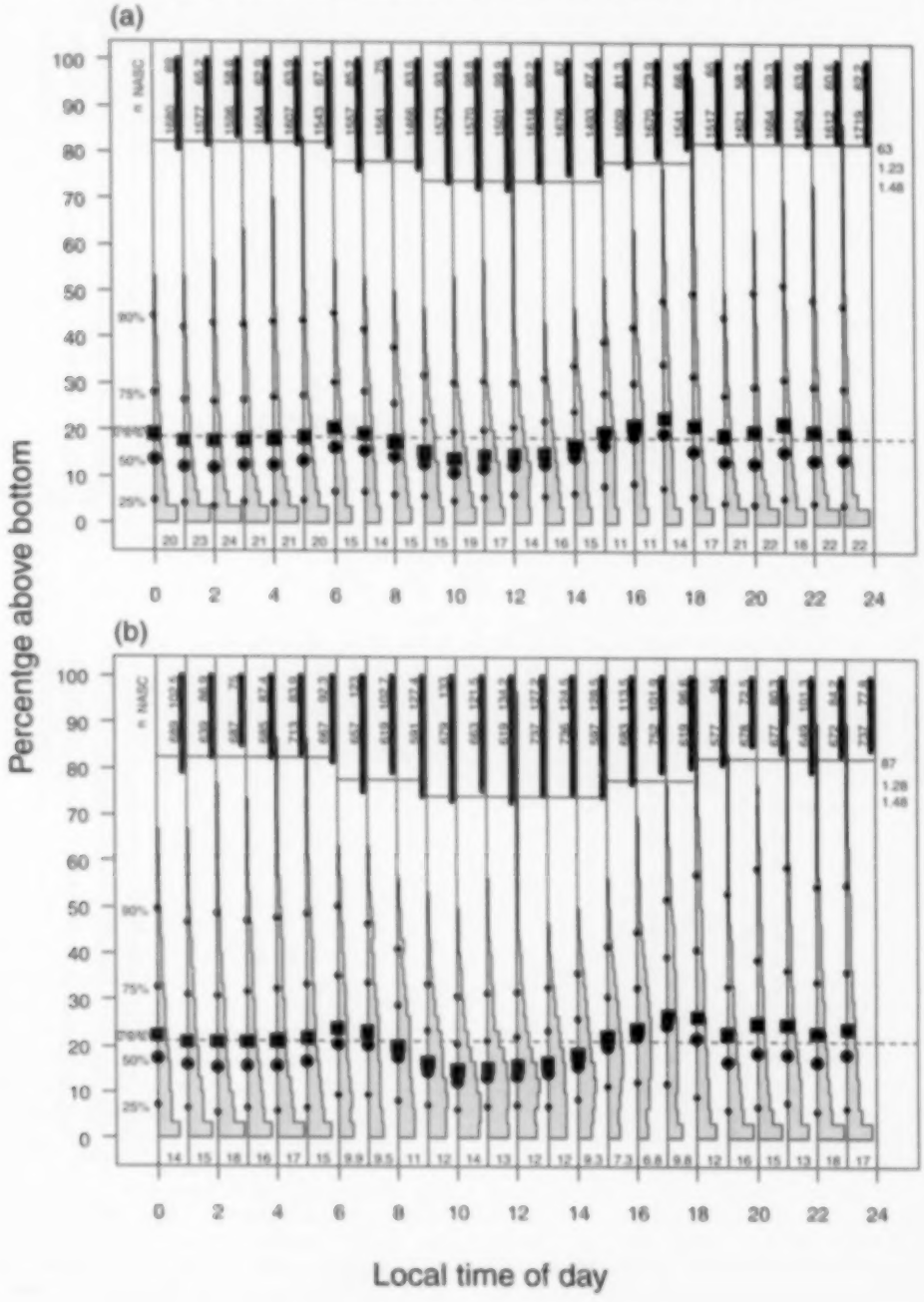

© 2004 NRC Canada

Fig. 6. Vertical density profiles all years joined together for (*a*) cod (*Gadus morhua*) only, all samples included; and for (*b*) plankton only, samples larger than the 99% quantile excluded. The area of each segment a profile is proportional to the average echo abundance over all samples taken in the actual time interval and the actual fraction of the water column. Small circles indicate the 25%, 75%, and 90% quantiles of the profiles; large circles indicate medians; and squares indicate means. The horizontal dotted line indicates the average of the means. The number of samples (*n*) and average echo abundance (nautical area scattering coefficient, NASC) in each time interval are given at top. The length of the solid bars at the top is proportional to the average echo abundance. The horizontal solid lines indicate the average echo abundance at night, dawn/dusk, and day. The corresponding numbers on the far right of the figure are the night average and the factors this must be multiplied with to get dawn/dusk and day averages. The number at the bottom of a profile indicates the percentage of the total echo abundance that is contained in the segment closest to bottom.

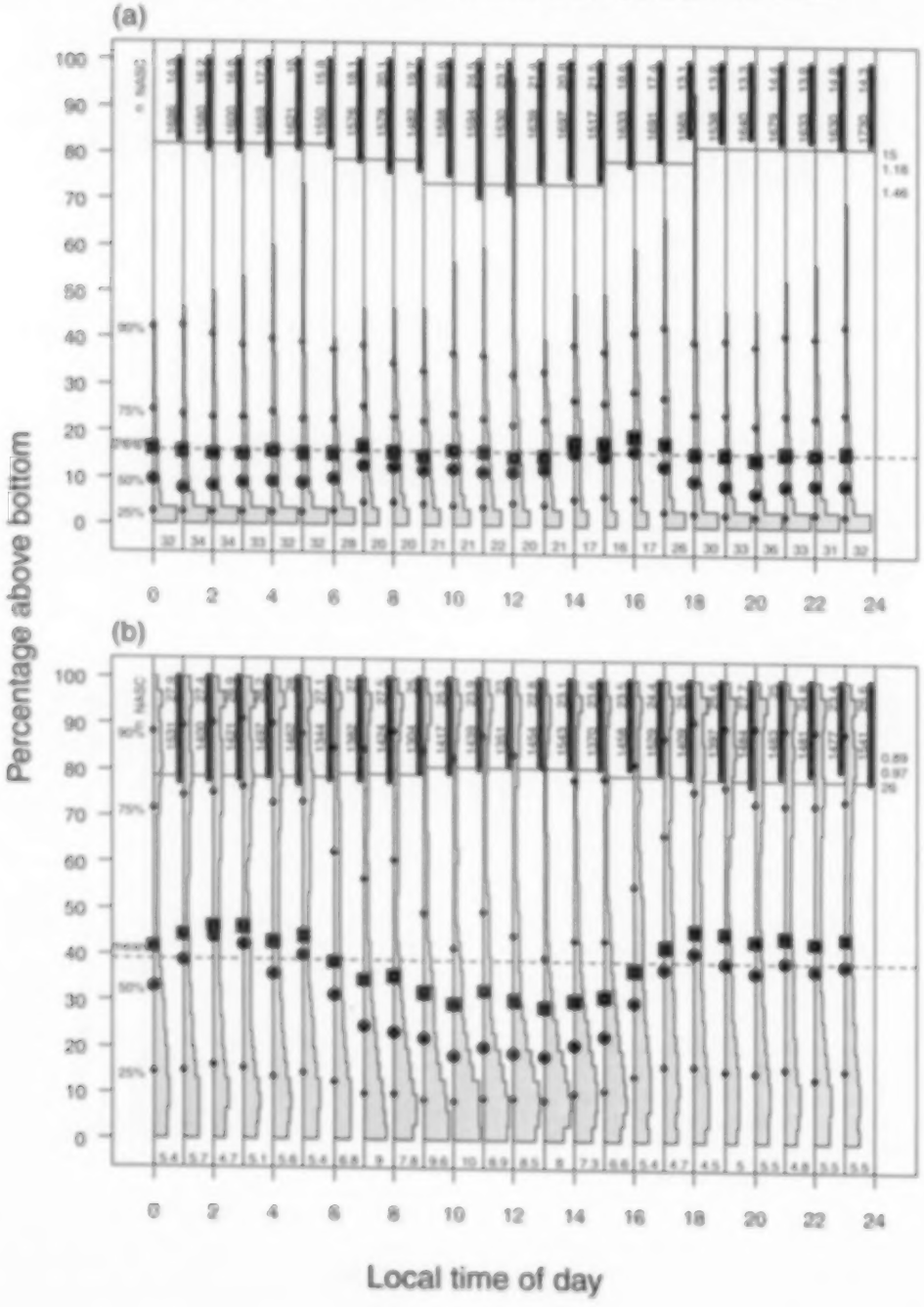

© 2004 NRC Canada

Fig. 7. Total echo abundance (upper bars) and 25%, 50%, 75%, and 90% quantiles of density profiles for the demersal category each year and for each species all years. The data are grouped in night (N, 1800–0600), dawn/dusk (U, 0600–0900 and 1500–1800), and day (D, 0900–1500) instead of in 24 one-hour intervals. The total echo abundance bars are scaled so that the night echo abundance bar is equal for all groups. Horizontal dotted lines are drawn at 100% and 150% of night echo abundance. The percentage of the samples used for each group is given in the bottom line. The species are as follows: demersal (dem), cod (*Gadus morhua*), haddock (had; *Melanogrammus aeglefinus*), redfish (red; *Sebastes marinus*), polar cod (pol; *Boreogadus saida*), blue whiting (blw; *Micromesistius poutassou*), others (oth), capelin (cap; *Mallotus villosus*), herring (her; *Clupea harengus*), and plankton (pla).

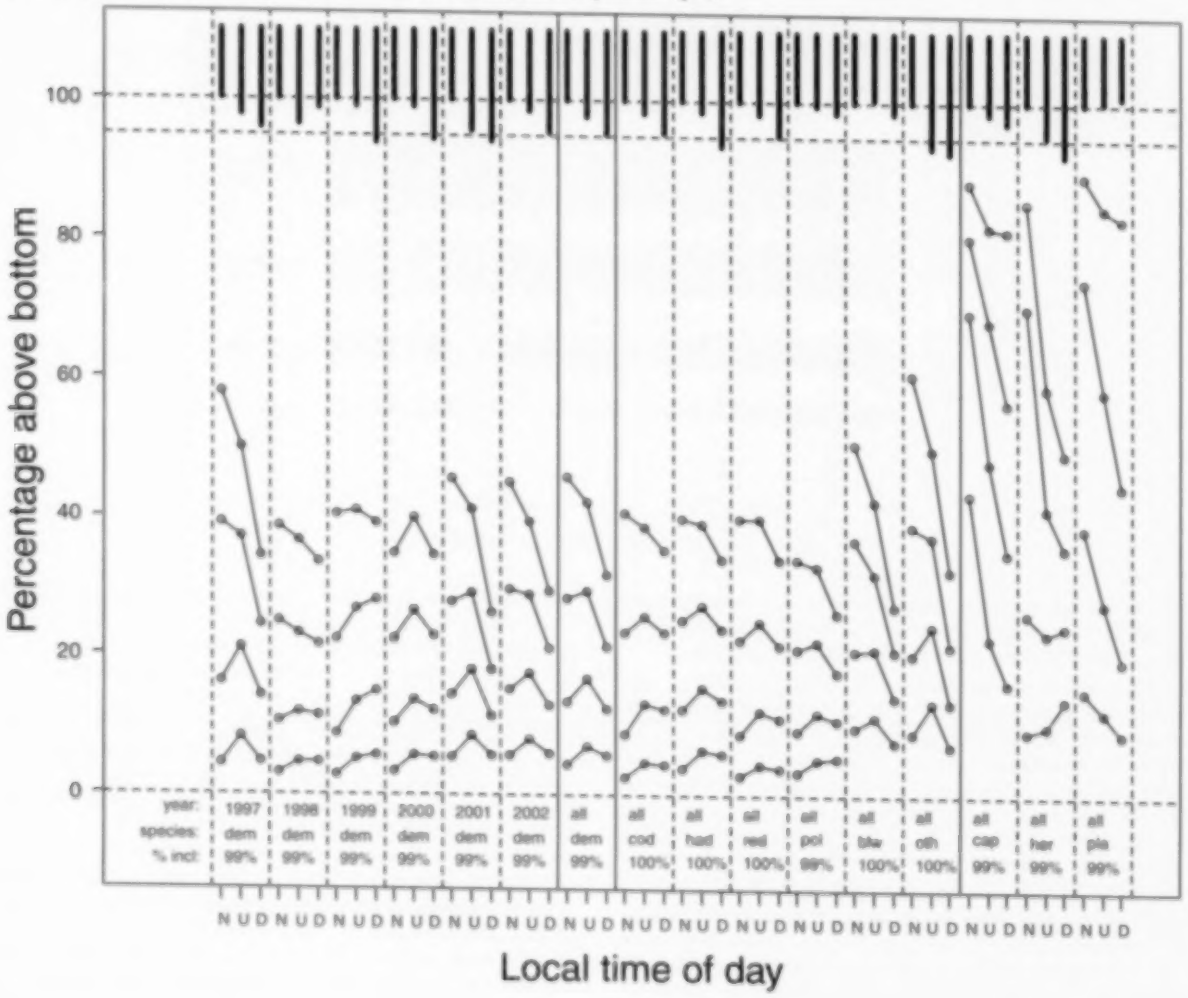
Percentage above bottom
100
80
60
40
20
0
year:
species:
% incl:
1997 dem 99%
1998 dem 99%
1999 dem 99%
2000 dem 99%
2001 dem 99%
2002 dem 99%
all dem 99%
all cod 100%
all had 100%
all red 100%
all pol 99%
all blw 100%
all oth 100%
all cap 99%
all her 99%
all pla 99%
N U D N U D N U D

Fig. 8. Randomized 95% confidence bands (shaded areas) for the total echo abundance and the 25%, 50%, 75%, and 90% quantiles of Fig. 5*b*. Data are based on 1000 randomizations. The right part of the figure shows the results when the data were distributed on three groups (i.e., night (N, 1800–0600), dawn/dusk (U, 0600–0900 and 1500–1800), and day (D, 0900–1500)) instead of on 24 one-hour groups.

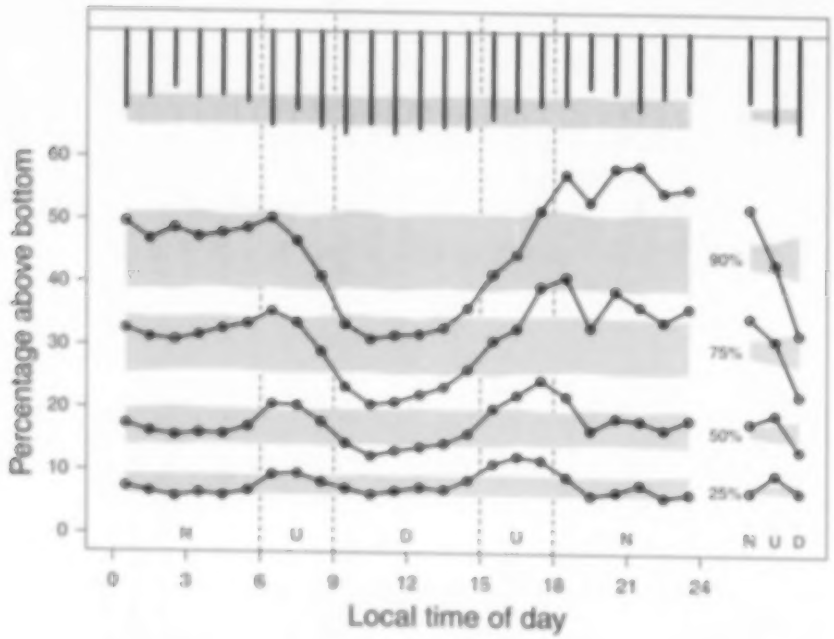

with the results of Aglen et al. (1999), who, in a much more limited 10-day experiment, observed the lowest echo abundance (virtually zero) during the dawn/dusk periods.

The plankton group follows a different pattern, with slightly less echo abundance during the day than at night. However, this is not unexpected, since most plankton is not susceptible to diurnal variation through tilt angle and swim bladder changes. This applies even though in our case the plankton is indeed a complex group of species, which may to some extent include small fish, since it includes all targets not identified as belonging to the fish groups.

As with the variation of echo abundance, there is a high degree of consistency in all species and groups with respect to vertical migration. For all groups, the biomass distribution is more widespread during the night. The slightly delayed descent of the demersal group compared with the near-surface plankton group might reflect a delay in reaction time to light with increasing depth. The hourly quantiles of the fish density are generally highest at dawn/dusk and lowest around noon, independent of their vertical distribution, but there are some exceptions. Monitoring cod fitted with data storage tags has demonstrated that individual cod may perform an extensive vertical migration without any diurnal pattern (Godø and Michalsen 2000). This is consistent with the weak diurnal pattern we observed for cod.

The patterns in total echo abundance and vertical distribution profiles of cod, haddock, redfish, and polar cod appear similar. The 25% and 90% quantiles are further apart at night than during the day, indicating a diurnal migration dynamics where the fish disperse in the water column during darkness and concentrate more in daytime. In contrast, blue whiting and the "other" group display stronger diurnal oscillations, moving towards the bottom in daytime and ascending and spreading out in the water column at night and are thus behaving more like the pelagic fish and plankton.

Based on combined observations from acoustics and pelagic trawling over 10 days, Aglen et al. (1999) suggested that patterns in the vertical migration of gadoids depend on fish size. Hjellvik et al. (2001) also demonstrated that the diurnal variation of bottom-trawl catches of small cod and haddock generally exceeded those of larger fish. As small fish (e.g., age 1 and 2 cod and haddock) feed on plankton (Mehl and Sunnanå 1991), it is expected that they might have behavioural characteristics similar to pelagic fish and plankton. Unfortunately, our acoustic data on the cod group are not easily resolved between large and small individuals. The smallest gadoids may occasionally be difficult to allocate to species in the interpretation of the acoustic signals because of their low backscattering strength and the fact that they are often underrepresented in the catches (Godø and Walsh 1992). Therefore, one cannot rule out the possibility that some of the small cod and haddock may have been wrongly included in the "other" group.

Why do we see less in the dark?

Three factors of potential importance to the diurnal variability have already been introduced: (*i*) fish are inaccessible to acoustics if located in the bottom or surface dead zones; (*ii*) fish TS depends on the tilt-angle distribution; and (*iii*) fish TS changes because of pressure effects on the swim bladder during vertical migration. In this paper, we give no further consideration to the surface zone, since the available

© 2004 NRC Canada

Table 4. Results from randomization tests of the null hypothesis of no diurnal variation against the alternative hypotheses H_1 and H_2.

Species	Depth		q_{25}	q_{50}	q_{75}	q_{90}	Mean	Total
Empirical *p* values								
All	>300	H_1	0	0	0	0	0	0
		H_2	0	0	0	0	0	0
	>0	H_1	0.001	0	0	0	0	0
		H_2	0.002	0	0	0	0	0
Demersal	>300	H_1	0	0	0	0	0	
		H_2	0	0	0	0	0	0
	>0	H_1	0	0	0	0	0	0
		H_2	0	0	0	0	0	0
Cod	>300	H_1	0	0	0.230	0	0.033	0.006
		H_2	0	0	0.066	0	0.009	0.001
	>0	H_1	0	0	0.208	0.020	0.053	0
		H_2	0	0	0.230	0.006	0.092	0
Plankton	>0	H_1	0	0	0	0	0	0.822
		H_2	0	0	0	0	0	0.452
$\hat{L}_i / \max \hat{L}_i^*$								
All	>300	H_1	1.90	1.94	2.44	2.65	2.49	1.58
		H_2	1.77	1.64	2.76	2.90	2.35	2.06
	>0	H_1	—	1.73	3.74	3.77	3.25	1.86
		H_2	—	2.18	4.83	5.02	3.82	2.27
Demersal	>300	H_1	2.42	1.52	2.44	2.98	2.51	1.27
		H_2	2.48	1.69	3.08	3.90	2.84	1.35
	>0	H_1	2.89	1.94	2.25	3.22	2.28	2.88
		H_2	2.84	2.35	2.63	3.83	2.93	3.58
Cod	>300	H_1	1.52	1.32	—	1.08	—	—
		H_2	1.80	1.15	—	1.29	—	—
	>0	H_1	1.66	1.77	—	—	—	1.94
		H_2	1.82	2.41	—	—	—	2.12
Plankton	>0	H_1	1.79	2.66	2.94	1.76	3.21	—
		H_2	2.86	3.40	3.33	2.30	3.69	—

Note: H_1: there is some diurnal variation; H_2: there is a symmetric diurnal variation. H_1 and H_2 are tested using the test statistics $\hat{L}_1$ and $\hat{L}_2$, respectively. See eqs. 1 and 2 for definitions of $\hat{L}_1$ and $\hat{L}_2$, respectively. The results are based on 1000 replicates. In the lower half of the table, the ratios $\hat{L}_1/\max \hat{L}_1^*$ and $\hat{L}_2/\max \hat{L}_2^*$ are given for H_1 and H_2, respectively. The term $\max \hat{L}_i^*$, $i = 1,2$ is the maximum value of $\hat{L}_i^*$ for the randomized samples. This is only given for cases with zero *p* values.

vertical profiles indicate that only plankton is likely to be much affected, although it is uncertain in which direction. Naturally, the hypotheses are not mutually exclusive. The observed pattern can be the result of a combination of all of the three options, although for pelagic fish the dead zone option is hardly a viable alternative.

The day–night variation in records of demersal fish biomass has often been explained by losses in the bottom dead zone (Aglen 1996; Aglen et al. 1999). In our case, this implies a higher concentration and loss of fish in the bottom dead zone during the night. Studying the vertical profiles for demersal fish in more detail (Fig. 9), we can see that a substantial amount of fish (48% of the total) has to dive into the dead zone at night to equal the daytime results. This comes in addition to the amount that already is in the dead zone during daytime. The percentage in the deepest layer is slightly higher at night than at day (Fig. 9*a*), and the same holds for the 10 m closest to bottom (Fig. 9*b*). The thickness of the dead zone with 0.5 m bottom offset is, for a transducer with beam width 14.2° and pulse duration 1 ms, about $0.875 + 0.00283d$, where d is bottom depth (Ona and Mitson 1996). That is, for 85% of the samples, the dead zone is between 1 and 2 m thick. The exponential increase with proximity to the bottom observed in the lowermost layers certainly suggests that there is much more fish in the dead zone than just above it, but in fact the exponential increase is stronger at day than at night (at day the echo abundance in the deepest layer is 2.4 times that in the second deepest; at night the ratio is 2.2, and at dusk/dawn it is 2.1 (Fig. 9*b*)). The profiles give little or no indication that the nighttime density in the dead zone by itself would be sufficient to explain the large discrepancies in nighttime and daytime echo abundance. At the very least, it would have to be combined with other effects. Also, it is interesting to note that the concentration in the dead zone seems to be minimum at dawn/dusk (Fig. 9). This is consistent with the general appearance of the vertical profiles in Fig. 5, but contrary to the results from the data of Aglen et al. (1999), who, for that particular data set, suggested that at dusk and dawn nearly all the fish seem to be hidden in the dead zone. Finally, if fish were go-

© 2004 NRC Canada

Fig. 9. (*a*) Density profiles for the data on which Fig. 5 is based, grouped in night (1800–0600), dawn/dusk (0600–0900 and 1500–1800), and day (0900–1500). The numbers to the right of the bins indicate the cumulative percentage of the total observed echo abundance. The numbers at the bottom indicate the percentage that must be added to the total observed echo abundance to reach the day level of total echo abundance. (*b*) The same data are shown for the 10 m closest to bottom.

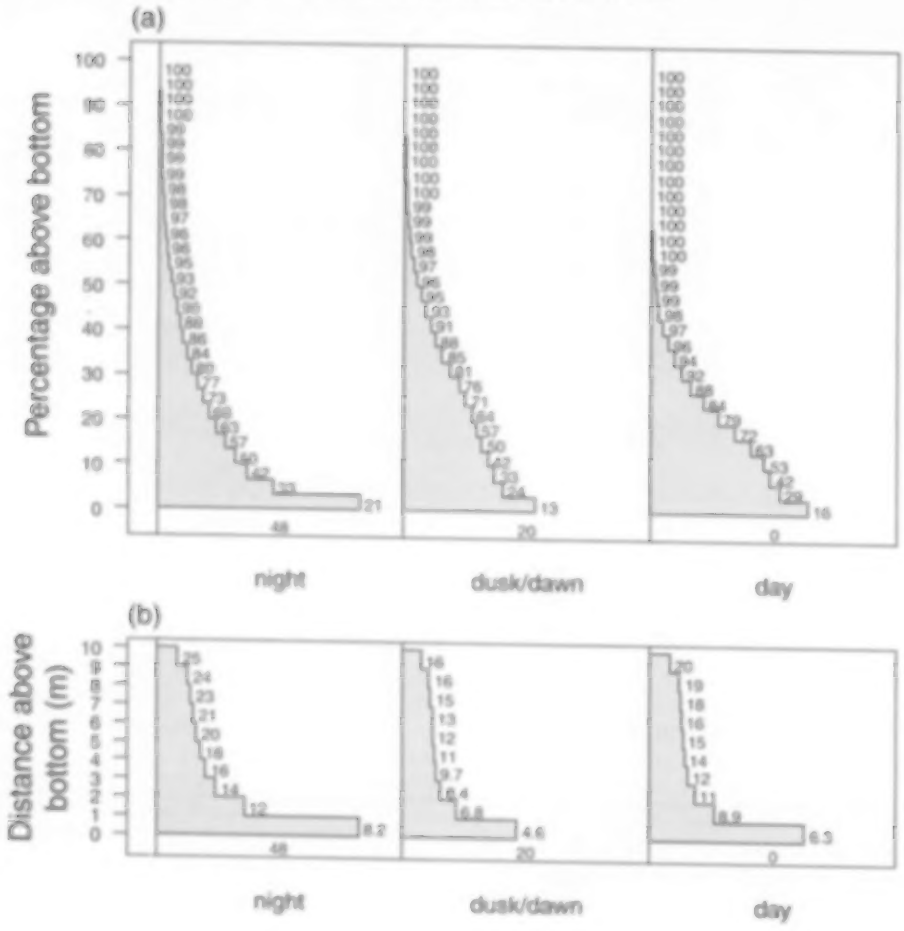

ing into and out of the dead zone at dusk and dawn, one would expect a higher density just above the dead zone at these times, whereas the opposite is the case.

An all-out dead zone explanation also conflicts with the fact that many studies report higher trawl catches by day than by night (Engås and Soldal 1992; Hjellvik et al. 2001, 2002). This may partly be explained by a higher catchability in daytime because of more effective herding. However, any difference in herding efficiency must be substantial indeed to compensate for the 48% of fish that are supposed to enter the dead zone at night (Fig. 9). Finally, a much stronger concentration of fish in the dead zone during the night should result in a higher proportion of large trawl catches associated with low acoustic densities at night. However, this is not the case (Fig. 10).

Aglen et al. (1999) and Stensholt et al. (2002), for instance, suggest that large and small demersal fish behave differently, with large fish moving up from the bottom (i.e., out of the dead zone) into the water column during the day, and small fish doing so during the night. If large fish also tended to disperse in the water column while they were off the bottom less than small fish, this might explain the observed patterns. As we do not know the length distribution of the fish in the acoustic data, this hypothesis is not easy to check directly. However, we can get a rough idea by analysing the eastern and western parts of the survey area separately, since the abundance of small fish is relatively larger in the eastern part. Setting the limit at 35°E, the root mean square length of demersal fish in the trawl catches is about 28 and 22 cm in the western and eastern parts, respectively. However, evaluation of differences in distribution and densities from these two areas gives no univocal response supporting a major impact of the small–large fish hypothesis.

The third option is to explain diurnal variation in total echo abundance by the pressure-related swim bladder volume changes. We note that fish that undertake substantial di-

© 2004 NRC Canada

Fig. 10. Catches of demersal fish taken at trawl stations with small demersal echo abundance as a function of local time of day. A NASC (nautical area scattering coefficient) value of 1 $m^2 \cdot n.mi.^{-2}$ corresponds to a fish density of about 200 cod with a mean length of 50 $cm \cdot n.mi.^{-2}$. Stations with $0 \leq NASC \leq 5$ are represented by solid circles; stations with $5 < NASC \leq 10$ are represented by open circles.

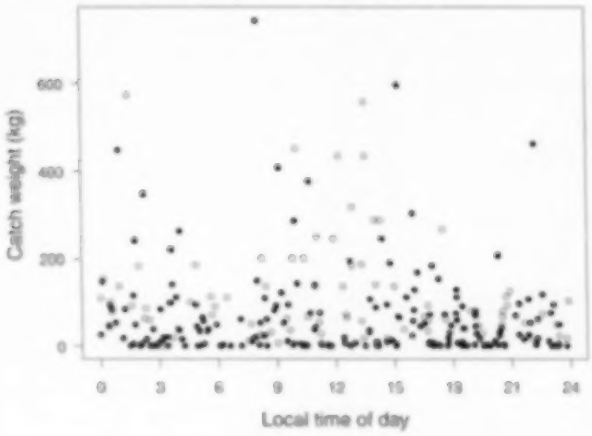

urnal vertical migrations may not be able to compensate their buoyancy by gas secretion and excretion. Thus, the fish will be negatively buoyant in the deepest parts of their depth range (see Arnold and Greer Walker 1992; Godø and Michalsen 2000). If one assumes a constant tilt-angle distribution at all times, this would in our case imply lower daytime than nighttime echo abundance values, which contrasts the actual observations. However, a negatively buoyant fish might be forced to swim at an acoustically favourable angle to maintain its position in the water column. Thus, it is difficult to estimate the combined direct and indirect effect of swim bladder volume changes. However, since the major species disperse in the water column at night and concentrate during the day, with little change in their mean depth, we think that the swim bladder effect is of minor importance.

Having discussed options (*i*) and (*iii*) as causes for diurnal variation in echo abundance, we now come to option (*ii*): diurnal variation in acoustic target strength because of light-controlled behavioural change. There is some evidence of this effect, mainly from fish in captivity. The fish is certainly a directive acoustic target, and the tilt angle of the body is an important determinant of the reflected energy (Nakken and Olsen 1977). A less organised behaviour at night, resulting in a more variable tilt angle, will cause a substantial reduction in echo abundance, as has been shown in model experiments (MacLennan and Simmonds 1992; McClatchie et al. 1996; Huse and Korneliussen 2000). McClatchie et al. (1996) examined the relationship between the standard deviation of the tilt-angle distribution and the average target strength. When the standard deviation increased from 5 to 15 degrees, they found that the average target strength decreased by about 2–3 dB. This corresponds to about 37%–50% reduction in echo abundance.

Cod is a visual feeder (Anthony 1981), and it is thus likely that nighttime behaviour is more relaxed and less directed. In a food search experiment reported by Løkkeborg and Fernö (1999), cod exhibited a diurnal activity rhythm, with higher swimming speeds and a larger range during the day than at night. Lawson and Rose (1999) reported energetic and directed swimming by cod in the daytime, while at night the fish remained motionless or circled slowly with no sustained directionality. Studies of captive cod have shown how that sort of behavioural change from day to night is associated with a reduction in the mean TS (E. Ona, Institute of Marine Research, P.O. Box 1870 Nordnes, N-5817 Bergen, Norway, personal communication). While we do not rule out that the dead zone alternative plays a role, we think that of the options discussed above, this last effect (which we call the TS–TA (target strength – tilt angle) link) is the heaviest contributor to the observed diurnal variation in echo abundance. The TS–TA link also provides a simple explanation of the gradual increase of total echo abundance during the dawn period as the fish gradually respond to increased light intensity by adopting a more uniform tilt-angle distribution and the corresponding decrease of echo abundance during the dusk period. Moreover, if we look at capelin, for which any dead zone effect is considered negligible (Fig. 11), it is interesting to note that the diurnal total echo abundance profile is about the same as that of demersal fish. It is hard to reconcile these facts with an all-out dead zone explanation. In contrast, for plankton (whose tilt angle is irrelevant at 38 kHz), the total echo abundance is about the same at all times. Finally, it is interesting to note that the TS–TA link may help to explain the minor but recurring peak in the quantiles at dawn and dusk, observed for all fish groups. With light as the controlling factor, the fish will organise themselves and their target strength will increase progressively with depth. Assuming the TS–TA link is dominant, the result will be higher echo abundance in shallow water first, with associated peaks in the quantiles, as we have observed. If this conclusion holds, the dawn/dusk effects may partially be artefacts of varying target strength.

Consequences and future research

The observed variation in acoustic backscattering has serious implications for the consistency of results from acoustic surveys and is an important consideration for the calibration of trawl catches against acoustic measurements. It is essential to understand the mechanisms behind the observed variation, and the validation of our hypothesis is thus an important task for future research. This could be done by further investigations on fish held in captivity under controlled conditions, and similar techniques might be used for in situ observations (e.g., Huse and Ona 1996). Based on such results, diurnal-modulated TS models can be developed (McClatchie et al. 1996).

The above discussion assumes that the number of fish in the dead zone is correlated with that just above the dead zone and that the fish in the dead zone do not greatly outnumber those above the dead zone. The observed correlation between acoustic recordings and trawl catches, roughly 0.5 on the log scale (Hjellvik et al. 2003), indicates that this assumption is to some extent justified. However, to decide the exact contribution of the bottom dead zone to the variation in echo abundance, studies should be done with autonomous underwater vehicles (Fernandes et al. 2000*a*, 2000*b*; Patel et al. 2004) or other means of placing the transducer close to

© 2004 NRC Canada

Fig. 11. Density profiles for capelin (*Mallotus villosus*), grouped in night (1800–0600), dawn/dusk (0600–0900 and 1500–1800), and day (0900–1500). The numbers to the right of the bins indicate the cumulative percentage of the total observed echo abundance. The numbers at bottom indicate the percentage that must be added to the total observed echo abundance to reach the day level of total echo abundance. Samples larger than the 99% quantile have been removed.

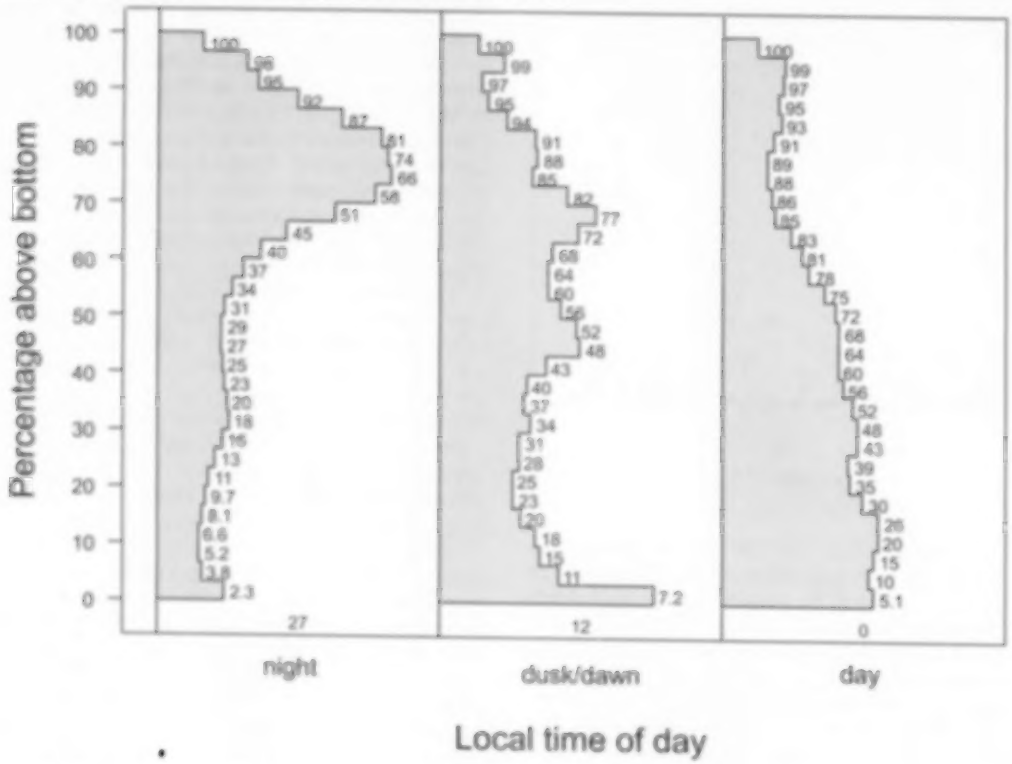

the bottom. Such studies, including the tracking of individual fish (Handegard et al. 2003), will elucidate the dynamics of echo abundance close to the bottom. Preliminary evidence does not suggest differences in vertical diving velocity as a response to trawling in nighttime and daytime, but these results are limited to tracking of individual fish and do not necessarily apply to high fish densities (Handegard 2004). Also, if combined with photographic techniques (Lawson and Rose 1999), more information on the species composition in the bottom zone could be obtained if one could ensure representative observations without avoidance. This would substantially assist our interpretation of the acoustic signals, which can be difficult, especially for small gadoids that are often underrepresented in trawl catches (Godø and Walsh 1992). Since higher-frequency echo sounders are more sensitive to changes in tilt angle, one would expect a larger day–night difference in total echo abundance at high frequencies if the difference is due to a greater variation of the tilt angle at night. Thus, if several transducers with different operating frequencies were used during the survey, a frequency-response analysis could improve our understanding of these phenomena.

Trawl catches in the Barents Sea vary systematically between day and night (Engås and Soldal 1992; Hjellvik et al. 2001, 2002), with lower catch rates at night. A meaningful comparison of the trawl and acoustic survey techniques and a thorough investigation of the observed variation in trawl catchability should be done, taking the inherent temporal variability of both techniques into account. Statistical compensation models can certainly improve this comparison. However, further studies of the kind suggested above will facilitate the development of combined models that incorporate knowledge of fish behaviour. Developments along these lines will be important for future field-monitoring programmes aimed at ecosystem health rather than at single-stock dynamics. For that purpose, a quantitative understanding of fish behavioural dynamics as well as species interactions in time and space will be crucial for the reliability of such programmes.

The answers to complex problems are often found in the interaction among several factors. Studies of such problems, in our case acoustic back scattering variability, often concentrate on single factors as evaluated from small-scale, short-term experiments. Such approaches may be seriously biased by the conditions during observation and may not necessarily give a representative picture applicable for a complete survey. In this paper, we have developed statistical approaches for utilizing data collected from the whole survey and during several years. We think that this gives not only a more representative and comprehensive picture of the problems, but should also be an important provider of priorities for further research.

© 2004 NRC Canada

Acknowledgments

We thank the staff at the section of electronic instruments at Institute of Marine Research for providing the acoustic data, Asgeir Aglen and Egil Ona for useful discussions, David N. MacLennan for comments on the paper, EU for financial support through the CATEFA (Combined Acoustic and Trawl data for Estimating Fish Abundance) project (Q5RS-2001-02038), and the Norwegian Research Council for support through the Strategic institute programme "Absolute abundance estimation of fish" (143249/140).

References

Abe, K., Iida, K., and Maukai, T. 1999. Diurnal changes in area backscattering coefficient during the acoustic surveys of walleye pollock. Nippon Suisan Gakkaishi, **65**: 252–259.

Aglen, A. 1994. Sources of error in estimation of fish abundance. *In* Marine fish behaviour in capture and abundance estimation. *Edited by* A. Fernö and S. Olsen. Fishing News Books, Oxford. pp. 107–133.

Aglen, A. 1996. Impact of fish distribution and species composition on the relationship between acoustic and swept-area estimates of fish density. ICES J. Mar. Sci. **53**: 501–506.

Aglen, A., Engås, A., Huse, I., Michalsen, K., and Stensholt, B. 1999. How vertical fish distribution may affect surveys results. ICES J. Mar. Sci. **56**: 345–360.

Anthony, P.D. 1981. Visual contrast thresholds in the cod (*Gadus morhua* L.). J. Fish Biol. **19**: 87–103.

Arnold, G.P., and Greer Walker, M. 1992. Vertical movements of cod (*Gadus morhua* L.) in the open sea and the hydrostatic function of the swim bladder. ICES J Mar. Sci. **49**: 357–372.

Carlstein, E., Do, K.A., Hall, P., Hesterberg, T., and Künsch, H.R. 1998. Matched-block bootstrap for dependent data. Bernoulli, **4**: 305–328.

Casey, J.M., and Myers, R. 1998. Diel variation in trawl catchability: is it as clear as day and night? Can. J. Fish. Aquat. Sci. **55**: 2329–2340.

Demer, D.A., and Hewitt, R.P. 1995. Bias in acoustic biomass estimates of *Euphausia superba* due to vertical migration. Deep-Sea Res. Part I, **42**: 455–475.

Engås, A., and Godø, O.R. 1986. Influence of trawl geometry and vertical distribution of fish on sampling with bottom trawl. J. Northw. Atl. Fish. Sci. **7**: 35–42.

Engås, A., and Soldal, A.V. 1992. Diurnal variations in bottom trawl catch rates of cod and haddock and their influence on abundance indices. ICES J. Mar. Sci. **49**: 89–95.

Fernandes, P.G., Brierley, A.S., Simmonds, E.J., Millard, N.W., McPhail, S.D., Armstrong, F., Stevenson, P., and Squires, M. 2000a. Oceanography: fish do not avoid survey vessels. Nature (London), **404**: 35–36.

Fernandes, P.G., Brierley, A.S., Simmonds, E.J., Millard, N.W., McPhail, S.D., Armstrong, F., Stevenson, P., and Squires, M. 2000b. Addendum: fish do not avoid survey vessels. Nature (London), **407**: 152.

Fernö, A., and Olsen, S. 1994. Marine fish behaviour in capture and abundance estimation. Fishing News Books, Oxford.

Foote, K.G., Knudsen, P., Korneliussen, R.J., Nordbø, P.E., and Røang, K.S.O. 1991. Postprocessing system for echo sounder data. JASA, **90**: 37–47.

Godø, O.R., and Michalsen, K. 2000. Migratory behaviour of northeast Arctic cod, studied by use of data storage tags. Fish. Res. **48**: 127–140.

Godø, O.R., and Walsh, S.J. 1992. Escapement of fish during bottom trawl sampling — implications for resource assessment. Fish. Res. **13**: 281–292.

Handegard, N.O. 2004. Cod reaction to an approaching bottom trawling vessel investigated using acoustic split-beam tracking. Ph.D. thesis, Department of Mathematics, University of Bergen, Norway.

Handegard, N.O., Michalsen, K., and Tjøstheim, D. 2003. Avoidance behaviour in cod (*Gadus morhua*) to a bottom-trawling vessel. Aquat. Living Resour. **16**: 265–270.

Hjellvik, V., Godø, O.R., and Tjøstheim, D. 2001. Modelling diurnal variation of marine populations. Biometrics, **57**: 189–196.

Hjellvik, V., Godø, O.R., and Tjøstheim, D. 2002. Diurnal variation in bottom trawl catches: does it pay to adjust? Can. J. Fish. Aquat. Sci. **59**: 33–48.

Hjellvik, V., Michalsen, K., Aglen, A., and Nakken, O. 2003. An attempt at estimating the effective fishing height of the bottom trawl using acoustic survey recordings. ICES J. Mar. Sci., **60**: 967–979.

Huse, I., and Korneliussen, R.J. 2000. Diel variation in acoustic density measurements of overwintering herring (*Clupea harengus* L.). ICES J. Mar. Sci. **57**: 903–910.

Huse, I., and Ona, E. 1996. Tilt angle distribution and swimming speed of overwintering Norwegian spring-spawning herring. ICES J. Mar. Sci. **53**: 863–873.

Jakobsen, T., Korsbrekke, K., Mehl, S., and Nakken, O. 1997. Norwegian combined acoustic and bottom trawl surveys for demersal fish in the Barents sea during winter. ICES C.M. 1997/Y:17.

Johannesson, K.A., and Mitson, R.B. 1983. Fisheries acoustics. A practical manual for aquatic biomass estimation. Food and Agriculture Organization (UN), Rome. FAO Fish. Tech. Pap. No. 240.

Karp, W.A., and Walters, G.E. 1994. Survey assessment of semipelagic Gadoids: The example of Walleye Pollock, *Theragra chalcogramma*, in the Eastern Bering Sea. Mar. Fish. Rev. **56**: 8–22.

Knudsen, F.R., and Sægrov, H. 2002. Benefits from horizontal beaming during acoustic survey: application to three Norwegian lakes. Fish. Res. **56**: 205–211.

Korsbrekke, K., and Nakken, O. 1999. Length and species dependent diurnal variation in catch rates in the Norwegian Barents Sea bottom trawl surveys. ICES J. Mar. Sci. **56**: 284–291.

Lawson, G.L., and Rose, G.A. 1999. The importance of detectability to acoustic surveys of semi-demersal fish. ICES J. Mar. Sci. **56**: 370–380.

Løkkeborg, S., and Fernö, A. 1999. Diet activity pattern and food search behaviour in cod, *Gadus morhua*. Environ. Biol. Fishes, **54**: 345–353.

MacLennan, D.N., and Simmonds, E.J. 1992. Fisheries acoustics. Chapman & Hall, London; McGraw-Hill, New York. Fish and Fisheries Series No. 5.

McClatchie, S., Alsop, J., Ye, Z., and Coombs, R.F. 1996. Consequence of swim bladder model choice and fish orientation to target strength of three New Zealand fish species. ICES J. Mar. Sci. **53**: 847–862.

McQuinn, I.H., and Winger, P.D. 2003. Tilt angle and target strength: target tracking of Atlantic cod (*Gadus morhua*) during trawling. ICES J. Mar. Sci. **60**: 575–583.

Mehl, S., and Sunnanå, K. 1991. Changes in growth of Northeast Arctic cod in relation to food consumption in 1984–1988. ICES Mar. Sci. Symp. **193**: 109–112.

Michalsen, K., Godø, O.R., and Fernö, A. 1996. Diel variation in the catchability of gadoids and its influence on the reliability of abundance indices. ICES J. Mar. Sci. **53**: 389–395.

© 2004 NRC Canada

Nakken, O., and Olsen, K. 1977. Target strength measurements of fish. Rapp. P.-V. Reun. Cons. Int. Explor. Mer, **170**: 52–69.

Neilson, J.D., and Perry, R.I. 1990. Diel vertical migrations of marine fishes: an obligate or facultative process? Adv. Mar. Biol. **26**: 115–168.

Ona, E., and Mitson, R.B. 1996. Acoustic sampling and signal processing near the seabed: the dead zone revisited. ICES J. Mar. Sci. **53**: 677–690.

Orlowski, A. 2000. Diel dynamics of acoustic measurements of Baltic fish. ICES J. Mar. Sci. **57**: 1196–1205.

Patel, R., Handegard, N.O., and Godø, O.R. 2004. Behaviour of herring (*Clupea harrengus* L.) to an approaching autonomous unverwater vehicle. ICES J. Mar. Sci. **61**: 1044–1049.

Smart, W.M. 1977. Textbook on spherical astronomy. Cambridge University Press, Cambridge, UK.

Stensholt, B.K., Aglen, A., Mehl, S., and Stensholt, E. 2002. Vertical density distributions of fish: a balance between environmental and physiological limitation. ICES J. Mar. Sci. **59**: 679–710.

© 2004 NRC Canada

A long-term rusty crayfish (*Orconectes rusticus*) invasion: dispersal patterns and community change in a north temperate lake

Karen A. Wilson, John J. Magnuson, David M. Lodge, Anna M. Hill, Timothy K. Kratz, William L. Perry, and Theodore V. Willis

Abstract: Rusty crayfish (*Orconectes rusticus*) were first observed in Trout Lake, Wisconsin, in 1979 and took 19 years to completely disperse around the littoral zone, advancing at an average rate of 0.68 km·year^{-1}. With the invasion of rusty crayfish, we found that fishes that share prey taxa with crayfish declined in numbers over time, but piscivorous fish species did not change in abundance. Snails declined from >10 000 to <5 snails·m^{-2} in one of the first invaded areas. Mean abundance of Odonata, Amphipoda, and Trichoptera decreased significantly lake-wide. Resident crayfish species nearly disappeared, although total crayfish abundance, driven by high abundances of rusty crayfish, continued to rise. Submerged macrophyte species richness declined by as much as 80% at some locations. Together these responses demonstrate dramatic long-term changes in the littoral zone biota of Trout Lake. Continued invasions of similar lakes in the region suggest that these impacts are occurring on a region-wide basis with potentially irreversible effects on communities and ecosystems. Only through long-term natural experiments such as this study can researchers ascertain the full extent of invasions and their impacts on community and ecosystem process that respond at spatial and temporal scales not captured in mesocosm studies.

Résumé : Les écrevisses américaines (*Orconectes rusticus*) ont été observées pour la première fois en 1979 dans le lac Trout, Wisconsin, et elles ont mis 19 ans à se disperser autour de l'entière zone littorale du lac, progressant à une vitesse moyenne de 0,68 km·an^{-1}. Après l'invasion de l'écrevisse américaine, les poissons qui partagent les proies de mêmes taxons que l'écrevisse ont subi un déclin de densité dans le temps, alors que les espèces de poissons piscivores n'ont pas changé d'abondance. Les gastéropodes sont passés de >10 000 à <5 individus·m^{-2} dans l'une des premières régions à être envahies. Les abondances moyennes des odonates, des amphipodes et des trichoptères ont baissé significativement dans tout le lac. Les espèces d'écrevisses indigènes ont presque disparu, bien que l'abondance totale des écrevisses, à cause des fortes abondances de l'écrevisse américaine, aient continué à augmenter. La richesse en espèces des macrophytes submergées a baissé de jusqu'à 80 % dans certains sites. Dans leur ensemble, ces réactions démontrent l'existence de changements spectaculaires à long terme chez les organismes de la zone littorale du lac Trout. L'invasion se poursuit dans des lacs semblables de la région, ce qui indique que de tels impacts se réalisent à l'échelle de toute la région avec des effets potentiellement irréversibles sur les communautés et les écosystèmes. C'est seulement à l'aide d'expériences en nature à long terme comme la nôtre que les chercheurs peuvent évaluer l'étendue complète des invasions et leur impact sur les mécanismes des communautés et des écosystèmes, car ceux-ci réagissent à des échelles spatiales et temporelles qui ne sont pas perçues dans les études de mésocosmes.

[Traduit par la Rédaction]

Introduction

Rusty crayfish (*Orconectes rusticus*), like many crayfish species, are strong interactors in many freshwater systems and, as a consequence, may have disproportionately large effects on invaded systems. For many North American streams and lakes, invasions of rusty crayfish result in a substantial disturbance through modification of complex trophic interactions and physical habitat (reviewed in Lodge et al. 2000). Crayfish are large and often abundant, comprising important elements of lentic and lotic benthic food webs (Lodge et al. 2000). Most crayfish, including *O. rusticus*, are trophic gen-

Received 10 November 2003. Accepted 16 September 2004. Published on the NRC Research Press Web site at http://cjfas.nrc.ca on 1 February 2005.
J17831

K.A. Wilson,[1,2] **J.J. Magnuson, T.K. Kratz, and T.V. Willis.** Center for Limnology, University of Wisconsin, 680 N. Park St., Madison, WI 53706, USA.
D.M. Lodge. University of Notre Dame, Notre Dame, IN 46556, USA.
A.M. Hill. The University of Louisiana at Monroe, Monroe, LA 71209-0520, USA.
W.L. Perry. Illinois State University, Normal, IL 61790-4120, USA.

[1]Corresponding author (e-mail: k.wilson@utoronto.ca).
[2]Present address: Department of Zoology, University of Toronto, 25 Harbord Street, Toronto, ON M5S 3G5, Canada.

 doi: 10.1139/F04-170 © 2004 NRC Canada

eralists, readily consuming terrestrial leaf litter (France 1996), benthic algae (Luttenton et al. 1998), macrophytes (Lodge and Lorman 1987; Nyström and Strand 1996; Wilson 2002), aquatic invertebrates (Momot 1995; Nyström et al. 1996), fish eggs (Horns and Magnuson 1981), and detritus (Momot 1995). Small crayfish are more likely to be carnivorous and consumed themselves by many species of fish, whereas large crayfish are more omnivorous and often obtain a size and behavioral refuge from all but the largest fishes (Stein and Magnuson 1976; Momot 1995; Whitledge and Rabeni 1997). Crayfish integrate into foods web at many levels and can persist on the substantial energy reserves of the detrital pool (France 1996), making crayfish good candidates for invading aquatic systems (Moyle and Light 1996).

In short-term laboratory, pond, and field studies, researchers have chronicled a myriad of direct and indirect effects of crayfish on subsets of aquatic communities (e.g., Rickett 1974; Lodge et al. 1994; Nyström et al. 1996), but these sometimes complex interactions have not been investigated at larger scales. The lack of long-term studies on crayfish invasions and the complex trophic and behavioral interactions inherent to natural systems make it unclear how crayfish invasions affect lake littoral communities over time spans of multiple generations.

The rusty crayfish is a highly visible invader in northern Wisconsin, spreading from a historical range in the Ohio River drainage over the last 40–50 years (Hobbs et al. 1989). Rusty crayfish may have been introduced by anglers emptying their bait buckets after fishing (Capelli 1982; Hobbs et al. 1989; Ludwig and Leitch 1996), well-intentioned lake users desiring to rid their lake of nuisance weeds (Magnuson et al. 1975), or intentional releases by commercial crayfish harvesters. Capelli and Magnuson (1983) found that human activity and lack of geographic isolation best explained the presence of rusty crayfish in 67 lakes in Vilas County, northern Wisconsin. Once established, rusty crayfish may spread from lake to lake via streams and rivers or through intentional or unintentional movement by humans.

Rusty crayfish were first detected in Trout Lake, Vilas County, Wisconsin, in 1979 (Lodge et al. 1986) near a heavily used boat landing. We suspect that rusty crayfish were introduced to the lake sometime between 1973 and 1979 based on historical trapping data (Lodge et al. 1986). In 1981, researchers with the North Temperate Lakes Long-Term Ecological Research (NTL-LTER) group began a monitoring program designed in part to track changes in lake biota as rusty crayfish spread from a known introduction point around the littoral zone of Trout Lake (Lodge et al. 1986). This presented a unique opportunity to observe temporally and spatially sequential invasions in the same environment, thus avoiding the confounding effects of comparing invasions in multiple systems.

Here we document the invasion of Trout Lake by *O. rusticus* and effects of this invasion on the resident crayfish, fish, macroinvertebrate, and macrophyte communities in the lake. We focused our efforts on changes in species richness, biomass (when available), and abundance.

With increases in rusty crayfish abundance, we expected that (*a*) the abundance of other crayfish species, as direct competitors, would decrease, (*b*) crayfish prey species would decrease in abundance and species richness (i.e., snails, other macroinvertebrates, macrophytes), and (*c*) fish species (Centrarchidae) that closely interact with rusty crayfish would increase if the species consumed crayfish and decrease if the species competed with crayfish for food or had nests vulnerable to crayfish predation. We investigated two scales of response: (*i*) at the individual-site level as rusty crayfish arrived and established local populations and (*ii*) at the whole-lake scale for which we summed species richness and biomass for all sites.

Methods

Site description

Trout Lake (46°2′N, 89°40′W; Fig. 1) is a 1608-ha mesotrophic lake located in the Northern Highlands Lake District of Wisconsin within a matrix of forested land and small lakes, rivers, and streams. Its 26-km shoreline consists primarily of sand and cobble substrates, with scattered areas of submerged macrophytes and muck (Wilson 1941). The littoral zone (defined here as ≤5 m deep) occupies approximately 21% of the lake area. Mean depth is 14.6 m; maximum depth is 35.7 m. Physiochemical conditions in Trout Lake have remained similar throughout this study (Bowser et al. 1999; Magnuson et al. 1999).

Sampling methods

Crayfish invasion data

To monitor the dispersal of rusty crayfish around the lake littoral zone, an average of 73 traps (±0.68 standard error (SE) resulting from loss of traps in the field) were set roughly equidistant (0.39 km ± 0.014 SE) around the lake shore and islands once annually from 1983 to 1999 by Lodge, Kratz, and associates. In some years (1984, 1985, 1988, 1989), trapping was concentrated around the edges of the invasion front to better characterize crayfish species distributions and consisted of fewer traps (21, 35, 25, and 45 traps, respectively). The invasion front was defined as more than one *O. rusticus* per trap. Distances were calculated as straight lines between traps and therefore represented minimum distances traveled. We assumed that the origin of the rusty crayfish invasion was at the mouth of Allequash Creek (Fig. 1), which was the midpoint in the initial distribution of rusty crayfish in 1983.

To trap crayfish, we used modified minnow traps (entrance holes ~5 cm diameter) baited with 120 ± 10 g of beef liver and set for 24 h in 1.5–2 m of water. Crayfish were trapped during the period of late July to late August to minimize the number of molting (and therefore inactive) individuals in the population. Traps select for adult male rusty crayfish over other crayfish species (Olsen et al. 1991) and may underestimate abundances of other crayfish. Olsen et al. (1991) used one-half of the adult rusty crayfish males caught as a conservative estimate of rusty crayfish numbers relative to congeners. Here we present total rusty crayfish per trap to facilitate direct comparisons between the Lodge–Kratz data set and the NTL-LTER data set (discussed below).

NTL-LTER data

The abundance of crayfish, fish, and macroinvertebrates was measured annually at six permanent sampling sites (A–

© 2004 NRC Canada

Fig. 1. Rusty crayfish (*Orconectes rusticus*) invasion of Trout Lake, Vilas County, Wisconsin, in 2-year time blocks. Arrows tracing the shoreline indicate the spatial distribution of *O. rusticus* through time, where the edge of the *O. rusticus* distribution is defined as >1 *O. rusticus*·trap^{-1}. Rusty crayfish reached the Trout River by 1995 and completely surrounded the lake in 1997 (arrow not shown for clarity) when they reached North Creek. North Temperate Lakes Long-Term Ecological Research (NTL-LTER) sampling sites are lettered in the order in which they were invaded. Rusty crayfish were first detected near site A in 1979. The lake's distinct north and south basins are separated by a deep narrow constriction. Four streams enter the lake and the Trout River exits the lake. The lake's deepest point (star) is located at 46°01.756′N, 89°39.901′W. The diamond denotes a heavily used public boat landing.

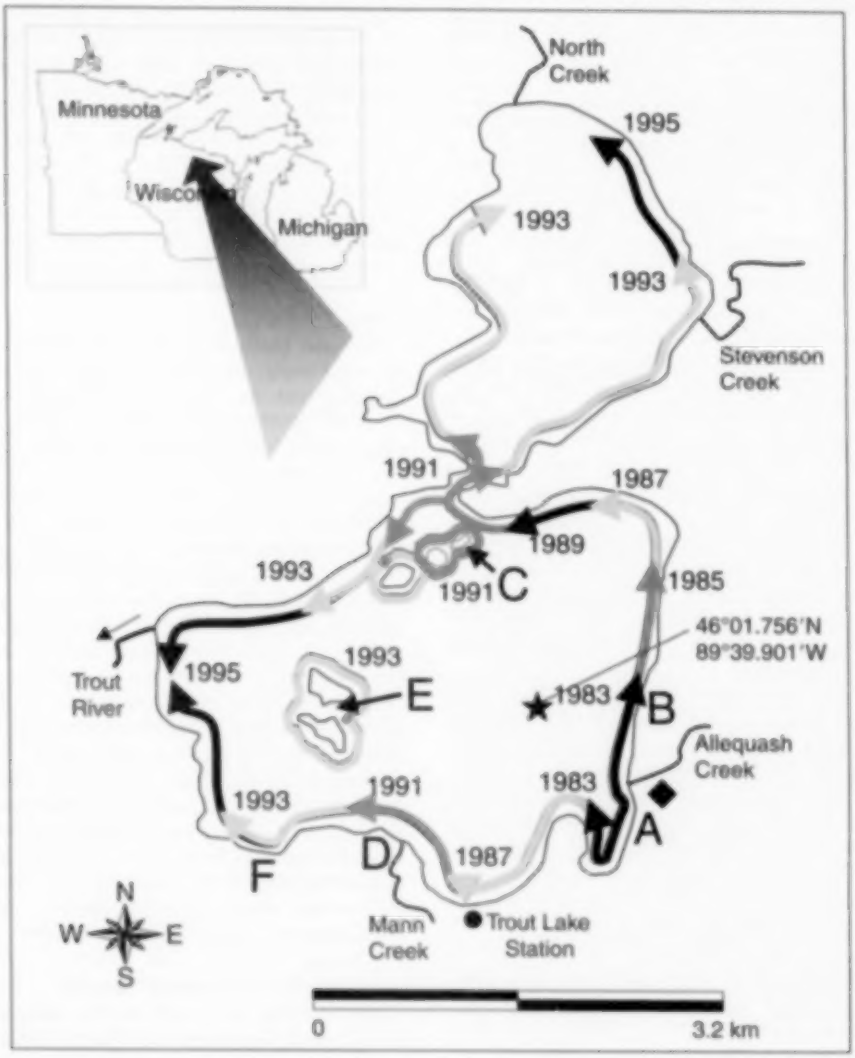

F; see Fig. 1 and Table 1) in the south basin of Trout Lake as part of NTL-LTER research group's annual sampling (1981 to present; data presented are through 1999). The NTL-LTER sampling sites are lettered in order of rusty crayfish invasion. NTL-LTER data are archived at http://limnosun.limnology.wisc.edu/.

Crayfish

To compare the change in crayfish abundances with other lake biota, we used the NTL-LTER data (Magnuson and Kratz 1999*a*) instead of the crayfish invasion data because these six sites correspond spatially and temporally to littoral zone macrophyte, macroinvertebrate, and fish sampling sites and so best represented site-specific crayfish abundances relative to other biota. Five crayfish traps were set at each LTER site until 1997, when effort was reduced to three crayfish traps per site to reduce operating costs. Traps were set within 10 m of a fyke net at the same time as the annual fish sampling (see Fish below). Crayfish were trapped in the same manner as described above.

Fish

Yearly fish sampling (1981–1999) was conducted by NTL-LTER at the same six sites where crayfish were sam-

© 2004 NRC Canada

Table 1. North Temperate Lakes Long-Term Ecological Research (NTL-LTER) sampling site characteristics.

Site	NTL-LTER site name	Primary substrate	Resident crayfish abundance (±1 SD)	Year[a]
A*	7	Sand	3.3 (2.3)	1988
B	17	Cobble	9.6 (7.5)	1988
C*	31	Sand–cobble	8.0 (3.7)	1993
D*	56	Sand	1.5 (1.1)	1995
E	67	Sand	5.4 (3.9)	1995
F*	50	Sand–muck	3.1 (1.5)	1996

Note: Sites at which macrophytes were also sampled are indicated with an asterisk (*). Resident crayfish (*Orconectes propinquus* + *O. virilis*) trap catches were averaged over the years before *O. rusticus* reached >9 crayfish·trap^{-1}. SD = standard deviation.

[a]Year *O. rusticus* reached >9 crayfish·trap^{-1}.

pled in the south basin of Trout Lake in mid- to late July (Magnuson and Kratz 1999*b*). For site-specific comparisons, we present only data from the night seines (three per site) and fyke nets (one 24-h set per site). To better characterize annual variation in species abundance in whole-lake catches, we combined all beach seine and fyke net catches, as well as trammel net and electroshocking catches from sites that did not necessarily overlap spatially with the six main sampling sites. Because trapping effort varied slightly from year to year, we calculated abundances as the number of fish caught divided by the number of sets of a gear in the lake for a year (i.e., catch per unit effort, CPUE). We then summed the CPUEs across gear types because fishing gears differ in their proficiency for catching different species and size classes of fish and thus may not be directly comparable (Weaver and Magnuson 1993).

We removed young-of-the-year (YOY) centrarchids from the analysis because their abundance can depend strongly on fluctuations in spring and summer temperature during spawning (Casselman 2002). Young-of-the-year were removed from the analysis by visually inspecting the size distribution and choosing a length that distinguished the YOY from juveniles (1+-year-olds) and adults for as many years as possible. Length criteria (millimetres total length) were similar to published size-at-age records (Becker 1983): smallmouth bass (*Micropterus dolomieu*) ≤80, largemouth bass (*Micropterus salmoides*) ≤80, rock bass (*Ambloplites rupestris*) ≤65, pumpkinseed (*Lepomis gibbosus*) ≤75, bluegill (*Lepomis macrochirus*) ≤75. Only a subsample of the fish caught in the field were measured, so that at times, individual fishes of a given length represented many unmeasured, but counted, fish of that length class. We thus adjusted the data for (*i*) changes in sampling effort over time (CPUE) and (*ii*) additional unmeasured fish of a given size class.

Macroinvertebrates

Invertebrates were sampled by NTL-LTER using modified Hester–Dendy artificial substrate samplers set in mid-August and pulled in mid-September of each year at each of the six main sampling sites (1981 or 1982 to 1999). The Hester–Dendy samplers consisted of a 7.26 cm × 7.26 cm × 10.2 cm high sandwich of interspersed components (six wide-meshed squares, four narrow-meshed squares, two tempered hardboard squares, and one plastic scrubber puff) to provide a variety of interstitial structure and substrate for macroinvertebrates. Three Hester–Dendy samplers were set at a depth of 1 m at each site; however, not all samplers were recovered in all years. Macroinvertebrates were identified to order.

Because the Hester–Dendy macroinvertebrate data were highly variable over time, we compared the mean abundance of macroinvertebrates in years of low rusty crayfish abundance and years of high rusty crayfish abundance. We defined low (≤9 crayfish·trap^{-1}) and high (>9 crayfish·trap^{-1}) rusty crayfish abundances based on the rapid increase in rusty crayfish abundance after ~9 crayfish·trap^{-1} were observed at most sites (see Fig. 2). We felt that this was an ecologically significant breakpoint, because at abundances of >9 crayfish·trap^{-1}, rusty crayfish were from two to six times more abundant than average abundances of resident crayfish before the rusty crayfish invasion (Table 1).

Snails

Because snails were not well sampled by the NTL-LTER Hester–Dendy samplers, we relied on core sampling conducted under the auspices of other projects (e.g., Lodge et al. 1987, 1994) to characterize changes in snail abundance. Snails were sampled on five occasions in the southeast bay of the South Basin. For the years 1995–2000, sediments were cored using a polyvinyl chloride pipe (inside diameter 15.22 cm) with a leading metal edge. The corer was pushed 5 cm into the sediments, and then sediments were contained by a metal plate slipped into a slot at the bottom of the corer. In 1984, samples were collected using a smaller corer (inside diameter 6.25 cm) (for details, see Lodge et al. 1994).

Macrophytes

Macrophytes at four of the six sites (sites A, C, D, and F) were assessed annually in mid-August (1982–1999) for species presence and biomass (Kratz 1999). Species presence in 0.25-m^2 quadrats was assessed by SCUBA divers at 1- or 2-m intervals along a permanent transect located along the substrate from 0.5 to 5 m in depth. Five above-sediment biomass samples (0.25 m^2 each) were taken adjacent to the permanent transects at depths of 1.5, 2.5, and 4 m for a total of 15 biomass samples per site. Biomass samples were separated by species, dried at least 24 h at 60 °C, and weighed.

Calculations and statistical analyses

We checked for evidence of temporal autocorrelation using partial autocorrelation plots (SPSS Inc. 2000). Autocorrelations were present in the macrophyte biomass times series (site B only) and the macrophyte species richness time series (sites A, B, and C), as well as rusty crayfish abundance times series at all sites and the whole lake. In all cases, autocorrelation occurred at a lag of 1 year, suggesting that values in these time series can be predicted, to some extent, by the value from the year before. However, because we were interested in how values changed in concert with increasing rusty crayfish abundance rather than predicting future change and because rusty crayfish abundance was highly correlated with time, we did not remove this time trend from the data. The data do not fit all assumptions of traditional parametric statistics; we used the nonparametric

© 2004 NRC Canada

Fig. 2. Rusty crayfish (*Orconectes rusticus*) trap catches over time for each North Temperate Lakes Long-Term Ecological Research sampling site. The dotted line denotes 9 crayfish·trap^{-1}. Each lettered panels corresponds to the same sampling site (sites A–F).

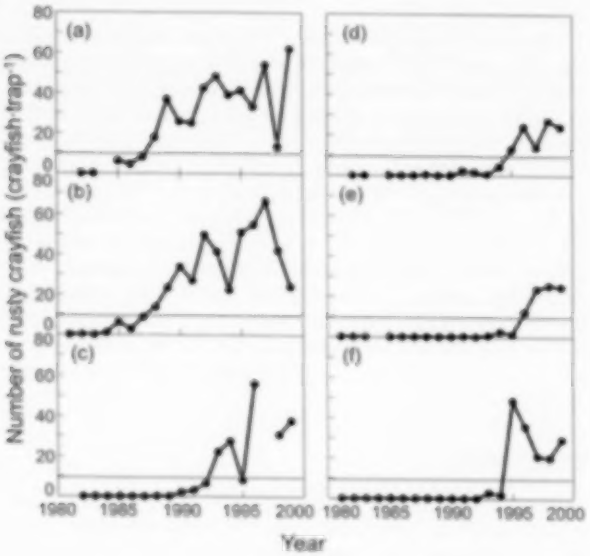

Spearman's rank coefficient (r) to describe correlations between crayfish abundance and other taxa.

Mean abundance of macroinvertebrates from years of low and high rusty crayfish abundance were compared using analysis of variance (ANOVA) to test for effects of site and level of rusty crayfish abundance. Data were $\ln(x + 1)$ transformed to achieve normality. We calculated individual ANOVAs for each macroinvertebrate order that tested the contribution of site and level of rusty crayfish abundance to variation in abundance ($N = 87$). Replicates in this case were the average macroinvertebrate abundance for each year. We assumed sites were independent because it took several years for crayfish to spread between sites and macroinvertebrates are relatively immobile (although adult forms are not).

To reduce the possibility of type I errors resulting from multiple comparisons, we used the sequential Dunn–Šidák method to calculate more conservative α values for an experiment-wise $\alpha = 0.05$ (Sokal and Rohlf 1995). Tests are considered significant if p values are less than the Dunn–Šidák associated α value (D–Š α).

Results

Rusty crayfish invasion

By 1983, rusty crayfish were well established in the southeast corner of Trout Lake (Fig. 1). The *O. rusticus* population dispersed along the shores of Trout Lake at an average rate of 0.68 km·year^{-1} (±0.14 SE). By 1990, they had crossed to the opposite shore of Trout Lake at the constriction between the two basins, traveling to depths greater than 12 m. The invasion front continued north along both shores of the North Basin and west along the north shore of the South Basin. Islands were invaded within 2 years after the arrival of *O. rusticus* on the corresponding shoreline. Rusty crayfish reached all sections of the lake by 1997.

Fig. 3. Change in whole-lake crayfish trap catches over time. Total crayfish (solid line) is the sum of the abundance of all three species of crayfish. Individual species are *Orconectes rusticus* (●), *O. propinquus* (▲), and *O. virilis* (★).

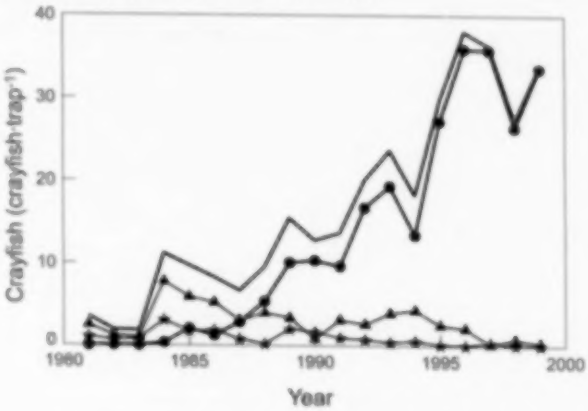

The NTL-LTER data and Lodge–Kratz data generally agreed on annual estimates of crayfish abundance. At the six different NTL-LTER sites, Pearson pairwise correlations between the NTL-LTER trap catches and five nearby crayfish invasion traps ranged from 0.42 to 0.90 for *O. rusticus*, 0.11 to 0.94 for *O. propinquus*, and –0.19 to 0.93 for *O. virilis*. At the whole-lake scale, correlations were 0.79 ($p = 0.003$) for *O. rusticus*, 0.67 ($p = 0.05$) for *O. propinquus*, and 0.71 ($p = 0.02$) for *O. virilis*. Lower correlations may be attributable in part to the different spatial extents of the data sets; for any given year, *O. rusticus* could have reached the NTL-LTER sample site but not all of the Lodge–Kratz traps. In particular, this may be true for estimates of *O. propinquus* and *O. virilis* abundances because trapping may underestimate the abundance of these species in the presence of *O. rusticus* (Olsen et al. 1991).

Orconectes rusticus abundance increased slowly at newly invaded sites but often rapidly at sites behind the invasion front (Fig. 2). A sharp rise in abundance at a site often occurred once *O. rusticus* reached an abundance of 9 crayfish·trap^{-1}. In some cases, abundances reached >60 crayfish·trap^{-1}. Despite the almost complete elimination of *O. propinquus* and *O. virilis* from Trout Lake, total crayfish abundance in the lake continued to increase (Fig. 3). Increases in total crayfish abundance were particularly dramatic at sandy-sediment sites, where total crayfish abundance went from <5 crayfish·trap^{-1} to 20 or more (see Table 1 for abundances of resident crayfish at these sites). At individual sites, *O. propinquus* and *O. virilis* abundances decreased exponentially with increases in *O. rusticus* abundance: *O. propinquus* (crayfish·trap^{-1}) = $3.455e^{(-0.026\ O.\ rusticus)}$, $R^2 = 0.40$; *O. virilis* (crayfish·trap^{-1}) = $1.473e^{(-0.112\ O.\ rusticus)}$, $R^2 = 0.49$.

In addition to our trapping, commercial crayfish harvesting has occurred in the lake since approximately 1990. Most of the commercial trapping effort is concentrated in areas of high rusty crayfish abundance (sites A and B, see Fig. 1) at depths between 2 and 3 m.

© 2004 NRC Canada

Fig. 4. Whole-lake abundance of centrarchid species vs. rusty crayfish (*Orconectes rusticus*) abundance. Young-of-year fishes are excluded. Fish species are (*a*) smallmouth bass (*Micropterus dolomieu*), (*b*) pumpkinseed sunfish (*Lepomis gibbosus*), (*c*) bluegill sunfish (*Lepomis macrochirus*), (*d*) rock bass (*Ambloplites rupestris*), and (*e*) largemouth bass (*Micropterus salmoides*).

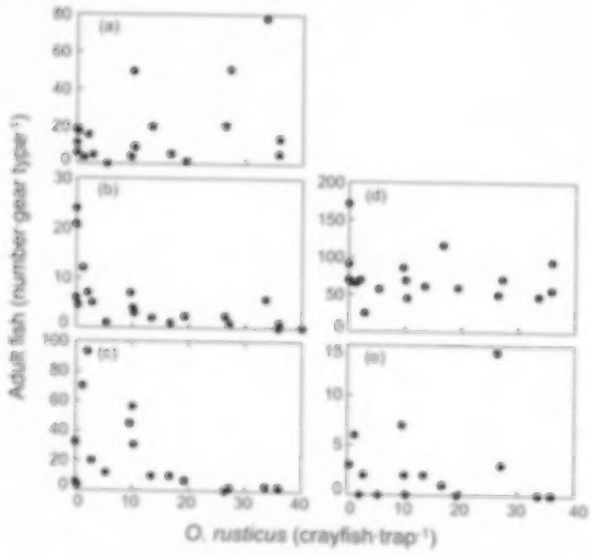

Fish

At the whole-lake scale, catches of smallmouth bass, rock bass, and largemouth bass were not correlated with increases in *O. rusticus* abundance, but bluegill (*Lepomis macrochirus*; $r = -0.63$, $p = 0.004$, D–Ŝ $\alpha = 0.009$) and pumpkinseed sunfish (*Lepomis gibbosus*; $r = -0.75$, $p < 0.001$, D-Ŝ $\alpha = 0.007$) were significantly negatively correlated (Fig. 4). Fish response was highly variable at individual sites.

Macroinvertebrates

Most invertebrate groups decreased in abundance with increases in rusty crayfish abundance. Total whole-lake macroinvertebrate abundance was not significantly correlated with increases in *O. rusticus* abundance ($r = -0.47$, $p = 0.05$, D–Ŝ $\alpha = 0.01$). Results from ANOVAs for Odonata, Amphipoda, and Trichoptera demonstrated that low abundance (pre-invasion) *O. rusticus* years boasted significantly higher counts of these macroinvertebrates than high abundance (post-invasion) *O. rusticus* years (Table 2; Fig. 5), despite significant site-to-site variation in mean abundance. Interaction terms for Amphipoda and Tricoptera were marginally significant and nonsignificant when sequential Dunn–Šidák corrections to the α value were applied. There was no significant variation for Diptera and Ephemeroptera between high and low rusty crayfish years.

Snails

Snail abundance also decreased with increasing *O. rusticus* abundance (Fig. 6). High snail abundances recorded in 1984 and 1986 were consistent with qualitative observations (D.M. Lodge, personal observation) of many snails in 1983 and 1985 in the site A area. Snails in this area declined sharply as *O. rusticus* became abundant, and by 2000, almost no snails were observed.

Macrophytes

Macrophyte species richness remained steady throughout the lake until 1996 when *O. rusticus* abundances reached high levels (>9 crayfish·trap^{-1}) at all four macrophyte sites. All sites eventually exhibited losses in macrophyte species richness with increasing *O. rusticus* abundance (Fig. 7), although this pattern was only significant in site A ($r = -0.85$, $p < 0.001$, D–Ŝ $\alpha = 0.006$) and site C ($r = -0.78$, $p < 0.001$, D–Ŝ $\alpha = 0.009$). Macrophyte species richness has remained low in recent years at site A (Fig. 8), as well as at site C, despite annual fluctuations in *O. rusticus* abundance. With increasing *O. rusticus* abundance, mean total macrophyte biomass decreased significantly at site C ($r = -0.81$, $p < 0.001$, D–Ŝ $\alpha = 0.007$) and marginally at site D ($r = -0.60$, $p = 0.015$, D–Ŝ $\alpha = 0.01$), was variable at site A, and steady at site F (Fig. 9).

Discussion

Rusty crayfish have had a profound effect on their competitors and prey in Trout Lake. Macroinvertebrate, snail, macrophyte, and crayfish species richness and, in some cases, abundance decreased within a few years of rusty crayfish arrival at sampling points around the lake. More sedentary or short-lived species, e.g., snails and some macroinvertebrates, exhibited dramatic whole-lake and site responses to increasing *O. rusticus* abundance, whereas more mobile and (or) long-lived species, e.g., fishes, macrophytes, and crayfish, required several years of exposure to increasing *O. rusticus* abundance before responding at either the local or whole-lake spatial resolution. Changes in taxa apparent at the site level often were masked at the whole-lake level, in part because of the slow *O. rusticus* invasion rate, which resulted in areas of the lake free of rusty crayfish until late in the time series.

Dispersal

The dispersal of rusty crayfish around Trout Lake was relatively slow compared with invasive species with pelagic life stages (e.g., zebra mussels, *Dreissenia polymorpha*) and considering the distances that crayfish can move in short time periods. Rusty crayfish completely encircled Trout Lake in a minimum of 16 years (1981–1997), traveling up to 9.8 km from the point of first introduction. Evidence from other area *O. rusticus* introductions suggests that *O. rusticus* invasion rates are highly variable (Olsen et al. 1991). Byron and Wilson (2001) found that *O. rusticus* moved on average 29 m·day^{-1} (at ~20 °C) between traps in Trout Lake; in the same study, several crayfish traveled up to 200 m in 48 h. Others have reported similar rates of movement for other crayfish species in ponds (15–20 m·day^{-1}, Camougis and Hichar 1959; 62 m·day^{-1}, Momot and Gowing 1972). Using this estimate for Trout Lake during the months of June, July, and August, when *O. rusticus* are most active (Lorman 1980), rusty crayfish could move 2.7 km·year^{-1} and might have encircled the lake in approximately 3 years. Clearly,

© 2004 NRC Canada

Table 2. Sources of variation in macroinvertebrate abundance (ln(x + 1) transformed).

Source	Sum of squares	df	Mean square	F ratio	P value	Associated α
Ephemeroptera (multiple R^2 = 0.40)						
Site	23.94	5	4.79	7.51	<0.001	0.006
O. rusticus	0.85	1	0.85	1.34	0.251	0.025
Site × *O. rusticus*	5.06	5	1.01	1.59	0.174	0.013
Error	47.8	75	0.637			
Odonata (multiple R^2 = 0.52)						
Site	7.32	5	1.47	7.82	<0.001	0.005
O. rusticus	2.34	1	2.34	12.48	0.001	0.006
Site × *O. rusticus*	1.67	5	0.33	1.78	0.127	0.010
Error	14.06	75	0.19			
Trichoptera (multiple R^2 = 0.71)						
Site	31.86	5	6.37	17.3	<0.001	0.004
O. rusticus	11.85	1	11.85	32.18	<0.001	0.003
Site × *O. rusticus*	4.16	5	0.83	2.26	0.057	0.009
Error	27.63	75	0.37			
Diptera (multiple R^2 = 0.45)						
Site	46.16	5	9.23	9.04	<0.001	0.005
O. rusticus	0.31	1	0.31	0.31	0.581	0.050
Site × *O. rusticus*	7.66	5	1.53	1.5	0.2	0.017
Error	76.6	75	1.02			
Amphipoda (multiple R^2 = 0.57)						
Site	22.95	5	4.59	10.59	<0.001	0.004
O. rusticus	6.71	1	6.71	15.49	<0.001	0.004
Site × *O. rusticus*	5.1	5	1.02	2.35	0.049	0.007
Error	32.49	75	0.43			

Note: "*O. rusticus*" is a binary effect representing low (≤9 crayfish·trap^{-1}) or high *Orconectes rusticus* abundance. N = 87 for each ANOVA; replicates are mean invertebrate abundance by year. P values less than the sequential Dunn–Šidák associated α are considered significant at an experiment-wise α = 0.05.

factors other than mobility slowed *O. rusticus* establishment and spread.

Although our data cannot distinguish between factors influencing invasion speed, we suspect that availability of cobble habitat, the presence of predatory fishes, and interactions with conspecifics were critical factors influencing how quickly rusty crayfish spread throughout Trout Lake. The lake's littoral zone is a mosaic of patchy macrophytes and cobble interspersed with substantial stretches of sand (Wilson 1941). In northern Wisconsin lakes, crayfish densities are consistently higher in cobble substrates (Lorman 1980; Kershner and Lodge 1995), where predation risk is low for smaller crayfishes (15- to 18-mm carapace length) relative to sand or macrophyte habitats (Kershner and Lodge 1995). Cobble areas are also nursery habitats for egg-bearing females and YOY crayfish (Lorman 1980). Perry et al. (2001*a*) found that rusty crayfish marked near the leading edge of the Trout Lake invasion front (in 1995) tended to disperse back to the nearest cobble habitat rather than forward into new, sandy habitat.

The presence of abundant predatory fishes in Trout Lake was likely an additional factor slowing the spread of rusty crayfish. Many larger fish species in Trout Lake are effective predators of small or molting crayfish (reviewed in Dorn and Mittelbach 1999), and smaller fishes like bluegill and pumpkinseed eat YOY crayfish when available (T.V. Willis, personal observation). In laboratory experiments, the presence of predatory fishes reduced foraging and other activity of *O. rusticus* (Stein and Magnuson 1976; Hill and Lodge 1994), especially over substrates that provided little refuge. However, laboratory experiments have demonstrated that *O. rusticus* generally displaces other *Orconectes* species from preferred refuge (Hill and Lodge 1999), which may increase the rate of predation on crayfish other than rusty crayfish (Capelli and Munjal 1982; DiDonato and Lodge 1993; Garvey et al. 1994) and contribute to the rapid extirpation of native crayfishes. This conspecific–predator interaction may release rusty crayfish from competition with their congeners (*O. propinquus* and *O. virilis*) and over time compensate for the inhibitory effect of predatory fishes. In addition, interbreeding between male *O. propinquus* and female *O. rusticus* is thought to have sped the establishment of rusty crayfish at, and ahead of, the invasion front (Perry et al. 2001*a*). *Orconectes rusticus* – *O. propinquus* hybrids are fecund and more competitive than either parent species (Perry et al. 2001*a*) and composed at least 6% of the Trout Lake crayfish population (F_1 hybrids) during the rusty crayfish invasion (Perry et al. 2001*b*).

© 2004 NRC Canada

Fig. 5. The mean abundance of macroinvertebrate orders (ln(x + 1) data) for years with low abundances of rusty crayfish (dotted line with triangles) and years with high abundances of crayfish (solid line with circles). High *O. rusticus* abundance was >9 crayfish·trap^{-1}. Error bars represent ±1 standard error. In a two-way analysis of variance, crayfish abundance (high or low) explained significant variation in (*d*) odonate, (*e*) trichopteran, and (*a*) amphipod abuadance. (*c*) Ephemeropterans and (*b*) dipterans varied significantly between sites only.

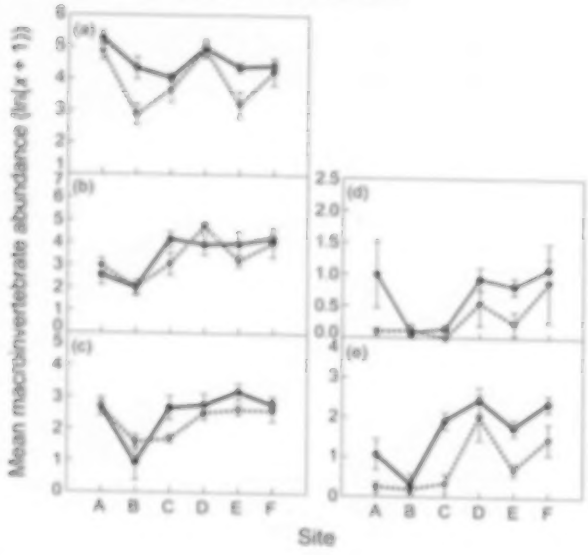

Fig. 6. Change in snail (Gastropoda) abundance over time (1984, 1986, 1989, 1990, 2000) on sandy sediments in the southeast bay of Trout Lake (near site A). Line indicates *Orconectes rusticus* abundance at site A over the same time period. Data from 1984 are from Lodge et al. (1987). Error bars represent ±1 standard error (SE). A measure of sampling error was not available for 1984.

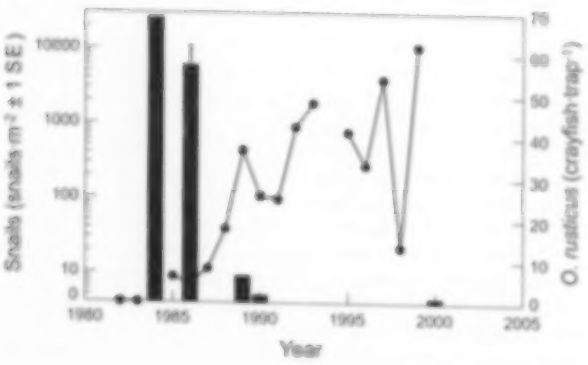

Biological impacts

In north temperate lakes, rusty crayfish and its native congeners occupy similar ecological niches, although rusty crayfish reach abundances far greater than those of the native species. In Trout Lake, we measured trap catches of rusty crayfish 2–18 times greater than the historical catches of native crayfishes, and these catches were sustained in some cases for 10 years or more (e.g., site A). Despite the differential trapability among crayfish species (Olsen et al. 1991), the increase in trap catches suggests a strong increase in total crayfish abundance. Negative impacts were generally observed at rusty crayfish catches >9 crayfish·trap^{-1}, suggesting that above this threshold value, we should expect observable changes in invaded systems. In addition, rusty crayfish consume more macroinvertebrates and macrophytes by weight than the native crayfish species (Olsen et al. 1991), adding to the impact of the sheer numbers of rusty crayfish present in invaded systems.

Fig. 7. Macrophyte species richness vs. *Orconectes rusticus* abundance at the four macrophyte sites, calculated as the species richness for post-*O. rusticus* years divided by the mean species richness for pre-*O. rusticus* years: (*a*) site A, (*b*) site C, (*c*) site D, (*d*) site F. In some years, species richness is greater than one because species richness was still high (and variable) during the early years of *O. rusticus* invasion.

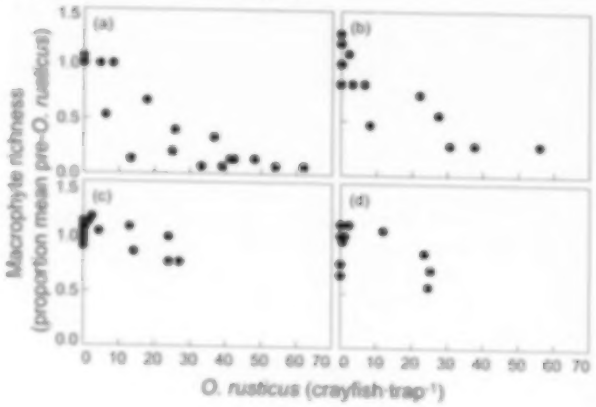

Fig. 8. Time series of macrophyte species richness at site A vs. *Orconectes rusticus* abundance. Notice the variation in crayfish abundances in later years and low variation in macrophyte species richness. The vertical solid line denotes the abundance of *O. rusticus* after which *O. rusticus* abundance increased (often sharply) at all sites.

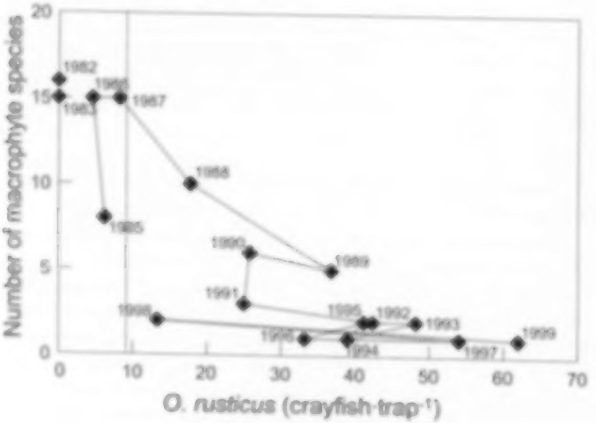

© 2004 NRC Canada

Fig. 9. Mean total macrophyte biomass (g dry weight·m^{-2}) vs. *Orconectes rusticus* abundance for each of the four macrophyte sites: (*a*) site A, (*b*) site C, (*c*) site D, (*d*) site F. Values for site F are 100 times the labeled value.

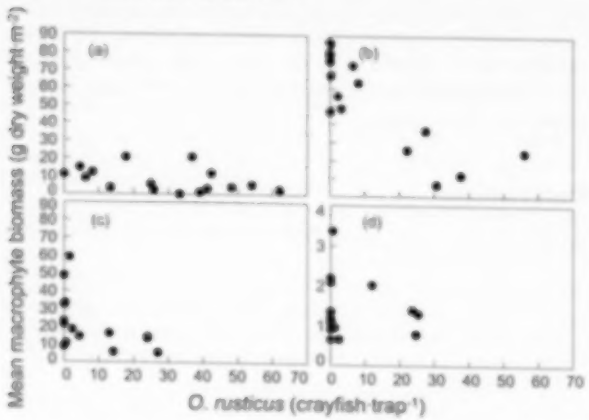

The most visible impact of rusty crayfish in Trout Lake was a shift to lower macrophyte abundance and species richness. Negative effects of crayfish on macrophytes are well documented (Lodge and Lorman 1987; Hanson and Chambers 1995; Nyström and Strand 1996). In experimental work, rusty crayfish have reduced macrophyte abundance as a result of nonconsumptive destruction (Lodge et al. 1994). Crayfish may also cause damage while grazing on periphyton or physically uproot seedlings or established plants in the process of digging burrows or foraging. In Trout Lake, loss of macrophyte species was not mirrored by decreases in macrophyte biomass at all sites, suggesting that persistent species were larger or that the loss of more vulnerable species allowed the remaining species to increase in abundance. Because some of the species lost from the lake represent highly complex and valuable habitat for macroinvertebrates, shifts in the macrophyte community to robust, often single-stemmed species likely reduced available refugia for both macroinvertebrates and fishes (e.g., Chick and McIvor 1994). Fluctuations in rusty crayfish abundance (i.e., site A) were not accompanied by recovery of the macrophyte community, suggesting that macrophyte recovery may require substantial and prolonged reductions in rusty crayfish abundance.

Short-term reductions in macroinvertebrate abundance in the presence of high densities of crayfish have been documented in a variety of experimental and natural settings (Hill and Lodge 1995; Charlebois and Lamberti 1996; Nyström et al. 1996), although reductions in non-gastropod invertebrates are less common (Lodge et al. 1994; Perry et al. 1997). In almost all cases, macroinvertebrate response to crayfish is highly variable. In this study we saw significant reductions in dipterans, odonates, and amphipods and large reductions in dipterans and ephemeropterans at some sites in years with high (>9 crayfish·trap^{-1}) rusty crayfish abundance. Although crayfish directly consume most invertebrates, reductions in numbers over long time periods may have also occurred from loss of macrophyte habitat or, in the case of predatory odonates, for example, competition for prey with rusty crayfish. The use of artificial substrates in this study may have overestimated the number of macroinvertebrates present at the different sites within the lake, because the samplers represent a more complex substrate than available in some sites (i.e., sand) or sites where macrophytes were lost over time. Rickett (1974) and Nyström et al. (1996) found that sediment-dwelling invertebrates (e.g., many Diptera, especially Chironimidae) dominated invertebrate communities in the presence of crayfish. Although we did see reductions in dipterans at some sites, Hester–Dendy samplers do not quantify sediment-dwelling organisms well and so would not have detected changes in sediment-dwelling dipterans. However, if sediment dwellers are surface grazers or detritivores, we would expect their numbers to decrease in direct competition with crayfish for prey items or reductions in detritus.

Constraints imposed by the limited spatial and temporal extent of field and laboratory experiments have prevented exploration of the impacts of rusty crayfish on long-lived and (or) highly mobile fish species (Dorn and Mittelbach 1999). Our results represent the first evidence that rusty crayfish have had long-term negative impacts on populations of bluegill and pumpkinseed sunfish populations, likely through reductions in habitat (submerged macrophytes), competition for invertebrate prey, and direct predation on eggs. Lake-wide reductions in odonates, trichopterans, amphipods, and snails represent a significant reduction in the availability of macroinvertebrate prey. Snails in particular are preferred prey for both crayfish (Lodge et al. 1998) and pumpkinseed sunfish. Pumpkinseed sunfish are rarely found in lakes containing abundant crayfish (Lodge et al. 1998) and in Trout Lake exhibited the greatest loss in abundance with increases in rusty crayfish numbers. Bluegill and pumpkinseed sunfish may also have experienced increasing frequency of nest predation by rusty crayfish (Dorn 2003). Although larger centrarchids (e.g., smallmouth bass and rock bass) can intimidate or physically remove all but the largest crayfish from their nests, pumpkinseeds (and presumably bluegill) do a poor job of defending their eggs from crayfish, especially at night (J.J. Magnuson, personal communication). In the summer of 1998 and 1999, both bluegill and pumpkinseed were observed nesting within open crayfish exclosures in Trout Lake, but nowhere nearby (Wilson 2002). Rock bass were also seen successfully nesting in heavily vegetated crayfish exclosures in 2001 and 2002 (K.A. Wilson, personal observation). We presume that these fish nested within the exclosures because of low rusty crayfish densities (Dorn 2003). In contrast to decreases in smaller centrarchid species, we detected no significant response in the abundance of adult predatory centrarchids. Before the invasion of rusty crayfish, smallmouth bass and rock bass diets in Trout Lake included 60–100% *O. propinquus* (Stein 1977). In 1990, when rusty crayfish were present only along the eastern shore of the South Basin, Garvey et al. (2003) found that rusty crayfish occurred in fish diets in proportion to their relative abundance in the lake, suggesting that rusty crayfish presently compose a large proportion of fish diets. We would expect that high availability of rusty crayfish as prey should benefit the larger centrarchids; however, competition for invertebrate prey between YOY centrarchids and crayfish, as well as loss of macrophyte habitat, may have counteracted any positive influence of increasing crayfish abundance.

© 2004 NRC Canada

The accumulated change in Trout Lake observed during the invasion of rusty crayfish represents significant changes in the forage base of Trout Lake, with the potential to modify pathways of energy transfer at the whole-lake scale. Decreases in the abundance of macroinvertebrates may disrupt trophic links and energy passage from primary producers and detritus up to higher consumers by forcing juvenile and adult centrarchids to feed on pelagically derived food sources (e.g., zooplankton, pelagic minnows; Vander Zanden et al. 1999). Alternatively, many larger fish species in Trout Lake are effective predators of small or molting crayfish (Rach and Bills 1989; Dorn and Mittelbach 1999; Weidel et al. 2000), and smaller fishes like bluegill and pumpkinseed eat YOY crayfish when available (T.V. Willis, personal observation). Under conditions of high crayfish abundance, centrarchids may switch to a crayfish-dominated diet. Under both scenarios, rusty crayfish invasions have the potential to greatly alter benthic–pelagic linkages in aquatic systems (Schindler and Scheuerell 2002; Vadeboncoeur et al. 2002). Some authors have gone further to suggest that the loss of benthic prey items may destabilize food webs by removing alternate prey items for pelagic species (Post et al. 2000; Schindler and Scheuerell 2002).

In conclusion, the invasion of Trout Lake by rusty crayfish was a slow process, with over 19 years from first detection in 1979 to eventual dominance throughout the littoral zone. Drastic declines of biota above a threshold of rusty crayfish abundances >9 crayfish·trap^{-1} suggest that high abundance is a primary reason for the large impacts of rusty crayfish, even in lakes with pre-existing crayfish populations. Sustained high abundances of rusty crayfish in the earliest invaded sites and the persistence of rusty crayfish in other regional lakes (Olsen et al. 1991) suggest that rusty crayfish will remain permanent and abundant residents of Trout Lake. The impacts observed in this study are not unique to Trout Lake; in Vilas County (Wisconsin) alone, rusty crayfish have been documented in over 40 lakes (Perry et al. 2002; Wilson 2002), and many of these lakes exhibit signs of rusty crayfish impacts (Wilson 2002). Potential for further spread is great, for example, approximately 70% of lakes located in the Canadian shield are vulnerable to rusty crayfish invasions based on pH and Ca^{2+} tolerances (although not on geographic isolation) (Vander Zanden et al. 2004), and rusty crayfish continue to spread throughout eastern North America (Lodge et al. 2000). Impacts of rusty crayfish are likely to be compounded by other human-induced stresses to aquatic ecosystems such as reductions in water quality and the loss of macrophytes from recreational boats and clearing in front of cabins (Radomski and Goeman 2001). Through shifts in littoral food web structure and energy flows, rusty crayfish have the potential for impacting recreational fisheries and rare native communities, including extirpation of native crayfish species.

Acknowledgements

We thank the staff at the University of Wisconsin's Trout Lake Station for field assistance and support over many years. B. Benson and D. Balsinger provided invaluable North Temperate Lakes Long-Term Ecological Research (NTL-LTER) database support. We also thank the many people who helped with fieldwork over the years. The manuscript was improved with comments from C. Holt and four anonymous reviewers. K.A.W., T.V.W., J.J.M., and T.K.K. were supported in part by National Science Foundation (NSF) (DEB 9632853; NTL-LTER) and the University of Wisconsin. D.M.L., A.M.H., and W.L.P. were supported by NSF (BSR85-00775, BSR89-07407, DEB 91-07569, DEB 94-08452), EPA (CR820290-01-0), NOAA Sea Grant (PU/643-1577-10), USGS/IWRRC (PU/561-1284-0432), and the University of Notre Dame.

References

Becker, G.C. 1983. Fishes of Wisconsin. University of Wisconsin Press, Madison, Wisconsin.

Bowser, C.J., Armstrong, D.E., Magnuson, J.J., and Kratz, T.K. 1999. LTER chemical limnology. North Temperate Lakes Long-Term Ecological Research Program, NSF, Center for Limnology, University of Wisconsin, Madison. Available at http://www.limnology.wisc.edu.

Byron, C.J., and Wilson, K.A. 2001. Rusty crayfish (*Orconectes rusticus*) movement within and between habitats in Trout Lake, Vilas County, Wisconsin. J. North Am. Benthol. Soc. **20**: 606–614.

Camougis, G., and Hichar, J.K. 1959. Some studies on crayfish distribution in a small pond. Am. Midl. Nat. **62**: 227–231.

Capelli, G.M. 1982. Displacement of northern Wisconsin crayfish by *Orconectes rusticus* (Girard). Limnol. Oceanogr. **27**: 741–745.

Capelli, G.M., and Magnuson, J.J. 1983. Morphoedaphic and biogeographical analysis of crayfish distribution in northern Wisconsin. J. Crustac. Biol. **3**: 548–564.

Capelli, G.M., and Munjal, B.L. 1982. Aggressive interactions and resource competition in relation to species displacement among crayfish of the genus *Orconectes*. J. Crustac. Biol. **2**: 486–492.

Casselman, J.M. 2002. Effects of climate and global warming on year-class production of warm-water, cool-water, and cold-water fishes in the Great Lakes basin. *In* Proceedings of American Fisheries Society Symposium 32, Fisheries in a Changing Climate, 20–21 August 2001, Phoenix, Arizona. *Edited by* N.A. McGinn. American Fisheries Society, Bethesda, Md. pp. 39–59.

Charlebois, P.M., and Lamberti, G.A. 1996. Invading crayfish in a Michigan stream: direct and indirect effects on periphyton and macroinvertebrates. J. North Am. Benthol. Soc. **15**: 551–563.

Chick, J.H., and McIvor, C.C. 1994. Patterns in the abundance and composition of fishes among beds of different macrophytes: viewing a littoral zone as a landscape. Can. J. Fish. Aquat. Sci. **51**: 2873–2882.

DiDomato, G.T., and Lodge, D.M. 1993. Species replacements among *Orconectes* crayfishes in Wisconsin lakes: the role of predation by fishes. Can. J. Fish. Aquat. Sci. **50**: 1484–1488.

Dorn, N.J. 2003. Effects of omnivorous crayfish on fish populations and the structure of littoral communities. Ph.D. thesis, Michigan State University, Lansing, Michigan.

Dorn, N.J., and Mittelbach, G.G. 1999. More than predator and prey: a review of interactions between fish and crayfish. Vie Milieu, **49**: 229–237.

France, R. 1996. Ontogenetic shift in crayfish delta^{13}C as a measure of land–water ecotonal coupling. Oecologia, **107**: 239–242.

Garvey, J.E., Stein, R.A., and Thomas, H.M. 1994. Assessing how fish predation and interspecific prey competition influence a crayfish assemblage. Ecology, **75**: 532–547.

Garvey, J.E., Rettig, J.E., Stein, R.A., Lodge, D.M., and Klosiewski, S.P. 2003. Scale-dependant associations among fish

© 2004 NRC Canada

predation, littoral habitat, and distributions of crayfish species. Ecology, **84**: 3339–3348.

Hanson, J.M., and Chambers, P.A. 1995. Review of effects of variation in crayfish abundance on macrophyte and macroinvertebrate communities of lakes. ICES Mar. Sci. Symp. **199**: 175–182.

Hill, A.M., and Lodge, D.M. 1994. Diel changes in resource demand: competition and predation in species replacement among crayfishes. Ecology, **75**: 2118–2126.

Hill, A.M., and Lodge, D.M. 1995. Multi-trophic-level impact of sublethal interactions between bass and omnivorous crayfish. J. North Am. Benthol. Soc. **14**: 306–314.

Hill, A.M., and Lodge, D.M. 1999. Replacement of resident crayfishes by an exotic crayfish: the roles of competition and predation. Ecol. Appl. **9**: 678–690.

Hobbs, H.H., Jass, J.P., and Huner, J.V. 1989. A review of global crayfish introductions with particular emphasis on two North American species (Decapoda, Cambaridae). Crustaceana, **56**: 299–316.

Horns, W.H., and Magnuson, J.J. 1981. Crayfish predation on lake trout eggs in Trout Lake, Wisconsin. Rapp. P.-V. Reun. Cons. Int. Explor. Mer, **178**: 299–303.

Kershner, M.W., and Lodge, D.M. 1995. Effects of littoral habitat and fish predation on the distribution of an exotic crayfish, *Orconectes rusticus*. J. North Am. Benthol. Soc. **14**: 414–422.

Kratz, T.K. 1999. LTER aquatic macroflora. North Temperate Lakes Long-term Ecological Research Program, NSF, Center for Limnology, University of Wisconsin, Madison. Available at http://www.limnology.wisc.edu.

Lodge, D.M., and Lorman, J.G. 1987. Reductions in submersed macrophyte biomass and species richness by the crayfish *Orconectes rusticus*. Can. J. Fish. Aquat. Sci. **44**: 591–597.

Lodge, D.M., Kratz, T.K., and Capelli, G.M. 1986. Long-term dynamics of three crayfish species in Trout Lake, Wisconsin. Can. J. Fish. Aquat. Sci. **43**: 993–998.

Lodge, D.M., Brown, K.M., Klosiewski, S.P., Stein, R.A., Covich, A.P., Leathers, B.K., and Bronmark, C. 1987. Distribution of freshwater snails: spatial scale and the relative importance of physiochemical and biotic factors. Am. Malacol. Bull. **5**: 73–84.

Lodge, D.M., Kershner, M.W., Aloi, J.E., and Covich, A.P. 1994. Effects of an omnivorous crayfish (*Orconectes rusticus*) on a freshwater food web. Ecology, **75**: 1265–1281.

Lodge, D.M., Stein, R.A., Brown, K.M., Covich, A.P., Bronmark, C., Garvey, J.A., and Klosiewski, S.P. 1998. Predicting impact of freshwater exotic species on native biodiversity: challenges in spatial scaling. Aust. J. Ecol. **23**: 53–67.

Lodge, D.M., Taylor, C.A., Holdich, D.M., and Skurdal, J. 2000. Nonindigenous crayfishes threaten North American freshwater biodiversity: lessons from Europe. Fisheries, **25**: 7–19.

Lorman, J.G. 1980. Ecology of the crayfish *Orconectes rusticus* in northern Wisconsin. Ph.D. thesis, University of Wisconsin–Madison, Madison.

Ludwig, H.R., and Leitch, J.A. 1996. Interbasin transfer of aquatic biota via anglers' bait buckets. Fisheries, **21**: 14–18.

Luttenton, M.R., Horgan, M.J., and Lodge, D.M. 1998. Effects of three *Orconectes* crayfishes on epilithic microalgae: a laboratory experiment. Crustaceana, **71**: 845–855.

Magnuson, J.J., and Kratz, T.K. 1999*a*. LTER crayfish. North Temperate Lakes Long-Term Ecological Research Program, NSF, Center for Limnology, University of Wisconsin, Madison. Available at http://www.limnology.wisc.edu.

Magnuson, J.J., and Kratz, T.K. 1999*b*. LTER fish. North Temperate Lakes Long-Term Ecological Research Program, NSF, Center for Limnology, University of Wisconsin, Madison. Available at http://www.limnology.wisc.edu.

Magnuson, J.J., Capelli, G.M., Lorman, J.G., and Stein, R.A. 1975. Consideration of crayfish for macrophyte control. *In* The Proceedings of a Symposium on Water Quality Management. *Edited by* P.L. Brezonik and J.L. Fox. University of Florida, Gainsville, Fla. pp. 66–74.

Magnuson, J.J., Bowser, C.J., and Kratz, T.K. 1999. LTER physical limnology. North Temperate Lakes Long-Term Ecological Research Program, NSF, Center for Limnology, University of Wisconsin, Madison. Available at http://www.limnology.wisc.edu.

Momot, W.T. 1995. Redefining the role of crayfish in aquatic systems. Rev. Fish. Sci. **3**: 33–63.

Momot, W.T., and Gowing, H. 1972. Differential seasonal migration of the crayfish *Orconectes virilis* (Hagen) in marl lakes. Ecology, **53**: 479–483.

Moyle, P.B., and Light, T. 1996. Biological invasions of fresh water: emperical rules and assembly theory. Biol. Conserv. **78**: 149–161.

Nyström, P., and Strand, J.A. 1996. Grazing by a native and an exotic crayfish on aquatic macrophytes. Freshw. Biol. **36**: 673–682.

Nyström, P., Bronmark, C., and Graneli, W. 1996. Patterns in benthic food webs: a role for omnivorous crayfish? Freshw. Biol. **36**: 631–646.

Olsen, T.M., Lodge, D.M., Capelli, G.M., and Houlihan, R.J. 1991. Mechanisms of impact of introduced crayfish (*Orconectes rusticus*) on littoral congeners, snails, and macrophytes. Can. J. Fish. Aquat. Sci. **48**: 1853–1861.

Perry, W.L., Lodge, D.M., and Lamberti, G.A. 1997. Impact of crayfish predation on exotic zebra mussels and native invertebrates in a lake-outlet stream. Can. J. Fish. Aquat. Sci. **54**: 120–125.

Perry, W.L., Feder, J.L., Dwyer, G., and Lodge, D.M. 2001*a*. Hybrid zone dynamics and species replacement between *Orconectes* crayfishes in a northern Wisconsin lake. Evolution, **55**: 1153–1166.

Perry, W.L., Feder, J.L., and Lodge, D.M. 2001*b*. Implications of hybridization between introduced and resident *Orconectes* crayfishes. Conserv. Biol. **15**: 1656–1666.

Perry, W.L., Lodge, D.M., and Feder, J.L. 2002. Importance of hybridization between indigenous and nonindigenous freshwater species: an overlooked threat to North American biodiversity. System. Biol. **51**: 255–275.

Post, D.M., Conners, M.E., and Goldberg, D.S. 2000. Prey preference by a top predator and the stability of linked food chains. Ecology, **81**: 8–14.

Rach, J.J., and Bills, T.D. 1989. Crayfish control with traps and largemouth bass. Prog. Fish. Cult. **51**: 157–160.

Radomski, P., and Goeman, T.J. 2001. Consequences of human lakeshore development on emergent and floating-leaf vegetation abundance. N. Am. J. Fish. Manag. **21**: 46–61.

Rickett, J.D. 1974. Trophic relationships involving crayfish of the genus *Orconectes* in experimental ponds. Prog. Fish-Cult. **36**: 207–211.

Schindler, D.E., and Scheuerell, M.D. 2002. Habitat coupling in lake ecosystems. Oikos, **98**: 177–189.

Sokal, R.R., and Rohlf, F.J. 1995. Biometry. 3rd ed. W.H. Freeman and Company, New York.

SPSS Inc. 2000. SYSTAT Version 10. SPSS Inc., Chicago, Ill.

Stein, R.A. 1977. Selective predation, optimal foraging, and the predator–prey interaction between fish and crayfish. Ecology, **58**: 1237–1253.

© 2004 NRC Canada

Stein, R.A., and Magnuson, J.J. 1976. Behavioral response of crayfish to a fish predator. Ecology, **57**: 751–761.

Vadeboncoeur, Y., Vander Zanden, M.J., and Lodge, D.M. 2002. Putting the lake back together: reinventing benthic pathways into lake food web models. BioScience, **52**: 44–54.

Vander Zanden, M.J., Casselman, J.M., and Rasmussen, J.B. 1999. Stable isotope evidence for the food web consequences of species invasions in lakes. Nature (Lond.), **401**: 464–467.

Vander Zanden, M.J., Wilson, K.A., Casselman, J.M., and Yan, N.D. 2004. Species introductions and their impacts in North American Shield lakes. *In* Boreal shield watersheds: lake trout ecosystems in a changing environment. Chapter 13. *Edited by* J.M. Gunn, R.J. Steedman, and R.A. Ryder. CRC Press, Boca Raton, Fla. pp. 239–264.

Weaver, M.J., and Magnuson, J.J. 1993. Analyses for differentiating littoral fish assemblages with catch data from multiple sampling gears. Trans. Am. Fish. Soc. **122**: 1111–1119.

Weidel, B.C., Josephson, D.C., and Krueger, C.C. 2000. Diet and prey selection of naturalized smallmouth bass in an oligotrophic Adirondack lake. J. Freshw. Ecol. **15**: 411–420.

Whitledge, G.W., and Rabeni, C.F. 1997. Energy sources and ecological role of crayfishes in an Ozark stream: insights from stable isotopes and gut analysis. Can. J. Fish. Aquat. Sci. **54**: 2555–2563.

Wilson, K.A. 2002. Impacts of the invasive rusty crayfish (*Orconectes rusticus*) in northern Wisconsin lakes. Ph.D. Dissertation, University of Wisconsin, Madison.

Wilson, L.R. 1941. The larger aquatic vegetation of Trout Lake, Vilas County, Wisconsin. Trans. Wisc. Acad. Sci. Arts Lett. **33**: 135–146.

© 2004 NRC Canada

Przemyslaw G. Bajer, Gregory W. Whitledge, and Robert S. Hayward	**2158–2167**	Widespread consumption-dependent systematic error in fish bioenergetics models and its implications
Przemyslaw G. Bajer, Robert S. Hayward, Gregory W. Whitledge, and Richard D. Zweifel	**2168–2182**	Simultaneous identification and correction of systematic error in bioenergetics models: demonstration with a white crappie (*Pomoxis annularis*) model
David A. Crook	**2183–2193**	Movements associated with home-range establishment by two species of lowland river fish
Claude Savenkoff, Martin Castonguay, Alain F. Vézina, Simon-Pierre Despatie, Denis Chabot, Lyne Morissette, and Mike O. Hammill	**2194–2214**	Inverse modelling of trophic flows through an entire ecosystem: the northern Gulf of St. Lawrence in the mid-1980s
Timothy E. Essington and Sture Hansson	**2215–2226**	Predator-dependent functional responses and interaction strengths in a natural food web
Juha Lilja, Timo J. Marjomäki, Juha Jurvelius, Tuomo Rossi, and Erkki Heikkola	**2227–2236**	Simulation and experimental measurement of side-aspect target strength of Atlantic salmon (*Salmo salar*) at high frequency
Vidar Hjellvik, Olav Rune Godø, and Dag Tjøstheim	**2237–2254**	Diurnal variation in acoustic densities: why do we see less in the dark?
Karen A. Wilson, John J. Magnuson, David M. Lodge, Anna M. Hill, Timothy K. Kratz, William L. Perry, and Theodore V. Willis	**2255–2266**	A long-term rusty crayfish (*Orconectes rusticus*) invasion: dispersal patterns and community change in a north temperate lake

NRC Research Press 75th Anniversary

Since the publication of the first issue of the *Canadian Journal of Research* in 1929, the National Research Council has provided scientists and engineers in Canada and elsewhere with a means to communicate with their peers in the international research community through the production of high-quality journals. NRC Research Press is proud to celebrate 75 years of science and technology publishing in Canada.

Le 75e anniversaire des Presses scientifiques du CNRC

Depuis la parution du premier numéro du *Canadian Journal of Research* en 1929, le Conseil national de recherches du Canada publient des revues savantes de qualité grâce auxquelles les chercheurs et ingénieurs du Canada et d'ailleurs peuvent partager les résultats de leurs recherches avec leurs pairs de la collectivité scientifique internationale. Les Presses scientifiques du CNRC sont fières de célébrer 75 ans d'édition scientifique et technique au Canada.

National Research Council Canada
Ottawa, Canada K1A 0R6

Conseil national de recherches Canada
Ottawa, Canada K1A 0R6

Postage paid at Ottawa
Publications mail
Registration No. 40062591

Port payé à Ottawa
Poste-publication
Enregistrement n° 40062591

USPS periodical postage paid at Champlain, NY 12919, USA

Canadian Journal of Fisheries and Aquatic Sciences

Volume 61, Number 11, November 2004

Journal canadien des sciences halieutiques et aquatiques

Volume 61, numéro 11, novembre 2004

ARTICLES		ARTICLES
Trip W. Armstrong and Roland A. Knapp	**2025–2037**	Response by trout populations in alpine lakes to an experimental halt to stocking
Francesca Vidussi, Suzanne Roy, Connie Lovejoy, Marie Gammelgaard, Helge Abildhauge Thomsen, Beatrice Booth, Jean-Eric Tremblay, and Behzad Mostajir	**2038–2052**	Spatial and temporal variability of the phytoplankton community structure in the North Water Polynya, investigated using pigment biomarkers
Lynda D. Rodwell and Callum M. Roberts	**2053–2068**	Fishing and the impact of marine reserves in a variable environment
David A. Witting, R. Christopher Chambers, Keith L. Bosley, and Sam C. Wainright	**2069–2084**	Experimental evaluation of ontogenetic diet transitions in summer flounder (*Paralichthys dentatus*), using stable isotopes as diet tracers
John M. Buffington, David R. Montgomery, and Harvey M. Greenberg	**2085–2096**	Basin-scale availability of salmonid spawning gravel as influenced by channel type and hydraulic roughness in mountain catchments
Edward A. Trippel and Steven R.E. Neil	**2097–2110**	Maternal and seasonal differences in egg sizes and spawning activity of northwest Atlantic haddock (*Melanogrammus aeglefinus*) in relation to body size and condition
Richard P. Barbiero and Marc L. Tuchman	**2111–2125**	Changes in the crustacean communities of Lakes Michigan, Huron, and Erie following the invasion of the predatory cladoceran *Bythotrephes longimanus*
Z. Zhang, W. Hajas, A. Phillips, and J.A. Boutillier	**2126–2134**	Use of length-based models to estimate biological parameters and conduct yield analyses for male Dungeness crab (*Cancer magister*)
Nathan J. Dorn and Gary G. Mittelbach	**2135–2143**	Effects of a native crayfish (*Orconectes virilis*) on the reproductive success and nesting behavior of sunfish (*Lepomis* spp.)
Brian D. Wisenden, Josh Klitzke, Ryan Nelson, David Friedl, and Peter C. Jacobson	**2144–2150**	Predator-recognition training of hatchery-reared walleye (*Stizostedion vitreum*) and a field test of a training method using yellow perch (*Perca flavescens*)
Anders Gravbrøt Finstad and Ole Kristian Berg	**2151–2157**	Bimodal population size distributions and biased gillnet sampling

Continued on inside back cover / Suite au verso

Printed in Canada by / Imprimé au Canada par
NRC Reprographic Services / Service de reprographie CNRC
Page production by / Mise en page par
NRC Research Press / Presses scientifiques du CNRC

0706-652X(20041)61:11;1-8